Imperial College London

A combined approach on the impact of EP300 overexpression on drug resistance, invasion and stemness in breast cancer

Roman Jugov

Supervisor: Dr. Ernesto Yagüe

Department of Surgery & Cancer
Imperial College London
ICTEM Building
Hammersmith Hospital Campus
London W12 0NN

A thesis submitted in accordance with the requirements of
Imperial College London for the degree of
Doctor of Philosophy

Faculty of Medicine

December 2020

Dedication

I dedicate this thesis to my parents. It would not be possible without you.

Jevgenia & Oleg

Declaration

I hereby declare that the contents of this entire thesis including the original data is my own work and that all the resources used in the thesis and all the assistance received at the professional and personal levels, for the completion of the study, have been appropriately acknowledged.

Roman Jugov
December 2020

Copyright

Roman Jugov
December 2020

Acknowledgements

Foremost, I would like to express my gratitude to my supervisor, Dr Ernesto Yagüe for his continuous support, encouragement and patient guidance for the duration of my PhD project.

Many thanks to Prof. Andy Stoker at UCL for providing the laboratory with HEK 293T cells which were used for viral transfections- and who's lab I had the pleasure of working in. Many thanks also to Dr Stelios Chrysostemou for providing unique insights on methodology for migration and invasion assays, Dr Claire Fletcher for the methodology for miR PCR analysis, Dr Giacomo Corleone and Dr Alex De Giorgio on their advice on computational analysis using R.

I would also like to thank Stephen Rothery at the Facility for Imaging by Light Microscopy, for his invaluable expertise on cell imaging and image analysis macro scripts and James Elliot at the MRC Flow Cytometry facility, for his advice on setting up the machines. I would also like to extend a special thanks to Prof. Georgios Giamas, Prof. Justin Stebbing and Dr Aleksandra Filipovic for initially inspiring me to pursue this journey during my MRes programme.

I would like to specially thank my fellow laboratory members and previous PhD students whose work this study was built upon. Note of appreciation goes to Leona Keung for motivating me and offering help when in need. Finally, I would like to express my gratefulness to Breast Cancer Now, who funded this work and allowed me to undertake this research successfully.

Abstract

Triple negative breast cancer, characterized by absence of estrogen and progesterone receptors and human epidermal growth factor receptor 2 (HER2), is very aggressive, and often progresses to metastasis. The absence of druggable targets implies that conventional chemotherapeutic agents do not work. Recent genomic studies show that epigenetics play a complicated role in maintaining healthy gene expression.

This thesis attempted to demonstrate a link between E1A binding protein P300 (EP300), epithelial to mesenchymal transition (EMT), drug resistance and cancer stem cell (CSC) traits by using breast cancer cell line models with EP300 overexpression (CAL51 and MDA-MB-231), short hairpin RNA (shRNA) lentiviral knockdown EP300 (T47D and MCF7), and EP300 knockout in colorectal cancer (HCT116). Techniques such as flow cytometry, migration/invasion assays and short/long term drug resistance assays were used to demonstrate these traits. This study also employed reverse transcription quantitative real-time PCR (RTqPCR) and RNA sequencing (RNA-seq) gene expression analysis for evaluating a gene signature and miR expression.

The study demonstrated positive regulation of EP300, forkhead box O3a (FOXO3a) and GATA binding protein 3 (GATA3) by miR-25 in minimally transformed mammary epithelial cancer (MTMEC) model. Neither RNA-seq nor RTqPCR demonstrated any correlation between cancer subtype and our gene signature. However, we confirmed that EP300 overexpression resulted in E-cadherin (CDH1) upregulation in CAL51 and MDA-MB-231. EP300 knockdown in T47D resulted in decreased expression of CDH1 and upregulated expression of FOXO3a. EP300 knockout in HCT116 downregulated CDH1. EP300 overexpression in MDA-MB-231 improved drug sensitivity to paclitaxel and doxorubicin. EP300 overexpression reduced aldehyde dehydrogenase + (ALDH) populations in MDA-MB-231 and CAL-51 cell lines, while EP300 modulation had a variable effect on CD44 antigen $(CD44)^{high}$/CD24 antigen $(CD24)^{low}$ subpopulations in these cell line models. Finally, overexpression of EP300 in MDA-MB-231 demonstrated a decrease in motility and invasion.

Table of contents

List of figures **xix**

List of tables **xxi**

Nomenclature **xxiii**

1 Introduction **1**

1.1 Breast Cancer Statistics 1

1.1.1 Breast Cancer Incidence 1

1.1.2 Breast Cancer Risk Factors 1

1.1.3 Molecular Subtypes of Breast Cancer 2

1.1.4 Methods of Detection, Diagnosis and Classification 2

1.1.5 Therapy and Management of Breast Cancer 5

1.1.6 Hallmarks of Cancer 8

1.2 Epithelial to Mesenchymal Transition (EMT) 11

1.2.1 Transcription Factors 13

1.2.2 Plasticity and CSC Characteristics 13

1.2.3 Invasion and Migration 15

1.2.4 Intravasation 16

1.2.5 Circulating Tumour Cells -the Seed Hypothesis 17

1.2.6 Micrometastasis, Drug Resistance and Relapse 19

1.3 Markers and Predictors of Drug Resistance and Metastasis 20

1.3.1 Stem Cells 20

1.3.2 Cancer Stem Cells (CSCs) 21

1.3.3 Cancer Stem Cell Maintenance 21

1.3.4 Cancer Stem Cell, EMT and Microenvironment 22

1.3.5 Cancer Stem Cell and Drug Resistance 23

1.3.6 Relevance of Markers for Stemness, EMT and Drug Resistance . . 23

1.3.7 Regulatory Pathways Involved in EMT and Stem Cell Phenotypes . 24
1.3.8 Relevance of Pathways to EMT 30
1.3.9 Relevance of Pathways to CSCs 33
1.4 EP300 and its Involvement in Transcription 35
1.4.1 Hypothesis 35
1.4.2 Transcription Factors and Drug Resistance 35
1.4.3 EP300 Function as a Transcriptional Co-activator 35
1.4.4 Structure of the EP300 Gene 42
1.4.5 Protein Structure of EP300 43
1.4.6 Functions of EP300 46
1.4.7 EP300 Mutations in Cancer 49
1.4.8 Aim 49

2 Methods **51**
2.1 Cell Culture and Maintenance 51
2.1.1 Cell Freezing and Thawing Procedure 51
2.1.2 Generating Knock-down Cell Lines with RNA Interference (RNAi) 52
2.1.3 Generating Overexpression Cell Lines 53
2.1.4 Cloning Vectors 53
2.1.5 Plasmid DNA Isolation, Digestion and Purification 54
2.1.6 Plasmid Isolation 54
2.1.7 Sequencing 54
2.1.8 Transfection Methods 55
2.1.9 Antibiotic Selection and Cell Culture Maintenance 55
2.2 Analysis of Protein Expression 56
2.2.1 Cell Lysis Procedure 56
2.2.2 Protein Concentration Estimation Using the BCA Assay 57
2.2.3 SDS-Polyacrylamide Gel Electrophoresis (SDS-PAGE) 57
2.2.4 Electroblotting by Wet Transfer Method 57
2.2.5 Western Blotting 57
2.3 Analysis of mRNA Expression by Real Time Quantitative Polymerase Chain Reaction (RTq PCR) 58
2.3.1 mRNA Extraction Method (RNeasy) 58
2.3.2 Quantification of mRNA Using NanoDrop® 58
2.3.3 Reverse Transcription of RNA for cDNA Synthesis 59
2.3.4 Real Time Quantitative Polymerase Chain Reaction (RTqPCR) . . . 59
2.3.5 Data Analysis 60

2.4 RNA-seq Data Analysis . . . 60
2.4.1 Survival Analysis . . . 60
2.4.2 RNA Sequencing Data Analysis . . . 62
2.4.3 Statistics and Plots . . . 62
2.5 Short- and Long-Term Drug Sensitivity Assays . . . 63
2.5.1 Cell Viability Assay for Drug Sensitivity . . . 63
2.5.2 Clonogenic Assay for Drug Resistance . . . 63
2.5.3 Sulphorhodamine B (SRB) Assay for Population Doubling Time . . . 64
2.6 Flow Cytometry Analysis by FACS . . . 64
2.6.1 CD44-APC and CD24-PE Assay . . . 64
2.6.2 Aldefluor Dehydrogenase (ALDH) Assay . . . 65
2.7 Cell Migration and Invasion Assay . . . 65
2.7.1 Cell Tracking Assay . . . 65
2.7.2 Wound Healing Assay . . . 65
2.7.3 Matrigel Cell Invasion via Chemotaxis . . . 66
2.8 Statistical Analysis . . . 66

3 Micro RNA and its Effect on EP300 69
3.1 Introduction . . . 69
3.1.1 What is micro RNA? . . . 69
3.1.2 Structure and Biogenesis . . . 69
3.1.3 Mechanism of Action . . . 70
3.1.4 General Overview of miR Function . . . 71
3.1.5 MiRs Involved in Epithelial to Mesenchymal Transition . . . 72
3.1.6 MiRs Involved in Chemoresistance . . . 73
3.1.7 MiR-25 . . . 74
3.1.8 MiR-27a . . . 76
3.1.9 MiR-23a . . . 80
3.2 Analysis of miRs 23a,25,27a . . . 82
3.2.1 Background . . . 82
3.2.2 Hypothesis . . . 84
3.2.3 Aim . . . 84
3.2.4 Results . . . 85
3.2.5 Discussion . . . 103
3.2.6 Future Potential Work . . . 107
3.2.7 Overall Conclusion . . . 108

4 Gene Signature Linked to EP300 **109**
4.1 Introduction . . . 109
4.1.1 ABCG2 . . . 109
4.1.2 ARHGAP20 . . . 111
4.1.3 BCL2 . . . 113
4.1.4 BMP4 and BMP7 . . . 114
4.1.5 CAPN9 . . . 116
4.1.6 Cadherins . . . 118
4.1.7 CEACAM5 . . . 121
4.1.8 CNN2 . . . 122
4.1.9 EFEMP1 . . . 124
4.1.10 EPHA4 . . . 125
4.1.11 FGFR2 . . . 127
4.1.12 FOXA1 . . . 129
4.1.13 FOXO3a . . . 131
4.1.14 GATA3 . . . 133
4.1.15 HEY2 . . . 135
4.1.16 HMCN1 . . . 136
4.1.17 ITGA2 and ITGA3 . . . 137
4.1.18 MUC5B . . . 140
4.1.19 PLS3 . . . 142
4.1.20 SGCG . . . 144
4.1.21 SNAI2 . . . 144
4.1.22 TGFβ2 . . . 145
4.1.23 TNFRSF1B . . . 148
4.1.24 VIM . . . 149
4.1.25 WIPF1 . . . 151
4.1.26 ZEB1 and ZEB2 . . . 152
4.2 Analysis of EP300 Gene Signature in Breast Cancer Cell Lines . . . 156
4.2.1 Hypothesis . . . 156
4.2.2 Aim . . . 157
4.2.3 Results . . . 157
4.2.4 Discussion . . . 194
4.2.5 Overall Conclusion . . . 198

5 Analysis of EP300 and CHD1 expression in breast cancer patient population 199
5.1 Introduction . . . 199
5.1.1 EP300 Influencing Transcription . . . 199
5.1.2 Enhancer Regions and Transcription . . . 199
5.1.3 Genomic Databases . . . 201
5.2 Analysis of Breast Cancer Patient Datasets . . . 202
5.2.1 Hypothesis . . . 202
5.2.2 Aim . . . 202
5.2.3 Results . . . 203
5.2.4 Discussion . . . 226
5.2.5 Future Potential Work . . . 228
5.2.6 Overall Conclusion . . . 229

6 EP300 and its Involvement in Drug Resistance 231
6.1 Introduction . . . 231
6.1.1 Pactlitaxel and Doxorubicin Mode of Action . . . 231
6.1.2 Drug Resistance . . . 231
6.1.3 Mechanisms of Drug Resistance . . . 232
6.2 Analysis of EP300 expression on Drug Resistance . . . 238
6.2.1 Hypothesis . . . 238
6.2.2 Aim . . . 238
6.2.3 Results . . . 238
6.2.4 Discussion . . . 248
6.2.5 Future Potential Work . . . 251
6.2.6 Overall Conclusion . . . 253

7 EP300 and Breast Cancer Stem Cells 255
7.1 Introduction . . . 255
7.1.1 Cancer Stem cells . . . 255
7.1.2 Molecular Markers of CSCs . . . 255
7.1.3 Marker Expression in Breast Cancer . . . 256
7.2 Analysis of EP300 on Breast Cancer Stem Cells . . . 261
7.2.1 Hypothesis . . . 261
7.2.2 Aim . . . 261
7.2.3 Results . . . 262
7.2.4 Discussion . . . 302
7.2.5 Future Potential Work . . . 306

7.2.6 Overall Conclusion 308

8 EP300 influence on Migration and Invasion 309
8.1 Introduction 309
8.1.1 Types of Migration 309
8.1.2 EMT and Migration 311
8.1.3 Genetic Expression of Metastatic Cells 311
8.1.4 Epigenetic Factors 312
8.1.5 Cancer Cell Invasion -ECM Remodelling 312
8.1.6 Changes in the Environment 313
8.1.7 Gene Expression in Migration 313
8.2 Analysis of EP300 on Migration and Invasion 314
8.2.1 Hypothesis 314
8.2.2 Aim 314
8.2.3 Results 315
8.2.4 Discussion 359
8.2.5 Future Potential Work 365
8.2.6 Overall Conclusion 367

9 Concluding Remarks 369

10 References 375

Appendix A Conferences and Publications 519
A.1 Breast Cancer Now Conference 2016 519
A.2 Oncogenic EP300 can be targetted with inhibitors of aldo-keto reductases . 520

Appendix B Scripts 535
B.1 Migration Cell Tracking R Script 535
B.2 Invasion Assay Image post processing on Fiji Macro Script 541
B.3 Invasion Assay Image Analysis Object Counter Fiji Macro Script 542
B.4 TCGA Data Analysis R Script 544

List of figures

1.1 Diagram of histone epigenetics 37
1.2 Diagram of EP300 gene structure 42
1.3 Diagram of EP300 protein structure 44
1.4 Diagram of the EP300 functional domains 47

2.1 Map of vectors and constructs used for EP300 knockdown 52
2.2 Plasmid constructs used in transfection 53
2.3 Sequence chromatograms indicating the START and STOP codons of the inserts 55

3.1 Visual representation of the miRs mechanism of action 83
3.2 MTMEC miR expression 87
3.3 MiR expression in 5 breast cancer cell lines 90
3.4 Gene expression in an MTMEC breast cancer cell line 91
3.5 Gene expression in 5 breast cancer cell lines 94
3.6 Effects of Doxorubicin and Taxol on miR expression in MCF7 97
3.7 Effects of Lapatinib on miR expression in BT474 99
3.8 Effect of Doxorubicin,Taxol and Lapatinib on gene expression 102
3.9 miR-25 interaction with Ep300 and CDH1 104
3.10 Effect of drug resistance on miR expression 106

4.1 Gene expression in CAL51 with EP300 overexpression 172
4.2 Gene expression in MDA-MB-231 with EP300 overexpression 176
4.3 Gene expression in HCT116 with EP300 knockout 182
4.4 Gene expression in a T47D with EP300 downregulation 187
4.5 Cell proliferation in breast cancer cell lines 190
4.6 Cell proliferation in T47D with EP300 downregulation 193

5.1 Kaplan-Meier survival curves 210

5.2 RNAseq tissue expression of EP300 and CDH1 223
5.3 TCGA gene expression analysis 225

6.1 Short-term drug sensitivity in MDA-MD-231 with EP300 overexpression . 240
6.2 Short-term drug sensitivity in T47D cells with EP300 downregulation . . . 244
6.3 Long-term drug resistance in MDA-MD-231 with EP300 overexpression . . 247

7.1 ALDH expression in CAL51 with EP300 overexpression 264
7.2 ALDH expression in MDA-MB-231 with EP300 overexpression 267
7.3 ALDH expression in drug resistant MCF7 270
7.4 ALDH expression in HCT116 with EP300 knockdown 273
7.5 $CD44^{high}/CD24^{low}$ populations in MDA-MB-231 with EP300 overexpression 278
7.6 $CD44^{high}/CD24^{low}$ populations in CAL51 with EP300 overexpression . . . 283
7.7 $CD44^{high}/CD24^{low}$ populations in MCF7 with EP300 downregulation . . . 288
7.8 $CD44^{high}/CD24^{low}$ populations in T47D with EP300 downregulation 292
7.9 $CD44^{high}/CD24^{low}$ populations in HCT116 with EP300 knockout 296
7.10 $CD44^{high}/CD24^{low}$ populations in drug resistant MCF7 301

8.1 Wound healing in CAL51 with EP300 overexpression 318
8.2 Wound healing in MDA-MB-231 with EP300 overexpression 322
8.3 Wound healing in MCF7 with EP300 downregulation 325
8.4 Wound healing in T47D with EP300 downregulation 328
8.5 Wound healing in HCT116 with EP300 knockout 331
8.6 Migration tracking in CAL51 with EP300 overexpression 336
8.7 Migration tracking in MDA-MB-231 with EP300 overexpression 340
8.8 Migration tracking in HCT116 with EP300 knockout 344
8.9 Migration tracking in MCF7 with EP300 downregulation 348
8.10 Migration tracking in T47D with EP300 downregulation 352
8.11 3D invasion through Matrigel in MDA-MB-231 with EP300 overexpression 355
8.12 3D invasion through Matrigel in HCT116 with EP300 knockout 358

List of tables

1.1 Surface receptor expression profiles of breast cancer. 2
1.2 Examples of post-translational modifications. 39

2.1 Commonly used protease and phosphatase inhibitors. 56
2.2 Antibodies used in western blotting technique. 58
2.3 Primers used in Real time PCR. 61

4.1 List of genes of interest. 159
4.2 Pathway analysis. 162

5.1 Normal tissue expression of EP300 and CDH1. 212
5.2 Expression of EP300 and CDH1 by cancer type. 218

Nomenclature

Acronyms / Abbreviations

α-SMA	α smooth muscle actin
ABCA9	ATP-binding cassette sub-family A member 9
ABCB1	ATP-binding cassette sub-family B member 1
ABCC1	Multi drug resistance associated protein
ABCC2	ATP binding cassette subfamily C member 2
ABCC3	ATP binding cassette subfamily C member 3
ABCC4	ATP binding cassette subfamily C member 4
ABCC5	ATP binding cassette subfamily C member 5
ABCG2	ATP-binding cassette super-family G member 2
ABCG5	ATP binding cassette superfamily G member 5
ACAP4	ArfGAP with coiled-coil, ankyrin repeat and PH domains 4
ACVR2A	Activin receptor type-2A
ADD	Reader domain
ADDATRX	Reader domain
AHNAK	Neuroblast differentiation-associated protein
AI	Aramatose inhibitor
AIL	Auto-inhibitory loop
AKR1C1	Aldo-keto reductase family 1 member C1
AKT	Protein kinase B
ALDH1A1	Aldehyde dehydrogenase 1 family, member A1
ALDH	Aldehyde dehydrogenase
ALK	Anaplastic lymphoma kinase
AMHR2	Anti-mullerian hormone receptor type 2
AMIDAS	Additional regulatory site adjacent to MIDAS
AML	Acute myeloid leukaemia
AMPK	AMP-activated protein kinase
ANGPTL4	Antiopoetin like 4

ANP32E	Acidic nuclear phosphoprotein 32 family member E
ANTXR1	Anthrax toxin receptor 1
AP-2β	Transcription factor AP-2 β
APAF1	Apoptotic protease activating factor 1
APC	Adenomatous polyposis coli
aPKC	Atypical protein kinase C
APLF	Aprataxin
ARG2	Argonaute protein 2
ARG	Argonaute Protein
ARHGAP20	Rho GTPase activating protein 20
ARP2	Actin-related protein
ASF1	ASF1 like histone chaperone
ASK1	Apoptosis signal-regulating kinase 1
ASPP2	Apoptosis-stimulating of p53 protein 2
ATF2	Activating transcription factor 2
ATM	ATM serine/threonine kinase
ATRX	Reader domain
AXL	AXL receptor tyrosine kinase
B-LINK	Basement membrane adhesion complex
BAC	Bcl-2 homologous antagonist killer
BAH	Bromo adjacent homology
BAX	BCL2 associated X protein
BCL-XL	B-cell lymphoma-extra large
BCL2	B-cell-lymphoma 2
BCL9	BCL9 Transcription Coactivator
BCT	Breast conservation therapy
BIM	BCL2 like 11
BL2	Bell-like homeodomain protein 2
BMI1	B lymphoma Mo-MLV insertion region 1 homolog
BMP4	Bone morphogenetic protein 4
BMP7	Bone morphogenetic protein 7
BRAF	Proto-oncogene B-Raf
BRCA1	Breast cancer 1, early onset
BRCA2	Breast cancer 2, early onset
BRCT	BRCA1 C-terminus domain
BRD4	Bromodomain-containing protein 4

BRG1	Brahma-related gene-1
BROMO	Bromodomain
BTG1	B-cell translocation gene 1
BTG2	BTG anti-proliferation factor 2
c-IAP1	Cellular inhibitor of apoptosis protein 1
C-KIT	Proto-oncogene c-KIT
C-MET	Tyrosine-protein kinase Met
C-SRC	Proto-oncogene tyrosine-protein kinase Src
C/EBPb	CCAAT/enhancer binding protein B
CAF	Cancer associated fibroblasts
CAPN9	Calpain 9
CBD	P300-P/CAF binding domain
cbEGF	Calcium-binding EGF-like
CCC	Cytoplasmic cell adhesion complex
CCL2	C-C motif chemokine ligand 2
CDG	Growth and differentiation factors
CDH11	Cadherin 11
CDH1	E-cadherin
CDH2	N-cadherin
CDK1	Cyclin dependent Kinase 1
CDK2	Cyclin dependent kinase 2
CDK4	Cyclin-dependent kinase 4
CDK6	Cyclin-dependent kinase 6
CDKN1C	Cyclin dependent kinase inhibitor 1c
CDKN2A	Cyclin dependant kinase inhibitor 2A
CEACAM5	The human carcinoembryonic antigen cellular adhesion molecule 5
CENPA	Centromere protein A
CH1	Cysteine/histidine-rich region 1
CHF	Helix loop helix factor
CID	CtBP interaction domain
CK1	Casein kinase 1
CK5	Keratin 5
CK6	Keratin 6
CKS1B	Cyclin-dependent kinases regulatory subunit 1
cMET	Tyrosine-protein kinase Met
CNB	Stereotactic guided core biopsy

CNN2	Calponin 2
co-SMAD	Common mediated SMAD
COUP-TFII	COUP transcription factor 2
COX2	Prostaglandin-endoperoxide synthase 2
CRB3	Crumbs 3
CREB	Cyclic AMP response element-binding
CRISPR	Clustered regularly interspaced short palindromic repeats
CSC	Cancer stem cell
CSF1	Colony stimulating factor 1
CSF2	Colony stimulating factor 2
CSL	Suppressor of hairless
CTBP1	C-terminal binding protein 1
CTBP2	C-terminal binding protein 2
CTC	Circulating tumour cell
CTGF	Connective tissue growth factor
CXCL12	C-X-C motif chemokine 12
CXCL1	Chemokine (C-X-C motif) ligand 1
CXCL5	Chemokine (C-X-C motif) ligand 5
CXCL6	Chemokine (C-X-C motif) ligand 6
CXCL7	Chemokine (C-X-C motif) ligand 7
CXCR1	CXC chemokine receptor 1
CXCR4	C-X-C motif chemokine receptor 4
CYR61	Cysteine-rich angiogenic inducer 61
DAAM1	Disheveled-associated activator of morphogenesis 1
DAB2	Disabled homolog 2
DAG	Diacylglycerol
DAP	Dystrophin associated protein
DAXX	Death domain associated protein
DCIS	Ductal carcinoma *in situ*
DDR1	Discoidin domain receptor 1
DEK	DEK proto-oncogene
DGCR8	DiGeorge Syndrome Critical Region 8
DHH	Desert Hedgehog
DLL1	Delta-like 1
DLL2	Delta-like 2
DLL4	Delta-like 4

DMD Dystrophin
DNMT1 DNA methyltransferase 1
DNMT3 Reader domain
DNMT3L Reader domain
DOT1L Disruptor silencing 1 like
DRAL Four and a half LIM domains 2
DVL2 Dishevelled segment polarity protein 2
DVL3 Dishevelled segment polarity protein 3
DVL Dishevelled proteins
E2F1 E2F transcription factor 1
E2F3 E2F transcription factor 3
ECM Extracellular matrix
EFEMP1 Epidermal growth factor-containing fibulin-like extracellular matrix protein 1
EGFR Epidermal growth factor
ELF5 E74-like factor 5
EMT Epithelial to Mesenchymal Transition
EpCAM Epithelial cell adhesion molecule
EPCR Endothelial protein C receptor
EPHA4 EPH Receptor A4
EPh Erythropoeitin-producing hepatocellular
ERα Estrogen receptor α
ERBB2 HER2
ERE Estrogen response elements
ER Estrogen
ERK Extracellular signal regulated kinase
ESPRP1 Epithelial splicing regulatory protein 1
EZH2 Enhancer of zeste homolog 2
FACT Facilitates chromatin transcription
FAK Focal adhesion kinase
FARP ARH/RhoGEF and pleckstrin domain protein
FBXW7 F-Box and WD repeat domain containing 7
Fen1 Flap endonuclease-1
FGFR1 Fibroblast growth factor receptor 1
FGFR2 Fibroblast growth factor receptor 2
FKH Forkhead winged helix turn helix DNA binding domain
FKHR Forkhead box protein O1

flt3	Cluster of differentiation antigen 135
FNAC	Fine needle aspiration cytology
FOSL1	FOS like 1, AP-1 transcription factor subunit
FOXA1	Forkhead box A1
FOXC1	Forkhead box C1
FOXC2	Forkhead box protein C2
FOXF2	FOXF2 encodes forkhead box F2
FOXG1	Forkhead box G1
FOXM1	Forkhead box protein M1
FOXO1	Forkhead Bbox O1
FOXO3a	Forkhead box O3
FOXP2	Forkhead box protein P2
FOXQ1	Forkhead box Q1
FRAS1	Fraser extracellular matrix complex subunit 1
FRS2	Fibroblast growth factor receptor substrate 2
FXR1	FMR1 autosomal homolog 1
G-CSF	Human granulocyte colony-stimulating factor
G6PC	Glucose 6 hosphatase
G9a	Euchromatic histone-lysine N-methyltransferase 2
GATA3	GATA Binding Protein 3
GBD	GTPase-binding domain
GDF	Growth differentiation factor
GDNF	Glial cell line derived neurotrophic factor
GDP	guanosine-5'-diphosphate
GFE	Guanine nucleotide exchange factor
GF	Growth factor
GFP	Green fluorescent protein
GLI1R	Glioma associated oncogene 1 receptor
GLI	Glioma associated oncogenes
GnRH	Gonadotropin-releasing hormone
GPI	Glycophosphatidyl-inositol
GRb2	Growth factor receptor-bound protein 2
GSK3α	Glycogen synthase kinase-3 α
GSK3β	Glycogen synthase kinase 3 β
GSTP1	Glutathione S-transferase π
GTP	Guanosine-5'-triphosphate

H2BK120ub Ubiquitination of lysine 120 on histone H2
H3K18ac Acetylation of lysine 18 on histone 3
H3K27ac Acetylation on lysine 27 on histone 3
H3K36me3 Tri-methylation at the 36th lysine residue of the histone H3
H3K39me5 Methylation on lysine 39 on histone 3
H3K3m1 Monomethylation of the 3rd lysine residues of histone H3
H3K4ac Acetylation of lysine 4 on histone 3
H3K4me1 Monomethylation of the4th lysine residues of histone H3
H3K79me3 Tri-methylation at lysine 79 on histone 3
H3K9ac Acetylation on lysine 9 on histone 3
H3K9me2 Di-methylation at the 9th lysine residue of the histone H3
H4K16ac Acetylation of lysine 16 on histone 4
H4K8ac Acetylation on lysine 8 on histone 4
HA Hyaluronic acid
HAS2 HA synthase 2
HAT Histone acetyltransferase
HAV Histidine alanine valine domain
HAX1 HS-1-associated protein X-1
HDAC1 Histone deacetylase 1
HDAC2 Histone deacetylase 2
HDAC7 Histone deacetylase 7
HD Homeodomain
hDlg Homolog of disc-large tumor suppressor
HER2 Human epidermal growth factor receptor 2
HES Hes family BHLH transcription factor
HEY2 Hairy/enhancer-of-split related with YRPW motif protein 2
HEY Hairy/enhancer-of-split related with YRPW motif protein
HEYL Hairy/enhancer-of-split related with YRPW motif-like protein
HGF Hepatocyte growth factor
HIF1α Hypoxia-inducible factor 1-α
HIF2 Hypoxia inducible factor 2
HIPK1 Homeodomain interacting protein kinase 1
HJURP Holliday junction recognition protein
HLH Helix loop helix
HMCN1 Hemicentin-1
HMGA2 High mobility group AT-hook 2

HMGB1 High mobility group box 1
HPC Hematopoietic progenitor cell
HPSE Heparanase
HRAS Transforming protein p21
HSP27 Heat shock protein 27
hTERT Telomerase reverse transcriptase
HUGL2 Scribble cell polarity complex component 2
I-SMAD Inhibitory SMAD
IBiD IRF3 binding domain)
ICAM1 Endothelium associated intercellular adhesion molecule 1
ICM Inner cell mass
ID1 Inhibitor of DNA Binding 1
IDR Intrinsically disordered regions
IF Intermediate filament
IGF-1R Insulin like growth factor-1
IGF1 Insulin-like growth factor 1
IHH Indian hedgehog
IL-1α Interleukin 1β
IL-1β Interleukin 1β
IL-17-b Interleukin 17b
IL-17A Interleukin 17A
IL10 Interleukin 10
IL6 Interleukin 6
IL8 Interleukin 8
ILR6 Interleukin 6 receptor
IM Immunomodulary
IRS-1 Insulin receptor substrate 1
ITGA2 Integrin subunit alpha 2
ITGA3 Integrin subunit alpha 3
ITGA6 Integrin subunit α 6
ITGA6 Integrin subunit alpha 6
ITSN1 Intersectin 1
JAG1 Jagged 1
JAG2 Jagged 2
JAK1 Janus Kinase 1
JAK Janus kinase

JNK c-Jun N-terminal kinases
KAT2B Lysine acetyltransferase 2
KDM4A Lysine demethylase 4A
KDM Lysine demethylase
Ki67 Ki67 proliferation index
KIX Kinase inducible domain of CREB interacting domain)
KLF4 Kruppel-like factor 4
KLF5 Kruppel-like factor 5
KLF8 Kruppel like factor 8
KMT Lysine methyltransferase
KRAS Kirsten rat sarcoma viral oncogene homolog
KRTHB1 Keratin, type II cuticular Hb1
LANA2 Latency-associated nuclear antigen 2
LAR Luminal androgen receptor
LATS1 Large tumor suppressor kinase 1
LATS2 Large tumor suppressor kinase 2
LBD Ephrin-ligand binding domain
LCIS Lobular carcinoma *in situ*
LEF Lymphoid enhancer-binding factor
LHRH Luteinizing hormone releasing hormone
LIMK1 Lim kinase 1
LLC Large latent complex
lncRNA GAS5 Long non-coding RNA growth arrest specific 5
lncRNA Long non-coding RNA
LOH Loss of heterozygosity
LOX Lysyl oxidase
LR Local occurrence
LRP Low density lipoprotein receptor-related protein 1
LSD1 Lysine-specific histone demethylase 1A
LY6E Lymphocyte Antigen 6 family member E
M-CSF Macrophage colony stimulating factor
M-RIP Myosin phosphatase Rho interacting protein
MAPK Mitogen activated protein kinase
Max MYC-associated protein X
MBT Malignant brain tumour
MCM7 Minichromosome maintenance complex component 7

MCT1	Monocarboxylate transporter 1
MDM2	Mouse double minute 2 homolog
Med1	Mediator of RNA polymerase II transcription subunit 1
MEK	Mitogen-activated protein kinase kinase
MENA	Mammalian-enabled (MENA) protein
MiRISC	miRNA-induced silencing complex
miR	Micro RNA
miRSNP	miR specific single nucleotide polymorphism
MKK3	Mitogen-activated protein kinase 3
MLCK	Myosin light-chain kinase
M	Mesenchymal
MMP2	Matrix Matrix Metallopeptidase 2
MMP3	Matrix metallopeptidase 3
MOAP1	Modulator of apoptosis 1
MOMP	Mitochondrial outer membrane permeabilization
MRE	MiRNA response elements
mRNA	Messenger RNA
MSC	Mesenchymal stem cells
MSL	Mesenchymal stem cell like
MST1	Macrophage stimulating 1
MSX2	Homeobox protein MSX-2
MT1-MMP	Membrane type 1-matrix metalloproteinase
MT2-MMP	Membrane type 2-matrix metalloproteinase
MT2A	Metallothionein 2A
MT3-MMP	Membrane type 3-matrix metalloproteinase
MTg-AMOs	Multiple-target anti-miRNA antisense oligo-deoxyribonucleotides
mTOR	Mammalian target of rapamycin
MTSS1	MTSS I-BAR domain containing 1
MUC1	Mucin 1
MUC5B	Mucin 5b
MYC	MYC proto-oncogene
MYO10	Filopodia inducing motor protein myosin-X
MYT1	Myelin transcription factor 1
NANOG	Homeobox protein NANOG
NBD	Nucleotide binding domains
Nedd9	Neural precursor cell expressed, developmentally down-regulated 9

NES	Nuclear export sequence
NF-$\kappa\beta$	Nuclear factor $\kappa\beta$
NF2	Neurofibromatosis 2
NFAT	Nuclear factor of activated T-cells
NIM	Nucleosome remodelling deacetylase interaction motif
NLS	Nuclear localisation sequences
NPM1	Nucleophosmin
NRID	Nuclear receptor interaction domain
NWASP	Neural Wiskott-Aldrich syndrome protein
OCT4	(Octamer-binding transcription factor 4
OS	Overall survival
p110	Phosphatidylinositol-4,5-bisphosphate 3-kinase
P4HA2	Prolyl 4-hydroxylase subunit alpha-2
p55	Membrane palmitoylated Pprotein 1
p85	Phosphoinositide 3-kinase
PAR-3	Partitioning defective 3
PARP9	Poly(ADP-ribose) polymerase family member 9
PARPG	Poly(ADP-ribose) glycohydrolase
PARP	Poly(ADP-ribose) polymerase
PATJ	PATJ crumbs cell polarity complex component
PBZ	PAR binding zinc finger
PCR1	Polycomb repressive complex 1
PCR2	Polycomb repressive complex 2
PDCD4	Programmed cell death 4
PDGF-BB	Platelet-derived growth factor subunits BB
PDGF-C	Platelet-derived growth factor C
PDGFR	Platelet derived growth factor
PEAK1	Pseudopodium enriched atypical kinase 1
PEF	Penta EF hand
PGC-1α	Peroxisome proliferator activated receptor γ coactivator 1α
PGE2	Prostaglandin E_2
PHD	Plant homeodomain
PHLPP2	PH domain and leucine rich repeat protein phosphatase 2
PH	Phosphatidylinositol phosphate binding protein domain
PI3K	Phosphoinositide 3-kinase
PIK3CA	Phosphatidylinositol-4,5-bisphosphate 3-kinase catalytic subunit α

Pin1	Propyl-isomerase
PIP2	Phosphatidylinositol 4,5 biphosphate
PIP3	Phosphatidylinositol 3,4,5 triphosphate
PKHD1L1	Polycystic kidney and hepatic disease 1-like 1
PK	Protein kinase
PLAG1	Pleomorphic adenoma gene 1
PLC	Phospholipase C
PLD1	Phospholipase D1
PLD2	Phospholipase D isoform 2
PlGF	Placental growth factor
PLK-1	Polo-like kinase 1
PLS3	Plastin 3
PMP22	Peripheral myelin protein 22
PN	Peripheral neuropathy
POU5F1	POU class 5 homeobox 1
PP2A	Protein phosphatase 2A
PPP2R1A	Protein phosphatase 2 scaffold subunit alpha
PPP2R1B	Protein phosphatase 2 scaffold subunit beta
PP	Protein phosphatase
pRb	Phosphorylated retinoblastoma protein
Pre-miR	Precursor Micro Ribonucleic Acid
Pri-miR	Primary Micro Ribonucleic Acid
PR	Progesterone
PSEN1	Presenilin-1
PSG	Pregnancy specific glycoproteins
PSI	Plexin sempaphorin integrin
PSPC1	Paraspeckle component 1
PTCH-1	Patched homolog-1
PTCH	Co receptor patched
PTEN	Phosphatase and tensin homolog
PTGR1	Prostaglandin reductase 1
PTHLH	Parathyroid hormone like hormone
Pygo	Pygopus Family PHD Finger 1
RAB40B	RAB40B, member RAS oncogene family
RAD51	RAD51 recombinase
RAF1	Raf-1 Proto-Oncogene

Raf1	RAF proto-oncogene serine/threonine-protein kinase
Rap1	Ras-proximate-1 or Ras-related protein 1
RA	RA domain which binds Rap1
RARRES3	Retinoic acid receptor responder protein 3
Ras	Ras oncogene
RASSF1A	Ras association domain family 1 isoform A
RB1	Retinoblastoma
Recq14	RecQ protein-like-4
RELN	Reelin
RFS	Relapse free survival
RHOA	Ras homolog family member A
RhoGDI1	Rho GDP dissociation inhibitor alpha
RING	Really interesting new gene (RING) domain
RMT	Arginine methyltransferase
ROCK2	Rho associated coiled-coil containing protein kinase 2
ROCK	Rho-associated protein kinase
ROR1	Receptor tyrosine kinase like orphan receptor 1
RSMAD	Receptor regulated SMAD
RTK	Receptor tyrosine kinase
RUNX3	RUNX family transcription factor 3
RYR3	Ryanodine receptor 3
S1PR1	Sphingosine 1 phosphate receptor
S1P	Sphingosine 1 phosphate
SAM	Sterile motif
SARA	Transcriptional regulator SarA
SAV1	Salvador family WW domain containing protein 1
SBD	SMAD binding domain
SET	Protein SET
SFRP1	Secreted frizzled related protein 1
SGCG	γSarcoglycan
SGK	Serine/threonine-protein kinase
SGPP1	Sphingosine 1 phosphate
SHH	Sonic hedgehog
shRNA	Short Hairpin RNA
SID	SMAD interaction domain
SIM2	SIM BHLH transcription factor 2

siRNA Small interfering RNA
SIX1 Sine oculis homeobox 1
SLNB Sentinel lymph node biopsy
SMAD2 Mothers against decapentaplegic homolog 2
SMAD3 Mothers against decapentaplegic homolog 3
SMAD4 Mothers against decapentaplegic homolog 4
SMAD7 Mothers against decapentaplegic homolog 7
SMO Smoothed homolog precursor
SNAI1 Snail family transcriptional repressor 1
SNAI2 Snail family transcriptional repressor 2
SNP Single-nucleotide polymorphism
SOD2 Superoxide dismutase 2
SOS Son of sevenless homolog
SOX3 Transcription factor SOX-3
SPFFbxo45 Ubiquitin E3 ligase
SPRY2 Sprouty 2
STAT3 Signal transducer and activator of transcription 3
STAT Signal transducer and activator of transcription
STK11 Serine/threonine kinase 11
SUFU SUFU negative regulator Of hedgehog signaling
T315I Threonine 315 to isoleucine mutation
TAD Transactivation domain
TAK1 Mitogen-activated protein kinase kinase kinase 7
TAM Tumor associated macrophage
TARG1 Terminal ADP ribose protein glycohydrolase
TAZ2 Transcriptional adaptor zinc finger domain 2
TAZ Tafazzin
TBO TATA-binding protein
TCF T-cell factor
TEAD1 TEA domain transcription factor 1
TERT Telomerase reverse transcriptase
TE Trophectoderm
TF Transcription factor
TGFβ2 Transforming growth factor β2
TGF-β1 Transforming growth factor β 1
TGFB1I1 Transforming growth factor beta 1 induced transcript 1

TGFBR1	Transforming growth factor beta receptor I
Tid1	Tumorous imaginal disc 1
TIMP1	TIMP metallopeptidase inhibitor 1
TK1	Cytoplasmic tyrosine kinase domain 1
TKI	Protein kinase inhibitors
TLTBP	Latent TGFβ binding protein
TMD	Transmembrane domains
TNFR1	Tumor necrosis factor receptor 1
TNFRSF1B	Tumour necrosis factor receptor 2
TNM	TNM classification of malignant tumors
TOP2A	DNA Topoisomerase II Alpha
TPX2	Targeting protein for Xklp2
TRAF2	TNF receptor associated factor 2
TRAF6	TNF receptor associated factor 6
TRAIL	TNF related apoptosis inducing ligand
TRBP	Transactivation Response Element RNA binding Protein
TRIM33	Tripartite motif containing 33
TSC1	TSC complex subunit 1
TSP1	Thrombospondin 1
TTN	Titin
TUBB3	Tubulin beta 3 class III
TWIST1	Twist family BHLH transcription factor 1
TWIST	Twist-related protein
USP22	Ubiquitin specific protease 22
UTR	Untranslated region
VEGFR1	Vascular endothelial growth factor receptor 1
VEGFR2	Vascular endothelial growth factor receptor 2
VEGF	Vascular endothelial growth factor
VIM	Vimentin
VWA	Von WIlllerband A
WH1	WSP homology1
WIPF1	WAS/WASL interacting protein family member 1
WIRE	WIP-like protein
WNT	WNT signaling pathway
XIAP	X-linked inhibitor of apoptosis protein
YAP1	Yes associated protein 1

YAP	Yes-associated protein
ZBTB10	Zinc finger and BTB domain containing 10
ZEB1	Zinc finger E-box binding homeobox 1
ZEB2	Zinc finger E-box binding homeobox 2
ZF	Zinc finger
ZNF2	Zinc finger motif 2
ZZ	ZZ type zinc finger domain

Chapter 1

Introduction

This thesis is concerned with, the underlying biochemical mechanisms behind metastasis, drug resistance and stem cell maintenance and generation uncovered through our work on E1A Binding Protein P300 (EP300).

1.1 Breast Cancer Statistics

1.1.1 Breast Cancer Incidence

Among cancers, breast cancer is second in incidence rates around the world and is the most common cause of cancer death in the developed world, with 198,000 cases compared to lung cancer (Murray and Lopez, 1997; Ferlay, Steliarova-Foucher et al., 2013). Breast cancer incidence rate is set to increase to 3.2 million by 2050 (Hortobagyi et al 2005). Around 55,000 of these women are diagnosed with breast cancer every year in the UK (Downs-Holmes and Silverman, 2011; Kotiyal and Bhattacharya, 2014). Additionally, 7400 women are diagnosed with a non-invasive form of breast cancer. CRUK cites an increase in survival rates, 78% of cases have a 10-year disease-free survival. However, high incidence rates are still present in most new cases which are located in less developed countries (Ferlay, Soerjomataram et al., 2015).

1.1.2 Breast Cancer Risk Factors

Risk factors for the disease include: age of onset (usually over 50), genetic mutation in Breast cancer type 1 susceptibility protein (BRCA1) and Breast cancer type 2 susceptibility protein (BRCA2), length of time from onset of menstrual cycles to menopause, will increase exposure to hormones and risk. Familial history of breast cancer also plays a role: the

Table 1.1 Surface receptor expression profiles of breast cancer.

Subtype	Occurrence%	ER	PR	HER2	CK5/6	EGFR	Ki67
Luminal A	40	+	+/-	-	Varies	Varies	Low
Luminal B	20	+	+/-	+	Varies	Varies	High
HER2	∼10-15	-	-	+	Varies	Varies	Varies
Basal like	∼15-20	-	-	-	+(if not EGFR)	+(If not CK5/6)	Varies
Normal breast	∼5-15	-	-	-	-	-	Varies

Source (Voduc, Cheang et al., 2010; Michiels et al., 2012).

likelihood of developing the disease increases if a first-degree relative has had it, disease recurrence is also more likely than once. There is also an association between receiving radiotherapy before the age of 30 and having a history of use of diethylstilboestrol that increases breast cancer risks. Lifestyle factors is also influential: low physical activity, obesity, hormone replacement or oral contraceptive use, high alcohol consumption and late pregnancy all place an individual at a higher risk of developing the disease (Garcia-Closas, Brinton et al., 2006).

1.1.3 Molecular Subtypes of Breast Cancer

The most common molecular subtypes of breast cancer are Luminal A, Luminal B, human epidermal growth factor receptor 2 (HER2) enriched, normal-like and triple negative. Triple negative have been further identified as basal-like 1 (BL1), basal-like 2 (BL2), immunomodulatory (IM), mesenchymal (M), mesenchymal stem cell like (MSL) and Luminal androgen receptor (LAR) (Lehmann, Bauer et al., 2011; Cancer Genome Atlas, 2012). These tumours can be identified through multiparameter profile testing (Bastien, Rodriguez-Lescure et al., 2012). Depending on their subtype, this alters their expression profile for surface receptors useful for therapies, such as Estrogen (ER), Progesterone (PR), HER2, cytokeratin 5 and 6 (CK5/6), epidermal growth factor receptor (EGFR) and the Ki67 marker of proliferation (**Table 1.1**).

1.1.4 Methods of Detection, Diagnosis and Classification

Breast cancer diagnosis is assessed by taking an ultrasound of the breast tissue, pathological assessment of a tumour tissue sample taken by a stereotactic guided core biopsy (CNB), fine needle aspiration cytology (FNAC) or sentinel lymph node biopsy (SLNB) (Senkus,

Kyriakides et al., 2015). The approach differs based on whether: (1) it is necessary to see lymph node involvement in a follow-up patient (Hammon, Dankerl et al., 2015); or (2) it is a new patient for whom it is necessary to predict metastasis to lymph nodes (Ahn, Kim et al., 2013).

Tumours are classified by their histology, grade, stage of the tumour, or by determination of DNA makeup or receptor status, as mentioned in the previous section. The difference between these is that staging is a rating system determined by a physician on the extent of the spread of the tumour and its size. These determinants include blood tests, histology testing and risk factors. They are important for patient prognosis, as a physician will be able to determine whether more testing is necessary. Alternatively, it can also be a useful metric to assess treatment results between patient groups undergoing clinical trials. Staging is the size of a tumour and how far it has spread. This is important while grade determines how the cancer cells appear under the microscope and how fast they proliferate. Finally, receptor status determines whether hormone therapy can be used. Altogether, these determine the therapy that a patient receives.

The patient's expression of ER, PR, HER2 receptors is determined by immunohistochemistry, and other proliferation markers such as Ki67 provide additional information on prognosis (Dowsett, Nielsen et al., 2011). The receptor status and pathological assessment is followed by a gene expression profile test such as Mammaprint™, OncoVue® Test, Oncotope DX (Zoon, Starker et al., 2009). The gene expression profile tests help mitigate recurrence of disease through tailored treatment plans based on individual profiles, advancing in one of the many steps in the direction of personalised healthcare.

Histology examines the epithelial lining and ducts of the breast to see the morphology of the cells and whether there is any spread to surrounding tissue or vasculature, e.g. the case of carcinoma *in situ* and invasive carcinoma. Grading depends on appearance compared to normal breast tissue, and this will compare whether cells are losing their differentiation, divide uncontrollably and if they have double the amount of DNA (diploid). In general, the greater differences between surrounding cells, the worse the prognosis.

Staging is conducted via TNM staging system which was originally defined by the American Joint Committee on Cancer (AJCC). It includes the extent or size of a primary tumour (T1-T4), lymph node involvement (N1-N3) and presence of metastasis (M). There is also a score for when a tumour or lymph node cannot be evaluated, TX and NX, or when there is no evidence of a primary tumour (TO) and no regional lymph node involvement (NO). Once every category is scored, an overall stage is given. Stage 0 is considered precancerous, stage 1 – 3 has lymph node involvement, whereas stage 4 is metastatic and has the worst prognosis (Sawaki, Shien et al., 2018; Edge, Hortobagyi et al., 2019). This staging can either

be clinical or pathological. The difference between the two is that pathological staging is done once the tumour has been surgically removed, and not used if surgical intervention is not necessary. There is also a possibility of underestimating tumour stage if pathological staging is preceded by chemotherapy.

Receptor status detects the presence of nuclear or cytoplasmic hormone receptors which bind hormones, the most common of which are estrogen receptor (ER), progesterone receptor (PR) and HER2. These are significant to determine which type of therapy would be effective; the types of therapy will be covered later in other chapters. However, a method for standardising their use as a predictive biomarker is yet to be achieved (Martinez-Perez, Turnbull et al., 2019).

Commonly, breast cancers fall under ductal or lobular carcinoma textitin situ and invasive ductal or lobular carcinoma (Li, Uribe et al., 2005), which will be further discussed below. Ductal carcinoma *in situ* (DCIS) (stage 0) is non-invasive and confined to the mammary ducts or tissue where they originated. Disease progression varies, notably low-grade DCIS will progress to invasive. 60% of the time in a 40-year follow-up and there is also a small potential for overdiagnosis of such cases. The chance for five-year survival is around 83%. (Yen, Tabar et al., 2003; Gorringe and Fox, 2017) Invasive lobular carcinoma is the second most common type of breast cancer diagnosed, comprising around 10% of all invasive breast cancer. The cancer originates in the lobules and presents much later than ductal carcinoma, in early 60s patients versus mid to early 50s. Lobular carcinoma *in situ* is diagnosed between the ages of 40 – 50 and is benign. Lobular carcinoma *in situ* is difficult to diagnose as it has no symptoms. (Oppong and King, 2011) Invasive ductal carcinoma has no distinct features and is classified based on ruling out all other specific forms; it is the diagnosis in 55% of cases (Eheman, Shaw et al., 2009). The survival rate is high and the likelihood of progression of invasion is low in cases of ductal, mucinal, cribriform and tubular carcinomas. However, there exist rare subtypes like inflammatory carcinoma that have a higher chance of invasion progression. Prognosis depends on the tumour size (T1a-T4), lymph node involvement (N0-N2), grade, vascular invasion, hormone receptor status and oncogene upregulation. The phenotype can be observed as forming tubular structures, an increased rate of cell division as well as different nuclear size. As mentioned above, the subtype can be further divided into ductal, mucinal, cribriform and tubular carcinomas.

Metastatic breast cancer spreads to the liver, bone, brain and lungs, this type of cancer is stage 4. The main mode of therapy as adjuvant chemotherapy, which is given to triple negative tumours, HER2 overexpressing tumours and sometimes to luminal cancers if they have a high grade (G3) with multiple node involvement and high ki-67 proliferation index (Coates et al 2015). In this case, adjuvant chemotherapy has been helpful in decreasing

breast cancer mortality (Weigelt et al 2005). A retrospective study has shown that of 2956 cases analysed, of which 86.5% were invasive ductal carcinoma, 50% of these cases had lymph node involvement and 19.9% of the total cases were triple negative (Copson et al 2013). This triple negative phenotype is often characteristically similar to the basal molecular subtype, which is present in 34% of young patients (Azim et al 2012). However, this is not the only contributing factor, as gene expression was also related to poorer prognosis (Anders et al 2008). It is clear from recent literature that cancer is heterogenous and requires multiple approaches for better classification and prediction. A recent study outlined that a combination of molecular classification and clinical parameters yields better decision making (Taherian-Fard et al 2015).

1.1.5 Therapy and Management of Breast Cancer

Earlier detection aims to prevent disease progression, which is difficult to treat. After the main patient assessment is completed as previously described, the patient will be advised to modify their lifestyle through alterations in diet and physical activity (Cuzick, DeCensi et al., 2011). The focus will then be dependent on whether the disease is diagnosed in the early or late stage, which determine the employment of local or approach which is targeted on multiple sites, with potential surgical excision of diseased tissue. (Harris, Fritsche et al., 2007) This section will outline the different treatment approaches.

Local Treatments

Local treatments comprise localised radiotherapy and mastectomies (i.e. surgical removal of diseased tissue), lumpectomy or breast conserving therapy. In early cases, this is conducted with adjuvant radiotherapy simultaneously. (Franceschini, Martin Sanchez et al., 2015). Tumour margin is important in reducing local occurrence (LR) in patients that need breast conservation. Yet, there is no consensus as to what the margin should be, which results in repeat surgery for 25% of patients with invasive carcinoma and 33% of patients with DCIS (McCahill et al 2012). The margin is however less important than tumour biology, and while no link on tumour for invasive carcinoma and 2 mm margin on DCIS is the guideline principle, widening margins has not shown to reduce LR (Park et al 2000). In terms of cosmetic outcome, breast conservation surgery is the most favourable, especially patients with larger breast size (Senkus, Kyriakides et al., 2015).

Mastectomy is the complete removal of breast tissue, this is done in the most severe cases usually followed by breast reconstruction. This can be operated either completely or involve some form of sparing procedure of the skin or nipple (Atiyeh, Dibo et al., 2014).

DCIS patients under the age of 40 will benefit from this procedure (Meijnen, Oldenburg et al., 2008), whereas patients with invasive cancer will not (Ananthakrishnan and Lucas, 2008). Breast reconstruction therapy can be carried out immediately after a mastectomy or delayed based on whether the tumour margin needs to be increased or further radiotherapy is necessary. In these cases, a space filler is used in place of where the implants will be placed (Ananthakrishnan and Lucas, 2008).

A lumpectomy is the excision of a portion of the breast and falls under breast conservation therapy (BCT). It is one of the methods used for early stage breast cancer. Previous data showed that lumpectomy combined with radiotherapy is comparable to mastectomy outcome in DCIS (Fisher, Redmond et al., 1989).

Adjuvant Therapy

Adjuvant therapy is given to patients with early stage cancer who are due to undergo surgery or to those patients that are receiving radiotherapy. The goal of adjuvant therapy is to work alongside the primary therapy to improve disease-free survival. This can be implemented within two to six weeks post-surgery (Lohrisch, Paltiel et al., 2006). The implementation time is on a case by case basis but usually dependent on tumour size, grade and lymph node involvement. Age, the overall health of the patient and co-morbidity, drug sensitivity, pros and cons of using particular therapies, and the risk of relapse are also relevant. (Lohrisch, Paltiel et al., 2006; Hernandez-Aya & Gonzalez-Angulo, 2013; Senkus, Kyriakides et al., 2015). An extensive list of recommendations for adjuvant therapy is given by Hernandez-Aya and Gonzalez-Angulo (2013).

In the case of triple negative cancers, cytotoxic chemotherapy with anthracycline and taxane is used. ER-negative, HER2-positive or ER-positive and HER2-positive cancers do not require systemic therapy when there is no lymph node involvement. Chemotherapy plus trastuzumab is prescribed at T1 b, c and a higher T/N stage is given anthracycline and taxane with concurrent trastuzumab over 12 months; whereas ER-positive and HER2-negative (luminal) without markers, will require endocrine therapy. In the case of pre- and post-menopausal low risk groups, it will require five years of tamoxifen treatment with extended therapy offered in case of luminal B-like sub type or higher risk in pre-post menopause. (Coates, Winer et al., 2015)

Neoadjuvant Therapy

Neoadjuvant therapy is used on inoperable cancers, which tend to be of larger tumour size. Neoadjuvant therapy can come in the form of chemo, endocrine therapy and targeted

therapy (Senkus, Kyriakides et al., 2015). Systemic therapy administered prior to surgery can decrease time spent in surgery and increase likelihood of operating on inoperable tumours by decreasing the cancer stage (Gralow, Burstein et al., 2008; Senkus, Kyriakides et al., 2015). If such preoperative therapy is successful, this would give vital information on favourable response to therapy and disease-free survival in earlier stage breast cancer for future references (Gradishar, Anderson et al., 2015).

Endocrine Therapy

Hormone therapy can be used for ER positive breast cancer. Pre-menopausal patients account for 20% of all breast cancers. For these patients, the main mode of therapy is a five year cycle of tamoxifen monotherapy (EBCTCG et al., 2005), in some cases combined with gonadotropin-releasing hormone (GnRH) (Cuzick et al., 2007), or with suppression of ovarian function (Pagani et al., 2014). Although in these patients, HER2 overexpression and PR negative status is associated with aggressive disease, no alternative protocol exists. Tamoxifen has been shown to have a benefit across age groups, and with a 41% reduction of annual recurrence rate and 34% reduction of annual mortality (EBCTCG et al., 2005). There is also a study on combining tamoxifen with anthracycline therapy, which improved disease free survival (IBCSG et al., 2006). Initially, the use of aromatase inhibitors (AI) were not beneficial and were observed to have an adverse effect, through an estrogen surge (Smith et al., 2003). However, recent studies have shown that the combined use of luteinizing hormone releasing hormone (LHRH) with Aramatose Inhibitors (AI), produce better estrogen suppression (Pistelli et al., 2018).

In post-menopausal patients, the treatment is similar, and tamoxifen has been the preferred treatment, showing a 41% risk reduction in patients regardless of ER status (EBCTCG et al., 2005). It has, however, recently been replaced by third generation AIs, which have improved response rates and time to progression, disease free survival. The main difference as to why this works better is perhaps explained by the difference in how pre-post-menopausal patients respond to estrogen. Premenopausal women experiment estrogen in a systematic way and under the influence of the hypothalamic pituitary ovarian axis. Whereas in postmenopausal patients, the effect is localised to the tissue in which estrogen is synthesised, and therefore the tissue concentration is fold higher than the systemic (Simpson et al., 2003)

The treatment works by: (1) blocking the ovarian function by using GnRH agonists or LHRH agonists which interfere with the pituitary gland signals, negating the feedback loop to produce estrogen; (2) blocking estrogen production through AIs by blocking aromatase enzymes. (3) using selective estrogen receptor modulators and interferes with the ability of

estrogen to regulate growth of breast cells through the binding to estrogen receptors directly. Alternatively, anti estrogen drugs are used to function as estrogen agonists in the last case.

1.1.6 Hallmarks of Cancer

The initial hallmarks of cancer were first described as the ability to generate self-sufficient growth signals, insensitivity to anti-growth signals, evasion of apoptosis, uncontrolled replication, angiogenesis and invasion and metastasis into tissues (Hanahan et al., 2000). Two more hallmarks were later added: the ability to reprogram energy metabolism and the evasion for the immune response (Weinberg et al., 2014). However, some disagree with these definitions on the basis that, with the exclusion of invasion and metastasis, other hallmarks are shared by non-malignant, benign, conditions (Wilbur et al., 2017). Having said that, they are the best approximation of what cancer is. This will briefly describe the hallmarks below.

Self-sufficient Growth

The self-sufficiency in growth signals can be gained through autocrine signalling of mitogenic growth factors (GF), such as platelet derived growth factor (PDGF) and tumour growth factor α (TGFα) (Fedi et al., 1997), a process by which the tumour produces its own signalling. Alternatively, they can stimulate the tumour microenvironment to produce these GFs (Cheng et al., 2008). In the same way, the receptors that respond to GFs can also be upregulated and overcome the ligand threshold for receptor stimulation ligand-independent signalling (DiFiore et al., 1987). Alternatively, through the expression of pro-growth integrins that activate the Salt Overly Sensitive (SOS)-Rat sarcoma (RAS)-rapidly accelerated fibrosarcoma (RAF)- mitogen-activated protein (MAP) kinase pathway (Giancotti et al., 1999). In a similar way, ligand receptors can be circumvented altogether via the stimulation of the downstream pathways. This is a result of the accumulation of somatic mutations which leads to aberrant signalling of pathways, such as Phosphoinositide 3-kinase (PI3K) (Jiang and Liu, 2009). Feed-back loops are also important and loss of function mutations in phosphatase and tensin homolog (PTEN) and mammalian target of rapamycin (mTOR) prevent the signal shut down of PI3K (Jiang and Liu, 2009; Sudarsanam and Johnson, 2010). Overall, these processes result in uncontrolled cell proliferation and growth.

Avoidance of Growth Inhibitors

As previously mentioned, growth and division are tightly controlled processes, regulated by tumour suppressors. The growth inhibitory signalling is achieved by inhibition of

transforming growth factor β (TGFβ) mediated effects on phosphorylated retinoblastoma protein (pRb) (Moses et al., 1990). This in turn disables cell cycle checkpoints at the G1 phase and promotes E2F transcription factors, resulting in loss of growth inhibition. There is also avoidance of differentiation through promotion of the Myelocytomatosis (MYC)/MYC Associated Factor X (MAX) complexes (Foley and Eisenman, 1999). Such processes are altered or switched off in cancer cells. Alternatively, there is also an interruption of contact inhibition.

Apoptosis

Apoptosis is the process by which cells undergo self-destruction as a response to DNA damage, cell signalling, hypoxia, or infection (Evan, Littlewood et al., 1998). The evasion of apoptosis is mainly through the upregulation of B-cell lymphoma 2 (BCL2), an inhibitor of apoptosis as it prevents the effectors of apoptosis BCL-2-like protein 4 (BAX) and BCL-2 homologous antagonist killer (BAK) from functioning (Adams & Cory, 2007). The upregulation of these anti apoptotic regulators, and the upregulation of pro-survival signals via extracellular insulin-like growth factor 1 (IGF1) can initiate the PI3K-Protein kinase B (AKT) pathway to prevent apoptosis. Additionally, suppression of pRB and tumour protein P53 (p53), which are also regulators of apoptosis (Symonds et al., 1994; Sherr et al., 2002), or via the loss of PTEN (Cantley & Neel, 1999). There are also other cell death mechanisms avoided such as autophagy and necrosis. Autophagy has the same PI3K and mTOR signalling pathways (Levine et al., 2008); whereas necrosis relates to another hallmark, avoidance of the immune system.

Limitless Proliferation

Cancer cells also have limitless replicative potential due to them being able to avoid the cell senescence by elongating their telomeres (Blasco et al., 2005). These telomeres normally shorten each cell division cycle, after which the limit is reached and the cell can no longer divide, normally within 70 doublings (Wyllie et al., 1980). Telomerase Reverse Transcriptase (TERT), the telomerase enzyme is also implicated in regulating the Wingless-related integration site (WNT) pathway (Park et al., 2009). Such an advantage is gained through the inhibition of pRB and p53 tumour suppressors. The pRB protein is responsible for regulating the growth and division cycle, which it regulates by sensing growth inhibition signals (Burkhart & Sage, 2008). While p53 can either halt growth or initiate apoptosis by reacting to intracellular response to stress and abnormality, i.e. monitoring glucose or oxygenation levels (Sherr et al., 2002). A further mechanism of control that is lost is cell

contact inhibition, the loss of Neurofibromatosis 2 (NF2) and Serine/threonine kinase 11 (STK11) which both promote contact inhibition (Curto et al., 2007; Shaw, 2009).

Angiogenesis

Tumours also require vast amounts of nutrients and it is done through angiogenesis. Under normal circumstances, new vessel formation is restricted to embryogenesis and wound healing. These processes are manipulated by a tumour to induce the tumour microenvironment to form new vessels. It begins with the entry into blood vessels, travel down the circulation and into new tissues. It is mainly through the actions of vascular endothelial growth factor (VEGF) 1/2/3 (Ferrara et al., 2009) and fibroblast growth factor 1 and 2 (FGF1/2) (Baeriswyl, Christofori et al., 2009), while downregulating inhibitors of angiogenesis like thrombospondin 1 and β-interferon (Ribatti et al., 2009). There is also evidence that transforming oncogenes such as RAS and MYC, are also implicated. There is also interplay with the avoidance of immunity, as tumours also use macrophages to initiate neovascularization in its microenvironment (Ferrara et al 2010).

Invasion and Metastasis

The final hallmark, invasion and metastasis, is defined as the ability to enter nearby tissues, and determines the malignant nature of a tumour. This involves the deregulated expression of cell adhesion molecules, notably E-cadherin (Berx, van Roy et al., 2009), as well as upregulation of α β integrin subunits utilised in migration, and degradation of the extracellular matrix (ECM) through protease expression (Varner et al., 1996). This is a multistep process through which a signalling cascade is initiated (Talmadge, Fidler et al., 2010), and results in the intravasation into the vasculature and dissemination into other tissues. A process largely regulated by the epithelial to mesenchymal transition (EMT).

Deregulated Metabolism

Deregulated metabolism refers to cancer cells utilising the Warburg effect, in which they thrive in hypoxic conditions. These cells upregulate glycolysis and lactic acid fermentation and prevent any kind of aerobic activity exerted by the mitochondria, which results in conversion of pyruvate into more material for cell growth and division.

Avoidance of the Immune Response

Avoidance of the immune system is the mechanism where the tumour prevents lymphoid cells to detect it, or by recruiting them to reshape the tumour microenvironment. Avoidance of necrosis is one such mechanism (Galuzzi & Kroemer, 2008).

1.2 Epithelial to Mesenchymal Transition (EMT)

EMT is the process in which epithelial characteristics are lost and the cell is transformed into a mesenchymal state which allows it to migrate to a new site. A reverse process exists called the Mesenchymal to Epithelial transition (MET) and it is believed that by this process migrating cancer cells form new micro metastatic niches at distal sites form the primary tumour. The EMT process itself has roots in embryogenesis, whereby migrating neurons and epithelial cells form new tissues like the neural crest. It is also where the origin of Snail family transcriptional repressor 1 (SNAI1) as master regulators of EMT occurs, and MET lays the foundation for cell differentiation (Nieto et al., 2009). Processes such as wound healing and gastrulation are heavily reliant on EMT (Thiery et al 2009). Even more so in cancer progression, where it is seen that EMT is the driving process in which most carcinomas begin, among them breast cancer (Ye et al., 2015).

A regular epithelial cell maintains its apical basal polarity through adhering to adjacent cells through links such as: desmosomes, tight junctions, adherens junctions. These are all maintained in some way or another, through the expression of E-cadherin. Others also exist but the loss of E-cadherin expression is canonical to the EMT process. Simultaneously, the loss of E-cadherin is followed by overexpression of mesenchymal markers in the form of N-cadherin, vimentin and fibronectin (Kalluri et al., 2009). This also alters the cellular morphology and the overall shape of the cell through reorganisation of the cytoskeletal fibres. As well as enabling the cell to migrate, invade and adopt stem like characteristics (Scheel et al., 2011). The process in which EMT begins is very complex but it involves the expression and activation of EMT transcription factors. Often described as master regulators of EMT, genes like *SNAI1*, Snail family transcriptional repressor 2 (*SNAI2*), Twist family BHLH transcription factor 1 (*TWIST1*), Zinc Finger E-Box Binding Homeobox 1 (*ZEB1*), Zinc Finger E-Box Binding Homeobox 2 (*ZEB2*), Forkhead box Q1 (*FOXQ1*), Forkhead Box C2 (*FOXC2*), Krueppel-like factor 8 (*KLF8*) can repress E-cadherin expression through epigenetic silencing of its promoter region (Wang et al., 2007; Zhang et al., 2011; Ocana et al., 2012).

The EMT process consists of several stages, initiation begins as paracrine and autocrine signalling forcing partial EMT and loss of epithelial characteristics. This paracrine signalling

can come in the form of transforming growth factor β (TGF-β), which is through the action of its two receptors, phosphorylates SMAD proteins, Mothers against decapentaplegic homolog 2 3 and 4 (SMAD2/3/4). This pathway is a common pro-invasion and metastasis pathway with control over cell fate (Han et al., 2005). Some of these SMADS even have epigenetic regulatory mechanisms, such as opening chromatin through tripartite motif containing 33 (TRIM33), as well as decreasing H3K9me2 (di-methylation at the 9th lysine residue of the histone H3) H3K36me3 (tri-methylation at the 36th lysine residue of the histone H3) (McDonald et al., 2011; Xi et al., 2011). Altogether, this activates transcription of otherwise switched off genes, resulting in the EMT cascade.

The second paracrine signalling pathway is WNT, which activates tumour progression through glycogen synthase kinase 3 β (GSK3-β) inhibition. This induces SNAI1 to associate with β-catenin and promote EMT (Kim et al., 2004; Zhou et al., 2004; Bachelder et al., 2005; Zhou et al., 2005). Without this GSK3-β phosphorylation, SNAI2 would undergo β-Transducin Repeat Containing E3 Ubiquitin Protein Ligase (βTRC) dependent ubiquitination (Wu et al., 2012). Paracrine signalling also comes in the form of activated receptor tyrosine kinases (RTKs) through growth factor stimulation, such as platelet derived growth factor (PDGFR) and epidermal growth factor (EGFR) (Jechlinger et al., 2006; Hardy et al., 2010).

Another way by which these pathways are stimulated is under hypoxic conditions. During which, there is stimulation of Hypoxia-inducible factor 1-alpha (HIF1-α) ,which upregulates SNAI1/SNAI2 (Imai et al., 2003; Lester et al., 2007). Notch signalling assists by binding to the SNAI1 gene promoter to induce transcription, as well as expressing a stabiliser protein, Lysyl oxidase (LOX) (Timmerman et al., 2004; Sahlgren et al., 2008). The final way in which the EMT process is triggered is through interaction with the tumour microenvironment. Namely, through stromal cells such as cancer associated fibroblasts, CD4 Molecule (CD4)+ helper T cells, CD8 Molecule (CD8)+ cytotoxic T cells, tumour associated macrophages and myeloid derived suppressor cells, which secrete a number of growth factors and interleukins that promote the expression of the EMT associated transcription factors (Shibue et al., 2017).

The reversal of this process is coined Mesenchymal to Epithelial transition (MET). There is evidence of this mechanism in early embryonic development of epithelial sheets (Dressler et al., 2006), as well as gaining stem cell like characteristics in de-differentiation of fibroblasts (Li et al., 2011). This process is in the later stages of cancer cells arriving at distal metastasis sites (Pattabiram et al., 2016), where the epithelial characteristics previously lost during EMT are re-gained, such as expression of E-cadherin versus N-cadherin and repression of EMT inducing transcription factors.

1.2.1 Transcription Factors

A number of transcription factors are known to be involved in stimulating or initiating the EMT process. Some of these are referred as master regulators due to the ability to interact with the E-cadherin (CDH1) promoter through the E-box nucleotide sequence. The repression of CDH1 transcription then requires their continued expression and recruits further chromatin remodelling enzymes which result in epigenetic silencing, such as trimethylation of lysine 27 on histone 3 (H3K27) (Zarek et al., 2011).

The most studied EMT transcription factors are SNAI1/ SNAI2, followed by TWIST1/ TWIST2, ZEB1 and ZEB2. All of these transcription factors work synergistically. Besides binding to the E-cadherin promoter, they can also regulate each other, and are responsible for different parts of the EMT process. SNAI1/2, stimulated through the TGF-β, Notch, WNT pathways, can induce EMT and chemoresistance (Gupta et al., 2009). Stemness, such as CD44 antigen^{high}(CD44)/CD24 antigen^{low}(CD24) status, can be controlled by octamer-binding transcription factor 4 (OCT4) (Mani et al 2008; Guo et al., 2012; Hu et al., 2012).

TWIST1 can regulate SNAI2 transcription by binding to its promoter (Casas et al., 2011). It is also paramount in migration and degradation of the ECM through formation of invadopodia structures (Eckbert et al., 2011). Further promotion of EMT generated from the overexpression of Ras-related C3 botulinum toxin substrate 1 (RAC1) which also aids in migration, invasion and repression of p16^{INK4a}, an inhibitor of cyclin-dependent kinase. It helps in bypassing oncogene induced senescence as well (Ansieau et al., 2008). Both SNAI1 and TWIST genes can be stimulated upon hypoxic conditions through different means. HIF1-α induces TWIST transcription by direct binding and promotes SNAI1 transcription through protein stabilisation (Imai et al., 2003; Lester et al., 2007; Yang et al., 2008). Along with the overexpression of transcription factors, there is also frequent loss of SNAI1 repressors such as SIM BHLH transcription factor 2 (SIM2), E74-like factor 5 (ELF5), forkhead box A1 (FOXA1), Kruppel-like factor 4 (KLF4) and SRY-Box Transcription Factor 3 (SOX3) in breast cancer. Both SNAI1 and TWIST are involved in proper early breast development (Laffin et al., 2008; Chakrabarti et al., 2012).

1.2.2 Plasticity and CSC Characteristics

Cells in the EMT state retain plasticity, so they are able to transition between EMT to MET. Friedl et al (2011) has written a review on the effects of this plasticity. The stability of this plasticity is governed by epigenetic markers, which shift as the cell goes from Epithelial to Partial EMT to Mesenchymal to and Mesenchymal Stable. This expression of epithelial

markers can also be controlled through methylation and acetylation, among other epigenetic silencing mechanisms.

Some studies show that the initial loss of E-cadherin is controlled by expression of the polycomb group of proteins which are epigenetic regulators involved in stem cell differentiation (Sparmann et al., 2006). Polycomb Repressive Complex 1 (PCR1) and Polycomb Repressive Complex 2 (PCR2) transcription factors are the most interesting as they are involved in EMT (Sparmann et al., 2006). PCR2's link to EMT is through interaction with the EZH2 protein. EZH2 drives H3K27 methylation which results in transcriptional silencing of CDH1 (Onder et al., 2008). The activation of PCR2 can also activate PCR1 which contains a functional subunit Bombyx mori nucleopolyhedrovirus orf11 (BM11). This subunit is often dysregulated in cancers and is related to stem cell characteristics (Park et al., 2004; Lobo et al., 2007). BM11 participates in EMT through stabilisation of the transcription factor SNAI1, and BM11 is itself stabilised by TWIST, another EMT transcription factor (Song et al., 2009; Yang et al., 2010).

Other mechanisms of genetic silencing of canonical EMT switches involve histone deacetylases (HDACs). HDACs are a group of enzymes that remove acetyl groups from N acetyl lysine amino acids located on histones. Through this action, the DNA is wrapped more tightly around histones, the opposite function to histone acetyltransferases. Acetylation of lysine residues can lead to histone modification and transcriptional repression of target genes. There are some examples of such repression mediators: histone deacetylase 1 (HDAC1) and histone deacetylase 2 (HDAC2), which were found to silence the CDH1 promoter through deacetylation (von Burstin et al., 2009).

Another mechanism by which genes can be controlled is histone demethylation of lysine. This is done through demethylases, which remove methyl groups from nucleic acids of histones and DNA, regulating the open and closed conformation of DNA. A group of histone demethylases, such as Lysine-specific histone demethylase 1A (LSD1), can remove methylation on tri-methylation at the 4th lysine residue of the histone H3 (H3K4me3). In particular, LSD1 has been shown to be overexpressed in ER- breast cancers and can silence E-cadherin, claudins and cytokeratins (Lim et al., 2010, Lin et al., 2010). However, LSD1 has multiple functions and both suppresses and promotes metastasis due to its involvement in conversion of dimethhylation of lysine 4 on histone 3 (H3K4me2) to a mono methylation of lysine 4 on histone 3(H3K4me1), as well as demethylation of lysine 9 on histone 3 H3K9me2 (Metzger et al., 2005).

The stable modification of histones and changing of chromatin structure to open euchromatin for gene transcription is the classic way by which genes are regulated by epigenetic mechanisms, such as the stable trimethylation of H3K9. SNAI1 is one of those genes that

is regulated by euchromatic histone-lysine N-methyltransferase 2 (G9a), a histone methyltransferase that is involved in this trimethylation (Dong et al., 2012). However, a bivalent state exists in which the genes are not actively repressed, which means that these bivalent domains, such as H3K4me3 and tri-methylation at the 27th lysine residue of the histone H3 (H3K27me3), have both a repressor and an antagonist acting on it simultaneously. Most bivalent domains are associated with embryonic stem cells, adding to their plasticity and pluripotency, such as with the case of ZEB1 (Chaffer et al., 2013). Evidence is shown in $CD44^{high}$ breast cancer cells where E-cadherin exists in a bivalent repressed state, through expression of both H3K4me3 and H3K27me3 (Maruyama et al., 2011).

This previously mentioned bivalency and expression of transcription factors such as ZEB1/SNAI1 and SNAI2, offers resistance to chemotherapy, often with the overexpression of genes involved in stem cell maintenance and cell fate (Guo et al., 2012; Lim et al., 2013), as well as gain of ABC transporters which efflux any chemotherapy targeting a cell. This stem-like phenotype is often followed by overexpression of markers like $CD44^{high}CD24^{low}$ or aldehyde dehydrogenase (ALDH), among others (Morel et al., 2008). There is also evidence of a mechanism by which cells within tumours can gain this stem like phenotype (Chaffer et al., 2011). However, only a subpopulation of cells exhibit this property, which further raises the possibility of gene bivalency and their association with multiple EMT states (Bierie et al., 2017).

1.2.3 Invasion and Migration

In the initial stages of invasion and migration, cells must traverse the basement membrane, a thick barrier that separates the epithelial layer and the interstitial layer of tissue made up of type I collagen. The basement membrane forms a scaffold by cross linkage of various extracellular proteins (such as laminin, type IV collagen), (Hohenester, Yurchenko et al., 2013). The cell begins its migration by forming a leading protrusion consisting of pseudopodia and terminal filopodia, which form connections with the ECM (Rhee et al., 2007). The mechanism of this movement is complex as it involves a number of receptors and interactions with the ECM. Cells move individually through a Ras homolog family member A (RA)-Rho-associated protein kinase (ROCK) and myosin II dependent manner to induce contraction, or as a multicellular sheet, which requires more of the ECM remodelling (Friedl et al., 2010). The sheet moves by as the leading cell paves the way through proteolytic activity, removing the barrier and the trailing macrocrack widens the gap created (Llina et al., 2011). This movement is aided by Matrix metalloproteases (MMP) expression which acts by dissolving or reorganising the ECM, studies have shown the relation of membrane type 1-matrix metalloproteinase (MT1-MMP), membrane type 2-matrix metalloproteinase

(MT2-MMP) and membrane type 3-matrix metalloproteinase (MT3-MMP) in a breast cancer cell line model (Hotary et al., 2006). MMP mediated reorganisation is controlled by adhering of $\beta 1$ integrin, and Ras-related C3 botulinum toxin substrate 1 (Rac1) dependent lamellipodia (Sanz-Moreno et al., 2008), as well as through focal adhesions (Bonnans et al., 2014). Additionally, there is a large involvement of integrins through integrin cycling, cell contraction and apoptosis resistance that many reviews have covered (Hood et al., 2002).

1.2.4 Intravasation

A cancer cell travels through the lymphatic or blood vessel system. The former is easier to penetrate due to the absence of interendothelial junctions present in blood vessels and having a lower rate of circulating fluid. For most cases, the first point of metastasis is the sentinel lymph node, where cancer cells accumulate, then travel down the thoracic duct and spread to further sites. To do this, it needs to undergo a process called intravasation, its opposite is extravasation, which is the exit of the cell from a blood vessel. The difference between the two lies in the formation of invadopodia for intravasation while the latter can do without (Roh-Johnson et al., 2014). The switch from migration to intravasation in breast cancer cells is thought to be TGF-β-mediated and results in the expression of various signalling proteins like EGFR, Neural Precursor Cell Expressed, Developmentally Down-Regulated 9 (Nedd9), Myosin phosphatase Rho-interacting protein (M-RIP), ARH)/RhoGEF And Pleckstrin Domain Protein (FARP) and Ras homolog gene family, member C (RhoC) (Giampieri et al., 2009).

In terms of blood vessels, the tumour cells can be assisted by macrophages, which form a chemokine concentration gradient along which the cells can migrate towards (Pollard et al., 2008), such as through secretion of EGF or colony stimulating factor 1 (CSF1) (Lin et al., 2002). This creates a paracrine loop, therefore stimulating synergy between macrophages, which form podocytes and invadopodia on cancer cells through the WIP pathway (Van Nguyen et al., 2002). A suggested mechanism for this process is by circulating monocytes exposed to C-X-C Motif Chemokine Receptor 4 (CXCR4) and their differentiation into macrophages. which are then recruited to the perivascular space by tumour associated fibroblasts expressing C-X-C motif chemokine 12 (CXCL12) (Arwert et al., 2018). These macrophages then change the permeability of the vessels and promote intravasation through Vascular endothelial growth factor A (VEGF-A) stimulated interendothelial junction removal.

Indeed, the tumour microenvironment plays a large role in promoting tumorigenesis. There has been a large amount of research conducted regarding tumours adapting to their environment. In terms of breast cancer microenvironment, it was found that there was an association between the tumour and mammalian-enabled (MENA+) cells, CD68 Molecule

(CD68)+ macrophages and CD31 Molecule(CD31)+ endothelial cells, promotion of blood / lymph node metastasis (Robinson et al., 2009; Harney et al., 2015), and relation between tumour associated macrophages and ER+/ HER2- breast cancer (Rohan et al., 2014). Paradoxically, patients that have undergone neoadjuvant chemotherapy can generate a chemo resistant cancer subpopulation. The neoadjuvant therapy was found to increase the amount of these macrophages and macrophage assisted metastasis, despite obvious positive benefits of the therapy (Karagiannis et al., 2017). However, it also seems that intravasation events are a result of newly formed immature blood vessels, promoted through excretion of EGFR by the primary tumour (Deryugina et al.,I 2017). Experiments have shown that EMT versus non-EMT cancer cells were able to invade but not able to form metastasis when administered intravenously, whereas the latter could (Lyons et al., 2008). This bolsters the argument that subpopulation of cells switch between EMT and MET under different conditions. A third final method of intravasation is through vascular mimicry, as lots of tumours have been demonstrated to be able to generate their own blood vessels to improve survival (Shen et al., 2017).

Intravasation is easily observed with the migration of mature T lymphocytes from the lymphoid organ into the system (Matlobian et al., 2010). In this case much of it is to do with a concentration gradient of sphingosine 1 phosphate (S1P), which has low concentration in tissues versus high concentration in blood and lymph. This forces the lymphocytes expressing sphingosine 1 phosphate receptor (S1PR1) to migrate towards a high S1P concentration region (Resop et al., 2015). This S1P and S1PR1 interaction is also a known mechanism by which dying epithelial cells are shed and replaced through Ras homologous (Rho) -mediated actin contraction (Gu et al., 2011). It is likely that tumour cells expressing S1P can interact with the perivascular endothelium which expresses S1PR1, thereby facilitating intravasation by hijacking this mechanism. Other examples exist, such as reverse endothelial migration during the inflammatory response, which in the same way is due to the expression of a receptor CXC chemokine receptor 1 (CXCR1) and endothelium associated intercellular adhesion molecule 1 (ICAM1) (Joly et al., 2003).

1.2.5 Circulating Tumour Cells -the Seed Hypothesis

Once the tumour cell enters the blood vessel, it becomes a circulating tumour cell (CTC), which was discovered as far back as 1869 by Thomas Ashworth. They have since been used as predictors of patient's prognosis and treatment outcome in a number of cancers such as ovarian, colon, pancreatic cancers among others (Sefrioui et al., 2017; Giannopoulou et al., 2018; Poudineh et al., 2018; Soler et al., 2018;). The presence of five or more circulating tumour cells per 7.5 ml of peripheral blood decreased progression-free survival and overall

survival. A study using green fluorescent protein (GFP) tags on CTCs, eliminated the cells in mice. This demonstrated that removal of CTCs had decreased metastasis and improved the survival (Kim et al., 2018). CTCs have a high level of plasticity as well as several different subpopulations. A study had sleeved CSCs with a specific signature associated with brain metastasis: HER2+/ EGFR+/ Heparanase (HPSE)+/ Notch Receptor 1 (NOTCH1)+. These cells were up to 80% more likely to form brain metastasis than the other sub populations of CTCs when injected into mice (Zhang et al., 2013). Another study specific to breast cancer shows the existence of subpopulations within CTCs that cause metastasis, characterised by epithelial cell adhesion molecule (EpCAM)+, CD44+, CD47 Molecule (CD47)+, MET proto-oncogene, MET receptor tyrosine kinase +/−) (Baccelli et al., 2013). There is also some evidence that a portion of CTCs expresses the $CD44^{high}$ marker which increased with disease progression (Baccelli et al., 2013). This marker is related to cancer stem cells and might indicate that some of these CTC populations are also chemoresistant. This, along with another breast cancer study (Sparano et al., 2018), indicates that CTCs are useful for prediction of therapy response Indeed, there is evidence in several cancers that patient CTCs have the same chemoresistance as small cell lung cancer (Hodgkinson et al., 2014). As an outcome of this, there are 3D models designed to culture CTCs (organoids) for predicting response to anaplastic lymphoma kinase (ALK) receptor tyrosine kinase inhibitors (Zhang et al., 2017).

The link to EMT plasticity comes in the study of cancer CTCs clusters. One of such studies showed dynamic EMT properties (Yu et al., 2013). CTC clusters were shown to be more potent initiators of metastasis (Aceto et al., 2014). Further research into this phenomenon found an interesting finding relating hypomethylation states of transcription factor binding sites on CTCs. CTCs exhibited hypomethylation of OCT4, homeobox protein NANOG (NANOG), SRY (sex determining region Y)-box 2 (SOX2) and SIN3 transcription regulator family member a (SIN3a), which are involved in proliferation and stemness (Gkountela et al., 2019).

Also, during this process of CTC movement, they are protected from circulating leukocyte mediated cell death, e.g. by Natural Killer cells and from mechanical stress of shear forces in the fluid they travel (blood or lymph) (Palumbo et al., 2005). For the most part, they recruit platelets and neutrophils through expression of tissue factor and P-selectin (Labelle et al., 2012; Gong et al., 2012). Platelets can act both by forming a physical barrier against Natural Killer cells and excrete PDGF and TGF-β, which inhibits Natural killer cell activity (Palumbo et al., 2005; Kopp et al 2009). They are also instrumental in forming points of attachment on the vascular endothelium for CTCs to initiate extravasation (Palumbo et al.,

2005). The same E- and P-selectin on CTCs are also responsible for this adhesion to the endothelial wall (Kohler et al.,2010).

1.2.6 Micrometastasis, Drug Resistance and Relapse

CTCs exit the blood vessels and into surrounding tissues through a process called extravasation. Even though the rate of CTCs forming metastatic niches is low and their half-life in the blood is rather short, which makes them hard to detect, they are still able to form metastatic niches. The seeding occurs more likely on endothelial junctions and at sites where inflammation is occurring, such as initiated by proinflammatory cytokines and nitric oxide (Lala et al., 1998), as well at sites of tissue injury (Cho et al., 2010). During this stage, CTCs initiate MET to re-gain an epithelial phenotype.

Much of the migration through stroma and recruitment of tumour associated macrophages occurs in the same way as during earlier migration steps. Much of this signalling is from the stroma (Giancotti et al, 2013). Some examples are excretions from cancer cells that stimulate the microenvironment to change forcing thrombospondin-1 expression by fibroblasts by prostate cancer cells to induce neo-angiogenesis (Kang et al., 2009). Other examples are cells from the same tumour signalling each other by secretion of osteopontin that recruit progenitor hematopoietic cells to the secondary tumour site and secrete granulin which can promote collagen-rich stroma (McAllister et al., 2008; Elkabets et al., 2011). There is also evidence that activation on one metastatic site can initiate another (Gao et al., 2008). In the example of bone metastasis by breast cancer, TGF-β induces the expression of Jagged and Notch, which in turn signals the neighbouring osteoblast cells to produce interleukin 6 (IL6) (Sethi et al., 2011).

Furthermore, there is also evidence of pre metastatic niches, whereby primary tumours remodel the environment of distal metastatic sites before the CTCs seed that site. Initial experiments with vascular endothelial growth factor receptor 1 (VEGFR1) positive hematopoietic progenitor cells (HPCs) are recruited to these pre metastatic niches by VEGF signalling and placental growth factor (PlGF) (Kaplan et al., 2005). This remodelling is also completed through extracellular vesicle signalling like exosomes which deliver their signals to distal stroma and endothelial cells (Minciacchi et al., 2015; Liu et al., 2016). Colonisation by micrometastasis requires a favourable environment and growth of the secondary tumour beyond 1 mm requires angiogenesis for access to nutrients and oxygen. They can also utilise a process called anastomosis, by which they form tubular structures to connect to capillaries.

The seed and soil hypothesis is now widely used to describe the process of secondary tumour formation showing specificity between cancers. For example, it is known that breast cancer has a preference to form tumours in the bone, brain, lungs and the liver. And once a

cell is seeded it can lay dormant until it is activated through cell signalling (Janni et al., 2005). For example, metastatic relapse can occur 10 years after diagnosis in breast cancer (Hanrahan et al., 2007). It is demonstrated that CTCs exhibit a growth arrest at G0-G1 phase (Vishnoi et al., 2015). They exit from this dormancy state once their microenvironment is remodelled through angiogenesis, which suppresses thrombospondin 1 (TSP1), which is secreted by the endothelial microenvironment (Ghajar et al., 2013). However, little is known about how these dormant cells are activated, but it is likely to occur through the recruitment of the tumour misgovernment or stem like properties of the seeded cells. Relapsed and secondary tumours are usually drug resistant (Steeg et al., 2016) and exhibit characteristics of stemness, as well as upregulated transporters for drug, and other advantages of chemoresistance previously outlined.

1.3 Markers and Predictors of Drug Resistance and Metastasis

Despite the diagnostic significance of markers such as ER, PR, HER2 and Ki67 to classify tumours, they are a brief snapshot of a much larger tumour landscape, the hallmarks of cancer highlighting the complexity of this. Thus, there is a need for developing new biomarkers to tackle specific traits such as metastasis and drug resistance. Attempts have been made to unveil sophisticated gene expression techniques, such as sequencing and arrays, to shed light on molecular targets for drug development. They are vital to stratify patients according to their subtypes, and aid in prognosis.

1.3.1 Stem Cells

Drug resistance traits have long been associated with a stem cell-like phenotype. Firstly, a stem cell is an unspecialised cell with the limitless capacity for self-renewal, having a function in early embryogenesis and in the adult organism. With each differentiation step, a totipotent cell, a cell which can differentiate into many types of cells, reduces in its capacity to do so. This capacity is reflected in methylation of its DNA and the cell with limited differentiation potential is now called unipotent (Kang et al., 2007). There is also a small distinction between totipotent and pluripotent cells. While both have high differentiation potential and can form any cell type, only the totipotent cells can form extra embryogenic structures. The next level down is multipotent cells, whereby the differentiation is more specialised to particular cell lineage, e.g. haematopoietic stem cells that form white and red blood cells.

To understand stem cells, we need to look at their basic function. In early embryogenesis, two distinct cell populations exist: the inner cell mass (ICM) and trophectoderm (TE). While the TE continues to differentiate and form the various extraembryonic structures and tissue types, the classic pluripotent stem cell is considered to be from the ICM (Sukoyan et al., 1993). In a fully developed organism, the stem cell acts as a source of new cells to replace the old, and their rate of division is dependent on which organ they are located in. They can be divided into, mesenchymal, neural, haematopoietic and skin stem cells. Although the process seems to be linear, there are ways to return differentiated cells back to their pluripotent potential, notably through the introduction of oncogenes MYC and KLF4 and suppression of p53 (Quinlan et al., 2011). This differentiation is documented to involve a number of signalling molecules, such as fibroblast growth factors (Turner et al., 2010), WNT family proteins (Rao et al., 2010), TGF-β family proteins (Moustakas et al., 2009) and bone morphogenic proteins (BMPs) (Moustakas et al., 2009).

1.3.2 Cancer Stem Cells (CSCs)

Throughout the years, there has been an increased interest in stem cells in cancer research due to the revelation of cancer stem cells (CSC), first isolated in acute myeloid leukaemia for the ease of establishing hierarchy in these types of cancers (Bonnet & Dick, 1997). Their role in solid tumours is more controversial as it is harder to isolate the subpopulation due to the loss of cell surface markers used to identify them. Since then, different models have been described as to how they function in cancer. Some argue that CSCs have different subpopulations and therefore functions, i.e. self-renewal and migration (Brabletz et al., 2005). Others cite CSCs as subpopulations representing different stages of tumorigenesis (Diaz-Cano et al., 2012). Other more relevant to breast cancer, suggests that CSCs represent dormant populations of cells that are involved in relapse of disease (Zimmerlin et al., 2011). CSCs can recruit mesenchymal stem cells (MSCs) from either the circulation or from the tumour stroma (Krampera et al., 2007; Karnoub et al., 2007). These same MSCs can promote metastasis and stemness through upregulation of BMPs (Cuiffo et al., 2014).

1.3.3 Cancer Stem Cell Maintenance

The stem cell phenotype is maintained as a feedback loop between the population of CSCs and recruited mesenchymal stem cells (MSC). Cancer cells promote the secretion of transforming growth factor β 1 (TGFβ1), VEGF and two platelet-derived growth factor subunits BB (PDGF-BB) which stimulate the chemotactic migration of MSCs towards the cancer niche (Klopp et al., 2007). This relationship is maintained by secretion of growth

factors, miRs, cytokines and signalling proteins. MSCs secreting bone morphogenetic protein 2 (BMP2) and bone morphogenetic protein 4 (BMP4) have been shown to increase CSCs populations (McLean et al., 2011). There have also been in vivo models showing secretion of chemokine (C-X-C motif) ligand 1 (CXCL1), ligand 5 (CXCL5), ligand 6 (CXCL6), and ligand 7 CXCL7 by MSCs, which increases the CSC population. Furthermore, secretion of interleukin 10 (IL-10), interleukin 17b (IL-17-b) and EGF by MSCs increases the breast cancer CSCs (Esquivel-Valazquez et al., 2015). MSCs also secrete miR-199 and miR-214 which promote metastasis and the CSC phenotype through upregulation of Forkhead box protein P2 (FOXP2) (Cuiffo et al., 2014). These stemness characteristics have been shown to be stimulated by interleukin 1 α (IL-1α) and interleukin 1 β (IL-1β), which promote the production of Prostaglandin E_2 (PGE2), interleukin 6 (IL-6) and interleukin 8 (IL-8) by MSCs, which are known stimulators of IL-6, CXCL1, CXCL8 that control stemness (Li et al., 2012). MSCs directly influence the expression of cell surface markers of stemness, such as ALDH (Liu et al., 2011) and CD133 antigen (CD133) (Tsai et al., 2011). ALDH is maintained through CXC chemokine receptor 2 (CXCR2)-mediated upregulation of OCT4 and SOX2 in breast cancer (Liu et al., 2011), while CD133 antigen is maintained in colorectal cancer through IL-6 stimulation (Tsai et al., 2011).

1.3.4 Cancer Stem Cell, EMT and Microenvironment

CSCs can recruit a number of cell types to help them, such as MSCs, cancer associated fibroblasts (CAFs) and tumour associated macrophages (TAMs) among others. All these cell types can affect the microenvironment by remodelling the ECM through the expression of collagen, and inflammatory cytokine production. Cytokines can promote: neovascularisation growth and even an EMT switch (Yamashita et al., 2012, Junttila et al., 2013).

MSCs can also upregulate the Notch signalling pathway to promote EMT (Kabashima-Niibe et al., 2013). This has also been the case in breast cancer where MSC-related activation of EMT was associated with their secretion of BMPs, as well as promoting pro-invasive Rho related proteins and focal adhesion kinase and MMPs (McAndrews et al., 2015). Interestingly, there seems to be a feedback loop in which cancer cells undergo an EMT switch stimulated by the MSCs and CAFs they recruit. MSCs travel to the tumour niche on a chemotactic gradient towards the cancer cells expressing chemokine (C-X-C motif) ligand 16 (CXCL16). Once there, they recruit CAFs to stimulate the release of CXCL12, forcing cancer cells to undergo EMT and express CXCR4, and to invade the surrounding vasculature (Maxwell et al., 2014).

CSCs are also crucial for remodelling of the tumour microenvironment as MSCs recruited to the primary tumour site are stimulated to release growth factors. In the case of pro-tumour

survival characteristics, one of these is neovascularisation. MSCs achieve this through the expression of angiopoietin-1 and IL-6, inducing the expression of VEGF that promotes the formation of tumour vasculature (Mao et al., 2013). Breast cancer CSCs originating in adipose tissue promote cells to differentiate into pericytes, which enforces the narrative that CSCs are involved in neovascularisation (Orecchioni et al., 2013). This also reinforces all the other signalling pathways as it results in more recruitment of MSCs and CAFs. However, this is not always the case, as colorectal cancer has been shown to thrive in hypoxic conditions (Mao et al., 2013).

1.3.5 Cancer Stem Cell and Drug Resistance

CSCs are also associated with a drug resistance trait; in fact their isolation in solid tumours is aided by their expression of ABC transporters (Tirino et al., 2013). Experimental models showed that healthy stem cell populations can be induced to transform into CSCs through the methylation of tumour suppressor genes (Daverey et al., 2015). CSC presence upregulates WNT, Notch, Hedgehog pathway signalling as well as modulates tumour response to chemotherapy through the release of platelet-derived growth factor C (PDGF-C), Hepatocyte growth factor, nitric oxide and interleukin 17a (IL-17A) (Shi et al., 2017).

1.3.6 Relevance of Markers for Stemness, EMT and Drug Resistance

Canonical clinical markers used to subtype tumours, such as ER, PR, HER2 and EGFR (Adamczyk, Niemiec et al., 2012), are also relevant to EMT, drug resistance and CSCs. estrogen receptor α (ERα) and estrogen receptor β (ERβ) expression is associated with the suppression of EMT (Chang et al., 2006; Guttilla et al., 2012; Bouris et al., 2015). ERα does this in two ways, firstly by modulating TGF-β signal transduction through mothers against decapentaplegic homolog 2 (SMAD2) and mothers against decapentaplegic homolog 3 (SMAD3) degradation, which favours the epithelial phenotype (Ito et al., 2010). Secondly, ERα expression is inversely correlated with nuclear factor kappa-light-chain-enhancer of activated B cells (NF-$\kappa\beta$) Re1B subunit, which is associated with promotion of EMT transcription factors such as SNAI1 and ZEB1 (Wang et al., 2007; Scherbakov et al., 2012). PR promotes EMT by increasing β-catenin signalling which suppresses E-cadherin. It promotes components of the EMT cascade during breast development (Fernandez-Valvidia et al., 2009; Brisken et al 2000). The expression of E-cadherin, TWIST, vimentin, cytokeratin 19, EpCAM have been associated with early detection of CTCs (Chen, Zou et al., 2010; Kallergi, Papadaki et al., 2011; Zhao, Yang et al., 2013). This was discussed earlier and shown to predict EMT and drug resistance. HER2 expression was also shown to induce EMT

in a stem cell like breast cancer cell line (Ingthorsson et al., 2015). All three receptors are involved in CSCs modulation. Lack of PR and ER receptors and increased HER2 expression is correlated with higher CSCs (Zhou et al., 2010), while Ki67 and cytokeratin 5/6 are markers for proliferation, invasion and metastasis (Hicks, Short et al., 2006; Dede, Gumuskaya et al., 2013). These CSCs can be identified through the expression of stem cell markers such as ALDH (Liu et al.,2011), $CD44^{high}$ (Schabath et al., 2006), $CD24^{low}$ (Jaggupilli et al., 2012), CD133+ (Sin et al., 2017), integrin alpha 6 (CD49f)+ (Sin et al., 2017) and Thy-1 Cell Surface Antigen (CD90)+ (Schabath et al., 2006). Which also correlaes with drug resistance traits in the form of increased drug transporters like ATP-binding cassette super-family G member 2 (ABCG2) (Sicchieri, da Silveira et al., 2015), and resistance to apoptosis (Nadler, Camp et al., 2008).

The interplay of these markers is important to the establishment of EMT, cancer stem cells and drug resistance (Singh & Settleman, 2010).

1.3.7 Regulatory Pathways Involved in EMT and Stem Cell Phenotypes

Referring back to the 6 hallmarks of cancer reviewed earlier, the section below will outline some of these pathways deregulated in cancer separated by hallmarks they promote, followed by their relevance to EMT and CSCs.

Self-sufficient growth is mainly achieved by switching one of the mitogen signalling pathways (Ras-Raf-MEK-ERK). This pathway mainly works through the binding of an extracellular growth factor such as EGF/ VEGF to its growth factor receptors. This in turn will initiate the guanosine-5'-diphosphate (GDP) to Guanosine-5'-triphosphate (GTP) swap by Ras which activates downstream mitogen activated protein kinase (MAPK). MAPK then activates MYC, effectively driving transcriptional changes, which regulates events such as cell cycle progression, as extracellular-signal-regulated kinase 1 (ERK1)/extracellular-signal-regulated kinase 2 (ERK2) is known to hyper-phosphorylate cyclin D (CCND1) and cyclin-dependent kinase 4 (CDK4) and cyclin-dependent kinase 6 (CDK6) (Chambard et al 2007). These will subsequently destabilise the pRB protein, detaching it from E2F and allowing the cell to return to S-Phase to return to initiate the cycle again. This signalling also has dynamic control, pending on the concentration of the growth factor, which determines gene expression through bursts of signalling. The ERK signalling produces feedback control loops on E2F, firstly through direct stimulation by MYC, secondly through Rb-mediated activation of E2F leading E2F to also have a positive feedback loop on itself through the expression of Cyclin E and cyclin dependent kinase 2 (CDK2). This pathway can also

be activated through HER2 (Burgess et al., 2008). Finally another way in which the cell cycle control is deregulated is through the translocation of ERα, affecting estrogen response elements (EREs) (Renoir et al., 2013). Some of the genes that ERα regulates in this way is cyclin D1, an activator of the cyclin dependant kinase that controls the cell cycle (Cicatiello et al., 2004).

Avoidance of growth inhibitors is mainly achieved by the TGF-β pathway. The pathway splits into SMAD-dependent and SMAD-independent. The first one is regulated by three types of SMAD proteins: receptor regulated (RSMAD), inhibitory SMADS (I-SMAD) and common mediated (co-SMAD). RSMADs contain mothers against decapentaplegic homolog 1 (SMAD1), SMAD2, SMAD3, mothers against decapentaplegic homolog 5 (SMAD5) and mothers against decapentaplegic homolog 8 (SMAD8), which phosphorylate upon signal transduction from membrane-bound receptors (Heldin et al., 1997). Two RMADs then recruit the co-SMAD, which translocate to the nucleus and activates transcription of genes. This part of the pathway is known to activate oncogenes such as SNAI1/2 . I-SMADS containing mothers against decapentaplegic homolog 6 (SMAD6) and mothers against decapentaplegic homolog 7 (SMAD7) are negative regulators of RSMADS and prevent transcription of genes to occur. This pathway promotes tumour progression, however it can also inhibit it, as it has been described to induce cell cycle arrest and growth inhibition , mostly through the action of SMAD genes, indicating that they are also mutated in cancer . This inhibition of the cell cycle is also down through the interaction of SMADs2/3/4 and EP300, which activates downstream cell cycle inhibitors $p15^{INK4b}$ and cyclin-dependent kinase inhibitor 1 (p21). Other inhibitory functions such as apoptosis were also known to be induced by this pathway. Its promotion of EMT tumour progression is through activation of transcription factors such as SNAI1/SNAI2 and TWIST. TGF-β ligands which include BMPs, growth differentiation factors (GDFs) and TGF-β, will bind to the type II receptor and initiate phosphorylation of the type I receptor. This formation of the receptor hetero tetrameric complex will initiate phoshprylation of RSMAD, which dissasociates from transcriptional regulator SarA (SARA), the mediator of the TGFβ pathway. RSMAD then forms a complex with coSMAD which initiates transcription at promoter sites of target sequences (Hill et al., 2009). In particular, the SMAD-dependent pathway activates SMAD4 and SMAD7, which are known to promote growth and prevent apoptosis (Halder et al., 2005) by inhibition of TGFβ growth inhibition functions. The SMAD independent pathway activates the mitogen activated pathway that promotes self sufficient growth (Derynck et al., 2003). The avoidance of growth inhibition mentioned earlier is also partly controlled by an interaction of AKT mediated SMAD3/4 (Conery et al., 2004). Additionally, activation of a pro survival signaling pathway nuclear factor kappa B (NF-κB) (Lu et a., 2004), and initiating pro survival signalling my modulating

the tumour microenvironment via recruitment of leukocytes which express cytokines (Bierie et al., 2006).

Avoidance of apoptosis inhibitors is mainly achieved by the PI3K/AKT/mTOR pathway, which is one of the most common genetic abnormalities in breast cancer and is activated in about 30-40% of cases. It is deregulated by mutations as the phosphatidylinositol-4,5-bisphosphate 3-kinase, catalytic subunit α (PIK3CA) that results in a loss of function of PTEN (Raphael et al., 2018), amplification of PI3K or activation of upstream oncogenes and tyrosine kinase growth factor receptors (Stemke-Hale et al., 2008, Zhou et al., 2000). The PI3K pathway is well studied and regulates many regulators of apoptosis which have been described (Duronio, 2008). In triple negative breast cancers (TNBC), the pathway is responsible for downregulation of its own regulators such as EGFR and proline rich inositol polyphosphatases, as well as activating the PIK3CA mutation (Costa et al., 2018). The pathway can be activated through external stimuli such as growth factors, cytokines and constitutively active Ras (Takahashi et al., 2005). In this pathway, AKT and protein kinase B (PKB) are proteins that directly influence cell survival and apoptosis (Takahashi et al., 2005). AKT is responsible for inactivating tumour suppressor p53, which regulates BCL2 and BAX genes, and inactivating the proapoptotic protein BCL2 associated agonist of cell death (BAD) (del Peso et al., 1997). Briefly, the PI3k is a group of plasma membrane associated lipid kinases that consist of 3 catalytic subunits, phosphoinositide 3-kinase (p85), membrane palmitoylated Protein 1 (p55) and phosphatidylinositol-4,5-bisphosphate 3-kinase (p110) (Donahue et al., 2012). PI3Ks are divided into 3 classes: type I, type II and type III. Under normal conditions, the p85 forms a dimer with p110, and when activated, these separate and catalyse the phosphorylation of PtdIns(4,5)P2(PIP2) into PtdIns(3,4,5)P3(PIP3). This secondary messenger recruits proteins via their pleckstrin homology domains or lipid binding domains, such as the AKT and 3-phosphoinositide-dependent protein kinase-1 (PDK1) proteins, which activate cell survival (Manning et al., 2007). The previously mentioned PTEN protein regulates this by dephosphorylating PIP3 to PIP2 (Hennessy et al., 2005). This pathway can also be activated by HER2 signalling (Mayer et al., 2016).

Limitless proliferation is gained by switching one of the WNT pathways. The pathway is divided up into the canonical β-catenin and independent pathways. In the absence of stimulus, β-catenin is phosphorylated by a destruction complex which includes glycogen synthase kinase-3 α (GSK3α), Axin, Adenomatous polyposis coli (APC) and Casein kinase 1 (CK1), which leads to ubiquitination by β-TRC (Latres et al., 1999), and recruitment by T-cell factor (TCF) and lymphoid enhancer-binding factor (LEF) in the nucleus of HDACS for repressing β-catenin target genes. The canonical pathway involves the attachment of WNT ligands to frizzled receptors and low density lipoprotein receptor-related protein 1

(LRP) co receptors. Upon attachment, the LRP receptors will recruit dishevelled proteins (DVL) that will inactivate the destruction complex, leading to an accumulation of β-catenin in the nucleus and recruits co-activators such has EP300, brahma-related gene-1 (BRG1), B-Cell CLL/Lymphoma 9 Protein (BCL9), Pygopus Family PHD Finger (Pygo), which are then responsible for activation of transcription of target genes. (Lien & Fuchs, 2014). The non-canonical pathway involves attachment to the receptor tyrosine kinase-like orphan receptors (ROR) to activate DVL, which in turn binds to Rho GTPAse. This triggers a signalling Disheveled-associated activator of morphogenesis 1 (DAAM1) -ROCK- c-Jun N-terminal kinase (JNK) cascade, which initiates transcription via jun proto-oncogene (JUN) and activating transcription factor 2 (ATF2). Alternatively, phospholipase C can initiate a G protein-mediated WNT/calcium, signalling that results in initiation of transcription through nuclear factor of activated T-cells (NFAT). In terms of breast cancer, the Wnt pathway is activated in 50% of cancers (Lin et al., 2000) and its aberrant signalling is responsible for poor prognosis in triple negative breast cancer (Xu et al., 2015). This extends to other breast cancer types (Li et al., 2014). Deregulated signalling is mainly a result of overexpression of wnt ligands (Liu et al., 2010; Howe et al., 2014) and silencing of antagonists (Klarmann et al., 2008). The signalling results in activation of TERT gene that maintains telomere length (Park et al., 2009). Models have also shown that WNT signalling along with NF-κB will induce dedifferentiation into stem cells in an intestinal model (Schwitalla et al., 2013), implicating these pathways in modulation of the tumour microenvironment to favour a stemlike niche. This has been confirmed in several subsequent studies in colorectal cancer (Vermeulen et al., 2010), breast (Malanchi et al., 2012) with overexpression of microenvironment secreted molecules like periostin and matrix metallopeptidase 3 (MMP3). Furthermore, this pathway upregulates miRs which are responsible for stability of β-catenin such as miR-146 (Hwang et al., 2014). A second pathway involved is the Hippo pathway. Inhibition of this cascade begins with macrophage stimulating 1 (MST1), macrophage stimulating 2 (MST2) kinase and salvador family WW domain containing protein 1 (SAV1) which form a complex. This complex function is to phosphorylate large tumor suppressor kinase 1 (LATS1) and large tumor suppressor kinase 2 (LATS2), which is controlled by phosphatases as well as integrity of the cytoskeleton (Badouel et al., 2011). LATS1/2 in turn inhibits the yes-associated protein (YAP) and tafazzin (TAZ) transcription factors, which are the effectors of the hippo pathway. YAP/TAZ are also regularly ubiquitinated when they are not active, which further regulates this pathway (Zhao et al., 2010). When YAP/TAZ are not phosphorylated by the complex, they translocate to the nucleus to initiate transcription through interaction with other transcription factors like TEA domain transcription factors 1 (TEAD1), TEA domain transcription factors 2 (TEAD2), TEA domain transcription factors 3 (TEAD3) and TEA

domain transcription factors 4 (TEAD4). Apart from these, there are also upstream signalling molecules that can initiate the MST1 and MST2 such as Merlin and Kibra (Yu et al., 2013).

Angiogenesis is initiated through the VEGF, and RAS, MYC pathways as well as Notch. Both VEGF and Notch signalling pathways are involved in the formation of new vessels, their maturation and specialisation. VEGF has 6 ligands (A, B, C, D, E, F PIGF) (Hellstrom et al., 2014). Their expression guides endothelial cells to form vessels (Gerhardt et al., 2003). Notch signalling involves two cells carrying the complementary receptor and ligand. There are 4 heterodimeric transmembrane notch receptors (1-4) and 5 ligands: delta-like 1 (DLL1), delta-like 2 (DLL2), delta-like 4 (DLL4) and Jagged 1 and 2 (JAG1/JAG2). Upon binding the intracellular domain (NICD) of Notch, it translocates to the nucleus and binds to a transcription factor suppressor of hairless (CSL), subsequently forming a transcriptional activation complex. This includes EP300, among others, which activates transcription of genes such as hes family BHLH transcription factor (HES) and hairy/enhancer-of-split related with YRPW motif protein (HEY). The balance between these two signalling pathways determines the endothelial cell shift between the "tip" or the growing end of the vessel, or the "stalk" which proliferates in the lumen of the cell. Both of these differ by their expression of vascular endothelial growth factor receptor (VEGFR), tips express vascular endothelial growth factor receptor 2/3 (VEGFR2)/(VEGFR3) while stalks express VEGFR1 (Dufraine et al., 2008). In cancer progression, tumours utilise the overexpression of VEGFs and DLLs as well as shift the balance of tip and stalk cells (Capaccione et al., 2013; Kontomanolis et al., 2014). The tumours of larger sizes will also display abnormal vasculature (Eilken et al., 2010). The expression of Notch is regulated by cytokines IL-1, IL-6 and leptin (Hellstrom et al., 2014), and the absence of regulators of the notch pathway is seen in 50% of breast cancer cases (Pece et al., 2004). Most cases are activated in the luminal A subtypes through Notch 3-mediated transactivation of ER-α (Dou et al., 2017), partly due to HES and HEY genes being mediators of estrogen, which promotes notch receptor and ligand expression (Soares et al., 2004). While triple negative breast cancers revealed to have a preference for higher notch 1 activity (Wang et al., 2015), there is also some crosstalk between notch and WNT pathways (Prosperi et al., 2010). Out of all of the Notch signalling ligands, the most interesting is DLL4 which functions both as a negative regulator of tumorigenesis and positive regulator of tumour progression, by both restricting formation of new vessels, and simultaneously forming larger diameter vessels (Hellstrom et al., 2014). The TGFβ pathway is involved in promoting angiogenesis and macrophages that stimulate angiogenesis to the tumour site (Roberts et al., 1986, Sunderkotter et al., 1991). TGFβ acts either through the activin receptor-like kinase 1 (ALK1) and activin receptor-like kinase 5 (ALK5) receptors. ALK1 would activate SMAD1 and SMAD5 which would promote angiogenesis (Ota et al., 2002); whereas ALK5

directly phoshphorylate SMAD2 and SMAD3 and promotes proinvasive characteristics (Ota et al., 2002). Furthermore, because angiogenesis is largely a process driven by angiogenic factors like VEGF and CTGF. TGFβ stimulates their production in surrounding epithelial and fibroblast cells (Shimo et al., 2001).

Invasion and metastasis is gained on multiple fronts, on one end, migration is driven by MAPK RAS/ MEK-ERK signalling and integrin cycling, and in another, the major EMT shift is done through the TGF-β/WNT and SHH pathways. TGF-β helps with cell migration by activating the PI3K/AKT and MAPK pathways, as well as mediating the cell contraction at the leading edge through Rho GTPases, potentially through SMAD4 phosphorylation (Tsapara et al., 2010). It also inhibits anti migratory microRNAs which target RhoA such as miR-155 (Kong et al., 2008). TGF-β effects on invasion are by remodelling the ECM by promotion of MMPs (Wiercinska et al., 2011) and the promotion of transcription of $\alpha 3\beta 1$ integrins that help advance through the basement membrane (Giannelli et al., 2002). This TGF-β-mediated invasion seems to be also directly correlated to p21 levels (Dai et al., 2012). Through the SMAD-independent pathway, TGF-β regulates tumour migration and invasion pathways, such as PI3K/AKT, MEK/ERK, RHO-A, and JNK/p38 mitogen-activated protein kinase (p38). The PI3K/AKT pathway bolsters the signalling from the SMAD dependent pathway to induce EMT as well as inhibits the growth, and apoptosis arrest that TGF-β can induce , whereas, the MEK/ERK contributes to EMT through cell motility and removing cell adherens junctions and cytoskeleton reorganisation inhibition of apoptosis. Cell motility is further increased by RHO-A-stimulated stress fibre formation, which helps the invading cells contract ; whereas the JNK pathway can promote more R-SMAD signalling, which would result in more pro oncogenic transcription factors (70). Overall TGF-β becomes pro tumourigenic once oncogenic transcription factors go over a threshold, at which point, the pathway becomes tumour promoting. Furthermore, it seems that the Hippo pathway is also implicated in this process by way of contact inhibition, which controls the cell proliferation response as a result of higher threshold for mitogenic growth factors. This decreases the growth factors necessary to promote proliferation and migration at the leading edge of the cell (Gumbiner et al., 2014). Briefly, the hedgehog pathway consists of 3 secreted ligands: sonic hedgehog (SHH), Indian hedgehog (IHH), Desert Hedgehog (DHH), and 2 transmembrane receptors: co receptor patched (PTCH) and smoothed homolog precursor (SMO). The effectors of this pathway are the glioma associated oncogene transcription factors 1 (GLI1), 2 (GLI2) and 3 (GLI3). During the inactive state, PTCH localises to the cilium, preventing SMO activation while the GLIs are phosphorylated to their repressor forms e.g. glioma associated oncogene 1 receptor (GLI1R). In the situation when Hh ligands bind to PTCH, SMO translocates from the cilium, this in turn separates SUFU negative regulator Of

hedgehog signaling (SUFU) bound GLIs, which then undergo proteolytic processing to form a full length GLI transcription factor. This GLIA will then activate the transcription of target genes. This pathway can be regulated by phosphorylation of GLIs such as by protein kinase A (PKA) and GSK3α (Tempe et al., 2006, Varjosalo et al., 2008). Other modifications of GLI include acetylation (Canettieri et al., 2010, Coni et al., 2013). This pathway is also known to be regulated by the MAPK, PI3K, TGF-β pathways through modulation of the receptors and ligands (Ji et al., 2007; Stecca et al., 2007; Seto et al., 2009; Goel et al 2013). The hedgehog pathway has both canonical and non-canonical signalling. In the canonical signalling, ligand-dependent autocrine signalling occurs when the cancer cell is activated upon being stimulated by an Hh ligand (Liu et al., 2014) and this can occur both in a paracrine and autocrine manner (Li et al 2014). Ligand-independent signalling occurs when the Hh ligand has no role in the activation of GLI as it either has a somatic mutation (Gailani et a l., 1996) or loss of function mutation (Raffel et al 1997) or there is an amplification of GLI (Stecca et al., 2007). The most common in triple negative breast cancer is the ligand dependent autocrine/paracrine signalling cascade. Non canonical signalling is controlled by the PTCH (type I), in which inhibition of apoptosis occurs through disruption of four and a half LIM domains 2 (DRAL)-caspase interaction or disrupting transforming protein p21 (HRAS) signalling through tumorous imaginal disc 1 (Tid1) (Wakabayashi et al., 2007; Mille et al., 2009). Some findings also show that PTCH can control ERK1 and ERK2 signalling (Chang et al., 2012). Furthermore, the SMO-dependent (type II) pathway in non-canonical signalling promotes cell migration through Rho and Rac1 GTPases (Chinchilla et al., 2010; Polizio et al., 2011; Razumilava et al., 2014). Of course, this is not the full story, as there are now emerging hallmarks being discussed in literature. Namely the deregulated metabolism and avoidance of the immune response. Which are vital for the cancer survival but are out of the scope of this thesis.

1.3.8 Relevance of Pathways to EMT

According to Miettinen et al. (1994), TGF-β can induce EMT, and more TGF-β is observed at the leading edge of cells. The upregulation of SMAD signaling leads to the active transcription of pro-EMT genes, such as SNAI1, SNAI2, ZEB2 and TWIST, as well as upregulating FOXC2 (Thualt et al., 2006, Brabletz et al., 2018). The upregulation of SNAI1/2 is also assisted by the Notch, Hedgehog and the WNT pathways (Zhan et al., 2017), which represses E-cadherin and disrupts cell adherens junctions and desmosomes, with the loss of cell adhesion. This is also assisted by the phosphorylation of Par6 by the type II TGF-β receptor (Ozdamar et al., 2005). It is also known that the TGF-β pathway contributes to EMT signalling by promoting pathways such as Ras/PI3K, RhoA, mTOR, ERK, P38 (Bakin et al.,

2002; Bhowmick et al., 2001; Larue et al., 2005; Lamouille et al., 2007; Grande et al., 2007). Furthermore, TGF-β signaling also controls microRNA expression which contributes to EMT by repressing inhibitory signalling. Evidence of this is primarily from the suppression of the miR-200 family, leading to the upregulation of ZEB2 and smad interacting protein 1 (SIP1) (Burk et al., 2008; Korpal et al., 2008).

The SHh pathway upregulates pro-EMT transcription factors, and when inhibited, the pathway promotes the loss of the mesenchymal phenotype through the upregulation of E-cadherin (Dan et al., 2013; Lei et al., 2015). It also influences migration, invasion and proliferation of triple negative breast cancer (Kwon et al., 2011; Harris et al., 2012), and contributes to the other hallmarks such as angiogenesis (Harris et al., 2012). It contributes to invasiveness through upregulation of matrix metalloproteinase 11 (MMP11) (Kwon et al., 2011), VEGF-A, and CD24 signalling (Cao et al., 2012). Cells exhibiting the EMT phenotype induced through SHH also promote a paracrine signalling loop promoting GLI1 in nearby cells (Neelakantan et al., 2015). Furthermore, metastasis is induced through the GLI signalling by promoting CXCR4 (Ciucci et al., 2013), a receptor for CXCL12 chemokine that is expressed highly in metastatic niches (Muller et al., 2001). Finally, under hypoxic conditions, HIF1-α can promote GLI expression in cancer associated fibroblasts which will promote the tumour progression (Spivak-Kroizman et al., 2013). The inhibition of the SHH/GLI1 signalling has been shown to downregulate the migration and invasion of breast cancer cells (Riaz et al., 2019).

The MAPK and PI3K/AKT pathway work with the TGF-β pathway as both of these are part of the SMAD-independent pathway (Derynck et al 2003). SMADS have a complex relationship between these two pathways. MAPK is known to phosphorylate RSMADs independently of TGF-β, which activates downstream transcription. While SMADS also interact with transcription factors in the MAPK pathway (Derynck et al 2003). Furthermore, TGF-β activates all downstream signalling in the MAPK pathway, such as ERK, p38 and JNK (Burch et al., 2010; Mao et al., 2011). The ERK activation could be through the stimulation of Ras (Yue et al., 2000), while p38 activation is through TGF-β activated kinase 1 (TAK1) which is downstream of all TGF-β receptors (Yamaguchi et al., 1995), as well as mitogen-activated protein kinase 3 (MKK3)/mitogen-activated protein kinase 6 (MKK6) (Bhowmick et al., 2001). TAK1 is also significant in the epithelial phenotype by maintaining E-cadherin expression (Strippoli et al., 2010). Lastly, JNK activation can be activated by the TGF-β downstream effector mitogen-activated protein kinase 4 (MKK4) (Frey et al., 1997).

Another important mediator of these two pathways is the TNF receptor associated factor 6 (TRAF-6). TRAF activates mitogen-activated protein kinase kinase kinase 7 (TAK1), mentioned earlier (Sorrentino et al., 2008), and its inhibition has a similar effect on TGF-

β-mediated EMT, and comparable to p38 or MKK3 knockdown (Yamashita et al., 2008). P38 is important in the EMT process as it reorganises the actin cytoskeleton upstream of RhoA/ROCK (Edlund et al., 2002) due to p38 influencing heat shock protein 27 (HSP27) (Hedges et al., 1999). In addition, it contributes to TGF-β signalling, as its effectors, activating transcription factor 2 (ATF2) and Sp1 transcription factor (SP1), promote transcription of TGF-β target genes (Hu et al., 2000). Furthermore, its direct influence over α-smooth muscle cell actin (α-SMA) leads to activation of the TGF-β SMAD network. This action results in the reorganisation of the ECM and ,in some cases, fibrosis (Lv et al., 2011).

Synergy is also seen among these multiple pathways, a study on EMT reversal using the coenzyme Qo (CoQo inhibitor), reversed the effects of EMT and induced apoptosis. This was achieved through demonstrated inhibition of the WNT/β-catenin pathway, while the reversal of EMT was achieved through the downregulation of matrix metallopeptidase 9 (MMP9) by the inhibition of PI3K/AKT/mTOR pathway (Yang et al., 2019). The PI3K/AKT/mTOR pathway is one of those pathways that is activated by TGF-β and promotes a more stable EMT process (Lamouille et al., 2012). This stable EMT phenotype could only be reversed by blocking mTOR, as blocking SMAD was no longer effective for this cell population (Katsuno et al., 2019). This confirms previous findings that EMT is initiated through TGF-β-mediated activation of the AKT/mTOR pathway (Hamidi et al., 2017), and its importance in the stable EMT phenotype explains how the activation of this pathway leads to resistance to inhibitors of BRAF/MEK/ERK/MAPK/PI3K, and CDK inhibitors (Guri et al., 2016).

PI3K activation can also result from the deletion of the tumour suppressor PTEN. Compared to 40.4% of the PIK3CA mutation previously mentioned, the loss of this gene, which is roughly 30.4% in primary and metastatic breast cancer (Gonzalez-Angulo et al., 2011), leads to the accumulation of PIP3 and the activation of the downstream effector genes, such as AKT/PKB. Some studies show that homozygous PTEN loss is associated with triple negative breast cancer (Carnero et al., 2014). This pathway promotes EMT through upregulation of cell proliferation, inhibition of apoptosis phosphorylation of BAD, caspase 9 and forkhead box protein O1 (FKHR) activation of Fas ligand (Vara et al., 2003).

Its influence on EMT could come in several ways. ERK activation could promote the loss of E-cadherin (the canonical mark of EMT), induce actin stress fibres, which would aid the cell in migration through contraction of the cytoskeleton, and promote MMP activity (Santamaria et al., 2010, Zuo et al., 2011). It is achieved through its control on cell adherens junctions, as well as promoting transcription of target genes which influence ECM interaction and integrin cycling to promote migration (Zavadil et al., 2001). Furthermore, it has been demonstrated that the MAPK pathway directly impacts the SNAI2, a major promoter of EMT. Experimental models showed that MEK and JNK inhibitors down regulate SNAI2

expression (Choi et al., 2007). In breast cancer, this activation is also dependant on RAS and RAF signalling (Xie et al., 2004).The previously mentioned WNT pathway is also involved in EMT, as its signalling stabilises SNAI2 through the inhibition of GSK3α (Wu et al., 2012). A regulator of the EMT process is apoptosis-stimulating of p53 protein 2 (ASPP2), which exerts its influence on EMT through inhibition of β-catenin phosphorylation and formation of an E-cadherin / β-catenin complex which results in inhibition the transcription of pro invasive genes such as ZEB1 (Wang et al., 2014). The effect of this pathway is also cell type context dependent, as the non-canonical pathway has been implicated in colorectal cancer by promoting PI3K and AKT inhibitor resistance (Tenbaum et al., 2012).

1.3.9 Relevance of Pathways to CSCs

Most of the pathways previously mentioned in EMT are also involved in the generation of breast cancer stem cells, including WNT, TGF-β, Hedgehog, Notch and receptor tyrosine kinase pathways (Liu et al., 2006; Morel et al., 2008; Scheel et al., 2011; Hinohara et al., 2012, D'Angelo et al., 2015). Other pathways, such as PI3K/AKT/mTOR, have been shown to be involved through their regulation of pluripotent stem cells, as inhibition of this pathway led to apoptosis (Hossini et al., 2016).

Most breast cancer stem cells have been shown to display a phenotype which expresses the $CD44^{high}/CD24^{low}$ glycoproteins (Wright et al., 2008). CD44 is responsible for cell adhesion, migration and invasion through its interaction with osteopontin (Herrara-Gyol et al., 1999, Ranganswami et al., 2006). While CD24 is responsible for tumour growth and metastasis, another marker often used is the ALDH (Balicki et al., 2007), its role is primarily in converting retinaldehyde into retinoic acid.

Overall, breast cancer stem cells are thought to promote cell survival by their upregulation of DNA repair, utilisation of reactive oxygen species (ROS) scavenging, dampen the effects of cytotoxic drugs and mediate metastasis (Al-Ejeh et al., 2011). The promotion of these traits is through three main pathways: Notch, Hedgehog and WNT (Karamboulas et al., 2013).

The Notch pathway has several ways by which it can upregulate the CSC population. The expression of Notch has been shown to correlate highly with the expression of HER2. Studies show that notch can bind to the HER2 promoter, thereby regulating its expression (Magnifico et a.,l 2009). Further experimentation showed that blocking HER2 expression through the downregulation of notch, resulted in a reduction in mammosphere formation (Magnifico et al 2009). Furthermore, upregulation of Notch increased the number of multipotent cells (Dontu et al 2004). Studying this phenomenon specific to breast cancer revealed that there is an upregulation of NICD, and Hes genes which were responsible for mammosphere formation

(Farnie et al., 2007). A later study showed that Notch 4 downregulation had a significant impact on upregulating this stem cell population. This was due to the proximity of notch to the ER promoter as notch inhibitors block estrogen activity and reduce its frequency in ER- stem cells (Harrison et al., 2013).

The hedgehog pathway is pivotal to cell growth, differentiation and embryonic tissue formation (Ingham et al., 2001). Its downstream target patched homolog-1 (PTCH-1) is responsible for breast formation and defects frequently observed in breast cancer (Fiaschi et al 2007). The overexpression of PTCH1, hedgehog and other downstream effectors of this pathway were highly correlated with invasive traits in breast cancer (Jeng et al., 2013). While upregulation of this pathway results in CSC traits, its inhibition will lead to downregulation in CSC markers such as ALDH1 and $CD44^{high}/CD24^{low}$ (Colavito et al., 2014; Sun et al., 2014; Han et al., 2015). Further evidence to this pathway supporting the CSC phenotype is given by p63 (a member of the p53 family), which promotes expression of the Hh ligands and PTCH1, GLI1/2 (Memmi et al., 2015).

This pathway is also linked to drug resistance as GLI1 overexpression has been shown to be involved in doxorubicin, paclitaxel and cisplatin resistance through the modulation of MDR1 gene (Das et al., 2013), and through the upregulation of pro EMT genes, such as SNAI1 and EGFR by GLIs (Rudolph et al., 2018). Much of this resistance is via crosstalk with the PI3K/AKT pathway in hormone receptor positive breast cancer (Ramaswamy et al., 2012). It is noteworthy that triple negative breast cancer expresses higher levels of GLI1/2 which could contribute to more pro EMT genes (Koike et al., 2017), through the upregulation of transcription factors like forkhead Box C1 (FOXC1) (Chung et al., 2017).

The PI3K/mTOR pathway deregulation can cause the promotion of basal mammary progenitor cells that have multipotent potential (Koren et al., 2015), while the downstream effectors, such as AKT and mTOR, are responsible for endocrine resistance (de Graffenried et al., 2004; Kim et al., 2011).

The TGF-β pathway is also important as it stabilises the CSC population through upregulation of $CD44^{high}/CD24^{low}$ markers, which it maintains through the expression of NANOG, SOX2, OCT4. This phenotype is inhibited upon targeting the mTOR pathway (Katsuno et al., 2019). This same study showed that prolonged TGF-β exposure was also responsible for doxorubicin and cisplatin resistance (Katsuno et al., 2019).

The development of EMT begins with β-catenin levels increasing in the nucleus, regulating the transcription of other genes, significantly those in the pro-invasive pathways like SNAI1, along with the downregulation of E-cadherin (Wang & Zhou, 2011). Other functions of the Wnt pathway include cell fate determination and skewing the cell towards EMT (Kotiyal & Bhattacharya, 2014). Both notch and TGF-β pathways work in conjunction

to suppress E-cadherin expression through SMAD3 upregulation of SNAI2, SNAI1 and TWIST (Leong, Niessen et al., 2007; Wang and Zhou., 2011). Furthermore, cross talk between the aforementioned pathways can produce an EMT phenotype, specifically WNT, notch, β-catenin, receptor tyrosine kinase (RTK) and NF-κB (Wang & Zhou, 2011).

1.4 EP300 and its Involvement in Transcription

1.4.1 Hypothesis

The general aim of this thesis was to explore the role of EP300 in the context of drug resistance, stemness and invasive cell properties. It is expected that EP300 and CDH1 should act as inhibitors on these traits in mesenchymal breast cancer cell lines. Whereas, the knockdown of EP300 and CDH1 should do the opposite in epithelial breast cancer cell lines.

1.4.2 Transcription Factors and Drug Resistance

Cellular gene expression is regulated in various ways. This is initiated through external or internal stimulus, which results in transcription of factors and effector proteins (Johnson & Carroll, 2015). Generally, transcription factors (TF) function by binding to enhancer or promoter sequences, located upstream or downstream of the gene being transcribed. However, there are instances when transcription factors aid in the formation of the transcription initiation complex through the binding of promoter sequences at the start site. There are also those that bind to regulatory sequences, which can influence gene expression either through stimulation or repression. Specifically, this process is coregulated with the help of cofactors, which initiate the activity of RNA polymerase II to begin translation (Carrera & Treisman, 2008).

Drug resistance to chemotherapy can be a result of deregulated gene expression. Influenced by upstream signalling pathways, a transcription factors own influence on the downstream signalling, or a combination of both. The canonical hallmarks of cancer described by Hannah and Weinberg (2000) are mainly regulated by transcription factor influence on signalling pathways.

1.4.3 EP300 Function as a Transcriptional Co-activator

DNA is tightly wound around histone and non-histone proteins, forming the chromatin fibre. The DNA bound histones form an octamer, called a nucleosome, consisting of H2A, H2B, H3 and H4 histones (Singh et al., 2018). A chain of these nucleosomes is

linked together with H1 histones and wrapped around a 30 nm solenoid spiral structure to maintain the structure (Szerlong et al., 2011). This control of DNA between the open conformation (euchromatin) or in a tightly packed closed conformation (heterochromatin) regulates transcription events by providing access for transcription factors to the promoter or enhancer regions (Das et al., 2010). Histones are important in this process due to their many modifications and interactions with histone chaperones that act as recruiters, resulting in different patterns of gene expression. Irregular patterns or disrupted epigenetic modifications of histones have been observed in breast cancer (Burgess et al., 2013).

Figure1.1 summarizes the epigenetic control of transcription . The first layer comprises the histone chaperones, which are responsible for nucleosome disassembly and the replacement of histones during the cell cycle and DNA replication (Valieva et al., 2016). A number of chaperones have been implicated in triple negative breast cancer and breast cancer metastasis: holliday junction recognition protein (HJURP) (Hu et al., 2010, McGovern et al., 2012), aprataxin (APLF) (Majumder et al., 2018), death domain associated protein (DAXX) (Hoelper et al., 2017), DEK proto-oncogene (Hollenbach et al., 2002), facilitates chromatin transcription (FACT) (Attwood et al., 2017), ASF1 like histone chaperone (ASF1) (Corpet et al., 2011), acidic nuclear phosphoprotein 32 family member E (ANP32E) (Xiong et al., 2018) and nucleophosmin (NPM1) (Zeng et al., 2018). The loss of the same APLF chaperone results in CDH1 overexpression through the activity of FOXA1 (Majumder et al., 2018). DAXX and DEK are interesting for acetylation, as DAXX is known to interact with HDAC2 and repressing the oncogene tyrosine-protein kinase Met (c-MET) (Hoelper et al., 2017), therefore has tumour suppressor functions (Morozov et al., 2008), while DEK interacts with histone acetyltransferase (HAT) inhibitors (Kappes et al., 2011), preventing acetylation and associating with metastatic breast cancer (Hollenbach et al., 2002). Finally, NPM1 acetylation by EP300 results in enhanced transcription (Swaminathan et al 2005), therefore it has wide implications for the transcriptional landscape.

The second layer comprises the histones themselves, which are split into canonical and non-canonical histones (regulatory histone variants). Canonical histones maintain the chromatin state (Venkatesh et al., 2015). The variants differ by a few residues and are integrated into the structure during different phases of the cell cycle, which likely represents their function (Quenet et al., 2018). Several histone variant families exist such as H2A (H2A.Z, MacroH2A, H2AX), H2B (HIS1H2BJ, HIS1H2BE), H4 (H4G) and H3 centromere protein A (CENPA-A), all of these have been implicated in promoting breast cancer. The H2A.Z variant has function in regulating the cell cycle, through cellular MYC proto-oncogene, BHLH transcription factor (c-Myc) mediated downregulation of p21 (Gevry et al., 2007), and through direct transcriptional repression of p21 and p53 (Rangasamy et al., 2010).

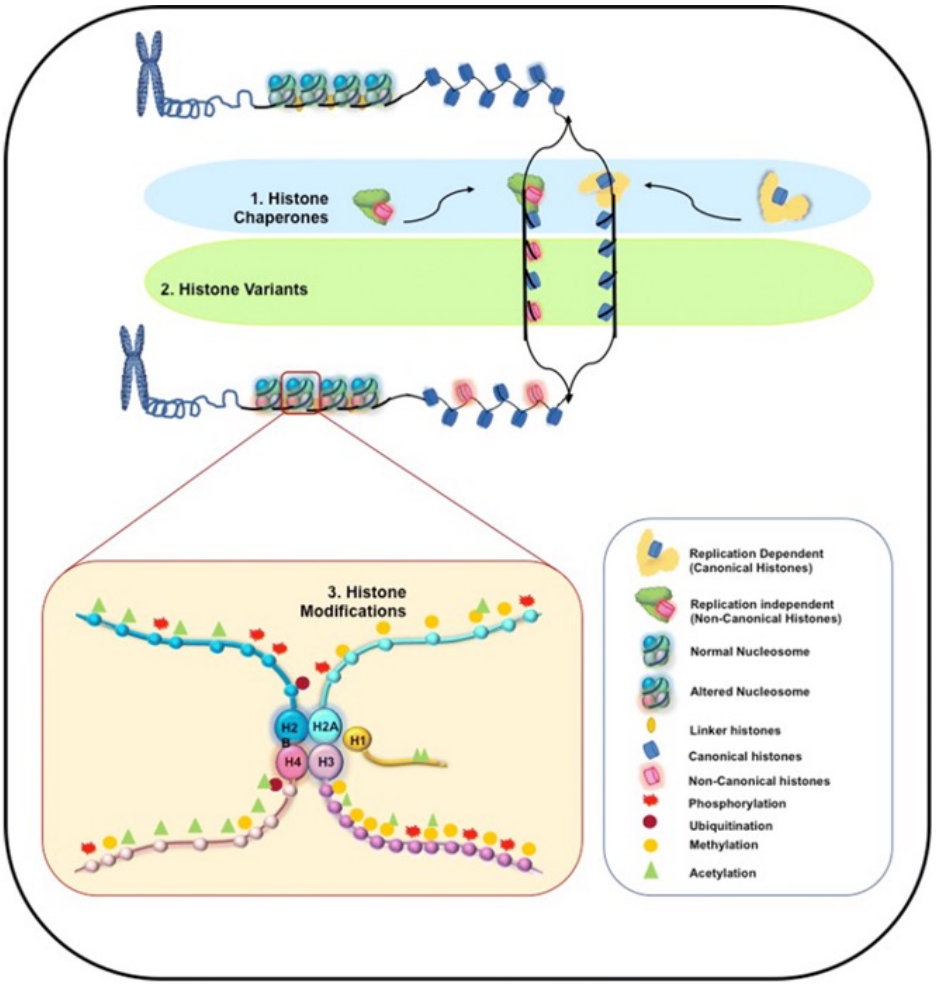

Fig. 1.1 Histone epigenetics showing the three layers of epigenetic control. (1) Histone chaperones (2) Histone variants and (3) Histone modifications (Nandy et al 2020).

Furthermore, the depletion of this histone variant has been associated with a phenotype similar to EMT (Domaschenz et al., 2017). MacroH2A is implicated in metastasis, the downregulation of its A1.1 variant induces EMT by downregulation of E-cadherin (Lavigne et al., 2014), whereas the A1.2 variant is a transcriptional repressor of metastasis (Kim et al., 2018). Variant H2A.X is often seen in triple negative cancer (Wang et al., 2019) associated with HIF1α expression (Razaeian et al., 2017). Hypomethylated HIS1H2BJ is associated with brain metastasis of breast cancer (Salhia et al., 2014), while its HIS1H2BE variant is associated with estrogen deprivation (Nayak et al., 2015). CENP-A is expressed higher in ER- breast cancers, higher proliferation rates and worse patient survival outcomes (McGovern et al., 2012). The third and final layer which we will explore in more detail, comprises the histone modifications themselves.

Chromatin remodelling is the modification of the chromatin architecture, allowing for transcription machinery to access the coding sequences. This modification is a catalysed addition or removal of a chemical group (acetyl, methyl, phosphoryl, ADP-ribose) onto the histone. This can be achieved by a number of molecules such as: HATs, histone deacetylases (HDACs), methyltransferases and protein kinases (Kouzarides et al., 2007). These modifications then affect the overall histone structure, opening binding sites for transcription factors, histone chaperones or histone modifying enzymes (Kouzarides et al., 2007, Nandy et al., 2020). A summary of their functions and domains they work on is listed in **Table 1.2**.

Table 1.2 Examples of post-translational modifications.

Histone Modification	Change	Modified Residue	Writer	Eraser	Reader Domain	Reference
Acetylation	Neutralisatio of positive charge	K	HAT	HDAC	Bromodomain	DesJarlais and Tummino 2016
Methylation	No charge change, increase of volume and hydrophobicity	K and R	KMT and RMT	KDM	Chromodomain domain, PHD finger domain, MBT domain, WD40r domain, PWWP, BAH, Ankyrin, ADD, Zinc finger CW domain	DesJarlais and Tummino 2016
Phosphorylation	Addition of negative charge	S, T, Y and H	PK	PP	14-3-3. BRCT	Rosetto et al 2012
ADP-ribosylation	Addition of volume and negative charge	E,K and S	PARP	PARG, MacroD1, D2, TARG1	Macro domain, WWE domain, PBZ	Barkauskaite et al 2015

Modified residue: E, glutamic acid; H, histidine; K, lysine; R, arginine; S, serine; T, threonine; Y, tyrosine. Writer and eraser: HAT, histone acetyltransferase; HDAC, histone deacetylase; KDM, lysine demethylase; KMT, lysine methyltransferase; PARP, poly(ADP-ribose) polymerase, PARPG, poly(ADP-ribose) glycohydrolase; PK, protein kinase; PP, protein phosphatase; RMT, arginine methyltransferase; TARG1, terminal ADP-ribose protein glycohydrolase. Reader domain: ADD, ATRX–DNMT3–DNMT3L, ADDATRX; BAH, bromo adjacent homology; BRCT, BRCA1 C terminus domain; MBT: malignant brain tumor; PBZ, PAR-binding zinc finger; PHD, plant homeodomain.
Source (Delphine Quenet 2018).

Each group has its own function and corresponding writer, eraser and reader, which corresponds to the addition, deletion and recognition of the groups. Phosphorylation is the most common post translational modification, and can occur on serine, threonine, tyrosine or histidine residues. This modification is involved in the DNA damage response, transcription, chromatin organisation and cell division. The phosphorylation of the linker H1 histone has different patterns of phosphorylation in different breast cancer cell lines (Harshman et al., 2014). Phosphorylations such as γH2A.X are used to diagnose breast cancer (Yang et al., 2017). Other phosphorylations exist, such as H3, which was implicated in breast cancer by increasing proliferation (Cui et al., 2015). Other modification, such as PARylation, is the transfer of an ADP ribose to an arginine, aspartate, glutamate, lysine or serine residues and is associated with DNA repair. The Poly(ADP-Ribose) Polymerase Family Member 9 (PARP9) modification is associated with metastasis in breast cancer (Tang et al., 2018). Many studies focused on this as a clinical target via Poly(ADP-ribose) polymerase (PARP) inhibitors, while ubiquitination is mainly observed on histones H2A and H2B and this modification is usually associated with protein degradation. In breast cancer, the level of activity of ubiquitin specific protease 22 (USP22), has been shown to correspond to cancer type, as the level of ubiquitin in H2 histone is lower in triple negative cancer (Prenzel et al., 2011) than in luminal (Prenzel et al., 2011). Methylation, depending on which lysine residue is methylated, can have different effects on chromatin. This methylation can be mono-methylated, demethylated, trimethylated on σ-amine of the lysine or mono-methylated, and symmetrically or asymmetrically dimethylated on guanidynil groups (Greer, Shi et al., 2012). This modification is involved in nucleosome stability and providing access for protein to recognise methyl groups. The relationships between these methylations on histones, DNA methylation determines gene transcription based on 3 transcriptional states: active poised or silent. Many histones methylations exist and have different functions. Lysine 4 of histone 3 (H3K4), lysine 36 of histone 3 (H3K36) and lysine 79 of histone 3 (H3K79) have been associated with active transcriptional states, whereas lysine 9 of histone 3 (H3K9) and lysine 27 of histone 3 (H3K27) and lysine 20 of histone 4 (H4K20) are associated with silencing (Black et al., 2012). Although exceptions to this rule exist, methylation of histones has been implicated in breast cancer progression and metastasis (Michalak et al., 2016; Su et al., 2018). The demethylation of H3K4 by pRB protein results in the repression of many target genes of transcription factor E2F1 (E2F1) (Chang et al., 2019), which removes cell cycle checkpoint inhibition and avoidance of apoptosis. The H3K27 trimethylation is caused by the EZH2 methyltransferase which promotes EMT (Gan et al., 2018). This tri methylation is also responsible for transcriptionally repressing EMT suppressive and cell proliferation control genes such as FOXC1, RAD51 recombinase (RAD51), CDH1 and RUNX Family

Transcription Factor 3 (RUNX3) (Yoo et al., 2012). A methyltransferase of interest is the disruptor silencing 1 like (DOT1L). When DOT1L is repressed, it is known to inhibit self-renewal of breast cancer CSCs and migration and invasion (Zhang et al., 2015). DOT1L forms a transcriptional active complex with c-MYC and EP300 and promotes derepression of EMT transcription factors through H3K27 trimethylation and H3 acetylation (Cho et al., 2015), which shows an interaction between methylation and acetylation states.

Acetylation of the lysine residue on histones leads to the opening of the chromatin structure, transcriptional activation and is a significant post translational regulatory mechanism with wide regulatory abilities (Verdone et al., 2006). EP300 is a transcriptional co-activator protein that controls and integrates multiple signal dependent transcription events (Goodma & Smolik, 2000). It influences transcription through chromatin remodelling, via acting as either a histone acetyltransferase (HAT) or lysine (K) acetyltransferase (KAT3B) (Chan & La Thangue, 2001). HAT's main function is to add an acetyl group from acetyl CoA to a lysine on the histones, which forms ε-N-acetyl lysine, subsequently unwinding the DNA coiled around the histone, allowing the genes located in that section to be transcribed. This can result in a myriad of biological effects, ranging from cell proliferation, cell growth to motility. The function of EP300 as a HAT has similar consequences. Acetylation in breast cancer is linked to the repression of tumour suppressor genes and activation of oncogenes (Liu et al., 2017). An example of pro EMT characteristics gained from acetylation are H3 acetylation within the SNAI2 promoter, a known EMT gene (Karadedou et al 2012), and the induction of VEGF through forkhead box protein M1 (FOXM1) mediated acetylation of the VEGF promoter within H3 and H4 (Yao et al 2014). Previously mentioned, the ER-α receptor is vital in cancer progression and therapy choice, and ER-α levels have been shown to be affected by the acetylation of H3 and H4 (Macaluso et al., 2003). This acetylation is also responsible for HER2 overexpression (Guo et al., 2018). Repression of ER-α in triple negative cell lines like MDA-MB-231 is maintained by the active DNMT1 obstruction of EP300 from binding to the ER-α promoter (Macaluso et al., 2003). Acetylation becomes even more important when observing the differential expression patterns of acetylation marks during different cancer stages (Elsheikh et al., 2009). Many acetylation marks exist. The acetylation of lysine 16 on histone 4 (H4K16ac) is associated with lymph node metastasis and angiogenesis (Elsheikh et al., 2009, Halasa et al., 2019). This acetylation actively influences pro EMT and inhibits oncogenes. The acetylation of lysine 18 on histone 3 (H3K18ac) promotes carcinogenesis by repressing gene promoter regions and is associated with high grade tumours (Messier et al., 2016). The acetylation of lysine 4 on histone 3 (H3K4ac) mark has been shown to have a high correlation with metastatic breast cancer (Halasa et al., 2019). The effect of this mark is cell type context dependent as it promotes acetylation of the promoter regions

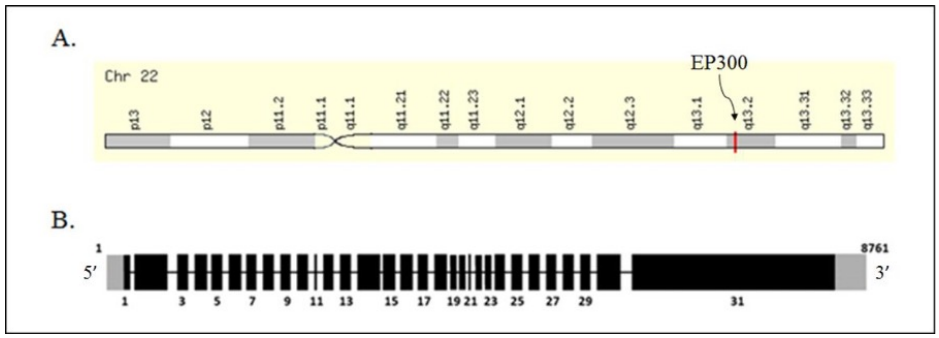

Fig. 1.2 Diagram of the chromosome location and the structure of EP300 gene. (A) The cytogenetic band which shows the location of EP300 (Human Gene Database, GeneCards). (B) Diagram representing the EP300 gene. Exons are shown as black boxes, both the 3' and 5' UTRs are shown as grey boxes. Adaptation from the Atlas of Genetics and Cytogenetics in Oncology and Haematology (http://atlasgeneticsoncology.org/Genes/P300ID97.html).

of pro invasive genes such as vimentin (Bellucci et al., 2013) in MDA-MB-231, while also promoting acetylation of epithelial markers such as GATA Binding Protein 3 (GATA3) and FOXA1 in MCF7 (Bellucci et al., 2013). Further role in EMT is seen with the mark H3K27ac by promoting these pro invasive genes (Halasa et al., 2019), as well as promoting drug resistance and avoidance of apoptosis through activation of p21 (Dong et al., 2019). Overall, these modifications are responsible for regulating transcription on multiple levels, and EP300 is known for at least 2 of these acetylation and interaction with methylation states.

1.4.4 Structure of the EP300 Gene

The EP300 gene (ENTREZ Gene ID 2033) is located on chromosome 22q13.2. It is 88,293 base pairs long containing 31 exons, and the section which encodes the transcriptional co activator. According to the Atlas of Genetics and Cytogenetics in Oncology and Haematology (2014), EP300 only has a single splice variant, its mRNA is 9585 bp long with a 3'-UTR of 1121 nt and a 5'-UTR of 1219 nt. There have been reports of rare translocations of chromosome 22 due to somatic mutations. Such a translocation has been observed in acute myeloid leukaemia (AML) with translocations between chromosomes 8 and 22 (Chaffanet et al., 2000). Another observed translocation between chromosomes 11 and 22 was also observed in AML patients as a result of chemotherapy (Ohnishi et al 2008). Somatic mutations of EP300 have also been observed in many other solid tumours, many of which involve inactivation of the HAT function (Duex et al., 2018). Furthermore, these mutations are associated with antitumour immunity and tumour burden in bladder cancer (Zhu et al., 2020).

1.4.5 Protein Structure of EP300

The EP300 protein (KAT3B) is a 264 kDa protein that belongs to the HAT or KAT3 family of proteins (Valor, Vioska et al., 2013). EP300 molecular functions relate to its structural and functional domains. The protein consists of the chromatin association and modification region, which includes in itself, the bromodomain/ PHD finger module and HAT domains. These are preceded by four Transactivation domains (TADs) (Bedfored & Bridle, 2012; Wang Marshall et al., 2013). The functions of each will be explained further and illustrated in **Figure 1.3** below.

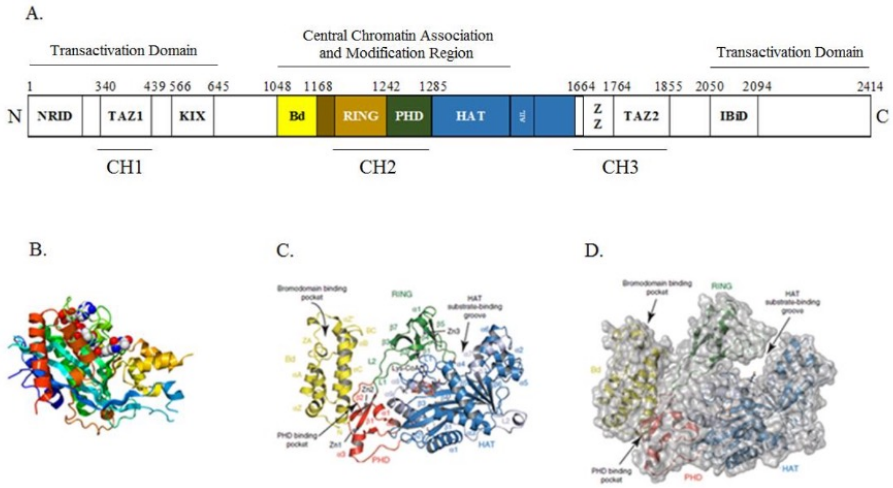

Fig. 1.3 Illustration of the EP300 core structure. (A) Architecture of all the domains of EP300. Showing NRID (nuclear receptor interaction domain), CH1 (cysteine/histidine-rich region 1, also known as transcriptional−adaptor zinc−finger domain 1 or TAZ1), KIX (kinase inducible domain of CREB interacting domain), BROMO (bromodomain), PHD (plant homeodomain finger), HAT (histone acetyltransferase domain), AIL (auto-inhibitory loop), ZZ (ZZ−type zinc finger domain), TAZ2 (transcriptional-adaptor zinc−finger domain 2; ZZ and TAZ2 together are sometimes referred to as CH3 or cysteine/histidine−rich region 3), and IBiD (IRF3−binding domain). These amino acid positions were adapted from UniGene NP_001420.2. (B) Diagram of the HAT domain of EP300 using crystallography. (N- terminus = blue, C-terminus = red) is complex with the inhibitor lysine-CoA (space-filling model, carbon = white, oxygen = red, nitrogen = blue, phosphorous = orange). (C and D) Ribbon and surface representations of the EP300 core structure with labeling of secondary- structure elements. The bromodomain (Bd), RING and PHD domains are shown in yellow, green and red, respectively. The N and C subdomains of the HAT domain are shown in blue and gray, respectively. Figures modified from (Delvecchio, Gaucher et al. 2013).

The bromodomain plays a pivotal role in attachment of EP300 to chromosomal sites, it operates by controlling EP300 attachment to acetyl groups (CH3CO) on acetylated histones, nucleosomes and transcription factors (Kalkhoven, 2004; Rack, Lutter et al., 2014), that are otherwise known to be in an opened conformed or activated state. The bromodomain works in tandem with the HAT domain for substrate acetylation. Without a bromodomain, there is no transcriptional activity or substrate specificity in EP300 (Delvecchio, Gaucher et al., 2013). Another integral part of the catalytic core of EP300 is the plant homeodomain finger (PHD). It is involved in substrate recognition of histone and non-histone substrates for acetylation, including auto-acetylation, and is associated with the bromodomain (Kalkhoven, 2004; Wankg, Marshall et al., 2013; Rack, Lutter et al., 2014).

The HAT domain is able to initiate auto acetylation of EP300, including histone and non-histone proteins. It is also crucial acetylation of promoter bound histones and modulation of transcription (Ito, Ikehara et al., 2000). The HAT domain is also able to acetylate the Cysteine/histidine-rich region 1 (CH1) otherwise known as transcriptional-adaptor zinc-finger domain 1 (TAZ1), Cysteine/histidine-rich region 2 (CH2), which is made up of the Really Interesting New Gene (RING) domain, the PHD finger and Cysteine/histidine-rich region 3 (CH3), encompassing the transcriptional adaptor zinc finger domain 2 (TAZ2) and ZZ-type zinc finger domain (ZZ) regions which are 3 cysteine/histidine-rich, giving them the ability to bind zinc for protein-protein interactions (Wang, Marshall et al., 2013; Valor, Viosca et al., 2013).

The RING domain has E3 ligase activity which binds E2 ubiquitin-conjugating enzymes for the transfer of ubiquitin. The structure of the HAT domain is a central β-sheet that is made up of 7 βstrands that are surrounded by 9 α-helices, with 1 β strands from the C subdomain (Liu, Wang et al., 2008). Altogether, these form a bromodomain, RING-PHD (BRP) module, this module closely associated with the HAT domain, and is juxtaposed with the HAT substrate binding site (Delvecchio, Gaucher et al., 2013). Through its many domains: CH1, kinase inducible domain of CREB interacting domain (KIX), CH3 and nuclear receptor coactivator binding domain (NCBD), EP300 interacts with transcription factors, transcriptional co-activators, and basal transcription machinery (Goodman and Smolik, 2000), which allow it to mediate epigenetic and transcriptional regulation of genes.

Posttranslational regulation of EP300 occurs through acetylation and deacetylation (Delvecchio, Gaucher et al., 2013), methylation (Lee, Coonrod et al. 2005), sumoylation (Girdwood, Bumpass et al., 2003), ubiquitination (Shima, Shima et al., 2008) and phosphorylation (Yang, Hong et al., 2001). It also shares homology with cyclic AMP response element-binding (CREB), binding protein (CBP) (Wang, Marshall et al., 2013), with 63% of its sequence identity and 75% similarity of amino acids (Wang, Marshall et al., 2013).

Due to their shared homology they also interact, one of these interactions is regulating the hypoxia pathway, as CBP/EP300 and hypoxia-inducible factor 1-α (Hif-1α) form a complex to initiate a hypoxic response, and recently this has been a target for therapy (Wei et al., 2018). However, EP300 has separate functions to CBP (Chan & La Thangue, 2001). Using lysine acetyltransferase activity, EP300 can regulate proteins, histones and non-histone substrates (Lee & Workman, 2007, Wang & Marshall et al., 2013).

1.4.6 Functions of EP300

Functions that separate EP300 from CBO are: histone modifications, chromatin remodelling, and acetylation of non-histone transcription factors. Firstly, histone modification by EP300 can occur on all four cores of the histone: H2A, H2B, H3 and H4. These cores have an N-terminal tail which is acetylated by the HAT domain, therefore uncoiling of the DNA happens through chromatin remodelling (Berdasco & Esteller, 2013; Wang, Marshall et al., 2013). Secondly, acetylation of non-histone transcription factors occurs through the action of the four TADs. They also have the function of interacting with TADs of transcription factors, otherwise known as intrinsically disordered regions (IDRs). The IDRs are known to recruit EP300 for acetylation as a response to internal or external stimuli, thus expressing the target genes that are coded for by the transcription factors (Wang, Marshall et al., 2013).

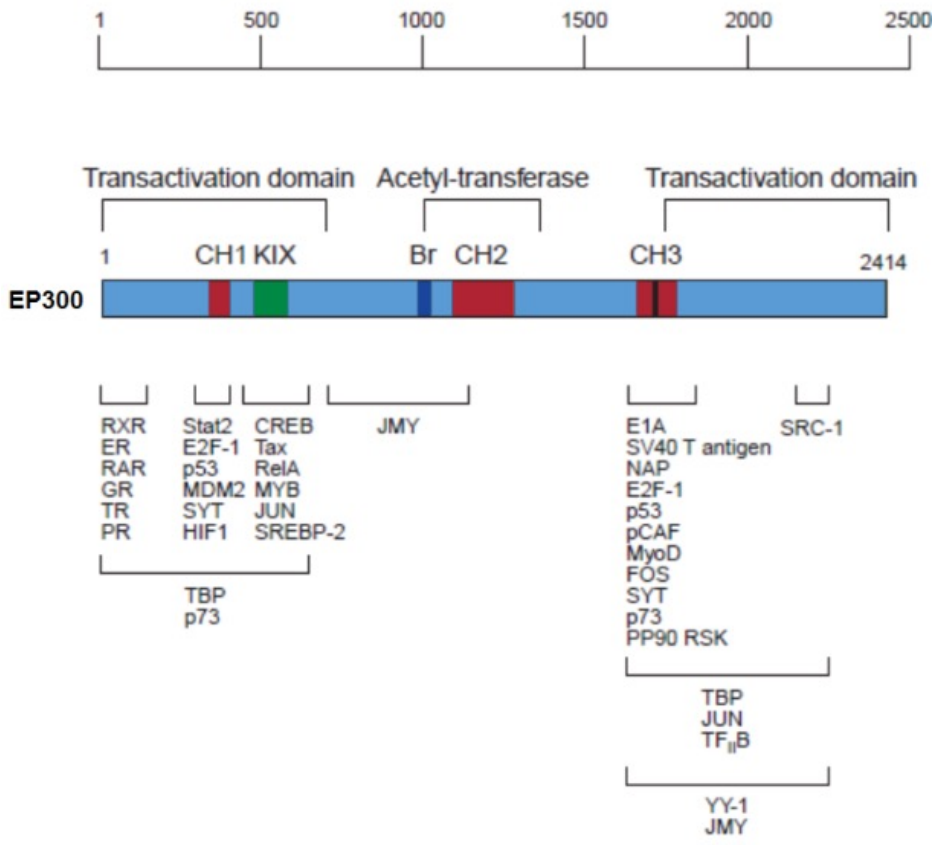

Fig. 1.4 Functional domains of EP300 and its interactive partners. The figure is taken from (Wang, Marshall et al. 2013).

The acetylation of non-histone substrates by EP300 can modulate transcription in both directions via four mechanisms: protein-protein interactions (activator of thyroid and retinoid receptors), protein-DNA interactions (the high mobility group protein), nuclear retention (hepatocyte nuclear factor 4) and protein half-life (E2F). As an example, EP300 modulated histone methyltransferases will condense chromatin and result in gene silencing. Therefore, not all functions of EP300 are promotion of transcription. EP300 functions as a bridge between DNA-bound transcription factors and direct interaction with transcription factor II D (TFIID): TATA-binding protein (TBP) and 13 TBP-associated factors and the pre-initiation complex (Wang, Marshall et al., 2013).

EP300 is an interesting protein as it has over 400 partner proteins (Bedford & Brindle, 2012). Notably, the EP300 interactome (Wang, Marshall et al., 2013) includes:

1. Oncoproteins and pro-proliferation proteins (cellular MYC (c-Myc), cellular MYB proto-oncogene (c-Myb), CREB, c-Jun N-terminal kinases (c-Jun), cellular Fos proto-oncogene (c-Fos)). The Myc proteins are involved in signal transduction, transcription, protein biosynthesis, cell adhesion and cytoskeleton formation, DNA repair, translation, metabolism, cell cycle, micro RNA, among other functions and deregulated in cancers (Chen et al., 2018). C-Jun and C-Fos are involved in proliferation, angiogenesis and invasion (Vleugel et al., 2006) and stemness (Muhammad et al., 2017).

2. Transforming viral proteins: Adenovirus early region 1A (E1A) and The Human Papillomavirus (HPV) E6 protein (E6). The expression of E1A is known to reduce tumorigenesis, proliferation and induce cell death as well as resensitise cells to chemotherapy (Chang et al., 2014). E6 inhibition leads to cell senescence due to the activation of pRb and p53 pathways (Pol et al., 2013).

3. Tumour suppressors and pro-apoptotic proteins: Forkhead Box O1 (FOXO1), Forkhead box O3a (FOXO3a), Forkhead box protein O4 (FOXO4), Signal transducer and activator of transcription 1 (STAT1), Signal transducer and activator of transcription 2 (STAT2), HIF-1α, BRCA1, Runt-related transcription factor 1 (RUNX1), E2F and SMAD proteins.

These are heavily involved in a variety of processes; the Forkhead box family of proteins on their own are involved in regulating transcription of many pro and anti-invasive genes. (HIF-1α regulates the hypoxic response, BRCA1 is the canonical gene of breast cancer, SMAD proteins operate downstream of the TGF-β pathway, STAT1/2 involved in cytokine and inflammatory response, while RUNX1 regulates EMT, while E2F regulates the cell cycle. The rest of the interactome is summarised in **Figure 1.4**.

EP300 plays a dual role in p53 regulation. Firstly, through the mouse double minute 2 homolog (MDM2) mediated ubiquitination of p53 resulting in its degradation, and EP300s CH1 region through its poly-ubiquitin ligase activity regulates this turnover. (Wang, Marshall et al., 2013). Secondly, EP300 acetylates p53, thereby activates its tumour suppressor activity (Lunning & Green, 2015). Cell cycle regulation takes place when EP300 associates with cyclin dependant kinase-2 (CDK2) (Wang, Marshall et al., 2013). Regulation of DNA repair happens when EP300 interacts with: DNA Polymerase b, Flap endonuclease-1 (Fen1), RecQ protein-like-4 (Recq14) and helicase and thymine DNA glycosylase (Dietschy, Shevelev et al., 2009). Lastly, nuclear import is controlled by EP300 through acetylation of its two main proteins: importin-α1, and importin-α7.

1.4.7 EP300 Mutations in Cancer

As previously mentioned, the EP300 gene is located at locus 22q13, this location allows frequent loss of heterozygosity (LOH) which had been reported in 36% of breast cases, 38% of colon and 49% of ovarian cancers (Bryan et al., 2002) as well as in gastric and colorectal carcinoma (Muraoka, Konishi et al., 1996). A genetic deletion or somatic mutation can cause the inactivation of the crucial HAT domain, previously mentioned to be involved in the acetylation of transcription factors. This deletion or somatic mutation has been reported in 39% of cases of diffuse large B-cell lymphoma, 41% of follicular lymphoma cases (Gayther, Butley et al., 2000; Pasquialucci, Dominguez-Sola et al., 2011), There are also some evidence that show EP300 can function as a tumour suppressor in epithelial cancers due to truncating mutations of EP300 being present in breast, colorectal primary tumours. Of the reported truncating mutations, three truncated EP300 upstream of the HAT domain result in a complete loss of function (Gayther, Batley et al., 2000).

1.4.8 Aim

1. To examine the role of EP300 in modulating or altering resistance to paclitaxel and doxorubicin by short-term drug sensitivity and long-term drug resistance assays.

2. To evaluate the effect of EP300 in modulating expression of EMT and CSC phenotypes by examining cell surface receptor expression with flow cytometry and invasion and migration assays.

3. To confirm the effect of EP300 and E-cadherin downregulation using stable transfection models in breast cancer cell lines.

Chapter 2

Methods

2.1 Cell Culture and Maintenance

Breast cancer cell lines MDA-MB-231, CAL-51, T47D, MCF7 and Hs578T (German Resource Centre for Biological Material, Braunschweig, Germany) and HEK-293-T (UCL) were cultured in Dulbecco's Modified Eagle Medium (DMEM) (Gibco®, U.K.) supplemented with 10% v/v Foetal Calf Serum (FCS) (Sigma-Aldrich, U.S.A) and 100 U/ml Penicillin (Sigma-Aldrich, U.S.A), 0.1 mg/ml streptomycin (Sigma-Aldrich, U.S.A) and 2 nM L-glutamine (Sigma-Aldrich, U.S.A). Colon carcinoma cell line HCT1106 was grown in McCoy's 5A modified medium (Gibco®, U.K.), supplemented with 10% v/v FCS (Sigma-Aldrich, U.S.A) and 100 U/ml Penicillin, 0.1 mg/ml streptomycin (Sigma-Aldrich, U.S.A) and 2 nM L-glutamine (Sigma-Aldrich, U.S.A). Minimally transformed mammary epithelial cells (MTMEC) were cultured in HuMEC basal serum free medium (Gibco®, U.K.) supplemented with 1% v/v HuMEC supplement (Gibco®, U.K.), 5% w/v bovine pituitary extract (Sigma-Aldrich, U.S.A), 10% v/v FCS (Sigma-Aldrich, U.S.A), 100 U/ml Penicillin (Sigma-Aldrich, U.S.A), 0.1 mg/ml streptomycin (Sigma-Aldrich, U.S.A) and 2 nM L-glutamine (Sigma-Aldrich, U.S.A). Cells were manipulated in a Class II laminar flow hood (BioMAT 2, Derby, U.K.) and maintained in a Galaxy 170R incubator (RS Biotech, Ayrshire, U.K.) at 37^{o}C and 4% CO_2. Cell lines with overexpression of EP300 and CDH1 were supplemented with 1 mg/ml G418 (Sigma-Aldrich, U.S.A) to maintain traits.

2.1.1 Cell Freezing and Thawing Procedure

When a 75 cm^2 flask (Corning®, USA) was at 80% confluence every five passages, cells were frozen in triplicate in 1ml of cryomedium. Cryomedium was composed of 90% v/v FCS and 10% v/v Dimethyl Sulfoxide (Sigma-Aldrich, U.S.A). Medium was aspirated

briefly, and cells were washed in Phosphate Buffered Saline (PBS), and trypsinised using EthylenediaminetetraAcetic Acid supplemented with 0.25% v/v trypsin (Sigma-Aldrich, U.S.A) for four minutes at 37°C, 4% CO_2. Cells were then quenched in DMEM (Gibco®, U.K.) containing 10% v/v FCS and 100 U/ml Penicillin, 0.1 mg/ml streptomycin, 2 nM L-glutamine, spun at 189 x g for three minutes and the pellet then divided equally among three vials. Cryotubes were transported to the liquid nitrogen storage facility inside a Mr FrostyTM (Thermo Fisher Scientific, UK) filled with 100% v/v isopropanol.

2.1.2 Generating Knock-down Cell Lines with RNA Interference (RNAi)

Cell lines were transfected at 60% confluency in a 75 cm^2 flask (Corning®, USA). Lipofectamine® (Invitrogen) was used to transduce shNCT into the colorectal carcinoma cell line HCT1806, while the lentiviral vector pGIPZ® (Thermo Scientific) containing EP300 and CDH1 consensus sequences(**Figure 2.1 A-C**), was used to transfect MTMEC, MCF7 and T47D breast cancer cell lines.

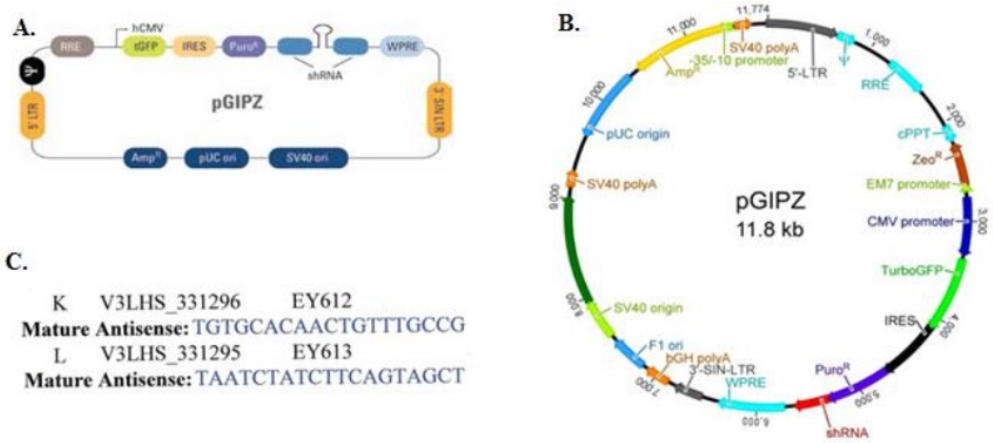

Fig. 2.1 Map of vectors and constructs. (A) A diagram of the pGIPZ lentiviral vector, (B) Diagram of pGIPZ in detail, (C) the sh constructs used for EP300 in pGIPZ.

2.1.3 Generating Overexpression Cell Lines

MDA-MB-231, and CAL51 breast cancer cell lines were used to generate stable expression of EP300 and CDH1 and empty pcDNA3.1 vectors as a negative control. The method is described below.

2.1.4 Cloning Vectors

The plasmids pcDNA3.1-EP300 (plasmid #23252) (Addgene, MA, USA) and hE-cadherin-pcDNA3 (plasmid #45769) (Addgene, MA, USA) (**Figure 2.2**) were purchased from Addgene. The empty vector pcDNA3.1 (Invitrogen) was purchased from Invitrogen. The plasmids were then cloned into an E.coli DH5α strain and then isolated using the QIAGEN plasmid purification kit (Qiagen, Hilden, Germany) according to the manufacturer's instructions.

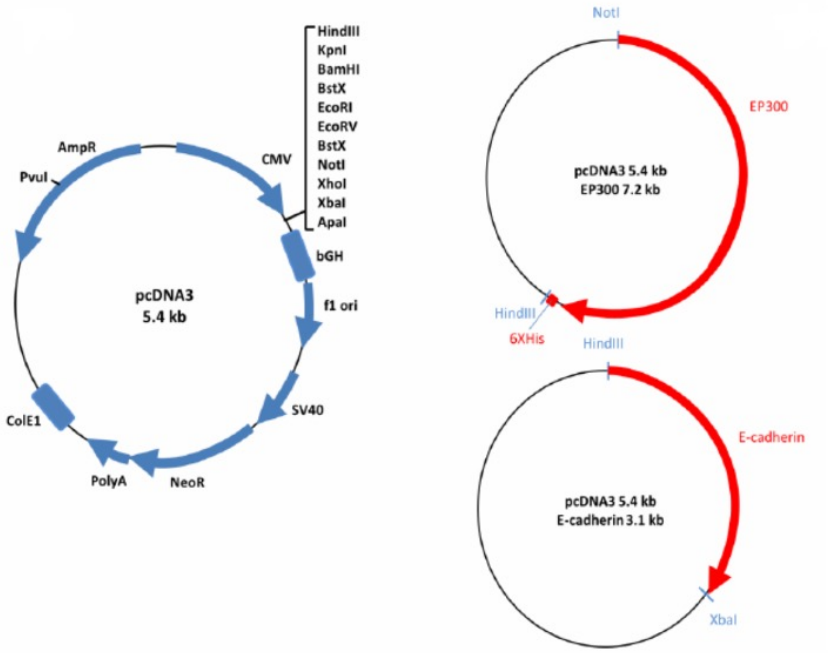

Fig. 2.2 Diagram representing the plasmid constructs used for transfection. Also shown in the diagram are the restriction enzyme cloning sites used for recombinant plasmid design in pcDNA3.1-EP300 and pcDNA3.1-hE-cadherin.

Plasmids that were used for the cloning procedures were the empty vector pcDNA3.1 (Invitrogen, USA) and the pcDNA3.1 with the EP300 inserts (Addgene, MA, U.S.A). Plasmids were cloned in E.coli DH5α (Sigma Aldrich, U.S.A) which were grown in a agar medium supplemented with the appropriate antibiotic at 37^{o}C and 4% CO^2. Plasmids were then purified using QIAGEN plasmid purification protocol (QIAGEN, Hilden, Germany).

2.1.5 Plasmid DNA Isolation, Digestion and Purification

Plasmid purification kit (Qiagen, Hilden, Germany) was used to isolate the plasmid from E.coli DH5α. All preparations were done in batches, using the same reagents and according to the manufacturer's instructions. Quality control was performed by using the A260/280 ratio of 1.8-2.0 on the Nanodrop ® absorption.

2.1.6 Plasmid Isolation

Plasmid isolation from E.coli DH5α was done using the QIAGEN plasmid purification kit® (QIAGEN, Hilden, Germany). The procedure described was done using miniprep: by inoculating a single bacterial colony from a pre-prepared ampicillin plate in 5 ml of Luria Bertani medium and subsequently harvested by centrifugation at 6800 x g for three minutes and resuspended in 250 μl of P1 buffer. The reaction which was followed by alkaline lysis, with 250 μl of P2 buffer for 5 minutes, followed with a neutralisation of the reaction with 350 μl of N3 buffer. The resulting mixture was then centrifuged at 13,500 x g to precipitate the DNA, the supernatant was added to a QIAprep® spin column and centrifuged at 13,500 x g for 30 seconds next, discarding the flow through. After, the column was washed with 750 μl of PE buffer, centrifuged at 13,500 x g for 30 seconds with an additional spin to remove any residual PE buffer. Elution of the DNA was carried out by adding 50 μl of EB buffer and one minute of centrifugation at 13,500 x g.

2.1.7 Sequencing

Upon plasmid isolation and concentration determination using NanoDrop ND1000® spectrophotometer (Thermo Scientific, Wilmington, U.S.A), 500 ng of each plasmid was used to check the integrity of its start and stop codons using 3.3 pM of the required primer (**Figure 2.3**). Samples were sent to the Genomics Laboratory (MRC Clinical Sciences Centre) for sequencing using an Applied Biosystems 3730xl DNA Analyser (Applied Biosystems, Carlsbad, U.S.A). The forward primer used for sequencing the two plasmids was 5'-CGCAATGGGCGGTAGGCGTG-3'. The sequences of the reverse primers used for the

pcDNA3.1-EP300 and pcDNA3-hE-cadherin plasmids were 5'- CCCCACTCCAGTCCTT CCCC-3' and 5'-TAGAAGGCACAGTCGAGG-3', respectively.

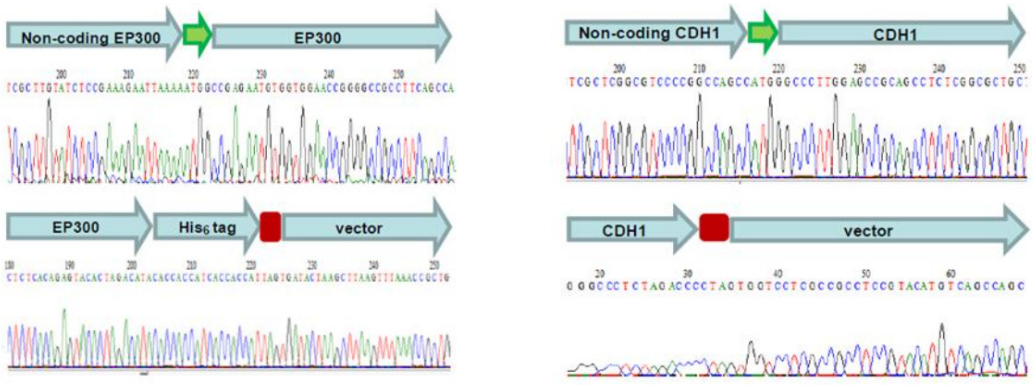

Fig. 2.3 The chromatograms shown indicate the START (green arrows) and STOP (red boxes) codons of the pcDNA3.1-p300 (A) and hE-cadherin-pcDNA3 (B) recombinant plasmids.

2.1.8 Transfection Methods

Overexpression of EP300 in CAL51 and MDA-MB-231 was performed using GenJet (SignaGen Laboratories, USA). A 25 cm^2 flask (Corning®, U.S.A) was grown to 90% confluence and transfected with a solution containing 250 μl serum-free DMEM with high glucose (4.5 g glucose/L), 5μg DNA and 20 μl of GenJet. Prior to transfection, the solution was separated 4:1, and the complex was allowed to form over 15 minutes at room temperature . Cells were trypsinsed, centrifuged at 150 x g, at room temperature . The cell pellet was then resuspended in 500 μl of the transfection reagent and allowed to incubate at 37^{o}C for 20 minutes. Cells were then plated onto another 25 cm^2 flask (Corning®, U.S.A) in 5 ml of fresh, pre-warmed DMEM (Gibco®, U.K.). Subsequent antibiotic selection was performed two days after transfection.

2.1.9 Antibiotic Selection and Cell Culture Maintenance

All cells, CAL51, MDA-MB-231, MCF7, HCT116 and HEK-293T (German Resource Centre for Biological Material, DSMZ, Braunschweig, Germany) were grown according to procedures described by the ATCC, using all safety protocols and performed under sterile conditions using disposable equipment. Cultured in DMEM (Gibco®, U.K.) containing 10% v/v FCS and 100 U/ml Penicillin, 0.1mg/ml streptomycin, 2 nM L-glutamine and 1mg/ml of G418® (geneticin). Cells were passaged every two to three days into sterile plastic-ware

(Corning®, U.S.A) with 0.25% v/v trypsin (Sigma-Aldrich, U.S.A). Cells were routinely tested for mycoplasma contamination using a MycoAlertTM (Lonza, CH) test kit.

2.2 Analysis of Protein Expression

2.2.1 Cell Lysis Procedure

Cell pellets were lysed on ice for five minutes, using RIPA buffer (Thermo Fischer Scientific, USA) which contained; 50 mM Tris-HCL pH=7 (Sigma Aldrich), 150 mM Sodium Chloride (NaCl) (Sigma Aldrich), 5 mM ethylenediaminetetraacetic acid (EDTA) (Sigma Aldrich), 5 mM dithiothreitol (DTT) (Sigma Aldrich), 1% v/v NP-40 (Sigma Aldrich). To prevent the proteolytic and phospholytic enzymes from degrading proteins, various phosphatase and protease inhibitors were added according to available literature (**Table 2.1**), such as 1 mM phenylmethylsulfonyl fluoride (PMSF) (Sigma Aldrich), 1 mM Sodium Fluoide (NaF) (Sigma Aldrich) and 1 mM Sodium Orthovanadate (Na3V04) (Sigma Aldrich), and samples were vortexed throughout. Lysates were then centrifuged at 15,000 x g for 10 min at 4^{o}C. The supernatant was then collected and stored at -80^{o}C. Protocol was adapted from (Krol et al., 2007).

Table 2.1 Commonly used protease and phosphatase inhibitors.

Inhibitor	**MW**	**Target Class**	**Type**	**Solubility (Solvent)**	**Typical Working Concentration**
Sodium Fluoride	42	Ser/Thr and acidic phosphatases	Irreversible	40mg/mL (H2O)	1 to 20mM
Sodium Orthovanadate	183.9	Tyr and alkaline phosphatases	Irreversible	20mg/mL (H2O)	1 to 100mM
EDTA	372.2	Metalloproteases (chelates cations)	Reversible	10g/100mL (H2O)	2 to 10mM
PMSF	174.2	Serine proteases	Reversible	18mg/mL (MeOH)	0.1 to 1.0mM

Source http://www.piercenet.com/browse.cfm?fldID=555B3262 -5056-8A76-4EA5-57A875C0B771

2.2.2 Protein Concentration Estimation Using the BCA Assay

The BCA assay (Thermo Scientific Pierce® BCA Protein Assay Kit) was performed according to manufacturer's instructions. Briefly, samples were diluted 1:5 with dH_20 and mixed with the reagents A and B mix supplied in the kit (200 μl of A and 1/50th amount of B). Samples were incubated for 30 minutes at 37^{o}C and then samples were analysed on a microplate reader (Tecan Sunrise®, Switzerland) plate reader at a wavelength of 562 nm.

2.2.3 SDS-Polyacrylamide Gel Electrophoresis (SDS-PAGE)

Samples are then denatured in 5x Laemmli buffer at 100^{o}C for five minutes. Stacking gels were set in at 4% v/v and Resolving gels were made at concentrations ranging from 4-10% v/v, according to the instructions of the manufacturer supplied with polyacrylamide gels (Pierce). The samples were loaded at a concentration of 20 μg per well, alongside 6 μl of Spectra™ Multicolor Broad Range Protein Ladder (Thermo Fisher Scientific, U.S.A) and run in running buffer (0.1% w/v SDS, 25 mM Tris, 190 mM glycine) for 60 minutes at 90V.

2.2.4 Electroblotting by Wet Transfer Method

20 μg of sample proteins was transferred to a nitrocellulose membrane (BioTrance®, N.T.) by using wet transfer method. Gel and membrane stacks were assembled and placed into transfer tanks, filled with a transfer buffer (25 mM Tris, 190 mM glycine, 20% v/v methanol). Tanks were running for 90 minutes at 90V on ice to prevent uneven transfer.

2.2.5 Western Blotting

Nitrocellulose membranes were dipped in Ponceau to visualise transferred protein bands. Afterwards, membranes were washed in dH_20 and then blocked for one hour at 4^{o}C in 5% w/v Bovine Serum Albumin diluted with 1x PBS-0.1% w/v Tween 20. Membranes were then washed in 1x PBS-0.1% v/v Tween 20 and incubated overnight with primary antibodies at a concentration of 1:1000 of primary antibody to 1x PBS-0.1% v/v Tween 20. β-actin was used as a loading control (mouse mAb 6276, abcam, 1:10,000). Membranes were then washed with 1x PBS-0.1% v/v Tween 20 and incubated with secondary antibody (Polyclonal goat anti mouse immunoglobulins HRP #P0447) and (Polyclonal goat anti rabbit Immunoglobulins HRP #P0448) for one hour at room temperature. Membranes were then washed a final time with 1x PBS-0.1% v/v Tween 20 and incubated for one minute with ECL (Perkin Elmer #NEL103001EA). Blots were then visualised on a film developer in a time interval of 1-4

minutes depending on signal intensity, and scanned according to the Abcam method. List of antibodies used can be seen in (**Table 2.2**).

Table 2.2 Antibodies used in western blotting technique.

Antibody	Species	Dilution	Manufacturer
EP300	Anti-rabbit	1:5000	Abcam, Cambridge, UK
E-cadherin	Anti-rabbit	1:1000	Cell Signalling, Heartfordshire, UK
βactin	Anti-mouse	1:20,000	Abcam, Cambridge, UK

2.3 Analysis of mRNA Expression by Real Time Quantitative Polymerase Chain Reaction (RTq PCR)

2.3.1 mRNA Extraction Method (RNeasy)

The cells were washed with PBS on ice and the media was removed from the flask. Cells were then scraped off using a cell scraper and reconstituted in 1ml of ice-cold PBS into a 1.5ml Eppendorf tube. These cells were then centrifuged at 10,000 x g for one minute at 4^{o}C. RNA was then extracted by using the protocol from (QIAGEN, Hilden, Germany). Next, pellets were suspended in 600 μl of RLT buffer (containing β mercaptoethanol). The mixture was subsequently shredded in a QIA shredder® column for two minutes at 12,500 x g. Samples were then mixed with an equal volume of 70% v/v ethanol and transferred to a QIA Spin® column and centrifuged at 9,500 x g for 15 seconds. The flow through was discarded and 700 μl of RW1 buffer was added to the same column and centrifuged at 9,500 x g for 15 seconds. The flow through was discarded and 500 μl of RPE buffer was added to the same column and centrifuged at 9,500 x g for two minutes, discarding the flow through after each centrifuge run. A final centrifugation was run at 12,500 x g for one minute, to get rid of any residual washing buffer. The RNA was then eluted by addition of 35 μl of RNA-se free dH_2O.

2.3.2 Quantification of mRNA Using NanoDrop®

RNA concentration and purity were determined by addition of 1.5 μl to the NanoDrop ND1000 spectrophotometer (Thermo Fisher Scientific, U.K.). RNA samples are all analysed according to their UV absorption measured at the 260nm/ 280nm and 260nm/ 230nm ratios.

Sample purity was selected based on their reading of 1.0 at 260nm (equivalent to $\sim$40μg/ml of pure RNA). While concentration of RNA was measured at 280nm, a good yield would be around $\sim$40μg/ml. Contaminants were also monitored by carefully monitoring the A260/A280 ratio.

2.3.3 Reverse Transcription of RNA for cDNA Synthesis

For mRNA detection, cDNA was generated from 1 µg of complementary isolated RNA using the high capacity RNA-cDNA master mix (Applied Biosystems, U.K.) according to the manufacturer's description. The thermal cycler settings were as follows: 40 cycles of primer annealing for five minutes at 20^{o}C, reverse transcription reaction for two hours at 37^{o}C, reverse transcriptase inactivation for 5 minutes at 85^{o}C and an incubation step indefinitely at 4^{o}C. Subsequent samples were then stored at -80^{o}C. For miR detection, cDNA was generated from 10ng of complementary isolated RNA using the Taqman MicroRNA Reverse Transcription Kit (Applied Biosystems, Life Technologies) according to the manufacturer's instructions. The thermal cycler settings were as follows: 40 cycles of primer annealing for thirty minutes at 16^{o}C, reverse transcription reaction for 30 minutes at 42^{o}C, reverse transcriptase inactivation for five minutes at 85^{o}C and an incubation step indefinitely at 4^{o}C. Subsequent samples were then stored at -80^{o}C.

2.3.4 Real Time Quantitative Polymerase Chain Reaction (RTqPCR)

RTqPCR for mRNA

The total reaction volume used was 10 μl, which contained 1x SYBR Green PCR Mix (Applied Biosystems, Carlsbad, U.S.A), 3.5 pM of primer mix and 1 μg of RNA. For this reaction, GAPDH or RPLO were used as normalizers. The reaction was set up on a thermocycler 9000HT (Applied Biosystems, SDS software version 2.4) for 40 cycles of: 10 minutes at 95^{o}C, 60 seconds at 95^{o}C, 30 seconds at 60^{o}C and for 30 seconds at 72^{o}C. A list of primers was selected based on genes we hypothesised to be modulated by EP300, based on previous findings (Asaduzzaman et al, 2017), the full list of primers can be found in (**Table 2.3**).

RTqPCR for miRNA

The total reaction volume used was 20 μl, which contained 10 μl TaqMan® Universal Master Mix, No AmpErarse® UNG 2X (Thermo Fischer Scientific, U.S.A), 1 μl TaqMan® Gene Expression Assay 20x primer (Thermo Fischer Scientific, U.S.A), 7.5 μl nuclease free

water, 1.5 μl of cDNA template (10 ng). The reaction was set up on a thermocycler 9000HT (Applied Biosystems, SDS software version 2.4) for 40 cycles of: two minutes at 50^{o}C, 10 minutes at 95^{o}C, 15 seconds at 95^{o}C and for 1 minute at 60^{o}C. A set of miR primers was selected based on findings (He et al 2015), the full list of primers can be found in (Table 4).

Prior to generating results, we diluted our control sample cDNA at 1, 1/10, 1/100, 1/1000 and 1/10000 to generate a log curve of dilutions against CT values and selected the dilution of 1/100 which best fit the CT range within 18-24. The same was done for each primer. Results generated were CT values (fluorescence 10 standard deviations above the average baseline threshold). For standardisation and quality assessment, we made sure to use a primer concentration between 150-250 nM for SYBR green primers to prevent primer dimerization. TaqMan® primers were used according to the manufacturer's instructions. Reference genes with the lowest CQ were carefully chosen to prevent variability within the sample, this was done by conducting an initial run on a control sample with non-template controls (NTC) and testing the reference gene primer at different concentrations. We also include multiple reference genes for the normalization step to improve reliability of results. To increase precision of measurements, the number of replicates for each gene was n=3, and the number of repeats of biological replicates was n=3 each repeat included an NTC.

2.3.5 Data Analysis

The comparative CT method used was developed by Schmittgen TD et al (2008) to analyse real time PCR data by comparative CT method. This method was used in this study to calculate the difference between the CT of the gene of interest and the reference gene. Firstly, the CT values of each gene were normalised to the reference gene intra sample. After, those normalised values were compared between inter samples which would estimate the relative amount of gene expression between treated and untreated samples. The statistical significance was measured by using the ANOVA method, supplemented with Tukey's test, with greater stringency ($P \leq 0.05$).

2.4 RNA-seq Data Analysis

2.4.1 Survival Analysis

Kaplan-Meier analysis was performed as described previously. For the expression of the genes, the median expression was used as the cutoff in a Cox regression analysis. The Kaplan-Meier survival plot, and hazard ratio with 95% confidence intervals and logrank P value were calculated and plotted in R using Bioconductor packages.

Table 2.3 Primers used in Real time PCR.

Gene Symbol	Forward Primer 5'-3'	Reverse Primer 5'-3'
ABCG2	GGGTCCTGCCTGCCTGTTTAGTCG	AAAAGAAAGCAGACTCAAAAC
ARHGAP20	CTCTCTCTCCTTCAGAGATAC	CTCTCTCAGAGCCAGTTATC
BCL2	GATTGTGGCCTTCTTTGAG	GTTCCACAAAGGCATCC
BMP4	AGAACATCTGGAGAACATCC	AATGTTTATACGGTGGAAGC
BMP7	TGGTTCCACTTCATCAACC	TTCTGTATTTCTTCAGGATGAC
CAPN9	CAAGCTAAATGGGAGCTATG	CTCTTTAGTTTGGAAGGTCTC
CDH1	GATTCTGCTGCTCTTGCT	GTCAAAGTCCTGGTCCTC
CDH11	AAGGTATTCCATCGATCGTC	TCTCTATCCAGAGGTTTTGTAG
CDH2	CTGGAACATATGTGATGACC	TGTAAACATGTTGGGTGAAG
CEACAM5	GTGATGTTGGAGATAAAGAGC	TCATCCTGAATGTCCTCTATG
CNN2	GGAACTATCTTATGCACACTC	ATGAAGTTGGACAGGTTTTC
EFEMP1	CGTAGACATAGATGAATGTACC	TGCACTGGCAATAAAATGAG
EP300	AGCCAAGCGGCCTAAACTC	TCACCACCATTGGTTAGTCCC
EPHA4	GGTGTAAGAACATATGTGGAC	AGGATGCGTCAATTTCTTTG
FGFR2	ATGAGGAATACTTGGACCTC	TTAACACTGCCGTTTATGTG
FOXO3a	GAATGTTGTTGGTTTGAACG	ATTTGGCAAAGGGTTTTCTC
GATA3	AAAATGAACGGACAGAACC	GGGGTCTGTTAATATTGTGAAG
HEY2	GGATTATAGAGAAAAGGCGTC	GTTTTTCAAAAGCAGTTGGC
HMCN1	AAGGATTACACAGAGGACTAC	TATAGTCAGATTCCACACAGG
ITAG2	GGTGGGGTTAATTCAGTATG	ATATTGGGATGTCTGGGATG
ITAG3	GGAAACAGCTACATGATTCAG	CCCAATATAGAGGTTTCCTTG
miR-23a	AUCACAUUGCCAGGGAUUUCC	
miR-25	CAUUGCACUUGUCUCGGUCUGA	
miR-27a	UUCACAGUGGCUAAGUUCCGC	

Table continues on the next page...

Gene Symbol	Forward Primer 5'-3'	Reverse Primer 5'-3'
MUC5B	TACGTTCTGTCCAAGAAATG	TAGATGGAGTTGAGGAACAC
PLS3	GAACACAGCATTCTTACTCAG	ACAAAGCACAATTCCATCAC
RPLPO	GCAGCATCTACAACCCTGAAG	CACTGGCAACATTGCGGAC
SGCC	GTCCCAAAATGGTAGAAGTC	CCCAGTTACTCGAAGTTTATC
TGFβ2	ATTTCTAAAGCAATAGGCCG	AGATTTGCAGGTATTGATGG
U6snRNA	GTGCTCGCTTCGGCAGCACATA TACTAAAATTGGAACGATACAG AGAAGATTAGCATGGCCCCTGC GCAAGGATGACACGCAAATTCG TGAAGCGTTCCATATTTT	
VIM	CATTTCACGCATCTGGCGTTC	AGTCCACTGAGTACCGGAGAC
WIPF1	TCTCCATGTGAAGATGAGTG	GTTTGCTGGGATAACTTTTG

2.4.2 RNA Sequencing Data Analysis

Fastq files obtained from TCGA, containing the sequence reads, obtained at the end of the sequencing, were mapped to the University of California at Santa Cruz (UCSC) human reference genome (hg19 assembly) as previously described (Pinho et al., 2013). The mapped bam files (obtained with TopHat version 1.4.1 http://ccb.jhu.edu/software/tophat/index.shtml) were cleaned from duplicates with Picard tools version 1.81 (http://picard.sourceforge.net) and then analysed using Cufflinks version 2.0.2 (http://cufflinks.cbcb.umd.edu) for transcript assembly, quantification and differential expression analysis (2.6.3 RefSeq genes version). The coordinates of the genes were downloaded from the UCSC genome browser (Fujita et al., 2011). A copy of the commands used can be seen in (**Appendix B.4**).

2.4.3 Statistics and Plots

All plots were drawn and statistics were performed using R. Heatmaps were drawn using the heatmap.2 function of the ggplots package. Statistics for expression data from TCGA were conducted using R computing environment (non-paramentric Mann-Whitney U test).

2.5 Short- and Long-Term Drug Sensitivity Assays

2.5.1 Cell Viability Assay for Drug Sensitivity

The Sulphordamine B assay was used to determine short-term sensitivity of the cells in response to chemotherapy drugs such as: doxorubicin, taxol and 5-fluorouracil (Vichai et al 2006). The method is widely used due to ease of availability and for cost effective testing and does not rely on metabolic activity measurement such as with the MTT assay, which requires extra steps for optimising protocol. Upon fixation with trichloroacetic acid, this increases the acidity of the cell membranes and exposes amino acids to which amino xanthene dye can attach via its sulphonic acid groups. The amount of dye accumulated is directly proportional to the cell mass, therefore, an accurate response to drug sensitivity can be estimated. Cells were plated in triplicate at a density of 3000 cells per well, onto a clear, flat bottomed 96 well plate (Corning®, U.S.A). Cells adhered overnight, and media was changed to that containing chemotherapeutic drugs such as paclitaxel (0-16nM) and doxorubicin (221-405 nM) in increasing concentrations, a serum free media was used as a control. The cell cycles were assumed to be synchronised as the same cell lines were used throughout and were cultured under the same conditions. Plates were fixed each day with 100 μl of 40% v/v trichloroacetic acid for one hour at 4^{o}C, to generate time points. Plates were then washed in dH_20 and dried overnight and stained with 100 μl of 0.4% w/v SRB (Sigma-Aldrich, Poole, U.K.) in 1% v/v acetic acid for 30 minutes at 37^{o}C. Plates were washed in dH_20 and dried overnight. The dry plates were then solubilised with 100 μl of 10 mM Tris-Base for one hour at 37^{o}C and optical density was measured on a microplate reader (Tecan Sunrise®, Switzerland) at 492 nm.

2.5.2 Clonogenic Assay for Drug Resistance

The principle of this assay is to monitor cell proliferation in response to chemotherapeutic agents over long term. Cells were incubated after treatment, the resulting colonies were counted after being stained in crystal violet. Cells were plated in triplicate at a density of 50,000 cells per 25 cm^2 flask (Corning®, U.S.A). Cells adhered overnight, and media was changed to that containing chemotherapeutic drugs in increasing concentrations (6-10 nM). Media was changed after five days to fresh DMEM (Gibco®, U.K.) supplemented with 10% v/v Foetal Calf Serum and 100 U/ml Penicillin, 0.1mg/ml streptomycin, 2 nM L-glutamine. Cells were left to proliferate for four weeks, cell conditions were monitored and media was changed every 1.5 weeks. After which the media was aspirated and cells were fixed in 100% v/v methanol for five minutes. The flask was then stained with 0.5% w/v

crystal violet (Sigma-Aldrich, U.S.A) in 25% v/v methanol for one hour. After, the flask was washed in dH2O and left to dry overnight. The next day, the colonies were counted and images were taken using a Carl Zeizz Microscope at a 10x magnification. The flask was then solubilised using 33% v/v acetic acid to measure the optical density on a microplate reader (Tecan Sunrise®, Switzerland) at 492 nm Flasks were imaged using a Canon 5D digital camera, and colonies were counted using Image J object tracker. Average colony numbers were then determined and statistical tests were performed.

2.5.3 Sulphorhodamine B (SRB) Assay for Population Doubling Time

The ability of the SRB to stain cellular protein can be employed to measure the population doubling time, i.e. the time by which the cell population doubles in number. This doubling time is an indication of how fast or how slow a particular cell can grow as they are cultured in-vitro and obviously varies from one cell type to the next. Various factors can affect the growth of cancer cells hence measuring the doubling time gives a clue to the effect produced by the specific factor influence on proliferation rate of cells. Cells were counted and seeded (500-100 cells/well, depending on the cell type) in six 96- well plates in replicas and one plate (Day 0) was fixed immediately on the same day after the cells were attached with 40% v/v TCA. The other plates were fixed each day until day 5. After all the plates were fixed, they were removed from the fixatives by washing under slow-running tap water and air-dried. Next, the plates were stained with SRB, rinsed off with 1% v/v acetic acid and left for drying overnight, and after which they were solubilised with 10 mM Tris and the OD readings were read at 492 nM using a microplate reader.

2.6 Flow Cytometry Analysis by FACS

2.6.1 CD44-APC and CD24-PE Assay

CD44 high and CD24 low cell surface receptor expression was quantified using a BD™ LSR II FACS machine, according to (Wenzhe et al., 2017). This is characteristic of a stem cell variant and has been previously shown in various types of breast cancer reference. Around 500,000 cells were added grown on 6 cm dishes, which were subsequently trypsinsed, counted and resuspended in 500 μl FACS buffers inside flow cytometry tubes. The following four conditions were used: unstained, CD44 and CD24 single stains, and double stains. The staining procedure was as follows: FACS buffer (500 ml PBS + 0.5% w/v BSA + 2 ml EDTA) was added to 100 μl of 106 cells and stained with 5 μl of CD44 or CD24 stain (BD Pharmingen®, U.S.A) for 30 minutes at 4^{o}C. Post incubation, the cells were centrifuged at

500 x g for 5 minutes and resuspended in a 500 μl FACS buffer. Subsequent readings were then taken using the FlowJo® software (Li et al 2019).

2.6.2 Aldefluor Dehydrogenase (ALDH) Assay

Aldehyde dehydrogenase activity assay was measured on a BD™ LSR II FACS machine, according to Wenzhe et al (2017). Briefly, 150,000 cells were plated on a 24 well, clear bottomed plate (Corning®, U.S.A) in fresh DMEM (Gibco®, U.K.) supplemented with 10% v/v Foetal Calf Serum and 100 U/ml Penicillin, 0.1 mg/ml streptomycin, 2 nM L-glutamine. The cells were allowed to adhere overnight, after which the media is removed from the flask and cells are washed with Phosphate Buffered Saline and trypsinsed using EthylenediaminetetraAcetic Acid supplemented with pancreatin for four minutes at 37^{o}C, 4% CO_2. Cells were then quenched in medium containing 10% v/v Foetal Calf Serum and 100 U/ml Penicillin, 0.1 mg/ml streptomycin, 2 nM L-glutamine, spun at 500 x g for three minutes. After, cells were counted and reconstituted in 2 ml phosphate buffered saline and spun at 500 x g for three minutes.

2.7 Cell Migration and Invasion Assay

2.7.1 Cell Tracking Assay

100,000 cells were plated on black, flat and clear bottomed 96 well plates (BD Biosciences). For this purpose, the cells selected were within 1-10 passages. Cells were allowed to adhere overnight. Time-lapse imaging was performed for 18 h (1 image/10 min) using a motorised-staged environment-controlled ImageXpress high content screening microscope powered by MetaXpress 2.0 (Molecular Devices). Three sites were acquired per well, and each condition was present in triplicate. To quantify the degree of migration, a minimum of 30 cells per condition were tracked using MetaXpress Track Points application. Tracks were analysed using a script written in (RStudio 0.99.89) by Dr Olivier E Pardo, Division of Cancer, Imperial College London, UK (o.pardo@imperial.ac.uk). A version of the script can be seen in (**Appendix B.1**).

2.7.2 Wound Healing Assay

100,000 cells were plated onto a 24 well, clear bottomed plate (Corning®, U.S.A). For this purpose, the cells selected were within 1-10 passages. Cells were cultured in fresh DMEM (Gibco®, U.K.) supplemented with 10% v/v FCS and 100 U/ml Penicillin, 0.1

mg/ml streptomycin, 2 nM L-glutamine. Media was then changed to 5 ml of serum-free DMEM and two crosses were scratched on each well with a sterile 200 μl pipette tip. Images were cantered and at 10x magnification using a Zeiss Axiovert 200M microscope equipped with a Zeiss AxopCam MRm camera (Carl Zeiss, AG, Switzerland). Cell migration rates were calculated with the formula: $(A0 - At)/ (A0 \times 100\%)$, where A0 represents the area of the scratch at 0 h, and At represents the area of the wound at indicated time point.

2.7.3 Matrigel Cell Invasion via Chemotaxis

10,000 cells were plated onto a 96 well, black bottomed plate (Corning®, U.S.A). For this purpose, the cells selected were within 1-10 passages. Cells were cultured in fresh DMEM (Gibco®, U.K.), supplemented with 10% v/v Foetal Calf Serum and 100 U/ml Penicillin, 0.1 mg/ml streptomycin, 2 nM L-glutamine. After cells have attached to the plate, 100 μl of type II rat tail collagen (Gibco Life technologies) was added into each well. The collagen was allowed to solidify at 37^{o}C, 4% CO_2. Afterwards, fresh 5x DMEM (20%) was added containing 0.01% v/v FCS and 1 μg/ml of Epidermal Growth Factor (EGF). After 48 hours, the cells were fixed in 4% w/v paraformaldehyde supplemented with 1.25 μM sytox green nuclear stain (ThermoFischer Scientific). Cells were then imaged using a Axio Observer Inverted Widefield Microscope with a Vivatome Spinning Disc System (FILM Institute, Imperial College London). Image stacks of 500 μm were taken at 9 sites per condition. Image stacks were then deconvoluted to improve image quality, using Huygens image software. Image analysis was performed using Fiji-Image J in the following manner: 3D plugin object counter and macro script (Stephen Rothery, FILM, Imperial College London, London, UK) The Z distances were normalised to median and subsequent averages normalised to the reference control using SPSS. A copy of both scripts can be seen in (**Appendix B.2 and B.3**).

2.8 Statistical Analysis

All data in the figures are presented as the mean ± standard error (SD) and assessed by using one-way ANOVA analysis followed by a Tukey's test (95% confidence) for multiple comparisons (SPSS version 17). P-value of ≤ 0.05 was considered statistically significant. Methods such as the t-test would yield one absolute t-value, which can confirm or deny a hypothesis at either tail. However, it cannot compare multiple groups (Kao et al., 2008). As we had multiple conditions to compare, we opted for ANOVA which yields an f-value which compares all groups simultaneously and shows the presence of a difference. With the

presence of multiple comparisons a greater probability of type 1 error, it leads to the false assumption that there is a difference. The ANOVA test can tell if the experiment is significant overall (Kao et al 2008), but it does not provide information on where the differences lie. The Tukey's honest significant difference test is a post-hoc test which shows which specific group's means are different when compared to each other. Post hoc analysis shows the exact groups which have the significant difference. Other methods exist such as Scheffe or Benferonni procedure, but Tukey's yields smaller confidence intervals.

Chapter 3

Micro RNA and its Effect on EP300

3.1 Introduction

3.1.1 What is micro RNA?

Micro RNAs (miRs) are 22 nucleotide long, non-coding RNA molecules which function in RNA silencing and post transcriptional gene expression (Bartel et al 2004). The first of which was called lin-4, was found to regulate transcription and translation (Lee et al 1993). Furthermore, they are key regulators of cancer and involved in EMT, metastasis and resistance to therapy (Weidle et al 2018, Satapathy et al 2019), and initiators of angiogenesis (Salinas-Vera et al 2018). The coding sequences of miRs are contained within intragenic or intergenic sequences, meaning inside: introns and in some cases exons of protein coding genes, or regulated by their own promoter and coding sequence (Denli et al 2004, de Rie et al 2017).

3.1.2 Structure and Biogenesis

The biogenesis pathway of miRs is relatively complex. The initial process is for the intragenic sequence to be transcribed by RNA polymerase II/III into a primary miR (pri-miR) in the nucleus. Following this process, a microprocessor complex processes the pri-miR strand. This complex is then formed from a ribonuclease III enzyme Drosha, and the RNA binding protein DiGeorge Syndrome Critical Region 8 (DGCR8). The DGCR8 recognises an N-6-methyl-adenylated GGAC sequence and the Drosha cleaves the pri-miR into a stem loop precursor-miR (pre-miR), which contains a double helix linked by a terminal loop of around 70 nucleotides long. This double stranded linked structure gets exported into the cytoplasm by exportin-5-Ran-GTP (Carrington et al 2013).

At this stage the pre-miR is cleaved into two strands by Dicer and transactivation response element RNA-binding protein (TRBP), which removes the loop. This produces two strands which are referred to in literature as the leading and lagging strands. The lead strand is more stable and is incorporated into the RNA-induced silencing complex (RISC). This RISC complex is made up of the lead strand and the Argonaute protein (Arg). As the lead strand passes through the RISC complex to become a mature miR, its passenger strand gets unwound and degraded (Winter et al 2009). However, there is also a variation of this process for different miR classes. Some strands can bypass Drosha, as is the case with mirtrons which are introns of spliced mRNA, or by 7 methylguanosine capped pre-miRs, both are immediately exported into the cytoplasm (Ruby et al 2007, Xie et al 2013). Alternatively, there is also short hairpin RNAs (shRNA) which are too short for Dicer to cleave, and therefore go directly to the RISC complex (Yang et al 2010).

There is also evidence of imprecise cleavage by Drosh and Dicer which can result in isoMirs, miRs closely related to their original output but with slight variations (Neilsen et al, 2012). Isomirs with a difference in one base mismatch or alteration can have a different inhibitory effect on the same target genes (Ma et al, 2019).

3.1.3 Mechanism of Action

As the function of any silencing mechanism mainly comes from base complementarity of adenine (A), uracil (U), guanine (G) , cytosine (C). The complementary mRNA strand is silenced either: by strand cleavage, shortening of the poly(A) tail which leads to strand destabilisation, or directly lowering efficiency of translation (Bartel et al 2004, Fabian et al 2010). This effect is modulated by direct interaction with target mRNA strands, in one of three ways: through interaction with the 3'-UTR, 5'-UTR or the promoter region.

Interaction with the 3'-UTR end induces deadenylation and decapping of the mRNA, in turn, which prevents translation of the transcript (Ipsaro et al 2015). This deadenylation and decapping process is mediated by the RISC complex, which is target specific for miRNA response elements (MREs), otherwise known as target mRNA (Jo et al 2015). The MRE is cleaved only when there is high complementarity with the leading strand. This MRE cleavage is controlled by Argonaute protein 2 (Arg2), which prevents further endonuclease activity on MRE by degrading the lead strand as it passes through the RISC complex. Subsequently, a complex recruitment of GW182 proteins by the RISC, and the poly(A) deadenylase complex: Poly(A) Specific Ribonuclease Subunit PAN2 (PAN2), Poly(A) Specific Ribonuclease Subunit PAN3 (PAN3) and Carbon Catabolite Repression—Negative On TATA-less (CCR4-NOT), finishes the process.

Interaction with the 5'-UTR can prevent gene expression (Zhang et al 2018). The process by which gene expression control is achieved is not well understood. There is potential for the miRNA-induced silencing complex (miRISC) to directly interact with actively transcribed regions of DNA, as it has been observed that miRISC localises in actively transcribed gene loci of euchromatin (Cernilogar et al, 2011). The miRISC complex is also present in many subcellular compartments of the cell such as Golgi apparatus or endoplasmic reticulum. This allows it to affect a wide range of mRNA, as well as provide quick transport into the extracellular space, where it affects its environment through paracrine or autocrine signalling (Iftikhar et al 2016).

Overall it seems that gene expression control is exercised through a combination of factors, such as MiRISC availability and its localisation at actively transcribed regions, the availability of (Drosha/Dicer), MRE strand affinity and complementarity with miRISC, and abundance of mRNA transcripts, whereas promotion of gene expression is through the interaction of miRISC with the promoter region (Dharan et al 2013). The translational activation is mediated by Arg2 and FMR1 autosomal homolog 1 (FXR1) (Truesdell et al 2012) or by ribosomal proteins attaching to the 5' UTR (Orom et al 2008).

In this way multiple miRs can affect one specific mRNA, or multiple mRNAs by a myriad of miRs, notably in the case of BRCA1 regulation by miR-24 and miR-545. This has led to the approach that miRs could be useful biomarkers for pathology or disease initiation. There is evidence of platelets releasing miRs into the microenvironment, affecting the surrounding endothelium through paracrine signalling (Gidlof et al 2013). Unsurprisingly, this phenomenon was also observed in the tumour microenvironment, facilitating tumour survival, through the transformation of the surrounding endothelium (Suzuki et al 2015).

3.1.4 General Overview of miR Function

Over the years, miRs involved in cancer have been termed oncomiRs (Krutovskikh et al 2010), due to the differential miR expression between cancer types (Tie et al 2009), and even between breast cancer subtypes (Blenkiron et al 2007). Global miR expression is augmented in cancer, miRs inhibit oncoproteins, while also inhibiting tumour suppressor genes. In breast cancer, there is an overall upregulation of miR-21, miR-145, miR-155, miR-184, miR-199, miR-572, miR-601 and miR-622, as well as a downregulation of miR-125b, miR-145, miR-221 and miR-328 (Hui et al 2009, Iorio et al 2005).

In invasive breast cancer, there are numerous miRs up and down regulated (Tahiri et al 2013). There was also an association between low endogenous levels of miR-203, miR-887, miR-3619 and increased Phospholipase (PLD) activity in invasive breast cancer cell lines

compared to luminal, a less aggressive type, which was found to be associated with the loss of E-cadherin (Fite et al 2015).

This augmented expression is also demonstrated in other tumours such as lung, colon, gastric, hepatocellular, prostate, pancreatic and myeloid cancers, among others (Yanaihara et al 2006, Yu et al 2008, Sarver et al 2009, Yu et al 2009, Jiang et al 2008, Wang et al 2008, Schaefer et al 2010, Lee et al 2007, Calin et al 2005).

MiR regulation is done in several ways, one of which is an autoregulatory loop with transcription factors (Tsang et al 2007), by extracellular signalling, or by an increase in signalling molecules like growth factors, cytokines, changes in environment like hypoxic conditions or mechanosensory stimuli (Gulaeva et al 2016). There is also epigenetic controls on miR expression in the form of methylation, acetylation or histone modifications, which appears to occur at higher frequencies for miRs (Goldberg et al 2007, Morales et al 2017) and influences the subsequent cancer phenotype (Scott et al 2006). MiRs can also exert epigenetic effects themselves through the modulation of histone methyltransferase, enhancer of zeste homolog 2 (EZH2). (Varambally et al 2008). MiRs are located at genetically fragile sites, therefore any mutation or alteration of these sequences will attenuate their expression (Calin et al 2004), such as copy number mutation in around 15% of cancers (Zhang et al 2006). Interestingly, there is miR specific single nucleotide polymorphism (miRSNP) which results in a loss of specificity or decreased affinity for their target MREs (Wilk et al 2018).

Some early work has been done to use miRs as a molecular biomarker in serum and blood samples (Zheng et al 2013). More interest as a likely biomarker is shown in exosomal miRs (An et al 2015) as their concentrations tend to correlate with tissue samples, at least in the case of lung cancer (Zhao et al 2015). And recently, miR-27a has been identified as one of seven miRS to be downregulated in the blood plasma of patients with highly invasive breast cancer (Jurkovicova et al 2017), as well as efforts to use miRs as a mode of therapy by delivering TargomiRs, which are miR mimics (Reid et al 2016). Both approaches have yet to be proven useful.

3.1.5 MiRs Involved in Epithelial to Mesenchymal Transition

Many miRs have already been implicated in EMT, metastasis, chemoresistance, stemness and migration/invasion such as with miR-10b, miR-19a/b, miR-21, miR-27a/b, miR-29, miR-143, miR-182, miR-183, miR-221, miR-222, miR-520 and let-7. Conversely, repression of this phenotype is observed with the upregulation or expression of miR-15b, miR-16, miR-20a/b, miR-31, miR-126, miR-141, miR-146a/b, miR-200a/b/c, miR-205 and miR-429 (Krutovskikh et al 2010). Let-7 is also known as a master regulator of self renewal and

seeding ability, one of the many ways cells can gain cancer stem cell phenotypes (Yu et al 2007), while the miR 200 family is very important for EMT transition (Burk et al 2008).

The Notch, Wnt and TGF-β pathways are canonical pathways towards EMT progression. Within those three pathways, there are 30 miRs that interact with all pathways. These miRs had eight common target genes between Wnt and TGF-β pathways: SMAD2, SMAD 3, SMAD4, Rho associated coiled-coil containing protein kinase 2 (ROCK2), ROHA, MYC, Protein Phosphatase 2 Scaffold Subunit Aalpha (PPP2R1A), Protein Phosphatase 2 Scaffold Subunit Abeta (PPP2R1B), five common genes between NOTCH, WNT, KEGG: C-terminal-binding protein 1 (CTBP1), C-terminal-binding protein 2 (CTBP2), Dishevelled segment polarity protein 2 (DVL2), Dishevelled segment polarity protein 3 (DVL3), and Presenilin-1 (PSEN1). And most significantly to our own research is that EP300 and CBP are shared between TGF-β, Notch, Wnt, and KEGG pathways (Zoni et al 2015). OncomiRs are miRs, which are overexpressed in cancers and can be attractive targets but they are offseted by challenges of systemic versus targeted delivery. Numerous examples of such miRs exist in the context of breast cancer (Helleman et al 2010, van Schooneveld et al 2015).

3.1.6 MiRs Involved in Chemoresistance

In terms of chemoresistance in breast cancer, there are many well known miRs involved. While miRs can exert control on ER-α, there is evidence of aberrant miR expression as a result of ER-α signalling in ER+ subtype of breast cancer (Howard et al 2017). This becomes more relevant when looking at resistance to tamoxifen, a common therapeutic treatment for this subtype. A number of miRs have been associated with this: overexpression of miR-101, miR-221/222, miR-301, and miRNAs- microRNA cluster on chromosome 19 (C19MC) (Sachdeva et al 2011, Shi et al 2011), and in downregulation in miR-15a, miR-16, miR-214, miR-320, miR-342, miR-451, miR-873, miRNA-375, miR-378a-3p, and miR-574-3p (Cui et al 2015, Cittelly et al 2010, Lu et al 2015,Liu et al 2016, Yu et al 2015, Ward et al 2012, Ikeda et al 2015, Ujihira et al 2015). Finally, there are also reports of trastuzumab resistance, a HER2 targeting therapy. Through the upregulation of miRs-21,221 and 375 was also observed (Gong et al 2011, Dall et al 2015, De Mattos-Arruda et al 2015, Ye et al 2014). Another common platinum based agent, cisplatin, resistance to which was associated with an upregulation in miR-345 and miR-7. And resensitised by upregulating miR-302b (Cataldo et al 2016, Pogribny et al 2010). Our labs past work, along with others has showed that paclitaxel resistance was associated with the downregulation of miRs-34a, miR-100 and mIR-30c. This resistance was reversed by upregulation of miR-139-3p (Zhang et al 2016,Yang et al 2015,Zhou et al 2010, Bockhorn et al 2013, Wu et al 2014). Downregulation of miR-505, miR-128, miR-145, resulted in doxorubicin resistance, another common chemotherapeutic

agent (Gao et al 2016, Yamamoto et al 2011, Zhu et al 2013). MiRs such as miR-663, miR-181a and miR-106b subsequently resensitise the cancer cells(Hu et al 2013, Zhu et al 2013, Zhou et al 2014).

Given that there is a growing amount of evidence for miRs function in cancer progression and survival through the gain of resistance traits. There is potential in their usage as a mode of therapy by attenuating tumorigenic signalling through the use of mimics (Badere et al 2010). Other possibilities exist, to compete for the MERs through the use of oligonucleotides, locked nucleic acids antisense oligonucleotides, miR sponges, multiple-target anti-miRNA antisense oligo-deoxyribonucleotides (MTg-AMOs), miRNA-masking and nanoparticles (Esau et al 2008, Elmen et al 2008, Krützfeldt et al 2005, Majid et al 2014).

3.1.7 MiR-25

Background

MiR-25 is part of the mIR-106b-25 cluster, which also includes miR-93 and miR-106. These miRs are on intron 13 of the Minichromosome Maintenance Complex Component 7 (MCM7) gene which is located on a 515-bp region of chromosome 7q22 (Petrocca et al 2008). This region is also regulated by MCM7. MCM7 is a frequently amplified gene in gastric and pancreatic cancers, and is associated with worse prognosis. MCM7 is activated by E2F1, a transcription factor that controls cells switching from G1-S phase. G1-S phase regulates the expression of the miR cluster located on the same region (Petrocca et al 2008). It is unclear whether it is controlling the whole transcript or interacting with the promoter region of the miRs as well. Both MCM7 and the cluster are induced by E2F1 and E2F3 transcription factors which are then upregulated by MYC (Bueno et al 2010). There were also studies on bromodomain-containing protein 4 (BRD4) which is a transcriptional activator along with MYC (Mertz et al 2011).

MiR-25 dysregulation has been shown in breast, colorectal, endometrial, oesophageal, gastric, liver, brain, lung, ovarian, prostate and renal cancers (Chen et al 2018, Li et al 2013, Zhao et al 2012, Kan et al 2009, Tamilzhalagan et al 2017, Suh et al 2012, Li et al 2009, Sardo et al 2017, Zhang et al 2012, Poliseno et al 2010, Boguslawska et al 2018). In breast cancer, the cluster was upregulated by TGF-β and c JUN pathways independent of MCM7, which shows there are other mechanisms for its activation (Gong et al 2015). Another interesting point is that miR-25 has been upregulated under hypoxic conditions, independently of HIF-1α (Wu et al 2017). MIR-25 upregulation was shown to promote the proliferation of triple negative breast cancer through BTG anti-proliferation factor 2 (BTG2) (Chen et al 2018), bypassing doxorubicin induced senescence, increasing motility and invasion (Zhou et al

2014), and regulating multidrug resistance through an ABC transporter independent manner (Hu et al 2016). It also regulates autophagy associated with chemoresistance (Wang et al 2014).

Role in Apoptosis

In apoptosis, mIR-106b-25 cluster is associated with the TGF-β pathway activation as miR-106b and miR-93 both silence p21, while miR-25 silences Bcl-2-like protein 11 (BIM) (Petrocca et al 2008). BIM silencing can inhibit TGF-β mediated apoptosis, conferring survival benefits to the cancer cells. Furthermore, when this cluster is knocked down with miR-17-92, it resulted in a more severe phenotype in mice experiments (Ventura et al 2008). This avoidance of apoptosis was shown to be due to miR-25 targeting of death receptor 4 (DR4), gaining protection from Tumour necrosis factor (TNF) related apoptosis inducing ligand (TRAIL) (Razumilava et al 2012). As well as having a link with BCL2 through targeting the modulator of apoptosis 1 (MOAP1), which is its binding partner in lung cancer (Wu et al 2015).

Role in Proliferation

Proliferation and cell cycle progression is mediated by the p53 activation of p21 which in turn controls the cyclin dependent kinases. miR-25 inhibition has been proven to directly increase p53 levels and promote apoptosis and cell cycle arrest (Kumat et al 2011). It does potentially alongside a p53 co activator lysine acetyltransferase 2 (KAT2B), which has been demonstrated in myeloma cells (Pichiorri et al 2008). A similar effect on p53 and the mTOR was demonstrated in glioblastoma where it was negatively regulated by MDM2 and TSC complex subunit 1 (TSC1) (Suh et al 2012). It also has an effect on cyclin dependent kinase inhibitor 1c (CDKN1C) (Zhang et al 2015). Furthermore, there has been a demonstrated effect on miR-25 associated proliferation through suppression of BTG2, a tumour suppressor protein in triple negative breast cancer(Chen et al 2018).

Role in Epithelial to Mesenchymal Transition

miR-25 is also heavily involved in EMT. For breast cancer it was demonstrated that the cluster directly interacted with the TGF-β pathway and inactivated SMAD7, which resulted in transforming growth factor beta receptor I (TGFBR1) upregulation (Smith et al 2012). It has also been shown in other forms of cancers and through different modes of action, such as activation of PTEN in oesophageal cancer (Zhang et al 2018), enhancement of SNAI1 expression in lung cancer (Savita et al 2013), inhibition of Rho GDP dissociation inhibitor

alpha (RhoGDI1) and the promotion of migration in hepatocellular carcinoma (Wang et al 2015).

Role in Promoting Stem Cells

Another thing that miR-25 regulates is cancer stem cell populations. The previously mentioned effect on SMAD7, also positively selects for CD44+ populations in gastric cancers (Yu et al 2014), and positively upregulates the WNT and β-catenin pathway through inhibition of GSK3β and selecting for the CD44+ cells (Zhang et al 2018). Furthermore, miR-25 upregulation seems to protect the CD133+ stem population from TRAIL induced apoptosis in liver cancer (Feng et al 2016), and from being associated with a more aggressive phenotype with low expression of miR-25 in colorectal cancer (Zoni et al 2015). Lastly, since the metastatic niche is associated with cancer stem cells, miR-25 has been associated with formation of this niche through mIR-25 exosomal signalling to the surrounding endothelium of colorectal cancer (Zeng et al 2018).

Role in Drug Resistance

These survival mechanisms also came with drug resistance. Whether mirR-25 is up (Zhou et al 2014, Hu et al 2016) or downregulated (Wang et al 2015), results in drug resistance to doxorubicin and epirubicin (Zhou et al 2014, Wang et al 2015, Hu et al 2016). Furthermore, high levels of miR-25 were associated with higher KRAS expression and increased docetaxel resistance in ovarian cancer (Rodriguez-Aguayo et al 2017). Additionally, these high levels of miR-25 result in resistance to cisplatin through the downregulation of FOXO3a in gastric cancers (He et al 2017). Its demonstrated role in drug resistance and detection in the patient serum of suspected aggressive cases suggests it is a good biomarker (Hesari et al 2018).

3.1.8 MiR-27a

Background

mIR-27 has two homologous genes, miR-27a and miR-27b. It clusters near miR-23 and miR-24 on chromosome 19p13.13 (Liang et al 2014). This miR has been shown to be dysregulated in many cancers, including those from breast, lung, prostate, cervix, stomach, and ovaries among many others, reviewed in Li et al (2019) and Zhang et al (2019). miR-27 Shows a variety of effects depending on tumour type, acting both to promote and inhibit tumorigenesis. It has also been widely demonstrated that it functions in tumorigenesis, proliferation, apoptosis, invasion, migration, angiogenesis, as well as drug resistance (Lin et

al 2009, Urbich et al 2012 and Veliceasa et al 2015), some of which seem to be dependent on the form of miR-27a expressed (Ma et al 2019). It has also been proposed as a prognostic marker for breast cancer progression and patient survival, as low expression of mIR-27a correlated with worse disease prognosis (Tang et al 2012, Li et al 2019).

Role in Tumourigenesis

Much like its effects on EMT, mir-27a has heterogenic effects on tumorigenesis. It's an inhibitor of growth in breast cancer through expression of transmembrane protein 170b (Li et al 2018). Its repression in xenograft models of breast cancer has been shown to be oncogenic, while its knockout in xenograft models decreased tumour growth (Hannafon et al 2019). However, it is involved in the initial tumour formation stages of mammary carcinoma through promotion of neovascularisation and increasing the p44/42 (MAPK) signalling involved in EMT by upregulating Sprouty 2 (SPRY2) (Li et al 2013). It also participates in targeting AKT in triple negative breast cancer to promote tumorigenesis (Wu et al 2017). Furthermore, knockout models of miR-23a and miR-27a showed their oncogenic role in the breast cancer cell line MCF7, decreasing proliferation, migration and invasion and clone formation, as well as reducing tumour growth *in vivo* (Hannafon et al 2019). What cements its role in tumorigenesis is that most primary tumours have a mutation in p53, a canonical tumour suppressor gene. MiR-27a, along with EGFR, are confirmed targets of p53, which is are upregulated upon introduction of a p53 mutation (Wang et al 2013). EGFR is also known to be inhibited by miR-27a in renal cell carcinoma (Li et al 2016). It represses VEGF upon its overexpression in ovarian cancer (Lai et al 2013) and has a controversial role in colorectal cancer, as it has been reported to both overexpressed in colorectal tumours and therefore oncogenic (Chintharlapalli et al 2009) and of very low expression in both human colorectal tumour tissue and colorectal cell lines such as HCT116 (Bao et al 2014).

Role in Epithelial to Mesenchymal Transition

Its functions in EMT progression, invasion and migration are widely associated with upregulation of oncogenic transcription factors. These are known to be regulated by an atypical ubiquitin E3 ligase complex Skp1-Pam-Fbxo45 (SPFFbxo45), as F-Box Protein 45 (Fbxo45) can be downregulated by miR-27a, thereby promoting EMT transcription factors (Xu et al 2015). In oral squamous carcinoma, the initiation of SNAI1/SNAI2 is thorough downregulation of miR-27a target yes-associated protein 1 (YAP1) (Zeng et al 2016), and it was also found to target tumour suppressor KRAS Proto-Oncogene (KRAS) (Jiang et al 2015). Similar to breast and gastric cancer, miR-27a increases proliferation and metastasis

by suppressing PH Domain And Leucine Rich Repeat Protein Phosphatase 2 (PHLPP2) and activation of AKT/GSK3β pathways (Ding et al 2017).

Well known EMT and migration pathways are also implicated with miR-27a upregulation, such as MEK/ERK through BTG Anti-Proliferation Factor 1 (BTG1) modulation (Bao et al 2014, Su et al 2019) and the WNT/β-catenin pathway through downregulation of Forkhead Bbox O1 (FOXO1) (Zhang et al 2019). This control on WNT/β-catenin pathways seems to be exerted through modulation of Secreted frizzled related protein 1 (SFRP1) in gastric cancer models (Wu et al 2017). Furthermore, another tumour suppressor, Transcription factor AP-2 β (AP-2β), is known to be targeted by miR-27, and downregulates canonical EMT transcription factors SNAI1 and SNAI2 (Yang et al 2018). This is also the case for breast cancer, where FOXO1 directly correlated to miR-27 (Liu et al 2012) and promoting EMT, invasion and metastasis through targeting of F-Box and WD repeat domain containing 7 (FBXW7), leading to activation of the same genes (Jiang et al 2018), as well as negatively regulating ERα receptor in ER+ breast cancer through Zinc finger and BTB domain containing 10 (ZBTB10) (Li et al 2010).

However, as mentioned before, there is a heterogenic function for miR-27a, as is seen from a study on hepatocellular carcinoma that showed promotion of metastasis through the upregulation of TWIST1, and BCL2 (Zhao et al 2015, Zhao et al 2016). In prostate cancer, miR27 induced metastasis through downstream targets of COUP transcription factor 2 (COUP-TFII), such as FOXM1 (Li et al 2016). Furthermore, there is evidence of promotion of metastatic behaviour in osteosarcoma (Salah et al 2015), which might be relevant to breast cancer, as the bones are one of the most common sites of metastasis from breast cancer.

Role in Proliferation and Apoptosis

There are studies of breast cancer, showing avoidance of cell cycle arrest by Myelin transcription factor 1 (Myt1) and previously mentioned ZBTB10 (Martens-Talcott et al 2007). Previous findings also showed miR-27a to be highly overexpressed in breast cancer and promoted proliferation through FOXO1 (Guttilla et al 2009). Other prevention of cell proliferation is seen through downregulation of WNT/β-catenin pathway and the tumour suppressor KRAS (Jiang et al 2015, Li et al 2018). The mechanism of this cell cycle arrest is thorough targeting cell cycle checkpoint inhibitors like cyclin D1 (CCND1), Cyclin dependent kinase 2 (CDK2), and upregulation of Cyclin-dependent kinase inhibitor 1B ($p27^{Kip1}$) (Li et al 2016). Similar effects on p21 and Cyclin-dependent kinase 1 (CDK1) were seen in gastric cancer (Zhao et al 2011), while in colorectal cancer, miR-27 modulates migration, proliferation and apoptosis through targeting effectors such as Sphingosine-1-Phosphate Phosphatase 1 (SGPP1) and SMAD2 (Bao et al 2014, Su et al 2019).

Role in Stemness and Angiogenesis

MiR-27a has a direct link to promoting stemness in multiple cancers. Multiple studies have shown that its upregulation is related to promotion of CSC subpopulations with expression of markers such as CD44, ALDH and CD133 (Li et al 2010, Luo et al 2018, Ueda et al 2020). It also has some function in regulating pluripotency of embryonal carcinoma cells (Fuchs et al 2014). It was observed that the upregulation of VEGF by breast cancer stem cells is through miR-27a signalling (Tang et al 2014). Both miR-27a and miR-23a recruit fibroblasts on the tumour endothelium and turn them into tumour associated fibroblasts (Wang et al 2018), as well as recruitment of lymphocytes such as CD8+ T cells, tumour associated macrophages (Chandran et al 2014, Ma et al 2016). Which suggests a role for these miRs in regulating the tumour microenvironment. Additionally, these miRs can suppress the immune response through the TGF-β pathway. Mainly by intervening in the B cell development and dendritic cell differentiation steps (Kong et al 2010, Min et al 2012).

Role in Drug Resistance

In terms of drug resistance, as previously mentioned there are multiple drug resistance genes involved in cancer such as ATP-binding cassette sub-family B member 1 (ABCB1) and ABCG2. MiR-27a seems to directly upregulate ABCB1 (Li et al 2010, Zhang et al 2011). Overexpression of ABCB1 leads to doxorubicin resistance in leukaemia (Feng et al 2011). Furthermore, another target of miR-27a, RUNX1 was responsible for drug resistance in bladder cancer (Deng et al 2015). It is also associated with chemoresistance in oesophageal cancer, development of many neoplasms (Tanaka et al 2015, Zou et al 2015, Liu et al 2016). And seems to act differently between tumour types as downregulation of miR-27a results in resistance to vincristine, Adriamycin and 5-fluorouracil through expression of ABCB1, activity of cyclin D1 and upregulation of p21 (Zhao et al 2011). There are some observations on adaptive response to cancer therapy, as it was seen that miR-27a levels increased as a response to cisplatin therapy, which resulted in resistance through directly targeting Raf kinase inhibitor protein (RKIP) (Li,Wang et al 2018, Li,Yu et al 2018). This response to miR-27a has shown it to be a viable target in breast cancer, as its downregulation can increase sensitivity to cisplatin, 5-fluorouracil, doxorubicin and paclitaxel (Zhou et al 2016, Ueda et al 2020).

3.1.9 MiR-23a

Background

As previously mentioned, miR-23a is found on chromosome 19, and clusters near miR-27a. It also functions as an oncomiR, and shaers up to 15% of miR-27a's targets (Chou et al 2016). Like miR-27a it is dysregulated in a number of cancers : breast, prostate, lung, gastrointestinal, gliomas (He et al 2012, Jin et al 2013, Pellegrino et al 2013, Ono et al 2014, An et al 2015, Huang et al 2015, Zhang et al 2011, Geng et al 2012). Notably, solid tumours of genitourinary origin seem to consistently have miR-23a downregulated (Cai et al 2015, Aghaee-Baakhtiari et al 2015). It also shares its dualistic role as both a promoter and inhibitor of proliferation, migration, invasion, metastasis, EMT, chemoresistance and cancer stem cell populations (Vaksman et al 2014, Tian et al 2013, Jin et al 2013, Qi et al 2015, Chen et al 2014, Zhou et al 2011, Wang et al 2010). MiR-23a is significant in clinical diagnosis, its expression has direct correlation with the stage, tumour size and depth of invasion, as well as presence of lymph node metastasis (Ma et al 2017, Qu et al 2015,Su et al 2018). Leading to it being used as a biomarker in patient serum (Wu et al 2012, Yong et al 2013, Frampton et al 2015). MiR-23 is largely regulated by p53 (Wang et al 2013,Huang et al 2015), Activator protein 1 (AP-1) (Zheng et al 2014), c-Myc (Poyyakkara et al 2018, Gao et al 2009) and NF-κB (Rathore et al 2012), which bind to its promoter region. However, it is also known to be regulated by epigenetic factors such as methylation (Xishan et al 2014, He et al 2015). In breast cancer, the suppression of miR-23a, which was found to be through lncRNA GAS5 via a sponge mechanism, initiated metastasis and was associated with higher tumour grade and poorer prognosis (Gu et al 2018).

Role in Tumourigenesis

MiR-23a is known to promote carcinogenesis in hepatocellular carcinoma. Its expression downregulates two proteins: Glucose 6 phosphatase (G6PC) and peroxisome proliferator activated receptor γ coactivator 1 α (PGC-1a) involved in the gluconeogenesis pathway (Wang et al 2012). Furthermore, there is evidence of miR-23a affecting the tumour microenvironment through tumour associated macrophages, such as the case in breast cancer, where miR-23a expression counteracts a immunosuppressed microenvironment. MiR-23a activates proinflammatory cytokines in the tumour associated macrophages through Tumor necrosis factor, alpha-induced protein 3 (A20) (Ma et al 2016), whereas in advanced lung cancer, high miR-23a exerted control on cytotoxic T cells by blocking granzyme B expression, leading to immunosuppression (Lin et al 2014).

Role in Proliferation

MiR-23a controls a plethora of genes involved in cell fate determination. In general, its regulation in cancer causes tumour specific effects on cell proliferation. One of its targets is Janus Kinase 1 (JAK1), which can lead to proliferative transformed cells in leukemia when miR-23a is downregulated (Su et al 2016). Another target is Interleukin 6 receptor (ILR6), which prevents activation of MAPK (Aghaee-Bakhtiari et al 2015). Overexpression of miR-23a resulted in cell senescence, preventing proliferation and promoted apoptosis. In pancreatic cancer cells, miR-23a induces expression of Polo-like kinase 1 (PLK-1), which promotes cell fate determinants like BCL2, cyclin B1, and BAX as well as other phenotypic changes like E-cadherin expression (Chen et al 2018). The same effect is achieved in gastric cancer through its target ILR6 (Zhu et al 2010). In gastric adenocarcinoma and pancreatic cancer, inhibition of miR-23a leads to suppression of proliferation as its expression prevents apoptosis through Programmed cell death 4 (PDCD4) and Apoptotic protease activating factor 1 (APAF1) (Liu et al 2014, Hu et al 2017, Yong et al 2014). Some of these effects may be abrogated by targeting Metallothionein 2A (MT2A), a target of miR-23a (Liu et al 2016). In fact, in most cancers types miR-23a interacts with the 3'-UTR of apoptosis activating targets (Huang et al 2015). Some of these anti proliferative effects of miR-23a are also linked to drug resistance to cisplatin through cell cycle arrest and possible links to ABCB1 expression (Jin et al 2015).

Role in Epithelial to Mesenchymal Transition

MiR-23a is also involved in the regulation of EMT related genes. It has been shown that it affects the EMT transition through the canonical loss of E-cadherin by directly regulating it, thereby promoting the Transforming growth factor β 1 (TGF-β1) pathway leading to cell invasion (Ma et al 2017). There are similar observations made in lung and neuroblastomas (Cao et al 2012, Cheng et al 2014). Lung cancer was also associated with the mesenchymal phenotype through increasing exosome expression of miR-23a (Hsu et al 2017).

There is a potential link to this process with Epithelial splicing regulatory protein 1 (ESPRP1) in pancreatic cancer (Wu et al 2017), and other known targets such as X-linked inhibitor of apoptosis protein (XIAP) (Chen et al 2017), MTSS I-BAR domain containing 1 (MTSS1) (Tang et al 2012), Insulin receptor substrate 1 (IRS-1) (Cao et al 2014), SPRY2 (Li et al 2013) and PTEN (Tian et al 2015). With proliferation, there is also a cancer dependent effect, and with its upregulation, its suppression can also lead to progression of EMT. In oesophageal cancer, miR-23a acts as a repressor and promote E-cadherin expression and downregulates markers of EMT such as vimentin, α-SMA by directly affecting SMAD3

(Liu et al 2016). A similar trend is seen in prostate and lung cancer, where miR-23a targets Lim kinase-1 (LIMK1), which prevents cell migration from occurring by suppressing the formation of actin stress fibres, which are used during contraction of the cell to induce movement (Cai et al 2015, Chien et al 2017).

Role in Drug Resistance and Stemness

With other miRs mentioned, it has some effects on the drug sensitivity and response to chemotherapeutic agents. In doxorubicin treatment, miR-23a can be both suppressed and induced, depending on the cancer type (Rizzo et al 2017). Imatinib is known to promote expression of miR-23a and its downstream effects on induction of apoptosis, therefore sensitising cells to the therapy, as seen in leukaemia (Farhadi et al 2016). This is a response to therapy in colon cancer, which opposes to the reduction in sensitivity to 5-fluorouracil caused by miR-23a expression (Shang et al 2014). It was shown that ABCB1 is one of the targets of miR-23a, and therefore is one of the reasons sensitivity is decreased as it modulates drug efflux (Li et al 2015). For breast cancer, cisplatin resistance was associated with the expression of oncogene CDC28 Protein Kinase Regulatory Subunit 1B (CKS1B), which regulated miR-23a expression by suppression of histone Lysine demethylase 4A (KDM4A) (Black et al 2016). There is also some evidence of miR-23a linked to cancer stem cells, as a high proportion of lung cancer stem cells were found to overexpress miR-23, which was correlated to erlotinib resistance (Han et al 2017). Therefore, there are suggestions that mechanisms of resistance and stemness could be linked through miR-23a expression.

3.2 Analysis of miRs 23a,25,27a

3.2.1 Background

Since this work has been undertaken at the start of the project, much of the work earlier mentioned has not yet been published (up to 2015). Therefore, we were working under assumptions drawn from data available at that time, as well as our published works. It is evident that due to their mechanism of action, miRs are able to silence and promote genes based on their specificity for the mRNA transcripts (MREs). Much of the earlier work cited, shows all three miRs to not only be aberrantly expressed in various cancers, but have cancer context dependent effects on migration, invasion, proliferation, tumorigenesis, stemness and chemoresistance.

Most of this thesis will be around our main target protein EP300, described in later chapters. **Figure 3.1** is a visual representation of a preliminary pathway for miR-25, miR-23a

and miR-27a. It explains how they repress or inhibit, through direct or indirect interaction with EP300 and E-cadherin to exert their influence on the phenotype, as well as properties such as EMT, stemness, migration and invasion. This chapter will show some preliminary results regarding miR expression and gene regulation in a panel of breast cancer cell lines MTMEC, MCF7 and BT474.

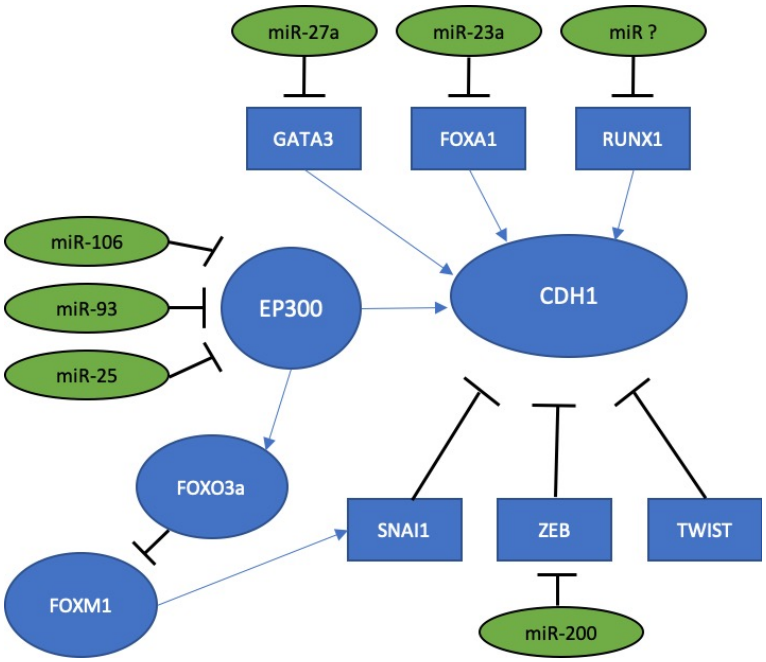

Fig. 3.1 Visual representation of the miRs mechanism of action. MiR-25, part of the miR-106b 25 cluster, actively repress EP300 which is the master regulator gene of CDH1, among other transcription factors like FOXO3a, while miR-27a and miR-23a exert their influence on CDH1 through direct interaction with GATA3 and FOXA1.

3.2.2 Hypothesis

Following these findings, we want to expand on the previous research done by our lab into the axis of activation of EMT and enrichment for the breast cancer stem cell population through the downregulation of CDH1 via EP300 (Zhou et al 2014). Primarily, looking into the impact of miR expression profiles in a panel of breast cancer cell lines and chemotherapy resistant variants. We will also look into positive regulators involved in these pathways such as forkhead box 03a (FOXO3a), GATA3, and RUNX1 among others (Lam et al 2013).

The hypothesis is that based on their bioinformatics information derived from several previous studies and public domains, suggests that miR-23a, miR-25, and miR27a have corresponding seed sequences to the 3'-UTR of FOXO3a and FOXA1. As these are important in breast cancer survival, it is likely they might have some impact on the activation of EMT, migration/invasion and chemoresistance.

3.2.3 Aim

1. 1. Elucidate the mechanism of action between miR-25 and FOXO3a and other genes of interest. We expect that miR-25 would have an effect on FOXO3a mRNA levels due to matched sequences to its 3'-UTR region. A down regulation in FOXO3a would decrease CDH1 levels through the FOXM1 -> SNAI1 axis and have an impact on apoptosis, DNA damage response and cancer stem cells.

    - RTqPCR of genes related to cancer stem cells and invasion, hypoxia and DNA damage response in the MTMEC cell line.
    - Western blot for protein levels of FOXO3a to show upregulation or inhibition of translation of FOXO3a.
    - Extend above two points to breast cancer cell lines MCF7, T47D, CAL51, MDA-MB-231 and Hs578T.

2. Elucidate the response mechanism of doxorubicin, paclitaxel and lapatinib on endogenous levels of miR-23a, miR-25 and miR-27a. As all miRs have been shown to have an effect on drug resistance on sensitivity, we expect miR expression to be upregulated or downregulated.

    - RTqPCR of miRs 23a, miR-25 an miR-27a in the MTMEC and BT474 breast cancer cell lines.
    - Extend above point to breast cancer cell line MCF7.

3.2.4 Results

MiR-25 Regulates EP300 and FOXO3a Expression

To discover the implication of miR-23a, mirR-25 and miR-27a in regulating FOXO3a, we generated a MTMEC cell line with overexpressed miR-23a (MTMEC-miR-23a), mirR-25 (MTMEC-miR-25) and miR-27a (MTMEC-miR-27a). **(Figures 3.2a)** shows the RTqPCR results for the miR expression in overexpressing cell lines relative to the wild type MTMEC cell line with empty vector control (MTMEC). Data for MTMEC-miR-23a and MTMEC-miR-27a shows no significance due to high variation between values in sample size (n=3). Data for miR-25 overexpression (MTMEC-miR-25) on MTMECs, shows a 5 fold increase ($p<0.01$) compared to MTMEC empty vector control (Figure3.2b). Following from this we decided to check whether the MTMEC cell line overexpressing miR-25 (MTMEC-miR-25) has any effect on the protein levels of FOXO3a using western blotting (**Figure 3.2c**). It shows the expression levels of FOXO3a to be inversely correlated to the expression of miR-25, while the control gene remains unchanged, showing good sample quality.

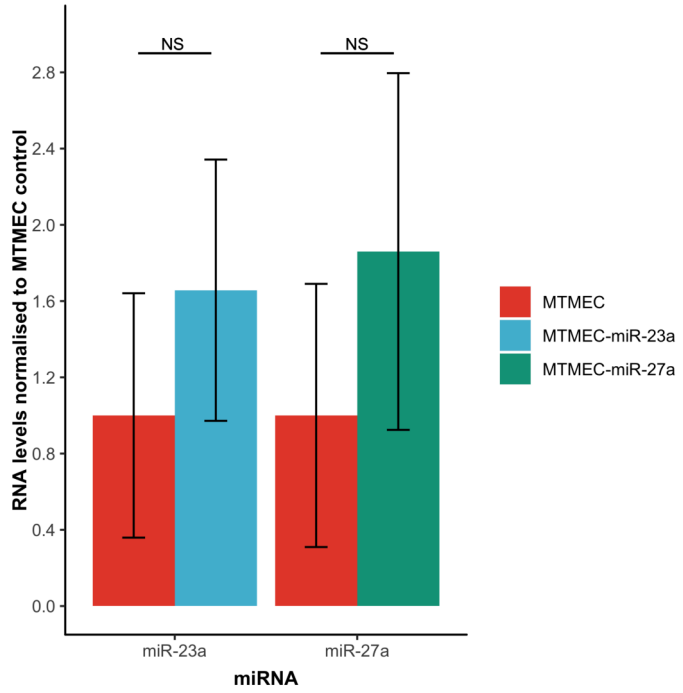
NS
NS
RNA levels normalised to MTMEC control
2.8
2.4
2.0
1.6
1.2
0.8
0.4
0.0
miR-23a
miR-27a
miRNA
MTMEC
MTMEC-miR-23a
MTMEC-miR-27a

(a)

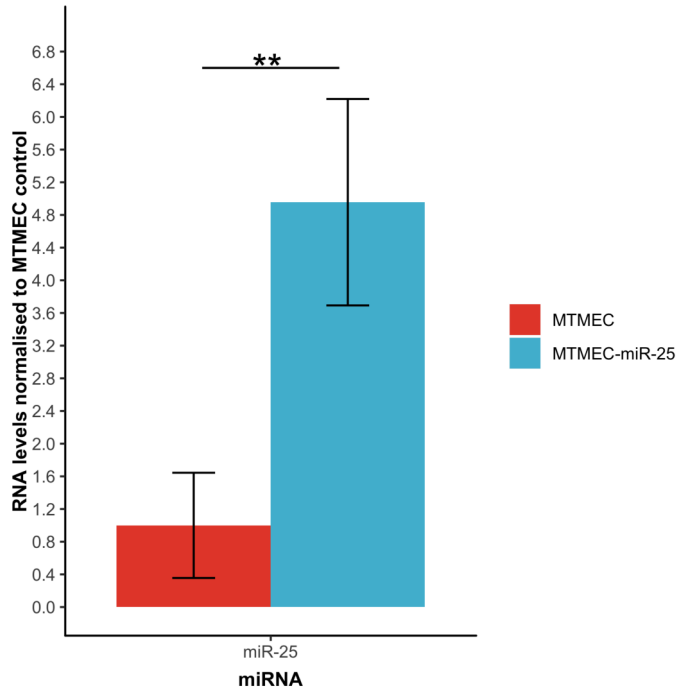
**
RNA levels normalised to MTMEC control
6.8
6.4
6.0
5.6
5.2
4.8
4.4
4.0
3.6
3.2
2.8
2.4
2.0
1.6
1.2
0.8
0.4
0.0
miR-25
miRNA
MTMEC
MTMEC-miR-25

(b)

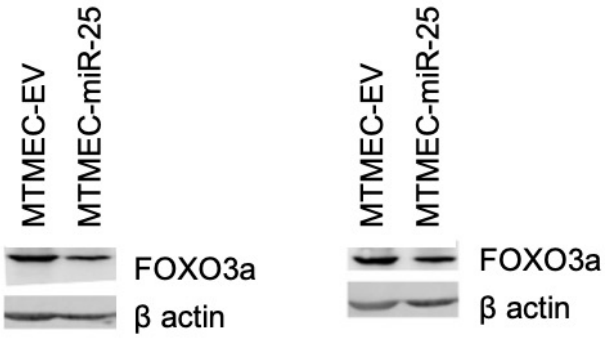

(c)

Fig. 3.2 Overexpression of miR-23a, miR-25 and miR-27a in an MTMEC breast cancer cell line. An MTMEC cell line was used to generate three separate overexpressions (MTMEC-miR-23a), (MTMEC-miR-25) and (MTMEC-miR-27a).The mRNA levels of each miR was detected in MTMEC (Control), MTMECs with miR-25 overexpression (MTMEC-miR-25), MTMECs with miR-23a overexpression (MTMEC-miR-23a) and), MTMECs with miR-27a overexpression (MTMEC-miR-27a) by RTqPCR analysis. Gene expression of each miR overexpression was demonstrated relative to the MTMEC control (wild type and empty vector control transfected cells). Gene expression was normalised to the U6 housekeeping gene. Panels show mRNA levels of (A) miR-23a and miR-27a (B) miR-25 and (C) shows two repeats of Western blotting analysis for the expression of FOXO3a of MTMEC breast cancer cells with Control and miR-25 overexpressing vectors, β-actin was used as an internal control. Data are shown as normalised to the control vector. The mean + SD of n=3 independent experiments is shown, NS Non-Significant, * $p \leq 0.05$, **$p \leq 0.01$, *** $P \leq 0.001$,****$p \leq 0.0001$ (ordinary one-way ANOVA following Dunnett's multiple comparison test).

MIR Expression in Breast Cancer Cell Lines

To discover if the expression of miR-23a, mirR-25 and miR-27a is feasible to explore in our further experiments, we compared the basal expression levels in a panel of breast cancer cell lines: MCF7, T47D, CAL-51, MDA-MB-231 and HS578T **(Figures 3.3)**. In **Figure 3.3a**, we compare MCF7 to the CAL-51 cell line. When comparing both cell lines, MiR-23a shows no significant difference, miR25 shows a fold increase of 1.6 ($p<0.05$), while miR-27a shows a fold increase of 1.7 ($p<0.05$). When only looking at CAL-51, miR-23a is the least expressed miR. Mir-27a is 1.7 fold times higher than miR-23a ($p<0.01$), while miR-25 is 0.6 fold higher than miR-23a ($p<0.05$). When comparing miR-23 and miR-25, there is no significant difference between their expression. In **Figure 3.3b**, we compare MCF7 to the MDA-MB-231 cell line. The expression of miR-23a is 2.1 fold higher ($p<0.05$) miR-25 is 0.4 fold lower ($p<0.05$) and 2 fold higher in miR-27a ($p<0.01$) in MDA-MB-231. When only looking at MDA-MB-231, we see miR-23a is 1.6 fold higher than miR-25 ($p<0.01$) and miR-27a is also 1.6 fold higher ($p<0.01$), with no significant difference shown between the expression of miR-23a and miR-27a. In **Figure 3.3c** we compare MCF7 to the HS578T cell line. The expression of miR-23a is 3.1 fold higher ($p<0.01$), miR-25 shows no significant difference and miR-27a is 6 fold higher ($p<0.001$). When comparing to the highest expressed miR-27a, it is 3 fold higher expressed than miR-23a ($p<0.01$), miR-27a is also 6 fold higher expressed than miR-25 ($p<0.001$), while miR-23a is 3 fold higher than miR-25 ($p<0.01$). In **Figure 3.3d**, we compare MCF7 to the T47D cell line. The expression of miR-23a is decreased 0.5 fold ($p<0.05$), miR-25 is decreased 0.45 fold ($p<0.05$), while miR-27a is decreased 0.1 fold ($p<0.05$). When comparing all miRs, miR-27a is 0.4 fold higher than miR-23a ($p<0.05$), while only having a 0.2 fold difference with miR-25. The 0.2 fold difference is shown between miR-23a and miR-25 ($p<0.05$).

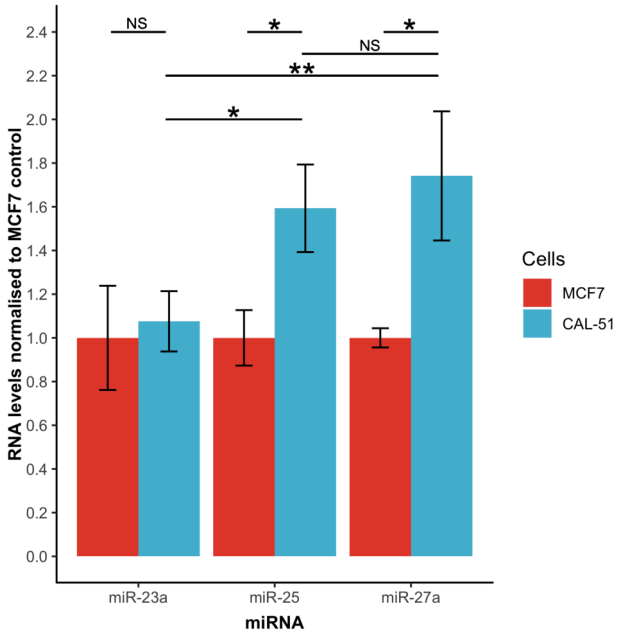
NS
*
*
NS
**
*
RNA levels normalised to MCF7 control
2.4
2.2
2.0
1.8
1.6
1.4
1.2
1.0
0.8
0.6
0.4
0.2
0.0
miR-23a
miR-25
miR-27a
miRNA
Cells
MCF7
CAL-51

(a)

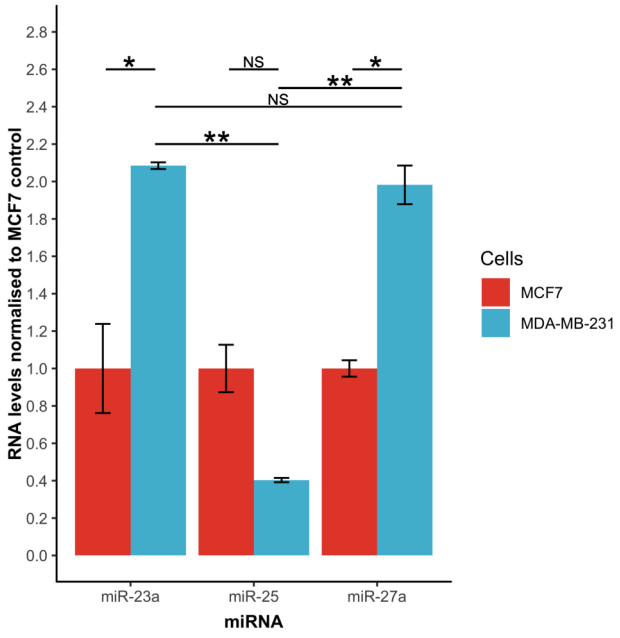
*
NS
*
**
NS
**
RNA levels normalised to MCF7 control
2.8
2.6
2.4
2.2
2.0
1.8
1.6
1.4
1.2
1.0
0.8
0.6
0.4
0.2
0.0
miR-23a
miR-25
miR-27a
miRNA
Cells
MCF7
MDA-MB-231

(b)

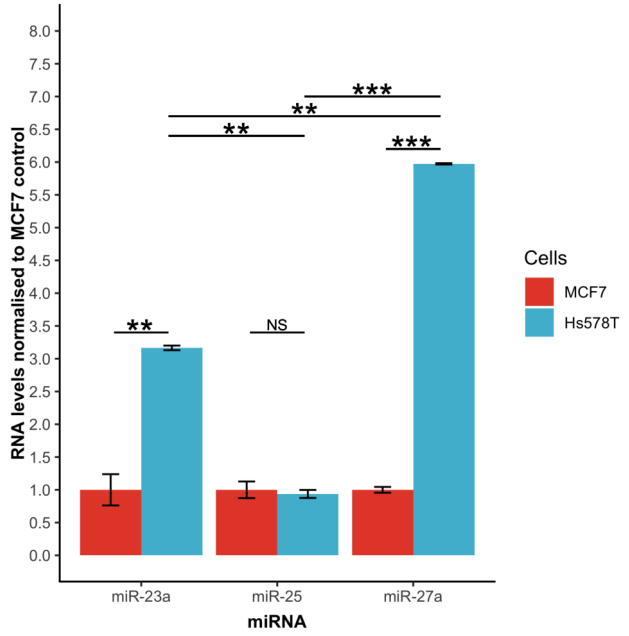

(c)

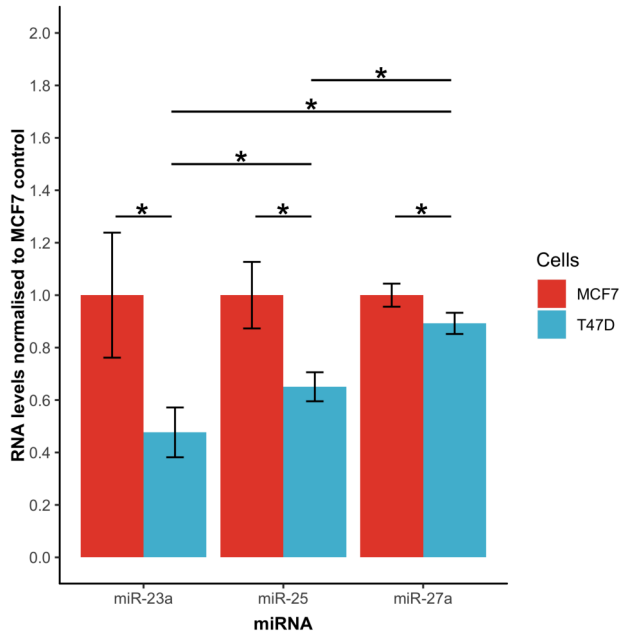

(d)

Fig. 3.3 MiR expression in 5 breast cancer cell lines. The mRNA levels were detected in MCF7, CAL-51, MDA-MB-231, Hs578T and T47D by RTqPCR analysis. Gene expression wild type cells were demonstrated relative to the respective control (MCF7 wild type). Gene expression was normalised to the RPS14 and RPLPO housekeeping genes. Panels show mRNA levels of (A) MCF7 vs CAL-51, (B) MCF7 vs MDA-MB-231, (C) MCF7 vs Hs578T and (D) MCF7 vs T47D. Data are shown as normalised to MCF7 cells. The mean + SD of n=3 independent experiments is shown, NS Non-Significant, * $p<0.05$, **$p<0.01$, *** $P<0.001$,****$p<0.0001$ (ordinary one-way ANOVA following Dunnett's multiple comparison test).

MiR-25 Effects on Downstream Targets

To see whether miR-25 has any potential to be a therapeutic target, we conducted a RTqPCR analysis (**Figure 3.4**) for the gene expression of CDH1, EP300, FOXA1, FOXO3a and GATA3. Here we can see that its effect is not significant on CDH1 and FOXA1 transcription levels, but shows 0.5 fold decrease in Forkhead Box 03a (FOX03a) ($p<0.05$), 0.5 fold decrease in GATA3 ($p<0.01$) and 0.5 fold decrease in EP300 ($p<0.01$). This is in line with our hypothesis as their seed sequences match miR-25, showing potential for miR-25 to regulate a myriad of genes for migration, invasion, EMT drug resistance and stemness.

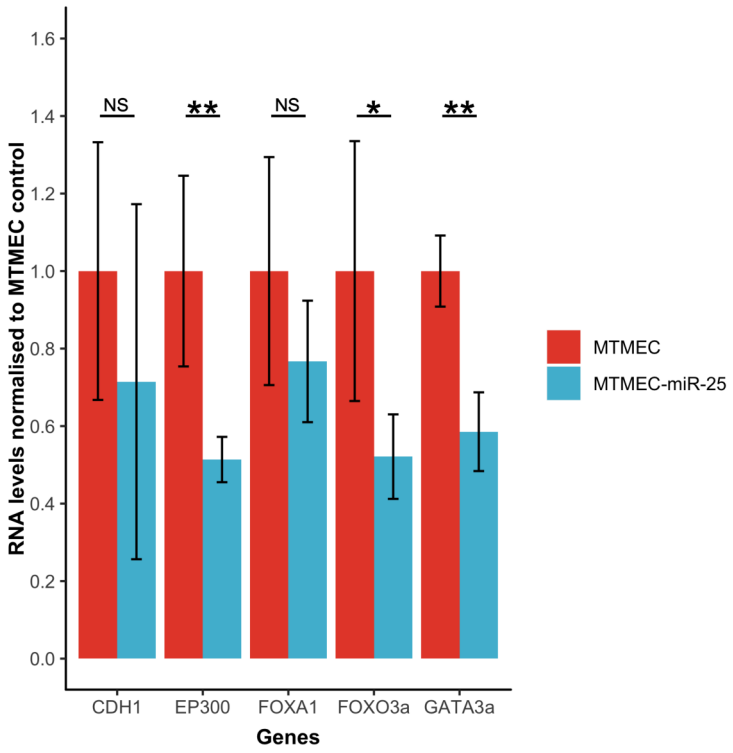

Fig. 3.4 Selected gene expression in an MTMEC breast cancer cell line as a response to miR-25 overexpression. The mRNA levels of miR-25 weres detected in MTMEC by RTqPCR analysis. Gene expression of miR-25 overexpressing MTMEC cells was demonstrated relative to the respective control (wild type and empty vector control transfected cells). Gene expression was normalised to the RPS14 and RPLPO housekeeping genes. Panels show mRNA levels of (A) miR-25. Data are shown as normalised to the control vector. The mean + SD of n=3 independent experiments is shown, NS Non-Significant, * $p\leq0.05$, ** $p\leq0.01$, *** $P\leq0.001$,**** $p\leq0.0001$ (ordinary one-way ANOVA following Dunnett's multiple comparison test).

MiR Effects on Downstream Targets in Breast Cancer Cell Line Panels

We have seen that miRs are expressed differently in our breast cancer cell line panel. Now the same panel is used to show if this influences CDH1, EP300, FOXA1, FOXO3a and GATA3. In **Figure 3.5a** we compared MCF7 to the CAL-51 cell line. Here we can see that the expression is decreased 1 fold CDH1 ($p<0.001$), 1 fold FOXOA1 ($p<0.001$), 0.7 fold FOXO3a ($p<0.05$) and 1 fold GATA 3 ($p<0.001$), while EP300 is increased 2.3 fold ($p<0.001$). In **Figure 3.5b** we compared MCF7 to the MDA-MB-231 cell line. Here we can see that the expression is decreased 1 fold CDH1 ($p<0.001$), 1 fold FOXOA1 ($p<0.001$), 0.5 fold FOXO3a ($p<0.01$) and 1 fold GATA 3 ($p<0.001$), while EP300 is increased 1.3 fold ($p<0.01$). In **Figure 3.5c** we compared MCF7 to the HS578T cell line. Here we can see that the expression is decreased 1 fold CDH1 ($p<0.001$), 1 fold decrease in FOXOA1 ($p<0.001$), FOXO3a shows non significant change, and GATA 3 has a 0.9 fold decrease ($p<0.001$), while EP300 is increased 2.3 fold ($p<0.001$). In **Figure 3.5d**, we compared MCF7 to the T47D cell line. Here we can see that the change of expression is not significant in CDH1, EP300 and GATA3, while it has a 0.5 fold decrease in FOXA1 ($p<0.001$) and a 0.6 fold in FOXO3a ($p<0.001$).

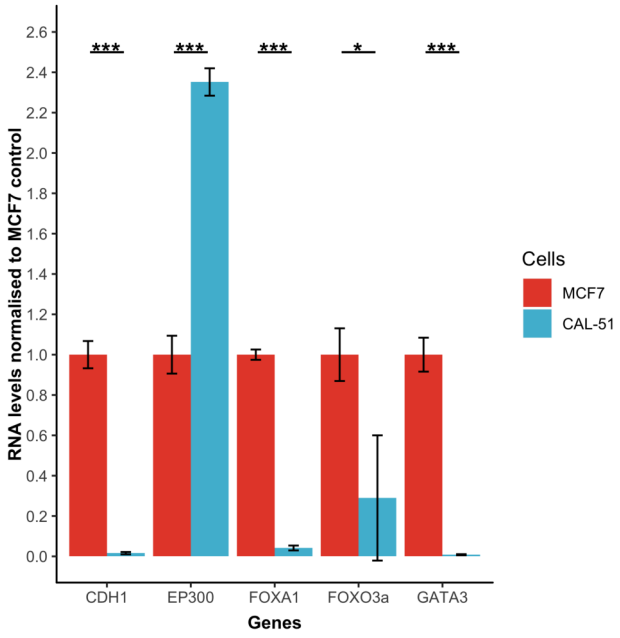
RNA levels normalised to MCF7 control
2.6
2.4
2.2
2.0
1.8
1.6
1.4
1.2
1.0
0.8
0.6
0.4
0.2
0.0
***
***
***
*
***
CDH1
EP300
FOXA1
FOXO3a
GATA3
Genes
Cells
MCF7
CAL-51

(a)

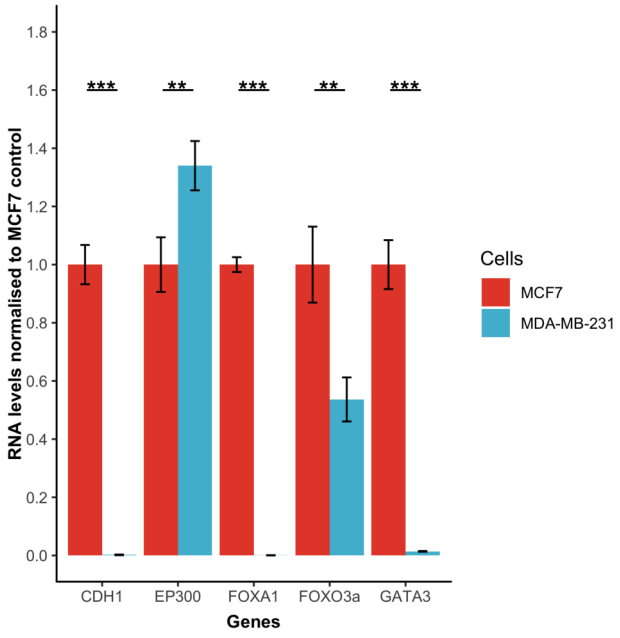
RNA levels normalised to MCF7 control
1.8
1.6
1.4
1.2
1.0
0.8
0.6
0.4
0.2
0.0
***
**
***
**
***
CDH1
EP300
FOXA1
FOXO3a
GATA3
Genes
Cells
MCF7
MDA-MB-231

(b)

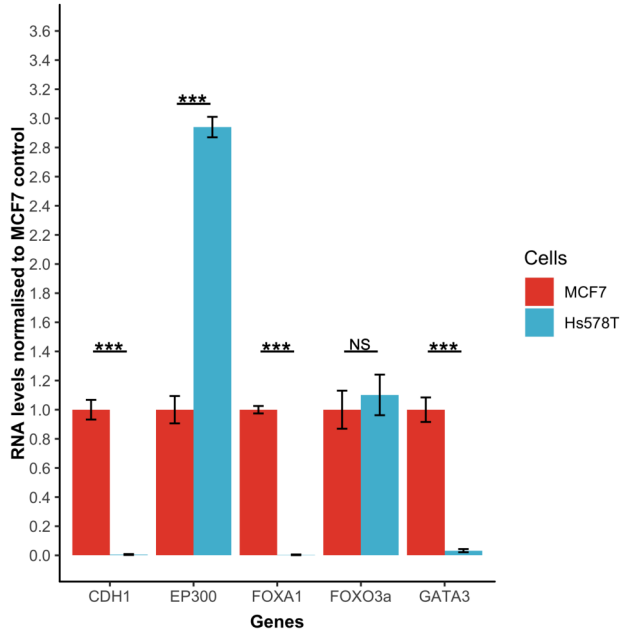

(c)

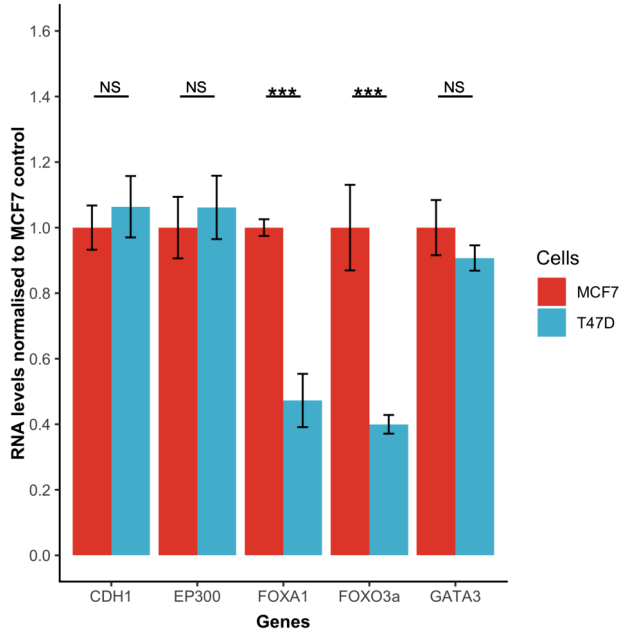

(d)

Fig. 3.5 Gene expression in breast cancer cell lines. The mRNA levels were detected in MCF7,CAL-51,MDA-MB-231,Hs578T and T47D by RTqPCR analysis. Gene expression wild type cells was demonstrated relative to the respective control (MCF7 wild type). Gene expression was normalised to the RPS14 and RPLPO housekeeping genes. Panels show mRNA levels of (A) MCF7 vs CAL-51, (B) MCF7 vs MDA-MB-231, (C) MCF7 vs Hs578T and (D) MCF7 vs T47D. Data are shown as normalised to MCF7 cells. The mean + SD of n=3 independent experiments is shown, NS Non-Significant, * p<0.05, **p<0.01, *** P<0.001,****p<0.0001 (ordinary one-way ANOVA following Dunnett's multiple comparison test).

Chemoresistance in Breast Cancer Affects miR Expression

To see whether chemoresistance has any effect on the expression of miR-23a, miR-25 and miR-27a, we tested our hypothesis by running a RTqPCR analysis of these miRs on MCF7 and BT474 breast cancer cell lines with long term chemoresistance to Doxorubicin, Paclitaxel **(Figure 3.6)** and Lapatinib **(Figure 3.7)**. There is a direct correlation between miR-23 levels and resistance as there is a significant 2.2 fold increase in miR-23a levels with Doxorubicin resistance ($p<0.001$) and 2.4 fold increase in Paclitaxel resistance ($p<0.001$) compared to the untreated control, while the difference between those two drugs is non-significant **(Figure 3.6a)**. There seems to be an inverse correlation between miR-25 levels and resistance as there is a significant 0.2 fold decrease in miR-25 levels with Doxorubicin resistance ($p<0.001$) and 0.18 fold decrease in miR-25 with Paclitaxel resistance ($p<0.001$) compared to the untreated control, while the difference between those two drugs is non-significant **(Figure 3.6b)**. In the case of miR-27a, it seems to follow the same pattern with miR-25. There is an inverse correlation between the levels of miR-27a and resistance as there is a significant 0.3 fold decrease in miR-27a levels with Doxorubicin resistance ($p<0.001$) and 0.48 fold decrease in Paclitaxel resistance ($p<0.001$) compared to the untreated control, while Doxorubicin seems to have a 0.18 fold difference in mIR-27a expression ($p<0.001$) compared to Paclitaxel **(Figure 3.6c)**. There is an interesting observation: miR-23a and miR-27a are located on the same cluster but seem to have a different response to Doxorubicin and Paclitaxel.

Moving on from this, we tested the same hypothesis on the drug Lapatinib, a platinum-based inhibitor in a BT474 breast cancer cell line. MiR-23a shows a significant 2.6 fold increase in expression levels ($p<0.001$) compared to the control **(Figure 3.7a)**. MiR-25 shows a significant 0.4 fold decrease in expression levels ($p<0.001$) compared to the control **(Figure 3.7b)** while miR-27a has a significant 1.32 fold increase in expression levels ($p<0.001$) compared to the control **(Figure 3.7c)**. When comparing all the miRs, the effect is significant between all three ($p<0.001$). However, there is a larger fold change in the levels of miR-23a.

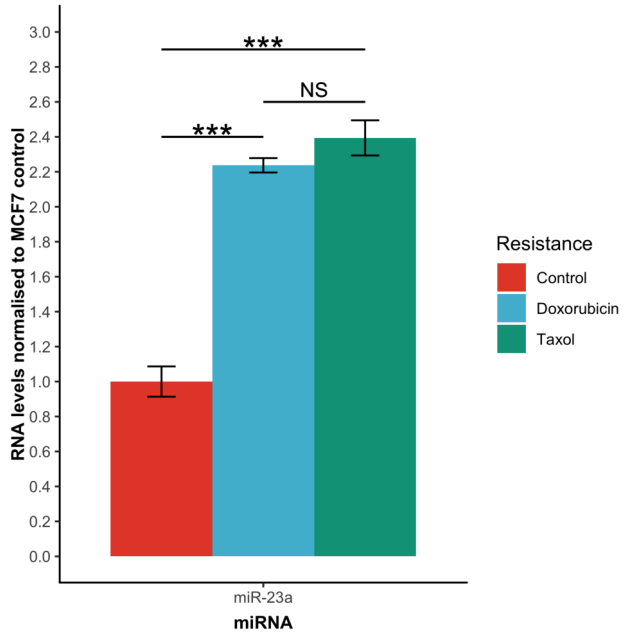
***
NS
***
RNA levels normalised to MCF7 control
3.0
2.8
2.6
2.4
2.2
2.0
1.8
1.6
1.4
1.2
1.0
0.8
0.6
0.4
0.2
0.0
miR-23a
miRNA
Resistance
Control
Doxorubicin
Taxol

(a)

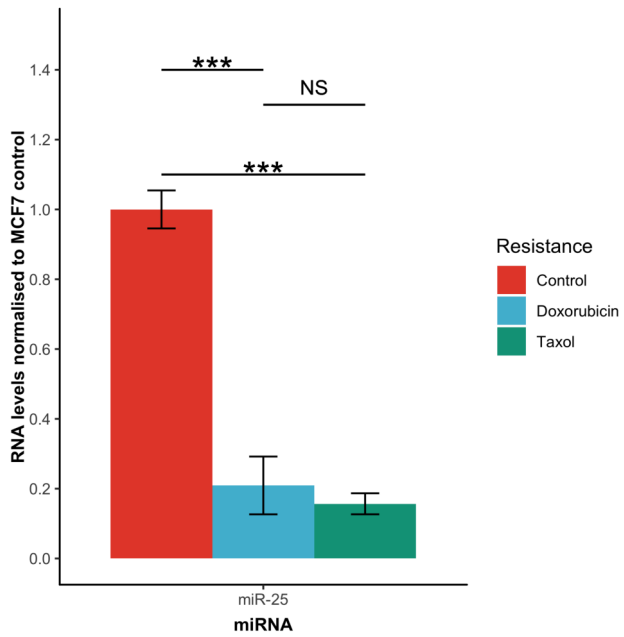
***
NS
***
RNA levels normalised to MCF7 control
1.4
1.2
1.0
0.8
0.6
0.4
0.2
0.0
miR-25
miRNA
Resistance
Control
Doxorubicin
Taxol

(b)

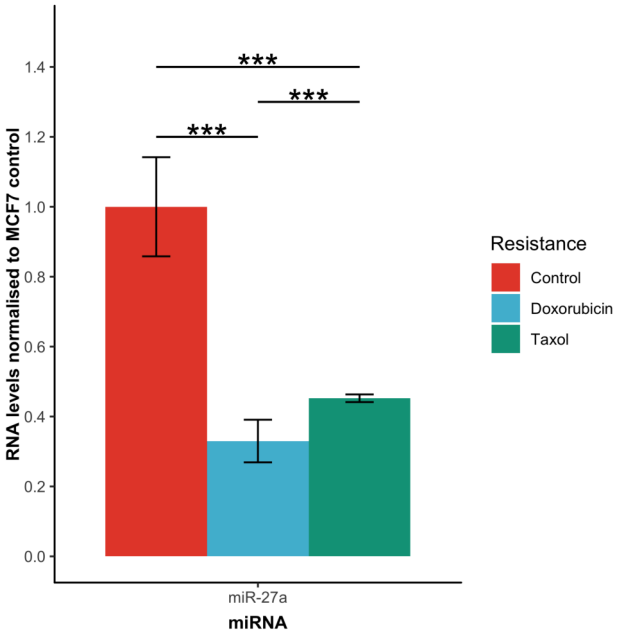

(c)

Fig. 3.6 Effects of Doxorubicin and Taxol resistance on miR-23a, miR-25 and mIR-27a expression in a MCF7 breast cancer cell line. The levels of the miRs were detected in MCF7 by RTqPCR analysis. Gene expression of Doxorubicin and Taxol resistant MCF7 cells was demonstrated relative to the respective control (wild type and empty vector control transfected cells). Gene expression was normalised to the U6 housekeeping gene. Panels show mRNA levels of (A) miR-23a, (B) miR-25 and (C) miR-27a. Data are shown as normalised to the control vector. The mean + SD of n=3 independent experiments is shown, NS Non-Significant, * p<0.05, ** p<0.01, *** P<0.001,**** p<0.0001 (ordinary one-way ANOVA following Dunnett's multiple comparison test).

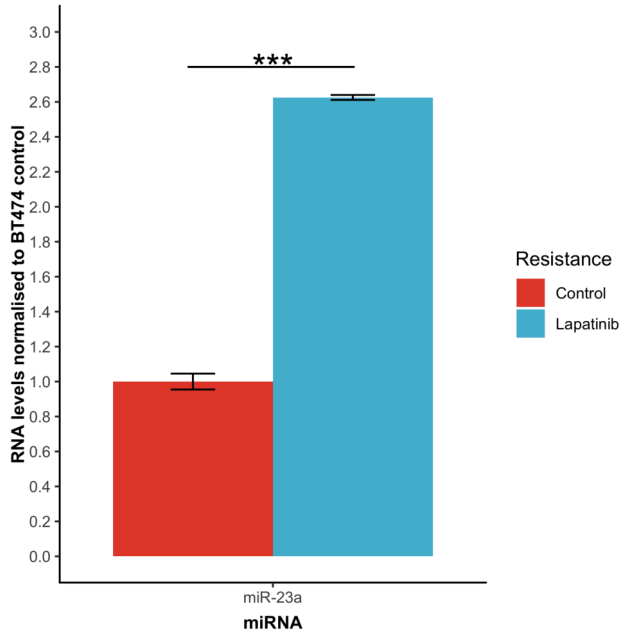
3.0
2.8
2.6
2.4
2.2
2.0
1.8
1.6
1.4
1.2
1.0
0.8
0.6
0.4
0.2
0.0
***
RNA levels normalised to BT474 control
miR-23a
miRNA
Resistance
Control
Lapatinib

(a)

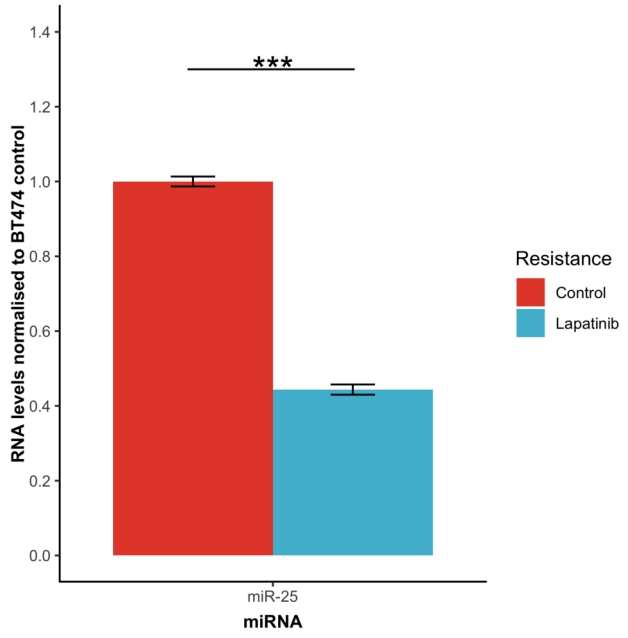
1.4
1.2
1.0
0.8
0.6
0.4
0.2
0.0
***
RNA levels normalised to BT474 control
miR-25
miRNA
Resistance
Control
Lapatinib

(b)

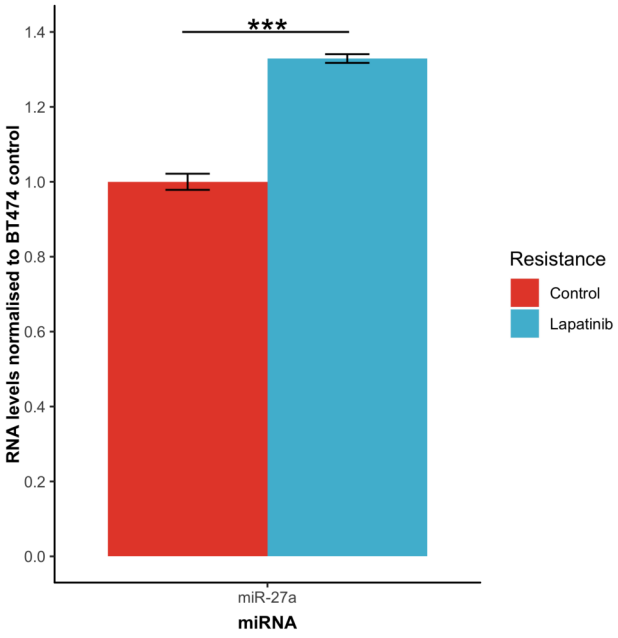

(c)

Fig. 3.7 Effects of Lapatinib resistance on miR-23a, miR-25, and mIR-27a expression in a BT474 breast cancer cell line. The level of the miRs was detected in BT474 by RTqPCR analysis. Gene expression of Lapatinib resistant BT474 cells was demonstrated relative to the respective control (wild type and empty vector control transfected cells). Gene expression was normalised to the U6 housekeeping gene. Panels show mRNA levels of (A) miR-23a, (B) miR-25 and (C) miR-27a. Data are shown as normalised to the control vector. The mean + SD of n=3 independent experiments is shown, NS Non-Significant, * p<0.05, ** p<0.01, *** P<0.001,**** p<0.0001 (ordinary one-way ANOVA following Dunnett's multiple comparison test).

Chemoresistance in Breast Cancer Affects Downstream miR Targets

To see whether chemoresistance has any effect on the downstream transcription factors, we tested our hypothesis by running a RTqPCR analysis of CDH1, EP300, FOXOA1, FOXO3a and GATA3 on a MCF7 with long term chemoresistance to Doxorubicin, Paclitaxel **(Figure 3.8a and 3.8b)** and BT474 breast cancer cell lines with long-term resistance to Lapatinib (Figure 3.8c and 3.8d). In **Figure 3.8a**, comparing the MCF7 cell line control, shows a 1.1 fold increase in EP300 with doxorubicin resistance ($p<0.001$), and a decrease of 0.5 fold with taxol resistance ($p<0.001$). FOXO3a decreases by 0.5 fold with doxorubicin resistance ($p<0.001$) and decreases by 0.7 fold with taxol resistance ($p<0.001$). When comparing the effects of the resistance, EP300 is 0.6 fold lower in taxol when comparing with doxorubicin ($p<0.001$). For FOXO3a, though both decrease compared to control, taxol resistance has a 0.2 fold lower than with doxorubicin resistance ($p<0.001$). **Figure 3.8b**, the MCF7 cell line shows a 1 fold decrease in CDH1 ($p<0.001$), 1 fold decrease in FOXA1 ($p<0.001$) and a 1 fold decrease in GATA3 ($p<0.001$) for both doxorubicin and taxol resistance. When comparing both drug resistances, there is no significant difference on these genes. In **Figure 3.8c**, the BT474 cell line shows a 0.7 fold decrease in EP300 ($p<0.001$) and a 0.9 fold decrease in FOXO3a ($p<0.001$) with lapatinib resistance. In **Figure 3.8d**, there was a 1 fold decrease in CDH1 ($p<0.001$), FOXA1 ($p<0.001$) and GATA3 ($p<0.001$) with lapatinib resistance.

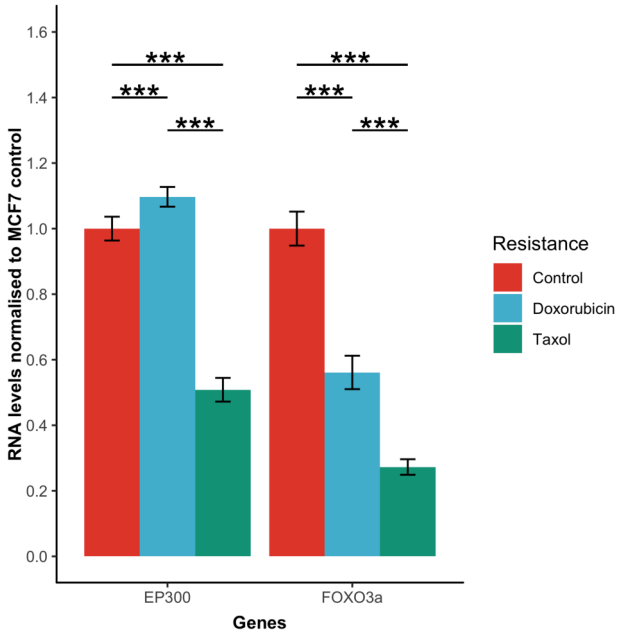
RNA levels normalised to MCF7 control
1.6
1.4
1.2
1.0
0.8
0.6
0.4
0.2
0.0
***
***
***
***
***
***
EP300
FOXO3a
Genes
Resistance
Control
Doxorubicin
Taxol

(a)

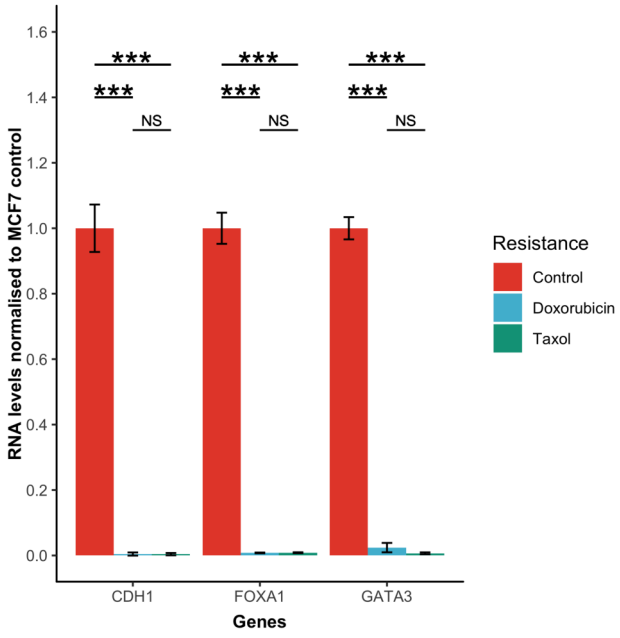
RNA levels normalised to MCF7 control
1.6
1.4
1.2
1.0
0.8
0.6
0.4
0.2
0.0
***
***
NS
***
***
NS
***
***
NS
CDH1
FOXA1
GATA3
Genes
Resistance
Control
Doxorubicin
Taxol

(b)

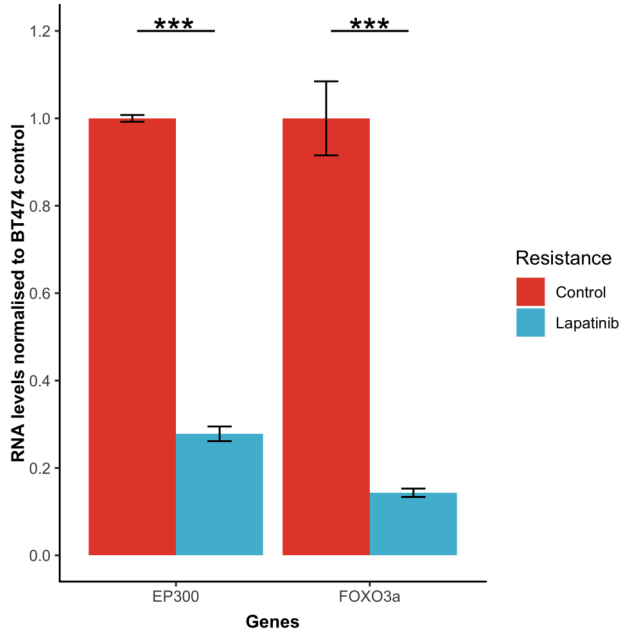

(c)

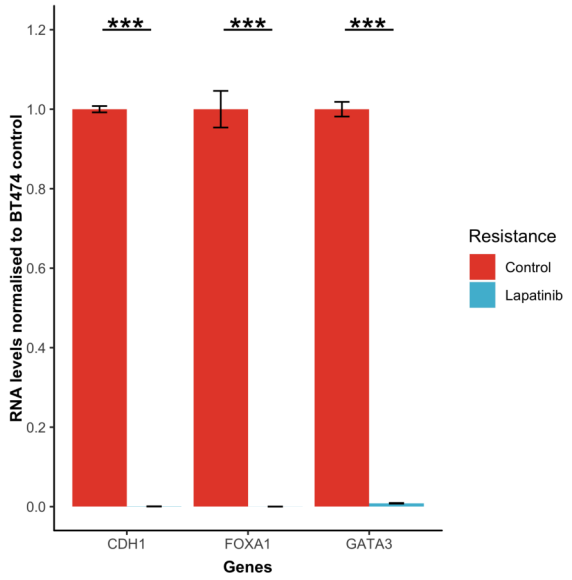

(d)

Fig. 3.8 Effects of Doxorubicin, Taxol and Lapatinib resistance on gene in MCF7 and BT474 breast cancer cell lines. The mRNA levels of selected genes were detected in breast cancer cell lines by RTqPCR analysis. Gene expression of resistant cells was demonstrated relative to the respective control (wild type and empty vector control transfected cells). Gene expression was normalised to the RPS14 and RPLPO housekeeping genes. Panels show (A) mRNA levels of EP300, FOXO3a in MCF7, (B) CDH1,FOXA1 and GATA3 in MCF7, (C) mRNA levels of EP300, FOXO3a in BT474, (D) CDH1,FOXA1 and GATA3 in BT474 . Data are shown as normalised to the Control vector. The mean + SD of n=3 independent experiments is shown, NS Non-Significant, * p<0.05, **p<0.01, *** P<0.001,****p<0.0001 (ordinary one-way ANOVA following Dunnett's multiple comparison test).

3.2.5 Discussion

The preliminary results on the miR-106b 25 cluster showed its upregulation as a response to doxorubicin resistance in MTMEC cells. Out of this cluster, miR-25 showed the most invasive phenotype (Zhou et al 2014). Along with these findings, the cluster is responsible for generating a phenotype capable of EMT and multidrug resistance, which bypasses doxorubicin and γ-radiation induced senescence through the modulation of EP300 and E-cadherin. This is also done independently of drug transporters like the ATP binding cassette (ABC) transporter ABCB1 and is thought to be through the evasion of apoptosis (Hu et al 2016). To this extent, it is more interesting to focus on miR-25 on how it regulates these effects through regulation of downstream pro invasive and antiapoptotic transcription factors. The others miR-27a and miR-23a have similar involvement in cancer, covered in the introduction.

Our results showed that miR-25 was successfully overexpressed in our MTMEC model **(Figure 3.2b)**, leading us to believe it might be the most promising target for us to investigate its effect on CDH1. We next moved onto mechanisms and targets by which miR-25 achieves its aggressive phenotype. For this demonstration, we chose FOXO3a, as it has a matching sequence with mIR-25. It is a transcription factor that is positively regulated by EP300 downstream of miR-25. FOXO3a, a pioneer factor from a well-established family of transcription factors, is involved in cell cycle regulation and initiation. As it was downregulated with miR-25 expression, it can be hypothesised that as FOXO3a is such a well-known antagonist to Forkhead Box M1 (FOXM1) (Lam et al 2013), it is one of the more important pathways through which miR-25 expression would affect the EMT phenotype. This is significant as FOXM1, being part of the same family, is an inducer of EMT through EMT transcription factors such as SNAI1 that are responsible for the canonical loss of E-cadherin.

Our model used the minimally transformed mammary epithelial cells (MTMECs) **(Figure 3.2a)**, which are representative of early tumorigenesis. The overexpression of miR-23a and miR-27a appears not working, which could be due to the efficiency of the transfection or other reasons. One of the reasons could be vector linearisation at the coding sequence or promoter site. This linearisation results in a population of cells that are resistant to our selection antibiotic but not expressing the miRs/GFP tag. Other potential mechanisms could be epigenetic silencing of an overactive promoter of our vector. We could consider improving our protocol by increasing the plasmid DNA concentration, which could increase the amount inside the cells. Improvements on the transfection method/transfection reagent could also be made, such as using lipofectamine 3000, or opting for DNA electroporation with cytomix buffers complemented with ATP. Alternatively, other reagents could be looked at such as the reduced serum Optimem. Freshness and batch quality could vary, a different batch could be

used to compare batch quality. Another way is improving efficiency could be done through changing to complete medium for longer than 72 hours post transfection, or via the addition of EDTA prior to transfection (Rybakovsky et al 2019).

Looking at **(Figure 3.4)**, the data shows that overexpressing miR-25 in MTMECs affects the expression of EP300, FOXO3a and GATA3. FOXO3a gene expression follows that of the protein expression, which suggests FOXO3a is regulated by miR-25. This could be due to miR-25s specificity for the 3' or 5'UTR of FOXO3a, interrupting translation from occurring (Ipsaro et al 2015). As FOXO3a is an important target, this could be one of the ways by which EP300 modulates EMT promoting transcription factors. Referring back to (Figure 1), we can see that the hypothesised control is via EP300. Interestingly, GATA3 should be regulated by miR-27a, but in our experiment it was downregulated with miR-25. This is probably due to the effects on EP300 or FOXO3a/FOXA1 which have many downstream targets, as miR-25 does not have a sequence match to GATA3. An updated network map summarising the effects of miR-25 is shown in **Figure 3.9**.

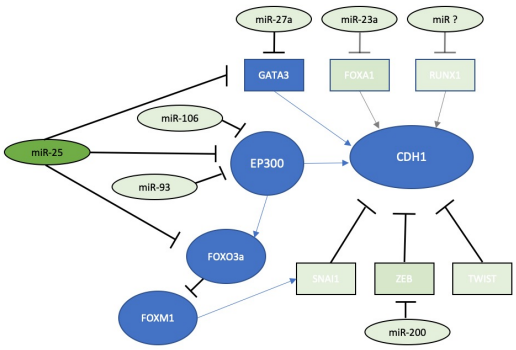

Fig. 3.9 Updated network map of miR-25 action based on RTqPCR data. MiR-25 represses GATA3 and FOXO3a.

Looking at **Figure 3.6** and **Figure 3.7**, all 3 miRs seem to be involved in multiple drug resistance. As shown in our MCF7 model, there is a decrease in miR-25 and miR-27a, while miR-25 is upregulated with doxorubicin and taxol resistance. All three drugs have different modes of action, therefore the way in which they modulate the miRs should be different. Doxorubicin acts on topoisomerase II mediated DNA repair by changing chromosome structure, as well as generating free radicals that damages the cell membrane (Thorn et al

2011). Its uptaken by the cell results in inhibition of cell proliferation through upregulation of p21 but other mechanisms are still to be determined (Patel et al 2012). Additionally, known mechanisms of resistance are upregulation of ABC transporters, amplification of TOP2A (Thorn et al 2011). Taxol stabilises the cells mitotic spindle assembly of the α and β tubulin heterodimers, induces cell cycle arrest and cell death. There is also an alternative theory as it is affecting interphase cells though controversial. Overall, the effects are hard to study due to differences in plasma and tumour concentration (Weaver et al 2014). At high concentrations, it arrests the cell cycle at G2 while at low concentration, it induces apoptosis through Raf-1 Proto-Oncogene (RAF1)/ p53/ p21 (Kampan et al 2015). Lapatinib is an inhibitor of tyrosine kinase activity, usually associated with EGFR and HER2 through binding to their ATP-binding pocket which prevents autophosphorylation. It arrests cell cycle arrest in sub G1 through upregulation of p38, p21 and p27, boosting apoptosis. Apoptosis is further promoted through upregulation of BIM, a promoter of apoptosis (Segovia-Mendoza et al 2015). As all three miRs are involved in cell cycle progression and apoptosis, it can be assumed that they are either recruited as a response to some mechanism involved in p21/ p38/ p53 or other transcription factors regulated by EP300.

Looking at these results in contexts of **Figure 3.8**, further complicates the narrative. FOXO3a is downregulated in response to doxorubicin and taxol, but it does so independently of miR-25, as miR-25 has low expression in MCF7. There is also an interesting downregulation of EP300 expression with Taxol resistance. MCF7 with doxorubicin and taxol resistance also seems to lose their epithelial characteristics as CDH1 is almost completely lost. This also seems independent of miRs-27a and miR-23a which regulate GATA3 and FOXA1 that are known CDH1 regulators, as they both have very low expression. BT474 shares the same expression profile as MCF7. There seems to be a shift towards a transitional mesenchymal state as CDH1 is lost with lapatinib resistance. Potentially, independent of miRs-27a and miR-23a as their effectors GATA3 and FOXA1 are downregulated. EP300 and FOXO3a is also lost, and might play a key role in the gain of resistance which needs to be investigated further. A summary of drug resistance to doxorubicin, lapatinib and taxol and its effects on our signalling network is summarised in **Figure 3.10**.

MiR expression is shown to vary between different cell lines **Figure 3.3**. Mesenchymal-like cell lines such as CAL51, seem to favour the expression of miR-25 and miR-27a. MDA-MB-231, while still mesenchymal-like has a different expression pattern, and favours miR-23a and miR-27a, while repressing miR-25. The same is seen in HS578T, though with a slightly higher expression of miR-27a. The epithelial cell lines, MCF7 and T47D do not seem to differ much in their expression of these miRs, although T47D seems to express them slightly less. As miR-23a and miR-27a are located on the same cluster, their differential

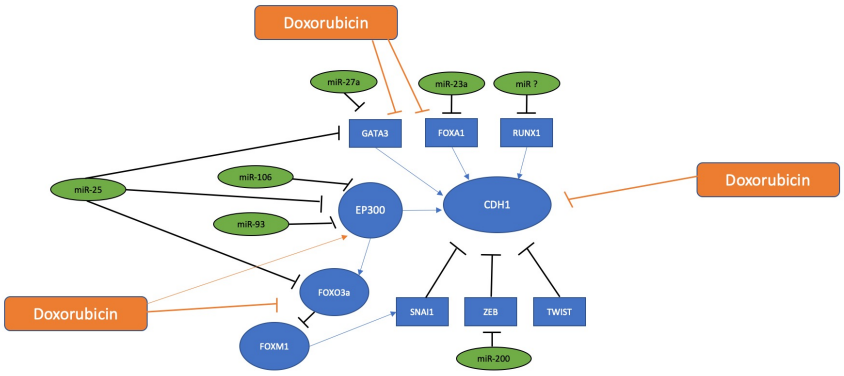

(a)

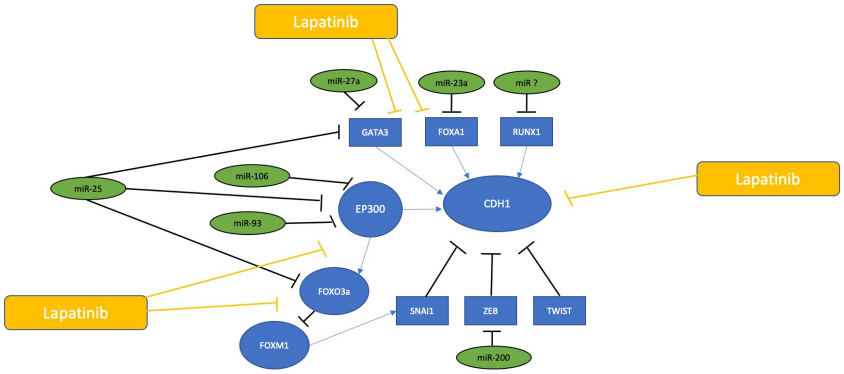

(b)

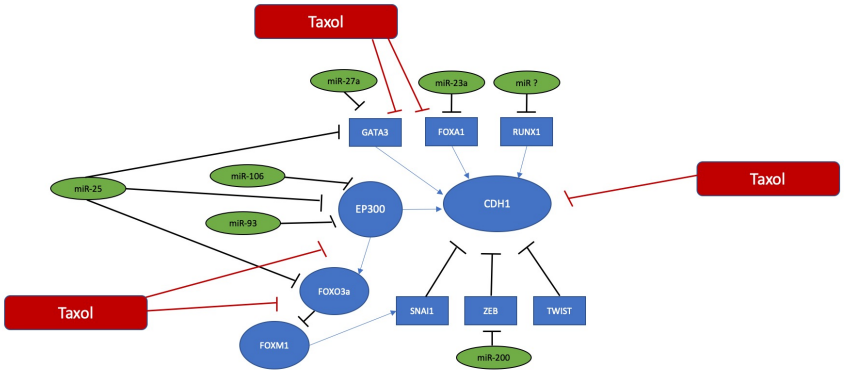

(c)

Fig. 3.10 The effect of drug resistance on gene and miR expression. Network map showing the effects of (A) doxorubicin, (B) lapatinib and (C) taxol.

expression could be due to the presence of another repressor or enhancer which favours the expression of one over the other. This leads us to **Figure 3.4**, which investigated the same cell lines for downstream effectors like EP300, FOXA1, FOXO3a and GATA3 that were tested in our MTMEC model.

Similar to the miR expression, mesenchymal-like cell lines CAL-51 and MDA-MB-231 have similar expression profiles. Oddly, while EP300 and miR25 expression is high in CAL51, it should follow that CDH1 and FOXO3a would also be increased as it is a downstream target of EP300. While FOXO3a downregulation cannot be explained by these data, it is likely CDH1 is repressed by the active expression of miR-23a and miR-27a which affect FOXA1 and GATA3 respectively, which in turn repress CDH1. More study is necessary to confirm this.In MDA-MB-231 cells, there is a different mechanism. miR-23a and miR-27a are located on the same transcript and therefore expressed together while miR25 is downregulated. In this case, FOXO3a and CDH1 downregulation could fit our hypothesis with miR-25 but unlikely the entire story. The same pattern is seen as with CAL-51, in terms of its GATA3 and FOXA1 expression, which could be attributed to miRs-27a and miR-23a. More study is necessary to explore these pathways.

With HS578T cells, miR-27a and miR-23a are expressed highly, and also a decrease in their targets GATA3 and FOXA1, which follows the logic of CAL-51 and MDA-MB-231. However, it expresses EP300 higher than the other cell lines, and this mechanism is not due to miR-25 as this miR is underexpressed. The other odd result is with T47D and MCF7 comparison as all the miRs are similarly expressed, although somewhat lower in T47D. However, FOXA1 and FOXO3a expression is lower with T47D, suggesting an alternative mechanism that functions there.

3.2.6 Future Potential Work

There is potential to look into the DNA damage response of triple negative breast cancer lines with depleted miRs, perhaps extended to miR200s, which would affect a wider range of regulatory pathways of EMT/tumorigenesis. Such studies could be done using the approach of abrogating function through targeting Dicer and Drosha. Previous studies showed siRNA targeted therapy, downregulates miR-27 and let-7 followed by a decrease in angiogenesis, implicating both (Kuehbacher et al., 2007). Alternatively, the miRs could be inactivated through the use of isomirs. As was shown in a recent study, where miR-27s isomirs have a variety of different effects on its target genes related to metabolism, depending on which base is substituted or altered (Ma et al., 2019). Otherwise an alternative pathway would be to look at the miR-25 effect on promoter activity of FOXO3a through bioinformatics studies; or to look at the effects of miR-25 on antiapoptotic genes such as BCL2, BAX.

3.2.7 Overall Conclusion

The investigation has led us to the results are inconclusive to support a general model of the way the miRs function in our cell panel. As the expression profiles seem so different even between mesenchymal-like and epithelial cell lines, such as with MDA-MB-231 vs CAL-51. This led us to abandon this line of investigation and move back to our primary investigation of EP300 and its effects on modulating transcription factors. Although there is some effect on miR expression along with our target effector genes in the chemo resistant cell line models, these should be investigated further to elucidate whether the potential gain/loss of function will reverse the phenotype. As drug resistance is related to stemness, EMT and invasive characteristics, it could also be of interest to investigate those in association with the gain and loss of function of these miRs. Whether the miR expression correlates with protein levels of FOXA1, EP300 and GATA3 is also of interest, which would give us more evidence to support this pathway. In **Chapter 4**, we will move from looking at miRs to the expression of other target genes potentially involved in the network.

Chapter 4

Gene Signature Linked to EP300

4.1 Introduction

The previous **Chapter 3** described the novel pathway controlling drug resistance. EP300 is associated with stem cell-like characteristics, and its downregulation raises the risk of tumorigenicity, while rescuing its ectopic expression in basal breast cancer cells, restores partially the epithelial phenotype and sensitivity towards paclitaxel. Through a genome wide expression profile analysis, performed on MCF7 breast cancer cell derivatives with EP300 knockdown and paclitaxel resistance, more than 4000 genes changed their expression, from which we selected those which were up or down regulated with the most significance (Asaduzzaman et al 2017). This next chapter will elucidate on this lists impact on EMT, drug resistance and stemness characteristics.

4.1.1 ABCG2

Background

The ATP binding cassette superfamily G member 2 (ABCG2) otherwise known as Breast cancer resistance protein (BRCP1), controls the availability of drugs through its localisation in the gastrointestinal tract and high specificity for substrates. This makes it important for pharmacokinetics of drugs in areas of : absorption, distribution, metabolism, excretion and toxicity (Hilgren et al 2013). As a consequence, it has been widely reported to be involved in multidrug resistance in cancer (Gottesman et al 2002, Sarkadi et al 2006, Gillet et al 2011, Sharom et al 2011). It has so far been identified as a marker for hematopoietic stem cells (Zhou et al 2001). ABCG2 and the other ABC transporters cause resistance to a wide list of substrates (reviewed by Ween et al 2015, Fletcher et al 2016, Beretta et al

2017). Some examples of these in breast cancer are: anthracyclines, taxanes, vinca alcoloids, camptothecins, epipodophyllotoxins and tyrosine kinase inhibitors (Sharom et al 2011). ABCG2 also has a number of other substrates, such as: indolocarbazole topoisomerase I inhibitors, methotrexate, mitoxanthrone, topotecan, irinotecan and flavopiridol (Mao et al 2015). Often this resistance is towards multiple substrates. Part of the reason for this multidrug resistance could be co-expression of more than one ABC transporter in solid tumours. The TCGA RNA-seq dataset reveals that ABCG2 is co-expressed 1000-fold along with ABCB1. Despite its obvious role in drug resistance, any effort to target this in a clinical setting has not been viable (Robey et al 2011 and Tamaki et al 2011). Loss of the ABC transporters can result in a number of genetic disorders, such as cystic fibrosis and tangier disease.

Structure

The ABC transporter family consists of 48 transporters, divided into 7 subfamilies (Moitra et al 2011). ABCG2 structure is similar to that of another member of the family, ATP binding cassette superfamily G member 5 (ABCG5) (Lee et al 2016). A 4 domain structure which contains: 4 nucleotide binding domains (NBD) and 2 transmembrane domains (TMD). A substrate binds to the binding pocket on the TMD, while the NBD hydrolyses ATP, which results in a conformational change in the transporter. The cycle then repeats once a new ATP molecule binds to the TMD (Dean et al 2001). The precise mechanism of conformation change in ABCG2 has not yet been determined (Taylor et al 2017).

Biological Function

ABCG2 plays a vital role in many physiological functions of the breast as well as numerous blood barriers (Cuperus et al 2014,Fetsch et al 2006, Diestra et al 2002, Robey et al 2009). MCF7 and MDA-MB-231 cells overexpressing ABCG2 gain resistance to mitoxanthone daunorubicin, doxorubicin and topotecan. Whereas resistance to cisplatin, paclitaxel, etoposide and vincristine were not present in control (Doyle et al 2003). ABCG2 has been first implicated in drug resistance in a canonical mouse study which showed phenotype reversal with ABCG2 inhibitor GF120918 (Allen et al 1999). Since then, its localisation in gut mucosa has led to numerous studies looking into drug absorption (Jonker et al 2000). As in the case of GF120918 which impacted availability of topotecan up to 97% (Kruijtzer et al 2002). Furthermore, there is reason to believe that ABCG2 could function as a stem cell marker. Not only is it is present in side populations with confirmed stem cell markers, but its silencing results in increased sensitivity to mitoxanthrone (Zhou et al 2001).

Paradoxically, ABCG2 levels were rather low when examining breast tumours with relapsed disease and post doxorubicin cycles (Faneyte et al 2002).

Therapy

A multitude of agents to target ABCG2 have been attempted such as bioenhancers such as Elacridar, tariquidar, biricodar and cyclosporin A (Minderman et al 2004, Robey et al 2004, Qadir et al 2005), but with little effect. Others in the form of RTK inhibitors show unexpected toxicity, which makes them problematic in therapy (Dy et al 2013). Examples of these are: lapatinib, apatinib, nilotinib (Dai et al 2008, Tiwari et al 2009, Mi et al 2010). Another type of therapy, used Ko143 inhibitor combined with Photodynamic Therapy (PDT), producing higher sensitivity to the PDT agent Aminolevulinic acid (ALA). (Palasuberniam et al 2015). It is noteworthy that the fluorescence exhibited by these cells differed between hormone receptor status, with the triple negative group displaying significantly lower fluorescence than even the HER2 compared to normal cells (Palasuberniam et al 2015).

4.1.2 ARHGAP20

Background

Rho GTPase Activating Protein 20 (ARHGAP20) regulates RHO related proteins, which are involved in cell processes, cell migration, and contraction of the cytoskeleton, growth, differentiation and development. They work antagonistically to guanine nucleotide exchange factors (GEFs), which act as activators of RHO proteins and enhance these processes. Its function in disease progression and cancer is not yet studied. But it has been implicated in neurite growth (Yamada et al 2005). And differentially expressed in a common deleted region associated with poorer survival in chronic lymphocytic leukaemia (Herold et al 2011).

Structure

ARHGAP20 is part of a large family of proteins consisting of 65 members. They are divided based on the G protein family they attach to: Rho family, Ras family, Ras-Related Protein Rab (Rab) family, RAs-related Nuclear protein (Ran) family and ADP ribosylation factor (Arf) family. The Rho family GTPase-activating proteins (GAPs) are : Rho GTPase Activating Protein 6 (ARHGAP6), Rho GTPase Activating Protein 10 (ARHGAP10), Rho GTPase Activating Protein 9 (ARHGAP9), Rho GTPase Activating Protein 15 (ARHGAP15), Rho GTPase Activating Protein 21 (ARHGAP21), ARHGAP20, Phosphatidylinositol 3-kinase regulatory subunit alpha (PIK3R1), Rho GTPase Activating Protein 4 (ARHGAP4),

Chimerin 1 (CHN), Rho GTPase Activating Protein 29 (ARHGAP29), BCR Activator Of RhoGEF And GTPase (BCR), Rho GTPase Activating Protein 1 (ARHGAP1), Rho GTPase Activating Protein 12 (ARHGAP12), Rho GTPase Activating Protein 27 (ARHGAP27), Rho GTPase Activating Protein 17 (ARHGAP17), Rho GTPase Activating Protein 26 (ARHGAP26), DLC1 Rho GTPase Activating Protein (DLC1), Inositol Polyphosphate-5-Phosphatase B (INPP5B), Myosin IXB (MYO9B), Rho GTPase Activating Protein 5 (ARHGAP5). The Ras family contains: TBC1 Domain Family Member 3C (TBC1D3C), TBC1 Domain Family Member 8 (TBC1D8), TBC1 Domain Family Member 9 (TBC1D9), TBC1 Domain Family Member 2 (TBC1D2), Small G Protein Signaling Modulator 2 (RUTBC1), Small G Protein Signaling Modulator 3 (RUTBC3), Ubiquitin Specific Peptidase 6 (USP6), TBC1 Domain Containing Kinase (MGC16169), TBC1 Domain Family Member 1 (TBC1D1). The Ran family contains a single member: Ran GTPase Activating Protein 1 (RANGAP1). The Arf family contains: Small ArfGAP 1 (SMAP1), ArfGAP With Dual PH Domains 2 (CENTA2), ArfGAP With GTPase Domain, Ankyrin Repeat And PH Domain 1 (CENTG2), ArfGAP With GTPase Domain, Ankyrin Repeat And PH Domain 5 (CTGLF2), ArfGAP With Coiled-Coil, Ankyrin Repeat And PH Domains 2 (CENTB2), GIT ArfGAP 1 (GIT1), ArfGAP With SH3 Domain, Ankyrin Repeat And PH Domain 2 (DDEF2) (Bos et al 2007). All members of the family share a RHO GAP domain, while ARHGAP20 contains a phosphatidylinositol phosphate binding protein domain (PH) and Ras associating (RA) domain which binds RAP1A, Member Of RAS Oncogene Family (Rap1). This RA domain serves as an autoinhibitory sequence and is released by Ras-proximate-1 or Rap1 upon binding (Yamada et al 2005).

Biological Function

ARHGAP20 stimulates the hydrolysis of the Guanosine-5'-triphosphate (GTP) to Guanosine diphosphate (GDP) which shuts off signal propagation for RHO proteins (Dvorsky et al 2004). This is done by supplying a stabilising arginine finger and changing the conformation of the G protein, which lowers the activation energy necessary for the hydrolysis to occur (Scheffzek et al 1998). Once the GTP is hydrolysed by the G protein, it is no longer activated. The exact specificity reasons for G proteins is unknown, yet there seems to be a mechanism by which G proteins and their G protein activating protein counterparts are co-expressed in the same location (Xie et al 2007). The family is regulated by protein-protein interactions (Yamada et al 2005), secondary messengers (Canagarajah et al 2004) or protein modifications such as phosphorylation (Avruch et al 2006).

4.1.3 BCL2

Background

B-Cell-Lymphoma 2 (BCL2) was the first discovered inhibitor of apoptosis (Vaux DL, et al 1988). Its role as an oncogene was confirmed, when co-expression of BCL2 with Myc resulted in faster progression of lymphoma (Strasser et al. 1990). This result later became useful as a marker for drug resistance and apoptosis (Nadler et al. 2008). It is also an independent prognostic marker for early breast cancer (Dawson et al. 2010), and low expression levels of BCL2 have been shown to correspond to more favourable outcomes for a subset of triple negative breast cancer (Bouchalova et al. 2014). In addition, BCL2 promotes EMT in the MCF10ATG3B mammary epithelial cell line (An et al. 2015).

Structure

BCL2 has homology motifs shared with the other members of the family, and correspond with their function. The family is subdivided into 3 groups: antiapoptotic BCL2 Like 1 (BCL-X), BCL2 Like 2 (BCL-W), MCL1 Apoptosis Regulator, BCL2 Family Member (MCL1), BCL2 Like 10 (BCL-B), pro-apoptotic effectors BAX, BAK, BCL2 Family Apoptosis Regulator BOK (BOK) and pro-apoptotic activators BH3 Interacting Domain Death Agonist (BID), BIM, BAD, Phorbol-12-Myristate-13-Acetate-Induced Protein 1 (NOXA), BCL2 Binding Component 3 (PUMA). External stress signals initiate the cascade of pro apoptotic activators, and if they are not impeded by BCL2, it will activate the downstream effectors and initiate the mitochondrial outer membrane permeabilization (MOMP) (Adams, J., Cory, S, 2018). The antiapoptotic group contains all 4 domains: Bcl-2 Homology domains 1 (BH1), Bcl-2 Homology domains 2 (BH2),Bcl-2 Homology domains 3 (BH3), Bcl-2 Homology domains 4 (BH4) and transmembrane domain (TM), this causes a hydrophobic tertiary structure that acts as a BH3 binding domain for the initiators (Shamas-Din, A et al. 2011) which inactivates them (Petros et al. 2000). By far, the most important domain which all interactions occur, is the BH3 domain, in which effectors like BAX/BAK are activated (Moldoveanu et al. 2013 and Czabotar et al. 2013).

Biological Function

Apoptosis is the normal cellular process during which cells shrink and destroy their DNA to be recycled by the phagocytes. It is one of the mechanisms of acquired drug resistance (Friedrich, Wieder et al. 2001). Our group has shown that suppression of apoptosis leads to chemotherapy resistance (Hu, Guo et al. 2015). BCL2 is in control of the intrinsic apoptosis

pathway through the mitochondrial outer membrane (MOM), while the extrinsic is controlled by the tumour necrosis factor receptor family. It is also known that BCL2 blocks both caspase 8 and caspase 9, which are the effector proteins in both pathways, through the reduction of cytochrome c (Li et al. 1997) and activates inhibitors of apoptosis (Watanabe, Yasuhira et al. 2013). It is demonstrated that BCL2 interferes with apoptosis in the case of cytotoxicity, radiation and stimulation from tumor necrosis factor alpha (TNFα) (Borner, C et al. 2003, Chipuk J, E, et al 2010, Cory, S et al. 2002). Both extrinsic and intrinsic pathways are later mediated by caspase 3, caspase 6 and caspase 7.

Therapy

Research into promotion of apoptosis led to the development of molecules such as Poly ADP ribose polymerase inhibitors (Munagala, Aqil et al. 2011), or small molecule inhibitors of Raf kinase, such as Soarenib (Bay 43-9006). Soarenib works by shutting down proliferation and angiogenesis through targeting VEGFR1, VEGFR2, VEGFR3, Platelet Derived Growth Factor Receptor Beta (PDGFR-b), Proto-oncogene c-KIT (c-kit), and Fms Related Receptor Tyrosine Kinase 3 (CD135) (Cadoo, Gucalp et al. 2014). Alternatively, there are cyclin dependant kinase inhibitors, such as Flavopiridol, which promote apoptosis through TRAIL; or histone deacetylase inhibitors like Vorinostat which shut down proliferation and differentiation (Munagala, Aqil et al. 2011). Overall, these approaches are still being tested.

4.1.4 BMP4 and BMP7

Background

Bone morphogenetic protein 4 (BMP4) and bone morphogenetic protein 7 (BMP7) are extracellular cytokines part of the TGF-β superfamily (Guo et al 2009). They are functional in developmental biology, tumour development and promotion of EMT and generating cancer stem cell populations. Both BMP4 and BMP7 are overexpressed in breast cancer compared to normal tissue (Alarmo et al 2007). The reduction of bone morphogenetic protein (BMP) receptors has been recently linked to impaired metastasis in mammary tumour models of mice (Pickup et al 2015). The role of BMPs in cancer remains controversial (Alarmo et al 2010) and depends on cancer type and cancer cell line type, as the same BMP may have a different function depending on pathway activation.

Structure

BMPs consist of 20 members, and some of them are subclassified as growth and differentiation factors (GDG) (Schmierer et al 2007). Members of the family share a structure consisting of, an N-terminal domain, a pro-domain and a C-terminal mature growth domain (Bragdon et al 2011). The prodomain is cleaved at a later maturing stage, but not in some cases for example it acts as a regulatory element on BMP activity (Constam et al 1999). They also contain a cysteine knot motif with 7 cysteine residues, the final of which is responsible for linking BMPs together into a mature dimer structure (Ducy et al 2000).

Biological Function

BMPs have 3 types of interacting partners that are classified as: antagonists, ligands or receptors. The antagonists can compete for BMPs to initiate BMP activation, whereas receptor antagonists are competitors for receptors and prevent BMP function (Rosen et al 2006). Complexes with BMP are formed in the pro-regions. Antagonists like Noggin and chordin are known to target a number of BMPs, including BMP4 and BMP7 (Bragdon et al 2011). Noggin has been extensively studied in cancer tumorigenesis and bone metastasis in breast cancer, where interacts with pathways such as WNT and sonic hedgehog (Shh) (Sharov et al 2009, Tarragona et al 2012). A third antagonist, Gremlin is involved in cancer stem cell development and linked with cell cycle progression through p21 (Yan et al 2014). In the case of receptors, BMPs function by binding to serine threonine kinase type II receptors: Activin A Receptor Type 1 (ACVRI) abd ALK1, bone morphogenetic protein receptor type 1A (ALK3), and Bone Morphogenetic Protein Receptor Type 1B (ALK6), which in turn phosphorylate the type I receptors: Activin receptor type-2A (ACVR2A), Activin A Receptor Type 2B (ACVR2B), Anti-mullerian hormone receptor type 2 (AMHR2) and form a complex. Through this process, there is activation and phosphorylation of SMADs (Bragdon et al 2011).

The role of BMPs is controversial, as they act both as promoters and inhibitors in the context of cancer, as outlined by several studies below. We will start with BMP4 which has been implicated in migration and invasion of cells in breast cancer (Guo et al 2012). This is supported by another study, where increasing migration and invasion but also produced an unexpected decrease in cell growth (Ketolainen et al 2010). Furthermore, BMP4 has also been shown to promote angiogenesis and invasion in breast cancer (Shon et al 2009, Farnsworth et al 2011). As an inhibitor, BMP4 has been implicated in downregulation of proliferation of mesenchymal breast cancer, through MMP expression (Ampuja et al 2013) and suppressed metastasis by inhibition of myeloid derived suppressor cells, through upregulation of human

granulocyte colony-stimulating factor (G-CSF)(Cao et al 2014). BMP7 has the same pattern, it suppresses primary breast cancer tumours while simultaneously promoting pro-osteoblast activity through VEGF. This dualistic role of BMP7 is confirmed in several studies where BMP7 expression confers resistance through avoidance of apoptosis and induction of EMT, migration and invasion (Feeley et al 2005, Yang et al 2006). BMP7 also showed the reverse, where proliferation, migration and invasion was inhibited upon its expression (Yang et al 2005, Ye et al 2007).

There is also some evidence that points to the involvement of BMPs in drug resistance in cancer. For example, resistance to epidermal growth factor (EGFR) tyrosine kinase inhibitors (TKIs) was demonstrated through BMP-mediated SMAD activation (Wang et al 2015). This is concurrent with a study where BMP4 overexpression led to resistance in small cell lung cancer (Xian et al 2014). This was largely attributed to the modulation of Acyl CoA synthetase long chain family member 4 and a downregulation of miR-139-5p (Bach et al 2018). Similar findings were seen in ovarian cancer, where BMP4 expression was modulated by the hedgehog signalling pathway (Coffman et al 2016). For BMP7, the link to resistance is largely cell type context dependent. The expression of BMP7 was both promoting the recurrence of resistance stem cells in prostate cancer through activation of p38 and p21 (Kobayashi et al 2011) and also inhibited stemness and tumour growth (Tate et al 2012).

Both BMP4 and BMP7 act through the ERK1/2, p38 and JNK pathways (Hu et al 2004, Otani et al 2007, Bragdon et al 2011). Both can be modulated by gene mutations, e.g. the canonical p53 gene mutation affects BMP expression through the WNT and β-catenin pathways (Voorneveld et al 2015), or by the activity and expression of miRs. These miRs can either target BMPs directly, such as miR-196a (Braig et al 2010) or miRs can target the BMP receptors (Li et al 2015). It is interesting to note that BMP4 has a suppressive effect on miR-21 (Ahmed et al 2011) which shows that the regulatory environment of BMPs is complex, as miR-21 is responsible for regulation of tissue inhibitors of TIMP metallopeptidase inhibitor 1 (TIMP1), TIMP Metallopeptidase Inhibitor 3 (TIMP3) and programmed cell death 4 (PDCD4).

4.1.5 CAPN9

Background

Calpain 9 (CAPN9) like other calpains is activated by the mitogen activated kinase pathway (Perrin et al 2002). They function in a variety of processes such as cytoskeleton remodelling, cell survival and apoptosis (Goll et al 2003). Certain diseases, such as limb-

girdle muscular dystrophy and cancer, result from calpain dysregulation. The predominantly studied members of the family are calpain 1 (CAPN1) and calpain 2 (CAPN2), which are useful patient prognosis predictors (Storr et al 2012). They are also involved in ER signalling through the activation of 17β estradiol (Hou et al 2012).

Structure

Calpains are calcium-dependent cysteine proteases, which exist as a heterodimer composed of two subunits: a large catalytic subunit (80 kD) and a small regulatory subunit (30 kD) (Saez et al 2006). The family is composed of 14 genes, divided into typical calpains: CAPN1, CAPN2, calpain 3 (CAPN3), calpain 8 (CAPN8), calpain 9 (CAPN9), calpain 11 (CAPN11), calpain 12 (CAPN12), calpain 13 (CAPN13) and atypical calpains: calpain 5 (CAPN5), calpain 6 (CAPN6), calpain 7 (CAPN7), calpain 8b (CAPN8b), (CAPN10a), and calpain 15 (CAPN15). Typical calpains share their structure with CAPN1/CAPN2 while atypical calpains lack domain IV (described later), therefore cannot interact with the 30 kD subunit. CAPN9 is made up of a regulatory N-terminal domain (Domain I), a protease domain (Domain II , with subdomains IIa and IIb), a C2-like Ca2+/phospholipid-binding domain (Domain III) and penta EF hand (PEF) (Domain IV) (Hata et al 2010). It is structurally different to CAPN1 and has different residues on its sites, which imply different function and substrate specificity (Moldeveanu et al 2004). It also has differences in its P1 and P2 residues (Davis et al 2007). CAPN9 is synthesized as an inactive enzyme, which upon calcium and phospholipid activation translocates to the cell membrane. The autocatalytic hydrolysis of its domain I, results in the 80 kD subunit to hydrolyse substrates on the cell membrane. There is also a second mechanism by which calpains activate, but it is only relevant to atypical calpains as they lack the 30 kD subunit (Ono et al 2012).

Biological Function

CAPN9 associates with CAPN4 (Lee et al 1999) and sometimes CAPN8 (Hata et al 2010). Very few studies have been done compared to CAPN1/CAPN2, so little is known about the interaction partners of CAPN9. However, it is known that it is involved in breast cancer cell lumen formation (Chen et al 2010). So far, CAPN9 knockdown in mouse fibroblasts has shown an increase in tumorigenesis (Liu et al 2000). An analysis of clinicopathological variables revealed that low CAPN9 expression is associated with smaller tumour size, tumour stage and that were ER+, while the average patients age range was higher (40+) (Davis et al 2014). The same study did not show any impact on overall survival, however there was an association between low CAPN9 and adverse disease specific survival with endocrine

therapy, though without conclusion as the study did not mention the enzymes activity levels which could have an impact (Davis et al 2014).

4.1.6 Cadherins

Background

The cadherin superfamily has 110 members (Hulpiau et al 2009, Oda et al 2011). They participate in cell adhesion through tight junctions, adherens junctions and desmosomes. The role of these structures defines the organisation of a cell into a tissue, organ or stroma. Of these junctions regulated by cadherins, the most important are adherens junctions and desmosomes (Perez-Moreno et al 2003). The extracellular portion of cadherins handles the homophilic attachment to ectodomains of other cadherins, while the intracellular portion deals with cell signalling, actin cytoskeleton filament crosslinking and reorganisation and cadherin trafficking via the endocytotic pathways (Bryant et al 2004, Mege et al 2006 and Yap and Covacs 2003). Cadherins interact with each other through homophilic interaction. The homophilic interaction is mediated throughout histidine alanine valine (HAV) domains, tryptophan residues and hydrophobic pockets in cadherin domains. The cadherin intracellular domain can form a cytoplasmic cell adhesion complex (CCC) with β and γ-catenins, which bind to the carboxyl termini on classical cadherins. Alternatively, it can bind to Catenin Delta 1 (p120) which has several binding sites on the cytoplasmic tail. A secondary function of the CCC facilitates the binding of β and γ-catenin to α-catenin, thereby linking the actin cytoskeleton (Yagi et al 2000, Perez-Moreno et al 2003).

Structure

The cadherin superfamily falls into classical (Type I and II) and non-classical cadherins. The latter includes desmosomal cadherins and protocadherins. Classical cadherins are further divided into type I cadherins and type II cadherins. Type I cadherins which include: CDH1, CDH2 (N-cadherin), cadherin 3 (CDH3), cadherin 4 (CDH4) and cadherin 15 (CDH15), share a short ectodomain with 5 extracellular cadherin repeats, stabilised by calcium ion binding. While type II cadherins include: cadherin 11 (CDH11) and cadherin 5 (CDH5) and form a distinct branch from type I. Through their distinct branch and distinct functions, they share domains for p120 and β-catenin.

All classical cadherins are composed of: five extracellular cadherin repeats, a transmembrane domain and a cytoplasmic domain. The cytoplasmic domain has binding sites for p120 catenin and β-catenin. This cytoplasmic domain signalling is largely mediated by cell adhesion, mechanotransduction and inhibition of EGFR and β-catenin (van Roy et al 2008).

Other cadherins exist, such as desmosomal cadherins, which include: desmoglein 3 (DSG3) and cadherin 13 (CDH13). These function by binding plakophilin and plakoglobin and are known to have a tumour suppressive role, mainly through loss of intracellular barriers, deregulation of WNT- β-catenin and inactivation of p53 mediated apoptosis through peripheral myelin protein 22 (PMP22) (Dusek et al 2011).

7D cadherins include: cadherin 16 (CDH16) and cadherin 17 (CDH17). These are structurally different to the other cadherins and have a characteristic seven vs the normal five units in the ectodomain, as well as a duplication of the first two cadherin repeats and a truncated cytoplasmic domain. Lastly, there are also protocadherins, the largest subgroup of 70, of which 50 are located on the same chromosome, which gives them their name clustered and non-clustered protocadherins. Their function is mainly involved in neural cells.

Biological Function

E-cadherin (*CDH1*) is a classical cadherin and the canonical gene lost during EMT progression, forcing cells to lose polarity and organisation, while its overexpression suppresses tumorigenicity, halts invasion and initiates apoptosis. The expression in differentiated tumours has an inverse relationship with tumour size, grade and mortality rates of patients (Birchmeier et al 1994, Hirohashi et al 1998). *CDH1* mutations have been found in gastric and lobular breast cancers (Strathdee et al 2002).

CDH1 is regulated by EMT promoters such as: SNAI1, SNAI2, SIP1, helix loop helix transcription factor E12 and E47. These all share their specificity for the E2 box on the *CDH1* promoter (Battle et al 2000, Cano et al 2000, Comjin et al 2001, Hajra et al 2002, Perez-Moreno et al 2001). Their binding to the *CDH1* regulatory region leads to promoter hypermethylation, a phenomenon observed in many cancers (Di Croce et al 2003). Interestingly, estrogen expression prevents loss of *CDH1* through metastasis associated 1 family member 3 (MTA3) mediated suppression of SNAI1 (Fujita et al 2003).

CDH1 loss also promotes invasion by upregulation of matrix metallopeptidase (MMPs) such as matrix metallopeptidase 2 (MMP2), matrix metallopeptidase 9 (MMP9) and matrix Mmetallopeptidase 14 (MMP14). These were all found in cancer cell cultures and tumour biopsies when the full length of *CDH1* is degraded (Nawrocki-Raby et al 2003). As mentioned, the role or CDH1 is vast, other examples of intracellular signalling partners are: protein tyrosine phosphatases and protein tyrosine kinases (Perez-Moreno et al 2003, McLachlan & Yap et al 2007), nd unsurprisingly, determinants of cellular polarity such as homolog of disc-large tumor suppressor (hDlg), a complex consisting of partitioning defective 3 (PAR-3), atypical protein kinase C (aPKC) and Par-6 family cell polarity regulator Alpha (PAR-6) (Laprise et al 2004, Iden et al 2006). CHD1 is also involved in growth factor

signalling, many epithelial tumours have high expression of EGF receptor EGFR (Bublil et al 2007), the importance of which for tumorigenesis was outlined earlier in this chapter. Secondly, CDH1 can modulate the cell response to EGF signalling (Qian et al 2004), either by autophosphorylating the receptor and increasing DNA synthesis or inhibiting EGF induced proliferation through an interaction of stat 5B (Perrais et al 2007).

Cadherin 2/N-cadherin (CDH2) has its function in neural tissues, and serves as an adhesion protein in synaptogenesis and organisation of the stress resistant intercalated discs of the heart important for heart muscle function. During EMT, the loss of CDH1 promotes expression of CDH2 as cells shift towards a mesenchymal state. CDH2 can bind to fibroblast growth factor receptor 1 (FGFR1) as a cis dimer, preventing ligand induced internalisation which keeps the signal switched on (Suyama et al 2002). FGFR activation, and ERK, MMP9 activity was shown to be an inducer of CDH2-mediated cell migration in mouse mammary tumour models (Qian et al 2013). In other cancers, such as pancreatic cancer, knockout models of CDH2 proved it was crucial for migration, invasion and metastasis (Shintani et al 2008, Su et al 2012). CDH2 overexpression is a response to an increase in type I collagen deposition on the ECM (Shintani et al 2006). It was also shown to be a viable target for melanoma and prostate cancer (Augistine et al 2008, Tanaka et al 2010). However, CDH2 expression can also prevent metastasis, as in the case of neuroblastoma (Lammens et al 2012). Interestingly during embryogenesis, it can also substitute some of the function of CDH1, but results in a lack of differentiated cell types of the intestine (Libusova et al 2010).

Cadherin 11 (CDH11) or otherwise known as osteoblast cadherin is also expressed in the mesoderm. Reported to have high expression in the stroma and epithelial cells in high grade prostate cancer, as well as being responsible for bone metastasis (Tomika et al 2000, Chu et al 2008), with the latter attributed to the homophylic attraction by CDH11 between cancer cells and bones, which normally have high ectopic expression (Chu et al 2008). There are also studies showing high expression of CDH11 in glioblastomas which when reduced, attenuated migration and cell survival (Kaur et al 2012). However, it is not limited to being a tumour promoter, there is also some evidence of CDH11 acting as a tumour suppressor in osteosarcomas, the further it was away from normal tissue, the less CDH11 was expressed (Nakajima et al 2008). This is probably due to normal bone cells having high expression. The same study suggests using CDH11 as a prognostic marker (Nakajima et al 2008).

Co-expression of CDH2 and CDH11 in mouse models of osteosarcoma lead to a reduction in lung metastasis (Kashima et al 2003). CHD11 is also silenced in lymph node metastasis of melanomas, head and neck cancers (Carmona et al 2012). When this expression was reintroduced, it reduced metastasis and tumour growth (Carmona et al 2012). CpG

methylation of the *CDH11* promoter occurs in breast cancer and in colorectal, liver, stomach, oesophaegeal and nasophasogeal cancers (Li et al 2012).

4.1.7 CEACAM5

Background

The human carcinoembryonic antigen (CEA) is related to a large superfamily divided into the 12 cellular adhesion molecules (CAM) and 10 pregnancy specific glycoproteins (PSG). The CEACAM is the Immunoglobulin subfamily of the CAMs which consist of immunoglobulins, integrins selections and cadherins. The CEACAMs play a role in tumour biology (Kuespert et al 2006), they are attached to the cell membrane through a glycophosphatidyl-inositol (GPI) anchor or a transmembrane domain. The members that are GPI linked are: CEA Cell Adhesion Molecule 1 (CEACAM1), CEA Cell Adhesion Molecule 3 (CEACAM3), CEA Cell Adhesion Molecule 4 (CEACAM4), CEA Cell Adhesion Molecule 5 (CEACAM5), CEA Cell Adhesion Molecule 6 (CEACAM6), CEA Cell Adhesion Molecule 7 (CEACAM7), CEA Cell Adhesion Molecule 8 (CEACAM8), CEA Cell Adhesion Molecule 19 (CEACAM19), CEA Cell Adhesion Molecule 20 (CEACAM20), and CEA Cell Adhesion Molecule 21 (CEACAM21). They utilise this GPI link to function as a cell adhesion molecule (Stanners et al 2007). CEACAM5 is a prognostic marker for pancreatic cancer with a correlation for shorter overall survival, and lymph node metastasis (Gebauer et al 2014).

Structure

Human carcinoembryonic antigen 5 (CEACAM5) consists of 7 domains which have a high association with the cell membrane and a complex expression between normal and tumour tissue. The structure is as follows, a variable like domain (N-domain), three repeating units of up to six constant C2-like Ig domains (A1, B1, A2, B2, A3, B3) (Beauchemin et al 2013). It also contains a 34-amino acid signal peptide.

Biological Function

CEACAM5 is overexpressed in gastrointestinal, lung, urinary and breast carcinomas (Shively e al 1985, Thompson et al 1991, Gold et al 1997, Hamarstom et al 1999). It has a similar function to CEACAM6, such as cellular adhesion, invasion and metastasis, which is achieved either through homophilic or heterophilic interaction (Benchimol et al 1989, Oikawa et al 1989 and Stanners et al 1998). The effect of CEACAM5 on invasion and

metastasis was first described in hepatocellular carcinoma and colorectal cancer (Thomas et al 1995, Yoshioka et al 1998). A recent RNA-seq study of patient derived xenograft (PDX) models of TNBC showed a metastatic driver role for CEACAM5. Its expression was inversely correlated with vimentin (mesenchymal marker). Furthermore, mouse models demonstrated high levels of CEACAM5 in metastasis sites compared to primary tumours, suggesting that its elevated levels promote MET, aiding the development of distal tumours (Powell et al 2018).

Therapy

A study looking into cancer cell lines from breast, pancreatic, colon and small cell lung carcinoma, has identified CEACAM6 as a highly expressed gene in these cell lines. By targeting CEACAM6 with a monoclonal antibody, they were able to yield a decrease in invasion, migration and cell adhesion (Blumenthal et al 2005). Through this early work, it is assumed that CEACAM5 could benefit from a similar approach. Other studies using CEACAM5 as a target show a benefit by reversing resistance to apoptosis and anoikis (Ordonez et al 2000, Soeth et al 2001). The benefit of such therapy is seen in an anti-CEA antibody called MN-14 has been shown to have favourable effects on the therapeutic effects of fluorouracil and Irinotecan (CPT-11) in colorectal cancer (Blumenthal et al 2004).

4.1.8 CNN2

Background

Calponin 2 (CNN2) is an actin filament associated with regulatory protein, with wide tissue distribution: smooth muscle, keratinocytes, fibroblasts, alveolar cells, endothelial cells, platelets, B lymphocytes myoblasts. Furthermore, the expression of CNN2 seems to be regulated by mechanotransduction. Initial experiments of cell culture on different substrates (hard vs soft) revealed less CNN2 expression on soft surfaces (Hossain et al 2005). Its distribution is related to its function in regulating the cytoskeleton and cell migration (Liu et al 2015). Other functions include: cell proliferation, cell adhesion and in the immune response (Huang et al 2008, Liu et al 2015).

Structure

As it is an actin filament associated with regulatory protein with 3 isoforms: calponin 1 (CNN1), calponin 2 (CNN2) and calponin 3 (CNN3), calponin has a structure with an N-terminal domain, a calponin homology (CH) domain, actin-binding surface 1 (ABS1) and

actin-binding surface 2 (ABS2) domains (which is part of the three repeating motifs), and a variable region which determines which isoform of calponin is made. CNN2 has a range of binding partners including actin, tropomyosin, tubulin, desmin, calmodulin, S100, myosin and phospholipids (Takahashi et al 1986, Childs et al 1992, Fuijii et al 1999, Mabuchi et al 1997, Fuijii et al 1994, Szymanski et al 1997, Bogatcheva et al 1995).

Biological Function

The promoter of *CNN2* contains a binding site for hairy and enhancer of split 1 (HES1). HES1 functions downstream of the Notch-Recombining binding protein suppressor of hairless (RBPJ) pathway, regulates gene transcription in response to external stimulus, like physical stress (Kageyama et al 1997, Morrow et al 2005). *HES1* deletion in mouse models corresponded with a high level of transcription for *CNN2* (Jiang et al 2014). CNN2 downregulation in prostate cancer leads to increased migration, proliferation and cell adhesion (Moazem et al 2014). An early mouse study suggested that the inhibitory effect is due to the effect of actin on myosin motor function, due to higher levels of activity of myosin II (Huang et al 2008). However, CNN2s effects are cell type context dependant as its expression promotes angiogenesis in endothelial cell lines (Tang et al 2006). CNN2 behaves differently in different primary tumours. In pancreatic ductal adenocarcinoma, CNN2 knockdown correlated with poor patient prognosis. This was followed with an upregulation of EMT associated signalling: PI3K/AKT, NF-$\kappa\beta$, vimentin, fibronectin, SNAI1, SNAI2, as well as a downregulation of E-cadherin (Qiu et al 2017). The opposite effect is seen in gastric carcinoma, where knockdown was associated with a reduction in those traits (Hu et al 2017). This suggests CNN2 behaves differently with different cancers. Few studies were done on breast cancer, only one suggests CNN2 as a potential marker, due to its high expression in PR- tumours and patients in the over 50 age group (Ji et al 2015).

Therapy

So far, no studies have been done on targeted therapy for CNN2. However, there are studies on CNN3 promoting drug resistance and invasion in colorectal cancer as its silencing increased sensitivity to 5-Fluorouracil, reduced mesenchymal markers and invasion (Nair et al 2019). Further studies on CNN1 revealed the same effect on apoptosis, invasion and cell adhesion, with a phenotype reversal seen by the binding of miR-106b-5p to CNN1 (Wang et al 2020). As CNN2 shares its structure with CNN1 and CNN3, it might have similar effects if targeted.

4.1.9 EFEMP1

Background

Epidermal growth factor-containing fibulin-like extracellular matrix protein 1 (EFEMP1), is a glycoprotein part of the fibulin family. It initially was identified as highly upregulated in Werner syndrome fibroblasts (Lecka-Czernik et al 1995), regulates MMP2 and matrix metallopeptidase 7 (MMP7) (Kim et al 2012). It has a wide distribution with some influence on body weight and behaviour (Lecka-Czernik et al 1995, Weedon et al 2008). Fibulins play a role in cell morphology, growth, adhesion and migration and with a dual role in tumorigenesis. In cancers, their functions are regulated by epigenetic mechanisms (Galagher et al 2005), which can partly explain why the same protein can have both tumour suppressive and oncogenic roles. For example, fibulin 1 (FLBN1), which has an inhibitory function in breast carcinoma motility with its variants 1D and 1C associated with breast tumours (Argraves et al 2003). An analysis of breast tumours had revealed a downregulation of EFEMP1 in over 60% of sporadic breast carcinoma cohort. Furthermore, this downregulation was mostly due to EFEMP1 promoter hypermethylation, and correlate highly with patient survival, and most pronounced in those under anthracycline adjuvant chemotherapy, leading the potential of EFEMP1 as a predictive marker for those patients (Saadr-Nabavi et al 2009).

Stucture

The family of glycoproteins contains five members, all sharing a tandem calcium binding epidermal growth factor EGF like modules, followed by a fibulin-type-C-terminal domain. They can be categorised as larger fibulins: FLBN1 and fibulin 2 (FLBN2), which contain an anaphylatoxin module which forms an extra domain, as well as containing more repeats of Calcium-binding EGF-like (cbEGF) modules. The structure varies between fibulins 1-5, with fibulins 3-7 having the shortest structure out of the rest of the family members, and consist of domains I-III. Both FLBN1 and FLBN2 are able to bind to ECM proteins like fibronectin, proteoglycans, tropoelastin, and other elastic fibres (Timpl et al 2003), in contrast to fibulin 3 (EFEMP1), which was shown to have weak binding to tropoelastin, and no binding to fibronectin, vitronectin, laminin-1, perlacan and nidogen-1 (Kobayashi et al 2007). Domain I consists of a cbEGF domain. Domain II contains 5 modified cbEGFs and a carboxy terminal domain III (Timpl et al 2003). Domain I of EFEMP1 has been described to have 5 splice variants (Lecka-Czernik et al 1995).

Biological Function

Literature shows that EFEMP1 promotes migration in gliomas (Hu et al 2009), which could partly be explained by its crosstalk with EGF receptors, which can activate the MAPK and AKT pathways (Camaj et al 2009). In breast cancer, EFEMP1 methylation results in downregulation and is associated with poor disease-free survival (Saadr-Nabavi et al 2009). Similar findings were found in colorectal, and hepatocellular carcinomas, which suggested a potential as a predictive marker (Nomoto et al 2010, Tong et al 2011). And more recently, it has been approved as a potential biomarker for prostate cancer (Shen et al 2017). It is involved in tumor progression of ovarian carcinoma (Chen et al 2013). Furthermore, traits like tumour progression, invasion, and lymph node metastasis were reversed in gastric cancer after the removal of the methylation (Zhu et al 2014).

EFEMP1s involvement with cancer stem cells is through activation of the hypoxia inducible factor 2 (HIF2)/EFEMP1 pathway. This promotes CSC renewal under hypoxic conditions. It has been shown that silencing EFEMP1 decreased tumour growth, CSC expression and chemoresistance (Kwak et al 2016). The restoration of EFEMP1 in breast cancer is thought to inhibit TGF-β, which abrogated the effects of EMT, and metastasis (Tian et al 2015). Potentially, this expression of EFEMP1 could be controlled through cancer exosomes (Qadir et al 2018).

4.1.10 EPHA4

Background

Erythropoeitin-producing hepatocellular (EPh) receptors are responsible for metastasis, cancer progression, angiogenesis and neovascularisation (Brantley-Sieders 2004, Brantley-Sieders et al 2004, Pasquale et al 2008), particularly in breast cancer (Vaught et al 2008). In invasive ductal carcinoma, EPH Receptor A4 (EPHA4) is highly overexpressed (Brantley-Sieders et al 2011). EPHA4 shows a high correlation with reduced overall survival, recurrence free survival and metastasis-free survival in patients with breast cancer (Brantley-Sieders et al 2011). The same is confirmed in colorectal cancer, with EPHA4 expression being a negative prognostic factor after concurrent chemoradiotherapy (CCRT) (Lin et al 2017). EPHA4 also appears to be a target for TGF signalling, later mentioned in this chapter. EPHA4 is required for TGF-mediated cell migration and is highly expressed in triple negative tumours. More importantly, the same study found that EPHA4 co-expressed along with TGFβ receptor type-2 (TGFβR2), and correlated with advanced tumour stage, tumour relapse and drug resistance (Hachim et al 2017). This coincides with previous findings, where EPHA4 expression is

associated with poor outcomes of breast carcinoma (Sun et al 2016). It is also implicated in enhancing migration of glioblastoma through EPHA4-FGFR1 signalling (Fukai et al 2008).

Structure

EPh receptors are the largest receptor tyrosine kinase family. Their ephrin ligands regulate cell-to-cell interactions (Himanen et al 2007 and Klein et al 2001). There are 16 Eph receptors and 9 ephrins which are divided into 2 subclasses: class A and class B (Himanen et al 2004). Class A interacts with glycosyl-phosphatidylinositol GPI linked class A nephrons and class B interacts with class B ephrins. Both interact with 8 ligands that are separated into five class A and 3 class B (Pasquale 2010). This gives very complex expression profile with multiple combinations of receptor-ligand interactions. Eph receptors structure is made up of a type I transmembrane proteins containing a N-terminal ectodomain. This ectodomain includes an ephrin-ligand binding domain (LBD), cysteine rich region, two fibronectin type III repeats. The ectodomain is separated by a transmembrane helix, which consists of: a juxtamembrane segment, a tyrosine kinase domain, sterile motif (SAM), PDZ binding motif. The basic function of the receptor is to bind using a hydrophobic ephrin loop into a ligands hydrophobic cavity (Himanen et al 2001).

Biological Function

They are involved in a lot of physiological processes such as bone formation, immune and inflammatory response, stem cell plasticity as well as vasculogenesis and angiogenesis (Pasquale et al 2008). They are frequently overexpressed in breast cancer and other solid tumours (Hafner et al 2004, Noblitt et al 2005, Sjoblom et al 2006). EPHA4 is the most interesting as it activates both A and B class ligands (Smith et al 1997, Egea et al 2005). A rarity despite both classes binding the same ligands, the signalling is usually class specific, mostly due to its ability to exist in two different conformations even in its unbound state (Singla et al 2010). Upon ephrin binding, EPHA4 forms signalling clusters at cell junctions and interaction with membrane proximal fibronectin domains (Xu et al 2013).

Therapy

A study done on the MCF7 and MDA-MB-231 cell lines, demonstrated that miR-335 expression inhibits cell proliferation, migration and invasion through downregulation of EPHA4 (Dong et al 2018). This is also the case when looking in context of chemotherapy sensitivity. EPHA4, along with other RTKS have been suggested to be involved in peripheral neuropathy (PN), a condition where the nervous system is damaged, something which occurs

with high doses of paclitaxel (a common chemotherapeutic agent for breast cancer). A recent study, looking into genetic variants of Eph receptors found EPH Receptor A5 (EPHA5) to be implicated in perineal neuropathy (Marcath et al 2019).

4.1.11 FGFR2

Background

Fibroblast Growth Factor Receptor 2 (FGFR2) is part of the FGF family and involved in a variety of cellular processes: embryogenesis, tissue homeostasis, carcinogenesis and oncogenesis of various tumour types (Eswarakumar et al 2005, Chaffer et al 2007, Dienstmann et al 2014). It is implicated in wound healing, angiogenesis, and cell migration (Ortega et al 1998, Campagni et al 2000) and recent studies showed also its implication in cell growth, differentiation and cell death (Turner et al 2010, Tout et al 2015, Zhao et al 2015). *FGFR2* amplification occurs in breast cancer but is uncommon, with only 2% of breast cancer cases and 4% of all triple negative breast cancers amplified (Turner et al 2010). Next generation sequencing reveals, the majority of FGFR mutations are only present in 7.1% of all cancers of which *FGFR2* represented 1.5% (Helsten et al 2016). This overexpression of FGFR2 was also confirmed in breast tumours (Sun et al 2010). However, it remains to be proved to have prognostic significance, as previous studies only showed associated lower overall survival and disease-free survival associated with lower FGFR2 expression (Sun et al 2012) and no effect on patient survival (Lee et al 2014). This contrasts to amplification of *FGFR1* which is reported in 15% of hormone positive breast cancer and 5% of triple negative breast cancers (Reis-Filho et al 2006 and Lee et al 2014). In MCF7 cells, FGFR2 mediated the upregulation of ADAM Metallopeptidase Domain 10 (ADAM10) and activated HER2 (Wei et al 2015 and Piasecka et al 2016).

Structure

FGFR2 is a member of the fibroblast growth factor receptor family, which is separated by ligand specificity and tissue localisation. Its extracellular region which interacts with fibroblast growth factors, consists of 3 immunoglobulin domains (D1-D3), a hydrophobic membrane spanning segment and a cytoplasmic tyrosine kinase domain 1 (TK1) and 2 (TK2), followed by a terminal carboxyl tail. It has two isoforms: FGFR2IIb and FGFR2IIIc. The former is found in the ectoderm and endothelial lining, and the latter is in the mesenchyme and craniofacial bone. There is also evidence of class switching between the two isoforms in prostate and bladder cancers (Carstens et al 1997, Chaffer et al 2007) which is followed by an increase in potential EMT.

FGFR2 shares its structure with FGFR1, Fibroblast Growth Factor Receptor 3 (FGFR3) and Fibroblast Growth Factor Receptor 4 (FGFR4) due to cytoplasmic tyrosine kinase domain and extracellular immunoglobulin-like domain (Ig-like). FGFR2 is either activated by fibroblast growth factor receptor substrate 2 (FRS2) or by others, with 4 main interacting pathways: mitogen-activated protein kinase(RAS-MAPK), Phospholipase C (PLC), Phosphoinositide 3-kinase (PI3K), Janus kinase/signal transducer and activator of transcription (JAK/STAT). Once a ligand binds to a receptor, causes dimerization and activation of the FGFRs. This in turn, phosphorylates FRS2 and fibroblast growth factor receptor substrate 3 (FRS3) and recruits Son of sevenless homolog (SOS) and growth factor receptor-bound protein 2 (GRb2) to activate MAPK, while growth factor receptor-bound protein 1 (GRb1) activates the PI3K pathway (Katoh et al 2006). PLC is an independent binding partner and binds to the autophosphorylated FGFR2, it enhances the MAPK signalling through the hydrolysis of phosphatidylinositol 4,5 biphosphate (PIP2), phosphatidylinositol 3,4,5 triphosphate (PIP3), diacylglycerol (DAG) and Protein kinase C (PKC), which in turn phosphorylate RAF.

Biological Function

FGFRs are responsible for crosstalk with the WNT, Notch and BMP pathways in carcinogenesis and cancer stem cell formation (Katoh et al 2006 and Katoh et al 2007). FGFR2 in turn has a vital role in proliferation, survival, differentiation and drug resistance (Fogarty et al 2007, Kunii et al 2008 and Yu et al 2014). There are nine FGFR2 single nucleotide polymorphisms (SNPs) that have been identified. (Easton et al 2007 and Hunter et al 2007). Single-nucleotide polymorphism (SNP) of intron 2 on FGFR2 has been associated with higher risk of breast cancer (Hunter et al 2007) which can increase susceptibility to the disease. Interestingly, differences are observed between breast cancer risk and expression of SNPs between populations (Chen et al 2016 and Butt et al 2012) and higher association with ER- and PR-positive disease (Garcia-Costas et al 2008). Two of these mutations, N550K and Y376C were shown to increase invasiveness in in vitro endometrial cancer models (Stehbens et al 2018). Point mutations on the other hand have been shown to be involved in drug resistance in breast cancer. Their effect takes place by increasing the capacity or specificity of the ligand binding to FGFR2. A study conducted by Byron et al (2013), showed 14 point mutations linked to dovitinib resistance, and are suggested to be induced through higher RTK activation and demonstrated that SNPs play a role in estrogen augmented response in breast cancer through the reversal of estrogen receptor 1 (ESR1) activation (Campbell et al 2016).

While a missense mutation of *FGFR2* has been identified in endometrial cancer and melanoma (Katoh et al 2014), activating mutations, which in *FGFR2* are more likely in

endometrial carcinomas and gastric cancer and occur in the kinase domain (Dutt et al 2008, and Greenman et al 2007) or chromosomal translocations, result in receptor dimerization without the ligand binding, the latter as a result of a part of the FGFR gene fusing with another protein. But these occur at low incidence rates (Wu et al 2013). Other ways in which FGFRs can be stimulated are due to autocrine signalling by the tumour or paracrine signalling from the tumour microenvironment. Secreted FGFs influence ligand specificity and receptor affinity by alternative splicing of the Ig III loop in the FGFR gene. FGF autocrine signalling can influence angiogenesis and EMT which is implicated in breast (Fillmore et al 2010), and other cancers (Shirakihara et al 2011).

Therapy

Small molecule inhibitors for FGFR2 in the form of protein kinase inhibitors (TKIs) have been described (Nobel et al 2004, Garber et al 2006). One of these is Ki23057 which targets FGFR2, FGFR2 and VEGF2. There were issues with TKIs, mainly in their toxicity and off target effects. Since then, other more advanced targeted therapies were seen in the form of next generation TKIs, small interfering RNA(siRNA), microRNA, and CRISPR with potent antiproliferative effects. TKIs, such as dovitinib and lucitanib, an antibody that targets both FGFR and VEGFR, is used in a clinical trial for breast cancer and other solid tumours as well as inhibitors ADZ4547 and BGJ398 (Andre et al 2013, Soria et al 2014, Tout et al 2015). Other alternatives such as monoclonal antibody drug conjugates of FGFR2 have been in testing (Sommer et al 2016).

4.1.12 FOXA1

Background

Forkhead box protein A1 (FOXA1) has strong expression in many cancers, and among them breast cancer. High expression has an association with good prognosis for the patients, and it is expressed in a lot of tissues e.g. breast, prostate, colon, and lung (Wolf et al 2007). It is very important in mammary gland development through regulation of the hormone response (Bernardo et al 2010). This protein was originally identified as a regulator of transthyretin and a1 antitrypsin in the liver (Costa et al 1989). FOXA1 is directly involved in breast development and is responsible for around 50% of ER-regulated genes (Carroll and Brown 2006). Silencing of *FOXA1* in ER+ breast cancer results in a reduction of almost all ER binding events (Hurtado et al 2011). This is a direct result of FOXA1, as studies have shown it not only directly binds to the *ESR1* promoter, thereby controlling ER expression

(Bernadro et al 2010), but also for its activity by allowing transcription of ER targets such as trefoil factor 1 (TFF1) (Beck et al 1999).

Structure

FOXA1 is a member of the FOXA family which is a member of the larger super family of forkhead box proteins. Its structure contains a DNA binding domain (Fox winged helix domain) which is unique to the fox proteins. The DNA binding domain is made of three α-helices and two wings. It also has conserved nuclear localisation sequence in its N- and C-terminal domains. What makes FOXA1 so special is its ability to open up chromatin for recruitment of transcriptional factors, which is why it is often referred as a pioneer factor (Bernardo and Keri, et al 2012). Its C-terminal domain interacts with histones H3/H4, and is functional in opening up chromatin (Cirillo et al 2002).

Biological Function

In cancer, FOXA1 has a dual role, both as a tumour promoter in the early stages of tumourigenesis and a suppressor at the later stages. For example, it can suppress the metastatic progression (Wolf et al 2007) though the overexpression of p27, a BRC1-associated cell cycle inhibitor, or directly increasing CDH1 expression. The expression of FOXA1 in breast cancer is around 70%, associated with the luminal subtype and not the triple negative breast cancers. Its expression highly correlates to tumour stage, size, lymph node involvement or overall survival and recurrence (Badve et al 2007). Interestingly, there were no survival benefits to adding cytotoxic drugs in combination with hormone therapy for HER2 negative patients with high FOXA1 expression (Hisamatsu et al 2012), however, high FOXA1 expression post treatment had an improved disease-free survival (Kawase et al 2013). It has also been shown to be highly correlated with androgen receptor expression in invasive breast cancer (Rangel et al 2018).

Furthermore, the downregulation of FOXA1 is associated with chemoresistance and stemlike characteristics. In a tamoxifen resistant ER+ breast cancer cell line, FOXA1 reduction increased IL6 expression and promoted tamoxifen resistance with higher mamosphere activity (Yamaguchi et al 2017). Studies show its importance in lineage switching and the EMT process of prostate cancer cells by controlling TGF-β signaling (Song et al 2018). In a breast cancer study, the overexpression of FOXA1 in a mesenchymal cell line MDA-MB-231 showed an increase in E-cadherin and decrease in SNAI2. The reverse effect was seen in an epithelial cell line MCF7 (Anzai et al 2017). Taken together it can be assumed it is involved in the progression of EMT. The same was found in gastric and pancreatic cancers, where

FOXA1 was associated with decrease in another EMT marker vimentin and proliferation (Lin et al 2018, Song et al 2010).

4.1.13 FOXO3a

Background

The FOXO family has a wide role in apoptosis (Chen et al 2017), proliferation (McClelland et al 2016) and the cell cycle (McGowan et al 2013), DNA damage response (Fluteau et al 2015) and tumorigenesis. It is also widely reported to be differentially expressed in primary tumours of the breast, colon, prostate, bladder and nasopharyngeal cancers. Primarily, its role is that of a tumour suppressor, and its inactivation leads to malignancy. First identified in the human placental cosmid, acts as a pioneer factor by affecting the expression and activity of target genes such as *CDH1*, the canonical gene responsible for EMT shift. It is also crucial for development of Alzheimer's disease and acute spinal cord injury and cardiovascular disorders (Wong et al 2013, Su et al 2009, Skurk et al 2005). Recently, it has become a biomarker for Hodgkin's lymphoma (Ikeda et al 2013) and other cancers (Qian et al 2017, Shou et al 2012, Rehman et al 2018, Ahn et al 2018, Yu et al 2015, Liu et al 2015, Jiang et al 2013, Lu et al 2012, Shi et al 2010, Fei et al 2009).

Structure

FOXO3a is part of the forkhead box protein family, which includes upward of 2000 members. The large family is subdivided into subfamilies: Forkhead transcription factor M (FOXM), Forkhead transcription factor K (FOXK), Forkhead transcription factor A (FOXA) and Forkhead transcription factor O (FOXO), the latter to which FOXO3a belongs. This subfamily has 4 members, Forkhead Box O1 (FOXO1), FOXO3a, Forkhead Box O4 (FOXO4), and Forkhead Box O6 (FOXO6). The structure contains 5 domains: the forkhead winged helix turn helix DNA binding domain (FKH), two nuclear localisation sequences (NLS), nuclear export sequence (NES), and a c terminal transactivation domain (TAD). The FKH domain is highly conserved and is responsible for binding to many of its DNA targets, while the NLS domain is responsible for FOXO3a translocation to the nucleus. Its TAD domain transactivates FOXO3a target genes. Some of its functions are to interact with ERα and p53 (Zou et al 2008, Wang et al 2008).

Biological Function

FOXO3a can be regulated in many ways, studies have demonstrated an upregulation of suppressor miRs result in downregulation of FOXO3a. For example, the case of miR-155, miR-132, miR-212 and miR-223 (Kong et al 2010) and miR-27a, whose attenuated expression directly correlates with FOXO3a expression (Ge et al 2013). Another example in breast cancer is the expression of miR-96 and its negative effect on FOXO3a targets, p27 and p21, which are checkpoint inhibitors for the cell cycle (Lin et al 2010, Nho et al 2014).

Other examples of regulation are shown in post translational modifications (Tikhanovich et al 2013, Sanphui et al 2013, Wang et al 2017), which affects the activity of FOXO3a and efficiency to how it binds to its interactive partners. Primarily, the main regulation is exercised through phosphorylation, which limits the translocation of the protein to the cytoplasm. This is achieved by PKB, ERK, Serine/threonine-protein kinase (SGK), Inhibitor Of Nuclear Factor κ B Kinase Subunit β (IKKβ) (Plas et al 2003, Finnberg et al 2004, Yang et al 2008, Luo et al 2016). Similarly, p38, macrophage Stimulating 1 (MST1) and AMP-activated protein kinase (AMPK) can phosphorylate FOXO3a and promote its nuclear import (Lehtinen et al 2006, Ho et al 2012, Sanchez et al 2012). The attenuated expression of all of these proteins shifts the balance between nuclear export and import, resulting in loss or gain of FOXO3a activity. This is not the full story, as the nuclear localised FOXO3a can also be modified by EP300 through acetylation and reversed by sirtuin 1 (SIRT1) and sirtuin 2 (SIRT2) (Giannakou et al 2012), which limits its DNA binding affinity for its target genes. There were examples of protein-protein interactions in cancer limiting FOXO3a activity, such as by c-Myc and latency-associated nuclear antigen (LANA2) causing avoidance of cell cycle arrest and avoidance of apoptosis (Chandramohan et al 2008). Other interactions like RUNX3 induce apoptosis through activation of BIM (Yamamura et al 2006).

The main step in which FOXO3a promotes carcinogenesis is by its phosphorylation and nuclear export into the cytoplasm, where it is subsequently ubiquitinated (Bader et al 2005, Guo et al 2013). As FOXO3a is an tumour suppressor, there are numerous examples of its activities influencing cancer survival traits. A known regulatory pathway is its control of apoptosis through promotion of miR-21, which activates Fas ligand, an initiator of apoptosis (Wang et al 2010). Similarly, FOXO3a limits oncogenic activities of MYC by directly repressing it (Delpuech et al 2007). In ER+ breast cancer, FOXO3a expression prevents cell survival by promoting cell cycle arrest through p21, p27 and p57 (Zou et al 2008). This same mechanism is activated by TGF-β mediated SMAD3 release and repressed by forkhead box G1 (FOXG1) (Seoane et al 2004); whereas its target RUNX3 is vital for the initiation of apoptosis in gastric cancer (Yamamura et al 2006). More importantly, FOXO3a has an antagonistic role with FOXM1 and both regulate ERα expression (Madureira et al 2006).

Other previous examples such as earlier mentioned FOXG1 (Seoane et al 2004), show an interplay between the FOX proteins.

Contrary to the function of FOXO3a as a suppressor of carcinogenesis, its expression and relationship to prognosis is cancer context dependent. Higher expression has been correlated with poor prognosis in triple negative breast cancer (Rehman et al 2018), hepatocellular carcinoma (Ahn et al 2018), glioblastoma (Qian et al 2017) and gastric carcinoma (Yu et al 2015), whereas low expression correlates to poor prognosis in glioma (Shi et al 2010) and ovarian cancer (Fei et al 2009).

As localisation of FOXO3a can reduce its activity, it is also useful for prognosis in luminal-like breast cancer (Habashy et al 2011), and helpful in determining chemotherapy response (Chen et al 2008, Kim et al 2017). Common chemotherapeutic agents used in breast cancer therapy also indirectly target FOXO3a and promote its activities, mostly through decreasing PKB phosphorylation and translocation of FOXO3a,leading to the potential of targeting FOXO3a for therapeutic purposes. An example of these is paclitaxel (Khongkow et al 2013), cisplatin (Wilson et al 2011), imatinib (Yang et al 2009) and lidamycin (Yang et al 2009).

4.1.14 GATA3

Background

GATA binding protein 3 (GATA3) is a master regulator, along with its other family members, and its loss in mouse models leads to embryonic lethality (Tsai et al 1994). It has been extensively studied due to its involvement in the development of the immune system (Tindemands et al 2014). All GATA proteins share some functional roles but also have distinct roles that are controlled by localised tissue expressed enhancers. This has been reflected in studies showing that while GATA3 is the main effector on interleukin 4, GATA binding protein 1 (GATA1), GATA binding protein 2 (GATA2) and GATA binding protein 4 (GATA4) can also activate its expression (Ranganath et al 2001). In the case of GATA3, these are in the urological, nervous system and endocardium and immune system, specifically in the natural killer cells (Lakshmanan et al 1999, Hosoya-Ohmura et al 2011). GATA3s main function is the development of lymphoid lineages and the haematopoietic progenitor stem cells (Fitch et al 2012, Tindemans et al 2014), such as regulating TH2 cells (Lee et al 2001), and if left unchecked, can lead to thymic lymphoblastoid tumours (Nawjin et al 2001).

Structure

GATA3 belongs to the family of zinc finger transcription factors which includes six members, GATA1, GATA2, GATA3, GATA4, GATA binding protein 5 (GATA5) and GATA binding protein 6 (GATA6). These transcription factors are known as master regulators. They all share a degree of homology, with GATA2 and GATA3 being 55% homologous. GATA3 contains a zinc finger motif 2 (ZNF2) on the C-terminus, which is responsible for binding to the promoter regions of target genes.zinc finger motif 1 (ZNF1) is at its N-terminus, and is responsible for interaction with nuclear factors. The zinc finger domains share 80% homology between all members. The C-terminal region is highly conserved in the family and has been shown to also be involved in chromatin remodelling of the *Th2* gene loci (Shinnakasu et al 2006). The binding of GATA proteins is determined by other co-regulatory proteins which modulate its activity through post translational modifications (Katsumara et al 2017). Studies have determined that GATA proteins can bind to DNA either as homodimers or heterodimers (Bates et al 2008). Low expression of GATA3 is a known predictor of poor survival and more aggressive disease (Oh et al 2006). GATA3 has a complex role in breast cancer, it can act both as a repressor and promoter of tumours (Eeckhoute et al 2007).

Biological Function

GATA3 has a crucial role in breast development, its expression is among the highest in the mammary epithelium (Kouros-Mehr et al 2006). Knockdown studies in mice have shown that it is responsible for proper formation of mammary ducts (Kouros-Mehr et al 2006) and is deleted in around 10% of breast cancers (Cancer Genome Atlas Network. 2012). Mouse models have demonstrated that its deletion results in tumour progression and migration (Kouros-Mehr et al 2008). Further studies showed that this is potentially done through promoting the expression of lysyl oxidase, a protein involved in matrix remodelling (Yan et al 2010, Chu et al 2011). When upregulated, it can result in the repression of metastasis transcription factors such as: inhibitor of DNA binding 1 (ID1), inhibitor of DNA binding 3 (ID3), keratin type II cuticular Hb1 (KRTHB1), lymphocyte antigen 6 family member E (LY6E), retinoic acid receptor responder protein 3 (RARRES3) (Dydensborg et al 2009). This repression is also known to act through its interactive partner BRCA1, an important gene in cancer progression. Through *BRCA1*, GATA3 repressses genes such as *FOXC1*, *FOXC2*, C-X-C Motif Chemokine Ligand 11 (*CXC11*) and *CDH3* to repress drug resistance and EMT (Tkocz et al 2011), as tumours are also known to hijack the inflammatory process to change the tumour microenvironment. The loss of GATA3s can also be another tumour survival mechanisms as it is known to regulate interleukin 4 (IL-4), interleukin 5 (IL-5)

and interleukin 13 (IL-13) (Kiwamoto et al 2006). Its role in EMT suppression is further bolstered by its activation of miR-29b, which is known to repress tumour metastasis and influence the tumour microenvironment (Chou et al 2013).

4.1.15 HEY2

Background

Hes Related Family BHLH Transcription Factor With YRPW Motif 1 (Hey1), Hes Related Family BHLH Transcription Factor With YRPW Motif 2 (Hey2) and Hes Related Family BHLH Transcription Factor With YRPW Motif Like (HeyL) are part of the helix loop helix factors (CHF) (Leimeister et al 1999). All of the genes have been identified in developmental tissues and can lead to organ defects if there is aberrant expression. The Hey genes can repress the transcription of cell fate regulators like achaete scute homolog 1, in doing so, they can maintain cells in an undifferentiated state (Sakomoto et al 2003). Furthermore, they also participate in early heart development by inducing epithelial to mesenchymal transition for differentiation of cells (Fischer et al 2003). The overexpression of HEY2 occurs in multiple cancers: prostate, hepatocellular, pancreatic ductal adenocarcinoma and hemangioma (Cavard et al 2009, Tradonsy et al 2012, Wu et al 2016). It is associated with poor survival in hepatocellular carcinoma and prostate cancers (Trodondsky et al 2012, Wu et al 2016).

Structure

Hey genes are homologs to the hairy and enhancer of split (Hes) family. They share 4 domains: basic, helix loop helix (HLH), Orange, and 2 C terminal motifs. They can attach to E-box DNA sequence through the glycine rich basic domain (Iso et al 2001). Their HLH domain can interact with cofactors, HEYL and HEY2. There is some evidence of transcriptional regulation of HEY2 (Lopez-Mateo et al 2016). With evidence that there is a variety of Hey variants, the regulation allows for dual nature of HEY gene repression and activation of the same genes in different contexts.

Biological Function

In regulating cancer metastasis, previous studies showed that HEY1 has a role in inducing EMT. HEY2 has a similar function. Both genes have been shown to promote MET in melanoma by repressing EMT genes SNAI2 and TWIST through their promoter regions (Bonyadi et al 2016). As Hey genes are involved in embryogenesis, and cancer cells hijack

the stem cell characteristics for survival. It is not surprising that their levels are elevated in tumour initiating cells or cancer stem cells compared to their non CSC counterparts (Yamamoto et al 2013). Furthermore, there is a role for Hey genes in proliferation as HEY2 overexpression increases the proliferation of cells in hepatocellular carcinoma (Kuo et al 2015). The other way in which Hey genes confer cancer adaptation is by promoting neovascularisaion. VEGFR2 has been shown to increase vascular sprouting, but its action were suppressed by HEY1 and HEY2 (Taylor et al 2002, Larrivee et al 2012). Some evidence shows this is due to the activation of the BMP and ALK pathway (Larrivee et al 2012, Ricard et al 2012).

Many pathways control HEY gene expression. The Notch pathway promotes invasion. Inhibition of Notch via a γ-secretase inhibitor, decreased invasion through decreased HEY gene expression (Chen et al 2010). The TGF-β pathway acts independently of Notch to activate the Hey genes. This was shown to be the case when Hey genes were activated by TGF-β1 induced SMAD3/4 under γ-secretase treatment (Zavadil et al 2004), as well as being activated by BMP9 through SMADs 1,5 and 8 (Sharff et al 2009, Larrivee et al 2012, Ricard et al 2012). HEYL, another member of the HEY family has been shown to promote breast cancer through Notch inhibition of TGF-β signalling (Han et al 2014). And more recently, HEY2 has been shown to be a co repressor of SMAD3 and SMAD4 in hepatocellular carcinoma which abrogates TGF-β signalling for growth inhibition (Wang et al 2019).

4.1.16 HMCN1

Background

Hemicentin-1 (HMCN1), also known as fibulin-6, is an extracellular matrix protein, first discovered in C.elegans. Initial studies were done on worms and it was found that HMC1 is responsible for maintaining structure and cell to cell and cell to ECM interactions. It also directs this attachment by forming tracks on both the basement membrane and the cell, to direct the position of the cell (Sherwood et al 2018). In a study on myocardial infarction, the tracks and remodelling of the myocardium is thought to be done through regulation of TGF (Chowdhury et al 2017). It plays an integral role in connecting tissues together through forming a basement membrane adhesion complex (B-LINK). However, the function of the B-Link complex has not been fully understood, although it is hypothesised that HMCN1 interacts with integrins, potentially as a ligand (Morrissey et al 2014). Other proteins can also be involved in this such as collagen $\alpha 3\alpha 4\alpha 5$(IV) (Keeley et al 2019). Another recent study pointed out HMCN1s potential function in podocyte dysfunction, as increased HMCN1

impedes TGF- mediated podocyte formation in diabetic glomerular disease (Toffoli et al 2018).

Structure

The structure of hemicentins consist of a Von WIlllerband A (VWA) domain, then a HMCN motif, followed by 48 immunoglobulin domains, 3 EGF repeats and lastly 1 fibulin-like carboxyl terminal module (Vogel et al 2006). The EGF and fibilun-like carboxyl terminal module help hemicentin monomers to interact and assemble (Dong et al 2006). The VWA domain is important for cell adhesion by interacting with ECM proteins as it exists among other ECM proteins (Whittaker et al 2002). This shared domain is likely a reason for its compensated function in knockout models, where no loss of function was seen in HMC1-/- mice (Lin et al 2020).

Biological Function

Few studies are available into the function of HMCN1 in cancer. An investigation into variant allele frequency of *HMCN1* in breast cancer, revealed that certain variants correlated with lymph node status but not tumour grade or size. However due to lack of availability of data for the survival time in datasets, the prognostic value of HMCN1 could not be determined (Kikutake et al 2018). However, an analysis by another group of using 4 datasets (including TCGA and METABRIC) found that HMCN1 was expressed highly in triple negative breast cancer along with titin (TTN), reelin (RELN), polycystic kidney and hepatic disease 1-like 1 (PKHD1L1), dystrophin (DMD), fraser extracellular matrix complex subunit 1 (FRAS1) and ryanodine receptor 3 (RYR3) (Saravia et al 2019). HMCN1 was also shown to promote ovarian cancer through cancer associated fibroblast invasion and migration (Liu et al 2019).

4.1.17 ITGA2 and ITGA3

Background

Integrin subunit alpha 2 (ITGA2) and Integrin subunit alpha 3 (ITGA3) are fundamental units in the cell adhesion process and regulate a lot of cell function in various scenarios (Hamidi et al. 2018, Winograd-Katz et al. 2014). The deregulation of integrins has been extensively addressed and linked with cancer (Seguin et al 2015, Hamidi et al 2016, Raab-Westphal et al 2017), where they have a dual function. Prominent members of the integrin family such as $\alpha 3\beta 1$ promote mammary tumorigenesis (White et al 2004, Cagnet et al 2014), while $\alpha 2\beta 1$ acts as a metastasis suppressor (Ramirez et al 2011). Other types of integrins

exist, such as the laminin binding integrins, also with a dual function in promotion and suppression of tumours (Ramovs et al 2011).

The $\beta 1$ subunit is highly correlated with the stiffening of ECM (Paszek et al 2005). This results in more formation of focal adhesion points at the leading edge of invading cells, which occurs with activation of focal adhesion kinase (FAK) and AKT (Rubashkin et al 2014). This stiffening of the ECM is promoted by $\alpha 2\beta 1$ through the upregulation of lysyl oxidase enzymes (LOX) (Gao et al 2016), an enzyme that induces cross linkage within the ECM (Cox et al 2013). The same can be said for integrins which act through the TGF-β pathway; cancers will be suppressed until they flip a biochemical switch and the same pathway will now promote growth (Moore et al 2014). In relation to EMT, $\beta 3$ initiates the process indirectly as a response to depletion of $\beta 1$ (Truong et al 2014). There is also extensive research on how integrins promote stemness (Seguin et al 2015) and how their high expression on exosomes is involved in priming the metastatic niche (Hoshino et al 2015).

Structure

Integrins are a family of 24 transmembrane heterodimers, which is a combination of 18α and 8β subunits. These can be further classified based on their interacting ligands. Such as: arginine-glycine-aspartic acid (RGD) peptide motifs, collagen receptors, laminin and leukocytes (Humphries et al 2006). Integrin expression can influence the formation of small nascent adhesion or large focal adhesions and rigidity sensing through myosin II (Schiller et al 2013). These subunits combine through non-covalent interactions to form a ligand binding head, two multi domains and two cytoplasmic tails. Each leg contains a thigh, Calf-1 and Calf-2 domains, supporting a ligand binding head (7 repeat b propeller). This propeller has calcium binding EF-hand domains which has an allosteric effect on ligand binding, and an additional αl domain that contains a metal ion dependant adhesion site (MIDAS). The β subunits are made up of 4 cysteine rich epidermal growth factor repeats, hybrid domain, I-like domain ($\beta 1$), and a plexin sempaphorin integrin (PSI) domain. It also contains a MIDAS and an additional regulatory site adjacent to MIDAS (AMIDAS). When a ligand binds with both $\beta 1$, al, the MIDAS then induces a conformational change. On the cytoplasmic side, the tail portion is assisted by adapter proteins such as talin, tensin, which link integrins to the cytoskeleton. Scaffolding proteins such as paxillin and kindlin connect it to the focal adhesion proteins, while catalytic adaptors such as FAK, integrin linked kinase (ILK) and SRC Proto-Oncogene, Non-Receptor Tyrosine Kinase (Src) aid in signal transduction from the adhesion site.

Biological Function

An integrin binds to the ECM through its globular head domain, it assembles direct and indirect links via its tail portion on the cytoplasmic side, containing scaffolding proteins, cytoskeletal proteins, and signalling proteins (Hynes et al 2002). They have a variety of functions: blocking apoptosis through PI3K and AKT, stimulating the cell cycle through ERK and cyclin D1 and controlling cytoskeletal reorganisation through ROCK, myosin light-chain kinase (MLCK). All of these are anchorage independent in cancer. They also have a secondary function recognising pathogens, toxins and viruses (Arruda Macedo et al 2015 and Hussein et al 2015). Integrins interpret the external stimulus, biochemical or mechanosensor, via inside-out and outside-in signalling. An initiated signal cascade can have implications on cell survival, migration, polarity and differentiation, and it can be a precursor to cancer progression (Winograt-Katz et al 2014). Integrins also promote ECM contraction and actin polymerization through interaction of FAK and filopodia which result in cell migration (Chan et al 2008, Gardel et al 2008). Alongside with this polymerization, there is also reorganisation of collagen, which serves as a good predictor for breast cancer migration (Provenzano et al 2006). Loss of E-cadherin is one of the hallmarks of the EMT switch, which is exhibited in all cancers This loss can be initiated by $\alpha 2\beta 1$ when it interacts with type I collagen (Wipff et al 2008). And when activated alongside discoidin domain receptor 1 (DDR1), it upregulates N-cadherin (Yasushi et al 2008). Furthermore, integrin links with fibronectin, another component of the ECM, that inhibits cell-cell adhesions (Borghi et al 2010) and junction stability (Canel et al 2010). A process, largely driven by $\beta 1$ activated src kinase which increases actomyosin contraction (Martinez-Rico et al 2010) and E-cadherin internalisation (Canel et al 2010).

During invasion, integrins assist in upregulating MMPs during intravasation of cancer cells (Munshi et al 2006, Yue et al 2012). This has been proven to be the case with ovarian (Ahmed et al 2002), colon (Gu et al 2002), breast (Baum et al 2007) and glioma (Kasenakurti et al 2013). Additionally, interaction with cancer associated fibroblasts can pave the way through the ECM with fibronectin (Gaggioli et al 2007). Once a cell arrives at a new distal site from the primary tumour, the cells undergo MET, which is induced partly by endocytosis of integrin $\beta 1$ and by hepatocyte growth factor (HGF) signalling (Barrow-McGee et al 2016). Integrin $\beta 1$-$\beta 4$ have shown to form a signalling complex with MET (Trusolino et al 2001, Mitra et al 2011, Yoshioka et al 2013). A zebrafish model of transendothelial migration established that $\beta 1$ is vital for the remodelling of the vascular endothelium and attachment to the blood vessels (Stolekov et al 2010). There was also evidence that $\beta 1$ was vital for dormant cancer cells to switch on their invasive properties (Barkan et al 2008). Inhibition of $\beta 1$ integrin is related to decreased metastasis in breast cancer (Huck et al 2010). Filopodia

inducing motor protein Myosin-X (MYO10) is another protein that accounts for motility and is reliant on integrin expression. A gene analysis of breast cancer revealed high expression of MYO10 in triple negative and HER2 breast cancer, and correlates with lung extravasation (Arjonen et al 2014). The integrin pathway is also hijacked by circulating tumour cells to avoid anoikis, the cell death process which is initiated after loss of anchorage to the ECM (Strilik et al 2017). Anoikis resistance occurs, at least partically, through other non-structural ECM components like cysteine-rich angiogenic inducer 61 (CYR61), that contains several integrin binding sites (Lau et al 2016). Elevated levels of CYR61 have been confirmed in advanced breast cancer (Xie et al 2001) and in triple negative breast cancer, serving as an activator of β1 and 5' AMPK, independent to AKT,FAK and ERK1/2 (Huang et al 2017).

Therapy

In relation to therapy, there have been mouse mammary tumour studies showing β1 integrin and src activity promotes resistance to trastuzumab, pertuzumab (both anti HER2) and buparlisib (anti PI3K) (Hanker et al 2017). Similar findings have demonstrated EGFR-targeting drugs in lung cancer (Kanda et al 2013), and resistance to radiotherapy in head and neck cancer (Eke et al 2015). Another example is αvβ3 integrin which confers resistance to RTK inhibitors in breast and lung cancer, as well as acquiring stemness properties (Seguin et al 2015). Initially, the targeting of integrins suggested tumours were sensitised to radiotherapy (Park et al 2008, Hu et al 2016). Regrettably, solely targeting integrins in clinical trials has not yielded favourable outcomes in glioblastoma (Mason et al 2015) and kirsten rat sarcoma viral oncogene homolog (KRAS) metastatic colorectal cancer (Elez et al 2015). This might be partly due to a tendency for integrin cycling in tumours, such as the case with breast cancer (Parvani et al 2013).

4.1.18 MUC5B

Background

Mucin 5b (MUC5B) is part of a family of mucins, heavily glycosylated proteins that have a key characteristic to form gel-like substances and aid cell signalling, as well as forming chemical barriers (Marin et al 2007). They are involved in reducing the immune response in two ways, they reduce the function of dendritic cells which present antigens to T cells, thereby preventing activation of other immune cells such as NK cells. Secondly, they lower the access of therapeutic drugs (Gottfried et al 2008, Jonckheere et al 2014). There are over 20 mucin genes, which include: Mucin 1, Cell Surface Associated (*MUC1*), Mucin 2, Oligomeric Mucus/Gel-Forming (*MUC2*), Mucin 3A, Cell Surface Associated

(*MUC3A*), Mucin 3B, Cell Surface Associated (*MUC3B*), Mucin 4, Cell Surface Associated (*MUC4*), Mucin 5AC, Oligomeric Mucus/Gel-Forming (*MUC5AC*), Mucin 5B, Oligomeric Mucus/Gel-Forming (*MUC5B*), Mucin 6, Oligomeric Mucus/Gel-Forming (*MUC6*), Mucin 7, Secreted (*MUC7*), Mucin 8 (*MUC8*), Mucin 12, Cell Surface Associated (*MUC12*), Mucin 13, Cell Surface Associated (*MUC13*), Mucin 15, Cell Surface Associated (*MUC15*), Mucin 16, Cell Surface Associated (*MUC16*), Mucin 17, Cell Surface Associated (*MUC17*), Mucin 19, Oligomeric (*MUC19*),Mucin 20, Cell Surface Associated (*MUC20*) and Mucin 21, Cell Surface Associated (*MUC21*) (Perez-Vilar et al 2004, Norman et al 2017). Mucins are produced in many adenocarcinomas such as lung, pancreas, breast, ovary and colon. A member of the family *MUC1*, has been linked to gastric cancer formation (Niv et al 2008) and is related to poor prognosis in breast cancer (Jing et al 2018). The highest expression of *MUC1* is in HER2+ tumours and is regulated by HER2 through the PI3K/AKT, independently of Ras/MEK pathways (Conley et al 2016).

Structure

Mucins have two regions aglycosilated region which contains cysteine rich amino acids, and a carboxy terminal region. It also contains a large central region, consisting of several repeats, each 10-80 residues long. Usually the repeats can consist of either O or N-linked oligosaccharides.

Biological Function

MUC5B can promote lung fibrosis in mice (Hancock et al 2018) and it is suggested that it is associated with idiopathic pulmonary fibrosis in humans with polymorphism of MUC5B (Armesto-Jimenez et al 2019). In lung cancer, MUC5B is among the most highly overexpressed proteins with potential as a biomarker (Li et al 2013). This overexpression is in part helped by its long non-coding RNA (lncRNA) MUC5B-AS1, which binds to MUC5 forming a duplex, increasing migration and invasion (Yuan et al 2018). The same lncRNA MUC5B-AS1 was found to be highly expressed in ER/PR+ breast cancer (Zaheed et al 2020). The study also confirmed MUC5B-AS1 overexpression in breast cancer cell lines MCF10DCIS, ZR-75-30, SK-BR-3 and MDA-MB-213 (Zaheed et al 2020). An earlier study found MUC5B overexpressed in primary tumours. However, out of all breast cancer cell lines, only MCF7 was found to express it (Berois et al 2002). This overexpression of MUC5B in MCF7 is related to a more aggressive phenotype (Valque et al 2012). Downregulation of MUC5B in gastric cancer reduces cell proliferation, migration and invasion, acting through the WNT/ β-catenin pathway (Lahdaoui et al 2017).

Overall, studies suggest MUC5B to be a marker of some importance in breast cancer. Further studies on breast cancer revealed that shRNA silencing of MUC5B decreased cell adhesion, proliferation and lower clonogenic efficiency. There was also increased sensitivity to 5-Fluorouracil and cisplatin (Garcia et al 2016). Previous studies of pancreatic cancer attributed this down regulatory effect of MUC5B on migration and growth due to a decrease in α- and β-integrins and VEGF (Yamazoe et al 2010, Hoshi et al 2011,). Furthermore, a number of malignancies including cancer are associated with O-glycosylation as one of the hallmarks of cancer (Weinberg et al 2015). A recent study outlined a link between MUC1 and EGFR signalling, which initiates this O-linked glycosylation (Tajadura-Ortega et al 2019). There is potential that MUC5B might share a similar function. Furthermore, there is also mucinous breast cancer, which represents about 4% of all breast cancers, which expresses all mucins highly, among them MUC5B. A comprehensive review was recently written (Marrazzo et al 2020).

4.1.19 PLS3

Background

Plastin 3 (PLS3), otherwise known as T plastin, is part of a family of plastins, whose main function is to bind to actin. They exist in 3 isoforms: Lymphocyte Cytosolic Protein 1/plastin L (LCP1), plastin T/PLS3 and plastin 1/fibrin (PLS1), and hare expressed in hematopoietic cells (Goldstein et al 1985), normal cells (e.g. endothelial, mesothelial) (Lin et al 1988) and in the small intestine (Bretscher et al 1980). There is also an I plastin isoform which is 86% identical to fibrin (Lin et al 1994). These plastins usually localise at place of contact and motility, such as focal adhesions, lamellipodia, filopodia, membrane ruffling and other microfilaments. Overexpression of PLS3 or L plastin had a cell type context dependent role. In fibroblasts, it prompted a round cell shape, reorganisation of actin stress fibres and less focal contacts; whereas in epithelial cells there was an increase in length and density of microvilli (Arpin et al 2008).

Structure

Plastins have a structure containing two amino terminal EF hands which are calcium binding, and two tandem actin binding domains, each subdivided into two calponin homology domains (CH) (Korenbaum et al 2002). The CH domains bind to actin and actin-related cytoskeletal proteins such as dystrophin, spectrin and α-actinin. The CH domain itself is composed of 4 α-helix segments, followed by extended or variable loops or 2 short helices. The complete structure of plastins is yet to be confirmed. Furthermore, the CH binding

domains CH1 and CH2, actin binding domain (ABD1), CH3 and CH4 and actin binding domain 2 (ABD2) have different conformations in which they attach (Garcia-Alvatez et al 2003, Klein et al 2004, Liu et al 2004). This follows previous evidence that the ABD1 attaches to two subdomains of actin (Hanein et al 1998).

Biological Function

Plastin function is regulated by calcium, as suggested by early studies such as that from Hanein et al (1998) although different isoforms seem to confer different responses to calcium (Giganti et al 2005). Otherwise, plastin function may be regulated by phospholipids and phosphorylation. Preliminary studies were exclusively done on L plastin and indicate some regulation on its binding to actin (Matsudaira et al 1979, Shinomiya et al 1995). PLS3 is involved in the binding of actin, its turnover, stabilisation and assembly (Giganti et al 2005); but it has low activity and is thought to be regulated through methylation of upstream CpG islands of its promoter (Liu et al 1999). In cancer, most focus was placed on researching L plastin. It has been shown to have an overexpression between transformed cells and controls (Leavitt et al 1982), and has been found upregulated in 68% of epithelial carcinomas and 53% of mesenchymal tumours (Lin et al 1993). It has since been considered a marker for cancers (Leavitt et al 1994). Recently, L plastin has been shown to regulate immune cell function by stabilising T cell synapses, migration of macrophages and priming neutrophils, reviewed by (Morley et al 2012, Morley et al 2013). Early studies of PLS3 suggested its association with cisplatin resistance due its higher expression in cisplatin resistant cell lines (Hisano et al 1996).

More recently, PLS3 has been identified as a marker for circulating tumour cells undergoing EMT in breast cancer patients, as well as predicting poorer prognosis when highly expressed (Yokobori et al 2013, Ueo et al 2015). It also correlated with other tumour associated markers in leukemic T cell lymphoma (Capriotti et al 2008). Follow up studies with a PLS3 targeting peptide PT1 show promise in identifying the circulating tumour cells (Shi et al 2019). It has also more recently been shown to be vital for basal membrane formation in mouse epithelium by controlling the localisation and activation of myosin II, as well as having secondary effects on cell polarity (Dor-On et al 2017). *PLS3* silencing in a triple negative breast cancer cell line MDA-MB-231 shows an increased sensitivity to paclitaxel through the p38 MAPK pathways (Ma et al 2019).

4.1.20 SGCG

Background

γSarcoglycan (SGCG) is part of a family of sarcoglycans (-) primarily expressed in striated muscle (Noguchi et al 1995). Their mutations are linked with muscular dystrophy and cause disruption in the dystrophin associated protein (DAP) complex (Vainzoff et al 1996). This DAP complex is essential for the stability of the muscle cell membrane and interaction between fibres. The main role of sarcoglycans is to stabilise dystrophin-glycoprotein complexes that associate with F-actin and helps interaction with the ECM. Other functions of SGCG have been proposed such as cell communication, metabolism and ion regulation (Ervasti et al 2008). SGCG mutations in particular, can lead to limb-girdle muscular dystrophy (Kerch et al 2014). In the context of cancers, the role of sarcoglycans has not been well studied. One study shows that breast cancer tissue has low expression of all the sarcoglycans, which suggests to be helpful in severing cell-cell adhesions (Arco et al 2012).

Structure

Initial structure of SGCG was described as a type II transmembrane protein, consisting of a casein kinase II phosphorylation site, and an N-linked glycosylation site (Campbell et al 1989). A purified SGCG has only just recently been isolated (Jamaleddine et al 2019).

4.1.21 SNAI2

Background

SNAI2 (slug) is one of three members of the snail family of zinc finger transcription factors. It is widely known to be the canonical EMT transcription factor (Barral-Gimeno et al 2005). SNAI2 has recently been found to act antagonistically with SNAI1 in highly invasive breast tumours through regulation of phospholipase D isoform 2 (PLD2) (Ganesan et al 2015). The usual tumorigenic advantages are gained with its overexpression, such as an increase in invasive capacity and migratory ability, combined with the loss of E-cadherin, leading to loss of cell adhesion and cell polarity (Hajra et al 2002, Bolos et al 2003). It is also a key player in developmental biology such as with the neural crest formation (Cobaleda et al 2007). A large body of evidence also shows the overexpression of SNAI2 in various cancers leads to poor prognosis (de Herros et al 2010, De Crane and Berx et al 2013). It is largely controlled by TGF-β, Notch and WNT pathways, as well as regulation by epidermal

growth factors. It is also associated with an aggressive phenotype in endocrine-resistant ER+ breast cancer (Alves et al 2018).

Structure

The structure of SNAI2 comprises five consecutive C-terminal zinc fingers which can bind to the E-box motif and an N terminal snag domain which can recruit chromatin regulators. The central region of SNAI2, differs from the rest of the family as it lacks a destruction box and nuclear export signal. Instead, it has a SLUG domain that interacts with cofactors such as SIRT2 that impact its function (Zhou et al 2016). SNAI2 has been known to silence genes such as *ESR1*, *CHD1* and *PUMA* (Bolos et al 2003, Wu et al 2005, Bai et al 2017).

Biological Function

As it has a role in developmental biology, SNAI2 controls lineage differentiation of hematopoietic stem cells (Perez-Losada et al 2002) and the differentiation of epidermal cells (Mistry et al 2014). Another function is to help progenitor cells to survive by inhibition of apoptosis through Signal Transducer And Activator Of Transcription 3 (STAT3) (Castillo-LLuvo et al 2015) and facilitating a DNA damage response (Gross et al 2019). Furthermore, in cancer biology, it confers stem cell survival characteristics, remodels vascular endothelium and induces the DNA damage response (Storci et al 2010, Whelch-Rheadon et al 2014, and Gross et al 2019). In breast cancer, SNAI2 was associated with stemness characteristics (Bhat-Nahkshatri et al 2010, Guo et al 2012). It is directly linked with basal characteristics in *BRCA1* mutation human mammary epithelium (Proia et al 2011). Furthermore, another characteristic advantage of SNAI2 overexpression is drug resistance. A number of studies have shown that SNAI2 depletion shows a reversal of this trait, in the case of radiosensitivity, RTK inhibitors, doxorubicin and cisplatin (Arienti et al 2013, Chang et al 2011, Dong et al 2016, Haslehurst et al 2012).

4.1.22 TGFβ2

Background

Transforming Growth factor $\beta 2$ (TGF$\beta 2$) is involved in apoptosis, proliferation and differentiation of cells (Derynck et al 2008). Initially isolated in transformed rat kidney fibroblasts (de Larco et al 1978) and described to be able to induce fibroblast growth (Roberts et al 1986), inhibit cell proliferation (Tucker et al 1984), it is involved in EMT, migration, differentiation and matrix formation (Moustakas et al 2005). TGFβ isomers have a function

related to their tissue localisation: TGFβ1 in cartilage, bone and skin (Dickinson et al 1990), TGFβ2 in glioblastoma cells, neurons and the embryonic nervous system (de Martin et al 1987) and Transforming Growth factor β3 (TGFβ3) in the lung, kidneys and umbilical cord (ten Dijke et al 1988). A recent study found higher levels of TGFβ1 and TGFβ3 in breast cancer patients, and this was associated with higher migration into lymph nodes and metastasis (Hachim et al 2017). The same study cites association isoforms and their receptors with cancer type. Expression of the ligands and receptors seems to correlate in solid tumours e.g. TGFβ1 and TGFβ3 are overexpressed with transforming growth factor, beta receptor II (TβRII), while TGFβ1 with transforming growth factor, beta receptor I (TβRI) (Hachim et al 2017).

Structure

The protein superfamily includes bone morphogenic proteins (BMPs), growth differentiation factors (GDFs), activin/inhibin, and the glial cell line derived neurotrophic factor (GDNF). The TGFβ family, can exist as homodimers, or heterodimer polypeptides (Ohta et al 1987), and consists of 3 isoforms: TGFβ1, TGFβ2 and TGFβ3 (Cheifetz et al 1987). The protein is composed of homodimers stabilised by disulphide bridges. The biogenesis of which begins with a pro-protein with latency associated proteins (LAP) amino terminal pro domains (Gray et al 1990). Once the pro-protein isoform forms a dimer, the LAP initiates folding of the tertiary structure. This dimer is then cleaved and at the same time associates with its pro-peptide as a large latent complex (LLC). The LLC as a finished product, gets secreted into the ECM, along with a latent TGFβ binding protein (TLTBP) (Miyazono et al 1988). The TLPBP is instrumental in TGFβ bioavailability as it acts as an intermediary for attachment to the ECM (Taipale et al 1994).

TGFβ acts through its associated receptors: TβRI, TβRII and transforming growth factor, beta receptor III (TβRIII), of which TβRIII is the more abundant and expressed by many cell types (Cheifetz et al 1988). These receptors can be regulated by post translational modifications which limit their availability e.g. phosphorylation, ubiquitination and sumoylation. Receptor activation through phosphorylation leads to TGFβ2 binding with TβRI and TβRII, forming a large ligand receptor complex (Shi et al 2003), except in the case of TGFβ1 and TGFβ3, which both bind exclusively to TβRII (Derynck et al 1997). This cascade of TGFβ activation can be initiated with a number of upstream proteins such as retinoic acid, fibroblast growth factor 2, plasmin, MMP-2 and MMP9 (Sato et al 1989, Flaumenhaft et al 1992, Kojima et al 1993, Yu et al 2000).

Activated TGFβ2 can initiate signalling through the canonical or non-canonical pathways. The canonical signalling pathway signal is propagated by the SMAD proteins, their effects

are cell type dependant. This pathway is initiated by DNA binding transcription factor families such as: forkhead box (FOX), Homeobox-leucine zipper protein (HOX), Runt-related transcription factor (RUNX), E2F Transcription Factor (E2F), Activator protein (AP1), cAMP response element binding protein (CREB)/Activating transcription factors (ATF) and Zinc-finger, among others (Messague et al 2015). Notably for our study, it is interesting to note the interaction between SMAD proteins MH1 domain and the transcriptional co-activators CBP and EP300 (Feng et al 1998, Pouponnot et al 1998, Topper et al 1998, Pearson et al 1999), which reveals another regulation on this pathway. The non-canonical pathway involves signal propagation through Wnt/β-catenin, nuclear factor$\kappa\beta$ (NF$\kappa\beta$), protein tyrosine kinase, GTP-binding proteins, AKT/PKB, MAPK and Notch pathways (Bakin et al 2002). The non-canonical pathway is responsible for differentiation and migration, which is largely through MAPK, ERK1/2, JNK and p38 PIK3 kinase signalling.

Biological Function

TGFβ has a dual role as a tumour suppressor and oncogene, depending on cell type and tumour stage (Bierie et al 2006 and Derynck et al 2001). An example on cell type dependant function of TGFβ, is it can promote mesenchymal cells, such as fibroblasts but suppresses endothelial, neural and hematopoietic cells. Its role as a suppressor functions through CDK inhibitors like $p21^{CIP1}$ $p15^{INK4B}$ and $p27^{KIP1}$. These affect the function of c-Myc and cyclin dependant kinases (Hannon et al 1994, Polyak et al 1994). P15 can also be upregulated by FOXO/SMADs by TGFβ to induce cytostatis in breast cancer (Gomis et al 2006).

TGFβ becomes an oncogene only when there is loss of heterozygosity, mutation or attenuated expression of the three TGFβ receptors or SMAD2 and SMAD4. As an oncogene, it can stimulate metastasis. It has been known to prime mammary carcinoma cells for seeding into the lungs by upregulation antiopoetin-like4 (Angptl4) (Padua et al 2008) and upregulates CXCL1, CXCL5 and Prostaglandin-Endoperoxide Synthase 2 (PTGS2) (Bierie et al 2008). Another study confirms this in breast cancer associated bone metastasis through the upregulation of parathyroid hormone like hormone (PTHLH), interleukin 11 (IL-11), connective tissue growth factor (CTGF) and JAGGED1 (JAG1) (Kang et al 2005,Sethi et al 2011). Furthermore, this seeding can give rise to a stemlike population, the isomer TGFβ2 has been implicated in expression of such characteristics (O'Brian et al 2015).

As mentioned previously TGFβ function can be attenuated through targeting of the receptors. Histone modifications, transcriptional repression of TβRII, as well as DNA methylation of TβRI and TβRII has been documented to have this effect (Kang et al 1999, Kim et al 2000, Hinshelwood et al 2007). The inactivation of TβRII, is frequent in breast, pancreatic and colon cancers (Gobbi et al 2000). But this inactivation is never associated

with mutations in TβRII promoter region (Barlow et al 2003). Loss of TβRII increases metastasis and progression in HER2 negative patient populations (Gobbi et al 2000) and leads to TGFβ resistance (Kalkhoven et al 1995). While expression of TβRIII decreases recurrence free survival (Dong et al 2007). In both those cases, elevated TGFβ expression has been shown to be unfavourable in lung, breast, prostate, colon and liver cancer (Teischer et al 2001). Another isomer, TGFβ1, has had conflicting reports. It was shown both to be a predictor of favourable prognosis (Marrogi et al 1997) and bad prognosis (Gorsch et al 1992 and Desruisseau et al 2006) and even connected to metastasis (Dalal et al 1993). Other determinants for the dual nature of TGFβ have been identified, such as pseudopodium enriched atypical kinase 1 (PEAK1), disabled homolog 2 (DAB2), sine oculis homeobox 1 (SIX1), Ras association domain family 1 isoform A (RASSF1A), CCAAT/enhancer binding protein B (C/EBPb), kruppel-like factor 5 (KLF5) and paraspeckle component 1 (PSPC1) with an extensive review into their functions (Yeh et al 2019).

4.1.23 TNFRSF1B

Background

Tumour necrosis factor receptor 2 (TNFRSF1B), otherwise known as TNFR2, is a membrane receptor that binds TNFα and is a member of the Tumour necrosis factor family. It functions by forming a heterocomplex which recruits cellular inhibitor of apoptosis protein 1 (c-IAP1) and cellular inhibitor of apoptosis protein 2 (c-IAP2) which then potentiate TNF induced apoptosis through ubiquitination of TNF receptor associated factor 2 (TRAF2).

Structure

It is a single pass transmembrane glycoprotein. It has about 28% homology with tumor necrosis factor receptor 1 (TNFR1) in the extracellular domain, both consisting of 4 cysteine rich motifs (Locksley et al 2001), whereas its intracellular domain lacks any homology (Lewis et al 1991). TNFRSF1B consists of an extracellular domain, transmembrane domain and cytoplasmic domain. Compared to TNFR1, TNFRSF1B does not contain an intracellular death domain. Its main interaction is with TNF receptor-associated factor 2 (TRAF2) (Wajant et al 2003), the domain for which is located in the cytoplasmic domain of TNFRSF1B.

Biological Function

TNFRSF1B is primarily expressed by regulatory T cells of the immune system (Grell et al 1998). As mentioned before, TNFR1 and TNFRSF1B share homology (Locksley et al

2001) but they are responsible for different functions. TNFR1 is responsible for signalling and cell death while TNFRSF1B is responsible for cell survival (Wajant et al 2003). The mode of action of TRAF2 is thorough binding to TNF receptor-associated factor 1 (TRAF1), TNF receptor-associated factor 3 (TRAF3) and cIAP1 (Rothe et al 1995). It acts through pathways such as the NF-κB and PI3K pathways (Rao et al 1995, Fischer et al 2014). The differences were further explored when a study was undertaken at the TNF-TNFRSF1B complex. The findings confirmed that there were differences between the two receptors, as well as the localisation of the complex on the cell membrane. Although no inferences could be made further as the domain structure of TNFRSF1B remains to be elucidated (Mukai et al 2010); recent analysis on therapeutic targets suggests that the region 3 of TNFRSF1B could have a potential for drug targeting (Shaikh et al 2018). Additionally, there could also be crosstalk between the two receptors which would add an additional regulatory component (Naude et al 2011), as seen with some upregulation of TNFR1 and caspase 8, as a response to TRAF2 depletion (Fotin-Mleczek et al 2002).

TNFRSF1B has been widely reported to promote tumour progression in skin, colorectal, renal, myeloma and T-cell lymphoma (Arnott et al 2004, Tanimura et al 2005, Johler et al 2004, Grotowski et al 2003 and Heeman et al 2012). It is also responsible for antigen stimulation and T cell activation (Kim et al 2006, Grell et al 1998). These studies observed that TNFRSF1B is implicated in transforming epithelial cells (Arnott et al 2004), promoting tumour cells growth.

In breast cancer, TNFRSF1B has been confirmed to have a positive association with larger tumour size, advance stage of disease and higher pathological grade (Yang et al 2017). It also promotes tumour growth through p42/p44 MAPK, JNK , AKT and NF-κB pathways (Rivas et al 2008), and avoids cell death and confers resistance to Adriamycin (Yang et al 2017). TNFRSF1B could likely become a good prognosticator due to its expression by the B lymphocytes of the breast tumour draining lymph nodes (Ghods et al 2018).

4.1.24 VIM

Background

Vimentin (VIM) is a structural protein part of the cytoskeleton and a type III intermediate filament (IF) expressed in mesenchymal cells. It is often used as a marker for initiation of EMT (Thiery et al 2002). VIM expression is functionally important in mammary gland development and stemness (Peuhu et al 2017), proliferation and differentiation through TGFβ signalling (Cheng et al 2016, Liana & Ahsan 2016), cell adhesion (Nieminen et al 2006), migration and invasion (Eckes et al 1998, Eckes et al 2000, Richardson et al 2018).

VIM expression has been studied in many solid tumours such as prostate, gastrointestinal, lung, melanoma (Kokkinos et al 2007).

Structure

VIM is part of a larger family of IFs, consisting of 70 members, distributed into six tissue specific classes. Types I and II are acidic and basic keratins (epithelial), type III are vimentin and desmin (mesenchymal), type IV are neurofilaments (neurons), type V are lamins (cell nucleus) and type VI are nestin (embryonic neuron). In addition, there are numerous IF associated proteins (Green et al 2002). The structure of vimentin comprises a conserved α-helical domain flanked by N and C terminal end domains, a head domain (77 residues) and tail domain (61 residues) (Goldie et al 2007). This structure then becomes a coil onto which the other IF family members attach (Fuchs et al 1983).

Biological Function

As mentioned previously, VIM is vital for functions such as adhesion and migration (Ivaska et al 2007). Loss of VIM results in a weaker wound healing response (Eckes et al 2000), renal failure and altering blood flow due to reduced arterial structure response (Terzi et al 1997, Schiffers et al 2000). In cell signalling, VIM prevents the dephosphorylation of activated ERK (Perlson et al 2006), a signaling protein regularly involved in cell migration. Furthermore, VIM also associates with Scribble Planar Cell Polarity Protein (SCRIB), another protein responsible for directed migration and invasion by preventing the proteolytic degradation of SCRIB (Phua at el 2009). VIM is also involved in EMT, which it initiates through upregulation of receptor tyrosine kinase Axl (AXL) and Ras (Vuoriluoto et al 2011). The role of VIM in directional migration is likely by influencing the microtubules responsible for the reorganisation and establishment of cell polarity, as well as interaction with actin which helps forming the lamellipodia (Battaglia et al 2018).

Increased VIM expression was documented in mesenchymal breast cancer cell lines MDA-MB-231, BT549, Hs578T, and MDA-MB-435 (Gilles et al 2003), which was preceded by a loss of cytokeratin, motivating an aggressive phenotype (Vora et al 2009). This phenotypic change is also accompanied by morphological changes to the cell, which is due to VIM helping the tumour cell resist stress and promoting migration through loss of cell contacts and increasing focal adhesion turnover (Tse et al 2012). Furthermore, the downregulation of VIM in MDA-MB-231 cells showed a decrease in invasive and migratory capacity, due to their associated morphological changes (Messica et al 2017). This cellular morphology change was also observed by Terriac et al (2019), who found intermediate filament ring

structures forming around the nucleus in the early stages of adhesion, the later stages will follow the deformation of the cell nucleus which they hypothesised could lead to some gene expression regulation. This increase of VIM in triple negative breast cancer is associated with high nuclei grade, high Ki67, poorer prognosis and overall survival. This contributes to an aggressive phenotype and chemoresistance (Yamashiata et al 2013). Breast cancer studies of breast carcinomas showed that low estrogen receptor expression correlated with high VIM expression in high grade tumours (Domagala et al 1990).

Therapy

There are few studies on VIM targeted therapy such as in the case of Withaferin-A, that works by binding vimentin in a pocket between heat to tail α-helical dimer. This compound was shown to induce apoptosis (Bargagna-Mohan et al 2007). There were also some effects on vimentin by salinomycin, an antibiotic which induced anti EMT phenotype reversal (Dong et al 2011). As well as efforts to look into micro RNA, showing a significant effect on VIM with miR-200 and miR-30 (Braun et al 2010).

4.1.25 WIPF1

Background

WAS/WASL interacting protein family member 1 (WIPF1) is important in actin cytoskeleton organisation (Moreau et al 2002). Its role extends into cell migration and invasion through its reorganisation and polymerisation of actin in the ECM (Ramesh et al 1997, Anton et al 1998, Donnelly et al 2013). Most notably it is implicated in Wiscott-Aldrich syndrome, an X linked recessive disorder (Volkman et al 2002). Other functions of WIPF1 include development of immune cells. Downregulation of WIPF1 reduces the function of NK cells (Krzewski et al 2008). While higher expression of WIPF1 correlated with better overall patient prognosis in breast cancer, colorectal cancer and glioma (Staub et al 2009).

Structure

The WAS family structure consists of a WSP homology 1 (WH1) domain at its N-terminal region and a GTPase-binding domain (GBD) which it uses to bind to CDC42. Its C-terminus includes a VCA domain, rich in proline this domain binds to SH3 containing molecules. These proteins are autoinhibited in resting cells, only activated once exposed or bound to Cell Division Cycle 42 (CDC42).

Biological Function

WIPF1 is responsible for invadopodia formation, which is achieved alongside Actin-related protein 2 (ARP2) and Actin-related protein 3 (ARP3) complex, fascin and cortactin (Calle et al 2008). Which is one of the formative structures responsible for cell movement at the leading edge. This invadopodium formation was later shown to be a result of the interaction of WIPF1 with intersectin 1 (ITSN1), intersectin 2(ITSN2) and WAS/WASL Interacting Protein Family Member 2 (WIPF2)/WIRE with neural wiskott-aldrich syndrome protein (NWASP). Both of which control the speed of migration and speed of matrix degradation associated with the movement (Gryaznova et al 2015, Garcia et al 2016). Its also responsible for initiating MET in MDA-MB-231 and Hs578T mesenchymal breast cancer cell lines. This is thought to be controlled by WIPF1 downregulation of VIM, influencing expression of epithelial markers such as E-cadherin and β-catenin and done independently of MMP concentration (Garcia et al 2014). Another function of WIP1 is driving tumour progression and activating the mutant p53 control of cancer stem cell formation (Gargini et al 2016, Escoll et al 2017). Furthermore, WIPF1 plays a role in promoting aggressive papillary thyroid cancer, mediated by B-Raf Proto-Oncogene, Serine/Threonine Kinase (BRAF) V600E hypomethylation of WIPF1 (Zhang et al 2017). It is reflected in similar findings in pancreatic ductal adenocarcinoma, where WIPF1 was targeted by a miR-141 and miR-200c, reducing migration and metastasis (Pan et al 2018).

4.1.26 ZEB1 and ZEB2

Background

Zinc finger E-box binding homeobox 1 (ZEB1) is a transcription factor responsible for repressing interleukin 2, a lymphocyte specific gene. It does so by binding to a negative regulatory domain near the transcription start site (Williams et al 1991). It is also implicated in neurogenesis, lymphopoiesis and development of the neural crest (Vanderwalle et al 2009). Most recently, its function in EMT has been reviewed by Zhang et al (2015). It is well known that it is regulated by several pathways such as the WNT, NF-$\kappa\beta$, TGF-β, prostaglandin-endoperoxide synthase 2 (COX2) and HIF signalling pathways. ZEB1s aberrant expression has had demonstrated effects in other cancers such as pancreatic, lung, liver, gastric, colon, among others (Wellner et al 2010, Zhou et al 2012, Okugawa et al 2012, Zhang et al 2013, Zhang et al 2013). In terms of clinical significance, elevated levels of ZEB1 a predictor of worse overall survival in solid tumours with potential to be used as a biomarker (Chen et al 2019).

The same can be said for Zinc finger E-box binding homeobox 2 (ZEB2) as it has also been associated with poor survival, higher malignancy and cell proliferation (Ellou et al 2005). The co-expression of both ZEB1 and ZEB2 correlates with poor prognosis for head and neck cancers (Chu et al 2013). ZEB2 alone has also been widely reported in many tumour types such as breast, pancreatic, squamous cell carcinoma, gastric cancer and liver cancer (Rosivatz et al 2002, Elloul et al 2005, Imamici et al 2007, Maeda et al 2007, Zhao et al 2018). It is alsos associated with higher malignancy, higher cell proliferation and poor patient survival. It is an important regulator of the TGF-β and BMP pathways, and in some ways acts antagonistically to ZEB1 by blocking transcription of TGF-β responsive genes (Postigo et al 1999). It can affect a variety of processes such as EMT, apoptosis, anoikis, regulation of tumour suppression proteins and cyclin dependant kinase inhibitors (Stankiewicz et al 2014). It also functions as a transcriptional co-repressor, as TGFβ phosphorylates R-SMADs, ZEB2 controls the transcription of the R-SMADs. ZEB2 mutations are most prominent in Mowat-Wilson syndrome and Hirschsprung's disease, which results in improper organ development and nerves.

Structure

ZEB1 has seven zinc fingers and one homeodomain, while ZEB2 has eight zinc fingers and one homeodomain (Burglin 2016). These genes, including a third Zinc finger E-box binding homeobox 3 (ZEB3), belong to the ZEB family, which is a subdomain of the zinc finger homeodomain transcription factors. ZEB1 domains include the Smad interaction domain (SID), CtBP interaction domain (CID) and the p300-P/CAF binding domain (CBD). These domains help ZEB1 exert its regulatory effects on co activators and co repressors such as SMADs (Postigo et al 2003). ZEB2 contains a nucleosome remodelling deacetylase interaction motif (NIM), a SMAD binding domain (SBD), a homeodomain (HD), a CtBP interacting domain (CID), and 2 zinc finger clusters (ZF) at its N and C terminus. These ZF clusters contain three ZF domains with a Cys2-His2 (C2H2) motif, while the N terminal ZF cluster contains a CCHC motif (Remacle et al 1999). NIM and CID recruit co-repressors, while the ZF clusters bind the promoters of target proteins (Remacle et al 1999).

Biological Function

ZEB1 is involved in all aspects of tumour progression. It downregulates E-cadherin and induces EMT in breast carcinomas, promoting tumour cell differentiation and tumour progression (Mikula et al 2007, Pernaido et al 2007). This is partly done through its recruitment of CtBP co repressors and the chromatin remodelling protein BRG1 (Shi et

al 2003, Sanchez-Tillo et al 2010). The transformation from non-tumorigenic state to tumorigenic is owed to ZEB1 promoter region being in a bivalent chromatin configuration (Chaffer et al 2013). While the pivotal repression of E-cadherin is also epigenetically controlled by ZEB1, through its recruitment of HDACs, DNA methyltransferase and ubiquitin ligase (Zhang et al 2018).

ZEB1 has also been demonstrated to affect cell proliferation and initiate cell cycle arrest by modulating the expression of p21 and p15 (Liu et al 2008, Hu et al 2010). Furthermore, there is also evidence of avoidance of EGFR induced senescence through the repression of $p16^{INK4A}$ and p15 in oesophageal cancer (Ohashi et al 2010). The same is seen with ZEB2 effects on p15 and p21(Zanotto-Filho et al 2011). This is opposite to ZEB2 which seems to promote senescence through telomerase reverse transcriptase (hTERT) expression (Lin et al 2003). ZEB1s effects on cell survival is regulated by the p53/ mir-200 pathway (Hill et al 2012), as it has been shown that p53 controls the miR-200c, miR-141 and the miR-200a/ miR-200b/ miR-429 clusters (Fontemaggi et al 2005).

ZEB1 has been documented to promote metastasis in lung cancer (Liu et al 2014), as well as seeding bone metastasis in breast cancer by initiating MET and expressing BMP inhibitors (Eger et al 2005). The effects on EMT and metastasis are further propagated through its repression of scribble cell polarity complex component 2 (HUGL2), PATJ crumbs cell polarity complex component (PATJ) and Crumbs Cell Polarity Complex Component 3 (CRB3) (Aigner et al 2007). There is no surprise that it also affects migration by remodelling the basement membrane and downregulating MMP1, MMP9 and MMP14, leading to cell invasion (Brabletz et al 2010). This is largely achieved through upregulation of TGF-β targets and the recruitment of p300-P/CAF and SMADs (Postigo et al 2003). More binding partners of ZEB1 are being identified, many of which control cell migration, invasion, cell polarity and anchorage independent growth. A triple negative cancer model of Hs578T cells identified over 2000 ZEB1-regulated genes (Maturi et al 2018).

In terms of EMT progression, ZEB2s association with known promoters of EMT is well documented (Vanderwalle et al 2005, Puisieux et al 2014). This promotion is likely due to its interaction with SP1, increasing the activation of integrin $\alpha 5$ which increases metastasis. This is associated with poorer prognosis in colorectal cancer (Li et al 2017). Much of the effects are also due to ZEB2s regulation of the miR-200 family. Largely, the repression effects of ZEB2 act through its CtBPs recruitment of HDACs (Kuppuswamy et al 2008). The reversal of oncogenic traits upon ZEB2 knockdown or its interacting partners results in inhibition of migration (Hu et al 2010), reversal of EMT (Sathyanarayanan et al 2017) and initiation of apoptosis (Zhao et al 2018). Paradoxically, its knockdown also promotes hematological malignancy through increasing the cancer stem cell subpopulation (Gossens

et al 2015). This upregulation of CSCs was partly explained by the reduction of DNA methyltransferase 1 (DNMT1) and demethylation of the *ZEB2* promoter in prostate cancer (Lee et al 2016), adding another layer of epigenetic control on these traits.

As resistant cells often exhibit a higher DNA damage response to radiotherapy, ZEB1 promotes DNA damage repair through activation of Checkpoint Kinase 1 (CHK1), thereby increasing radioresistance, cell survival and cell cycle arrest in breast cancer cells. A process assisted by ATM serine/threonine kinase (ATM) phosphorylation and stabilisation of ZEB1 (Zhang et al 2014). Interestingly, the same study showed that ZEB1 was exclusively responsible for the radioresistance in the MCF7 breast cancer cell line, independently of EMT or other EMT inducers such as SNAI1 or TWIST. Resistance to various compounds have been confirmed. MiR-200c was shown to induce trastuzumab resistance in HER2+ breast cancer through TGFβ activation of ZEB1 (Bai et al 2014). ZEB2s role in multidrug resistance is seen in lung and gastric cancers (Fang et al 2014, Jiang et al 2017).

Docetaxel resistance in prostate cancer was recorded for both ZEB1 and ZEB2 overexpression (Hanrahan et al 2017). Similarly, both promoted gemcitabine resistance in pancreatic ductal adenocarcinoma (Wang et al 2017). This effect on resistance extends to other substances such as 5-fluorouracil, gemcitabine, paclitaxel, cisplatin and doxorubicin due to the widely reported association of resistance with the loss of miR-200 (Pogribny et al 2010, Senfter et al 2015), as ZEB1 and ZEB2 both regulate miR-200 expression.

Resistant cells often exhibit a stem like phenotype. ZEB1s promotes these traits in triple negative breast cancer cell lines upon TGFβ stimulation (Chaffer et al 2013). There is further evidence to this through ZEB1 repression of miR-200, miR-183, and miR-203 that can target SOX2 and KLF4 (Wellner et al 2009). All of which are inhibitors of stemness. Further evidence is seen in the utilisation of ZEB1 by normal stem cells. Its function is to prevent the effects of oxidative stress by promoting methionine sulfoxidase reductase (MSRB3) activity (Morel et al 2017). The regulation of ZEB2 can occur through transcription factors such as HIF-1α, TGF-β, SMAD, Ras, ERK, FOS Like 1, AP-1 Transcription Factor Subunit (FOSL1), NF-κB and WNT pathways (Dave et al 2011). Another interesting regulator of ZEB2 is FOXO1 which will be mentioned later, by binding to the *ZEB2* promoter (Dong et al 2017).

Therapy

Several studies into miR silencing experiments of ZEB1 revealed several miRs that resensitise cells to radiotherapy, such as miR-205 for breast, lung and osteosarcoma cell lines (Zhang et al 2014) and miR-200c for lung cancer in xenograft models (Cortez et al 2014). The same miR-200c was responsible for drug resistance by targeting ZEB2 (Jiang et al

2017). Other miRs like miR-200, abrogate the ZEB1 promoting loop of invasion, metastasis (Gibbons et al 2009). ZEB1 also confers resistance to immunotherapies such as with PD-L1 inhibitors, whose effects are abrogated by ZEB1 through its control of miR-200 (Chen et al 2014, Shibue et al 2017). The use of an HDAC inhibitor, mocetinostat, has shown to epigenetically repress ZEB1(Meifhof et al 2015). This could be another potential therapy to use to combat drug resistance.

4.2 Analysis of EP300 Gene Signature in Breast Cancer Cell Lines

4.2.1 Hypothesis

Drawing from conclusions in **Chapter 3**, the effect of the miRs and drug resistance was not as conclusive and needs further investigation. Therefore, moving back to our original line of inquiry, we are focusing on EP300 and a drug resistance regulated gene signature. The signature was derived from a differential expression of 4000 genes in an MCF7 cell line with EP300 knockdown and Taxol resistance, from which we generated a list of 15 most upregulated and 11 most downregulated genes that might have a connection to biological function. Moving forward, the hypothesis is based on the results of Gene Chip ® analysis of MCF7, we assume these same genes will have differential expression between cancer cell lines (breast/ colorectal) and cell type (epithelial/ mesenchymal).

In this chapter, we investigate whether there is any difference in basal expression patterns in mesenchymal versus epithelial cell lines. As cells undergo an EMT shift and lose epithelial markers as they approach mesenchymal status, it is expected that genes most upregulated or downregulated by MCF7 would have the opposite expression in mesenchymal subtypes like MDA-MB-231, CAL-51 and HCT116. Whereas, the T47D epithelial model would mimic the effects of the gene signature on the MCF7 cell line as they share the Luminal A subtype. Furthermore, this T47D model was generated using two vectors, shEP300 I and shEP300 II which were used to generate the MCF7 model in previous studies. The effectiveness of both vectors on the gene signature would be demonstrated using RTqPCR as well as the phenotypic effect on cell proliferation. It is expected that cell proliferation should increase upon EP300 downregulation by both vectors as the cell line would be drifting more towards EMT phenotype and losing its epithelial characteristics. Cell proliferation effects of EP300 and CDH1 overexpression would also be tested in an MDA-MB-231 model. It is expected that the overexpression would result in a migration towards epithelial characteristics, therefore a decrease in cell proliferation.

4.2.2 Aim

1. Test the gene signature from our Gene Chip ® results in mesenchymal breast cancer cell line models.
    - RTqPCR of genes most upregulated and downregulated in the MCF7 model and compared with the mesenchymal breast cancer cell line CAL51.
    - RTqPCR of genes most upregulated and downregulated in the MCF7 model and compared with the mesenchymal breast cancer cell line MDA-MB-231.
    - Compare gene signature between EP300 and CDH1 overexpression.
2. Test the gene signature from our Gene Chip ® results in colorectal cancer cell line models.
    - RTqPCR of genes most upregulated and downregulated in the MCF7 model and compared with the colorectal cancer cell line HCT116.
3. Test the gene signature from our Gene Chip ® results in epithelial breast cancer cell line models.
    - RTqPCR of genes most upregulated and downregulated in the MCF7 model and compared with the epithelial breast cancer cell line T47D.
    - Compare gene signature between EP300 knockdown using vectors shEP300 I and shEP300 II.
4. Investigate whether there is a pattern between gene signature and cancer type (breast/-colorectal) and cell type (epithelial/mesenchymal).
5. Elucidate whether the gene signature is regulated by EP300 and CDH1.
    - Monitor the effect of EP300 and CDH1 overexpression on cell proliferation by testing in a mesenchymal breast cancer cell line MDA-MB-231.
    - Monitor the effect of the EP300 knockdown on cell proliferation in an epithelial cell line T47D.

4.2.3 Results

EP300 has been established as a regulator of many transcription factors. Previously published findings by our lab indicated genes that are potentially regulated by EP300. These findings were generated through a Gene Chip ® whole transcript microarray of the MCF7

cell line with EP300 overexpression and long-term Taxol resistance. The summary of these results is demonstrated in **Table 4.1** and a brief summary of their function is shown in **Table 4.2**. For this chapter, we have selected these genes and will be investigating modulation of these genes as a response to downregulation and overexpression of EP300 and CDH1 in a panel of breast cancer cell line models: CAL-51, MDA-MB-231, HS578T, T47D and a colorectal cancer cell line model: HCT116.

Table 4.1 List of genes of interest.

Condition	Gene	sh EP300 I vs Control	sh EP300 II vs Control	Mean	p-value	Change
EP300	ABCG2	7.14603	7.72488	7.435455	9.84E-08	UP
EP300	BCL2	11.4333	14.3576	12.89545	1.40E-11	UP
EP300	BMP4	-3.00648	-3.12433	-3.065405	4.03E-08	DOWN
EP300	BMP7	-5.88559	-6.2225	-6.054045	4.25E-13	DOWN
EP300	CAPN9	-5.34713	-3.90685	-4.62699	4.66E-12	DOWN
EP300	CDH11	4.52923	5.11104	4.820135	1.78E-06	UP
EP300	CEACAM5	-32.6789	-20.6263	-26.6526	1.29E-08	DOWN
EP300	CNN2	-5.67638	-5.08862	-5.3825	4.02E-09	
EP300	EFEMP1	3.2339	5.11161	4.172755	3.89E-09	UP
EP300	EP300	-1.89938	-1.64523	-1.772305	7.09E-05	DOWN
EP300	EPHA4	8.64868	10.2864	9.46754	4.76E-11	UP
EP300	FGFR2	3.3111	6.32719	4.819145	6.63E-09	UP
EP300	HEY2	-6.06371	-4.88699	-5.47535	2.50E-09	DOWN
EP300	HMCN1	4.4454	4.75231	4.598855	1.03E-08	UP
EP300	ITGA2	2.50114	2.74064	2.62089	9.74E-09	UP
EP300	ITGA3	2.22857	2.34247	2.28552	1.89E-09	UP

Table continues on the next page...

Condition	Gene	sh EP300 I vs Control	sh EP300 II vs Control	Mean	p-value	Change
EP300	MUC5B	-5.40393	-6.75995	-6.08194	1.68E-09	DOWN
EP300	PLS3	-16.0606	-15.8059	-15.93325	1.11E-08	DOWN
EP300	SGCG	10.6904	11.5366	11.1135	1.16E-11	UP
EP300	TGFβ2	6.23349	8.69347	7.46348	6.76E-12	UP
EP300	TNFRSF11B	4.59912	8.1184	6.35876	5.82E-10	UP
EP300	WIPF1	7.68807	6.27784	6.982955	3.38E-06	UP
EP300 TaxR	ABCG2	5.39979	3.45269	4.42624	6.20E-06	UP
EP300 TaxR	ARHGAP20	-23.6458	-23.839	-23.7424	1.42E-09	DOWN
EP300 TaxR	BCL2	9.36195	10.0436	9.702775	9.80E-10	UP
EP300 TaxR	BMP4	-4.05436	-2.8025	-3.42843	1.67E-06	DOWN
EP300 TaxR	BMP7	-4.6073	-2.31274	-3.46002	3.20E-11	DOWN
EP300 TaxR	CAPN9	-5.02644	-4.11477	-4.570605	3.60E-09	DOWN
EP300 TaxR	CDH11	4.4511	5.40109	4.926095	3.71E-05	UP
EP300 TaxR	CEACAM5	-25.0994	-4.59832	-14.84886	8.23E-08	DOWN
EP300 TaxR	CNN2	-5.13855	-4.05614	-4.597345	4.49E-08	DOWN
EP300 TaxR	EFEMP1	5.9966	4.84404	5.42032	1.69E-08	UP

Table continues on the next page...

Condition	Gene	sh EP300 I vs Control	sh EP300 II vs Control	Mean	p-value	Change
EP300 TaxR	EP300	-1.61575	-1.55099	-1.58337	0.00128802	DOWN
EP300 TaxR	EPHA4	6.33952	7.54935	6.944435	5.76E-09	UP
EP300 TaxR	FGFR2	4.56188	5.73542	5.14865	4.91E-07	UP
EP300 TaxR	HEY2	-8.29284	-6.05543	-7.174135	1.83E-09	DOWN
EP300 TaxR	HMCN1	4.45937	5.99296	5.226165	1.78E-07	UP
EP300 TaxR	ITGA2	1.78222	3.59573	2.688975	0.00019532	UP
EP300 TaxR	ITGA3	2.13745	2.50416	2.320805	1.37E-06	UP
EP300 TaxR	MUC5B	-8.0819	-5.15303	-6.617465	8.50E-09	DOWN
EP300 TaxR	PLS3	-12.8653	-14.2251	-13.5452	2.67E-07	DOWN
EP300 TaxR	SGCG	9.5809	7.16039	8.370645	3.17E-10	UP
EP300 TaxR	TGFβ2	10.6569	16.1276	13.39225	3.49E-11	UP
EP300 TaxR	TNFRSF11B	2.84722	10.1387	6.49296	8.60E-06	UP
EP300 TaxR	WIPF1	6.83559	4.54568	5.690635	2.16E-05	UP
EP300 TaxR	ABCG2	5.39979	3.45269	4.42624	6.20E-06	UP

Source “Tumour suppressor EP300, a modulator of paclitaxel resistance and stemness, is downregulated in metaplastic breast cancer”, Asaduzzaman et al, 2017.

Table 4.2 Pathway analysis.

Gene Symbol	Status	Function	Notable Pathways
BCL2	Upregulated	Apoptosis	TP53 Network, Apoptosis and survival_Anti-apoptotic action of nuclear ESR1 and ESR2, Gemtuzumab ozogamicin Pathway, Pharmacokinetics/Pharmacodynamics, Hematopoietic Stem Cell Gene Regulation by GABP alpha/beta Complex, ATF-2 transcription factor network, IL2 signaling events mediated by PI3K, Interleukin-11 Signaling Pathway, Transcription_P53 signaling pathway, Apoptosis and survival Anti-apoptotic TNFs/NF-kB/Bcl-2 pathway, Hedgehog signaling pathway (KEGG), Apoptosis and survival Caspase cascade
ITGA2	Upregulated	Migration	Platelet Adhesion to exposed collagen, VEGFR3 signaling in lymphatic endothelium, Cell adhesion_Endothelial cell contacts by non-junctional mechanisms, Platelet Aggregation Inhibitor Pathway, Pharmacodynamics, Interleukin-11 Signaling Pathway, ECM proteoglycans, TGF-beta Signaling Pathway (WikiPathways), AKT Signaling Pathway, MET promotes cell motility, Regulation of actin cytoskeleton, MAPK-Erk Pathway, Focal Adhesion, Integrin Pathway, TGF-Beta Pathway
ITGA3	Upregulated	Migration	Cell adhesion_Endothelial cell contacts by non-junctional mechanisms, Cell adhesion_Cell-matrix glycoconjugates, Cell surface interactions at the vascular wall, AKT Signaling Pathway, MAPK-Erk Pathway, Focal Adhesion, Degradation of the extracellular matrix, Integrin Pathway, PI3K-Akt signaling pathway, TGF-Beta Pathway

Table continues on the next page...

Gene Symbol	Status	Function	Notable Pathways
TGFβ2	Upregulated	Invasion, Growth	Signaling events mediated by the Hedgehog family, IL-2 Gene Expression in Activated and Quiescent T-Cells, p38 MAPK Signaling Pathway (WikiPathways), ERK Signaling, TGF-Beta Pathway, Akt Signaling, Integrin Pathway, Toll-like Receptor Signaling Pathway, MAPK signaling pathway, Degradation of the extracellular matrix, MicroRNAs in cancer, Wnt / Hedgehog / Notch, SMAD Signaling Network, Cell cycle, FoxO signaling pathway, Angiogenesis (CST)
ABCG2	Upregulated	Drug Resistance	Abacavir transport and metabolism, Methotrexate Pathway, Pharmacokinetics, Uricosurics Pathway, Pharmacodynamics, Lamivudine Pathway, Pharmacokinetics/Pharmacodynamics, Erlotinib Pathway, Pharmacokinetics, Zidovudine Pathway, Pharmacokinetics/Pharmacodynamics, Doxorubicin Pathway, Pharmacokinetics, Ponatinib Pathway, Pharmacokinetics/Pharmacodynamics, Irinotecan Pathway, Pharmacokinetics, Pazopanib Pathway, Pharmacokinetics, Imipramine/Desipramine Pathway, Pharmacokinetics, Fluoropyrimidine Activity, Platinum Pathway, Pharmacokinetics/Pharmacodynamics, Antifolate resistance, Statin Pathway - Generalized, Pharmacokinetics
EPHA4	Upregulated	Cell Proliferation, Migration	G-protein signaling_RhoA regulation pathway, EPHA forward signaling, MAPK-Erk Pathway, Nanog in Mammalian ESC Pluripotency, Akt Signaling, TGF-Beta Pathway, ERK Signaling

Table continues on the next page...

Gene Symbol	Status	Function	Notable Pathways
WIPF1	Upregulated	Growth, Proliferation	Signaling by Rho GTPases, ERK Signaling, EphB-EphrinB Signaling
FGFR2	Upregulated	Proliferation, Growth, Apoptosis, Differentiation, Migration	Signaling by FGFR2, Angiogenesis, VEGF Signaling Pathway, mTOR signalling, MAPK Signaling: Mitogen Stimulation Pathway, PI3K/AKT activation, Signaling pathways regulating pluripotency of stem cells, Apoptosis Pathway
EFEMP1	Upregulated	Hypoxia, Growth, Proliferation	Elastic fibre formation, Degradation of the extracellular matrix, Integrin Pathway, ERK Signaling
SGCG	Upregulated	N/A	Arrhythmogenic right ventricular cardiomyopathy (ARVC), Dilated cardiomyopathy (DCM), Allograft rejection
HMCN1	Upregulated	Invasion, Metastasis	N/A
CDH11	Upregulated	Migration, EMT	Adhesion, Cell junction organization, WNT Signaling
CDH2	Upregulated	Migration, EMT	TGF-B Signaling in Thyroid Cells for Epithelial-Mesenchymal TransitionTGF-B Signaling in Thyroid Cells for Epithelial-Mesenchymal Transition, N-cadherin signaling events, Cell adhesion_Endothelial cell contacts by non-junctional mechanisms
VIM	Upregulated	Migration, EMT	Cell Adhesion Endothellial cell contacts by junctional mechanisms, Apoptosis related network due to altered Notch3 in ovarian cancer, TGFB signalling in Thyroid cells for epithelial-mesenchymal transition, Neural stem cell differentiation pathways and lineage-specific markers

Table continues on the next page...

Gene Symbol	Status	Function	Notable Pathways
CEACAM5	Downregulate	Metastasis	Cell adhesion cell matrix glycoconjugates, Adhesion, NF-kappaB Signalling, cell surface interactions at the vascular wall, Hematopoietic Stem Cell Differentiation and Lineage-specific markers
BMP4	Downregulate	Migration, EMT, Stemness	Human Early Embryo Development, Differentiation pathway, TGF-beta Pathway, Signaling pathways regulating pluripotency of stem cells, SMAD Signalling network,NF-kappaB Family, Wnt/Hedgehog/Notch
BMP7	Downregulate	Migration, EMT	ALK2 signalling events, Akt signalling, Wnt/Hedgehog/Notch , SMAD signalling network, TGF-beta signalling network
CAPN9	Downregulate	Apoptosis	Apoptosis Pathway
CNN2	Downregulate	Proliferation, Migration	Myometrial Relaxation and Contraction Pathways
MUC5B	Downregulate	Invasion, Migration, Growth	Defective GALNT12 causes colorectal cancer 1(CRCS1), IL-1 Family Signalling Pathways
PLS3	Downregulate	EMT, Stemness	N/A
ARHGAP20	Downregulate	Proliferation, Migration	Signalling by Rho GTPases
HEY2	Downregulate	EMT	Notch mediated HES/HEY network

Table continues on the next page...

Gene Symbol	Status	Function	Notable Pathways
EP300	Downregulate	Migration, EMT, Drug Resistance	P53/Notch/FoxO/TGF-beta and many others
CDH1	Downregulate	Migration, EMT	CDK-mediated phosphorylation and removal of Cdc6
SNAI2	Variable	EMT, Migration, Invasion	TGF-B Signalling in Thyroid Cells for Epithelial-Mesenchymal Transition/ Adherens Junction/Regulation of Wnt-Mediated beta catenin signalling and target gene transcription
TNFRSF11B	Variable	Tumorigenesis	Apoptosis Modulation and Signaling/ Osteoclast Signaling
ZEB2	Variable	Invasion, Migration	TGF-beta Receptor Signalling
ZEB1	Variable	Drug Resistance, Growth, Tumorigenesis, EMT	Hypoxia-mediated EMT and Stemness
FOXA1	Variable	Invasion, Migration, Drug Resistance	FOXA1 transcription factor network

Source “Tumour suppressor EP300, a modulator of paclitaxel resistance and stemness, is downregulated in metaplastic breast cancer”, (Asaduzzaman et al, 2017).

The overexpression of EP300 results in upregulation of CDH1 in mesenchymal breast cancer cell lines.

We tested our candidate gene signature in a breast cancer cell line CAL-51 which has mesenchymal characteristics and is triple negative. Otherwise known as not expressing the canonical markers ER+, PR+ and HER2. In **Figure 4.1**, we show the expression of the gene signature in CAL-51 in context of EP300 overexpression, CDH1 overexpression and compare it to the basal expression in the same cell line with a control empty vector.

As a result of EP300 overexpression in **Figures 4.1a** and **4.1b**, we see that ARHGAP20 has a 0.3 fold decrease ($p<0.01$), EFEMP1 has a 0.3 fold decrease ($p<0.01$), while CDH1 has a 4.3 fold increase ($p<0.01$). As a result of CDH1 overexpression (Figure 4.1a), we see that ARHGAP20 has a 132.8 fold increase ($p<0.001$), EFEMP1 has a 37 fold increase ($p<0.001$), while CDH1 has a 33 fold increase ($p<0.001$). In **Figures 4.1c** and **4.2d**, we see overexpression of EP300 results in a 0.2 fold decrease in CDH11 ($p<0.01$), a 0.2 fold decrease in HEY2 ($p<0.05$), a non significant change in ITGA2, a 0.4 fold decrease in TGFβ2 ($p<0.05$), a non-significant change in FGFR2 and GATA3. The overexpression of CDH1 results in a 14 fold increase in CDH11 ($p<0.001$), a 17 fold increase in FGFR2 ($p<0.001$), a non-significant change in GATA3, a 18 fold increase in HEY2 ($p<0.001$), a 9 fold increase in ITGA2 ($p<0.001$), and a 3.6 fold increase in TGFβ2 ($p<0.05$).

In **Figure 4.1e**, we see overexpression of EP300 results in no significant change in ABCG2, BMP4 and CAPN9. It decreases expression of BCL2 by 0.2 fold ($p<0.01$), BMP7 by 0.6 fold ($p<0.01$). It also increases expression of CDH2 by 1.4 fold ($p<0.01$), CEACAM5 by 1.7 fold ($p<0.05$), and CNN2 by 1.1 fold ($p<0.05$).The overexpression of CDH1 results in no significant change in BCL2, BMP4 and BMP7. It decreases the expression of CNN2 by 1 fold ($p<0.001$). It increases expression of ABCG2 by 2.4 fold ($p<0.05$), CAPN9 by 1.3 fold ($p<0.05$), CDH2 by 1.3 fold ($p<0.05$) and CEACAM5 by 2 fold ($p<0.01$). In **Figure 4.1f**, we see overexpression of EP300 results in no significant change in EPHA4, FOXO3a, PLS3, SGCG and VIM. There is a decrease by 0.3 fold in HMCN1 ($p<0.001$) and by 0.3 fold in ITGA3 ($p<0.05$). The overexpression of CDH1 results in no significant change in EP300, EPHA4, FOXO3a, HMCN1, ITGA3, PLS3 and SGCG and an increase by 1.9 fold in VIM ($p<0.001$). Our final panel in **Figure 4.1g**, is taken from our lab's publication (Asaduzzaman et al 2017), demonstrating the overexpression of EP300 in this cell line using western blot. Which as can be seen from our data, results in the upregulation of CDH1.

We move on to the second triple negative, mesenchymal-like, breast cancer cell line, MDA-MB-231 (**Figure 4.2**). As a result of EP300 overexpression (**Figures 4.2a** and **4.2b**), we see that there is a decrease by 0.32 fold in ABCG2 ($p<0.05$), by 0.43 fold in FGFR2 ($p<0.01$), by 0.6 fold in MUC5B ($p<0.001$) and an increase, as expected, by 3.8 fold in

CDH1 ($p<0.001$). No significant change was observed in CAPN9 and CEACAM5. With CDH1 overexpression resulted in reduction by 0.7 fold in ABCG2 ($p<0.001$), by 0.16 fold in CAPN9 ($p<0.05$), by 0.8 fold in MUC5B ($p<0.001$), an increase by 36.5 fold in CDH1 ($p<0.001$) and an increase by 25 fold in CEACAM5 ($p<0.001$). No significant change was found in FGFR2. In **Figures 4.2c** and **4.2d**, we see overexpression of EP300 results in no significant change in BMP7 and HEY2. It also resulted in a decrease in HMCN1 by 0.4 fold ($p<0.001$), by 0.5 fold in SGCG ($p<0.001$) and an increase by 3 fold in ARHGAP20 ($p<0.001$) and by 1.6 fold in TGFβ2 ($p<0.001$). Overexpression of CDH1 results in no significant changes in BMP7, HEY2 and SGCG. It also resulted in a decrease by 0.1 fold in ARGHAP-20 ($p<0.001$), by 0.3 fold in HMCN1 ($p<0.001$), by 0.1 fold in TGFβ2 ($p<0.001$).

In **Figure 4.2e**, we can see overexpression of EP300 resulted in no significant change in BCL2, EPHA4, FOXO3a, GATA3 and WIPF1. It resulted in higher expression of CDH2 by 6.3 fold ($p<0.001$). With CDH1 overexpression, there was an increase by 1.3 fold in CDH2 ($p<0.05$), by 2.7 fold in WIPF1 ($p<0.001$) and a decrease by 0.3 fold in GATA3 ($p<0.05$). In **Figure 4.2f**, we can see the overexpression of EP300 results in no significant change to ITGA3 and VIM. It resulted in a decrease by 0.27 fold in EP300 ($p<0.01$), by 0.34 fold in ITGA2 ($p<0.01$), and an increase by 1.2 fold in PLS3 ($p<0.05$). Overexpression of CDH1 resulted in no significant change in ITAG3 and VIM. As well as an increase in EP300 by 2 fold ($p<0.001$), by 1.4 fold in ITAG2 ($p<0.001$), by 1.8 fold in PLS3 ($p<0.001$). In **Figure 4.2g**, overexpression of EP300 resulted in no significant change to BMP4. It also resulted in a higher expression of CDH11 by 1.3 fold ($p<0.001$), by 1.8 fold in CNN2 ($p<0.001$) and lower expression in EFEMP1 by 0.3 fold ($p<0.05$). With overexpression of CDH1, there was an increase in CNN2 by 1.2 fold ($p<0.05$), and a decrease in BMP4 by 0.4 fold ($p<0.01$), by 0.2 fold in CDH11 ($p<0.05$) and by 0.4 fold in EFEMP1 ($p<0.001$). Our final panel in 4.2g, is taken from our lab's publication, demonstrating the overexpression of EP300 in this cell line using western blot (Asaduzzaman et al. 2017). Which as can be seen from our data, results in the upregulation of CDH1.

Thus overall the this set of results show that overexpression of EP300 in CAL-51 and MDA-MB-231 results in an upregulation of CDH1. Suggesting that EP300 could be a potential target, as the overexpression of CDH1 might also result in EMT reversal. Though these cell lines have distinct molecular signaling pathways as demonstrated by variable expression of all the reest of the genes.

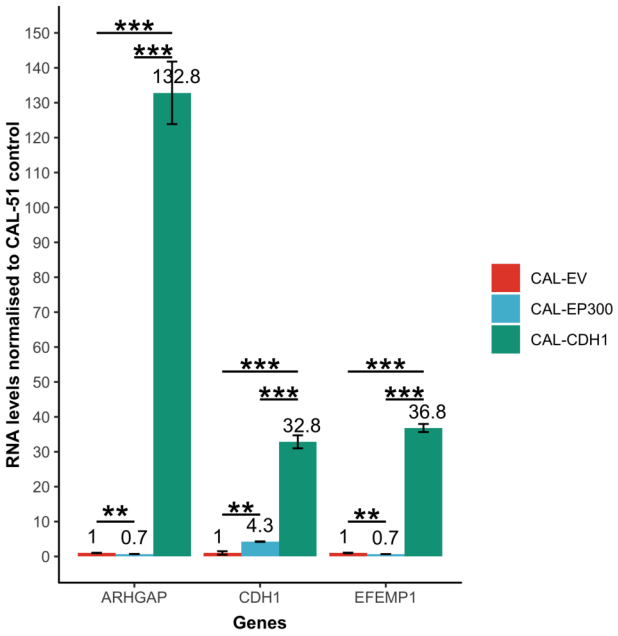
RNA levels normalised to CAL-51 control
Genes
ARHGAP
CDH1
EFEMP1
CAL-EV
CAL-EP300
CAL-CDH1
132.8
32.8
36.8
4.3
0.7
1
***
**

(a)

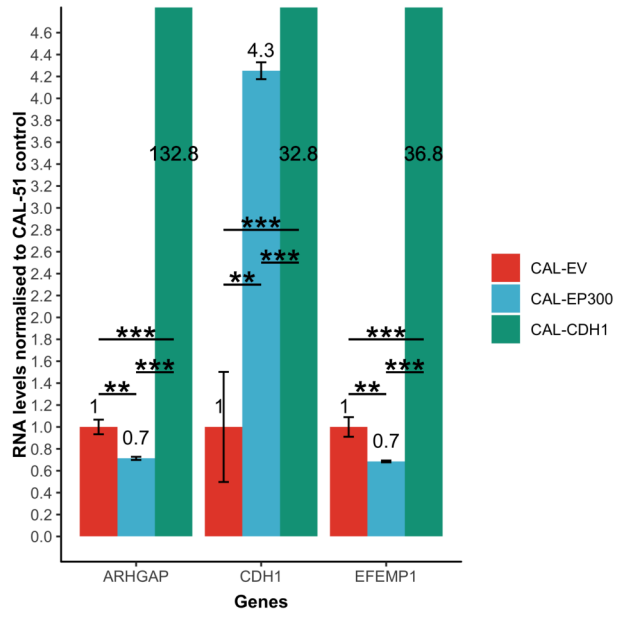
RNA levels normalised to CAL-51 control
Genes
ARHGAP
CDH1
EFEMP1
CAL-EV
CAL-EP300
CAL-CDH1
132.8
32.8
36.8
4.3
0.7
1
***
**

(b)

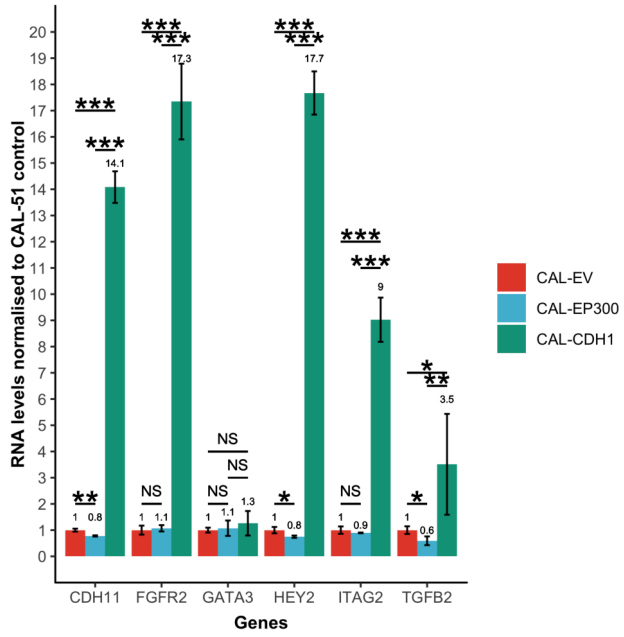
RNA levels normalised to CAL-51 control
Genes
CDH11
FGFR2
GATA3
HEY2
ITAG2
TGFB2
CAL-EV
CAL-EP300
CAL-CDH1

(c)

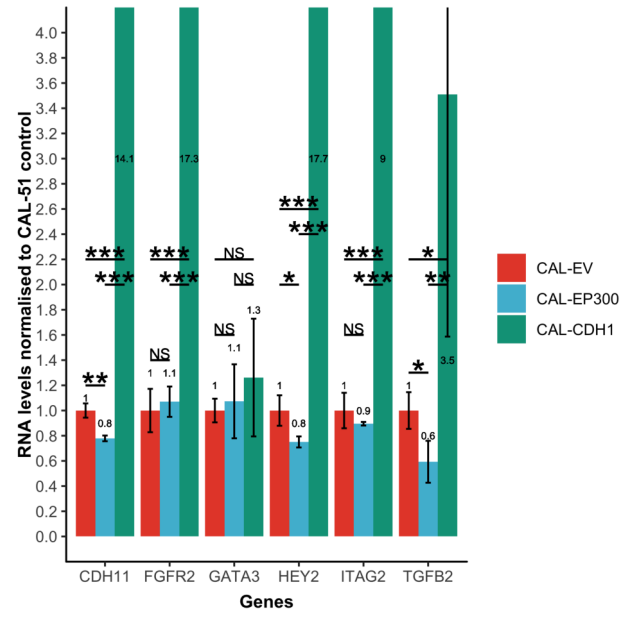
RNA levels normalised to CAL-51 control
Genes
CDH11
FGFR2
GATA3
HEY2
ITAG2
TGFB2
CAL-EV
CAL-EP300
CAL-CDH1

(d)

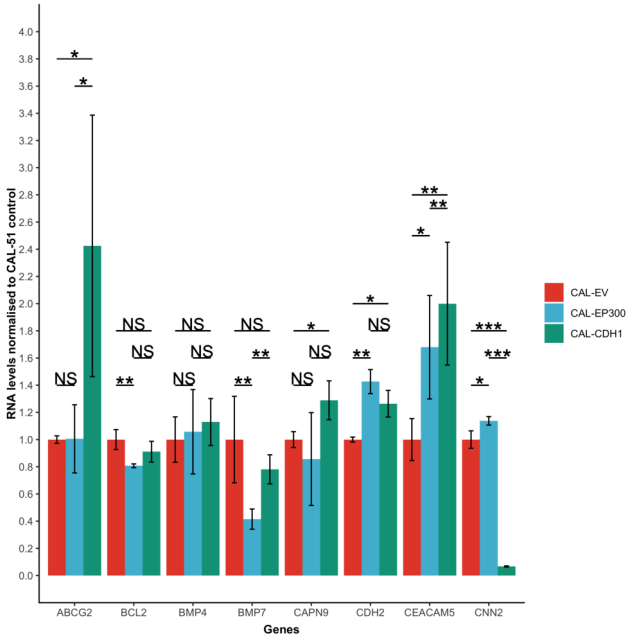
RNA levels normalised to CAL-51 control
Genes
ABCG2
BCL2
BMP4
BMP7
CAPN9
CDH2
CEACAM5
CNN2
CAL-EV
CAL-EP300
CAL-CDH1

(e)

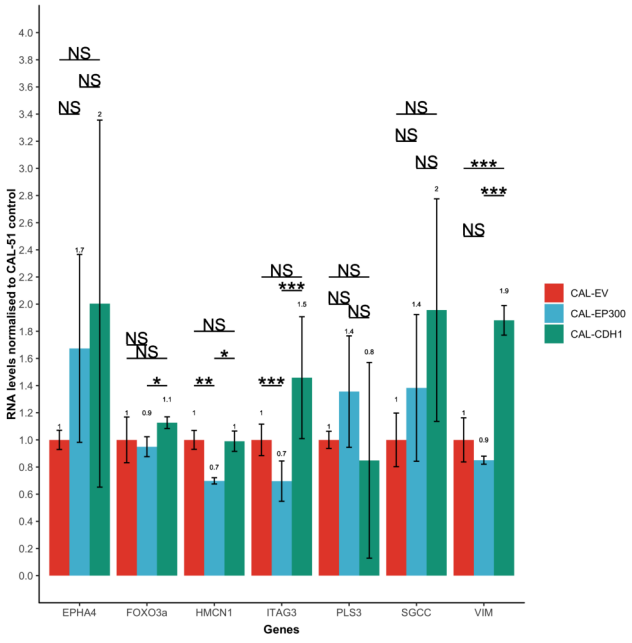
RNA levels normalised to CAL-51 control
Genes
EPHA4
FOXO3a
HMCN1
ITAG3
PLS3
SGCC
VIM
CAL-EV
CAL-EP300
CAL-CDH1

(f)

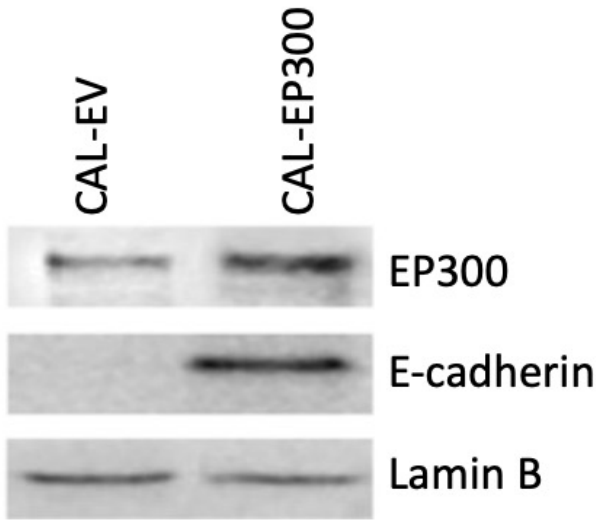

(g) Source : "Tumour suppressor EP300, a modulator of paclitaxel resistance and stemness, is downregulated in metaplastic breast cancer", (Asaduzzaman et al 2017).

Fig. 4.1 Gene expression in CAL51 breast cancer cell lines with EP300 overexpression. The mRNA levels were detected in CAL51 by RTqPCR analysis. Gene expression in EP300 (CAL-EP300) and CDH1 (CAL-CDH1) overexpressing cells was demonstrated relative to the respective control (wild type and empty vector control transfected cells). Gene expression was normalised to the RPS14 and RPLP0 housekeeping genes. Panels show mRNA levels in CAL51 (a-f). A western blot demonstrating the overexpression of EP300 and subsequent effect on E-cadherin is shown in CAL51 (g). Data are shown as normalised to CAL51 shEV empty vector expressing cells (CAL-EV). The mean + SD of n=3 independent experiments is shown, NS Non-Significant, * $p<0.05$, **$p<0.01$, *** $P<0.001$,****$p<0.0001$ (ordinary one-way ANOVA following Dunnett's multiple comparison test).

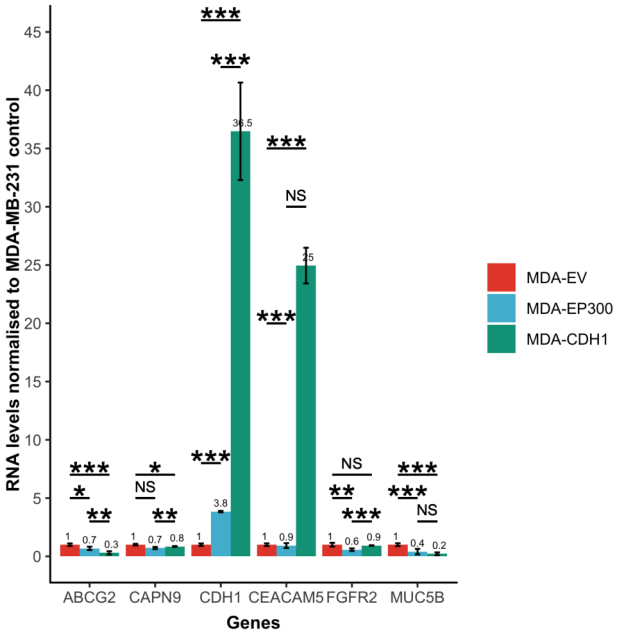
RNA levels normalised to MDA-MB-231 control
Genes
ABCG2
CAPN9
CDH1
CEACAM5
FGFR2
MUC5B
MDA-EV
MDA-EP300
MDA-CDH1

(a)

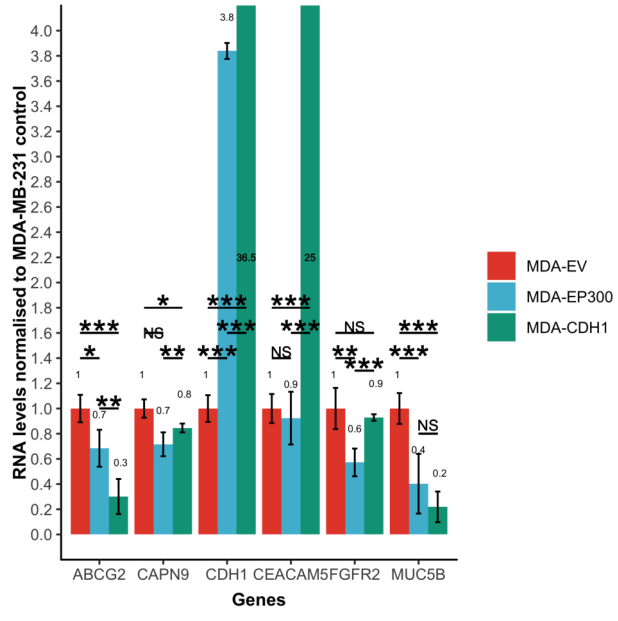
RNA levels normalised to MDA-MB-231 control
Genes
ABCG2
CAPN9
CDH1
CEACAM5
FGFR2
MUC5B
MDA-EV
MDA-EP300
MDA-CDH1

(b)

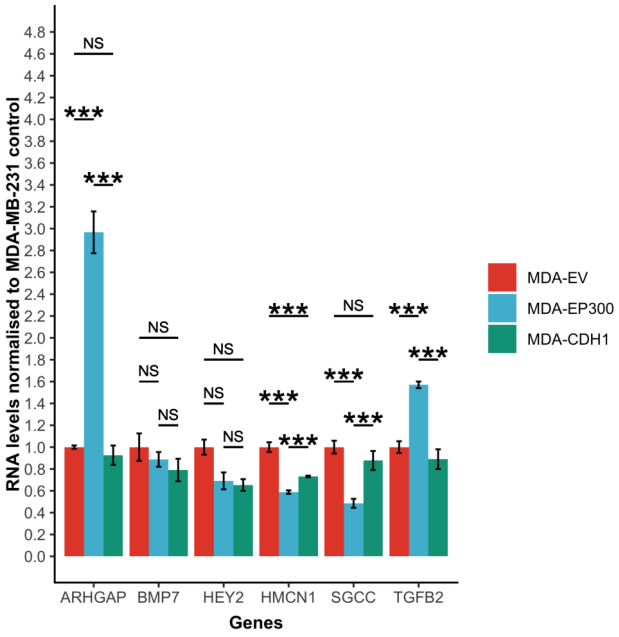
RNA levels normalised to MDA-MB-231 control
Genes
ARHGAP
BMP7
HEY2
HMCN1
SGCC
TGFB2
MDA-EV
MDA-EP300
MDA-CDH1
NS
***

(c)

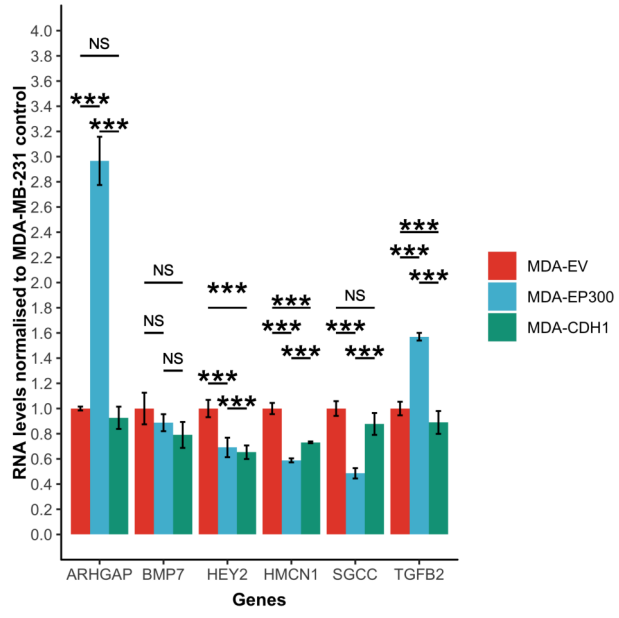
RNA levels normalised to MDA-MB-231 control
Genes
ARHGAP
BMP7
HEY2
HMCN1
SGCC
TGFB2
MDA-EV
MDA-EP300
MDA-CDH1
NS
***

(d)

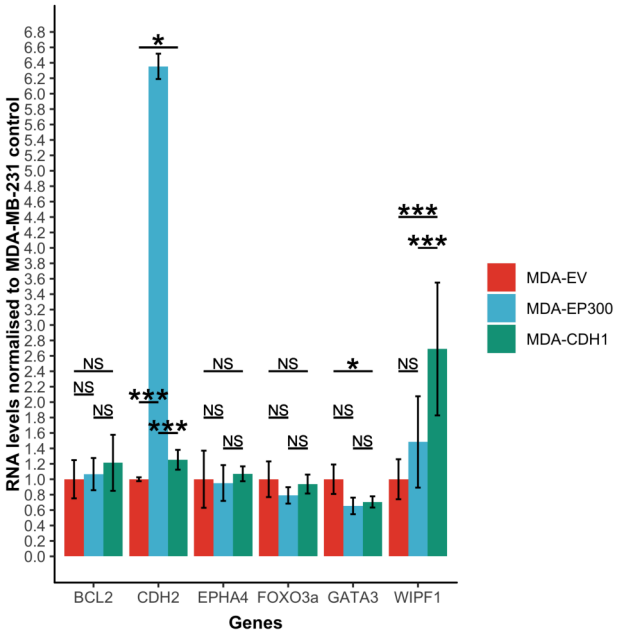
RNA levels normalised to MDA-MB-231 control
Genes
BCL2
CDH2
EPHA4
FOXO3a
GATA3
WIPF1
MDA-EV
MDA-EP300
MDA-CDH1

(e)

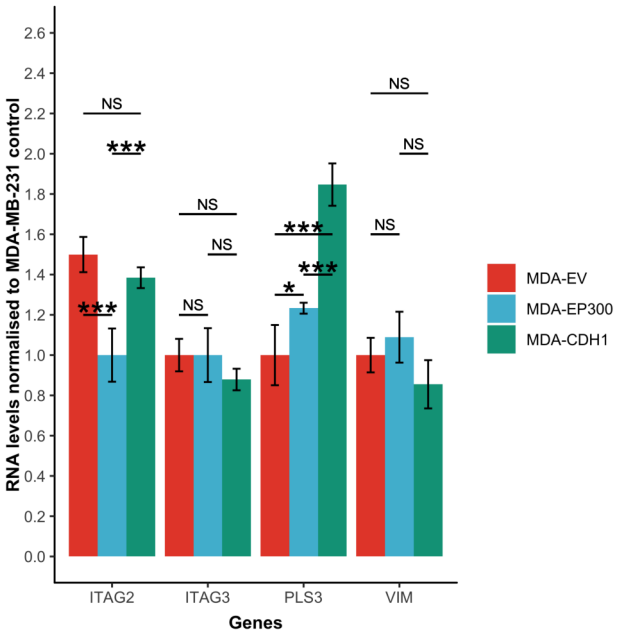
RNA levels normalised to MDA-MB-231 control
Genes
ITAG2
ITAG3
PLS3
VIM
MDA-EV
MDA-EP300
MDA-CDH1

(f)

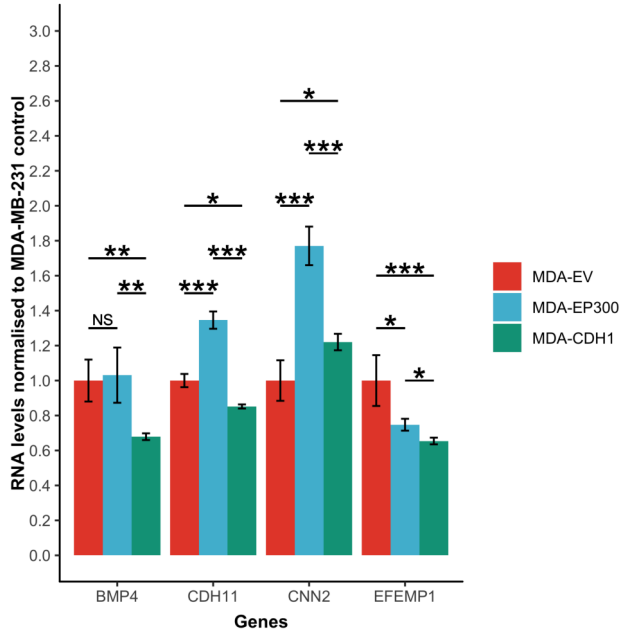

(g)

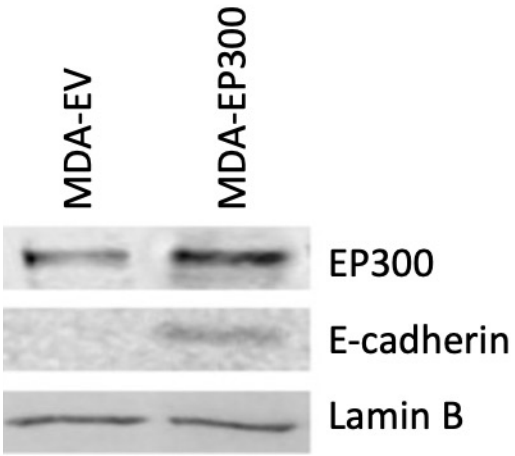

(h) Source : "Tumour suppressor EP300, a modulator of paclitaxel resistance and stemness, is downregulated in metaplastic breast cancer", (Asaduzzaman et al 2017).

Fig. 4.2 Gene expression in MDA-MB-231 breast cancer cells with EP300 overexpression. The mRNA levels were detected in MDA-MB-231 by RTqPCR analysis. Gene expression in EP300 (MDA-EP300) and CDH1 (MDA-CDH1) overexpressing cells was demonstrated relative to the respective control (wild type and empty vector control transfected cells). Gene expression was normalised to the RPS14 and RPLP0 housekeeping genes. Panels show mRNA levels in MDA-MB-231 (a-g). A western blot demonstrating the overexpression of EP300 and subsequent effect on E-cadherin is shown in MDA-MB-231 (h). Data are shown as normalised to MDA-MB-231 shEV empty vector expressing cells (MDA-EV). The mean + SD of n=3 independent experiments is shown, NS Non-Significant, * $p<0.05$, **$p<0.01$, *** $P<0.001$,****$p<0.0001$ (ordinary one-way ANOVA following Dunnett's multiple comparison test).

EP300 and CDH1 overexpression does not result in a similar gene expression profile in mesenchymal cell lines.

When comparing the overexpression of EP300 and CDH1 in CAL-51 (**Figure 4.1**), CDH1 has a significantly higher effect on 132 fold higher expression of ARHGAP20 ($p<0.001$), 36 fold higher expression of EFEMP1 ($p<0.001$) and 29 fold higher expression of CDH1 ($p<0.001$) (**Figures 4.1a** and **4.1b**). CDH1 also results in a 13 fold higher CDH11 ($p<0.001$), a 17 fold higher FGFR2 ($p<0.001$), a 17.8 fold higher HEY2 ($p<0.001$), a 9 fold higher ITGA2 ($p<0.001$), and a 2.6 fold higher TGFβ2 ($p<0.01$)(**Figures 4.1c** and **4.1d**). It also results in 2.4 fold higher ABCG2 ($p<0.05$), 0.4 fold higher CEACAM5 ($p<0.01$). Both EP300 and CDH1 have no effect on CDH2 and CAPN9 (**Figure 4.1e**). 1.9 fold higher expression of VIM ($p<0.001$). EP300 is lower by 0.4 fold in HMCN1 ($p<0.001$) and also higher by 1.1 fold in CNN2 ($p<0.001$) (**Figure 4.1f**).

The overexpression of EP300 and CDH1 in MDA-MB-231 (**Figure 4.2**) has a different effect in this cell line, compared to CAL51. There was no significant change between the two conditions in MUC5B. CDH1 overexpression resulted in higher expression by 0.13 fold in CAPN9 ($p<0.01$), by 33 fold in CDH1 ($p<0.001$), by 23 fold in CEACAM5 ($p<0.001$), by 0.3 fold in FGFR2 ($p<0.001$). Whereas overexpression of EP300 resulted in higher expression of ABCG2 by 0.3 fold ($p<0.01$) (**Figures 4.2a** and **4.2b**. EP300 overexpression resulted in a lower expression by 0.3 fold in HMCN1 ($p<0.001$) and by 0.4 fold in SGCG ($p<0.001$). It also resulted in a higher expression of ARGHAP-20 by 3.1 fold ($p<0.001$) and by 1.7 fold in TGFβ2 ($p<0.001$) (**Figures 4.2c** and **4.2d**). EP300 overexpression resulted in higher expression of CDH2 by 5.2 fold ($p<0.001$). While CDH1 overexpression resulted in lower expression of GATA3 by 0.1 fold ($p<0.05$) and higher expression of WIPF1 by 1.1 fold ($p<0.001$) (**Figure 4.2e**). CDH1 overexpression resulted in higher expression by 1.7 fold in ITGA2 ($p<0.001$) and by 0.5 fold in PLS3 ($p<0.001$) (**Figure 4.2f**). EP300 overexpression resulted in higher expression of BMP4 by 0.5 fold ($p<0.01$), by 1.5 fold in CDH11 ($p<0.001$), by 0.5 fold in CNN2 ($p<0.001$). While CDH1 overexpression resulted in a lower expression of EFEMP1 by 0.1 fold ($p<0.05$) (**Figure 4.2g**).

Overall while both cell lines share mesenchymal characteristics, which was extensively covered by other studies, we show that their responses to overexpression of EP300 and CDH1 results in a different expression pattern. This likely reflects the heterogeneity of cancer, and activation of multiple pathways. Furthermore, comparing both EP300 and CDH1 shows that they affect different genes. CDH1 seems to affect certain genes in a dramatic way, something which is not matched by EP300, despite it promomting CDH1 expression. This is likely due to two reasons. Firstly EP300 affects a much larger range of interactive partners, some of which might negate the effects on the genes we demonstrated CDH1 upregulates. Secondly,

EP300 overexpression while upregulating CDH1, does not bring it over the threshold of direct CDH1 overexpression, which is the most likely reason for such differences in signalling.

Knockout of EP300 in colorectal carcinoma cell line HCT116 promotes mesenchymal gene expression.

We now move on to our colorectal cancer cell line HCT116 of epithelial origin, which is characterised by a KRAS mutation and PIK3CA mutation. It also has a high basal level expression of EP300 (**Figure 4.3**). In **Figures 4.3a and 4.3b** knockout of EP300 showed no significant change in ABCG2. It did result in an upregulation of HMCN1 by 20.6 fold ($p<0.05$), by 17.3 fold of TGFβ2 ($p<0.001$) and by 6.4 fold of WIPF1 ($p<0.001$). There was also a decrease in ARHGAP20 by 0.5 fold ($p<0.05$).In **Figure 4.3c**, knockout of EP300 showed no significant change in CEACAM5 and SNAI1. There was also an upregulation of CAPN9 by 8.2 fold ($p<0.01$), by 14.3 fold of CDH11 ($p<0.001$), by 3.9 fold of CDH2 ($p<0.01$) and by 5.5 fold of EFEMP1 ($p<0.01$). In **Figure 4.3d**, knockout of EP300 showed no significant change in FOXA1 and GATA3. There was also an upregulation of BCL2 by 5.3 fold ($p<0.05$), by 4.5 fold in HEY2 ($p<0.001$), and a downregulation by 5.4 fold in SGCG ($p<0.05$). In **Figure 4.3e**, knockout of EP300 showed no significant change in BMP7, EPHA4, FGFR2, FOXO3a and ITGA2. There was upregulation in BMP4 by 7.9 fold ($p<0.001$). In **Figures 4.3f and 4.3g**, knockout of EP300 showed no significant change in ITGA3 and PLS3. There was downregulation of CDH1 by 0.7 fold ($p<0.001$), and upregulation by 2.2 fold in CNN2 ($p<0.05$) and VIM by 257 fold ($p<0.001$). In this section we also demonstrate the knockout of EP300 using a western blot showing the downregulated protein levels (**Figure 4.3h**). This was taken from our lab's publication (Asaduzzaman et al. 2017).

Overall the knockout of EP300 seems to result in a potentially more mesenchymal cell line. Suggesting that EP300 acts as a suppressor of favourable tumour characteristics. The overexpression of VIM, BMP4 and CDH11 shows that this cell line is progressing more towards its mesenchymal phenotype and perhaps even showing some stemness characterics as CDH11 controls stem cell fate. Furthermore, the upregulation in TGFβ2 promotes this view as the TGF-β pathway along with WNT signalling are involved in driving tumour inititation in vivo.

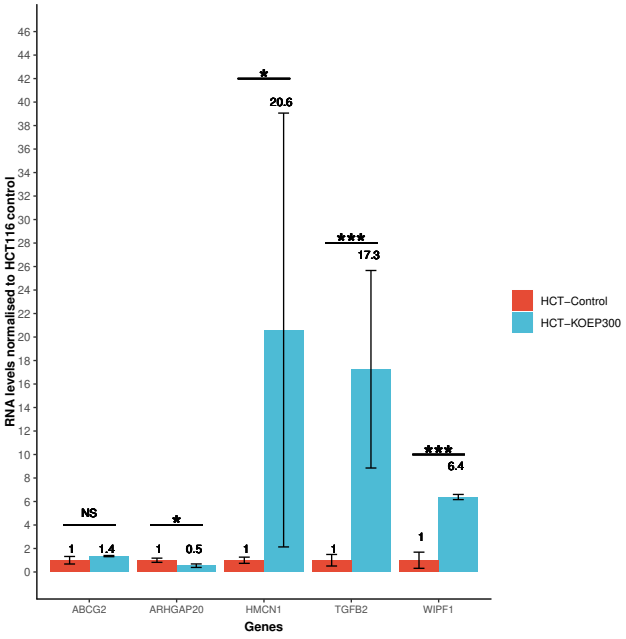
RNA levels normalised to HCT116 control
Genes
ABCG2
ARHGAP20
HMCN1
TGFB2
WIPF1
NS
*
20.6
***
17.3
***
6.4
1
1.4
0.5
HCT−Control
HCT−KOEP300

(a)

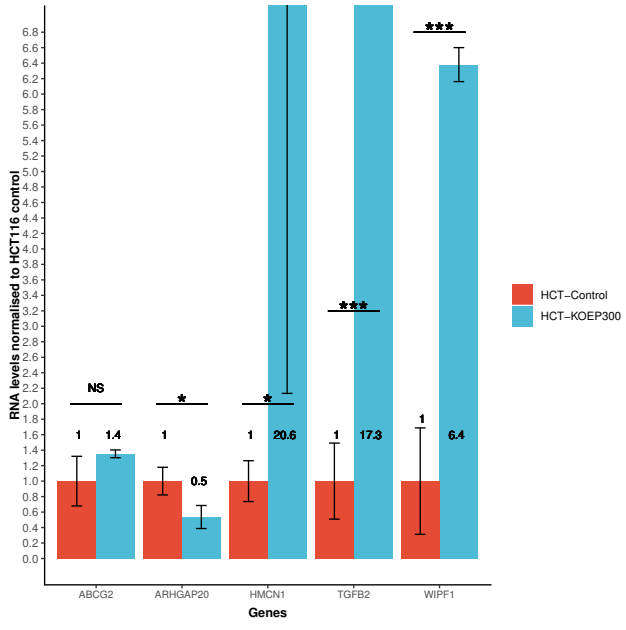
RNA levels normalised to HCT116 control
Genes
ABCG2
ARHGAP20
HMCN1
TGFB2
WIPF1
NS
*
20.6
***
17.3
***
6.4
1
1.4
0.5
HCT−Control
HCT−KOEP300

(b)

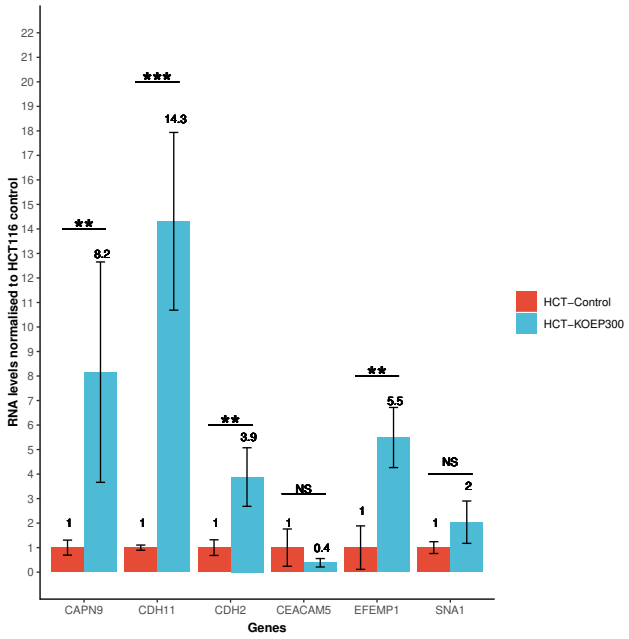
RNA levels normalised to HCT116 control
Genes
CAPN9
CDH11
CDH2
CEACAM5
EFEMP1
SNA1
HCT−Control
HCT−KOEP300
**
***
**
NS
**
NS
8.2
14.3
3.9
0.4
5.5
2
1

(c)

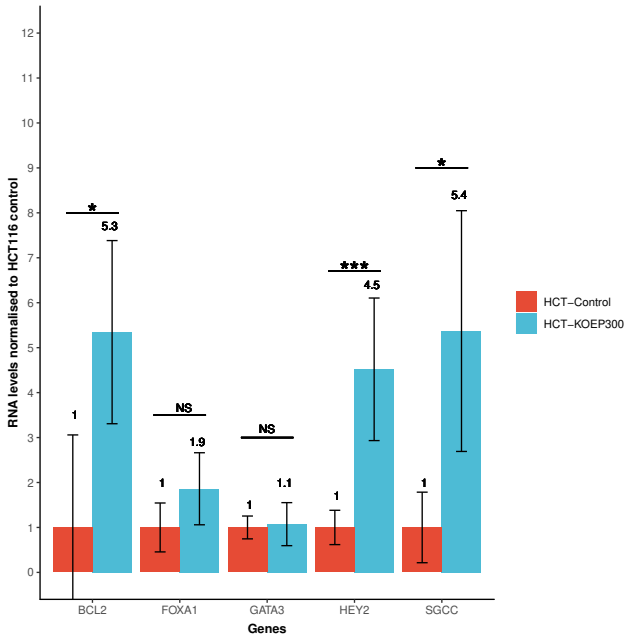
RNA levels normalised to HCT116 control
Genes
BCL2
FOXA1
GATA3
HEY2
SGCC
HCT−Control
HCT−KOEP300
*
NS
NS
***
*
5.3
1.9
1.1
4.5
5.4
1

(d)

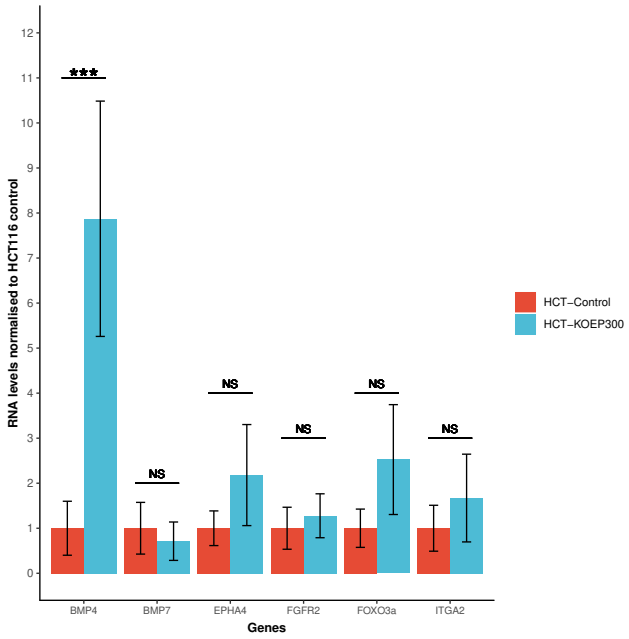
RNA levels normalised to HCT116 control
Genes
BMP4
BMP7
EPHA4
FGFR2
FOXO3a
ITGA2
***
NS
NS
NS
NS
NS
HCT−Control
HCT−KOEP300

(e)

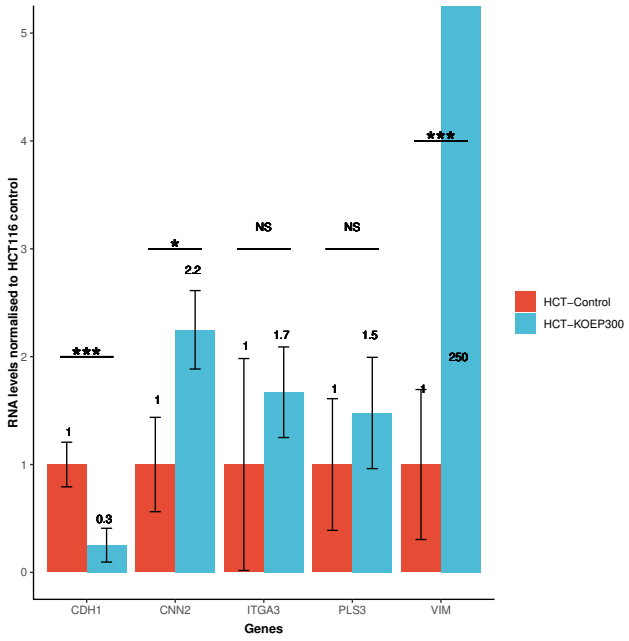
RNA levels normalised to HCT116 control
Genes
CDH1
CNN2
ITGA3
PLS3
VIM
***
*
NS
NS
***
1
0.3
1
2.2
1
1.7
1
1.5
1
250
HCT−Control
HCT−KOEP300

(f)

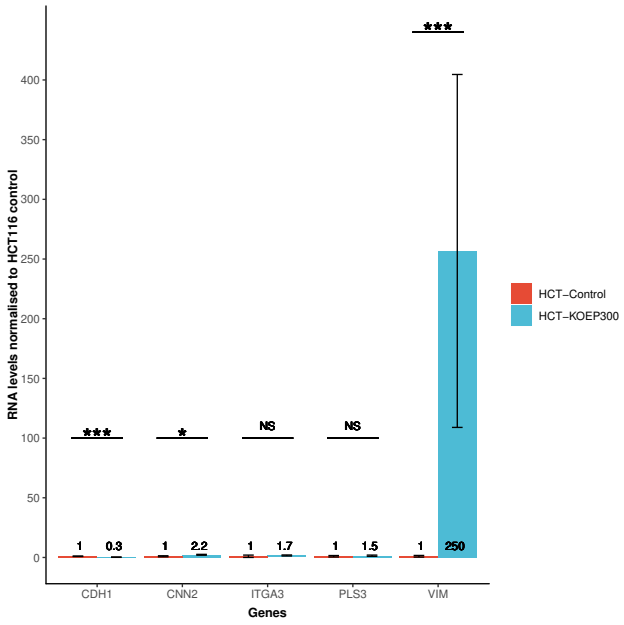

(g)

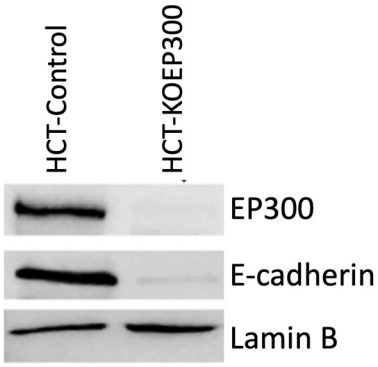

(h) Source : "Tumour suppressor EP300, a modulator of paclitaxel resistance and stemness, is downregulated in metaplastic breast cancer", (Assaduzzaman et al 2017).

Fig. 4.3 Gene expression in HCT116 colorectal cancer cells with EP300 knockout. The mRNA levels were detected in HCT116 by RTqPCR analysis. Gene expression in EP300 knockout cells (HCT-KOEP300) was demonstrated relative to the respective wild type control (HCT-Control). Gene expression was normalised to the RPS14 and RPLP0 housekeeping genes. Panels show mRNA levels in HCT116 (a-g). A western blot demonstrating the knockdown of EP300 is shown in HCT116 (h). Data are shown as normalised to HCT116 wild type cells (HCT-Control). The mean + SD of n=3 independent experiments is shown, NS Non-Significant, * p<0.05, **p<0.01, *** P<0.001,****p<0.0001 (ordinary one-way ANOVA following Dunnett's multiple comparison test).

The introduction of shEP300 vectors into the T47D breast cancer cell line, results in a potent downregulation of EP300.

The next cell line we will look at is of an epithelial characteristic, same to the MCF7 cell line used in the Gene Chip ®. Both the MCF7 and the T47D cell lines are of the luminal A subtype and express ER, PR and HER2- enrichment. The T47D expresses basal levels of EP300. In this experimental model, we will do the opposite to mesenchymal cells and attempt to induce a mesenchymal-like phenotype through the downregulation of EP300 by RNA interference using two different hairpins, shEP300 I and shEP300 II.

In **Figure 4.4a** the downregulation of EP300 with shEP300 I, resulted in no significant change in ARHGAP20, MUCS5B and WIPF1. There was upregulation of CDH11 by 2.6 fold ($p<0.001$), by 2.3 fold in HMCN1 ($p<0.05$) and SGCG by 2.2 fold ($p<0.05$). The downregulation of EP300 with shEP300 II, resulted in no significant change in HMCN1, SGCG and WIPF1. There was an upregulation of ARHGAP20 by 4.9 fold ($p<0.001$), by 1.7 fold in CDH11 ($p<0.05$), and a downregulation by 0.2 fold in MUCS5B ($p<0.05$). In **Figures 4.4b** and **4.4c** the downregulation of EP300 with shEP300 I, resulted in a significant decrease by 0.8 fold in EP300 ($p<0.001$), which is expected based on our previously published results for MCF7 (Asaduzzaman et al 2017). We also saw a 1.3 fold increase in FOXO3a ($p<0.01$), and a 0.8 fold decrease by 0.9 fold in GATA3 ($p<0.001$). No significant change was seen in CDH2, EPHA4 and HEY2. While there is an upregulation of PLS3 by 3.8 fold ($p<0.001$). The downregulation of EP300 with shEP300 II, also resulted in a significant downregulation by 0.9 fold in EP300 ($p<0.001$). We also saw a 1.3 fold increase in FOXO3a ($p<0.01$), and a 0.8 fold decrease in GATA3 by 0.9 fold ($p<0.01$). No change was seen in CDH2 and HEY2. There was also an upregulation in EPHA4 by 11.7 fold ($p<0.001$) and a downregulation in PLS3 by 0.7 fold ($p<0.001$). In **Figure 4.4d** the downregulation of EP300 with shEP300 I, resulted in a 1 fold decrease in CDH1 ($p<0.01$), a 0.9 fold decrease in GATA3 ($p<0.01$) and no significant change in CNN2, EFEMP1, FGFR2. The downregulation of EP300 with shEP300 II, resulted in 0.9 fold decrease in CDH1 ($p<0.001$), 0.8 fold decrease in GATA3 ($p<0.01$) and no significant change in CNN2, EFEMP1 and FGFR2.

Comparing the two vectors shEP300 I and shEP300 II seems to show they affect gene expression differently. The shEP300 I vector upregulates CDH11 by 1 fold ($p<0.001$), HMCN1 by 2.8 fold ($p<0.001$), SGCG by 1.1 fold ($p<0.01$) and more downregulation in MUCS5B by 0.2 fold ($p<0.05$). The shEP300 II vector upregulates ARGHAP-20 by 5.2 fold ($p<0.01$). Comparatively, shEP300 I resulted in higher expression of PLS3 by 4.1 fold ($p<0.001$) and shEP300 II resulted in higher expression of EPHA4 by 16.7 fold ($p<0.001$). Comparatively, shEP300 I resulted in higher expression of FGFR2 by 1.3 fold ($p<0.01$) while shEP300 II resulted in higher expression of CDH1 by 2.1 fold ($p<0.001$). There is also

no significant difference between the two vectors and expression of GATA3, FOXO3a and EP300.

Thus, to summarise we demonsrate a downregulation of EP300 as a result of our lentivarial transfection of shEP300 I and shEP300 II vectors. This also resulted in a downregulation in CDH1 and GATA3, which could suggest the loss of epithelial characteristics and mirrors the results of the previously published data on MCF7s shown in 4.4e (Asaduzzaman et al 2017). The differences in expression of other genes is likely due to different phases of the cell cycle in which the protein extraction took place. Alternatively the efficiency of vector uptake over the other might result in these differences.

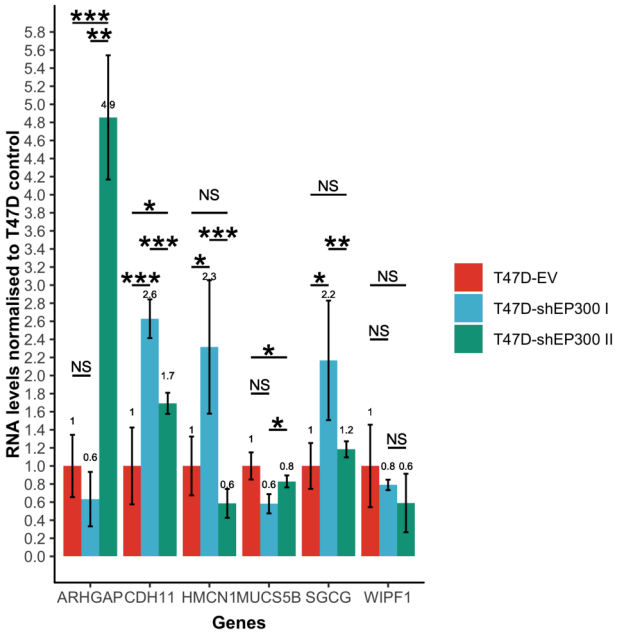
RNA levels normalised to T47D control
Genes
ARHGAP
CDH11
HMCN1
MUCS5B
SGCG
WIPF1
T47D-EV
T47D-shEP300 I
T47D-shEP300 II

(a)

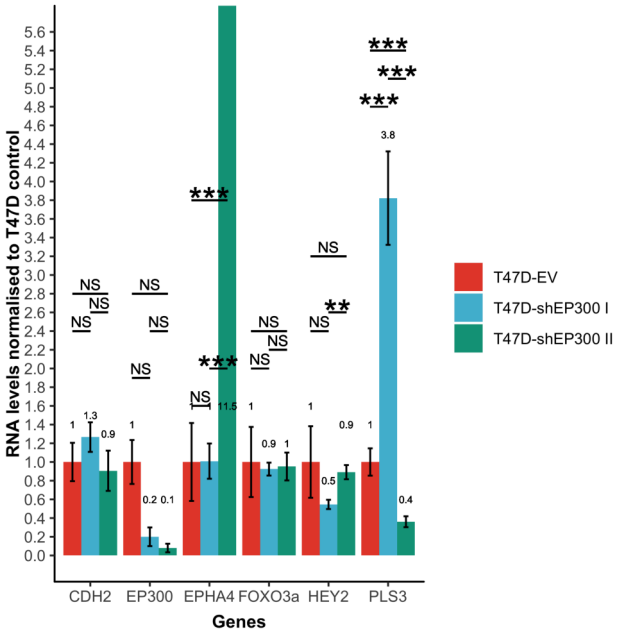
RNA levels normalised to T47D control
Genes
CDH2
EP300
EPHA4
FOXO3a
HEY2
PLS3
T47D-EV
T47D-shEP300 I
T47D-shEP300 II

(b)

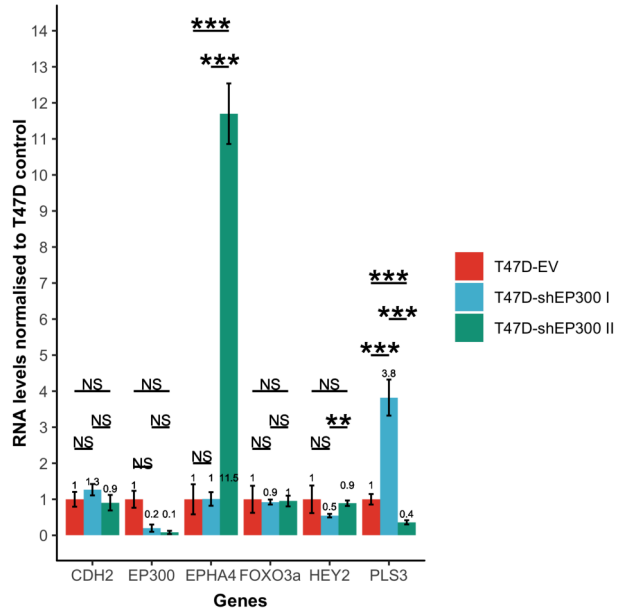
RNA levels normalised to T47D control
Genes
CDH2
EP300
EPHA4
FOXO3a
HEY2
PLS3
T47D-EV
T47D-shEP300 I
T47D-shEP300 II

(c)

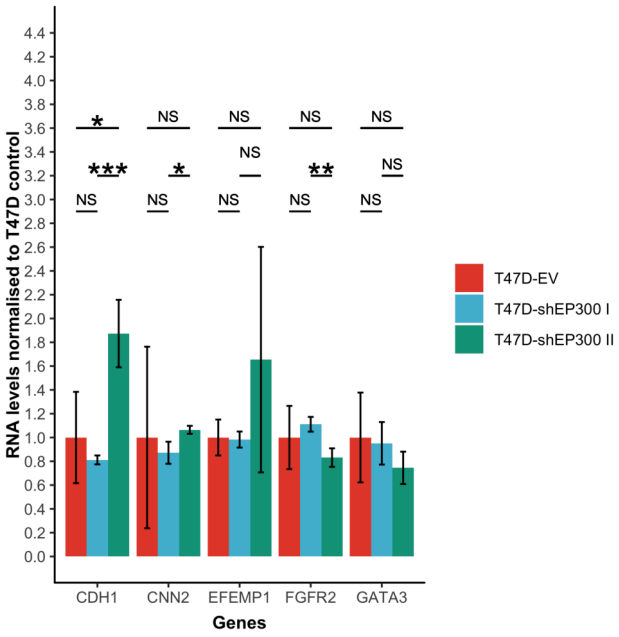
RNA levels normalised to T47D control
Genes
CDH1
CNN2
EFEMP1
FGFR2
GATA3
T47D-EV
T47D-shEP300 I
T47D-shEP300 II

(d)

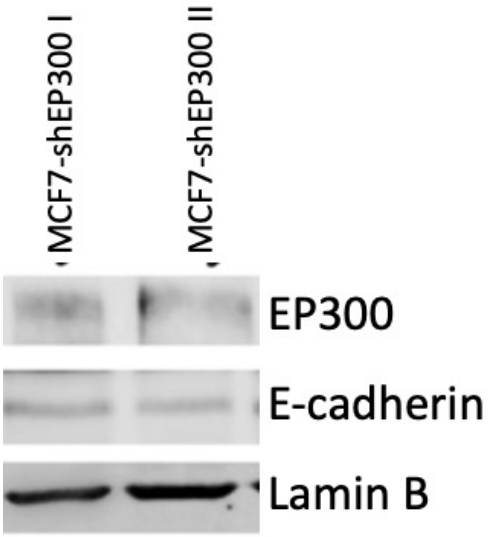

(e) Source : "Tumour suppressor EP300, a modulator of paclitaxel resistance and stemness, is downregulated in metaplastic breast cancer", (Asaduzzaman et al 2017).

Fig. 4.4 Gene expression in a T47D breast cancer cells with EP300 downregulation. The mRNA levels were detected in T47D by RTqPCR analysis. Gene expression of T47D cells transfected with two EP300 knockdown vectors (T47D-shEP300 I) and (T47D-shEP300 II) was demonstrated relative to the respective control (wild type and empty vector control transfected cells). Gene expression was normalised to the RPS14 and RPLP0 housekeeping genes. Panels show mRNA levels of T47D breast cancer cell line, transfected with EP300 overexpressing vectors sh EP300 I and sh EP300 II (a-d). A western blot demonstrating the knockdown of EP300 using shEP300 I and shEP300 II is shown in a comparable model of MCF7 (e). Data are shown as normalised to T47D shEV empty vector expressing cells (T47D-EV). The mean + SD of n=3 independent experiments is shown, NS Non-Significant, * $p<0.05$, **$p<0.01$, *** $P<0.001$,****$p<0.0001$ (ordinary one-way ANOVA following Dunnett's multiple comparison test).

Modulation of EP300 results in no change in cell proliferation.

As previous results showed potential for reversal of EMT through gene expression in CAL-51, MDA-MB-231 and potential promotion of EMT through gene expression in our epithelial cell lines, we moved on to attempt to see if this had any effect on proliferation. As one of the characteristics and hallmarks of cancer, cell proliferation is an important survival trait for cancer. We attempted to investigate this in our two models for EP300 and CDH1 overexpression in CAL-51 and MDA-MB-231.

In **Figures 4.5a** and **4.5b**, we see the effect of EP300 and CDH1 overexpression on cell proliferation in CAL-51 and MDA-MB-231. EP300 and CDH1 overexpression seem to follow the same upwards trend of proliferation as with the empty vector control. No significant difference is seen between conditions in either cell line. In **Figure 4.5c**, we see no effect of EP300 downregulation on cell proliferation in MCF7. EP300 knockdown with shEP300 I seems to follow the same upwards trend of proliferation as with the empty vector control, with no significant difference being seen between the two conditions. With shEP300 II, there seems to be a lower rate of proliferation from day 3 across to day 6 ($p<0.05$). In **Figure 4.5d** we observe no the effect of EP300 knockout on cell proliferation in HCT116. However, this cell line seems to generate an increase in proliferation between day 4-5.

Overall, we observe no correlation between modulation of EP300, in either of our two models. Suggesting that either our genes of choice have no effect on this trait, or we should look into alternative models for proliferation.

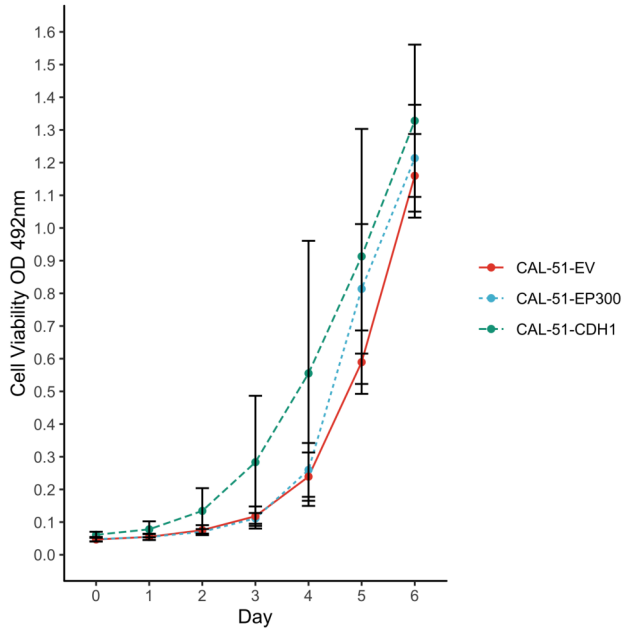
Cell Viability OD 492nm
Day
CAL-51-EV
CAL-51-EP300
CAL-51-CDH1

(a)

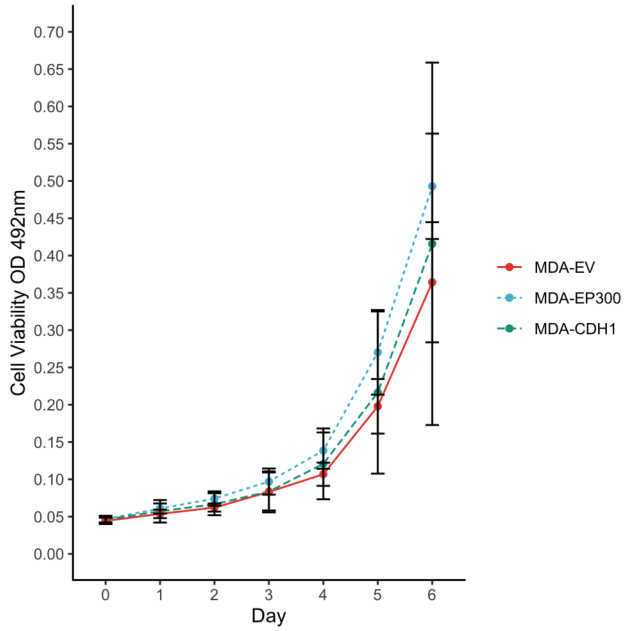
Cell Viability OD 492nm
Day
MDA-EV
MDA-EP300
MDA-CDH1

(b)

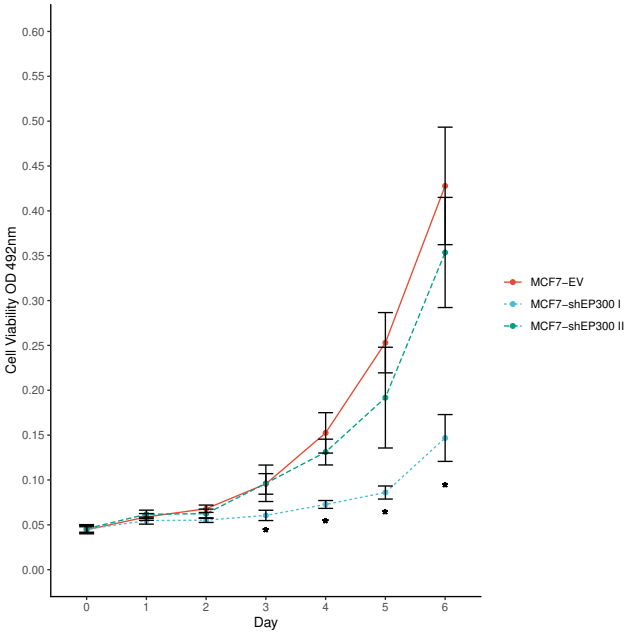

(c)

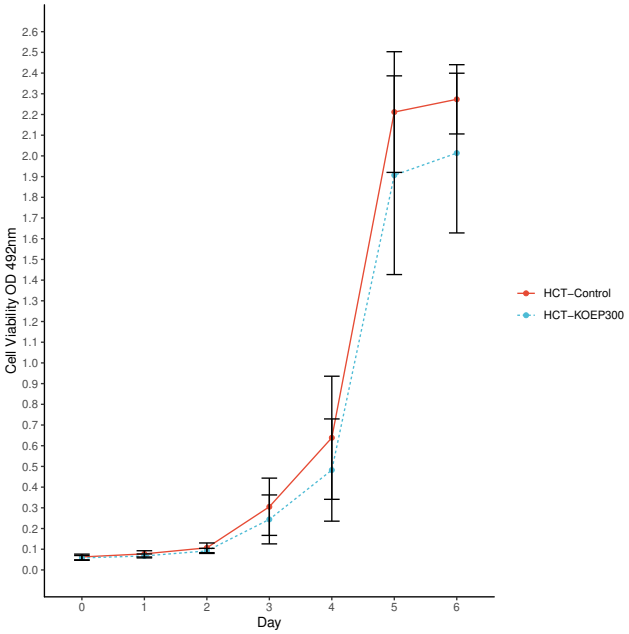

(d)

Fig. 4.5 Cell Proliferation In Breast Cancer Cell Lines. The cell proliferation was measured as OD value representative of crystal violet staining.Panels show cell viability (OD) values of (A) CAL51 overexpressing EP300 (CAL-EP300) and overexpressing CDH1 (CAL-CDH1) compared to CAL51 with an empty vector control (CAL-EV), (B) MDA-MB-231 overexpressing EP300 (MDA-EP300) and overexpressing CDH1 (MDA-CDH1) compared to MDA-MB-231 with an empty vector control (MDA-EV), (C) MCF7 cells with a downregulation in EP300 (shEP300 I and shEP300 II) compared to MCF7 with an empty vector control (MCF7-EV) and (D) HCT116 wild type cells (HCT-Control) compared to HCT116 with EP300 knockout (HCT-KOEP300). The mean + SD of n=3 independent experiments is shown, NS Non-Significant, * p<0.05, **p<0.01, *** P<0.001,****p<0.0001 (ordinary one-way ANOVA following Dunnett's multiple comparison test).

Effect of EP300 downregulation results in no change in cell proliferation in epithelial breast cancer cell lines.

In our investigation of the effects of EP300 on cell proliferation we tested our epithelial MCF7 and T47D model with shEP300 vectors. Followed by an alternative model in colorectal cancer where we induced a stable knockdown of EP300. In Figure 6, we try to replicate the experiment for MCF7 and see if our T47D knockdown of EP300 has any effect on cell proliferation. In **Figure 4.6a**, we tested the effect of EP300 knockdown on cell proliferation in T47D with a cell seeding density of 200 cells per well. There is no significant difference between shEP300 II and other conditions between days 0-3. There is no significant difference between shEP300 I and the control between days 0-5. There is a difference of 0.16 in cell viability at day 6 ($p<0.05$) and 0.34 at day 7 ($p<0.05$) of shEP300 I versus the empty vector control. With shEP300 II, there is an increase there is a difference of 0.3 at day 4 ($p<0.01$), 0.28 at day 5 ($p<0.05$), 0.6 at day 6 ($p<0.05$) and 0.68 at day 7($p<0.01$).

Comparing both vectors, shEP300 II has more effect on cell proliferation than shEP300 I. It is higher by 0.23 at day 4 ($p<0.01$), by 0.23 at day 5 ($p<0.05$), by 0.39 at day 6 ($p<0.05$) and by 0.34 day 7($p<0.01$). In **Figure 4.6b** we tested the effect of EP300 knockdown on cell proliferation in T47D with a cell seeding density of 500 cells per well. There is no significant difference between any conditions on any day. In **Figure 4.6c** we tested the effect of EP300 knockdown on cell proliferation in T47D with a cell seeding density of 700 cells per well. There is no significant difference between any conditions on days 0-4 and no significant difference between the control and shEP300 I on any day. On day 5, shEP300 II has higher cell viability to the control by 0.45 ($p<0.05$) and by 0.27 on day 6 ($p<0.05$). When comparing shEP300 I and shEP300 II, shEP300 II has a higher cell viability on day 5 by 0.44 ($p<0.05$) and by 0.27 on day 6 ($p<0.05$). In **Figure 4.6d** we tested the effect of EP300 knockdown on cell proliferation in T47D with a cell seeding density of 1000 cells per well. Between the days 0-4 and 6-7 there was no significant difference. On day 5 shEP300 I increased by 0.29 ($p<0.05$) and shEP300 II decreased by 0.21 ($p<0.05$) compared to the control. The difference between shEP300 I and shEP300 II on day 5 is 0.5 ($p<0.05$).

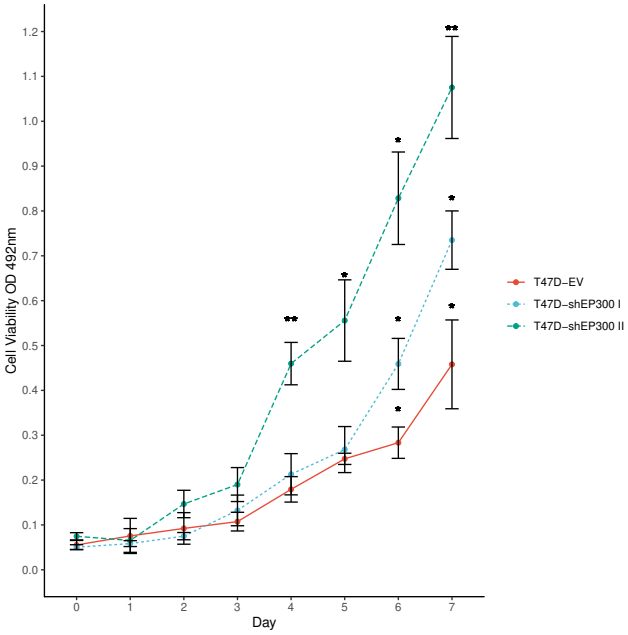
Cell Viability OD 492nm
Day
T47D−EV
T47D−shEP300 I
T47D−shEP300 II

(a)

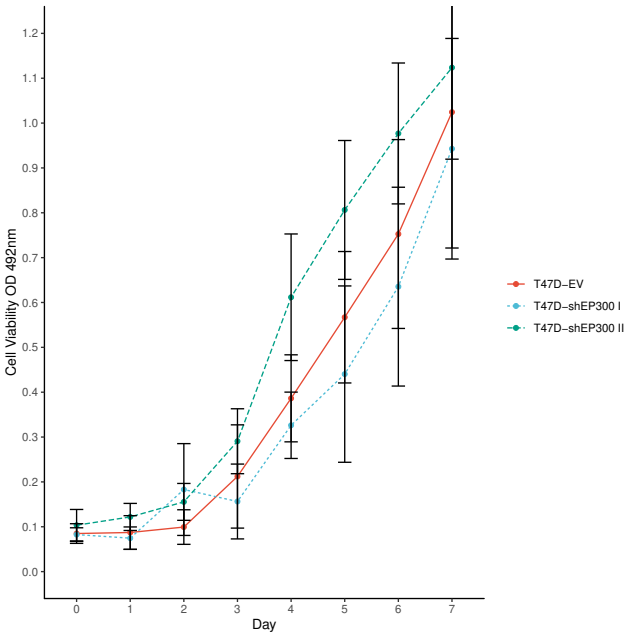
Cell Viability OD 492nm
Day
T47D−EV
T47D−shEP300 I
T47D−shEP300 II

(b)

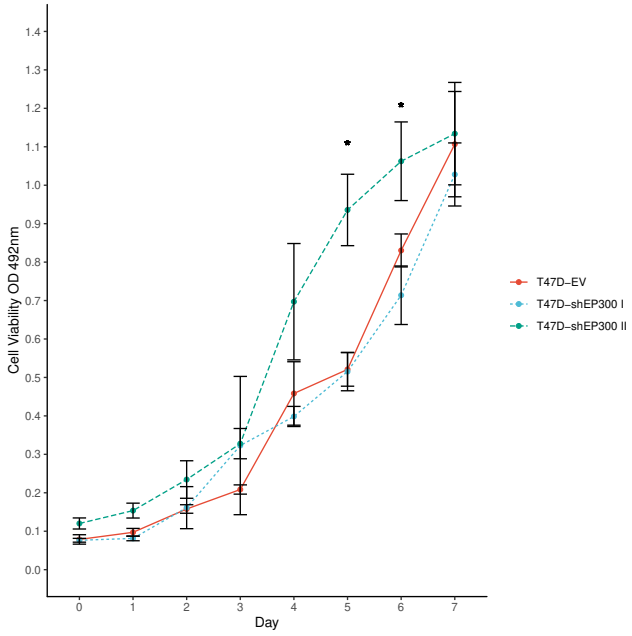

(c)

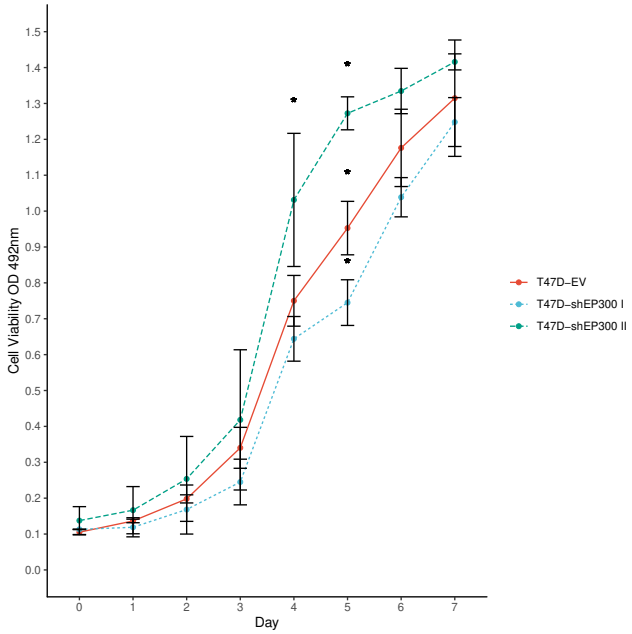

(d)

Fig. 4.6 Cell Proliferation in T47D with EP300 downregulation. The cell proliferation was measured as OD value representative of crystal violet staining. T47D cells transfected with two EP300 knockdown vectors (T47D-shEP300 I) and (T47D-shEP300 II) was demonstrated relative to the respective control T47D-EV (wild type and empty vector control transfected cells). Panels show seeding at cell density at 200 cells per well (A), 500 cells per well (B), 700 cells per well (C) and 1000 cells per well (D). All show cell viability (OD) values of T47D empty vector expressing breast cancer cell line (T47D-EV) versus its counterparts transfected with Ep300 downregulating vector (T47D-shEP300 I) and (T47D-shEP300 II) vectors. Data are shown as normalised to T47D empty vector expressing cell line (T47D-EV). The mean + SD of n=3 independent experiments is shown, NS Non-Significant, * p<0.05, **p<0.01, *** P<0.001,****p<0.0001 (ordinary one-way ANOVA following Dunnett's multiple comparison test).

4.2.4 Discussion

Mesenchymal gene signature.

Looking at the effect of EP300 overexpression on the CAL-51 cell line (Figure). Its overexpression effects are unknown as it controls a wide range of genes. As CDH1 is one of those genes that it controls, both directly and through a FOXO3a/FOXM1 loop, it could be that it will reverse the mesenchymal phenotype through CDH1, which we can see increased. Overall, the overexpression of EP300 and CDH1 do not affect the gene signature in the same way and results are inconclusive.

From what we have shown, CAL-51 and MDA-MB-231 overexpression of EP300 and CDH1 works well and affects the cell phenotype (Asaduzzaman et al 2017). In the results in this chapter we show that as a result of EP300 overexpression, we promote the upregulation of CDH1 and FOXO3a in both cell lines. Which provides evidence to support our hypothesis of EP300 modulating CDH1 and therefore plays some role in EMT switching. We also saw decrease in pro EMT genes which confirms this. However, it does not seem to regulate its expression through FOXO3a in this cell line, as its levels remain unchanged. Another mechanism independent of this gene should be looked into. Anomalies in gene expression could be explained by different regulatory mechanisms in place in this cell line being activated over time. The abundance of the EP300/CDH1 mRNA transcript in the cell could be causing a feedback loop, in which the protein level doesn't correspond to this. To confirm our findings for all genes up/down regulated we need to perform western blots. However, even in some cases the protein level doesn't correspond, and the mRNA levels can vary with time points (Fournier et al 2010). There are a variety of mechanism that can impede direct mRNA to protein translation, such as modifications, miR targeting of transcripts for degradation, not to mention proteins having different half-lives. However, differentially expressed mRNAs do seem to correlate better to protein expression than those not correlated (Koussounadis et al 2015).

Counterintuitively in our CAL-51 model, CDH2 and CDH1 are both upregulated with EP300 overexrression. These are reported to act antagonistically to each other, CDH2 being the marker for EMT, while CDH1 is the marker for epithelial phenotype. Nevertheless, an increase in cell adhesion molecules responsible for attachment to the ECM and impeding migration like CEACAM5 and CNN2 might have some effect on cell migration. This should be confirmed with a functional assay to monitor cell movement over time across conditions. Other genes such as ARHGAP20, EFEMP1, CDH11, HEY2,TGFβ2, BCL2, BMP7, HMCN1 and ITGA3 might not be an effect due to such low levels of downregulation. With the overexpression of CDH1, the phenotype should return to an epithelial. Cell adhesion

markers such as CDH1, CDH11, EFEMP1 and CEACAM5 are upregulated, which would increase capacity to bind and have effects on cell polarity. This is however not the full story as, this cell line also seems to upregulate EMT markers CDH2 and VIM, as well as downregulation in CNN2, a cell adhesion molecule.

EP300 expression leads to pro invasive characteristics?

In MDA-MB-231, there is an upregulation of CDH2 and CDH11, which doesn't disprove our hypothesis. Both are EMT markers and determinants of cell fate and regulate stemness. CDH2 is overexpressed in 47% of triple negative breast cancers (Alimperti et al 2015, Yang et al 2017). As PLS3 has been known to be involved in cisplatin and paclitaxel resistance (Hisano et al 1996, Ma et al 2019), and leads to poorer prognosis (Ueo et al 2015). Taking these three genes combined could mean that there is still a chemoresistant/ stem like population present in the cell culture, despite EP300 overexpression. Furthermore, the downregulation of HMCN1 could also produce an unfavourable phenotype, as it is often overexpressed in triple negative cancers (Saravia et al 2019) and leads to loss of cell-cell contacts. In this case TGFβ2 could be exerting pro metastatic effects, but is known to exert its influence in the opposite direction. Its effects are yet to be determined in this model.

EP300 expression leading to anti invasive characteristics?

An anti-metastatic effect might be contributed by a reduction in MUC5B and FGFR2. MUC5B is known for reducing proliferation (Lahdaoui et al 2017). Whereas FGFR2 is known to play a role in reducing proliferation and differentiation, as well as inhibiting apoptosis. An upregulation in ARHGAP20, could also prevent migration or invasion. It is a known pathway for inhibiting Rho GTPAses such as RhoA. A canonical protein involved in integrin cycling and metastasis (Chan et al 2010). No study has yet published any evidence between EP300 and ARHGAP20. There is very small downregulation of ABCG2, ITGA2 and EFEMP1. Other genes like CAPN9, CEACAM5, BMP7, HEY2, BCL2, EPHA4, FOXO3a, GATA3, WIPF1, ITGA3, VIM and BMP4 remain unchanged. Therefore, we cannot make nay assumptions, apart from that their regulation is different from MCF7 and that EP300 doesn't affect their expression. A role for SGCG could also not be inferred in this model. Due to the above, it might be worth exploring the idea that EP300 might have cell type dependant functions, in some cases promoting EMT.

CDH1 expression leading to anti-invasive characteristics?

Minor downregulation seen in CAPN9, ARHGAP20, HMCN1, TGFβ2, GATA3, and CDH11 is unlikely to be due to CDH1 overexpression. Likewise, there is also no effect on FGFR2, BMP7, HEY2, SGCG, ITGA2 and VIM. Downregulation of ABCG2, a known marker of drug resistance, is interesting and could be investigated further alongside with other markers of drug resistance. Upregulation of CDH1, confirms the overexpression worked, interestingly the levels of EP300 have also increased. This is an unexplained consequence of our transfection or a feedback loop exerted from CDH1. We could potentially study EP300 methylation levels in these cell lines, to see whether its promoter is activated as a result of our transfections or differences between cell lines. Otherwise we could check for presence of enhancer regions. Anti-proliferative effects could be exerted through downregulation of MUC5B. The upregulation of CEACAM5 and CNN2 might improve cell attachment, but as there is also an increase in ITGA2, this cell line might still be capable of cell migration.

There might be no effect on stemness, the increase in CDH2 and PLS3 could increase the stem like population. However, as we also see an increase in WIPF1 there could be no effect overall. WIPF1 upregulation in this cell line has been documented and decreased expression of VIM which promotes MET (Garcia et al 2014). As well as giving favourable prognosis in breast cancer (Staub et al 2009). However, in this context it might act with PLS3 and CDH2 to promote cancer stem cells and tumour progression, as there have been documented cases of WIPF1 promoting these effects (Escoll et al 2017).

Overall the gene signature doesn't seem to show any conclusive results as to what is happening with the overexpression of EP300 and CDH1, as these genes regulate a large landscape, the scope of this study is somewhat limited. It might benefit to research some of these genes with larger fold changes in functional assay experiments with gain/loss of function to see whether the phenotype of the cell changes. Perhaps with more targeted approaches such as Crispr Cas 9 or Crispr Cas 13. The latter of which has higher efficiency and specificity for RNA.

Gene signature in colorectal cell line

We chose the colorectal cell line HCT116 due to it being invasive and with high proliferation characteristics. The effects of which we were hoping would be reversed with knockout of EP300 as it has high basal levels and show a cell type context dependant effect of EP300. With the knockout of EP300, we can see this has an effect on CDH1, which suggests the epithelial characteristics are lost.

There is no change in integrin levels ITGA2, ITGA3, BMP7, EPHA4 and FGFR2 which could mean migration and apoptosis is unaffected. Other integrin genes could be looked into, as well as levels of BAX for apoptosis. However, ARHGAP20 is downregulated, which could mean the activation of Rho related proteins and more migratory capacity. The levels of which should be confirmed, along with MEK, ERK,AKT and PI3K. Markers of stemness and drug resistance: ABCG2 and PLS3, are also unaffected. Which either means there is no stem like population present, or there is no change. EMT markers like SNAI1 don't change, as are important pioneer transcription factors like FOXA1/FOXO3a which exert influence on a myriad of genes involved in EMT.

Potential for EMT is seen in the increase of CDH2, VIM and HEY2. In addition, the increased expression of TGFβ2 and CAPN9 shows tumourigenic potential. Further potential for an unfavourable phenotype could be gained through loss of cell-cell contacts with HMCN1. Increased BCL2 might help with avoiding apoptosis, while an increase in CDH2, CDH11 and BMP4 could contribute to promotion of stemlike qualities. WIPF1 is a known inhibitor of CDH2 and VIM, so their increase is confusing. A explanation is there is another mechanisms or cell line particularity. At this time the increase in SGCG is also unclear. Overall the knockout of EP300 in this model could lead to an unfavourable phenotype but this needs to be confirmed whether the protein level is altered and with functional assays on invasive and migration capacity.

Epithelial gene signature.

The T47D model while has the same marker profile as MCF7, does not behave in the same way. Transfection with shEP300 I and shEP300 II vectors produces vastly different results. This either due to transfection efficiency or the vector for shEP300 II having higher efficiency or specificity. When transfected with shEP300 I, no change is seen in the majority of genes: ARHGAP20, MUC5B, WIPF1, CDH2, EPHA4, HEY2, CNN2, EFEMP1, FGFR2 and GATA3. More importantly however, our genes of interest: CDH1 and EP300 are downregulated by this vector. As well as affecting FOXO3a upregulation and downregulation in GATA3. Suggesting that there is some credence to our hypothesis of pro EMT switch control of EP300 in epithelial breast cancer cell lines. CDH11 and PLS3 increases is also an indicator for this, as this would promote stem like populations. HMCN1 upregulation could mean loss of epithelial structure and cell to cell attachment.

The shEP300 II vector, also shows the same effects on CDH1,EP300,FOXO3a and GATA3 as shEP300 I . As a result of the transfection, there no change in HMCN1, SGCG, WIPF1, CHD2, CNN2, EFEMP1, FGFR2 and HEY2. Stemness characteristics are unaffected as CDH11 is upregulated while PLS3 is downregulated which exerts opposing effects. While

upregulation in ARHGAP20 and CDH1 upregulation could promote epithelial characteristics and decrease migration. Although, EPHA4 which is also upregulated, could promote migration but the activity of TGFβ2 should be looked into. There might also be an increase in proliferation due to MUC5B downregulation. No conclusion can be drawn from the gene signature in this cell line other than our transfection has worked and our target gene CDH1 is affected. Whether this has any effect on EMT characteristics is still to be determined. We should also consider extending the study to include other epithelial cell lines. In terms of the gene signature, no pattern can be seen in the cell lines we have used in the study. No conclusions can be drawn. Another gene signature should be used to test the hypothesis.

Effect of EP300 and CDH1 on cell proliferation.

Along with gene expression, we decided to test functional effects on phenotype such as higher cell proliferation. Which would be one of the first changes associated with an EMT phenotype. The cell proliferation was tested in cell lines: CAL-51, MDA-MB-231, MCF7, T47D and HCT116. There was no demonstrated effect in CAL-51 or MDA-MB-231, which could be a cell line particularity or EP300 and CDH1 expression not having an effect on these properties. The effect of EP300 and CDH1 knockdown in MCF7 and T47D also produced no effect on cell proliferation, though the later could be due to poor transfection efficiency. While the knockdown of Ep300 in colorectal cell lineHCT116 also has no effect. Overall no demonstrated effect on proliferation is seen in our experiments.

4.2.5 Overall Conclusion

To conclude this chapter, we have demonstrated that the overexpression of EP300 in mesenchymal cell lines CAL-51 and MDA-MB-231 induces CDH1 expression. This is a canonical marker for EMT and invasion, and while we also see the upregulation in cell adhesion mollecules. The expression of other genes which are involved in drug resistance, invasion and stemness, prevent us from drawing a conclusion about the cell lines phenotype. The same can be said for our T47D model, that while our downregulation of EP300 is confirmed by RTqPCR, the effect is not significant on CDH1. We should potentially repeat this experiment and also consider switching from a SYBR green system to Taqman for better accuracy of probes.

Chapter 5

Analysis of EP300 and CHD1 expression in breast cancer patient population

5.1 Introduction

Previously in **Chapter 4** we described a novel gene signature we attempted to attribute as the potential mechanism for regulating the shift from an epithelial phenotype. This chapter will try to investigate this in online datasets to see the prevalence of their modulation, specifically looking at data from the human protein atlas and the cancer genome atlas.

5.1.1 EP300 Influencing Transcription

EP300 loss of heterozygosity has been demonstrated in breast carcinomas and somatic mutations of EP300 have also been described in various solid tumours (Bryan et al 2002, Gayther et al 2000). In particular it has been shown that a loss of EP300 contributes to EMT in colon carcinona (Krubasik et al 2006). Recent studies have shown that inhibition of the EP300 catalytically active bromodomain, which is responsible for its acetylation function, if inhibited in ER-ve breast cancer, lead to inhibition of cell proliferation (Garcia-Carpizo et al 2019). These studies follow previous successful efforts of using HAT inhibitors as a therapeutic method for malignancies (Sante et al 2011, Yang et al 2013, Bowers et al 2010). Some of which are specific to the catalytically active bromodomain (Hay et al 2014).

5.1.2 Enhancer Regions and Transcription

Enhancers are DNA elements that can activate transcription of genes at distance, while groups of these in close proximity to each other are defined as super enhancers. Enhancers

contain binding sites for transcription co activators which allows them to interact with gene promoters located in other regions of DNA (Pott & Lieb 2015). As enhancer regions and super enhancer regions do not have a functional definition, it is hard to determine these in the genome. One way uses GRO-seq to predict enhancer sites through identifying actively transcribing RNA polymerase II (Core et al 2008). Reasoning being that these regions show more H3K4me1 and H3K27ac enhancer related modifications and would loop towards target genes promoters (Hah et al 2015). The most common method to identify these regions is the high abundance of acetylation at the 27th lysine residue of the histone H3 (H3K27ac) or the mono-methylation at the 3rd or 4th lysine residues of histone H3 (H3K3m1)/(H3K4me1) modifications (Hnisz et al 2013, Franco et al 2018), or abundance of Mediator of RNA polymerase II transcription subunit 1 (Med1), which is responsible for RNA polymerase II activity (Loven et al 2013).

A recent study on breast cancer cell lines showed that the expression of enhancers is cell type context dependant and will result in unique transcriptional events (Franco et al 2018). This study defines enhancer regions as regions which are high in RNA polymerase II activity, combined with enrichment of H3K4me1 and H3K27ac and presence of motifs which correlate to the expression of predicted transcription factors (Franco et al 2018). To help with transcription, these regions attract coactivators such as RNA polymerase II and EP300 (Hnisz et al 2013), which then initiate the transcription of downstream target genes. Of interest to breast cancer and other solid tumours, is that these enhancer regions are frequently upregulated in cancers and are more likely to be present on coding sites for oncogenes (Hah et al 2015). Of interest is the higher upregulation of transcription factors, Forkhead Box F2 (FOXF2), Forkhead Box Q1 (FOXQ1), Forkhead Box C1 (FOXC1), FOSL1 and Pleomorphic adenoma gene 1 (PLAG1) in triple negative tumours, while luminal tumours favoured Forkhead Box O11 (FOXO11), FOXA1 and Forkhead Box P2 (FOXP2) (Franco et al 2018).

FOXA1 was previously covered earlier in **Chapter 4**, while Forkhead box C1 (FOXC1) is involved in NF-κB signalling and is a predictor of poor survival (Wang et al 2012, Ray et al 2010). FOS Like 1 (FOSL1) is a key regulator of gene expression in cancer (Verde et al 2007), which can induce EMT (Bakiri et al 2015). While PLAG1 is a new zing finger transcription factor involved in tumour formation (Van Dyck et al 2007). Other examples exist such as the association of super enhancers with pluripotency genes, which are upregulated in breast cancer stem cells, e.g. *OCT4*, *SOX2*, *NANOG* (Whyte et al 2013). Taken together it is likely that expression of HATs like EP300 influence acetylation/methylation marks and thereby modulate not only access of transcription factors to active sites, but also indirectly influence regions they do not actively acetylate through modifying active status of enhancer regions.

This in turn would influence transcription events involved in EMT and stemness through its active bromodomain, by modulating their acetylation status. Breast cancer cell lines treated with a general inhibitor JQ1 and EP300 bromodomain specific inhibitor showed that its activity had a cell type specific influence on the expression of cancer associated enhancers. These superenhancer regions seemed to interact with the androgen receptor and therefore influence genes in this pathway, and each cell type had its own unique pathway profile (Garcia-Carpizo et al 2019). It is therefore of interest to look at EP300 expression status as it would have wide implications on pathway activation.

5.1.3 Genomic Databases

The human genome project was the very first effort to utilise computing to answer some of the basic biology questions, since its completion many thousands of other species have been sequenced. In bioinformatics, this would fall under 4 categories: assembly, resequencing, classification and quantification. Assembly is the nucleotide composition of a genome, resequencing is the identification of mutations and variations, classification is the determination of what species an organism belongs to, and quantification is the DNA sequencing for measuring functional characteristics of the cell. As the amount of data generated has increased exponentially with higher computing power and lower cost this has led to the widespread development of various sequencing techniques such as RNA-seq and Chip-seq etc. RNA-seq is the primary method to reveal the amount of mRNA, which measures it with higher accuracy than RT-qPCR. Newer methods exist which delve into the shape and function of RNA, such as SHAPE-seq and PARTE-seq etc, with many more constantly being developed to suit a biological question.

Efforts have been made to make the process of cataloguing and replication of experiments easier, such as the creation of online databases. One of the most heavily used is the Human Protein Atlas, a project started in 2003 in Sweden to map most of the omics approaches used for cell lines, tissue samples and other analytes, enabling easy access for academics and researchers. Since then, it has contributed to many publications such as Uhlen et al (2017) and Thul et al (2017). Another program that has been crucial for the study of cancer genomics is the cancer genome atlas (TCGA), which consists of 20,000 primary cancers with matched normal tissues. This program started in 2006 and has generated over 2.5 petabytes of data and generated numerous publications over its course (The Cancer Genome Atlas Network et al 2012, Tomczak et al 2015, Liu et al 2018).

5.2 Analysis of Breast Cancer Patient Datasets

5.2.1 Hypothesis

Drawing on evidence from previous research, we are shifting our focus back to the main regulators of the cell phenotype. In this chapter, we attempt to discover whether there is any difference in basal expression of EP300 and CDH1 in diseased tissue and normal mammary epithelium, and explore their influence on overall disease survival. It is expected that the expression of EP300 and CDH1 would be associated with better overall survival, as well as being attributed to normal tissue.

5.2.2 Aim

1. Look at the effects of modulated EP300 and CDH1 expression in the TCGA dataset. With the KM plotter investigate.
    - Trend in Overall survival.
    - Trend in Recurrence free survival.
2. Look at the expression profiles of EP300 and CDH1 in healthy and diseased tissue from the "Human Protein Atlas" dataset.
    - Investigate healthy tissue expression and how it might relate to function.
    - Investigate which tumour type is more prone to express or downregulate EP300 and CDH1.
    - Compare healthy tissue expression and tumour expression profile of EP300 and CDH1.
3. Investigate the relative mRNA expression in tumour types from the "Human Protein Atlas" dataset.
    - Show whether localisation relates to expression in tumour subtypes.
    - Show which tumour types express the most/least of EP300 and CDH1.
4. Investigate the gene signature identified in chapter 4 and identify expression patterns in the TCGA dataset.
    - Compare gene expression across cancer subtypes: Luminal A, Luminal B, Her2 and triple negative breast cancer.
    - Look at the global view and in subset.

5.2.3 Results

Figure 5.1 shows Kaplan Meier curves, demonstrating the relapse free survival (RFS). RFS is defined as the length of time after primary treatment for cancer ends and the patient survives without any symptoms. It also shows overall survival (OS): the length for time from diagnosis, or start of treatment that the patient is still alive. The Hazard ratio (HR): the association of risk to our event. A value greater than one is a greater risk, a value of one shows no risk, while smaller than one would mean a smaller risk.

In **Figure 5.1a**, it shows the RFS for all the patients and how this RFS is impacted by EP300 and CDH1 expression. We can see that with EP300 expression, the HR is 0.76 and the median RFS is around 50 months for high expression and less than 50 months for low expression. With CDH1 expression, we can see that the HR is 0.82, the median RFS is around 200 months for high expression and 240 months for low expression. In **Figure 5.1b**, it displays the OS in all patients and how this RFS is impacted by EP300 and CDH1 expressions. We can see that with EP300 expression, the HR is 1.23, the median OS is around 200 months for high expression and 300 months for low expression. With CDH1 expression, it is observed that the HR is 1.27, the median OS is around 300 months for high expression and 270 months for low expression.

Figure 5.1c shows the RFS in patients with triple negative breast cancer. We can see that with EP300 expression, the HR is 0.86, the median RFS is around 200 months for high expression and less than 200 months for low expression. With CDH1 expression, we can see that the HR is 1.37, the median RFS is around 200 months for high expression and 200 months for low expression. In **Figure 5.1d**, it demonstrates the RFS in patients with HER2+ breast cancer. We can see that with EP300 expression, the HR is 1.39, the median RFS is around 130 months for high expression and more than 200 months for low expression. With CDH1 expression, we can see that the HR is 1.85, the median RFS is around 70 months for high expression, and 170 months for low expression.

In **Figure 5.1e**, it shows the RFS in patients with Luminal B subtype breast cancer. We can see that with EP300 expression, the HR is 0.75, the median RFS is around 250 months for high expression and less than 120 months for low expression. With CDH1 expression, we can see that the HR is 1.3, the median RFS is around 150 months for high expression and 160 months for low expression.Figure 1F demonstrates the RFS in patients with Luminal A subtype breast cancer. We can see that with EP300 expression, the HR is 0.75, the median RFS is around 220 months for high expression and 230 months for low expression. With CDH1 expression, we can see that the HR is 1.25, the median RFS is around 250 months for high expression, and 220 months for low expression.

Thus to summarise the effects of EP300 and CDH1, high EP300 expression seems to be more prognostically favourable to high CDH1 expression. As it is associated with higher probability of patients with RFS in luminal A, B and Basal subtypes. However its expression correlated with lower RFS in the HER2 subtype. Interestingly the OS for all patients dropped after 200 months. CDH1 on the other hand was only prognostically fabourable for RFS in basal and HER2 subtypes.

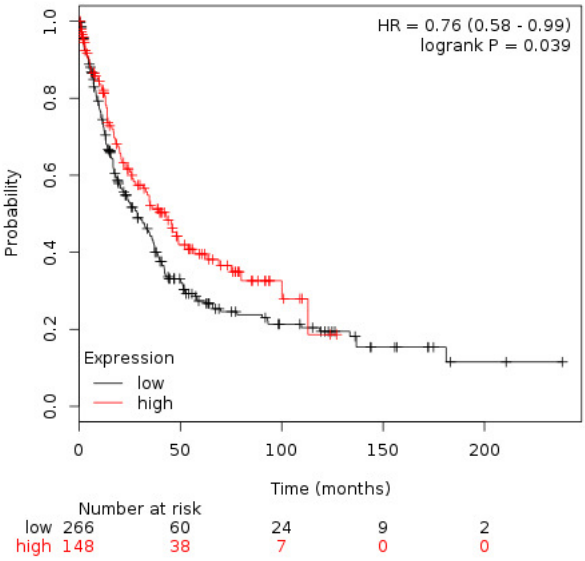

(a) RFS in all patients associated with EP300

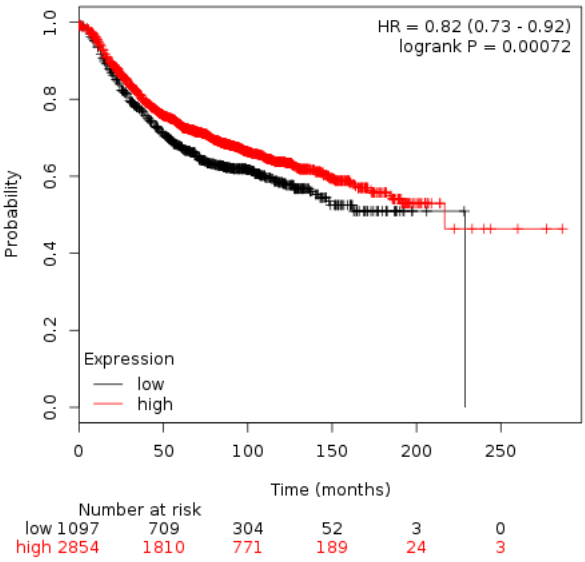

(b) RFS in all patients associated with CDH1

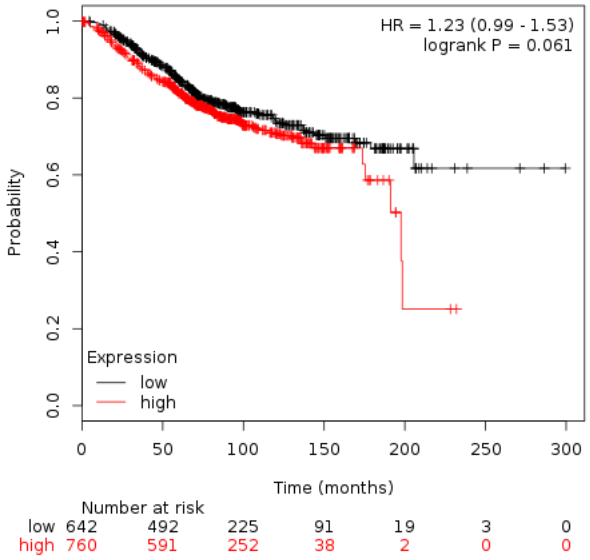

(c) OS in all patients associated with EP300

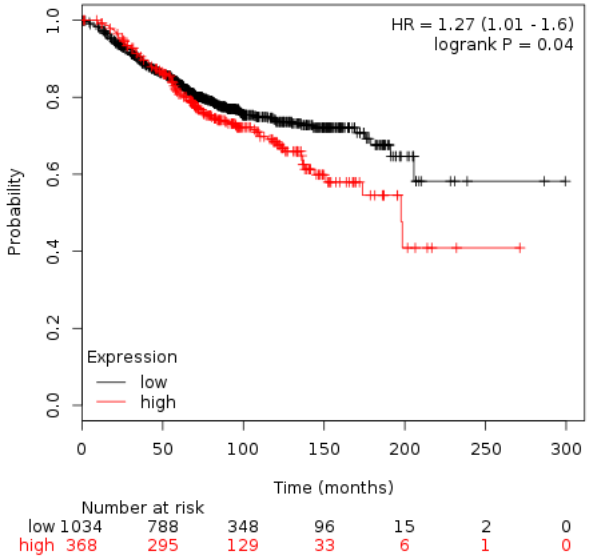

(d) OS in all patients associated with CDH1

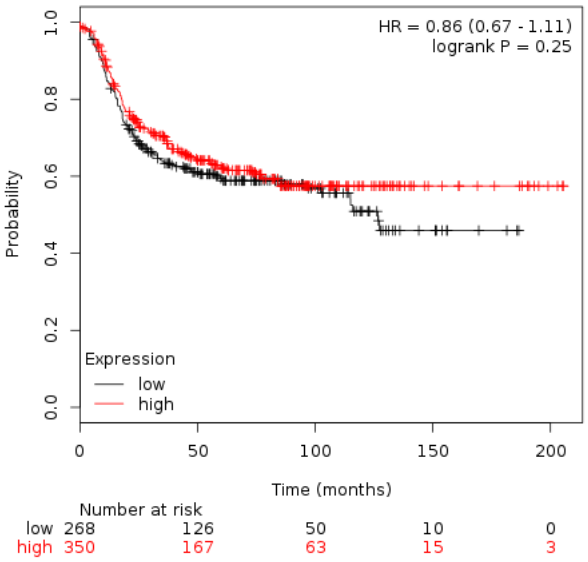

(e) RFS with EP300 in basal tumours

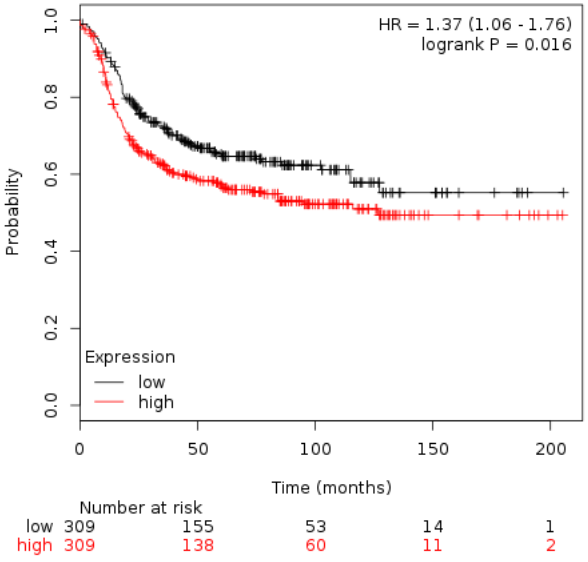

(f) RFS with CDH1 in basal tumours

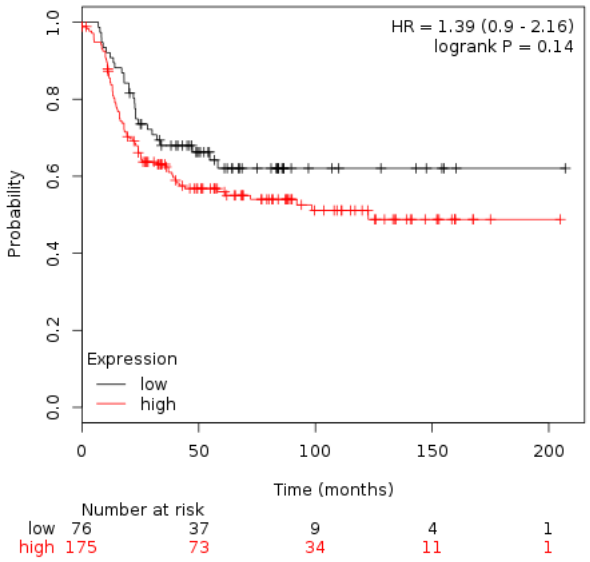

(g) RFS with EP300 in HER2 tumours

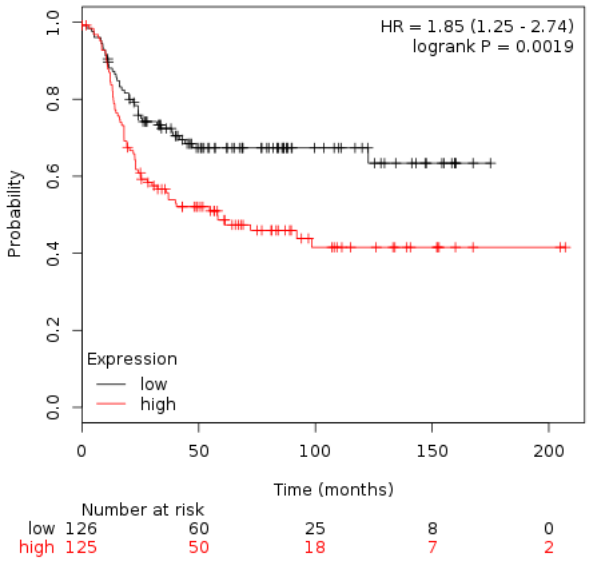

(h) RFS with CDH1 in HER2 tumours

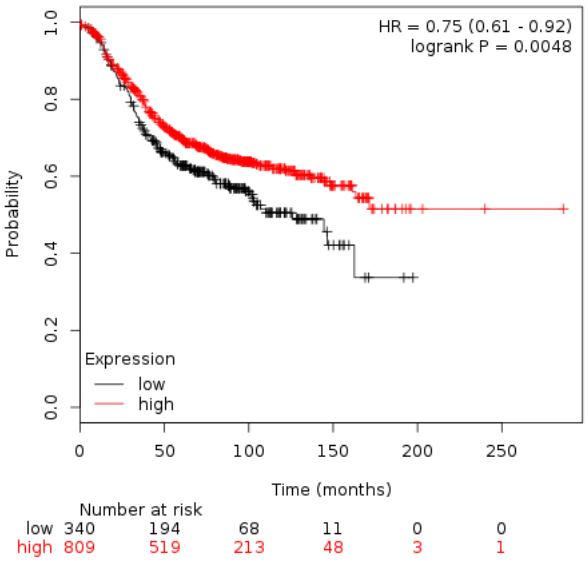

(i) RFS with EP300 in Luminal A tumours

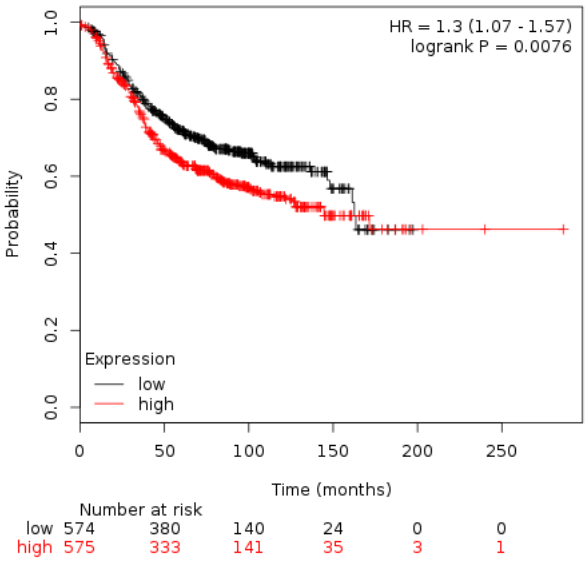

(j) RFS with CDH1 in Luminal A tumours

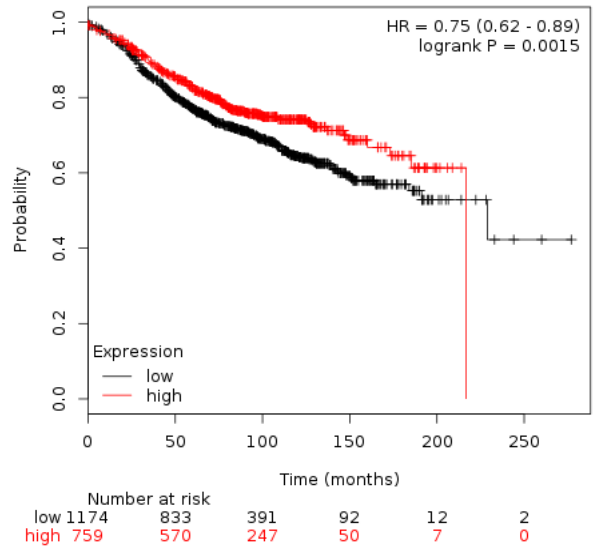

(k) RFS with EP300 in Luminal B tumours

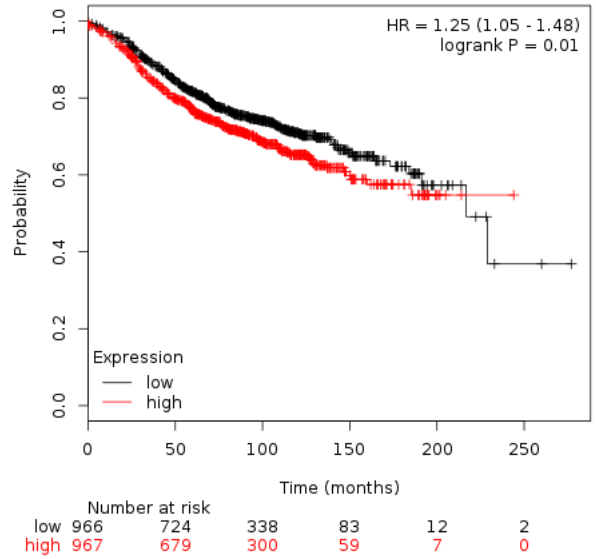

(l) RFS with CDH1 in Luminal B tumours

Fig. 5.1 Kaplan-Meier survival curves with EP300 and CDH1 expression of (a-b) RFS in all patients (c-d) OS in all patients (e-f) RFS in basal subtype (g-h) HER-2 subtype (i-j) luminal B subtype (k-l) luminal A subtype patients. Red line = high expression, above median group, black line = low expression, below median group. Kaplan-Meier plots were obtained from http://kmplot.com/.

Table 5.1 identifies the normal localised expression pattern of EP300 and CDH1 in normal tissue. From here it is observed that the highest expression of CDH1 is in the glandular cells, medium expression is in the myoepithelial cells and no expression in the adipocytes. Whereas the highest or rather medium expression of EP300 is in the glandular cells, and no expression in the adipocytes or myoepithelial cells. For CDH1, the tissues with the highest expression are in the glandular cells: colon, breast, duodenum, endometrium, epididymis, fallopian tubes, gallbladder, pancreas, parathyroid gland, prostate, rectum, salivary gland, seminal vesicle, stomach, thyroid gland. There was also a high expression in the squamous epithelium: cervix, oesophagus, oral mucosa, tonsil, vagina, and in the cells in tubules of the kidney, pneumocytes of the lung, respiratory epithelial cells of the nasopharynx, trophoblastic cells of the placenta, all cell types of skin and urothelial cells of the urinary bladder. This is reflected in the relative mRNA expression in **Figure 5.2**. The largest to smallest relative expression of EP300 and CDH1 across tissues. The breast is one of the tissues expressing the median amounts of both genes compared to other tissues.

This is important as it shows that while these proteins are localised in many tissues, their relatively high abundance in the breast. And their reregulated expression would have large effects, which is why targeted therapy would benefit breast cancer.

Table 5.1 Normal tissue expression of EP300 and CDH1.

Gene Name	Tissue	Cell Type	Level
CDH1	adipose tissue	adipocytes	Not detected
CDH1	adrenal gland	glandular cells	Not detected
CDH1	appendix	glandular cells	High
CDH1	appendix	lymphoid tissue	Not detected
CDH1	bone marrow	hematopoietic cells	Not detected
CDH1	breast	adipocytes	Not detected
CDH1	breast	glandular cells	High
CDH1	breast	myoepithelial cells	Medium
CDH1	bronchus	respiratory epithelial cells	Medium
CDH1	caudate	glial cells	Not detected
CDH1	caudate	neuronal cells	Not detected
CDH1	cerebellum	cells in granular layer	Not detected
CDH1	cerebellum	cells in molecular layer	Not detected
CDH1	cerebellum	Purkinje cells	Not detected
CDH1	cerebral cortex	endothelial cells	Not detected
CDH1	cerebral cortex	glial cells	Not detected
CDH1	cerebral cortex	neuronal cells	Not detected
CDH1	cerebral cortex	neuropil	Not detected
CDH1	cervix, uterine	glandular cells	Medium
CDH1	cervix, uterine	squamous epithelial cells	High
CDH1	colon	endothelial cells	Not detected
CDH1	colon	glandular cells	High
CDH1	colon	peripheral nerve/ganglion	Not detected
CDH1	duodenum	glandular cells	High

Table continues on the next page...

Gene Name	Tissue	Cell Type	Level
CDH1	endometrium 1	cells in endometrial stroma	Not detected
CDH1	endometrium 1	glandular cells	High
CDH1	endometrium 2	cells in endometrial stroma	Not detected
CDH1	endometrium 2	glandular cells	High
CDH1	epididymis	glandular cells	High
CDH1	oesophagus	squamous epithelial cells	High
CDH1	fallopian tube	glandular cells	High
CDH1	gallbladder	glandular cells	High
CDH1	heart muscle	myocytes	Not detected
CDH1	hippocampus	glial cells	Not detected
CDH1	hippocampus	neuronal cells	Not detected
CDH1	kidney	cells in glomeruli	Not detected
CDH1	kidney	cells in tubules	High
CDH1	liver	bile duct cells	Medium
CDH1	liver	hepatocytes	Medium
CDH1	lung	macrophages	Low
CDH1	lung	pneumocytes	High
CDH1	lymph node	germinal center cells	Not detected
CDH1	lymph node	non-germinal center cells	Not detected
CDH1	nasopharynx	respiratory epithelial cells	High
CDH1	oral mucosa	squamous epithelial cells	High
CDH1	ovary	follicle cells	Not detected
CDH1	ovary	ovarian stroma cells	Not detected
CDH1	pancreas	exocrine glandular cells	High

Table continues on the next page...

Gene Name	Tissue	Cell Type	Level
CDH1	pancreas	islets of Langerhans	Not detected
CDH1	parathyroid gland	glandular cells	High
CDH1	placenta	decidual cells	Not detected
CDH1	placenta	trophoblastic cells	High
CDH1	prostate	glandular cells	High
CDH1	rectum	glandular cells	High
CDH1	salivary gland	glandular cells	High
CDH1	seminal vesicle	glandular cells	High
CDH1	skeletal muscle	myocytes	Not detected
CDH1	skin 1	fibroblasts	Not detected
CDH1	skin 1	keratinocytes	High
CDH1	skin 1	Langerhans	High
CDH1	skin 1	melanocytes	High
CDH1	skin 2	epidermal cells	High
CDH1	small intestine	glandular cells	High
CDH1	smooth muscle	smooth muscle cells	Not detected
CDH1	soft tissue 1	fibroblasts	Not detected
CDH1	soft tissue 2	chondrocytes	Not detected
CDH1	soft tissue 2	fibroblasts	Not detected
CDH1	soft tissue 2	peripheral nerve	Not detected
CDH1	spleen	cells in red pulp	Not detected
CDH1	spleen	cells in white pulp	Not detected
CDH1	stomach 1	glandular cells	High
CDH1	stomach 2	glandular cells	High

Table continues on the next page...

Gene Name	Tissue	Cell Type	Level
CDH1	testis	cells in seminiferous ducts	Not detected
CDH1	testis	Leydig cells	Not detected
CDH1	thyroid gland	glandular cells	High
CDH1	tonsil	germinal center cells	Not detected
CDH1	tonsil	non-germinal center cells	Not detected
CDH1	tonsil	squamous epithelial cells	High
CDH1	urinary bladder	urothelial cells	High
CDH1	vagina	squamous epithelial cells	High
EP300	adipose tissue	adipocytes	Low
EP300	adrenal gland	glandular cells	High
EP300	appendix	glandular cells	Medium
EP300	appendix	lymphoid tissue	Medium
EP300	bone marrow	hematopoietic cells	High
EP300	breast	adipocytes	Low
EP300	breast	glandular cells	Medium
EP300	breast	myoepithelial cells	Low
EP300	bronchus	respiratory epithelial cells	Medium
EP300	caudate	glial cells	Medium
EP300	caudate	neuronal cells	Medium
EP300	cerebellum	cells in granular layer	Medium
EP300	cerebellum	cells in molecular layer	Medium
EP300	cerebellum	Purkinje cells	Medium
EP300	cerebral cortex	endothelial cells	Low
EP300	cerebral cortex	glial cells	Low

Table continues on the next page...

Gene Name	Tissue	Cell Type	Level
EP300	cerebral cortex	neuronal cells	High
EP300	cerebral cortex	neuropil	Not detected
EP300	cervix, uterine	glandular cells	Medium
EP300	cervix, uterine	squamous epithelial cells	Medium
EP300	colon	endothelial cells	Low
EP300	colon	glandular cells	High
EP300	colon	peripheral nerve/ganglion	Medium
EP300	duodenum	glandular cells	Medium
EP300	endometrium 1	cells in endometrial stroma	Medium
EP300	endometrium 1	glandular cells	Low
EP300	endometrium 2	cells in endometrial stroma	Low
EP300	endometrium 2	glandular cells	Low
EP300	epididymis	glandular cells	Medium
EP300	esophagus	squamous epithelial cells	High
EP300	fallopian tube	glandular cells	Medium
EP300	gallbladder	glandular cells	Medium
EP300	heart muscle	myocytes	Low
EP300	hippocampus	glial cells	Medium
EP300	hippocampus	neuronal cells	Medium
EP300	kidney	cells in glomeruli	Medium

Source" The Human Protein Atlas Dataset".
Breast tissue expression of EP300 is mainly restricted to the adipocyte(LOW), myoepithelial(MEDIUM) and glandular cells(LOW). While CDH1 expression is mainly restricted to the glandular(HIGH) and myoepithelial(MEDIUM).

EP300 is only highly expressed in the hematopoietic cells of the bone marrow, neuronal cells of the cerebral cortex, glandular cells of the colon and the squamous epithelium of the oesophagus. The majority of tissues express medium levels such as in the digestive system and brain. **Table 5.2** shows EP300 and CDH1 in context of prognosis across cancer subtypes. We can see that for breast cancer both EP300 and CDH1 are not prognostically favourable or unfavourable in this patient population. CDH1 and EP300 are prognostically favourable for renal cancer. CDH1 is unprognostic and unfavourable for breast cancer, cervical cancer, head and neck, ovarian, pancreatic, testicular cancer, thyroid cancer. Whereas EP300 is unprognostic and unfavourable for breast, liver, melanoma, ovarian, pancreatic, testicular, thyroid and urothelial cancers.

Table 5.2 Expression of EP300 and CDH1 by cancer type.

Gene name	Cancer	High	Medium	Low	Not detected	prognostic favourable	unprognostic favourable	prognostic unfavourable	unprognostic unfavourable
CDH1	breast cancer	8	1	0	2	NA	NA	NA	0.03954
CDH1	carcinoid	1	3	0	0	NA	NA	NA	NA
CDH1	cervical cancer	7	3	0	0	NA	NA	NA	0.1906
CDH1	colorectal cancer	12	0	0	0	NA	0.001119	NA	NA
CDH1	endometrial cancer	10	1	0	0	NA	0.1132	NA	NA
CDH1	glioma	0	0	0	11	NA	0.1418	NA	NA
CDH1	head and neck cancer	0	3	1	0	NA	NA	NA	0.2778
CDH1	liver cancer	5	6	0	0	NA	0.00504	NA	NA
CDH1	lung cancer	5	5	0	2	NA	0.1628	NA	NA
CDH1	lymphoma	0	0	0	12	NA	NA	NA	NA
CDH1	melanoma	2	5	2	3	NA	0.0547	NA	NA
CDH1	ovarian cancer	7	3	0	0	NA	NA	NA	0.2849
CDH1	pancreatic cancer	12	0	0	0	NA	NA	NA	0.01195
CDH1	prostate cancer	9	1	0	0	NA	0.3606	NA	NA
CDH1	renal cancer	0	3	1	8	0.0002059	NA	NA	NA
CDH1	skin cancer	3	7	1	1	NA	NA	NA	NA
CDH1	stomach cancer	7	2	1	2	NA	0.1208	NA	NA

Table continues on the next page...

Gene name	Cancer	High	Medium	Low	Not detected	prognostic favourable	unprognostic favourable	prognostic unfavourable	unprognostic unfavourable
CDH1	testis cancer	6	1	0	5	NA	NA	NA	0.2623
CDH1	thyroid cancer	4	0	0	0	NA	NA	NA	0.2506
CDH1	urothelial cancer	9	2	0	1	NA	0.0592	NA	NA
EP300	breast cancer	3	8	0	0	NA	NA	NA	0.07666
EP300	carcinoid	1	2	0	0	NA	NA	NA	NA
EP300	cervical cancer	2	10	0	0	NA	0.0556	NA	NA
EP300	colorectal cancer	3	7	0	1	NA	0.229	NA	NA
EP300	endometrial cancer	3	8	1	0	NA	0.2515	NA	NA
EP300	glioma	2	8	2	0	NA	0.006096	NA	NA
EP300	head and neck cancer	2	2	0	0	NA	0.1665	NA	NA
EP300	liver cancer	1	6	1	3	NA	NA	NA	0.02209
EP300	lung cancer	4	7	1	0	NA	0.2134	NA	NA
EP300	lymphoma	0	11	1	0	NA	NA	NA	NA
EP300	melanoma	4	8	0	0	NA	NA	NA	0.1545
EP300	ovarian cancer	1	10	0	0	NA	NA	NA	0.08972
EP300	pancreatic cancer	3	7	1	0	NA	NA	NA	0.01737

Table continues on the next page...

Gene name	Cancer	High	Medium	Low	Not detected	prognostic favourable	unprognostic favourable	prognostic unfavourable	unprognostic unfavourable
EP300	prostate cancer	4	8	0	0	NA	0.08536	NA	NA
EP300	renal cancer	4	7	0	0	7.45E-05	NA	NA	NA
EP300	skin cancer	0	12	0	0	NA	NA	NA	NA
EP300	stomach cancer	1	10	0	0	NA	0.07972	NA	NA
EP300	testis cancer	4	8	0	0	NA	NA	NA	0.1406
EP300	thyroid cancer	1	3	0	0	NA	NA	NA	0.1015
EP300	urothelial cancer	6	5	1	0	NA	NA	NA	0.08656

Source " The Human Protein Atlas".
EP300(Medium) and CDH1(HIGH) genes are expressed in breast cancer, and follow a similar pattern in cervical cancer.

Figure 5.3 shows a heatmap constructed from the RNA-seq data of the TCGA dataset. **Figure 5.3a** shows the global expression profile for all genes across the four breast cancer subtypes: Basal, HER2, Luminal A and Luminal B. There are no large differences observed. Within this patient cohort, we can see that the largest presented cases were of Luminal A subtype, while the second and third largest were Luminal A and Basal respectively. **Figure 5.3b** shows the expression profile for our gene signature from chapter 4, across the four breast cancer subtypes: Basal, HER2, Luminal A and Luminal B. Here we see that FOXO3a and SGCG have the lowest expression across all four subtypes. Similarly, no differences can be seen in BCL2, EFEMP1, ITGA3, CDH11, EP300, CNN2, PLS3, FGFR2, TGFB2, ITGA2, WIPF1, SNAI2, HMCN1, ZEB1 and ZEB2. Across all four subtypes, there is low expression of HEY2, EPHA4, CDH2, ARHGAP20, ABCG2, TNFRSF11B, BMP4, BMP7, CAPN9 and CEACAM5. It is interesting to note that Basal expression of CEACAM5 and CAPN9 seems to be lower than the other subtypes. Basal expression of MUC5B seems to be higher also compared to the other subtypes. VIM and CDH1 and seem to be uniformly expressed at high levels across all four subtypes. FOXA1 seems to follow a similar pattern, except with the basal subtype, where it seems to be expressed at much lower levels.

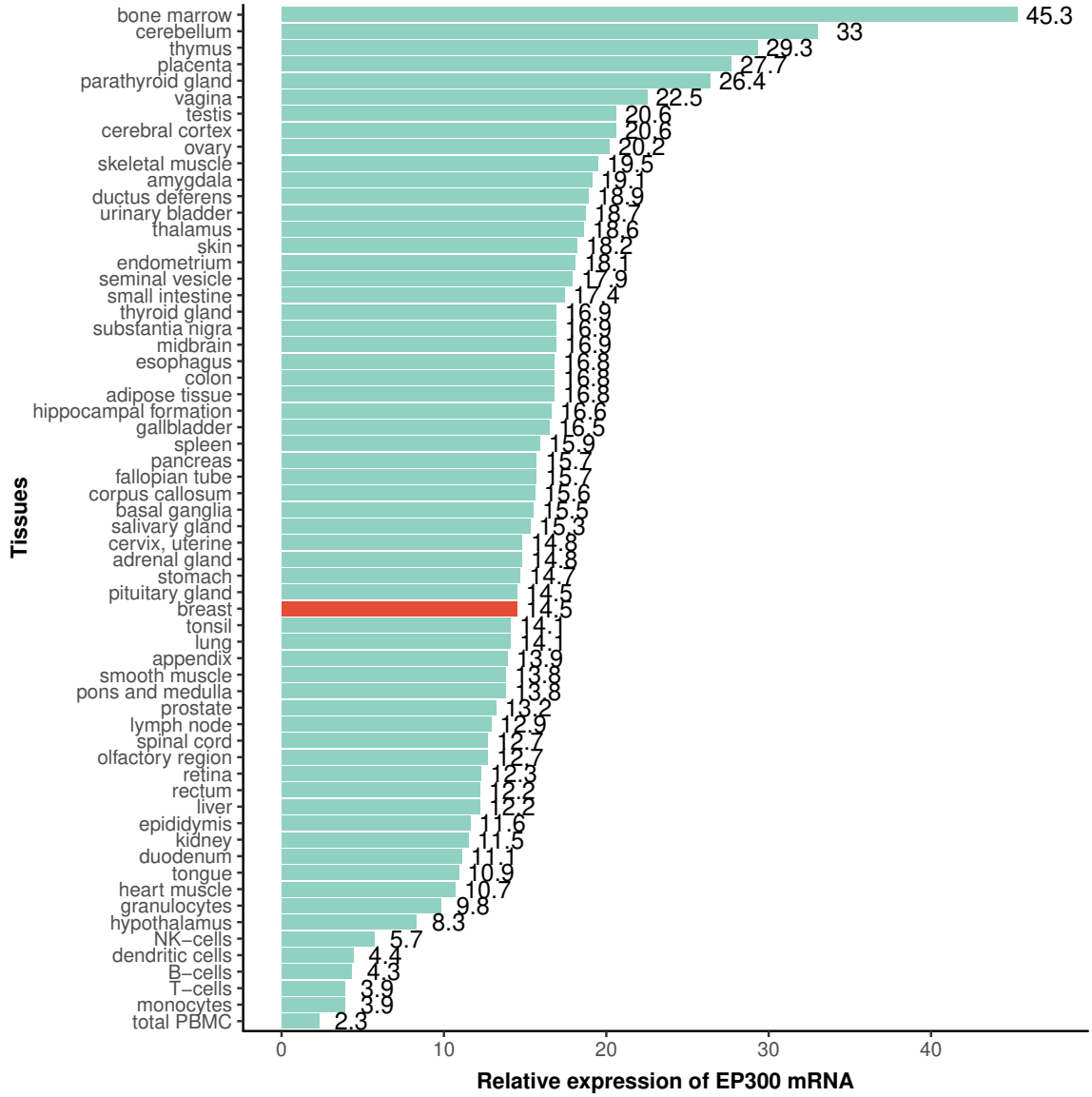
bone marrow 45.3
cerebellum 33
thymus 29.3
placenta 27.7
parathyroid gland 26.4
vagina 22.5
testis 20.6
cerebral cortex 20.6
ovary 20.2
skeletal muscle 19.5
amygdala 19.1
ductus deferens 18.9
urinary bladder 18.7
thalamus 18.6
skin 18.2
endometrium 18.1
seminal vesicle 17.9
small intestine 17.4
thyroid gland 16.9
substantia nigra 16.9
midbrain 16.9
esophagus 16.8
colon 16.8
adipose tissue 16.8
hippocampal formation 16.6
gallbladder 16.5
spleen 15.9
pancreas 15.7
fallopian tube 15.7
corpus callosum 15.6
basal ganglia 15.5
salivary gland 15.3
cervix, uterine 14.8
adrenal gland 14.8
stomach 14.7
pituitary gland 14.5
breast 14.5
tonsil 14.1
lung 14.1
appendix 13.9
smooth muscle 13.8
pons and medulla 13.8
prostate 13.2
lymph node 12.9
spinal cord 12.7
olfactory region 12.7
retina 12.3
rectum 12.2
liver 12.2
epididymis 11.6
kidney 11.5
duodenum 11.1
tongue 10.9
heart muscle 10.7
granulocytes 9.8
hypothalamus 8.3
NK−cells 5.7
dendritic cells 4.4
B−cells 4.3
T−cells 3.9
monocytes 3.9
total PBMC 2.3
Tissues
0
10
20
30
40
Relative expression of EP300 mRNA

(a)

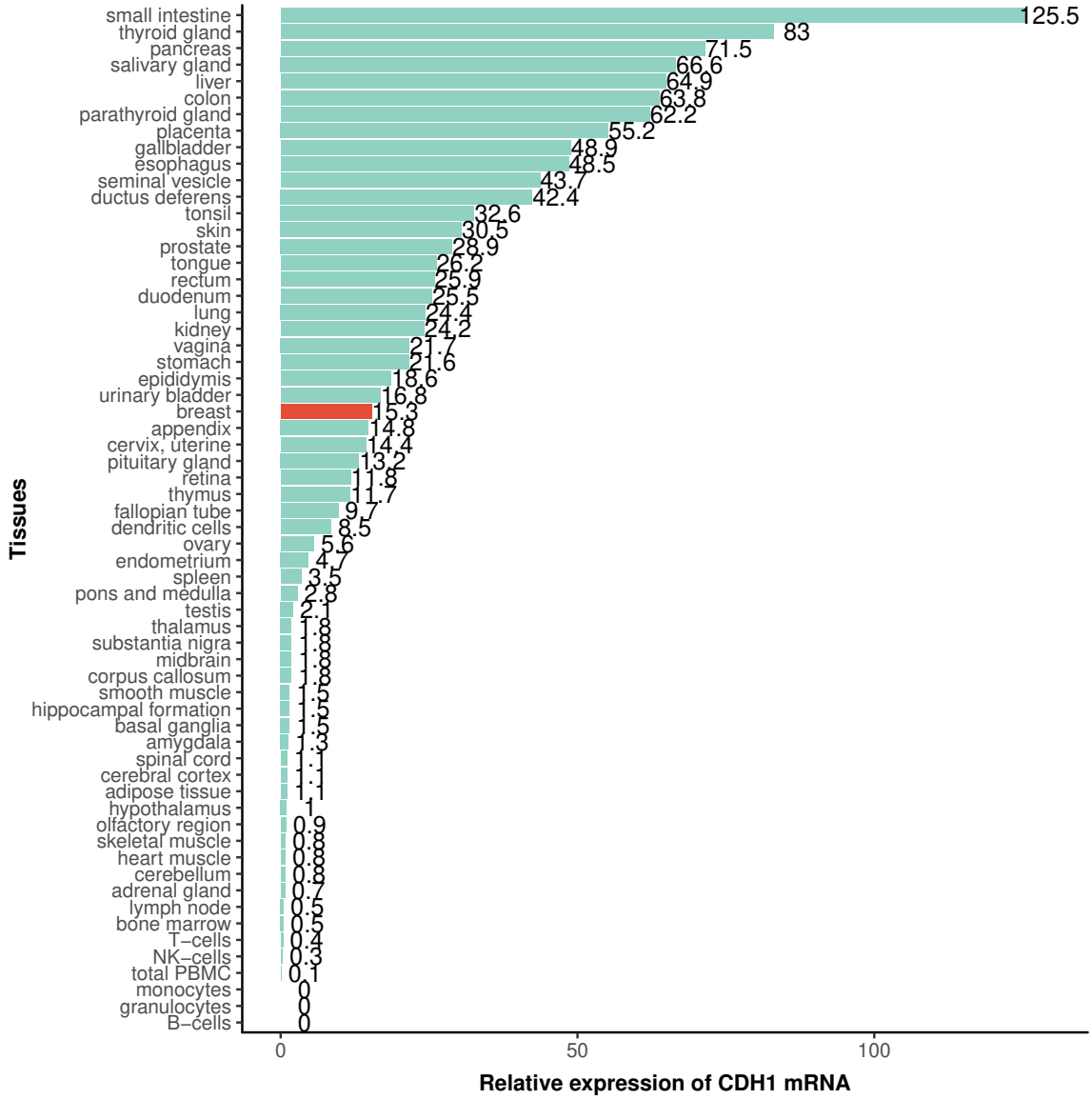

(b)

Fig. 5.2 RNAseq tissue expression of EP300 and CDH1. Source " The Human Protein Atlas". Relative expression of genes are shown across a variety of tumour types. Data are shown as normalised to the basal expression. The mean + SD of n=3 independent experiments is shown, NS Non-Significant, * p<0.05, **p<0.01, *** P<0.001,****p<0.0001 (ordinary one-way ANOVA following Dunnett's multiple comparison test).

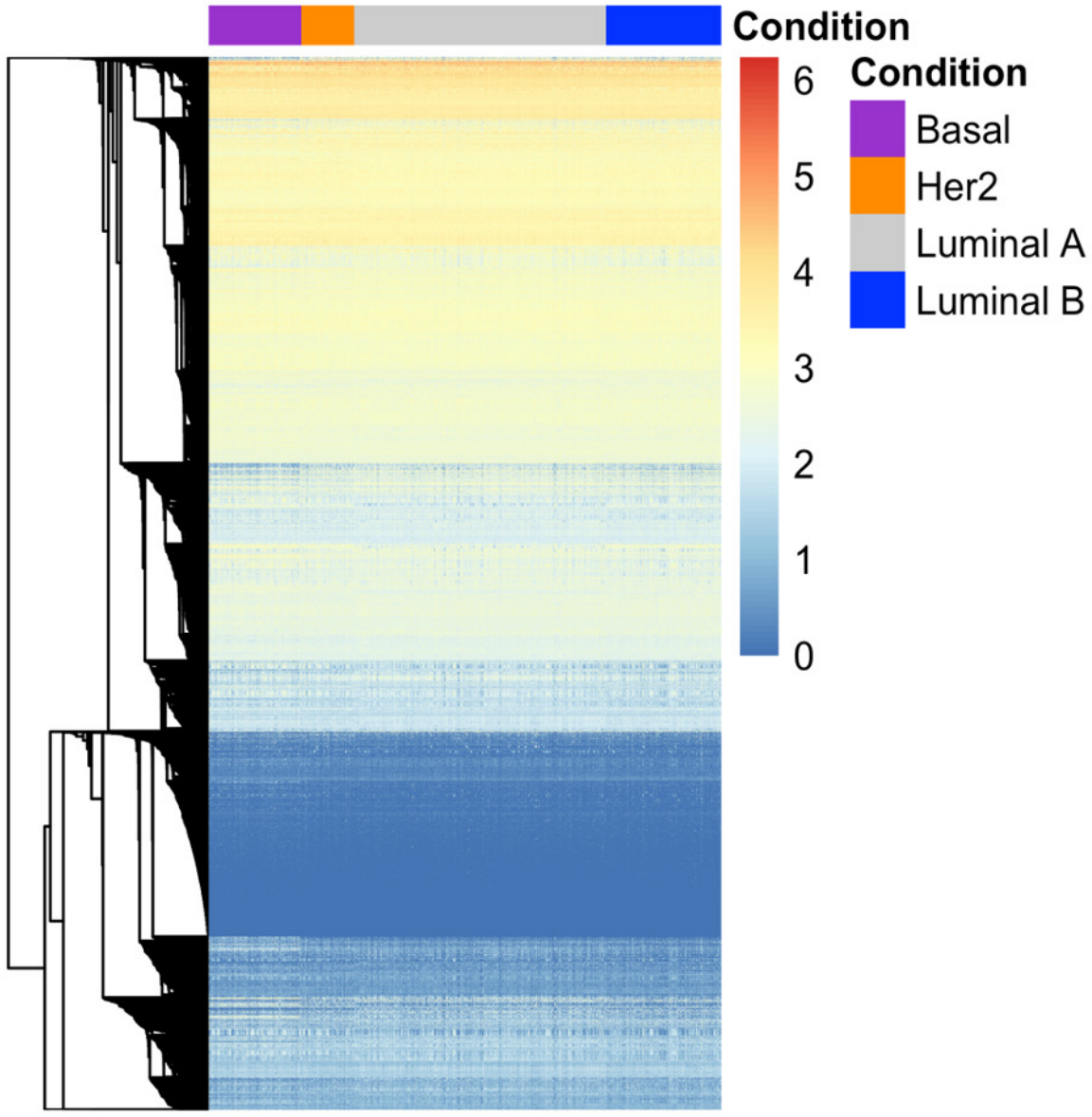
Condition
Condition
6
5
4
3
2
1
0
Condition
Basal
Her2
Luminal A
Luminal B

(a)

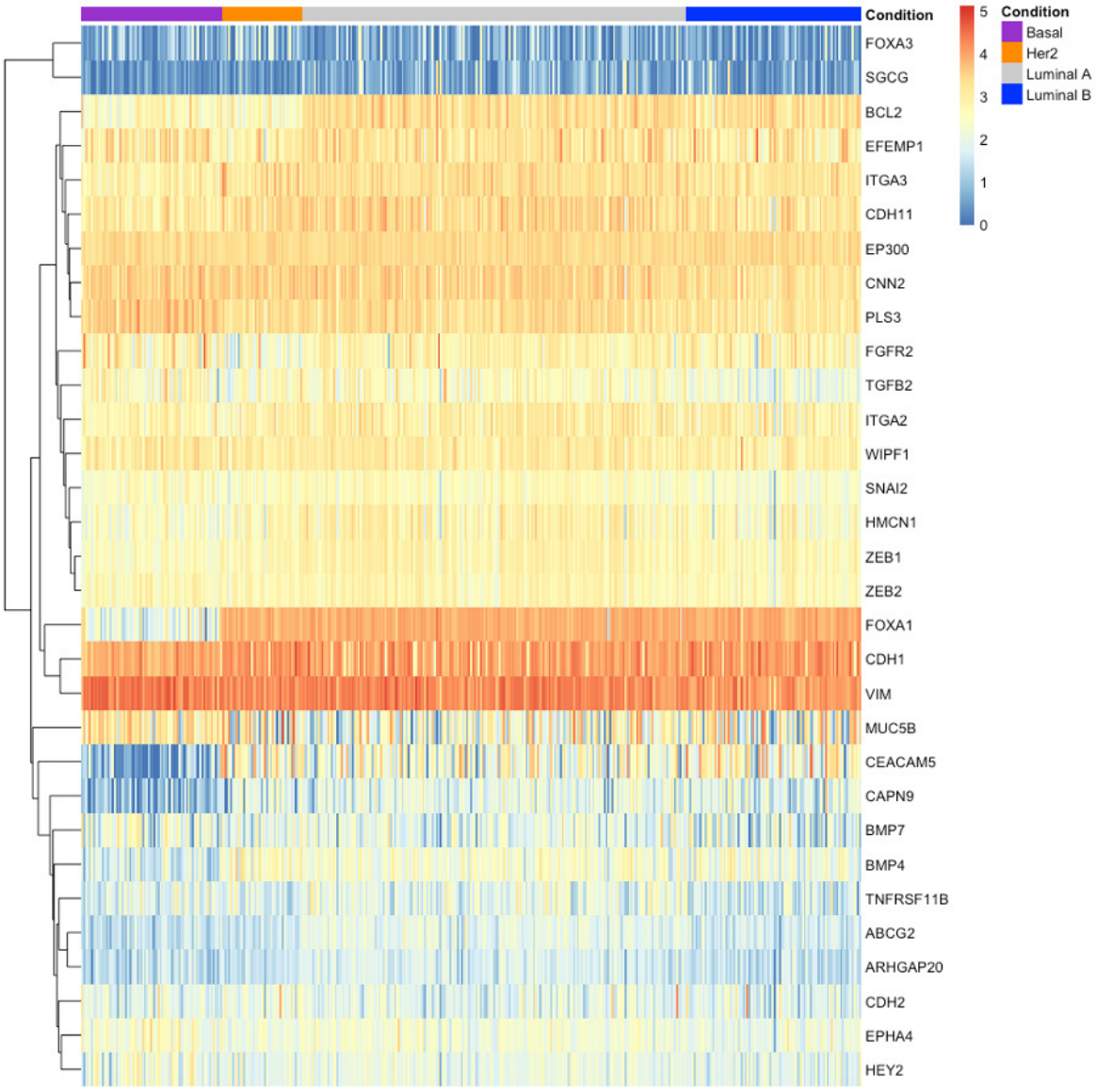

(b)

Fig. 5.3 TCGA gene expression analysis. (A) Global view of TCGA dataset showing the clusters zoomed out (B) Correlation of genes of interest across breast cancer subtypes: Luminal A(n=235), Luminal B(n=133), Her-2+(n=58), and basal(n=81). Heatmap was generated using the TCGA-BRCA dataset obtained from https://tcga-data.nci.nih.gov/tcga/. Data shown is a selected sample of n=948 with n=100 genes. Correlation statistical analysis was done using Pearson correlation test.

To conclude this results chapter, we have first demonstrated that EP300 has a prognostic value in RFS for three subtypes of breast cancer, basal, luminal A and B. Secondly we have shown the relative abundance of this protein in different tissue types, of which the breast is of relevance to our disease model. When exploring RNA-seq data, we attempted to apply our gene signature as well as EP300 to see if this had any differences between subtypes. While the signature did not produce any discernable patterns, it is worth noting that the sselected gene signature is too small for this purpose. It might be of more relevance to sequence our cell lines with EP300 overexpression (CAL51/MDA-MB-231-EP300) and EP300 knockdown (MCF7 and T47D-shEP300) to see whether there is an effect on global gene expression. From this we can also see whether there are any differences on enhancer regions or open/closed confirmations and acetylation status. Furthermore, a variety of novel techniques have developed for making this procedure easier, such as the development of deep learning. Which is a variation of machine learning, a technique by which a machine logically computes through computational layers to form the correct conclusion, based on access to a previous data model. It is particularly well suited for tackling genomic problems due as it does not require simplifying asumptions which is usually done in traditional statistical techniques. Four areas we propose are: 1. Investigating transcription factor binding, as we have earlier outlined that EP300 controls multiple transcription factors such as FOXO3a, ZEB1/2 etc. We can use deep learning to investigate the abundance of transcription factor motifs based on expression of EP300. For this purpose a convolutional neural network model could be used. 2. Earlier we mentioned that DNA accessibility is controlled by epigenetic mechanisms such as methylation and acetylation. The accessibility of these motifs for transcription factors can also play a role in protein expression. Therefore it might be worthwhile to look into. Examples of both of these approaches can be seen in published theoretical approaches (Ramsudar et al., 2019). With some labs using these approaches (Koo et al., 2020, Zheng et al., 2020)

5.2.4 Discussion

In **Figure 5.1a** we could see that for the whole patient population, both EP300 and CDH1 had very little risk associated with RFS. As expression of EP300 decreased, the RFS decreased. The difference is minimal, and no inference can be made. The reverse is seen with CDH1, whose lower expression showed higher RFS after it passed the median. This might suggest a shift towards MET (Friedl et al., 2011), where it might be beneficial to lose CDH1 to prevent activation of distal secondary tumour sites.

In **Figure 5.1b**, when looking at the whole patient cohort, we can see that EP300 and CDH1 expression has higher risk to OS. The median OS improved with lower EP300

expression, while the median OS improved for high CDH1 expression. This could suggest that an epithelial phenotype is favourable, it has less migratory capacity and less drug resistant traits (Friedl et al., 2011). The association of EP300 expression with less favourable OS is unclear, but could be due to many reasons such as a particularity of this patient cohort, or not being stratified by cancer subtype, thereby negating any effect. Another reason could be that EP300 affects such a wide range of transcription factors and miRs that it could have a net negative effect (Bedford & Brindle, 2012, Wang, Marshall et al., 2013).

When only looking at the triple negative breast cancer subset of the population in **Figure 5.1c**, EP300 has a smaller risk associated with RFS, while CDH1 has a higher risk associated with RFS. The RFS has a large decrease associated with a loss of EP300. This could be due to EP300 controlling a vast majority of EMT and drug resistance associated transcription factors (Dave et al., 2011), and with its loss there is even more activation of these. While the median RFS does not change with CDH1 expression, this could be easily explained as these types of tumours are highly aggressive and resistant to therapy, thereby being prognostically unfavourable (Coates, Winer et al., 2015).

When only looking at the HER2 positive breast cancer subset of the population in **Figure 5.1d**, both EP300 and CDH1 have a higher risk associated with RFS. The median RFS increases with lower expression of EP300 and CDH1, in which CDH1 has a bigger effect. We cannot make any inference as to what the reason is behind this at this point. When only looking at the Luminal B breast cancer subset of the population reflected in **Figure 5.1e**, EP300 has a small risk associated with RFS, while CDH1 has a higher risk associated with RFS. EP300 expression increases RFS, while CDH1 expression does not have much change. No inference can be made at this time. When only looking at the Luminal A breast cancer subset of the population in **Figure 5.1f**, EP300 has a small risk associated with RFS, while CDH1 has a higher risk associated with RFS. EP300 expression slightly increases RFS while CDH1 expression slightly decreases RFS. Similarly, no inference can be made at this time.

The results in **Table 5.1** show that both CDH1 and EP300 expression is mostly around the glands is not surprising as it is the most functional unit of the breast (Li, Uribe et al., 2005). Their presence is interesting as most carcinomas arise from the ductal tubules, a very loose hypothesis could be made that perhaps they are involved in some way with this process. The presence of EP300 and CDH1 in a variety of tissues, showing the wide-ranging function in various processes in the body. **Table 5.2** results suggest that neither gene is prognostic in this patient cohort, however multiple studies showed that this is not the case. Loss of CDH1 is a canonical marker for EMT and its prognostic significance has been previously discussed in (Birchmeier et al 1994, Hirohashi et al 1998). The same can be said for EP300. However, this could be reflected in the tumour heterogeneity and the difficulty in getting an accurate

biochemical representation of a tumour sample from one biopsy. As the expressions are averaged across the subtypes, any individual differences could be removed.

In **Figure 5.3** we can see that it is difficult to discern any differences across subtypes when looking at the global overview. We have decided to only focus on our gene signature that we have previously ruled out to be of any significance in **Chapter 4**. In the TCGA dataset, we can see that it also shows no significance within a patient population. What is interesting is the low expression of FOXA1, CEACAM5 and CAPN9 and a higher expression of MUC5B by the triple negative subtype. So far, there is no significance to this, but it might be related to a biochemical process which confers survival for this subtype of cancer.

5.2.5 Future Potential Work

As EP300 is an acetyl transferase, there is many ways in which its activity can be investigated. Potentially the methylation status of the EP300 promoter can be seen to see how much of it would be transcribed or active. This can be done through genotyping of bisufite converted genomic DNA at individual CpG sites (Moarii et al 2015, Bibikova et al 2011).

The TCGA dataset has a lot of information that further analysis can reveal, a recent study on tumour immune microenvironment subtypes (TIME) in head and neck squamous cell carcinomas investigated the role of EP300 in these subtypes (Krupar et al 2020). It found that EP300 was associated with an immune activated TIME, and its downregulation was associated with more anti-tumour activity, due to its association with metabolism (Krupar et al 2020). This not only confirms EP300 as a viable target, but shows potentially similar analysis could be done on molecular subtypes of breast cancer to identify a gene expression profile pathway that could be targeted.

MDA-MB-231 cells were shown to not be as sensitive to bromodomain inhibitors, with higher transcriptional responses shown to JQ1 inhibitors. Due to this overalap, they found that bromodomain inhibitors resulted in cell specific effects. Upregulated genes as a result of CBP30 were involved in mRNA processing, activation of pre replicative complex and transcription, while JQ1 targeted glycolysis and transcription. While downregulated genes targeted with CBP30 were involved in interferon alpha beta signalling, collagen formation, ncam1 interactions and class a1 rhodopsin like receptors. And the downregulated genes targeted with JQ1 were involved in the same, with the addition of DNA replication genes (Garcia-Carpizo et al 2019). Out of these genes 90 were cancer associated super enhancers when compared to normal human mammary epithelial cells, and 1522 super enhancers are shared with the normal human mammary epithelial cell (Garcia-Carpizo et al 2019). This might mean that it might be relevant to investigate each of our cell lines, and which specific pathways are activated or commonly shared in response to EP300 expression.

In breast cancer, ADP-ribosilation of EP300 might also be of interest as this modification has been shown to influence the modification of nucleosomes that are accessed by nucleosome-evicting brahma-related gene 1 (BRG1) mediated poly-ADP-ribose polymerase 1 (PARP1) transcriptional activation of the DNA repair pathway (Sobczak et al 2019). Alternatively we could look into the frequency and presence of EP300 mutations among our cell lines and patient samples to investigate. Which would probably involve collecting DNA from our cell line samples and performing deep analysis on gene expression. Performing principal component analysis with some screening and correlational analysis of expressed genes. Followed by exon expression, gene structure refinement, alternate splicing analysis of EP300, SNP detection, indel detection. After this it could also be possible to perform gene ontology enrichment analysis, pathway enrichment, cluster analysis and protein-protein interation network analysis to identify more transcription factors involved in EP300 (Bi et al 2019).

5.2.6 Overall Conclusion

From looking at just the expression profile of EP300 we can assume that its expression does not correlate with higher risk in RFS as CDH1 is a much better predictor of this overall. However it might be relavant for subtypes such as basal, luminal A and B. The abundance of EP300 in various tissues and its presence in other carcionomas, would suggest that it has an active role in the tumourigenic process. Therefore it would be of most interest to investigate EP300 by using other deeper bioinformatics methods to elucidate the role in which it modifies the landscape. And finally while RNA-seq data analysis was very limited, we hypothesise that investigating our cell lines in context of EP300 modulation would yield interesting results.

Chapter 6

EP300 and its Involvement in Drug Resistance

6.1 Introduction

6.1.1 Pactlitaxel and Doxorubicin Mode of Action

Paclitaxel belongs to the family of taxanes and is used in many cancers including breast, ovarian, lung and pancreatic tumours. This drug targets the cell cytoskeleton including tubulin, which results in inhibition of the mitotic spindle formation during cell division, and defects in chromosome segregation. It effectively freezes cell division and prevents cells to enter metaphase, which then triggers the apoptotic cell death response (Bharadwaj et al., 2004). Doxorubicin is also used to treat a wide variety of solid tumours including breast cancer. Doxorubicin on the other hand, inhibits macromolecular biosynthesis (Tacar et al., 2013), preventing the topoisomerase II enzyme to unwind DNA for transcription (Pommier et al., 2010). Furthermore, it freezes the topoisomerase complex which prevents unwound DNA from being resealed (Tacar et al., 2013).

6.1.2 Drug Resistance

Drug resistance can be both intrinsic and extrinsic. Intrinsic is when the cells are inherently resistant to therapy prior to any exposure, either a result of genetic mutations, tumour heterogeneity or activation of intrinsic drug resistance pathways. Examples of genetic mutation are seen in HER2 overexpressing tumours which have resistance to cisplatin (Huang et al 2016). This overexpression leads to promotion of EMT through upregulation of SNAI1 and SNAI2, as previously mentioned, and avoidance of p53 mediated apoptosis

and promotion of CSC self-renewal (Huang et al., 2016). Tumour heterogeneity has been a long problem in therapy, and a reason for relapse to remaining populations of resistant cells (Greaves et al., 2012). CSCs are thought to form part of the resistant population (Frank et al., 2010). The intrinsic pathways are upregulation of drug transporters and the glutathione S-transferase system, which will be discussed later. Acquired resistance is either through a proto oncogene that becomes an emerging driver gene for drug resistance, mutations in drug targets or through the tumour microenvironment. Examples of the first two can be found in acute myeloid leukaemia. Whole genome sequencing comparing primary and relapse tumours reveals novel gene mutations (Ding et al., 2012), while secondary mutations such as the threonine 315 to isoleucine (T315I) in BCR Activator Of RhoGEF And GTPase (BCR)-ABL Proto-Oncogene 1, Non-Receptor Tyrosine Kinase (ABL) gene appear as a result of tyrosine kinase inhibitors (Quintas-Cardama et al., 2009).

6.1.3 Mechanisms of Drug Resistance

There are many mechanisms for drug resistance in breast cancer, including and not limited to changes to the cell membrane which leads to efflux, through expression of glycoproteins (Wu et al., 2013). Otherwise, there are also enzymes that inactivate drugs or alter their metabolism. Finally, the availability or affinity of hormone receptors covered in **Chapter 1**, and expression of cancer associated genes involved in DNA repair, CSCs and microenvironment, will influence a tumor's response to therapy.

Upregulation of Drug Transporters

Many drug transporters exist such as ATP-binding cassette ABC transporters. These functions by ATP hydrolysis mediated export of drugs and lead to a decreased intracellular drug concentration. They are frequently cited as a major reason for chemoresistance (Wu et al., 2014). They include: ABCB1, multi drug resistance associated protein (ABCC1) and ABCG2 (Kort et al., 2015, Cole, 2014). ABCB1 is cited as having multiple binding sites which allow for its multidrug resistant function on a variety of substrates, including and not limited to doxorubicin, paclitaxel, etoposide and vinblastine (Vaidyananthan et al., 2016; Lagas et al., 2010; Lal et al., 2008; Sharom et al., 2008). ABCC1 also has multiple binding sites and is cited to be involved in the efflux of organic anionic substrates (Cole, 2014; Muller et al., 1994). ABCG2 is heavily implicated in breast cancer drug resistance and also a marker of CSCs. It has a wide range of substrates including mitoxantrone, bisantrene, epipodophyllotoxin, camptothecins, flavoridol and andtracyclines (Sharom et al., 2008), as well as tyrosine kinase inhibitors such as imatinib and gefitinib (Mao et al., 2015; Stacy

et al., 2013). Other known transporters are ATP binding cassette subfamily C member 2 (ABCC2) and ATP binding cassette subfamily C member 3 (ABCC3) which are involved in cisplatin, doxorubicin and etoposide transport (Balaji et al., 2016 Pan et al., 2016; Zhao et al., 2013). ABCB1 and ABCC1 are both regulated by p53 (Gao et al., 1998; Wang et al., 1998). ABCB1 is also regulated by NF-κB by attaching to its promoter region (Zhou et al., 1997; Gao et al., 2013). There is also transcriptional control over it through the PI3K/AKT, WNT/β-catenin and the MAPK pathways (Bargou et al., 1997; Yang et al., 2001; Lim et al., 2008). In particular, it has been shown that the EGFR/ HER-2, PI3K and MAPK pathways are implicated in tamoxifen resistance (Ziauddin et al., 2014).

Their function as mentioned is similar, ABCB1 is mainly responsible for enhanced DNA repair, glutathione metabolism. ABCC1 is responsible for altering intracellular drug distribution (Sodani et al., 2012). The activity of these differ in effectiveness between compounds, while ABCC1 is weaker than ABCB1 (Sodani et al., 2012), the ABCG2 gene is notably weaker with methotrexate and mitoxantrone derivatives (Vtorushin et al., 2014).

Altered Drug Resistance Targets

While the goal of many targeted therapies is a single target, a problem in resistance arises when the therapy causes a secondary mutation in the target or alteration in its expression levels. Examples of these can be seen with multiple generation of tyrosine kinase inhibitors, which solved the mutation of the previous, such as the loss of cysteine residues on EGFRs ATP site, targeted by the 3rd generation of TKIs versus the 4th generation of TKIs, which targets the allosteric site of EGFR (Jia et al., 2016; Wang et al., 2016). Another known mechanism of altered expression is seen in tamoxifen therapy, which results in mutations in the ER gene, or ER expression (MacGregor et al., 2000; Likhite et al., 2006). This is being circumvented with aromatase inhibitors (Avvaru et al., 2018).

Upregulation of Drug Metabolism Enzymes

Enzymes are important in detoxifying cells, and some of these can be utilised by cancer cells to improve drug resistance as a secondary mechanism to drug efflux. These include: ALDH, DNA topoisomerase, protein kinase C, dihydrofolate reductase and glutathione S-transferase (GST) (Hazarika et al., 2017). Glutathione S-transferase π (GSTP1) in particular, can influence the MAPK pathway signalling (Borrie et al., 2017), which improves drug resistance of a number of compounds such as cisplatin and Adriamycin (Sharma et al., 2017). It is also known for modulating the drug efflux properties of ABCB1 which can contribute to

the duration of effect of the drugs and their accumulation in target tissues (Al-Harras et al., 2016).

Changing Metabolism and Drug Resistance

Drug resistance can also be influenced by external stimuli, mainly coming from the changes in the microenvironment induced by paracrine signalling, hypoxic conditions and pH (Li et al., 2006; Nathanson et al., 2014). Under hypoxic conditions, cells are known to upregulate MRP, topoisomerase II which modulates the cells ability to respond to drugs (Xu et al., 2005). Furthermore, the main gene responsible for hypoxia is the hypoxia inducible factor-1 (HIF-1) which has been shown to regulate MDR1, the gene responsible for coding the ABC transporter cassette ABCB1 (Comerford et al., 2002; Martin et al., 2008). Although I will not review it in depth, pH balance involves proton pumps like (H+) vascular ATPase, which change the pH gradient between cell cytosol (alkaline) and extracellular (acidic). This results in inhibition of apoptosis (Ryder et al 2012; Daniel et al., 2013). This falls in line with the emerging hallmark of cancer, the Warburg effect and the overall shift to glycolysis due to increasing ATP demand by the tumour. This shift is not only responsible for drug resistance but helps in promoting metastasis and invasive capabilities of cancer cells through upregulation of RAS/MAPK. These influence downstream gene transcription such as MMP2/MMP9 (Cato et al., 2005, Cardone et al., 2005; Yang et al., 2010), which are responsible for matrix remodelling and VEGF which activates angiogenesis (Xu et al., 2002).

Tumour Microenvironment and Drug Resistance.

Previously, we showed that the tumour microenvironment is crucial for tumour survival through paracrine and autocrine signalling, resulting in recruitment of cancer associated fibroblasts and macrophages, which in turn release cytokines and growth factors that can lead to angiogenesis, avoidance of apoptosis and EMT promotion. It is also involved in drug resistance as tumour associated macrophages can negate the cytotoxic drug effects of paclitaxel through cathepsin-dependent functions (De Palma, 2011). Mesenchymal stem cells are also demonstrated to have a drug resistant effect (Bonomi et al., 2015). Other cell types like endothelial cells can be epigenetically altered by survivin (Virrey et al., 2008). These cells can upregulate RAF proto-oncogene serine/threonine-protein kinase (Raf1) and Apoptosis signal-regulating kinase 1 (ASK1) to improve avoidance of doxorubicin-induced damage (Alavi et al., 2007). Finally, to add to the diversity of cell types and drug responses, the final cell type is the cancer associated fibroblast (Park et al., 2015).

EMT and Upregulation of Transcription Factors

As both EMT and CSCs share similar activated pathways, such as TGF-β,WNT, hedgehog, and notch, the transcription factors they activate are also similar. Well-known EMT transcription factors such as TWIST, SNAI1, SNAI2, ZEB and FOXC2 are all linked to drug resistance phenotypes (Haslehurst et al., 2012; Zhou et al., 2015; Lazarova et al., 2017). They function through upregulation of ABC transporters. ABCB1 is controlled by TWIST, ZEB1/2, SNAI2 and SNAI1 (Li et al., 2011; Zhu et al., 2012, Tsou et al., 2015). ABCG2 is controlled by SNAI1, Homeobox protein MSX-2 (MSX2), SOX2 and ZEB1 (Chen et al., 2010; Hamada et al., 2012, Lee et al., 2014; Mato et al., 2014). Similar patterns are seen with ABCC1/ ABCC2/ ATP binding cassette subfamily C member 4 (ABCC4) and ATP binding cassette subfamily C member 5 (ABCC5) (Uchibori et al., 2012; Bhucanalakshmi et al., 2015; Sun et al., 2017).

Firstly, we previously mentioned genes involved in EMT such as TWIST. This gene is regularly upregulated by the NF-κB pathway and shares its function in drug resistance by downregulating ERα and upregulating drug resistance genes (Lo et al., 2007; Vesuna et al., 2011). Other genes such as ABCB1, which encodes P-glycoprotein, a key drug transporter, is regulated by p53, whose aberrant expression is responsible for a number of cancer hallmarks and GSTP1 (Gao et al., 2013). GSTP1 is involved in the phase two metabolism by which it forms a complex with the drugs and gets transported out of the cell through cell membrane pumps. Phase one metabolism acts on reactive oxygen species via the cytochrome p450 family (Allocati et al., 2019).

MiRs

mIRs also play a part in drug resistance, as previously mentioned, and the prototypical miR-200 family is responsible for regulating ABCB1. It is also responsible for paclitaxel resistance through ZEB1/ZEB2 and Tubulin Beta 3 Class III (TUBB3) (Park et al., 2008; Cochrane et al., 2009) Other targets such as ABCB1 and MDR have been responsible for doxorubicin resistance, as a result of mIR-451 and miR-326 (Kovalchuk et al., 2008; Liang et al., 2010). Not to mention, miR influenced endocrine resistance through targeting ER-α, doing so through post translational modification (Muluhngwi et al., 2015) and through direct action on its promoter by miR-221, miR-222, miR-342-3p (He et al., 2013).

DNA Repair Mechanisms and CSCs

Pertinent to compounds such as paclitaxel and doxorubicin is DNA repair mechanisms (Branham et al., 2004; Taymaz-Nikerel et al., 2018). In cancer cells, prevention of these

mechanisms is done through the promotion of CSCs (Nikitaki et al., 2015), which plays an important role in breast cancer drug resistance (Pavlopoulou et al., 2016). Some known mechanisms include: nucleotide excision repair, base excision repair which repair single strand breaks and / or oxidation, deamination and alkylation of bases (Krokan et al., 2013; Martejin et al., 2014). There is also homologous recombination and non homologous end joining, and these are responsible for double strand break repair and mismatch repair (Dietlein et al., 2014; Prakash et al.,2015).

The other way in which CSCs contribute is through their overexpression of the aforementioned drug transporters, as well as upregulation of antiapoptotic factors, including doxorubicin resistance (Zhou et al., 2016). These traits are particularly expressed through CSC markers such as Aldehyde Dehydrogenase 1 Family Member A1 (ALDH1) (Tanei et al., 2009) and $CD44^{high}/CD24^{low}$ (Liu et al., 2013) which will be covered in the next **Chapter 7** (Collina et al., 2015). With the CSC status comes the activation of the self-renewal pathways, as previously mentioned, such as Notch and Hedgehog and resistance pathways WNT/β-catenin. Modulating these pathways, such as via let-7 overexpression, resensitises CSCs to chemotherapy (Yu et al., 2007). Other examples of modulating drug resistance of CSC populations are seen with targets such as nicastrin, insulin like growth factor-1 (IGF-1R) and propyl-isomerase (Pin1) (Lombardo et al., 2012; Kotiyal et al., 2014).

How EP300 Affects Drug Resistance

In this chapter, we have described mechanisms of drug resistance such as: the upregulation of drug transporters, altered drug resistance targets, upregulation of drug metabolism enzymes, changing metabolism, tumour microenvironment impact, impact of EMT and CSC characteristics through transcription factor and miR expression and DNA repair. Epigenetic mechanisms such as methylation and acetylation have already been implicated in drug resistance (Ohata et al., 2017).

Such changes in methylation or acetylation states, otherwise known as epimutations, are maintained throughout each DNA replication and are therefore reversible (De Smedt et al., 2018). A portion of these epimutations are attributed to the maintenance of a CSC subpopulation and drug resistance (Wainwright et al., 2017). Hypoacetylation of chromatin regions is of particular interest as it has high association with cancer (Liu et al., 2017). The maintenance of this acetylation state is dependent upon the antagonistic function of histone acetyl transferases (HATs) and histone deacetylases (HDACs). HDACs are some of the most well studied epigenetic effectors. They have been implicated in regulating the CSC subpopulation in breast cancer through the repression of ESR1 and progesterone receptor (PGR) (Sulaiman et al., 2016). Furthermore, the maintenance of the CSC phenotype is

directly influenced by histone deacetylase 1 (HDAC1) and histone deacetylase 7 (HDAC7) in breast and ovarian cancer (Witt et al., 2017); while the pluripotency related transcription factors are regulated by HDAC1 and histone deacetylase 2 (HDAC2) (Jamaladdin et al., 2014).

Due to this direct involvement in drug resistance and CSCs, HDACs have been selected as a good target for therapy, epigenetic mechanisms being the first step or the overriding step in gene regulation. We will describe a few HDAC inhibitors which have had some early success in targeting these traits. Abexinostat, lowered the CSC subpopulation in breast cancer by promoting differentiation (Salvador et al., 2013). Others such as gemcitabine were used in pancreatic ductal carcinoma, showing a correlation of HDAC inhibition with downregulated EMT traits (Cai et al., 2018). These inhibitors also function by blocking key pathways which are known to regulate CSCs such as the WNT and Hippo pathways (Li et al., 2015; Cui et al., 2016). Unfortunately, HDAC inhibitors can also induce multi drug resistance despite their benefits (Kim et al., 2008). This is because while HDAC inhibitors target particular inhibitors, the blocking of an HDAC may have unpredictable consequences. FK228, a cyclic tetrapeptide based HDAC inhibitor, showed an undesirable upregulation of ABC transporters ABCC1 and ABCB1 (Dean et al., 2008; To et al., 2008). Since some efficacy is seen with HDAC inhibitors, but they result in unwanted effects, it might be worthwhile to explore the effects of HATs like EP300.

As EP300 is an acetyltransferase and its epigenetic impact has been shown to influence the acetylation states of specific amino acid residues both on the histones and on transcription factors, it promotes or alters the transcriptional landscape resulting in drug resistance. Multiple studies have demonstrated that EP300 has effects on drug resistance traits. Its downregulation in bladder cancer showed increased resistance to doxorubicin and cisplatin (Shiota, Yokomizo et al., 2010; Takeuchi, Shiota et al., 2012). In colorectal cancer, this effect is mainly as a result of ZEB1, a transcription which is controlled by EP300 acetylation (Lazarova et al., 2017).

Previously published findings from our lab support this as EP300 knockdown in MTMEC cells lead to an increase in long-term paclitaxel resistance and evasion of apoptosis (Hu, Li et al., 2015). The effects of the drugs were mitigated by a mechanism overcoming drug induced senescence (Zhou, Hu et al., 2014). Furthermore, the effects of EP300 vary between cell lines. Towards the end of this project, Aldo-keto reductase family 1 member C1 (AKR1C1), Aldo-keto reductase family 1 member C2 (AKR1C2) and Aldo-keto reductase family 1 member C3 (AKR1C3) which are aldo keto reductases were found to be effectors for drug resistance in breast cancer cell line HS578T, with an hypermethylated E-cadherin promoter (Mahmud et al., 2019). In light of these findings, we will be using breast cancer cell lines

MDA-MB-231 and CAL-51 with EP300 overexpression, as well as newly generated T47D breast cancer cell line with EP300 knockdown to demonstrate effects on drug resistance.

6.2 Analysis of EP300 expression on Drug Resistance

6.2.1 Hypothesis

The hypothesis for this chapter will be that in the mesenchymal breast cancer cell lines MDA-MB-231 and CAL51, which exhibit EMT and drug resistance traits, as well as an increased population of CSCs, the experimental overexpression of EP300 would re-sensitise the cells to paclitaxel and doxorubicin. Long-term exposure to these drugs in these cell lines would also negatively impact the number of colonies grown, which directly correlates to the CSC subpopulation and is related with drug resistance. The reverse is hypothesized in the epithelial breast cancer cell line T47D. The downregulation of EP300 would increase the drug resistance to these drugs as EP300 normally controls the EMT/CSC/drug resistant traits.

6.2.2 Aim

1. Investigate the effect of EP300 and CDH1 overexpression on short-term drug sensitivity in breast cancer cell line MDA-MB-231.
    - Find the concentration of paclitaxel at which the cell lines are sensitised.
    - Find the concentration of doxorubicin at which the cell lines are sensitised.
2. Investigate the effect of EP300 and CDH1 overexpression on long term drug resistance in breast cancer cell line MDA-MB-231.
    - Find the concentration of paclitaxel at which the cell lines form less colonies.

6.2.3 Results

EP300 and CDH1 overexpression shows no change in sensitivity to Paclitaxel in the MDA-MB-231 breast cancer cell line.

In order to study the effects of EP300 and CDH1 overexpression on sensitivity to paclitaxel and doxorubicin, we used some of the cell lines we had used previously for our gene expression analysis in **Chapter 4**. The hypothesis was tested in a mesenchymal breast cancer cell line MDA-MB-231 in context of EP300 overexpression, CDH1 overexpression and compared to the basal expression in the same cell line with a control empty vector.

In **Figure 6.1a**, we observe the breast cancer cell line MDA-MB-231 in three conditions: a control sample with an empty vector, an EP300 overexpression and a CDH1 overexpression. All three samples were treated with increasing concentrations of paclitaxel (0-16 nM) 48h post cell seeding. We see that overall, all conditions (control, EP300 overexpression and CDH1 overexpression) result in decreased cell survival. With EP300 overexpression, cell survival increases when compared to the control. At 12 nM it is 20% higher ($p<0.05$), at 14 nM it is 37% higher ($p<0.05$) and at 16nM it is 55% higher ($p<0.01$). With CDH1 overexpression, the results follow the same trend in cell survival compared to both control and EP300, at 6-10 nM. When comparing CDH1 and the control: at 6nM it is 30% lower ($p<0.01$), at 8nM it is 22% lower ($p<0.05$) and at 10nM it is 7% lower ($p<0.05$), after which there is no significant difference between samples. When comparing CDH1 and EP300 samples: at 6nM it is 45% lower ($p<0.01$), at 8nM it is 32% lower ($p<0.05$) and at 10nM it is 13% lower ($p<0.05$), after which there is no significant difference between samples. Overall, the concentration at which cell survival improves is not found yet, but is likely to sit between 10-16nM or higher.

In **Figure 6.1b**, we observe the breast cancer cell line MDA-MB-231 in three conditions: a control sample with an empty vector and EP300 overexpression. Both samples were treated with increasing concentrations of doxorubicin (221-405 nM) 48h post cell seeding. We see that overall, EP300 overexpression showed less cell survival when compared to its control counterpart. With EP300 overexpression, cell survival decreases when compared to the control. At 221 nM most cells survive, at 239 nM it is 18% lower ($p<0.05$) and at 258nM it is 14% lower ($p<0.05$), at 313nm it is 17% lower ($p<0.05$), 331nM it is 33% lower ($p<0.01$), 350nM it is 50% lower ($p<0.001$), 386nM it is 49% lower ($p<0.001$) and 405nM it is 58% lower ($p<0.001$). The maximum concentration at which doxorubicin survival improves is not yet found, higher concentration ranges must be explored.

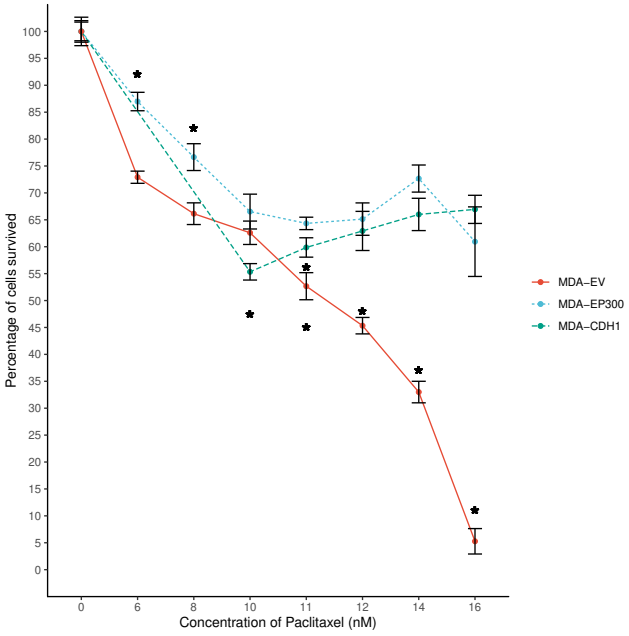

(a)

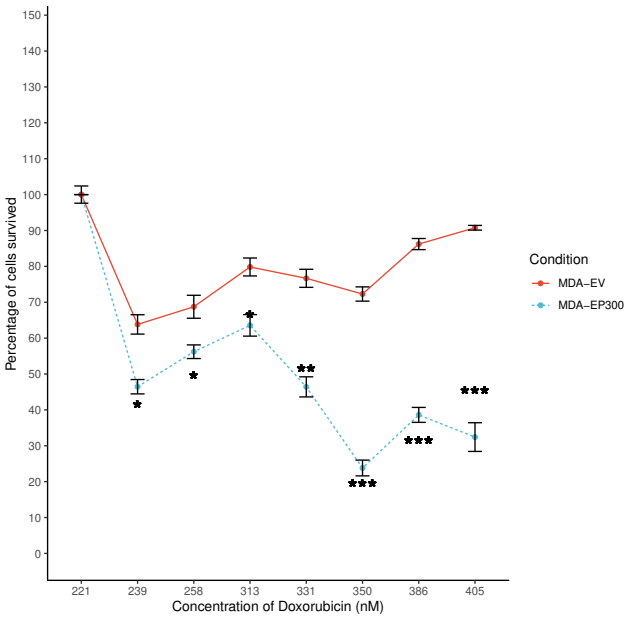

(b)

Fig. 6.1 Short-term drug sensitivity in MDA-MD-231 cells with EP300 overexpression. (A) Presents a sulphorhodamine B assay with paclitaxel sensitivity. (B) presents a sulphorhodamine B assay with doxorubicin sensitivity. Drug sensitivity in EP300 and CDH1 overexpressing cells was demonstrated relative to the respective control (wild type and empty vector control transfected cells). 3000 cells per well were seeded in triplicate, in a 96 well plate. After adhering overnight, and treated with pacliltaxel and doxorubicin in increasing concentrations (221-405nM). Plates were then fixed with 40% TCA, and stained with 0.4% SRB, the resulting total protein concentration which corresponds to the OD value was measured on a microplate reader at 492 nm. Statistical analysis was performed using a two way ANOVA test, comparing the control (empty vector), and cells overexpressing EP300 (MDA-EP300) and CDH1 (MDA-CDH1), (**P<0.01,***P<0.001). Data represents average number of resistant clones + SD from three independent experiments (n=3).

EP300 knockdown shows no change in sensitivity to Paclitaxel in a T47D breast cancer cell line.

In order to study the effects of EP300 knockdown on sensitivity to paclitaxel, we used some of the cell lines we had used previously for our gene expression analysis in **Chapter 4**. The hypothesis was tested in an epithelial breast cancer cell line T47D in context of EP300 knockdown using two EP300 vectors (sh EP300 I and sh EP300 II), and compared both of these to the basal expression in the same cell line with a control empty vector.

In **Figure 6.2**, we observe the breast cancer cell line T47D in three conditions: a control sample with an empty vector, an EP300 knockdown vector (sh Ep300 I) and another EP300 knockdown vector designated (sh Ep300 II). Each panel differs in the treatment cycle length (24-72 h). All three samples were treated with increasing concentrations of paclitaxel (0-10n M) 48h post cell seeding.

In **Figure 6.2a**, we observe the breast cancer cell line T47D in three conditions: a control sample with an empty vector, an EP300 knockdown vector (sh EP300 I) and another EP300 knockdown vector designated (sh EP300 II). All three samples were treated for a treatment cycle length of 24h with increasing concentrations of paclitaxel (0-5000 nM), 48h post cell seeding. We see that for all conditions (control, sh EP300 I and sh EP300 II) paclitaxel treatment results in decreased cell survival. At 1 nM, the control sample has 7% lower ($p<0.05$) cell survival compared to the other two conditions. At 5 nM, the same is seen, where the control sample is 10% lower ($p<0.05$) than shEP300 I and 23% lower ($p<0.05$) than shEp300 II. At this concentration, we can also see that shEp300 II performs better than shEp300 I by 13% ($p<0.05$). At 10 nM, we see an anomalous result where the control sample results are statistically insignificant. However, the survival of shEP300 I is 14% worse ($p<0.05$) than sh EP300 II. At higher concentrations, we see that the control sample performs much better than either two conditions. At 100 nM, the control cell survival is 9% higher ($p<0.05$) than shEp300 I, and 17% higher ($p<0.05$) than sh EP300 II. At this concentration, cell survival is also 8% higher ($p<0.01$) in shEP300 I. After this concentration, there are no differences in survival between shEP300 I and II. Both have 8% worse survival ($p<0.05$) at 500 nM. At 1000 nM, the control has 16% better survival ($p<0.01$) and 18% better survival ($p<0.01$) than shEP300 I and II. At 5000 nM, the control has 22% better survival ($p<0.01$) and 23% better survival ($p<0.01$) than shEP300 I and II.

In **Figure 6.2b**, we observe the breast cancer cell line T47D in three conditions: a control sample with an empty vector, an EP300 knockdown vector (sh EP300 I) and another EP300 knockdown vector designated (sh EP300 II). All three samples were treated for a treatment cycle length of 48h with increasing concentrations of paclitaxel (0-5000 nM), 48h post cell seeding. We see that overall, all conditions (control, sh EP300 I and sh EP300 II) result

in decreased cell survival. At 5 nM, the same is seen, where the control sample is 9% lower ($p<0.01$) than shEP300 II, with no difference seen between it and shEp300 II. At this concentration, we can also see that shEp300 II performs better than shEp300 I by 11% ($p<0.01$). At 100 nM, the control cell survival is 11% higher ($p<0.05$) than shEp300 I and 12% higher ($p<0.05$) than sh EP300 II. At 500 nM, the control cell survival is 18% higher ($p<0.01$) than shEp300 I and sh EP300 II ($p<0.01$). At 1000 nM, the control cell survival is 8% higher ($p<0.01$) than shEp300 I and 9% higher than sh EP300 II ($p<0.01$). At 5000 nM, the control cell survival is 18% higher ($p<0.01$) than shEp300 I and 19% higher than sh EP300 II ($p<0.01$).

In **Figure 6.2c**, we observe the breast cancer cell line T47D in three conditions: a control sample with an empty vector, an EP300 knockdown vector (sh EP300 I) and another EP300 knockdown vector designated (sh EP300 II). All three samples were treated for a treatment cycle length of 72h with increasing concentrations of paclitaxel (0-5000 nM), 48h post cell seeding. We see that overall, all conditions (control, sh EP300 I and sh EP300 II) result in decreased cell survival. At 10 nM, the same is seen, where the control sample is 10% lower ($p<0.01$) than shEP300 II, with no difference seen between it and shEp300 II. At this concentration, we can also see that shEp300 II performs better than shEp300 I by 21% ($p<0.01$). The same is seen at 50 nM, where the control sample is 9% higher ($p<0.01$) than shEP300 II, with no difference seen between it and shEp300 I. At this concentration, we can also see that shEp300 I perform better than shEp300 II by 8% ($p<0.01$). At 100 nM, the control cell survival is 13% higher ($p<0.01$) than shEp300 I, and 19% higher ($p<0.01$) than sh EP300 II. At 500 nM, the control cell survival is 20% higher ($p<0.01$) than shEp300 I and sh EP300 II ($p<0.01$). At 1000 nM, the control cell survival is 24% higher ($p<0.001$) than shEp300 I and 25% higher ($p<0.001$) than sh EP300 II. At 5000 nM, the control cell survival is 34% higher ($p<0.001$) than shEp300 I and sh EP300 II ($p<0.001$).

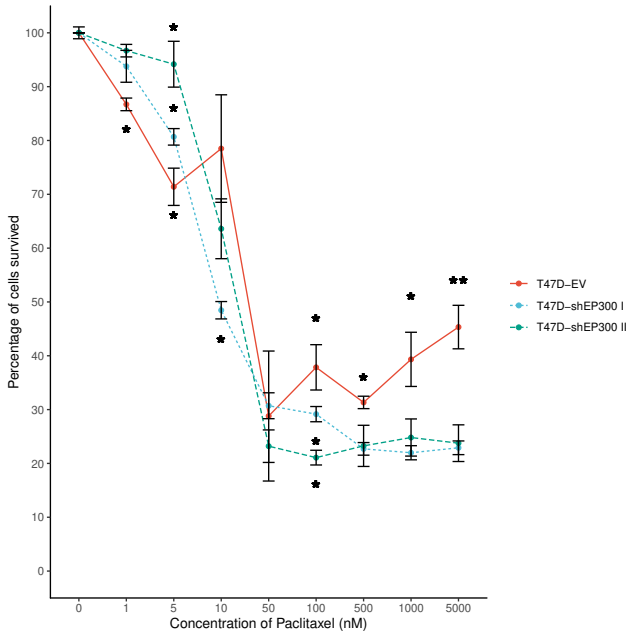
Percentage of cells survived
Concentration of Paclitaxel (nM)
T47D−EV
T47D−shEP300 I
T47D−shEP300 II

(a)

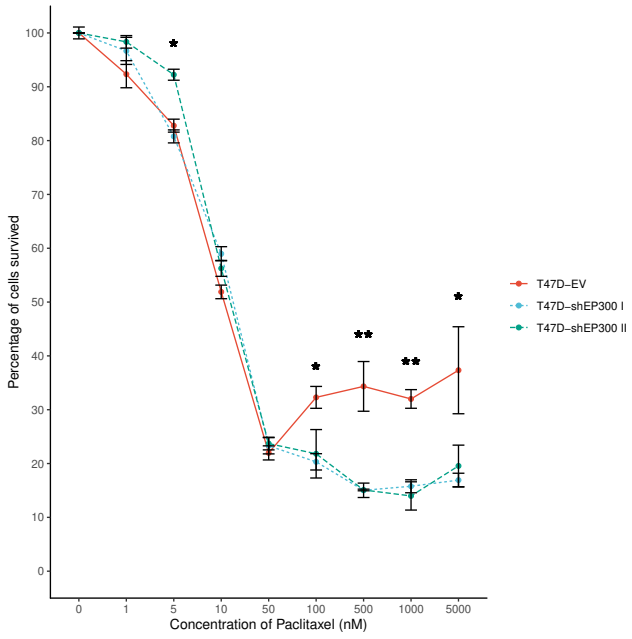
Percentage of cells survived
Concentration of Paclitaxel (nM)
T47D−EV
T47D−shEP300 I
T47D−shEP300 II

(b)

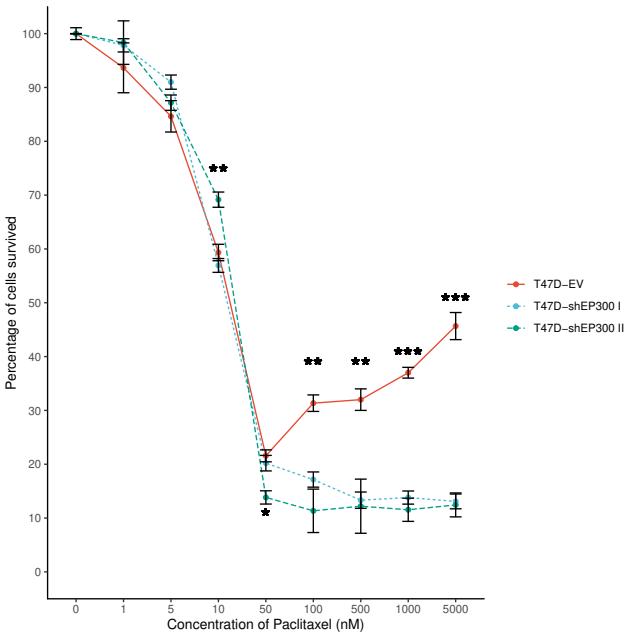

(c)

Fig. 6.2 Short-term drug sensitivity in T47D cells with EP300 downregulation. (A) Presents 24h treatment with paclitaxel, (B) 48h and (C) 72h treatment. Drug sensitivity in sh EP300 I and sh EP300 II knockdown cells was demonstrated relative to the respective control (wild type and empty vector control transfected cells). 3000 cells per well were seeded in triplicate, in a 96 well plate. After adhering overnight, and treated with pacliltaxel in increasing concentrations (0-5000 nM). Plates were then fixed with 40% TCA, and stained with 0.4% SRB, the resulting total protein concentration which corresponds to the OD value was measured on a microplate reader at 492 nm. Statistical analysis was performed using a two way ANOVA test, comparing the control (empty vector), and EP300 downregulation (T47D-shEP300 I) and (T47D-shEP300 II), (**P<0.01,***P<0.001). Data represents average number of resistant clones + SD from three independent experiments (n=3).

EP300 and CDH1 overexpression modulates long-term resistance to Paclitaxel in the MDA-MB-231 breast cancer cell line.

In order to study the effects of EP300 overexpression on long-term resistance to paclitaxel, we used some of the cell lines we had used previously for our gene expression analysis in **Chapter 4**. The hypothesis was tested in a mesenchymal breast cancer cell line MDA-MB-231 in context of EP300 and CDH1 overexpression (EP300, CDH1) and compared both of these to the basal expression in the same cell line with a control empty vector.

In **Figure 6.3a**, we observe a diagram of images to demonstrate the number of drug resistant formed by the breast cancer cell line MDA-MB-231 after treatment with increasing concentrations of paclitaxel. The breast cancer cell line MDA-MB-231 had three conditions: a control sample with an empty vector, an EP300 overexpression (EP300) and CDH1 overexpression (CDH1). All three conditions were treated for 2 weeks with increasing concentration of paclitaxel (6-12 nM), after which, the media was replaced every 6 days. Results show the number of colonies growing in response to the treatment and vector expression. In **Figure 6.3a**, it can be seen that the number of colonies starts to decrease at 8 nM and decreases dramatically at 10 nM, when comparing the 6 nM concentration across all 3 conditions.

Figure 6.3b shows a bar chart representation of the number of clones. Drug resistant clones were defined as a clone consisting of more than 50 cells. With EP300 overexpression no significant difference was seen when comparing the control and CDH1 overexpression, at concentrations lower than 7 nM. When comparing EP300 with the control sample, we can see at EP300 had 30 clones more at 7 nM ($p<0.001$), 40 clones more at 7.5 nM ($p<0.001$), 32 clones more at 8 nM ($p<0.001$), and 30 clones more at 10 nM ($p<0.001$). When comparing CDH1 with the control sample, we can see at CDH1 had 12 clones more at 7 nM ($p<0.01$), 30 clones more at 7.5 nM ($p<0.001$), 36 clones more at 8 nM ($p<0.001$), and 26 clones more at 10 nM ($p<0.001$). When comparing both EP300 and CDH1, there was no significant difference between the number of clones formed.

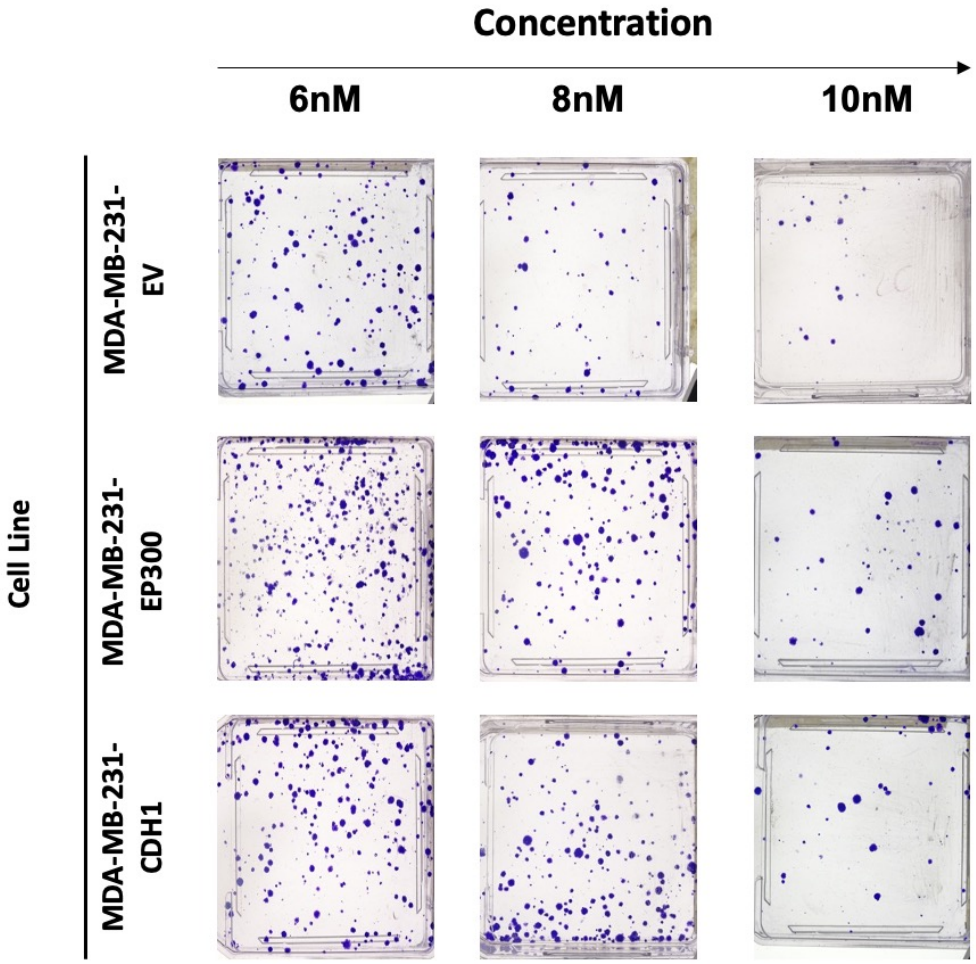
Concentration
6nM
8nM
10nM
Cell Line
MDA-MB-231-EV
MDA-MB-231-EP300
MDA-MB-231-CDH1

(a)

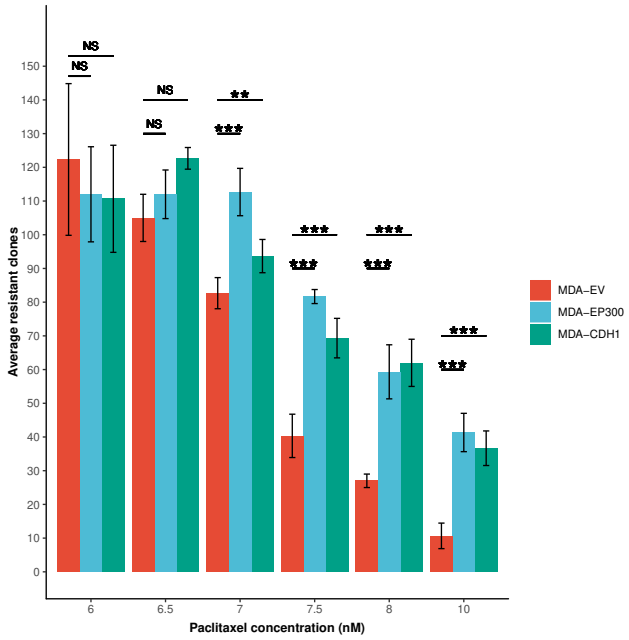

(b)

Fig. 6.3 Overexpression of EP300 increases long-term drug resistance in MDA-MD-231 cells. (A) Presents paclitaxel resistance clones under a microscope. (B) presents the number of resistant clones (upper panel) and absolute absorbance values at 490 nM (lower panel). Clones were grown over 40 days, following a 5 day treatment with paclitaxel at concentrations of 6, 6.5, 7, 7.5 and 10 nM. Statistical analysis was performed using a two way ANOVA test, comparing the control (empty vector), and cells overexpressing EP300 (MDA-EP300) and CDH1 (MDA-CDH1), (**P<0.01,***P<0.001). Data represents average number of resistant clones + SD from three independent experiments (n=3).

6.2.4 Discussion

In this chapter, we looked into the effects of EP300 and CDH1 overexpression on sensitivity to doxorubicin and paclitaxel in the MDA-MB-231 cell line, as well as the same effect of EP300 downregulation using our T47D cell line. While we see a decrease in cell survival with increasing concentrations of paclitaxel (**Figure 6.1**), we did not determine the concentration we achieve full cell death in the control sample, which is what would prove the hypothesis. Therefore, we should continue the test, in particular between the concentrations of 11-16 nM as the control sample experienced the largest drop in cell survival within this concentration range. This difference would be more pronounced if we expanded the titrations within this range. Neither EP300 nor CDH1 overexpression yielded better cell survival, although it is suspected that EP300 should offer more drug sensitivity. Likewise, as with the control sample, once we expand the drug concentration and allow cell survival to fall below 50%, we should see more of a difference. Anomolous results in this expriment could be explained as a likely issue with cell density. While the use of multi-pipettes should yield the same volumes, proper resuspension technique could get rid of this. Another least likely hypothesis is that due to the improper resuspension, the wells tested for in those concentrations received a portion of the cells with lower resistance. The long-term resistance with paclitaxel (**Figure 6.3**) does show that EP300 overexpression improves cell death, as the number of resistant clones decreases.

The rationalisation behind our choice of treatment concentrations comes from previous studies which used paclitaxel on MDA-MB-231, one quotes 30 nM as the half maximal inhibitory concentration (IC50) range (Jeong et al., 2016). Treatment with 100 nM paclitaxel increases G2 arrest by a factor of 3.9 in MDA-MB-231 and by 5 in T47D, followed by an increase in CDK1 in both cell lines while CDK2 increased only in T47D (Nakayama et al 2009). Other earlier studies reported the IC50 concentrations for MDA-MB-231, T47D to be 2.4 nM and 4.4 nM respectively (Nakayama et al., 2009). Further justification comes from previous studies demonstrating that low concentrations mimic clinical intratumoral treatment ranges of 1-9 nM, due to the way paclitaxel builds up in cells while showing low concentrations in the plasma (Zasadil et al., 2014).

Unfortunately, it seems that the 30 nM range results in residual highly proliferative CSC subpopulation of MDA-MB-231 cells (Jeong et al., 2016). This suggests that while effective, either combinational therapy or much higher doses is necessary for this triple negative cell line, they do not develop full resistance to doxorubicin. These cells develop a resistance to dasatinib (Jeong et al., 2016), highlighting that drugs share drug resistance pathways. Some through the expression of the same EMT and CSC promoting genes, which were also found to be overexpressed in this same study. Some of these were Proto-oncogene tyrosine-protein

kinase Src (c-Src), tyrosine-protein kinase Met (c-Met), Notch 1, c-Myc, Sox2, Oct3/4, Nanog, and E-cadherin (Jeong et al., 2016). Indeed, the activation of these pathways is also cell context dependent due to the heterogeneous nature of tumours. One likely unique target for MDA-MB-231 has been identified as Mammalian-enabled protein (MENA) and MENA invasive (MENAINV) (Oudin et al., 2017), this protein has a resistance mechanism independent of drug efflux or MENA-α5 interaction and in some way related to increased MAPK signaling (Oudin et al 2017). We can attempt to draw a link between this key driver protein of breast cancer metastasis that upregulated in many cancers (Gerler et al 2011), and as our lab's previous work highlighting paclitaxel resistance is due to downregulation of EP300 by the miR-106b$\sim$25 cluster (Hu et al 2015). The link might be the effect of EP300 directly on MENA expression or through acetylation of its promoter sequences.

Our lab's previous work highlights that MDR in MTMECs, including pactliaxel is a result of EP300 downregulation and avoidance of apoptosis (Hu et al., 2015). It would also be interesting to explore the apoptosis related genes such as BAD/BAX/BCL2 in relation to EP300 overexpression and in context of triple negative paclitaxel resistance. Also, how these relate to the NF-κB pathway, which was found to be upregulated in the 10 nM paclitaxel resistant MDA-MB-231 cell line (Calaf et al., 2018). The same study showed that apoptosis was only initiated at 8.6% in this cell line, as well as no PARP activation (Calaf et al., 2018), which is a target of caspase protease activity.

The results in **Figure 6.1b** show that EP300 overexpression resensitises the cells to doxorubicin, as the control sample has much better survival these concentrations than when EP300 is overexpressed, likely due to activation of proapoptotic pathways, reactive oxygen species damage and cell cycle checkpoints. The concentration at which doxorubicin becomes effective seems to be within 300-500 nM, that is around the concentration in a report concluded by Lovitt et al. (2018), between 0.5 and 2 μM, while another cited 1μM (Pilco-Ferreto et al., 2016). Therefore, we could assume that the lack of EP300 in mesenchymal cells does yield some survival benefits, which are abrogated upon its overexpression. We can attempt to confirm this using other mesenchymal cell lines such as CAL51, as well as attempting to target the EP300 bromodomain directly to see whether its acetylation activity is what is responsible for this survival. If proven, this could reverse doxorubicin resistance using acetylation. A study highlighted that acetylation plays a large role in doxorubicin resistance of MDA-MB-231, whereby high expression of H2B Clustered Histone 12 (HIST1H2BK) was targeted with and HDAC inhibitor suberoylanilide hydroxamic acid (SAHA), resensitising the cells to doxorubicin (Han et al., 2019). The expression of this HIST1H2BK is correlated with histone modification genes and leads to the overexpression of ABCB1 and ATP Binding Cassette Subfamily A Member 8 (ABCA8) which his an antiapoptotic gene, as well as

IL-6, Colony Stimulating Factor 2 (CSF2), and CXCR4 (Han et al., 2019). The activity and expression of these genes should be checked upon experimental overexpression of EP300. Alternatively, we have recently shown in our publication that the overexpression of Ep300 in Hs578T cells results in regulation of aldo keto reductases AKR1C1, AKR1C2 and AKR1C3 (Mahmud et al., 2019). These have been shown to reduce dexorobucin to a less toxic doxorubicinol form (Zeng et al., 2017, Hofman et al., 2014).

The doxorubicin resistance is likely due to expression of ABCB1, which has been shown to be responsible for poor nuclear translocation of doxorubicin in MDA-MB-231, the effects of which were reversed by MiR-298 (Bao et al., 2012). Besides ABC transporters and resistance in this cell line have been shown to be controlled by STAT 3, NOTCH1, and β-catenin genes (Alkaraki et al., 2020). There is also a link with CSC characteristics through upregulation of CD24, CD44, Integrin Subunit Alpha 6 (ITGA6), Integrin Subunit Beta 1 (ITGB1), POU Class 5 Homeobox 1 (POU5F1), NANOG, Aldehyde dehydrogenase 1 family, member A1 (ALDH1A1) (Pirsko et al., 2019). The secondary resistance mechanism is through the suppression of apoptotic initiators and upregulation of antiapoptotic proteins. There is demonstrated evidence that B-cell lymphoma-extra large (BCL-XL) and BCL2 are upregulated in MDA-MB-231 upon doxorubicin resistance (Lovitt et al., 2018). Paradoxically, another study found the same proteins to be downregulated (Pilco-Ferreto et al., 2016). Other apoptosis initiators such as caspase 3 (CASP3), caspase 8 (CASP8) and caspase 9 (CASP9) are also downregulated, which also followed higher hydrogen peroxide (H_2O_2) and Superoxide Dismutase 2 (SOD2) expression coupled with a decrease in NF-κB prevented reactive oxygen species damage (Pilco-Ferreto et al., 2016).

Effects of doxorubicin resistance seem to be influenced by the ECM environment. MDA-MB-231 cells grown in 3D environments and treated with 10 μM doxorubicin displayed disturbance of 3D architecture, a vital component which is thought to be β1 integrin (Lovitt et al., 2018). Giving credence to this idea, another scaffolding protein neuroblast differentiation-associated protein (AHNAK), was also found to contribute to this resistance in MDA-MB-231 by modulation of cleaved caspase 7, cell cycle arrest, while its overexpression decreased cleaved caspase 7 and cleaved PARP levels and induced S-phase arrest (Davis et al., 2018). This establishes a link between the ECM and apoptosis signalling. Further control of apoptosis in MDA-MB-231 is seen with the upregulation of HS-1-associated protein X-1 (HAX1), which induced the release of cytochrome c from mitochondria, resulting in the activation of caspases. Its knockdown sensitizes the cell to cisplatin and doxorubicin. (Yang et al., 2016)

The starting point for choosing the concentration for this cell line was our own earlier experiments with MCF7 cell lines, where doxorubicin resistance was tested at 30 nM

(Assaduzaman et al., 2017). Other studies showed that the IC50 concentration for the T47D cell line was 4.5 nM, while growth arrest was achieved at 100 nM (Nakayama et al., 2009). **Figure 6.2** show some potential for targeting EP300 in epithelial cell lines, as T47D survival decreases with EP300 knockdown under paclitaxel treatments. Because survival for both vectors shEP300 I/II seems to plateau at around 50 nM, we should expand on the concentration range of 10-50 nM, which was previously reported. The effects of paclitaxel resistance on T47D cell lines can in some ways be estimated through studies on MCF7 as they are from the same luminal A subtype. In fact their shared expression of ER-α, could be what represses paclitaxel induced apoptosis in these cell lines (Sui et al., 2007). As an example, treating the MCF7 cell line with paclitaxel can induce apoptosis in 85.5% of the cell population (Calaf et al., 2018). Due to their shared molecular signature, this could also potentially be the case with the T47D cell line. Some known effectors of T47D paclitaxel resistance are the tau protein, a microtubule protein involved in the cytoskeleton, which is expressed at high endogenous levels in this cell line (Rouzier et al., 2005). Another source of drug resitance in these cell lines could be aldo keto reductases AKR1C1, AKR1C2 and AKR1C3. Based on our own work as well, while EP300 has a link to drug resistance through aldo keto reductases (Mahmud et al., 2019). There are however no studies showing a link betwen paclitaxeland aldo keto reductase, except AKR1C1 which confers resistance to non substrates like cisplatin (Chen et al., 2013).

6.2.5 Future Potential Work

Short-term sensitivity should be followed up on, more concentration ranges between 12-20 nM should be used in paclitaxel to establish the IC50 for MDA-MB-231. After, we can repeat experiments with other mesenchymal cell lines such as CAL51. For doxorubicin, we should do the same but within the 300-1000 nM range. Once both IC50s are established, we can focus on using inhibitors of EP300 and CDH1, their active domains in particular. This would determine two things: if the effect is coming from EP300s modulation of CDH1, or if it is these two proteins' activity rather than their expression, which affects drug resistance. Furthermore, It would be beneficial to explore other common drugs to test such as 4 fluorouracil, cisplatin, perhaps even use TKIs or orthovanadate to check if tyrosine kinase pathways or phosphatase pathways are affected.

For long-term resistance, the study would benefit from using inhibitors of EP300 and CDH1 such as Y08197 (Zou et al., 2019). Furthermore, it would be worth checking which pathway is affecting this resistance by attempting to block ESR1 or PI3K. It would also be interesting to conduct western blotting experiments to see if our EP300 overexpression

has any effect on KRAS, Myc, P53 or proto-oncogene B-Raf (BRAF), which are known undruggable driver mutations of drug resistance.

Further explanation could also try WB and RTqPCR, alternatively, RNA-seq experiments for investigating expression levels of the following genes: ABCB1, ATP-binding cassette sub-family A member 9 (ABCA9), IL6, Colony Stimulating Factor 2 (CSF2), CXCR2, AHNAK, β1 integrin and HS-1-associated protein X-1 (HAX1). If ABC transporters are upregulated, we could check for Signal transducer and activator of transcription 3 (STAT3), Notch-1 and β-catenin. We could also check for components of the apoptotic pathway such as: BCL-XL and BCL2, caspase 3, 7, 8, 9, superoxide dismutase 2 (SOD2) and ($H2O_2$) levels. The presence and potential for CSCs should also be evaluated as these drug resistance traits are usually co expressed, therefore, expression levels of CD24, CD44, integrin Subunit α 6 (ITGA6), ITGB1, POU5F1, NANOG, ALDH1A1 should be assessed.

Furthermore, it would be beneficial to use RTqPCR and western blots to check for TWIST, which is known to contribute towards chemoresistance through the NF-κB pathway (Pham et al., 2007). Other potential targets could be GSTP1 and p53, which are genes involved in multi drug resistance (Gao et al., 2013).

Another novel target would be the prostate apoptosis response-4 (PAR-4), a pro apoptotic tumour suppressor protein. As its role has been recently identified in the inhibition of DNA damage induced apoptosis through preventing activation of caspase 8, a key regulator of the pathway in triple negative breast cancer (Guo et al., 2019), it is frequently downregulated in breast cancer (Satherley et al., 2016). In particular, it is downregulated in triple negative cancer and associated with poor outcome (Alvarez et al., 2013). Additionally, it is a known effector molecule for thrombin, a molecule known to improve metastatic capacity of tumours (Kondo et al., 2001). Thrombin itself would be an interesting target as it is known to upregulate MMP-2 (Maragoudakis et al., 2001), VEGF receptors: Kinase Insert Domain Receptor (KDR) and Fms Related Receptor Tyrosine Kinase 1 (FLT1) (Tsopanoglou et al., 1999).

Other targets such as drug efflux transporters are also of interest. Our previous findings found that in an MTMEC model, the miR-106b 25 cluster was responsible for multi drug resistance independently of ABCB1 (Hu et al., 2015), as well as identifying AKR1C1-3, an aldo-keto reductase which activates as a response to hypermethylated E-cadherin promoter, which is responsible for drug resistance to paclitaxel and doxorubicin in a HS578T breast cancer cell model (Mahmud et al., 2019).

6.2.6 Overall Conclusion

To conclude this chapter, while the influence of EP300 on drug resistance transcription factors, acetylation of histones remains an interesting and viable target, the current findings on EP300 overexpressing MDA-MB-231 are inconclusive and need to be repeated with both paclitaxel (10-40 nM) and doxorubicin (500-1000 nM). Other drugs should also be used to expand EP300s role in MDR, combined with studies on apoptosis related genes. The T47D EP300 knockdown experiment is also inconclusive and needs repeating, likely in the concentration range of 3-5 nM.

Chapter 7

EP300 and Breast Cancer Stem Cells

7.1 Introduction

7.1.1 Cancer Stem cells

Earlier chapters covered how breast cancer is categorised based on molecular subtypes such as luminal A/B, HER2 and triple negative, which represents the heterogeneity of cancer and its challenges in treating it. Matters are further complicated with the triple negative/basal subtype which has recently been identified to be heterogeneous within its own subtype based on the transcriptome: luminal androgen receptor, immunomodulatory, basal like immune suppressed and mesenchymal-like (Jiang et al., 2019).

This leads us to two distinct hypothesis on the origins of this heterogeneity. The first theory is the clonal evolution theory by which the heterogeneity in cells is a result of a mutation (Greaves et al., 2012). The second is the CSC model (Vermeulen et al., 2008), which places these pluripotent cell types as the origin of the heterogeneity, and maintain self-renewal properties and maintain the diverse population of heterogeneous cell types in tumours. As mentioned earlier in **Chapter 6**, they are postulated to be the origin of chemoresistance in breast cancer (Liu et al., 2010).

7.1.2 Molecular Markers of CSCs

The discovery of the CSC population has led to the expanding knowledge regarding markers for their identification. Many breast CSC markers are available such as: CD24, CD44, CD47, CD133, Activated Leukocyte Cell Adhesion Molecule (CD166), ALDH1, EpCAM and ABCG2 to name a few (Liu et al., 2013). $CD44^{high}/CD24^{low}$ (Shipitsin et al., 2007) and ALDH+ (Ginestier et al., 2007) are the two molecular markers which are most

commonly used. Early Investigations of cancer subtypes found that $CD44^{high}$ cells were more prevalent in the primary tumour, while CD24+ were seen more on distal metastasis sites (Bloushtain-Qimron et al., 2008; Shipitsin et al., 2007). This shows that the tumor's heterogeneous nature could be somehow due to expression of these markers. We will outline the three that were used in these experiments.

CD44 is a class I transmembrane glycoprotein (Naor et al., 2008). It is a receptor for hyaluronic acid and promotes migration (Ponta et al., 2003), while also maintaining other functions such as cell growth, proliferation, adhesion, angiogenesis, differentiation, motility and invasion, through its association with proteins (Naor et al.,2008). Other functions include presenting cytokines to transmembrane receptors and being involved in signalling cascades initiated from the cell membrane (Naor et al., 2008; Bourguignon et al., 2001).

CD24 is a cell surface protein molecule which is held in place with a glycosyl phosphatidylinositol, and involved in interactions with ECM (Kristiansen et al., 2003). Due to its glycosylated nature it acts as a ligand in a variety of processes (Fang et al., 2010). Shifting from DCIS to IDC results in membrane bound CD24 and is associated with poorer prognosis (Mylona et al., 2008), its overexpression also leads to motility and invasion (Baumann et al., 2005).

ALDH is a superfamily of enzymes involved in detoxification of aldehydes, as well as biosynthesis of retinoic acid. Apart from being a stem cell marker, this enzyme can regulate CSC properties such as self-renewal, clonal expansion, drug resistance and radio resistance (Vassalli, 2019).

7.1.3 Marker Expression in Breast Cancer

The expression pattern of these markers is complex and seems to represent two distinct CSC populations (Ginestier et al., 2007). This seems to be related to the two different EMT/MET states exhibited by CSCs (Pinto et al., 2013). The EMT phenotype expresses the $CD44^{high}/CD24^{low}$ and EpCAM+ markers, while MET promotes ALDH+ expression (Liu et al., 2013). As described earlier, cells can also exist in a transient EMT state, which further proves that these cells shift between these states. The switch is regulated through cytokine signalling (Stankic et al., 2013).

Cell Type Context Expression

However, as previously mentioned, the variety of markers exist and is likely cells are influenced by different cell types in which they are discovered as well as the microenvironment. Mouse studies of different mutations showed different CSC marker expressions. BRCA1

deficient mice exhibited CD133+ and $CD44^{high}/CD24^{low}$ (Wright et al., 2008), which has been shown to increase metastatic potential in another study (Vassipoulos et al., 2014). Wnt Family Member 1 (MMTV-WNT1) and p53 mutations showed expression of CD90 and Integrin Subunit Beta 3 (CD61) (Cho et al., 2008; Vaillant et al., 2008).

Expression of the CD44 and CD24 markers seems to vary even between cell lines in the same subtype, which causes difficulty using these as exclusive CSC markers (Stuelten et al., 2010). Cell type context-dependant expression of these markers is also demonstrated in various studies. MCF7 cells showed a preference for mucin 1 (MUC1) (Engelmann et al., 2008). A study analysing some of the more common cell lines showed that $CD44^{high}/CD24^{low}$ and ALDH+ expression is not universal. The flotillin 2 (FLOT2) marker is reported to be highly expressed and therefore more highly suited for MDA-MB-231, MCF7 and T47D cell lines. This is due to the variation in $CD44^{high}/CD24^{low}$ expression between these cell lines, as epithelial tend to be $CD44^{high}/CD24^{high}$ (Hwang-Verslues et al 2009). However, studies still rely on the classical markers such as $CD44^{high}/CD24^{low}$ to validate new markers like anthrax toxin receptor 1 (ANTXR1) or ABCG2 (Leccia et al., 2014; Chen et al., 2013).

Cancer Subtype Context Expression

Cell type context expression is also observed in breast cancer subtypes. The CSC population is proportionately higher in triple negative breast cancer and HER2-enriched, when comparing its luminal A/B counterparts (Brooks et al., 2015). This shows two distinct subpopulations of cloudin low and basal-like triple negative cancer, characterised by a high presence of $CD44^{high}/CD24^{low}$ and ALDH+ cells respectively (Brooks et al., 2015). The expression of both markers is shown to be the most aggressive with more tumorigenic potential (Liu et al., 2018). The same study also identified markers associated with CSC prognosis: Prolyl 4-hydroxylase subunit alpha-2 (P4HA2), prostaglandin reductase 1 (PTGR1) and Member RAS Oncogene Family (RAB40B). Furthermore, another study identified another marker, Receptor Tyrosine Kinase Like Orphan Receptor 1 (ROR1), highly associated with this phenotype (Zhang et al., 2019).

As mentioned $CD44^{high}/CD24^{low}$ are overexpressed in MDA-MB-231 and CAL-51 (Li et al., 2017; Yu et al., 2016; Samantha et al., 2014; Sheridan et al., 2006). Other subpopulations exist with this marker, which is also dependent on cancer subtypes, for example: luminal A cancers and the archetypal cell line MCF7 express $CD44^{low}/CD24^{high}$ (Li et al., 2017). Luminal A cancers are also more likely to express ALDH, and the coexpression of $CD44^{high}/CD24^{low}$ along with ALDH is more commonly seen in basal or HER2 subtypes (Park et al., 2010). HER2 amplification is one of those markers which directly impacts ALDH expression, which is why ALDH expression is frequently elevated in HER2 sub-

types (Korkaya et al., 2008). Another subpopulation, $CD44^{high}/CD24^{high}$ is considered to be non-tumorigenic or less than $CD44^{low}/CD24^{high}$ populations (Li et al., 2017). While $CD44^{high}/CD24^{low}$ might be indicative of CSCs, there is a degree of heterogeneity within this phenotype.

Gene Expression Influence on Marker Expression

Other gene expression influence is seen with GATA3, which is responsible for lumen cell differentiation and is frequently seen downregulated in $CD44^{high}$ versus $CD24^{high}$ side populations (Park et al., 2010; Kouros-Mehr et al., 2006). Shifting from DCIS to Invasive ductal carcinoma (IDC) results in membrane bound CD24, and is associated with poorer prognosis (Mylona et al., 2008; Kristiansen et al., 2003). Its overexpression leads to motility and invasion (Baumann et al., 2008). The same study found vimentin and GATA3, two of the genes we studied in **Chapter 4**, as well as Endothelial protein C receptor (EPCR). It revealed that vimentin was more expressed in basal like, while GATA3 was important for luminal epithelial cell differentiation (Kouros-Mehr et al., 2006), and its expression might explain why $CD24^{high}$ cells are in more differentiated tumours while $CD44^{high}$ are more stem cell side population.

Influence of miRs on CSCs

Part of the regulation of CSCs is the epigenetic influence of miRs. A large proportion of this regulation comes from the miR-200 family, such as miR-200c reducing the clonal population of breast cancer stem cells through its suppression of B lymphoma Mo-MLV insertion region 1 homolog (BMI1), a protooncogene (Shimono et al., 2009). BMI1 is important as its expression not only correlates with poor survival and a basal phenotype (Wang et al., 2012), but also promotes self-renewal of CSCs, and contributes to drug resistance through upregulation of ABC transporters (Paranjape et al., 2014; Wu et al., 2011).

MiR-200c is also responsible for the promotion of tumour heterogeneity and the EMT phenotype, which it activates through Homeodomain Interacting Protein Kinase 1 (HIPK1)/β-catenin signalling (Liu et al., 2018). The self-renewal properties of CSCs are also influenced by let-7 and miR-600 (Yu et al., 2010; Yu et al., 2007). Let-7 silences H-Ras and High Mobility Group AT-Hook 2 (HMGA2), while miR-600 targets UBC9 and ITGβ3, while simultaneously functioning as a switch for self-renewal and differentiation in CSCs through the WNT pathway (El Halou et al., 2017; Yu et al., 2010; Yu et al., 2007). Other aspects of such growth are targeted through the miR-200b-SUZ12-cadherin pathways (Iliopoulos et al., 2010).

Tumour Microenvironment Influence on CSCs

As discussed in previous sections, the tumour microenvironment is a complex network of mesenchymal cells, cancer associated fibroblasts, adipocytes, epithelial cells and immune cells, which communicate with each other either through physical interactions and responding to changes in the ECM components. They are responsible for paracrine and autocrine signalling with cytokines, growth factors and hypoxia inducing factors. Mesenchymal stem cells (MSCs) can promote the CSC population by IL-6 and CXCL7 signalling (Liu et al., 2011) and also represses FOXP2 by way of miR-199a binding to FOXP2 regulating the propagation traits (Cuiffo et al., 2014). Cancer associated fibroblasts (CAFs) are in a synergistic relationship with CSCs and they regulate each other. CAFs can release IL-6, IL-8 and C-C Motif Chemokine Ligand 2 (CCL2) (Tsuyada et al., 2012; Korkaya et al., 2011). Their release of High Mobility Group Box 1 (HMGB1) also promotes the CSC population and upregulates the markers previously discussed (Zhao et al., 2017). The regulation of CAFs is carefully controlled by CSCs through the hedgehog pathway (Valenti et al., 2017). CSCs also attract the tumour associated macrophages (TAMs) by secreting Macrophage Colony Stimulating Factor (M-CSF), these cells then promote the CSC population by inducing hypoxia and activating TGF-β (Plaks et al., 2015). They also maintain the population by their EGFR/STAT3/SOX2 signalling (Yang et al., 2013).

Tumour Heterogeneity and Invasive Capabilities

Firstly, not all $CD44^{high}/CD24^{low}$ cells are radioresistant (Zielske et al., 2011), and not all are CSCs, as earlier studies indicated very little correlation with event free and overall survival (Shipitsin et al., 2007; Abraham et al., 2005). This heterogeneity might be explained by the presence or absence of other CSC markers. Nevertheless, when comparing SEM images of all the possible CD44 and CD24 expression patterns, $CD44^{high}/CD24^{low}$ is indicative of higher migration and invasion capacity, as cells expressing this marker have more pseudopodia and microvilli. This is also seen in $CD44^{high}/CD24^{high}$, albeit in a lesser capacity (Yan et al., 2013). The other two combinations: $CD44^{low}/CD24^{low}$ and $CD44^{low}/CD24^{high}$ showed the smoothest cell structure with little or none protrusions, which indicates a reduced capacity to migrate (Yan et al., 2013). The presence of these different combinations is indicative of the variable EMT state ($CD44^{high}/CD24^{low}$ or $CD44^{high}/CD24^{high}$), the control over which seems to be determined by the expression of SNAI2 and TNF-α (Bhat-Nakshatri et al., 2010).

Therapeutic Targets for CSCs

PARP inhibitors have shown good efficacy against triple negative breast cancer tumours, drastically lowering the $CD44^{high}/CD24^{low}$ population (Shimo et al., 2014). However, in some cases there are residual resistant BRCA1 mutant populations (Liu et al., 2017). The demonstrated evidence proves there is clinical benefit to using PIK3 and EGFR inhibitors shows that CSCs are not only involved in the hallmark traits of cancer (Bendell et al., 2012; Carey et al., 2012) but also the targeting of EP300 might be a viable alternative due to the EGFR/NOTCH/PI3k/MAPK pathways. There is also a difference seen between subtypes. While a large portion of CSCs can be inhibited through AR-targeted and HIF-1α-targeted therapy (Barton et al., 2017; Samantha et al., 2014), luminal cancers seem to benefit more from CCND1, CDK4, CDK6 or mTOR inhibitors (Finn et al., 2009; Zhou et al., 2007).

We previously covered the importance of WNT, Notch and hedgehog pathways in CSCs. Next, we will briefly mention that they are also useful targets for therapy. In breast cancer, WNT target genes are activated by the nuclear translocation of β-catenin. These genes were found to be downregulated and suppressed once the WNT heterodimer receptor was targeted in triple negative breast cancer (King et al., 2012). A similar matter is being investigated with hedgehog target genes. Smoothened, Frizzled Class Receptor (SMO) is a regulator of GLI that activates these genes and overexpressed in the breast $CD44^{high}/CD24^{low}$ CSC population, which makes it a viable target (Cazet et al 2018). A direct effect on these hedgehog genes was already demonstrated by inhibiting GLI1 and GLI2 in triple negative breast cancer (Koike et al., 2017). Finally, the Notch pathway is known to contribute to brain metastasis of breast cancer through its notch receptor/ligand activated translocation of NCID (McGowan et al., 2011).

How EP300 Affects Stem Cells

It is likely that through the acetylation of histones, EP300 influences gene expression and expression of miRs, that activate pathways which will either promote EMT/MET shift, therefore influencing the cytoplasmic/membrane bound receptors such as CD44, CD24, and ALDH. A direct link is yet to be determined as to whether EP300 influences this directly or it is merely a consequence of the gene expression landscape. As CSCs and drug resistance are so intertwined (covered in the previous **Chapter 6**), it is a logical progression to check whether these traits would be affected as they are one of the challenges of therapy.

7.2 Analysis of EP300 on Breast Cancer Stem Cells

7.2.1 Hypothesis

The hypothesis is based on previous studies that show markers like $CD44^{high}/CD24^{low}$ and ALDH1 have been used to determine the presence of breast cancer stem cell populations (). These markers are not only important in identifying these traits but also the manifestation of these traits and promotion of others like EMT and drug resistance. The hypothesis is that as EP300 is an acetyltransferase responsible for modification of transcription events. Its overexpression should induce an overexpression in CDH1, as we have shown in our RTqPCR results in **Chapter 4**. This expression of CDH1 should promote a more epithelial phenotype. This would result in less CSC subpopulations and presence of ALDH+ and $CD44^{high}/CD24^{low}$ markers. The reverse is expected to happen in epithelial cell lines like MCF7 and T47D. Where we hypothesise the downregulation of EP300 would induce a downregulation in CDH1, thereby inducing an EMT phenotype and with it more subpopulations of CSCs exhibiting markers such as ALDH+ and $CCD44^{high}/CD24^{low}$.

7.2.2 Aim

1. Demonstrate a correlation between EP300 and CDH1 overexpression and $CD44^{high}/CD24^{low}$ status
    - Test effect of EP300 and CDH1 overexpression on $CD44^{high}/CD24^{low}$ populations in mesenchymal breast cancer cell lines: CAL51 and MDA-MB-231
    - Test effect of EP300 knockout on $CD44^{high}/CD24^{low}$ populations in colorectal cancer cell lines: HCT116
    - Test effect of EP300 knockdown on $CD44^{high}/CD24^{low}$ populations in mesenchymal breast cancer cell lines: MCF7 and T47D
2. Use a secondary marker ALDH to demonstrate the same correlation
    - Test effect of EP300 and CDH1 overexpression on ALDH+ populations in mesenchymal breast cancer cell lines: CAL51 and MDA-MB-231
    - Test effect of EP300 knockout on ALDH+ populations in colorectal cancer cell lines: HCT116
    - Test effect of EP300 knockdown on ALDH+ populations in mesenchymal breast cancer cell lines: MCF7 and T47D

3. Observe the effect of drug resistance on these markers to link drug resistance with breast cancer stem cells.

    - Test effect of paclitaxel resistance on ALDH+ populations in epithelial breast cancer cell lines: MCF7
    - Test effect of doxorubicin resistance on ALDH+ populations in epithelial breast cancer cell lines: MCF7
    - Test effect of paclitaxel resistance on $CD44^{high}/CD24^{low}$ populations in epithelial breast cancer cell lines: MCF7
    - Test effect of doxorubicin resistance on $CD44^{high}/CD24^{low}$ populations in epithelial breast cancer cell lines: MCF7

7.2.3 Results

Overexpression of EP300 and CDH1 downregulates ALDH+ cell populations in mesenchymal breast cancer cell lines.

In this experiment, we used our previously established breast cell line models from **Chapter 4**: CAL51 and MDA-MB-231. Which have 3 conditions: a control empty vector, an EP300 overexpression and a CDH1 overexpression. These cells were exposed to ALDH+ substrate for 45 minutes and separated into two aliquots: a positive control for presence of ALDH+ populations (without inhibitor) and a negative control with the presence of diethylamiobenzadeyde (DEAB) ALDH specific inhibitor. The cells were then run through a BD™ LSR II flow cytometer to determine the cell population percentages, and were then analysed on FlowJo software and represented in the figures below.

Figure 7.1a shows a panel demonstrating the percentage of cells testing positive for the ALDH marker of stemness. In this panel, we have the mesenchymal breast cancer cell line CAL51 with 3 conditions: a control empty vector, an EP300 overexpression and a CDH1 overexpression. Each condition was treated in the presence of DEAB inhibitor and without, the positive control (without inhibitor) shows the accurate ALDH+ breast cancer cell population.

The same data is represented in a bar chart in **Figure 7.1b** showing that under normal conditions (control), the percentage of ALDH+ cells is 2.5%. With EP300 overexpression, this decreases to 1.36% ($p<0.001$) and with CDH1 overexpression, this decreases to 1.6% ($p<0.001$). There are 0.2% less ALDH+ cells with EP300 overexpression ($p<0.05$), when comparing EP300 to CDH1 overexpression.

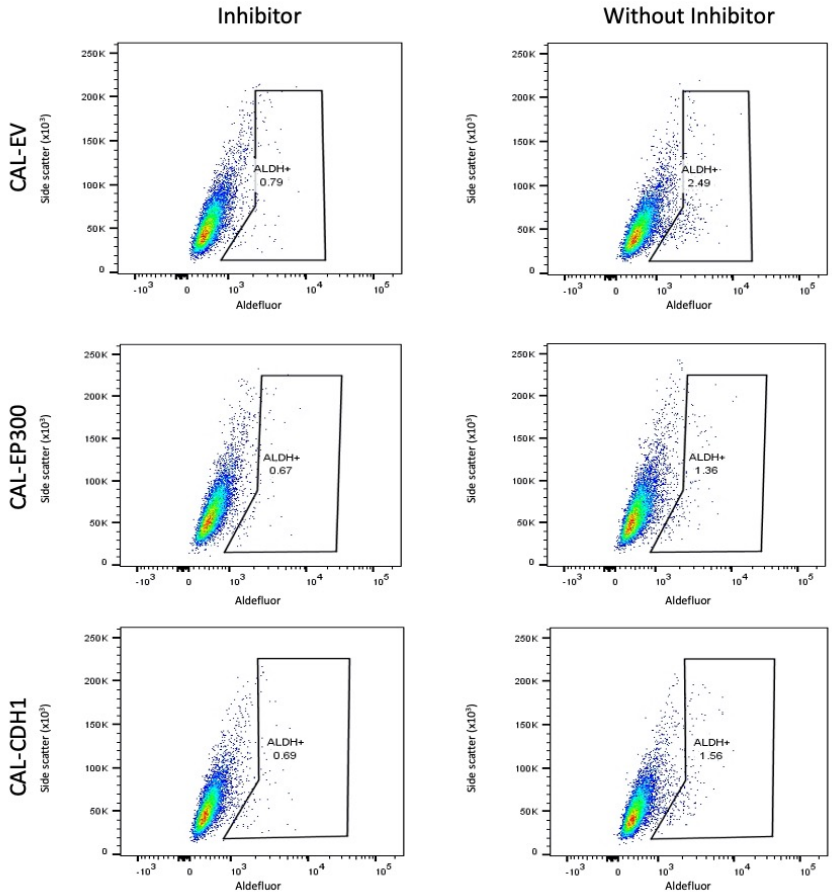
Inhibitor
Without Inhibitor
CAL-EV
CAL-EP300
CAL-CDH1
Side scatter (x10³)
Aldefluor
ALDH+
0.79
ALDH+
2.49
ALDH+
0.67
ALDH+
1.36
ALDH+
0.69
ALDH+
1.56

(a)

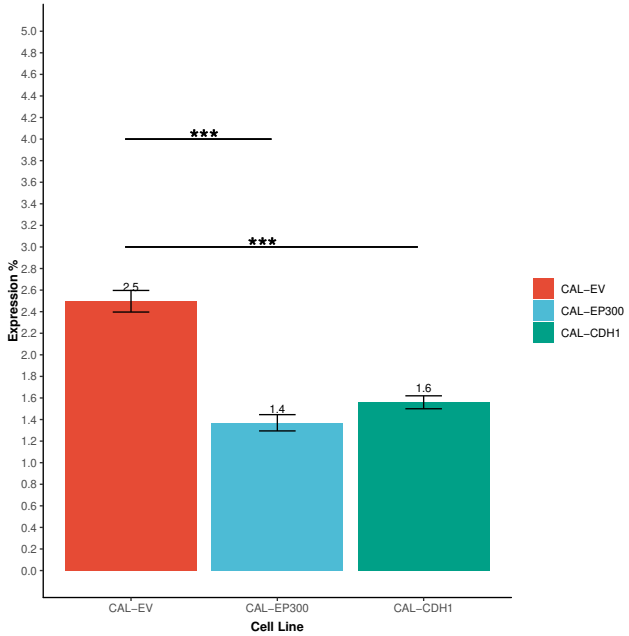

(b)

Fig. 7.1 Overexpression of EP300 decreases the ALDH+ cell population. (A) A selected representation of the flow cytometry plot for CAL51 cells with stable overexpression of EP300 (CAL-EP300) and CDH1 (CAL-CDH1). Cells were assessed for ALDH expression by flow cytometry using treatments of aldefluour agent on its own, and with the presence of ALDH inhibitor(DEAB). The figure is separated into cells without DEAB (top left) and (B) A bar chart representing the mean + SD of the % ALDH+ populations, representing 3 independent experiments (n=3). Statistical analysis was performed using one-way ANOVA, comparing control (CAL-empty vector), to EP300 overexpressing (CAL-EP300) and CDH1 overexpressing (CAL-CDH1) transfected cells. (**P$\leq$0.01, ***P$\leq$0.001).

Figure 7.2a shows a panel demonstrating the percentage of cells testing positive for the ALDH marker of stemness. In this panel, we have the mesenchymal breast cancer cell line MDA-MB-231 with 3 conditions: a control empty vector, an EP300 overexpression and a CDH1 overexpression. Each condition was with or without DEAB inhibitor, the positive control (without inhibitor) shows the accurate ALDH+ breast cancer cell population. The same data is represented in a bar chart in **Figure 7.2b**, which shows that under normal conditions (control), the percentage of ALDH+ cells is 2.7%. With EP300 overexpression, this decreases to 1.4% ($p<0.001$) and with CDH1 overexpression, this decreases to 1.5% ($p<0.001$). There are 0.1% less ALDH+ cells with EP300 overexpression ($p<0.05$) when comparing EP300 to CDH1 overexpression.

To summarise, the effect on mesenchymal cells such as CAL51 and MDA-MB-231 seems to be that ALDH+ subpopulations decrease with the overexpression of EP300 CDH1. Which provides evidence for our protein to be a regulator of CSC traits.

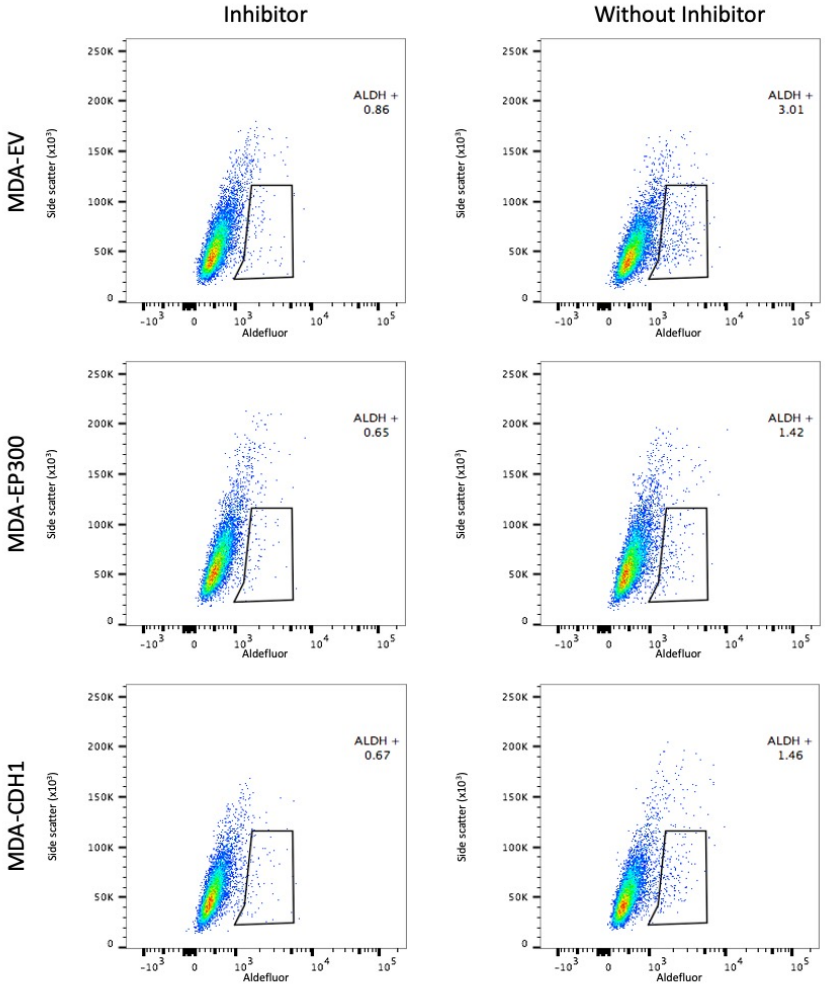
Inhibitor
Without Inhibitor
MDA-EV
MDA-EP300
MDA-CDH1
ALDH +
0.86
ALDH +
3.01
ALDH +
0.65
ALDH +
1.42
ALDH +
0.67
ALDH +
1.46
Side scatter (x10³)
Aldefluor

(a)

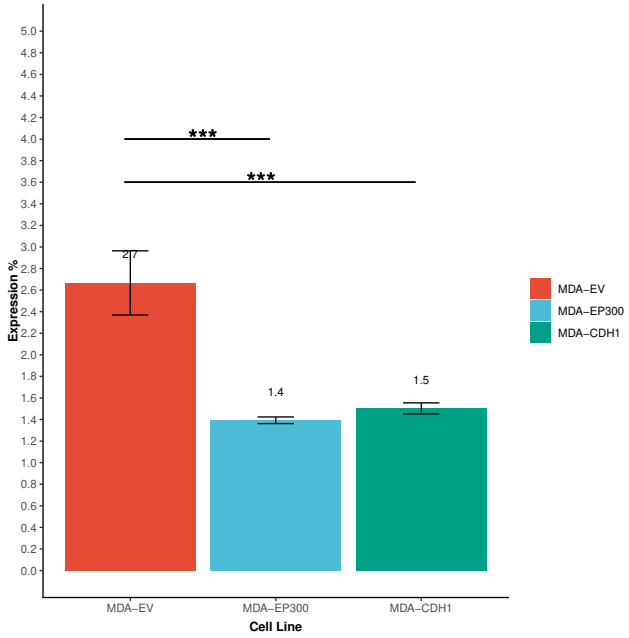

(b)

Fig. 7.2 Overexpression of EP300 decreases the ALDH+ cell population. (A) A selected representation of the flow cytometry plot for MDA-MB-231 cells with stable overexpression of EP300 (MDA-EP300) and CDH1 (MDA-CDH1). Cells were assessed for ALDH expression by flow cytometry using treatments of aldefluour agent on its own, and with the presence of ALDH inhibitor(DEAB). The figure is separated into cells without DEAB (top left) and (B) A bar chart representing the mean + SD of the % ALDH+ populations, representing 3 independent experiments (n=3). Statistical analysis was performed using one-way ANOVA, comparing control (MDA-empty vector), to EP300 overexpressing (MDA-EP300) and CDH1 overexpressing (MDA-CDH1) transfected cells. (**P$\leq$0.01, ***P$\leq$0.001).

ALDH+ populations are influenced by exposure to chemotherapeutic drugs

In this experiment, we used a previously established drug resistant MCF7 breast cell line from Eric Lam's group (Alasiri et al., 2019; de Moraes et al., 2015), which had 3 conditions: a control empty vector, long-term paclitaxel resistance and long-term doxorubicin resistance. These cells were exposed to ALDH+ substrate for 45 minutes, and separated into two aliquots: a positive control for presence of ALDH+ populations (without inhibitor) and a negative control with the presence of diethylamiobenzadeyde (DEAB) ALDH specific inhibitor. The cells were then run through a BD™ LSR II flow cytometer to determine the cell population percentages, which were then analysed on FlowJo software and represented in the figures below.

Figure 7.3a shows a panel demonstrating the percentage of cells testing positive for the ALDH marker of stemness. In this panel, we have the epithelial breast cancer cell line MCF7 with 3 conditions: a control empty vector, long-term paclitaxel resistance and long-term doxorubicin resistance. Each condition was treated in the presence of DEAB inhibitor and without, the positive control (without inhibitor) shows the accurate ALDH+ breast cancer cell population. The same data is represented in a bar chart in **Figure 7.3b** , which shows that under normal conditions (control) the percentage of ALDH+ cells is 1.3%. With paclitaxel resistance, this decreases to 0.9% ($p<0.001$) and with doxorubicin resistance, this increases to 4.9% ($p<0.001$). There are 4% more ALDH+ cells present in doxorubicin resistant cells ($p<0.001$) when comparing doxorubicin resistance to paclitaxel resistance. Thus chemotherapeutic drugs also influence ALDH cell populations, it can be seen that both doxorubicin and paclitaxel seem to have opposite effects on ALDH. Which might be due to the way they work on cells. Paclitaxel seems to have a better outcome for reducing CSC subpopulations expressing ALDH.

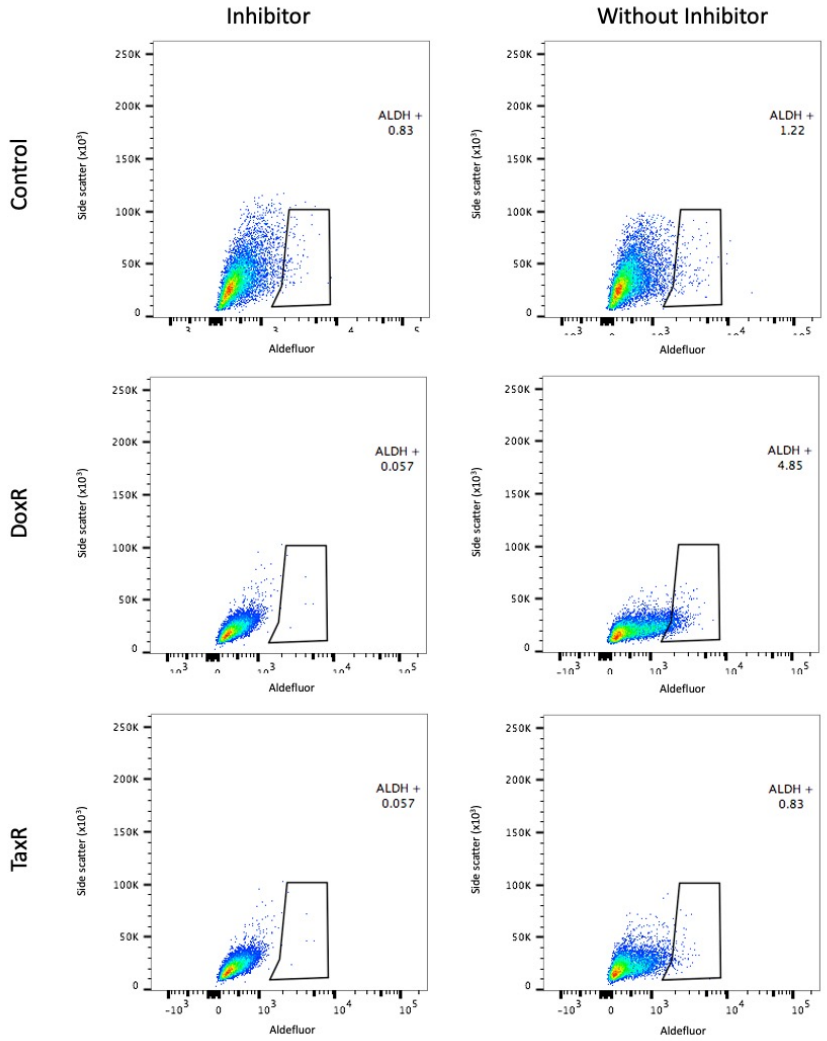
Inhibitor
Without Inhibitor
Control
DoxR
TaxR
ALDH +
0.83
ALDH +
1.22
ALDH +
0.057
ALDH +
4.85
ALDH +
0.057
ALDH +
0.83
Side scatter (x10³)
Aldefluor
250K
200K
150K
100K
50K
0

(a)

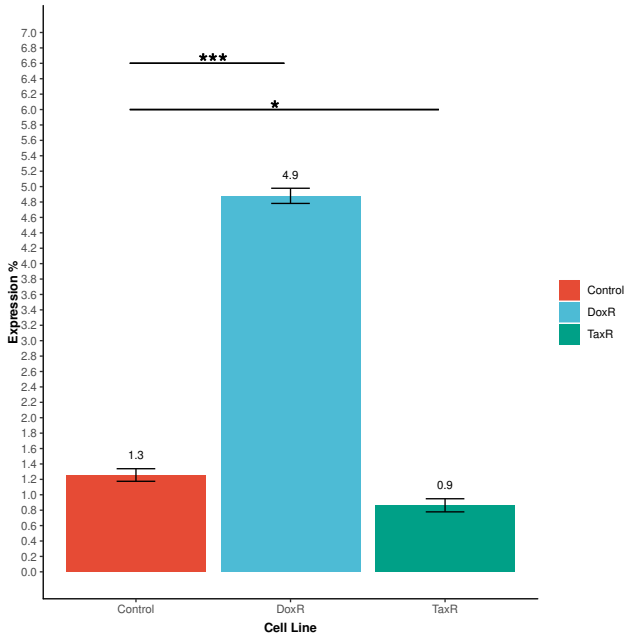

(b)

Fig. 7.3 ALDH expression in drug resistant MCF7.(A) A selected representation of the flow cytometry plot for MCF7 cells with doxorubicin resistance (DoxR) and paclitaxel resistance (TaxR). Cells were assessed for ALDH expression by flow cytometry using treatments of aldefluour agent on its own, and with the presence of ALDH inhibitor(DEAB). The figure is separated into cells without DEAB (top left) and (B) A bar chart representing the mean + SD of the % ALDH+ populations, representing 3 independent experiments (n=3). Statistical analysis was performed using one-way ANOVA, comparing control (naive wild type cells), doxorubicin resistance (DoxR) and paclitaxel resistance (TaxR). (**P$\leq$0.01, ***P$\leq$0.001).

Knockout of EP300 downregulates ALDH+ cell populations in colorectal cancer cells.

In this experiment, we used our previously established colorectal cell line model from the previous **Chapters 4**: HCT116. Which have 2 conditions: a control empty vector (HCT-EV) and EP300 knockout (HCT-KOEP300). These cells were exposed to ALDH+ substrate for 45 minutes, and separated into two aliquots: a positive control for presence of ALDH+ populations (without inhibitor) and a negative control with the presence of diethylamiobenzadeyde (DEAB) ALDH specific inhibitor. The cells were then run through a BD™ LSR II flow cytometer to determine the cell population percentages, which were then analysed on FlowJo software and represented in the figures below.

Figure 7.4a shows a panel demonstrating the percentage of cells testing positive for the ALDH marker of stemness. In this panel, we have the colorectal cancer cell line HCT116 with 2 conditions: a control empty vector (HCT-EV), an EP300 knockout (HCT-KOEP300). Each condition was treated in the presence of DEAB inhibitor and without, the positive control (without inhibitor) shows the accurate ALDH+ breast cancer cell population. The same data is represented in a bar chart in **Figure 7.4b**, which shows that under normal conditions (control), the percentage of ALDH+ cells is 67.8%. With EP300 knockout, this increases to 70.8% ($p<0.001$).

Thus our colorectal models seems to show that there is not much difference in the ALDH subpopulations with or without EP300 knockout. This is a particularity of this cell line and perhaps EP300 functions differently to our breast cancer models.

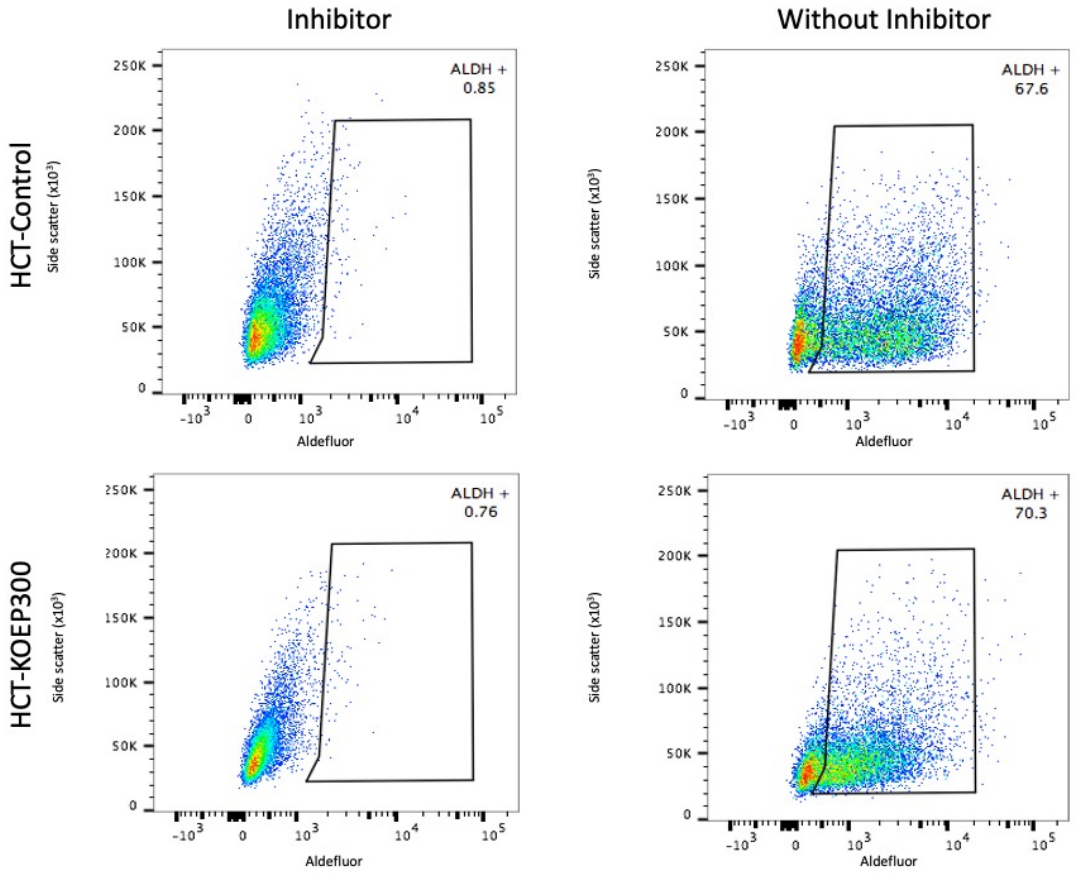
Inhibitor
Without Inhibitor
HCT-Control
HCT-KOEP300
ALDH +
0.85
ALDH +
67.6
ALDH +
0.76
ALDH +
70.3
Side scatter (x10³)
Aldefluor
250K
200K
150K
100K
50K
0
-10³
0
10³
10⁴
10⁵

(a)

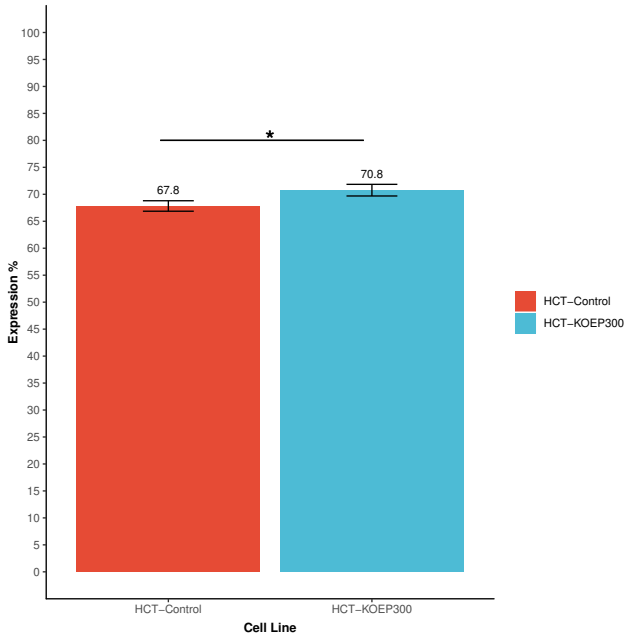

(b)

Fig. 7.4 Knockout of EP300 enriches the ALDH+ cell population. (A) A selected representation of the flow cytometry plot for HCT116 cells with knockout of EP300 (KO EP300). Cells were assessed for ALDH expression by flow cytometry using treatments of aldefluour agent on its own, and with the presence of ALDH inhibitor(DEAB). The figure is separated into cells without DEAB (top left) and (B) A bar chart representing the mean + SD of the % ALDH+ populations, representing 3 independent experiments (n=3). Statistical analysis was performed using one-way ANOVA, comparing HCT116 wild type control (HCT116-Control), to EP300 knockout cells (KO EP300). (**P$\leq$0.01, ***P$\leq$0.001).

Overexpression of EP300 and CDH1 modulates $CD44^{high}/CD24^{low}$ cell populations in mesenchymal breast cancer cell lines.

In this experiment, we used the same cell lines as for the ALDH+ experiment: CAL51 and MDA-MB-231, which have 3 conditions: a control empty vector, an EP300 overexpression and a CDH1 overexpression. These cells were exposed to anti CD44 and anti CD24 antibodies for 30 minutes, followed by Isotype APC or PE-labelled antibodies. Cells were separated into four aliquots: two positive controls for presence of a single CD44 or CD24 stain ($CD44^{high}$ and $CD24^{high}$) a negative unstained control, and a sample with both antibodies stained (Double stain). The cells were then run through a BD™ LSR II flow cytometer to determine the cell population percentages, which were then analysed on FlowJo software and represented in the figures below.

Figure 7.5a shows a panel demonstrating the percentage of cells testing positive for the $CD44^{high}/CD24^{low}$ markers of stemness. In this panel, we have the mesenchymal breast cancer cell line MDA-MB-231 with 3 conditions: a control empty vector, an EP300 overexpression and a CDH1 overexpression. Each condition was treated with a single CD44 or CD24 stain ($CD44^{high}$ and $CD24^{high}$), a negative unstained control and a sample with both antibodies stained (Double stain). The panels show the accurate $CD44^{high}/CD24^{low}$ breast cancer cell population.

The single stained sample data is represented as a bar chart in **Figure 7.5b**. The data shows that the control stained 74.3% as $CD24^{high}$ and 99.3% $CD44^{high}$. With EP300 overexpression, the staining for $CD24^{high}$ increased to 88.4% ($p<0.001$) and decreased $CD44^{high}$ staining to 99% (NS). With CDH1 overexpression, the staining for $CD24^{high}$ decreased to 38.9% ($p<0.001$) and decreased $CD44^{high}$ staining to 99% (NS). **Figure 7.5c** and **Figure 7.5d** show the double stained samples, it is split up into two panels. Both show the same data, the first panel shows all the phenotypes while the second panel focuses on the majority population.

In **Figure 7.5c**, The control did not stain $CD44^{low}/CD24^{low}$ or $CD44^{low}/CD24^{high}$, 39.5% for $CD44^{high}/CD24^{low}$ and 60.8% stained for $CD44^{high}/CD24^{high}$. With EP300 overexpression, $CD44^{low}/CD24^{low}$ and $CD44^{low}/CD24^{high}$ did not change, $CD44^{high}/CD24^{low}$ increased to 43.9% ($p<0.001$) and $CD44^{high}/CD24^{high}$ decreased to 57.1% ($p<0.001$). With CDH1 overexpression, $CD44^{low}/CD24^{low}$ and $CD44^{low}/CD24^{high}$ did not change, $CD44^{high}/CD24^{low}$ increased to 66.6% ($p<0.001$) and $CD44^{high}/CD24^{high}$ decreased to 33.4% ($p<0.001$). **Figure 7.5d** shows the majority of the population for the control sample is 60.8% $CD44^{high}/CD24^{high}$ and 39.5% $CD44^{high}/CD24^{low}$. With EP300 overexpression, this population shifts more towards the $CD44^{high}/CD24^{low}$ with an increase by 4.4% ($p<0.001$) and decreases by 3.7% ($p<0.001$) in $CD44^{high}/CD24^{high}$. With CDH1 overexpression, this population shifts

more towards the $CD44^{high}/CD24^{low}$ with an increase by 27.1% ($p<0.001$), and decreases by 27.4% ($p<0.001$) in $CD44^{high}/CD24^{high}$. When comparing both EP300 and CDH1, CDH1 overexpression has 22.7% ($p<0.001$) more population in $CD44^{high}/CD24^{low}$ and less $CD44^{high}/CD24^{high}$ by 23.7% ($p<0.001$).

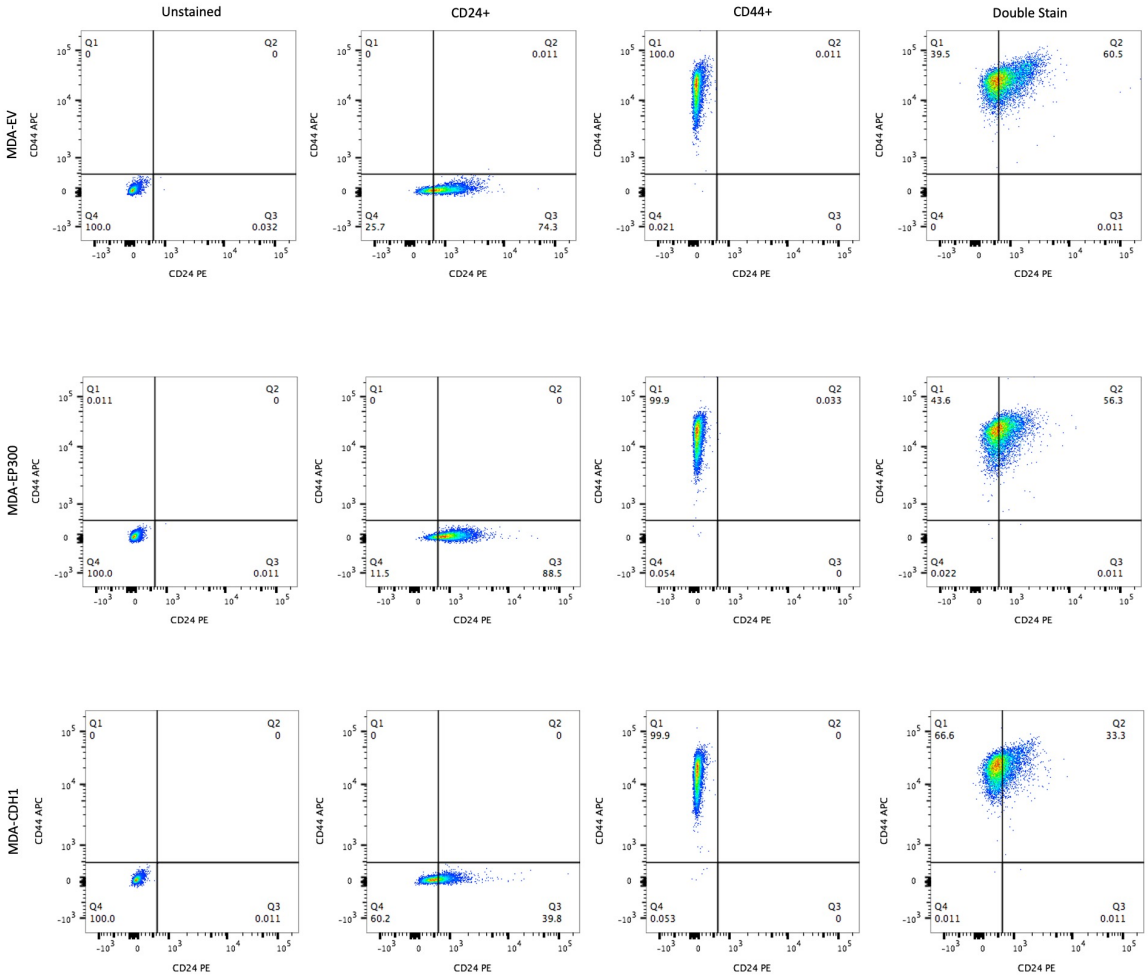
Unstained
CD24+
CD44+
Double Stain
MDA-EV
MDA-EP300
MDA-CDH1
CD44 APC
CD24 PE
Q1 0
Q2 0
Q4 100.0
Q3 0.032
Q1 0
Q2 0.011
Q4 25.7
Q3 74.3
Q1 100.0
Q2 0.011
Q4 0.021
Q3 0
Q1 39.5
Q2 60.5
Q4 0
Q3 0.011
Q1 0.011
Q2 0
Q4 100.0
Q3 0.011
Q1 0
Q2 0
Q4 11.5
Q3 88.5
Q1 99.9
Q2 0.033
Q4 0.054
Q3 0
Q1 43.6
Q2 56.3
Q4 0.022
Q3 0.011
Q1 0
Q2 0
Q4 100.0
Q3 0.011
Q1 0
Q2 0
Q4 60.2
Q3 39.8
Q1 99.9
Q2 0
Q4 0.053
Q3 0
Q1 66.6
Q2 33.3
Q4 0.011
Q3 0.011

(a)

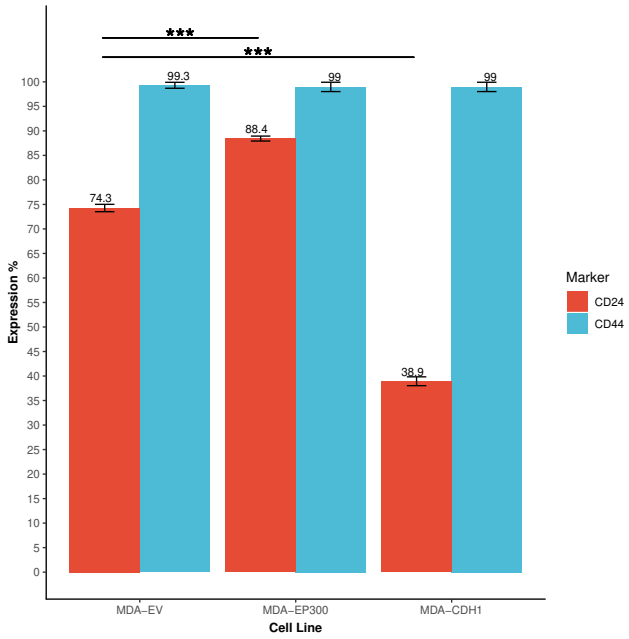
***
***
99.3
99
99
88.4
74.3
38.9
Expression %
Cell Line
MDA−EV
MDA−EP300
MDA−CDH1
Marker
CD24
CD44

(b)

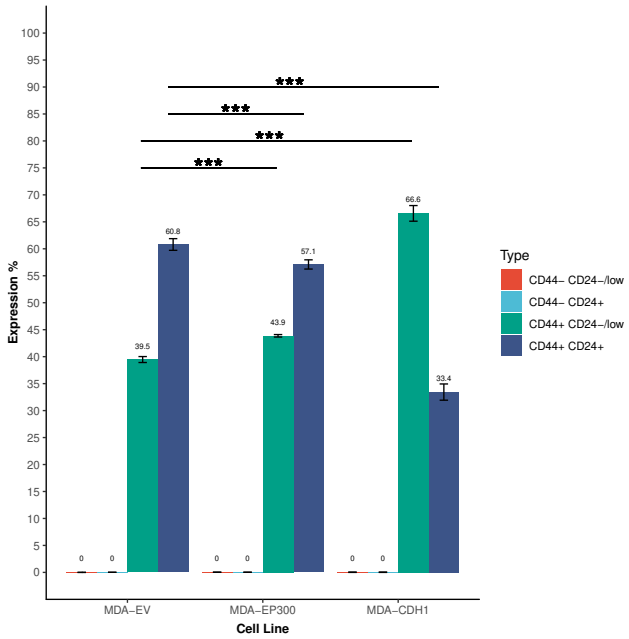
***
***
***
***
66.6
60.8
57.1
43.9
39.5
33.4
Expression %
Cell Line
MDA−EV
MDA−EP300
MDA−CDH1
Type
CD44− CD24−/low
CD44− CD24+
CD44+ CD24−/low
CD44+ CD24+

(c)

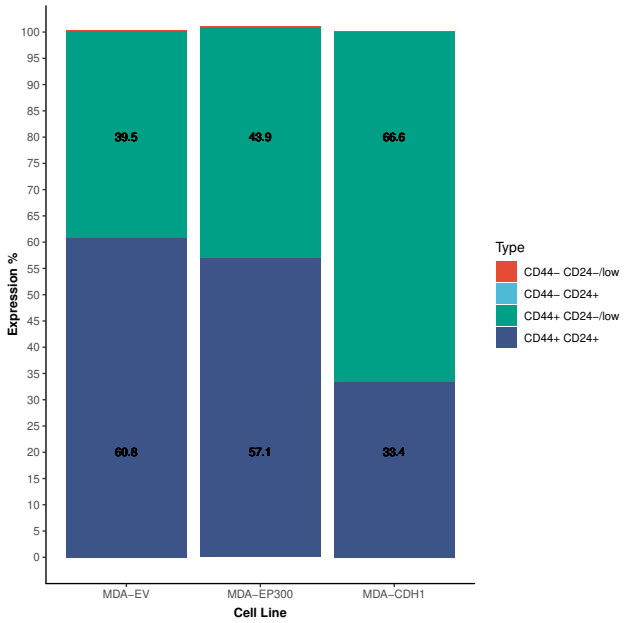

(d)

Fig. 7.5 Overexpression of EP300 enriches the $CD44^{high}/CD24^{low}$ cell population in MDA-MB-231 overexpressing EP300.(A) A selected representation of the flow cytometry plot for MDA-MB-231 cells with stable overexpression of EP300 (MDA-EP300) and CDH1 (MDA-CDH1). Cells were assessed for CD44 and CD24 expression by flow cytometry using a allophycocyanin (APC) and phycoerytrin (PE) – conjugated specific antibodies. The figure is separated into quadrants, positioned by placing 100% of unstained cells into Q4 (CD44-,CD24-). (B-C) A bar chart representing the mean + SD of the % of $CD44^{high}/CD24^{low}$ populations, representing 3 independent experiments (n=3). Statistical analysis was performed using one-way ANOVA, comparing MDA-MB-231 empty vector control (MDA-EV), to EP300 overexpressing (MDA-EP300) and CDH1 overexpressing (MDA-CDH1) transfected cells. (**P<0.01, ***P<0.001).

Figure 7.6a shows a panel demonstrating the percentage of cells testing positive for the $CD44^{high}/CD24^{low}$ markers of stemness. In this panel, we have the mesenchymal breast cancer cell line CAL51 with 3 conditions: a control empty vector, an EP300 overexpression and a CDH1 overexpression. Each condition was treated with a single CD44 or CD24 stain ($CD44^{high}$ and $CD24^{high}$), a negative unstained control, and a sample with both antibodies stained (Double stain). The panels show the accurate $CD44^{high}/CD24^{low}$ breast cancer cell population.

The single stained sample data is represented as a bar chart in **Figure 7.6b**. The data shows that the control stained 46.3% as $CD24^{high}$ and 0.2% $CD44^{high}$. With EP300 overexpression, the staining for $CD24^{high}$ decreased to 24.1% ($p<0.001$) and increased $CD44^{high}$ staining to 1.7% ($p<0.05$). With CDH1 overexpression, the staining for $CD24^{high}$ decreased to 36.7% ($p<0.001$) and increased $CD44^{high}$ staining to 0.4% (NS). **Figure 7.6c** and **Figure 7.6d** show the double stained samples, it is split up into two panels. Both show the same data, the first panel shows all the phenotypes while the second panel focuses on the majority population.

In **Figure 7.6c**, the control stained 51.6% as $CD44^{low}/CD24^{low}$, 48.5% $CD44^{low}/CD24^{high}$, none stained for $CD44^{high}/CD24^{low}$ and 0.2% stained for $CD44^{high}/CD24^{high}$. With EP300 overexpression, $CD44^{low}/CD24^{low}$ increased to 69.6% ($p<0.001$), $CD44^{low}/CD24^{high}$ decreased to 29.4% ($p<0.001$), $CD44^{high}/CD24^{low}$ increased by 0.8% (NS) and $CD44^{high}/CD24^{high}$ increased by 0.5% (NS). With CDH1 overexpression, $CD44^{low}/CD24^{low}$ decreased to 40.4% ($p<0.001$), $CD44^{low}/CD24^{high}$ increased to 59.7% ($p<0.001$), $CD44^{high}/CD24^{low}$ increased by 0.1% (NS) and $CD44^{high}/CD24^{high}$ increased by 0.1% (NS). **Figure 7.6d** shows the majority of the population for the control sample is 51.6% $CD44^{low}/CD24^{low}$ and 48.5% $CD44^{low}/CD24^{high}$. With EP300 overexpression, this population shifts more towards the $CD44^{low}/CD24^{low}$ with an increase by 18% ($p<0.001$) and decreases by 19.1% ($p<0.001$) in $CD44^{low}/CD24^{high}$. With CDH1 overexpression, this population shifts more towards the $CD44^{low}/CD24^{high}$ with an increase by 11.2% ($p<0.001$), and decreases by 11.2% ($p<0.001$) in $CD44^{low}/CD24^{low}$. When comparing both EP300 and CDH1, EP300 overexpression has 29.2% ($p<0.001$) more population in $CD44^{low}/CD24^{low}$ and less $CD44^{low}/CD24^{high}$ by 30.3% ($p<0.001$).

To summarise the effect of EP300 overexpression on $CD44^{high}/CD24^{low}$, we can see that mesenchymal cell lines do not have a universal response to EP300 expression. MDA-MB-231 surprisingly shows the overexpression of EP300 results in an upregulation in the $CD44^{high}/CD24^{low}$. Which means the CSC traits are positively regulated by EP300 and CDH1. CAL51 on the other hand does not show any $CD44^{high}/CD24^{low}$ populations, EP300 seems to only induce a very small portion of cells to express it, and even then it does not

compare to the increase in $CD44^{low}/CD24^{low}$ and $CD44^{low}/CD24^{high}$ populations. Likely these cells have different adaptive survival responses and these different subpopulations are reflective of this.

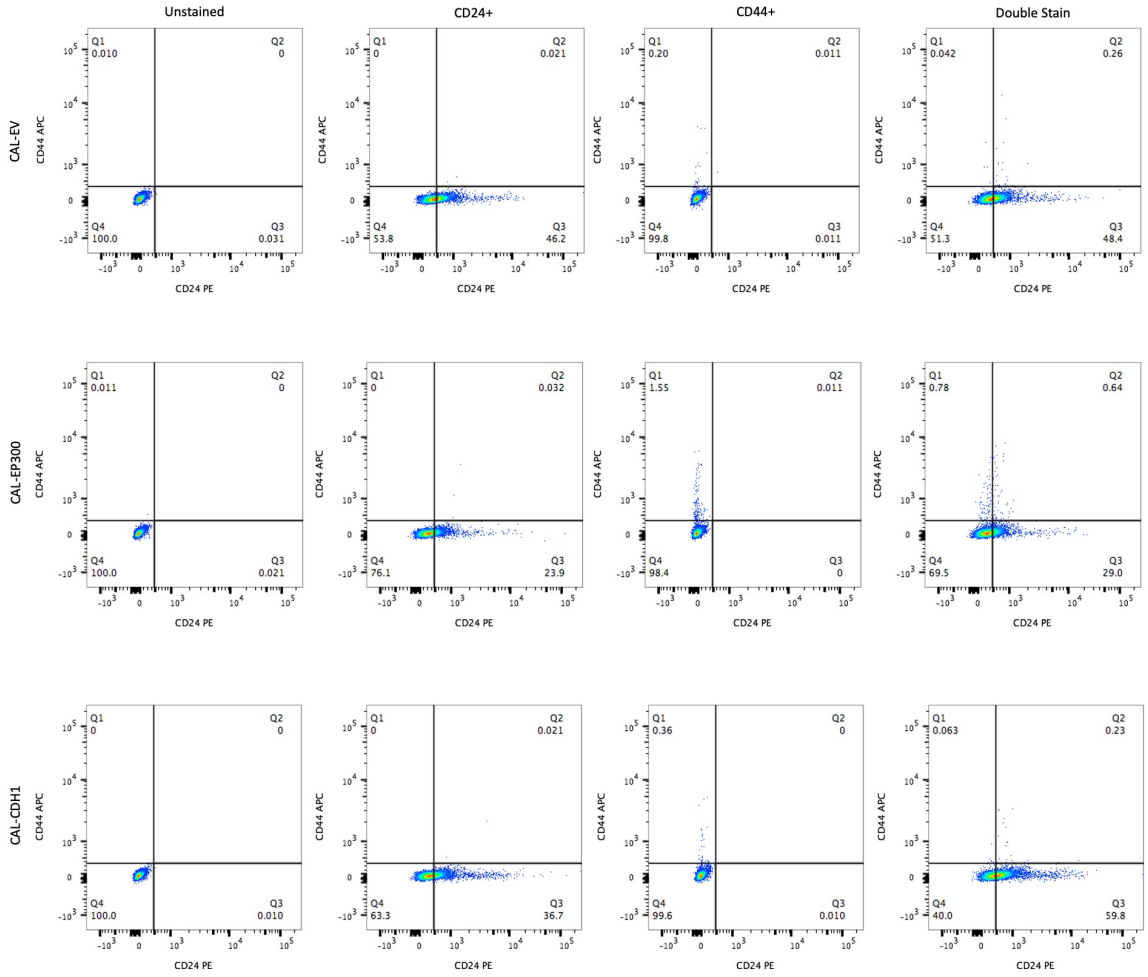
Unstained
CD24+
CD44+
Double Stain
CAL-EV
CAL-EP300
CAL-CDH1
CD44 APC
CD24 PE
Q1 0.010
Q2 0
Q4 100.0
Q3 0.031
Q1 0
Q2 0.021
Q4 53.8
Q3 46.2
Q1 0.20
Q2 0.011
Q4 99.8
Q3 0.011
Q1 0.042
Q2 0.26
Q4 51.3
Q3 48.4
Q1 0.011
Q2 0
Q4 100.0
Q3 0.021
Q1 0
Q2 0.032
Q4 76.1
Q3 23.9
Q1 1.55
Q2 0.011
Q4 98.4
Q3 0
Q1 0.78
Q2 0.64
Q4 69.5
Q3 29.0
Q1 0
Q2 0
Q4 100.0
Q3 0.010
Q1 0
Q2 0.021
Q4 63.3
Q3 36.7
Q1 0.36
Q2 0
Q4 99.6
Q3 0.010
Q1 0.063
Q2 0.23
Q4 40.0
Q3 59.8

(a)

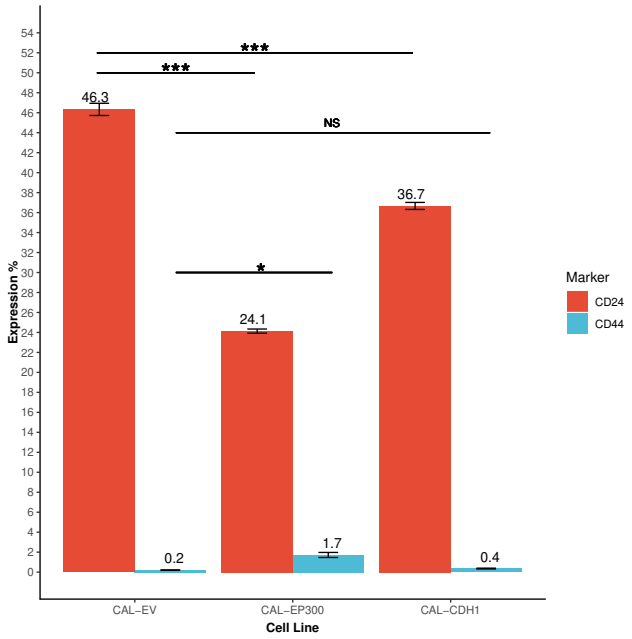
***
***
NS
*
46.3
0.2
24.1
1.7
36.7
0.4
Expression %
Cell Line
CAL−EV
CAL−EP300
CAL−CDH1
Marker
CD24
CD44

(b)

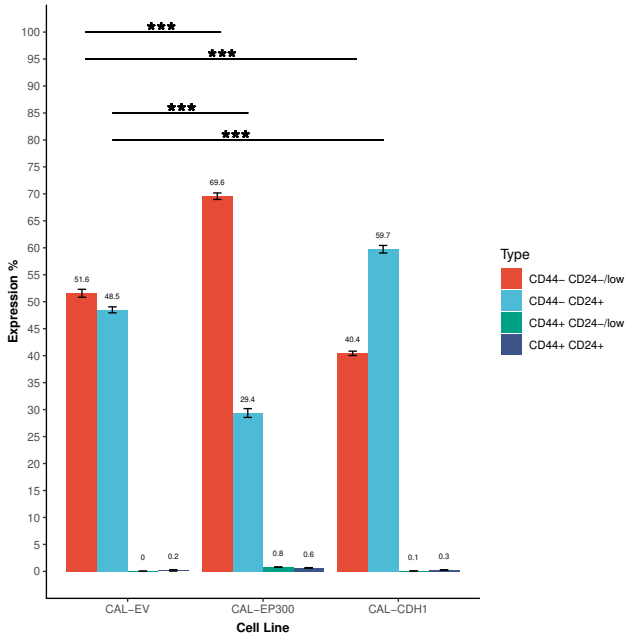
***
***
***
***
51.6
48.5
0
0.2
69.6
29.4
0.8
0.6
40.4
59.7
0.1
0.3
Expression %
Cell Line
CAL−EV
CAL−EP300
CAL−CDH1
Type
CD44− CD24−/low
CD44− CD24+
CD44+ CD24−/low
CD44+ CD24+

(c)

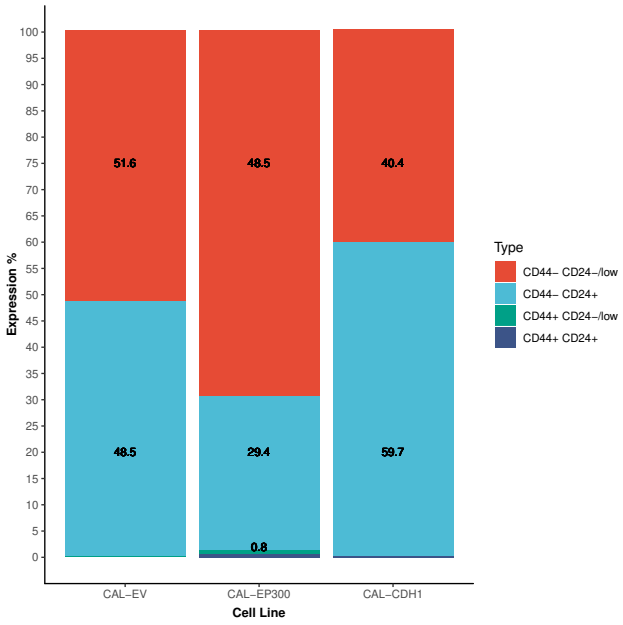

(d)

Fig. 7.6 Overexpression of EP300 enriches the $CD44^{high}/CD24^{low}$ cell population in CAL51 with EP300 overexpression. (A) A selected representation of the flow cytometry plot for CAL51 cells with stable overexpression of EP300 (CAL-EP300) and CDH1 (CAL-CDH1). Cells were assessed for CD44 and CD24 expression by flow cytometry using a allophycocyanin (APC) and phycoerytrin (PE) – conjugated specific antibodies. The figure is separated into quadrants, positioned by placing 100% of unstained cells into Q4 (CD44-,CD24-). (B-C) A bar chart representing the mean + SD of the % of $CD44^{high}/CD24^{low}$ populations, representing 3 independent experiments (n=3). Statistical analysis was performed using one-way ANOVA, comparing CAL51 empty vector control (CAl-EV), to EP300 overexpressing (CAL-EP300) and CDH1 overexpressing (CAL-CDH1) transfected cells. (**P$\leq$0.01, ***P$\leq$0.001).

Knockdown of EP300 modulates $CD44^{high}/CD24^{low}$ cell populations in epithelial breast cancer cell lines.

In this experiment, we used the same cell lines as for the ALDH+ experiment: MCF7 and T47D, which have 3 conditions: a control empty vector, an EP300 knockdown sh EP300 I and EP300 knockdown sh EP300 II. These cells were exposed to anti CD44 and anti CD24 antibodies for 30 minutes, followed by Isotype APC or PE-labelled antibodies. Cells were separated into four aliquots: two positive controls for presence of a single CD44 or CD24 stain ($CD44^{high}$ and $CD24^{high}$), a negative unstained control, and a sample with both antibodies stained (Double stain). The cells were then run through a BD™ LSR II flow cytometer to determine the cell population percentages, which were then analysed on FlowJo software and represented in the figures below.

Figure 7.7a shows a panel demonstrating the percentage of cells testing positive for the $CD44^{high}/CD24^{low}$ markers of stemness. In this panel, we have the epithelial breast cancer cell line MCF7 with 3 conditions: a control empty vector, a knockdown sh EP300 I and EP300 knockdown sh EP300 II. Each condition was treated with a single CD44 or CD24 stain ($CD44^{high}$ and $CD24^{high}$), a negative unstained control, and a sample with both antibodies stained (Double stain). The panels show the accurate $CD44^{high}/CD24^{low}$ breast cancer cell population.

The single stained sample data is represented as a bar chart in **Figure 7.7b**. The data shows that the control stained 98.3% as $CD24^{high}$ and 21.2% $CD44^{high}$. With sh EP300 I, the staining for $CD24^{high}$ decreased to 98% (NS) and decreased $CD44^{high}$ staining to 20.6% (NS). With shEP300 II overexpression, the staining for $CD24^{high}$ increased to 99% (NS) and increased $CD44^{high}$ staining to 47% ($p<0.001$). **Figure 7.7c** and **Figure 7.7d** shows the double stained samples, it is split up into two panels. Both show the same data, the first panel shows all the phenotypes while the second panel focuses on the majority population.

In **Figure 7.7c**, The control stained 0.2% as $CD44^{low}/CD24^{low}$, 78.1% $CD44^{low}/CD24^{high}$, none stained for $CD44^{high}/CD24^{low}$ and 22.2% stained for $CD44^{high}/CD24^{high}$. With sh EP300 I, $CD44^{low}/CD24^{low}$ decreased to 0.1% (NS), $CD44^{low}/CD24^{high}$ decreased to 41% ($p<0.001$), $CD44^{high}/CD24^{low}$ did not change and $CD44^{high}/CD24^{high}$ increased to 58.8% ($p<0.001$). With sh EP300 II overexpression, $CD44^{low}/CD24^{low}$ decreased to 0.1% (NS), $CD44^{low}/CD24^{high}$ decreased to 53.8% ($p<0.001$), $CD44^{high}/CD24^{low}$ did not change and $CD44^{high}/CD24^{high}$ increased to 46.8% ($p<0.001$). **Figure 7.7d** shows the majority of the population for the control sample is 78.1% $CD44^{low}/CD24^{high}$ and 22.2% $CD44^{high}/CD24^{high}$. With sh EP300 I, this population shifts more towards the $CD44^{high}/CD24^{high}$ with an increase by 36.6% ($p<0.001$) and decreases by 37.1% ($p<0.001$) in $CD44^{low}/CD24^{high}$. With sh EP300 II, this population shifts more towards the $CD44^{high}/CD24^{high}$ with an increase by

24.6% ($p<0.001$), and decreases by 24.3% ($p<0.001$) in $CD44^{low}/CD24^{high}$. When comparing both sh EP300 I and II, sh EP300 I has 12% ($p<0.001$) more population in $CD44^{high}/CD24^{high}$ and less $CD44^{low}/CD24^{high}$ by 12.8% ($p<0.001$).

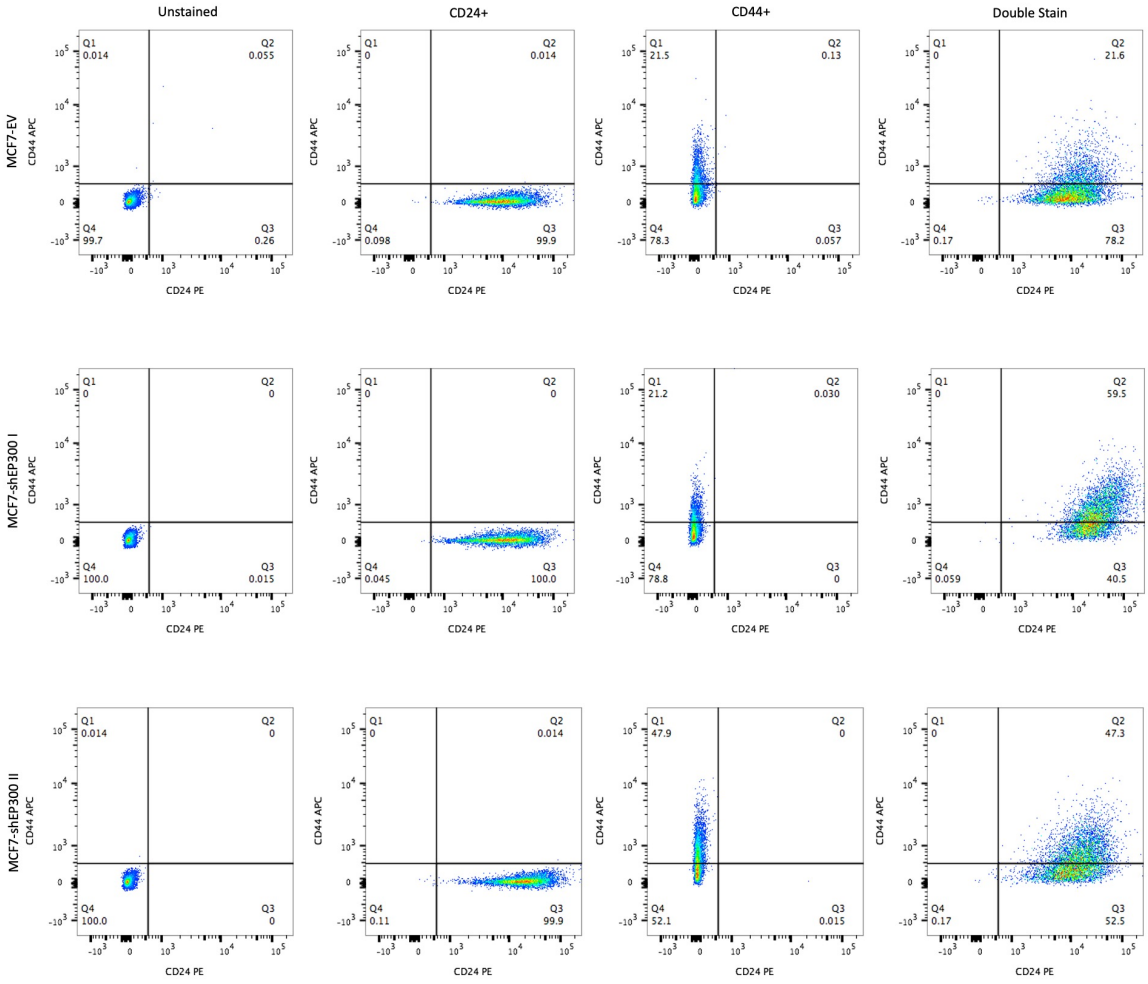
Unstained
CD24+
CD44+
Double Stain
MCF7-EV
MCF7-shEP300 I
MCF7-shEP300 II
CD44 APC
CD24 PE
Q1 0.014
Q2 0.055
Q4 99.7
Q3 0.26
Q1 0
Q2 0.014
Q4 0.098
Q3 99.9
Q1 21.5
Q2 0.13
Q4 78.3
Q3 0.057
Q1 0
Q2 21.6
Q4 0.17
Q3 78.2
Q1 0
Q2 0
Q4 100.0
Q3 0.015
Q1 0
Q2 0
Q4 0.045
Q3 100.0
Q1 21.2
Q2 0.030
Q4 78.8
Q3 0
Q1 0
Q2 59.5
Q4 0.059
Q3 40.5
Q1 0.014
Q2 0
Q4 100.0
Q3 0
Q1 0
Q2 0.014
Q4 0.11
Q3 99.9
Q1 47.9
Q2 0
Q4 52.1
Q3 0.015
Q1 0
Q2 47.3
Q4 0.17
Q3 52.5

(a)

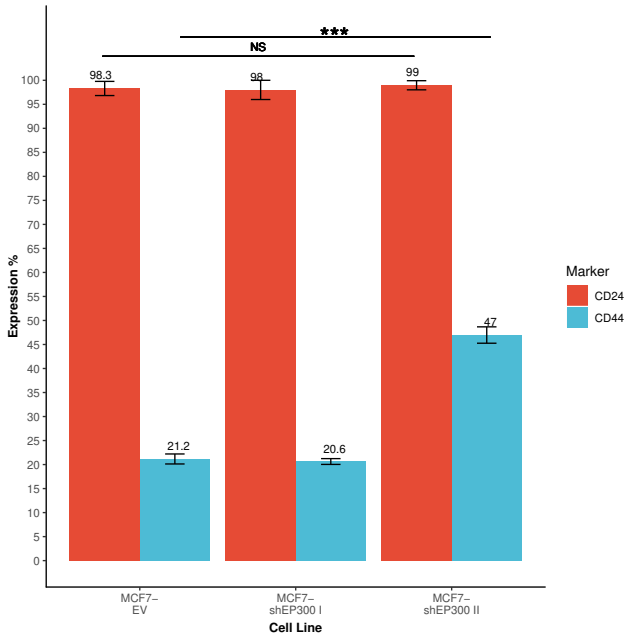
***
NS
98.3
98
99
47
21.2
20.6
Expression %
Marker
CD24
CD44
MCF7–
EV
MCF7–
shEP300 I
MCF7–
shEP300 II
Cell Line

(b)

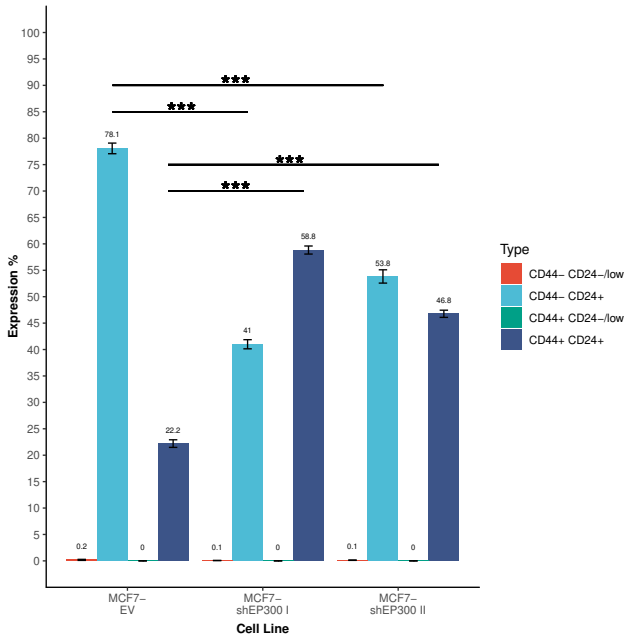
***
***
***
***
78.1
22.2
0.2
0
41
0.1
0
58.8
53.8
0.1
0
46.8
Expression %
Type
CD44– CD24–/low
CD44– CD24+
CD44+ CD24–/low
CD44+ CD24+
MCF7–
EV
MCF7–
shEP300 I
MCF7–
shEP300 II
Cell Line

(c)

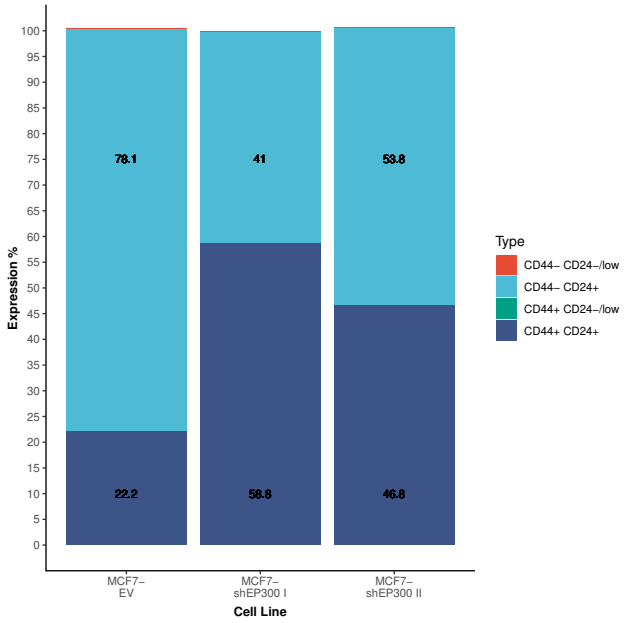

(d)

Fig. 7.7 Downregulation of EP300 enriches the $CD44^{high}/CD24^{high}$ cell population. (A) A selected representation of the flow cytometry plot for MCF7 cells with downregulation of EP300 (MCF7-sh EP300 I) and (MCF7-shEP300 II). Cells were assessed for CD44 and CD24 expression by flow cytometry using a allophycocyanin (APC) and phycoerytrin (PE) – conjugated specific antibodies. The figure is separated into quadrants, positioned by placing 100% of unstained cells into Q4 (CD44-,CD24-). (B-C) A bar chart representing the mean + SD of the % of $CD44^{high}/CD24^{low}$ populations, representing 3 independent experiments (n=3). Statistical analysis was performed using one-way ANOVA, comparing MCF7 shEV empty vector control (MCF7-EV), to EP300 downregulation (MCF7-shEP300 I) and (MCF7-shEP300 II) transfected cells. (**P$\leq$0.01, ***P$\leq$0.001).

Figure 7.8a shows a panel demonstrating the percentage of cells testing positive for the $CD44^{high}/CD24^{low}$ markers of stemness. In this panel, we have the epithelial breast cancer cell line MCF7 with 3 conditions: a control empty vector, a knockdown sh EP300 I and EP300 knockdown sh EP300 II. Each condition was treated with a single CD44 or CD24 stain ($CD44^{high}$ and $CD24^{high}$), a negative unstained control, and a sample with both antibodies stained (Double stain). The panels show the accurate $CD44^{high}/CD24^{low}$ breast cancer cell population.

The single stained sample data is represented as a bar chart in **Figure 7.8b**. The data shows that the control stained 97.3% as $CD24^{high}$ and 21.4% $CD44^{high}$. With sh EP300 I, the staining for $CD24^{high}$ decreased to 96.5% (NS) and increased $CD44^{high}$ staining to 25.9% ($p<0.05$). With shEP300 II overexpression, the staining for $CD24^{high}$ decreased to 95.7% (NS) and decreased $CD44^{high}$ staining to 10.9% ($p<0.001$). **Figure 7.8c** and **Figure 7.8d** shows the double stained samples, it is split up into two panels. Both show the same data, the first panel shows all the phenotypes, while the second panel focuses on the majority population.

In **Figure 7.8c**, The control stained 0.9% as $CD44^{low}/CD24^{low}$, 73% $CD44^{low}/CD24^{high}$, 0.1% $CD44^{high}/CD24^{low}$ and 24.29% stained for $CD44^{high}/CD24^{high}$. With sh EP300 I, $CD44^{low}/CD24^{low}$ decreased to 0.8% (NS), $CD44^{low}/CD24^{high}$ decreased to 66.5%, $CD44^{high}/CD24^{low}$ did not change and $CD44^{high}/CD24^{high}$ increased to 32.2% ($p<0.001$). With sh EP300 II overexpression, $CD44^{low}/CD24^{low}$ decreased to 0.5% (NS), $CD44^{low}/CD24^{high}$ increased to 85.4% ($p<0.001$), $CD44^{high}/CD24^{low}$ did not change and $CD44^{high}/CD24^{high}$ decreased to 14.4% ($p<0.001$). **Figure 7.8d** shows the majority of the population for the control sample is 73% $CD44^{low}/CD24^{high}$ and 24.9% $CD44^{high}/CD24^{high}$. With sh EP300 I, this population shifts more towards the $CD44^{high}/CD24^{high}$ with an increase by 7.3% ($p<0.001$) and decreases by 6.5% ($p<0.001$) in $CD44^{low}/CD24^{high}$. With sh EP300 II, this population shifts more towards the $CD44^{low}/CD24^{high}$ with an increase by 12.4% ($p<0.001$), and decreases by 10.5% ($p<0.001$) in $CD44^{high}/CD24^{high}$. When comparing both sh EP300 I and II, sh EP300 I has 17.8% ($p<0.001$) more population in $CD44^{high}/CD24^{high}$ and less $CD44^{low}/CD24^{high}$ by 18.9% ($p<0.001$).

Thus to summarise the effect on epithelial breast cancer cell lines, we see that both MCF7s and T47Ds do not express $CD44^{high}/CD24^{low}$, as expected due to their epithelial characteristics. The downregulation of EP300 in these cell lines seems to induce a shift from $CD44^{low}/CD24^{high}$ to $CD44^{high}/CD24^{high}$. Meaning that while it does not induce the invasive CSC subpopulation, it still has an effect on expression of these receptors. Probably allowing them to form niches in distal organs.

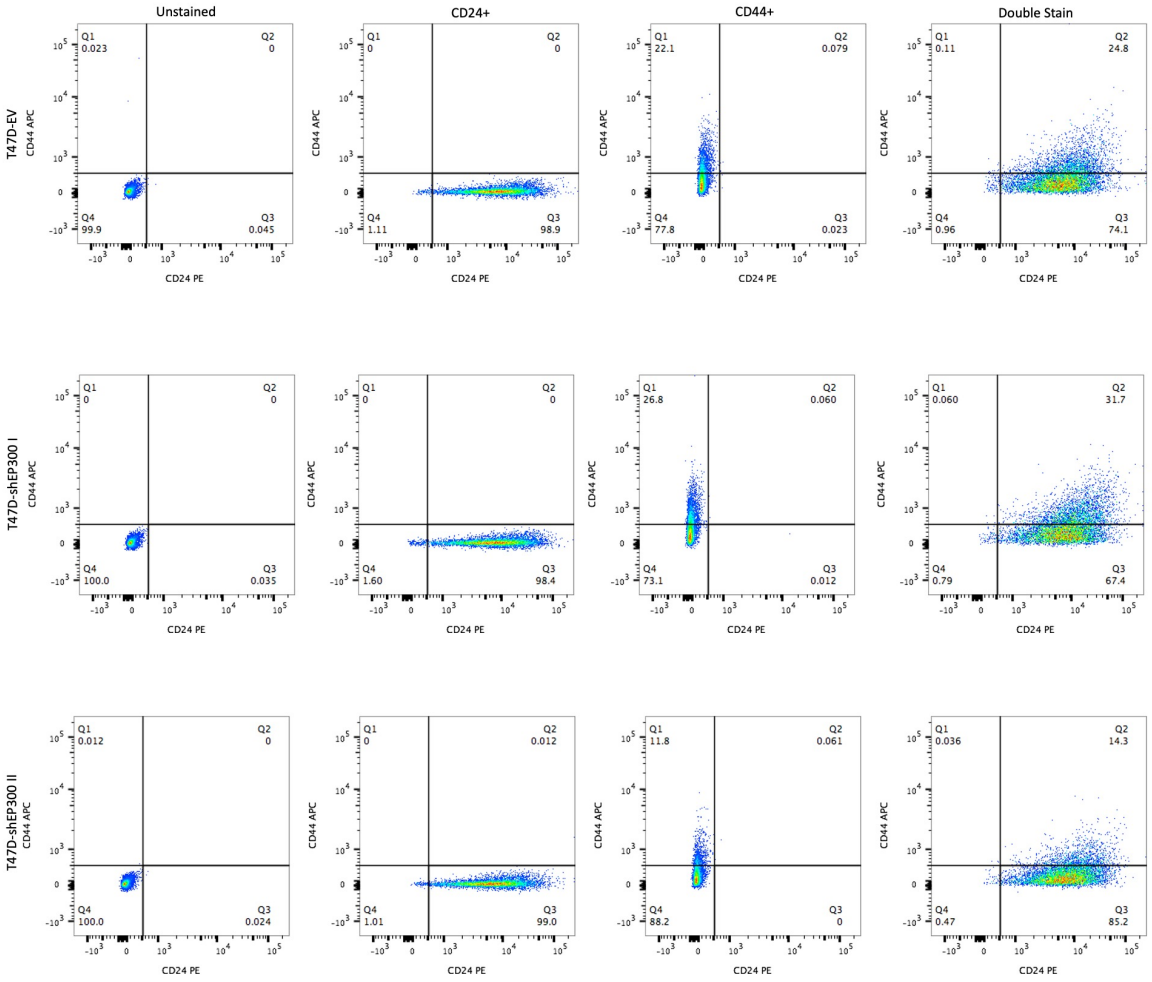
Unstained
CD24+
CD44+
Double Stain
T47D-EV
T47D-shEP300 I
T47D-shEP300 II
CD44 APC
CD24 PE
Q1 0.023
Q2 0
Q4 99.9
Q3 0.045
Q1 0
Q2 0
Q4 1.11
Q3 98.9
Q1 22.1
Q2 0.079
Q4 77.8
Q3 0.023
Q1 0.11
Q2 24.8
Q4 0.96
Q3 74.1
Q1 0
Q2 0
Q4 100.0
Q3 0.035
Q1 0
Q2 0
Q4 1.60
Q3 98.4
Q1 26.8
Q2 0.060
Q4 73.1
Q3 0.012
Q1 0.060
Q2 31.7
Q4 0.79
Q3 67.4
Q1 0.012
Q2 0
Q4 100.0
Q3 0.024
Q1 0
Q2 0.012
Q4 1.01
Q3 99.0
Q1 11.8
Q2 0.061
Q4 88.2
Q3 0
Q1 0.036
Q2 14.3
Q4 0.47
Q3 85.2

(a)

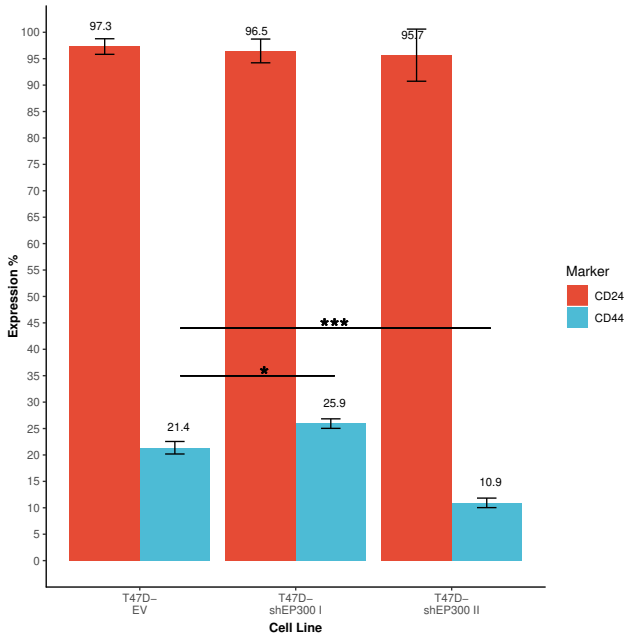
97.3
96.5
95.7
21.4
25.9
10.9
***
*
Expression %
Marker
CD24
CD44
T47D–
EV
T47D–
shEP300 I
T47D–
shEP300 II
Cell Line

(b)

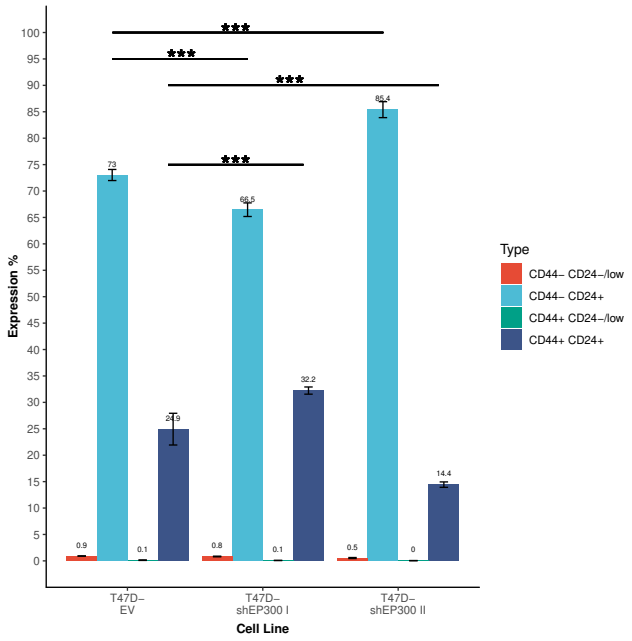
***
***
***
***
Expression %
Type
CD44– CD24–/low
CD44– CD24+
CD44+ CD24–/low
CD44+ CD24+
T47D–
EV
T47D–
shEP300 I
T47D–
shEP300 II
Cell Line

(c)

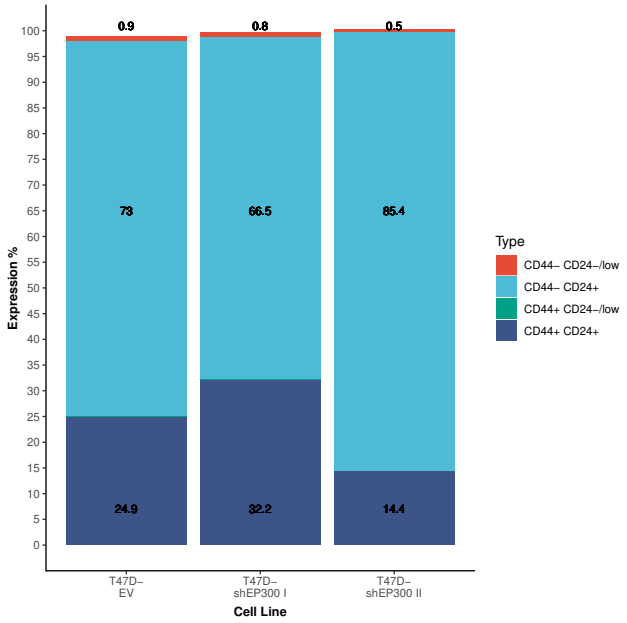

(d)

Fig. 7.8 Downregulation of EP300 enriches the $CD44^{low}/CD24^{high}$ cell population. (A) A selected representation of the flow cytometry plot for T47D cells with downregulation of EP300 (shEP300 I an shEP300 II)). Cells were assessed for CD44 and CD24 expression by flow cytometry using a allophycocyanin (APC) and phycoerytrin (PE) – conjugated specific antibodies. The figure is separated into quadrants, positioned by placing 100% of unstained cells into Q4 (CD44-,CD24-). (B) A bar chart representing the mean + SD of the % of $CD44^{high}/CD24^{low}$ populations, representing 3 independent experiments (n=3). Statistical analysis was performed using one-way ANOVA, comparing T47D shEV empty vector control (T47D-EV), to EP300 downregulation (T47D-shEP300 I) and (T47D-shEP300 II) transfected cells. (**P$\leq$0.01, ***P$\leq$0.001).

Knockout of EP300 modulates $CD44^{high}/CD24^{low}$ cell populations in colorectal cancer cell lines.

In this experiment, we used the same cell lines as for the ALDH+ experiment: HCT116, which has 2 conditions: a control empty vector and EP300 knockout. These cells were exposed to anti CD44 and anti CD24 antibodies for 30 minutes, followed by Isotype APC or PE-labelled antibodies. Cells were separated into four aliquots: two positive controls for presence of a single CD44 or CD24 stain ($CD44^{high}$ and $CD24^{high}$), a negative unstained control, and a sample with both antibodies stained (Double stain). The cells were then run through a BD™ LSR II flow cytometer to determine the cell population percentages, which were then analysed on FlowJo software and represented in the figures below.

Figure 7.9a shows a panel demonstrating the percentage of cells testing positive for the $CD44^{high}/CD24^{low}$ markers of stemness. In this panel, we have the colorectal cancer cell line HCT116 with 2 conditions: a control empty vector and an EP300 knockout. Each condition was treated with a single CD44 or CD24 stain ($CD44^{high}$ and $CD24^{high}$), a negative unstained control, a sample with both antibodies stained (Double stain) and the panels show the accurate $CD44^{high}/CD24^{low}$ colorectal cancer stem cell population.

The single stained sample data is represented as a bar chart in **Figure 7.9b**. The data shows that the control stained 8.4% as $CD24^{high}$ and 87.3% $CD44^{high}$. With EP300 knockout (KO EP300), the staining for $CD24^{high}$ decreased to 2.6% ($p<0.001$) and increased $CD44^{high}$ staining to 96.3% ($p<0.001$). **Figure 7.9c** and **Figure 7.9d** shows the double stained samples, it is split up into two panels. Both show the same data, the first panel shows all the phenotypes while the second panel focuses on the majority population.

In **Figure 7.9c**, the control stained 1.4% as $CD44^{low}/CD24^{low}$, 0.1% $CD44^{low}/CD24^{high}$, 89.3% $CD44^{high}/CD24^{low}$ and 8.7% stained for $CD44^{high}/CD24^{high}$. With KO EP300, $CD44^{low}/CD24^{low}$ decreased to 0.1% ($p<0.05$), $CD44^{low}/CD24^{high}$ remained unchanged, $CD44^{high}/CD24^{low}$ decreased to 85.6% ($p<0.01$) $CD44^{high}/CD24^{high}$ increased to 14% ($p<0.001$). **Figure 7.9d** shows the majority of the population for the control sample is 89.3% $CD44^{high}/CD24^{low}$ and 8.7% $CD44^{high}/CD24^{high}$. With KO EP300, the population remains largely $CD44^{high}/CD24^{low}$ with a decrease in this by 3.7% ($p<0.05$). A slight shift is seen towards the $CD44^{high}/CD24^{high}$ with an increase by 5.3% ($p<0.001$).

This knockout of EP300 in HCT116 converts some of the $CD44^{high}/CD24^{low}$ subpopulations into $CD44^{high}/CD24^{high}$. While this does not remove the CSC populations completely, the modulation of EP300 in this cell line might give us a clue as to which pathways promote this shift.

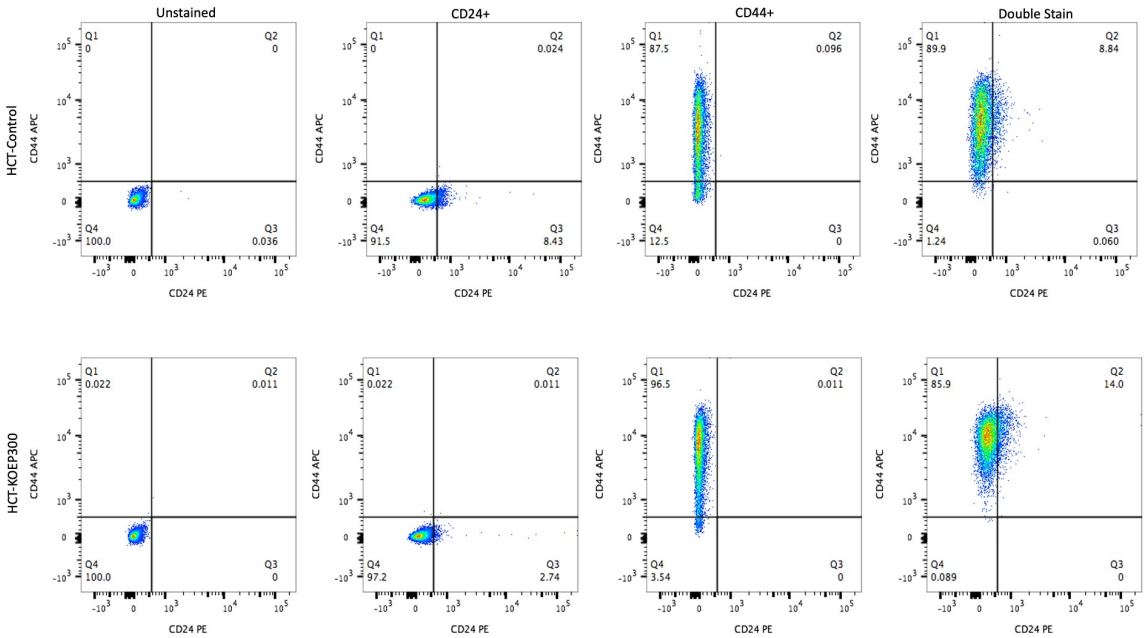
Unstained
CD24+
CD44+
Double Stain
HCT-Control
HCT-KOEP300
CD44 APC
CD24 PE
Q1 0
Q2 0
Q4 100.0
Q3 0.036
Q1 0
Q2 0.024
Q4 91.5
Q3 8.43
Q1 87.5
Q2 0.096
Q4 12.5
Q3 0
Q1 89.9
Q2 8.84
Q4 1.24
Q3 0.060
Q1 0.022
Q2 0.011
Q4 100.0
Q3 0
Q1 0.022
Q2 0.011
Q4 97.2
Q3 2.74
Q1 96.5
Q2 0.011
Q4 3.54
Q3 0
Q1 85.9
Q2 14.0
Q4 0.089
Q3 0

(a)

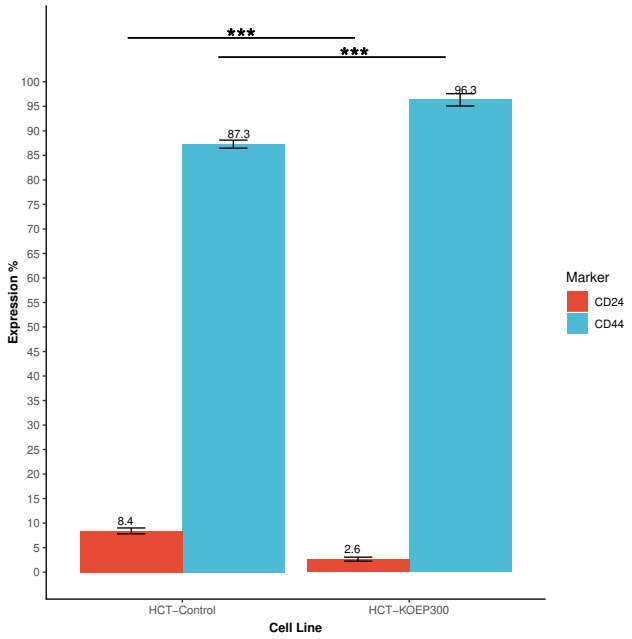
***
***
100
95
90
85
80
75
70
65
60
55
50
45
40
35
30
25
20
15
10
5
0
Expression %
96.3
87.3
8.4
2.6
HCT−Control
HCT−KOEP300
Cell Line
Marker
CD24
CD44

(b)

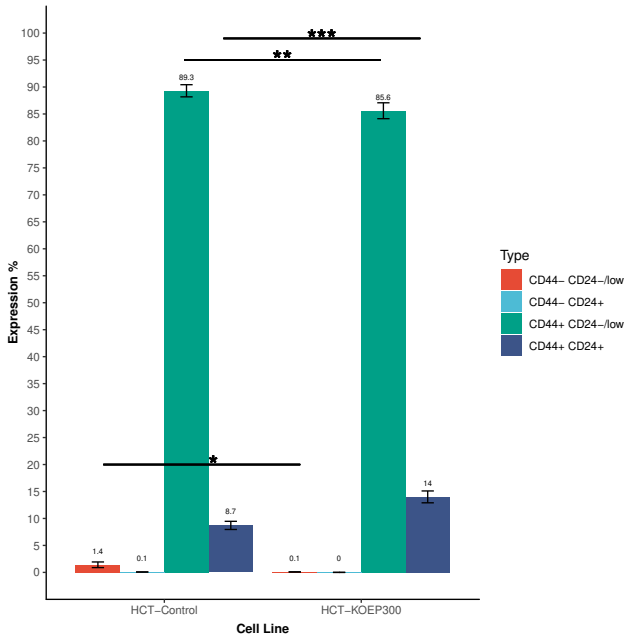
***
**
*
100
95
90
85
80
75
70
65
60
55
50
45
40
35
30
25
20
15
10
5
0
Expression %
89.3
85.6
14
8.7
1.4
0.1
0.1
0
HCT−Control
HCT−KOEP300
Cell Line
Type
CD44− CD24−/low
CD44− CD24+
CD44+ CD24−/low
CD44+ CD24+

(c)

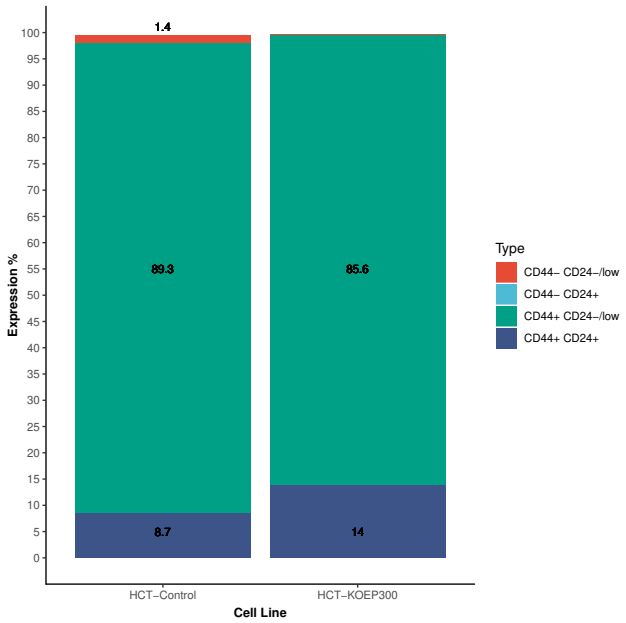

(d)

Fig. 7.9 Knockout of EP300 enriches the $CD44^{high}/CD24^{low}$ cell population.(A) A selected representation of the flow cytometry plot for HCT116 cells with knockout of EP300 (HCT-KOEP300). Cells were assessed for CD44 and CD24 expression by flow cytometry using a allophycocyanin (APC) and phycoerytrin (PE) – conjugated specific antibodies. The figure is separated into quadrants, positioned by placing 100% of unstained cells into Q4 (CD44-,CD24-). (B-C) A bar chart representing the mean + SD of the % of $CD44^{high}/CD24^{low}$ populations, representing 3 independent experiments (n=3). Statistical analysis was performed using one-way ANOVA, comparing HCT116 wild type control (HCT116-Control), to HCT116 with EP300 knockout (HCT-KOEP300) transfected cells. (**P$\leq$0.01, ***P$\leq$0.001).

Knockdown of EP300 modulates $CD44^{high}/CD24^{low}$ cell populations in paclitaxel resistant and doxorubicin resistant epithelial breast cancer cell lines.

In this experiment, we used the same cell lines established by Eric Lam Group (de Moraes et al., 2015; Alasiri et al., 2019) as for the ALDH+ experiment, which has 3 conditions: a control empty vector, a control empty vector, long-term paclitaxel resistance and long-term doxorubicin resistance. These cells were exposed to anti CD44 and anti CD24 antibodies for 30 minutes, followed by Isotype APC or PE-labelled antibodies. Cells were separated into four aliquots: two positive controls for presence of a single CD44 or CD24 stain ($CD44^{high}$ and $CD24^{high}$), a negative unstained control, and a sample with both antibodies stained (Double stain). The cells were then run through a BD™ LSR II flow cytometer to determine the cell population percentages, which were then analysed on FlowJo software and represented in the figures below.

Figure 7.10a shows a panel demonstrating the percentage of cells testing positive for the $CD44^{high}/CD24^{low}$ markers of stemness. In this panel, we have the MCF7 breast cancer cell line with 3 conditions: a control empty vector, long-term paclitaxel resistance and long-term doxorubicin resistance. Each condition was treated with a single CD44 or CD24 stain ($CD44^{high}/CD24^{high}$), a negative unstained control, and a sample with both antibodies stained (Double stain). The panels show the accurate $CD44^{high}/CD24^{low}$ colorectal cancer stem cell population.

The single stained sample data is represented as a bar chart in **Figure 7.10b**. The data shows that the control stained 98% as $CD24^{high}$ and 65.5% $CD44^{high}$. With Doxorubicin resistance (DoxR), the staining for $CD24^{high}$ decreased to 95.6% ($p<0.001$) and increased $CD44^{high}$ staining to 99% ($p<0.001$). With paclitaxel resistance (TaxR), the staining for $CD24^{high}$ decreased to 86% ($p<0.001$) and increased $CD44^{high}$ staining to 98.6% ($p<0.001$). **Figure 7.10c** and **Figure 7.10d** shows the double stained samples, it is split up into two panels. Both show the same data, the first panel shows all the phenotypes while the second panel focuses on the majority population.

In **Figure 7.10c**, the control stained 0.1% as $CD44^{low}/CD24^{low}$, 31.7% $CD44^{low}/CD24^{high}$, none stained for $CD44^{high}/CD24^{low}$ and 68.9% stained for $CD44^{high}/CD24^{high}$. With DoxR, $CD44^{low}/CD24^{low}$ and $CD44^{low}/CD24^{high}$ did not stain, $CD44^{high}/CD24^{low}$ increased to 2.3% ($p<0.001$), $CD44^{high}/CD24^{high}$ increased to 97.2% ($p<0.001$). With DoxR, $CD44^{low}/CD24^{low}$ and $CD44^{low}/CD24^{high}$ did not stain, $CD44^{high}/CD24^{low}$ increased to 11.3% ($p<0.001$), $CD44^{high}/CD24^{high}$ increased to 88.1% ($p<0.001$).

Figure 7.10d shows the majority of the population for the control sample is 31.7% $CD44^{low}/CD24^{high}$ and 68.9% $CD44^{high}/CD24^{high}$. With DoxR, the population remains largely $CD44^{high}/CD24^{hig}$ with an increase by 28.3% ($p<0.001$). A slight shift is seen towards

the $CD44^{high}/CD24^{low}$ with an increase by 2.3% ($p<0.001$). With TaxR, the population remains largely $CD44^{high}/CD24^{high}$ with an increase in this by 19.2% ($p<0.001$). A slight shift is seen towards the $CD44^{high}/CD24^{low}$ with an increase by 11.3% ($p<0.001$). When comparing DoxR with TaxR, DoxR has more $CD44^{high}/CD24^{high}$ populations by 9.1% ($p<0.001$), and TaxR has more $CD44^{high}/CD24^{low}$ population by 9% ($p<0.001$).

As with ALDH, the effects of doxorubicin and paclitaxel prove to be also different on the $CD44^{high}/CD24^{low}$ populations. The shift from $CD44^{low}/CD24^{high}$ to $CD44^{high}/CD24^{high}$, is seen with both drugs. However, they also seem to promote $CD44^{high}/CD24^{low}$ populations, of which paclitaxel has the larger effect.

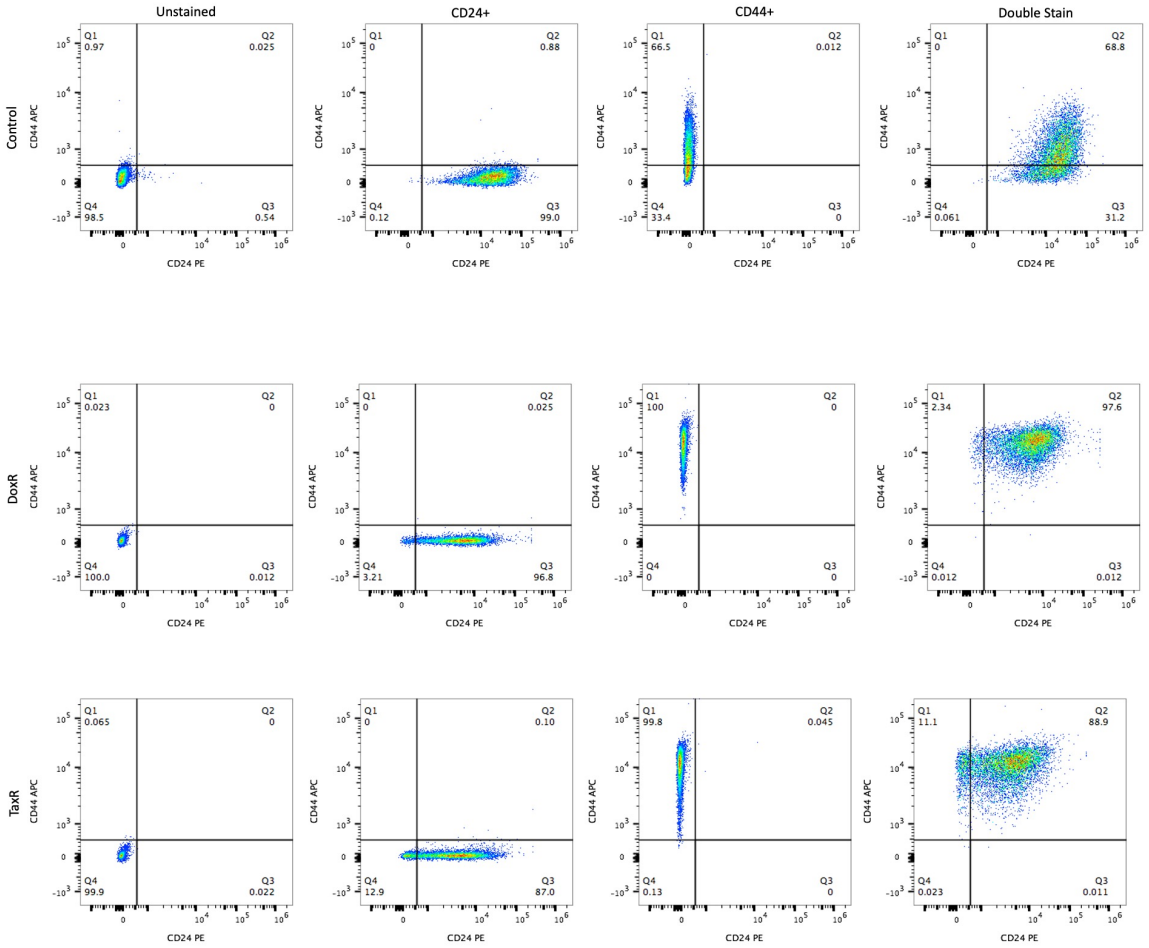
Unstained
CD24+
CD44+
Double Stain
Control
DoxR
TaxR
CD44 APC
CD24 PE
Q1 0.97
Q2 0.025
Q4 98.5
Q3 0.54
Q1 0
Q2 0.88
Q4 0.12
Q3 99.0
Q1 66.5
Q2 0.012
Q4 33.4
Q3 0
Q1 0
Q2 68.8
Q4 0.061
Q3 31.2
Q1 0.023
Q2 0
Q4 100.0
Q3 0.012
Q1 0
Q2 0.025
Q4 3.21
Q3 96.8
Q1 100
Q2 0
Q4 0
Q3 0
Q1 2.34
Q2 97.6
Q4 0.012
Q3 0.012
Q1 0.065
Q2 0
Q4 99.9
Q3 0.022
Q1 0
Q2 0.10
Q4 12.9
Q3 87.0
Q1 99.8
Q2 0.045
Q4 0.13
Q3 0
Q1 11.1
Q2 88.9
Q4 0.023
Q3 0.011

(a)

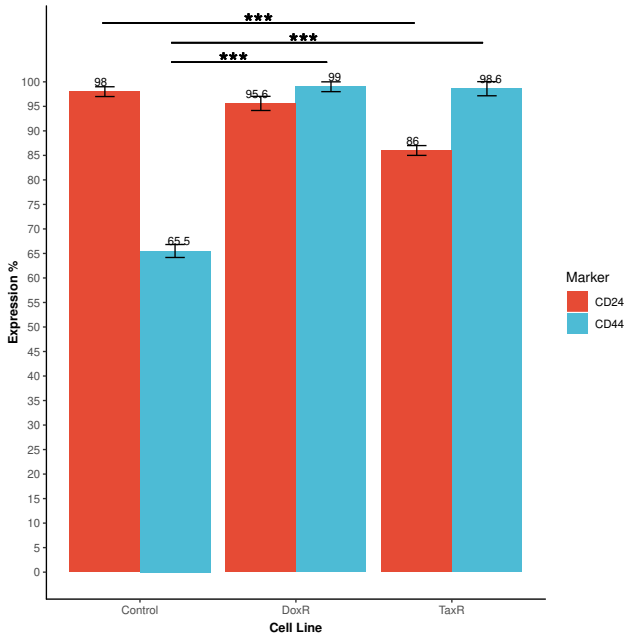
***
***
***
98
65.5
95.6
99
86
98.6
Expression %
Control
DoxR
TaxR
Cell Line
Marker
CD24
CD44

(b)

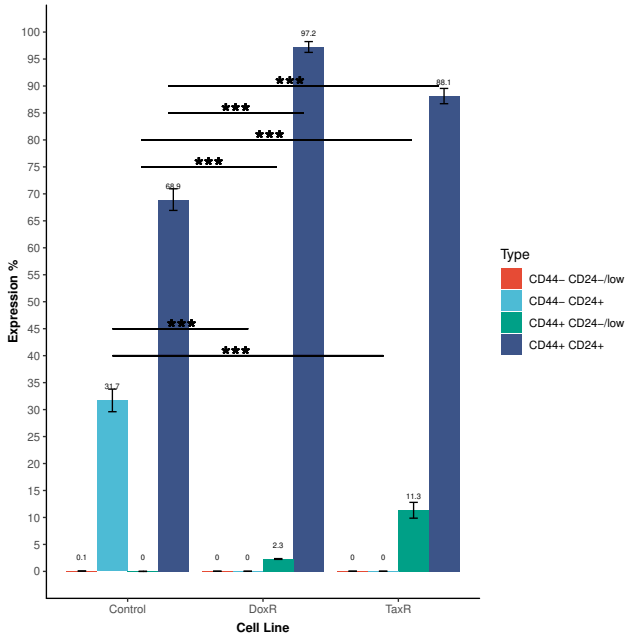
***
***
***
***
***
***
***
0.1
31.7
0
68.9
0
0
2.3
97.2
0
0
11.3
88.1
Expression %
Control
DoxR
TaxR
Cell Line
Type
CD44– CD24–/low
CD44– CD24+
CD44+ CD24–/low
CD44+ CD24+

(c)

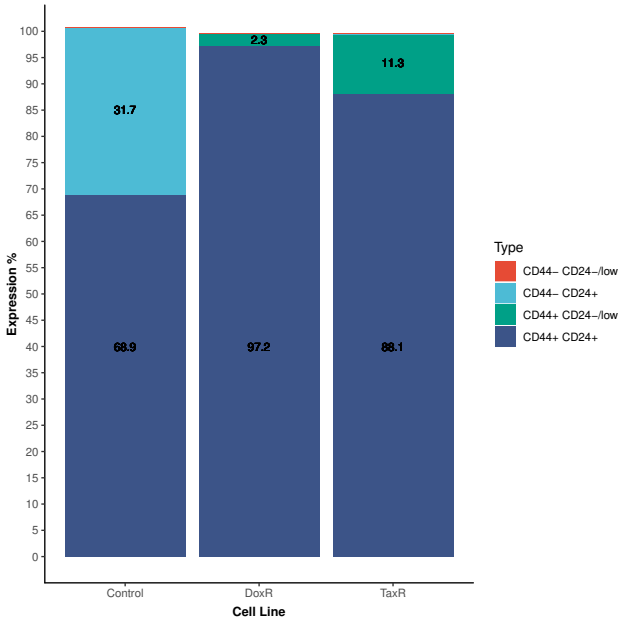

(d)

Fig. 7.10 Drug resistance to Paclitaxel enriches the $CD44^{high}/CD24^{low}$ cell population. (A) A selected representation of the flow cytometry plot for MCF7 cells with resistance to doxorubicin (DoxR) and Paclitaxel (TaxR). Cells were assessed for CD44 and CD24 expression by flow cytometry using a allophycocyanin (APC) and phycoerytrin (PE) – conjugated specific antibodies. The figure is separated into quadrants, positioned by placing 100% of unstained cells into Q4 (CD44-,CD24-). (B) A bar chart representing the mean + SD of the % of $CD44^{high}/CD24^{low}$ populations, representing 3 independent experiments (n=3). Statistical analysis was performed using one-way ANOVA, comparing wild type MCF7 control (Control), to MCF7 with doxorubicin resistance (DoxR) and MCF7 with paclitaxel resistance (TaxR). (**P$\leq$0.01, ***P$\leq$0.001).

7.2.4 Discussion

Previous findings show that CAL51 and MDA-MB-231 cells both contain ALDH+ and $CD44^{high}/CD24^{low}$ subpopulations (Sheridan et al., 2006; Samanta et al., 2014; Yu et al., 2016; Li et al., 2017). Among them, MDA-MB-231 cells expresses both markers at much higher levels than CAL51 cells. Previous findings by Yu et al. (2016) show CAL51 cells have 70% $CD44^{low}/CD24^{high}$, and 3-4% ALDH expression while MDA-MB-231 cells have 90% $CD44^{low}/CD24^{high}$ and 40% ALDH respectively.

In our findings, both mesenchymal MDA-MB-231 and CAL-51 cell lines have completely different responses to EP300 and CDH1 overexpression as well as their basal expression of the CD44/CD24 markers. However, they share very similar ALDH expression patterns. Both MDA-MB-231 and CAL-51 cell lines downregulate ALDH upon EP300 and CDH1 overexpression. We also found that while our findings confirm MDA-MB-231 expression of ALDH at higher levels than CAL51, both cell lines express ALDH at much lower levels than the other studies. We first examined the MDA-MB-231 cell line. The control sample shows that basal expression levels are mostly $CD44^{high}/CD24^{high}$ and a large part of the cells remain in this population, even with EP300 overexpression. A shift towards $CD44^{high}/CD24^{low}$ is only seen with CDH1 overexpression. This suggests that a larger part of our control and EP300 overexpressing conditions would be less tumorigenic, invasive and have impaired migration and less able to form metastasis, which is what is shown with previous research (Hu et al., 2015).

This result is interesting as there is a decrease of ALDH, while an increase in the $CD44^{high}/CD24^{low}$, suggesting there is a higher proportion of basal cells, which is counter-intuitive, as ALDH+ cells associate more with the MET phenotype (Liu et al., 2013). As $CD44^{high}/CD24^{low}$ are frequently seen in basal, while ALDH favour the HER2 subtype, it is unclear why the MDA-MB-231 CDH1 overexpression has a larger impact. Overexpressing CDH1 should induce epithelial characteristics; however, we see the opposite, with upregulation of CSC characteristics in the form of $CD44^{high}/CD24^{low}$ expression. Previous studies already have shown that $CD44^{high}/CD24^{low}$ can convert to $CD44^{high}/CD24^{high}$, and vice versa with EMT reversal.

When looking at CAL51, the control sample is largely made up of the $CD44^{low}/CD24^{high}$ which has been reported to be one of the least tumorigenic with smooth cell characteristics (Yan et al., 2013). Also, 50% of its subpopulation is negative for both markers. It is unclear whether this suggests that there is little migration/invasive capacity with respect to the control, and subsequent functional assays need to be performed to determine this. It also seems that EP300 overexpression results in a much larger population of non expressing cells, a decrease in $CD44^{low}/CD24^{high}$ as well as a very negligible increase in $CD44^{high}/CD24^{low}$

. CDH1 overexpression, on the other hand, seems to have a different effect. Similar to the MDA-MB-231 cell line. It is unclear why CDH1 overexpression has a larger impact. The small increase in $CD44^{high}/CD24^{low}$ might also have no impact on invasive characteristics.

In terms of ALDH expression for both cell lines, we are unable to determine whether these over expressions are enough on its own to decrease the CSC characteristics only based on the ALDH marker. It is unclear at this time whether it is because EP300 is exerting influence on CDH1 if they have a synergistic effect. We could test this by inhibition of EP300 and CDH1 to see their influence on ALDH. What does seem to be clear, is that the effect of EP300 overexpression is dependant on the cell line and this affects CSC markers differently. This can be seen in another model of EP300 overexpression. Based on my published FACS results show ALDH+ and $CD44^{high}/CD24^{low}$ population increase in Hs578T with EP300 overexpression (Mahmud et al., 2019). What is interesting is this also shows that the effect of EP300 overexpression is diminished when the *CDH1* promoter is hypermethylated. Implicating epigenetic control of these traits. These results can be seen in **Appendix A.1**. This sort of *CDH1* hypermethylation has been shown by other studies (Sarrio et al., 2003). This however might not be the case for our MDA-MB-231 cells as their *CDH1* promoter hypermethylation is just 13% (Reinhold et al., 2007). Alternatively reasons could be truncations of *CDH1* (Droufakou et al., 2001).

It would also be interesting to see the effect on HIF1α as paclitaxel is known to increase it, making it a good target (Samanta et al., 2014). With its involvement in hypoxia, and tumours favouring hypoxia, it would be interesting to investigate EP300s effect on the hypoxic response. We could conduct mammosphere assays to determine their ability to replicate, or assess the cells in 3D cultures to determine whether the ALDH expression in the necrotic core is affected. Usually, the ALDH is restricted to the inner tumour while $CD44^{low}/CD24^{high}$ is restricted to the leading invasive edge. Furthermore, similar to other studies, we have opted for $CD44^{low}/CD24^{high}$ as the secondary marker to validate our effect on CSC traits. This marker is highly correlated with basal/triple negative cell lines (Ricardo et al., 2011), a portion of these cells which also express ALDH are cited to be tumourigenic (Liu et al., 2014). Its knockdown has been shown to induce CSCs to differentiate into tumour cells without self-renewal capacity (Phame et al., 2011). Furthermore, the reason for a much less ALDH expression in these cell lines than previously reported is unknown. However, it could be an error in the antibody conjugation, which means the cells are there but not showing up. Alternatively, cell clumping can also occur and may result in less populations being recorded, which would reduce the population. A third reason could also be that these cell lines do not express it due to cell heterogeneity and difference of gene expression at different EMT states; or stem in the cell cycle could fluctuate the expression of genes/markers.

In either of those cases, appropriate steps will be taken to mitigate these errors as well as potential for use of alternative markers such as CD133, Integrin Subunit Beta 3 (CD61) (Sin et al., 2017). Integrin Subunit Alpha 6 (CD49f) and Integrin Subunit Beta 1 (CD29) are also shown to be involved in breast cancer stem cell generation (M. Cariati et al., 2008).

Colorectal carcinoma cell line HCT116 seems to express very high levels of ALDH, and knocking out EP300 only has a small effect on increasing this subpopulation. This seems opposite to previously published findings, where this cell line did not express ALDH (Feng et al., 2018). We also find that a large proportion of HCT116 cells express $CD44^{high}/CD24^{low}$, which has been published by another group reporting high levels of CD44 and EPcam expression (Kanwar et al., 2010).This should indicate a highly invasive and motile capability; whereas a small proportion of cells remains as $CD44^{high}/CD24^{high}$. This proportion of cells increases with knockout of EP300. This cell line follows our hypothesis more linearly as we would expect a knockout of EP300 to have reduction on CSC populations.

MCF7 and T47D cells show low expression of $CD44^{high}/CD24^{low}$, which makes it a bad marker for this cell line (Sheridan et al., 2006). Our results show this to be true, as neither the control, nor overexpression of EP300/CDH1 has any effect on increasing $CD44^{high}/CD24^{low}$ populations. Furthermore, the overexpression of EP300 and CDH1 seems to drive the population towards the least motile and more luminal A-like phenotype of $CD44^{high}/CD24^{high}$. This has no indication of whether there is any MET shift as these cells would still be highly epithelial. It is interesting to note that while they both T47D and MCF7 are of the luminal A subtype and ER+, they seem to have different expression profiles for the CD44/CD24 markers. T47D is more $CD44^{low}/CD24^{high}$ on the outset but EP300 overexpression also drives a shift towards $CD44^{high}/CD24^{high}$. Surprisingly, CDH1 overexpression has the opposite effect to EP300, suggesting other pathways that might be involved.

ALDH expression becomes interesting when taken in context of drug resistance traits. Our results show that doxorubicin and paclitaxel affect CSC traits in MCF7 cells in different ways. While doxorubicin increased ALDH+ populations, pactlitaxel decreased them. The overexpression of ALDH in doxorubicin resistant and pactlitaxel resistant MCF7 has been confirmed by other studies (Quayle et al., 2018; Reynolds et al., 2017; Manandhar et al., 2017). However, the decrease of paclitaxel resistant subpopulation through EP300 has not been published yet. This otherwise anomalous result could be due to drug behaviour in context of ER+ as well as their different modes of action. It will increase SOX2 expression, as SOX2 seems to follow an inverse relationship with ALDH in paclitaxel resistant MCF7s. MCF7s normally have high SOX2 expression, which is a marker for stemness, and it has been shown to decrease upon paclitaxel treatment in 2D/3D cultures (Reynolds et al., 2017).

Likewise, while doxorubicin increased ALDH+ cells, this might have further decreased SOX2 expression.

The results are more interesting when we look at the CD44/CD24 ratios. Doxorubicin treatment drives the shift from the $CD44^{low}/CD24^{high}$ population and increases proliferative properties of the cells through $CD44^{high}/CD24^{high}$ populations. A small fraction of highly invasive $CD44^{high}/CD24^{high}$ cells appear, which might explain drug resistance in context of this new invasive population capable of self renewal. This population increases even more dramatically with paclitaxel resistance. It is unclear why it has more effect but likely due to pathways such as MAPK/ AKT PI3K.

Why $CD44^{high}/CD24^{low}$ and ALDH is non conclusive.

Despite the usefulness of these markers illustrated earlier, they are far from the gold standard as some studies dispute their clinical relevance to metastasis (Sheridan et al., 2006; Abraham et al., 2005). Follow up studies have all called for novel markers in breast cancer due to variable $CD44^{high}/CD24^{low}$ expression (Ricardo et al., 2011; Mylona et al., 2008), while co-expression of ALDH and $CD44^{high}/CD24^{low}$ was found to be as little as 1%, which limits these markers used in the clinical setting (Ricardo et al., 2011). Other reasons for doubting their validity is that the $CD24^{high}$ subpopulations could actually be arising from the $CD44^{high}$ cells (Visvader & Lindeman, 2008). Other works by Croker et al. (2009) and Sheridan et al. (2006), suggesting that is conversion of $CD44^{high}/CD24^{low}$ to $CD44^{high}/CD24^{high}$ which results in metastasis.

Despite this, several cell lines, such as MDA-MB-468, show high expression for the $CD44^{high}/CD24^{high}$ marker (Ricardo et al., 2011), which proves potential for the theory that $CD24^{low}$ gets converted to $CD24^{high}$ and vice versa (Meyer et al., 2009), resulting in metastasis from an otherwise differentiated epithelial cell line. Nonetheless, CD44 and CD24 have been proven to play a vital role in metastasis (Hill et al., 2006; Baumann et al., 2005; Bourguignon et al., 2001). In mice experiments of primary xenografts, the co-expression of ALDH and $CD44^{high}/CD24^{low}$ has the greatest capacity for initiating tumours in immune deficient mice (Ginestier et al., 2007). Both of these markers were expressed in a variety of carcinomas such as pancreatic, colon, lung, ovary and prostate (Kryczek et al., 2012; Huang et al., 2009; Eramo et al., 2008; Li et al., 2007; Prince et al., 2007). ALDH+ CSCs are generated by hypoxia (Conley et al., 2012), while $CD44^{high}/CD24^{low}$ cells were located primarily at the tumor-invasive edge (Liu et al., 2014).

Analysis of mRNA expression profiles of 45 primary human breast cancers revealed that there are reciprocal expression patterns between the distinct ALDH and $CD44^{high}/CD24^{low}$ populations. While this was the case, they shared tumorsphere formation gene expression

profiles (Liu et al., 2014), suggesting both of these populations do have a stem-like characteristics , which seems to share a gene expression profile across molecular subtypes (Liu et al., 2014).

Genes like vimentin, ZEB1/ZEB2, β-catenin and MMP9 were enriched in $CD44^{high}$/ $CD24^{low}$ cells (Liu et al., 2014), alluding that it is an EMT phenotype. While the same genes were decreased in ALDH positive populations, however, these cells expressed a higher proliferative capacity through high ki67 expression and multilineage differentiation capacity (Liu et al., 2014), altogether, suggesting mesenchymal ($CD44^{high}$/$CD24^{low}$) and epithelial (ALDH) CSC populations. These distinct populations, and genetic differences outlining mesenchymal and epithelial characteristics, were seen in various established breast cancer cell lines such as SUM149 and MCF7 (Liu et al., 2014). Both cell populations, when purified and regrown on new media, gave rise to a heterogeneous population (Liu et al., 2014). These same distinct properties were also confirmed in the minimally transformed MCF10A cells, and $CD44^{high}$/$CD24^{low}$ and ALDH+ correspond to the mesenchymal EPCAM-/CD49f+ and epithelial EPCAM+/CD49f- (Liu et al., 2014).

The switch between these EMT and epithelial sets could be helped by the tumour microenvironment. Both TGF-β and IL-6 can induce EMT, while their inhibition promotes MET (Liu et al., 2012). This process could also be controlled by miRs (Liu et al., 2012). Linking these distinct populations with the mammary gland stem cells is hard. The mammary gland consists of both luminal and basal lineage (van Keymeylen et al., 2011) and both can generate a mammary tree network (Keller et al., 2012), indicating a high plasticity within both populations.

Early work by some groups indicates that the EPCAM-/CD49f+ population is where the BRCA1 breast carcinomas originate (Proia et al., 2011; Molyneux et al., 2010). However, taking the work done by Liu et al. (2014), it shows a heterogenous EPCAM-/CD49f+ population, and while they are luminal progenitors, they display a plasticity and capacity for self renewal in 6% of this population which is ALDH+ (Liu et al., 2014). These cells are more prone to mutations, and associate with loss of heterozygosity in BRCA1 (Liu et al., 2008)

7.2.5 Future Potential Work

Most studies are limited by the 2D planar growth of cells, which pushes them towards more proliferative characteristics compared to their 3D counterparts (Birgesdotter et al., 2005). These discoveries pushed for 3D cultures which mimic the complex environment of tumours, the gradients of proliferation, necrotic core and cell to cell contacts make it superior, with potentially different signalling mechanisms (Hirschhaeuser et al., 2010). In

fact, these models demonstrated their robustness in a drug resistance response in MCF7 cells (Zhang et al., 2016). When comparing 2D to 3D MDA-MB-231 cultures, paclitaxel treatment prevented microtubule disassembly, while in 3D cultures it prevented spheroid growth into the collagen matrix (Reynolds et al., 2017). 3D models of MDA-MB-231 were more viable after paclitaxel treatment than their 2D counterparts. The viability changed from periphery 34% to 97% in the necrotic core (Reynolds et al., 2017).

Furthermore, MDA-MB-231 3D cultures showed higher populations of ALDH+ cells compared to 2D cultures, with the necrotic core occupying a large part of these ALDH+ cells. These same cells formed more mammospheres (Reynolds et al., 2017). This was also reflected in higher expression of ALDH1A3, SOX2, OCT4 and Nanog in 3D cultures of MDA-MB-231 and these were enriched after treating with paclitaxel (Reynolds et al., 2017). A study investigated the effects of paclitaxel and cisplatin on 2D versus 3D (non diffuse and embedded) models. The results showed that not only do 3D cultures exhibit a heterogeneous response to chemotherapy (core versus periphery), they also exhibit higher CSC traits (Reynolds et al., 2017).

CSC populations can be tested in three ways: expression of CSC markers (Ginestier et al., 2007), testing for self-renewal capacity using mammosphere assays (Grimshaw et al., 2008) and RTqPCR for Aldehyde Dehydrogenase 1 Family Member A3 (ALDH1A3), SOX2, OCT4 and NANOG (Marcato et al., 2011; Charafe-Jauffret et al., 2009; Ben-Porath et al., 2008). To show further proof of EP300 modulating CSC properties, we should also include mammosphere assays, as well as testing for ALDH1A3, SOX2, OCT4 and NANOG. Paclitaxel resistance is related to the activation of the SET Nuclear Proto-Oncogene (SET)/Protein phosphatase 2 (PP2A)/AKT pathways (Zhang et al., 2015). What makes expression of these genes interesting is that OCT4/AKT is responsible for the self renewal of stem cells (Su et al., 2014), while PI3K/AKT are associated with drug resistance and inhibition of apoptosis (Nakanishi et al., 2012; Switzer et al., 2011). If EP300 acts on CSC properties, it could be through these genes. MCF7 cells express high levels of SOX2 and paclitaxel has been shown to decrease SOX2 expression (Reynolds et al., 2017). It is unclear at this time whether EP300s modulation of ALDH+ paclitaxel resistant cells would induce SOX2, or whether EP300s modulation of ALDH+ doxorubicin resistant cells would decrease SOX2. ALDH1A3 is known to be methylated in MCF7 cells (Shames et al., 2006). As there is some interaction between methylation and acetylation states, it would be interesting to see if the expression of this gene changes, while nanog mediates drug resistance and radio resistance in MCF7 (Harati et al., 2019; Jeter et al., 2011).

7.2.6 Overall Conclusion

Overall the results presented here are inconclusive and seem to reflect some of the concerns shown by other authors that these markers are inconsistent. Therefore, it would be beneficial to use a larger panel of markers, or solely focus on CSC traits through functional assays like mammosphere formation assays or colony formation in soft agar. A 3D culture would also be better reflective of the heterogeneous nature of the tumours.

Chapter 8

EP300 influence on Migration and Invasion

8.1 Introduction

8.1.1 Types of Migration

As covered earlier in the introductory **Chapter 1**, metastasis begins with invasion of the detached tumour cells into the stroma, leading up to the intravasation step into the blood. Metastasis is one of the hallmarks of cancer (Chaffer et al., 2011), and the very first step is for the cells to break through the basement membrane into the stroma. In many ways the tumour stroma and the microenvironment interact with the cells to promote this migration. Cell migration is vital in many steps of the progression of metastasis such as: local invasion, intravasation and extravasation of blood vessel and colonising secondary sites (Chaffer et al., 2011), which makes it an important characteristic to study.

Cancer cells are constantly adapting during their migration, and change their morphology during each stage of migration (Friedl et al., 2011). This migration can be both as an individual cell, or as a well organised sheet of cells. The choice between individual or organised migration is down to the cells molecular phenotype. Epithelial cells prefer to migrate in organised groups, whereas mesenchymal cells can also display individual migration. We will cover some of these now.

Single cell migration does not require cell-cell interaction or displays very little of it. There are different phenotypes within this characteristic, such as the amoeboid and mesenchymal phenotypes. The amoeboid display a round cell morphology and has three movement patterns. Cells can either have short protrusions and move fast (0.4-5 μm/min), show chaotic movement with blebs, or display proteolytic activity and move slowly at 0.1

μm/min. The mesenchymal phenotype on the other hand is more spindle shaped with long protrusions. They can either have a rapid movement pattern of protrusions 0.4 μm/min, or a relatively slow net movement of 0.2 μm/min due to the lagging rear of the cell. Multicellular streaming is something which is between a single and collective migration. These cells migrate together in one path at a rate of 1-2 μm/min, with a morphology between amoeboid and mesenchymal (Friedl et al., 2011). Collective migration involved cell-cell adhesions and follow a unidirectional movement. These can be as a sheet or a liner strand, or by multi cell diameter strands (Friedl et al., 2011). Their morphology can be both epithelial and mesenchymal. This migration type is the slowest due to the volume of cells involved, at a rate of 0.01-0.05 μm/min or 0.2-1μm/min (Alexander et al., 2013; Khalil et al., 2010; Prasad et al., 2007).

On an individual scale each cell migrates by increasing cell contraction through the Rho pathway. The rate of this contraction differs between amoeboid and mesenchymal which is much faster and with lower adhesion (Bergert et al., 2012; Sahai et al., 2003). One other distinction of the mesenchymal phenotype is that it can switch between single-cell, stream or collective migration by regulating N-cadherin levels (Shih et al., 2012). However epithelial origin tumours, such as breast cancer, are more likely to be display collective migration (Bronsert et al., 2014), which originate in a neoplastic gland and protrude out of the basement membrane in clusters, such as observed in colorectal and breast cancer (Lino-Silva et al., 2018; Scherz-Shouval et al., 2014). These invading cells will display the canonical EMT markers such as downregulated E-cadherin, upregulated N-cadherin, loss of apical basal polarity as well as changes in gene expression and morphology (Thiery et al., 2002). Despite these observations, mesenchymal cells are rarely observed in imaging studies (Bronsert et al., 2014). This relates to the unidentified as of yet origin of metastasis. Such as presence of stem cells, aggregated mutations, or intravasation of tumour cells into the circulation. There is a class of cells called the circulating tumour cells which have been observed to form tumours, it is unclear whether they are the primary cause at this time (Aceto et al., 2014). Nevertheless, there is a clear favour towards adopting the epithelial glandular morphology of the primary tumour, seen in secondary metastasis, which is either a result of the cell clusters migrating in sheets which preserves the structure, or the reversion into the MET phenotype (Brabletz et al., 2005). This intiation of invasion and migration might also be regulated by other factors such as asparaargine synthase, which is a metabolic enzyme that correlated with metastasis development (Knott et al., 2018).

8.1.2 EMT and Migration

EMT can drive local metastasis and invasion, as part of collective migration, the cells still express E-cadherin as a marker, cell junctions and adhesion markers, but their leading edge has epithelial plasticity and differs in marker expression (Friedl et al., 2009). Furthermore, single cell invasion is more likely to promote distal site metastasis (Hannahan et al., 2011), after which an MET programme is initiated to colonise the new site (Valastyan et al., 2011). This induction is mainly brought on by the TGF-β signalling, which is a vital pathway in this process. It has been shown that this pathway is activated by cells at the leading edge to promote epithelial plasticity, and allow them to switch between single-cell and collective migration (Giamperi et al., 2009). Notably, there are several morphological changes that TGF-β induces, especially in the cytoskeleton, which allows for intravasation and migration (Eckert et al., 2011; Yamguchi et al., 2005). These changes fall under the induction of invadipodia formation that aid movement through TGF-β mediated stimulation of transforming growth factor beta 1 induced transcript 1 (TGFB1I1) (Pignatelli et al., 2012). As well as a switch in its cytoskeleton from myosin IIC strands to myosin IIB and phosphorylation of myosin heavy chain IIA, which regulates filament dynamics and induces invasion (Beach et al., 2011). While EMT is involved in the metastatic process, no clear link is yet shown. An attempt is made to show the genetic diversity of metastatic cells to elucidate this link. EMT is also extensively discussed in the introduction.

8.1.3 Genetic Expression of Metastatic Cells

Metastasis is a complex process which can be inititated by somatic mutations in p53, cyclin dependant kinase inhibitor 2A (CDKN2A), phosphatase and tensin homolog (PTEN), phosphatidylinositol-4,5-bisphosphate 3-kinase catalytic subunit alpha (PIK3CA), and retinob lastoma (RB1), 75% of these gene defects were associated with DNA repair (Robinson et al., 2017; Birkbak et al., 2020). As previously described in **Chapter 7** on drug resistance and stemness, the intratumoural population is heterogenous, which makes studying genetic diversity of these cells challenging. This is somewhat tackled by attempting to show commonality in traits like adapting to hypoxia through HIF-α. Which not only primes the metastatic niche by secreting LOX, but also via its effector mediator AXL promotes metastasis and migration (Rankin et al., 2016). These cells thereby shift their metabolic needs by promotion of monocarboxylate transporter 1 (MCT1) by shifting away from glycolysis (Tasdogan et al., 2020).

8.1.4 Epigenetic Factors

Metastasis and indeed migration of these cells can be influenced by a patient's immune response (Kaur et al., 2019). This somewhat decreased immunity in elderly patients has a paradoxical effect by which there are fewer migration into the lymph nodes but more distal metastasis (Ecker et al., 2019). Likely reflective of a shift towards an MET or $CD44^{high}/CD24^{high}$ characteristic, which although has decreased migration capacity, can still form metastatic niches due to higher adhesion capabilities. This however could also be due to easier collagen tracks that these cells can navigate through in the lymph nodes of elderly individuals (Ecker et al., 2019). Similarly the same paper also discussed that other advantages such as epithelial cell permeability, as well as cadherin dependant cell-cell adhesion can also play a role in promoting these cells (Ecker et al., 2019).

8.1.5 Cancer Cell Invasion -ECM Remodelling

The migrating cells briefly mentioned earlier exert their influence on the ECM by remodelling collagen by affecting the stiffness forming cell tracks. A process that they hijack and which is usually regulated by matrikines (Maquart et al., 2004). One of the molecules that cells at the leading edge upregulate are MMPs ,which not only promote invasion and survival, but cell proliferation and degradation of the ECM (Moss et al., 2012). Various ECM associated proteins also promote cancer cell growth by providing nutrients and positive growth signalling. Suppressors of this movement are lunican, which can initiate MET and downregulate Matrix Metallopeptidase 14 (MM14) (Pietraszek et al., 2014; Karamanou et al., 2017) and hyaluronic acid (HA) which is a main component of the stroma and its expression is essential to interaction with CD44 receptors on cancer cells (Passi et al., 2019; Chanmee et al., 2016). HA can also enhance EMT through ZEB1 and HA synthase 2 (HAS2) (Zhang et al 2016). HAS2, which induces TGF-β (Porsch et al., 2013), interact with TAMs (Okuda et al., 2012). In particular, its low molecular weight HA counterpart, is vital in cell migration and invasion (Wu et al., 2015).

Integrins, which serve as a vital cell adhesion receptor, have a play a large role in tumour progression (Hamidi et al., 2018), including, but not limited to, influencing the growth factor receptor signalling to promote migration and invasion (Hamidi et al., 2018). E-cadherin is one of those key molecules that participates in this process. E-cadherin holds therapeutic importance not only in its role in EMT but as a mediator for attachment and dissemination of metastatic cells and promoting survival blocking of reactive oxygen species (Padmanaban et al., 2019). As such, the influence of EP300 on E-cadherin expression, might be a potential therapeutic target.

8.1.6 Changes in the Environment

As the tumour cells migrate, they influence their environment to clear their path. The stroma mainly consisting of collagen type I, is organised into a mesh, which is observed to have a more ordered straight morphology at the tumour border and provides cell tracks for invading cells to follow (Conklin et al., 2010). The reorganisation of this stroma is usually aided by cancer associated fibroblasts (CAFs), by secreting enzymes like LOX (Cox et al., 2013). This reorganisation results in a stiffer stroma and area of high tissue density in breast cancer (Ursin et al., 2005; Alowami et al., 2003). Otherwise, in areas of low density, results in reversed TGF-β signalling and low cell migration (Giamperi et al., 2009). The proximity towards blood vessels is also a vital factor for increasing cell migration due to the presence of chemokines and cytokines as well as nutrients (Gligorejevic et al., 2014). TGF-β seems to play an important role in initiating the switch towards amoeboid migration in mouse models of mammary tumours (Giamperi et al., 2010).

8.1.7 Gene Expression in Migration

The classical makers for cell migration and proliferation in breast cancer are ki67 and Targeting protein for Xklp2 (TPX2) (Li et al., 2015). These are known to be predictors of poor prognosis in patient survival. Currently there exists three gene signatures that correlate with cancer progression and formation of metastasis (Yu et al., 2007; Wang et al., 2005; van't Veer et al., 2002). Analysing the TCGA dataset, higher levels of migration are seen in Her2 and basal subtypes, as well as tumour grade increases, and correlates to patient overall survival (Nair et al., 2019). The same study found genes which suppress migration qualities in MDA-MB-231 cells and correlate with expression of genes involved in migration and invasion in breast cancer, as well as genes that regulate enhancers of migration, and cell adhesion and maintenance of cell junctions (Nair et al 2019). These same gene types involve in cell adhesion, cell junction and maintenance of the cytoskeleton have already been implicated by previous studies (Friedl et al., 2017; Nagano et al., 2012; Yamaguchi et al., 2007). The same study concluded that as migration levels are a good predictor of patient survival, those patients that have high predicted migratory potential, benefit from drugs targeting the cytoskeleton making it a good biomarker (Nair et al., 2019).

8.2 Analysis of EP300 on Migration and Invasion

8.2.1 Hypothesis

The hypothesis is that by overexpressing EP300 in the CAL51 and MDA-MB-231 mesenchymal cell lines we will induce an MET -to- EMT switch, reconstituting the expression of E-cadherin, by which we will have a less invasive cell line with less migratory capacity. We will try to demonstrate the opposite in the epithelial cell lines T47D and MCF7, where we will downregulate EP300 and try to induce an EMT-to-MET switch, which should result in a more invasive cell line with high migratory capacity.

8.2.2 Aim

1. Demonstrate a correlation between EP300 and CDH1 overexpression and directional migration.
    - Test the effect of EP300 and CDH1 overexpression on directional migration using a wound healing assay with the mesenchymal breast cancer cell lines: CAL51 and MDA-MB-231
    - Test effect of EP300 downregulation on directional migration using a wound healing assay with the epithelial breast cancer cell lines: MCF7 and T47D
    - Test effect of EP300 knockout on directional migration using a wound healing assay with a colorectal cancer cell lines: HCT116
2. Demonstrate a correlation between EP300 and CDH1 overexpression and random migration.
    - Test effect of EP300 and CDH1 overexpression on random migration using a cell tracking assay with the mesenchymal breast cancer cell lines: CAL51 and MDA-MB-231
    - Test effect of EP300 downregulation on random migration using a cell tracking assay with the epithelial breast cancer cell lines: MCF7 and T47D
    - Test effect of EP300 knockout on random migration using a cell tracking assay with the colorectal cancer cell lines: HCT116
3. Demonstrate a correlation between EP300 and CDH1 overexpression and chemotaxis mediated cell invasion.

- Test effect of EP300 and CDH1 overexpression on chemotaxis mediated cell invasion, using a matrigel assay with the mesenchymal breast cancer cell lines: CAL51 and MDA-MB-231
- Test effect of EP300 knockdown on chemotaxis mediated cell invasion, using a matrigel assay with the epithelial breast cancer cell lines: MCF7 and T47D
- Test effect of EP300 knockout on chemotaxis mediated cell invasion, using a matrigel assay with the colorectal cancer cell lines: HCT116

8.2.3 Results

Overexpression of EP300 and CDH1 leads to decreased directional migration in mesenchymal breast cancer cell lines.

In order to study the effects of EP300 and CDH1 on wound closure, we used some of the cell lines we had used previously for our gene expression analysis in **Chapter 4**. The hypothesis was tested in a mesenchymal breast cancer cell line CAL51 in context of EP300 overexpression, CDH1 overexpression and compared to the basal expression in the same cell line with a control empty vector.

In **Figure 8.1**, we observe the breast cancer cell line CAL51 in three conditions: a control sample with an empty vector (CAL-EV), an EP300 overexpression (CAL-EP300) and a CDH1 overexpression (CAL-CDH1). In **Figure 8.2**, we observe the breast cancer cell line MDA-MB-231 in three conditions: a control sample with an empty vector (MDA-EV), an EP300 overexpression (MDA-EP300) and a CDH1 overexpression (MDA-CDH1). All three samples were seeded at a density of 100,000 cells per well into a 96 well plate, from which 5 positions were selected, and 1 image was taken for each well and respective position every 30 minutes for 24 hours. The images were then analysed, by monitoring the wound closure using the formula : $(A0-At)/ (A0 \times 100\%)$, where A0 represents the area of the scratch at 0 h, and At represents the area of the wound at indicated time point. The methodology is based on previously published research by (Holand et al., 2014).

Figure 8.1a is a visual representation of one well analysed for this experiment in CAL51. The area highlighted in yellow, represents the wound. Each panel represents the respective conditions and the time point of 0 h at the start and 24 h at the end of the experiment. **Figure 8.1b** shows the compiled data for three replicates for CAL51 and demonstrates a decrease in wound closure when EP300 and CDH1 is reintroduced into the cell line. At 12 h the control sample is 13% wound closure, EP300 has 14% wound closure and CDH1 has 6%. There is no significant difference between the control and EP300 sample at this time point. While when comparing CDH1 with the control sample it is 7% less ($p<0.001$), and 8% less

($p<0.001$) than EP300. At 24 h the control has 27% wound closure, EP300 has 23.8%, while CDH1 has 12.5%. There is no significant difference between the control and EP300 sample at this time point. While when comparing CDH1 with the control sample it is 14.5% less ($p<0.001$), and 11.3% less ($p<0.001$) than EP300. After 48 h the control has 47% wound closure, EP300 has 36%, while CDH1 has 24%. There is a significant difference between the control and EP300 sample, as EP300 is 11% less ($p<0.001$). While when comparing CDH1 with the control sample it is 23% less ($p<0.001$), and 12% less ($p<0.001$) than EP300.Overall CDH1 has the slowest rate of wound closure and smallest total overall area of wound closed in CAL51 cells.

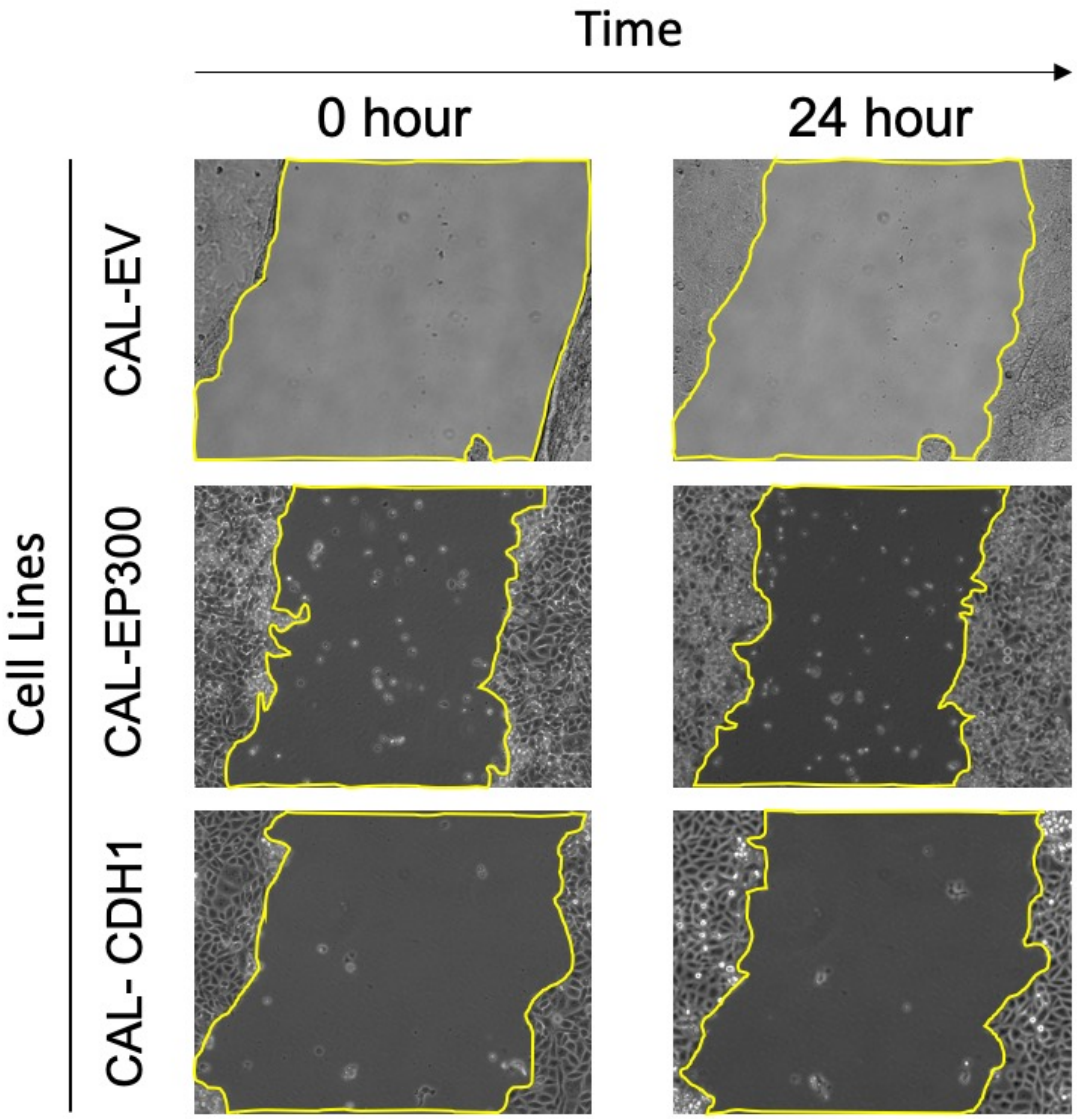

(a)

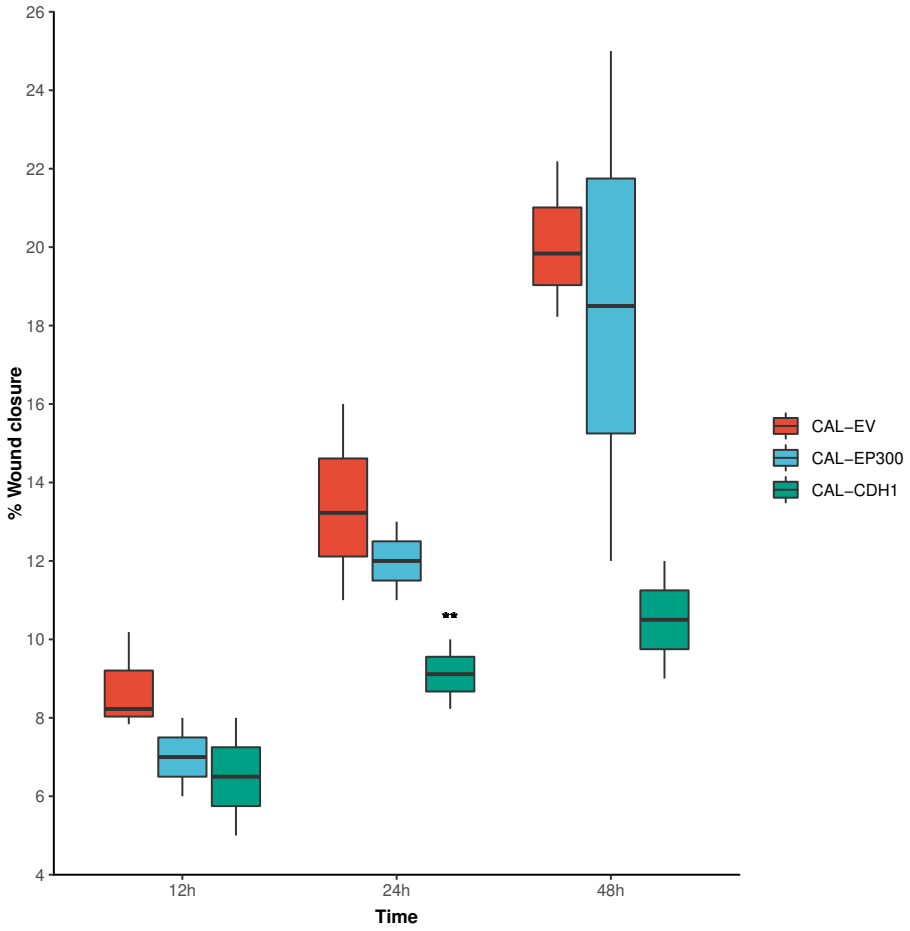

(b)

Fig. 8.1 Overexpression of EP300 decreases wound healing in CAL51 breast cancer cells. (A) Images show CAL51 cell lines transfected with empty vector control (CAL-EV), EP300 overexpressing (CAL-EP300), and CDH1 overexpressing (CAL-CDH1), plated onto 6 well plates and imaged over 24 h, over a 2-hour interval. Quantification of the wound closure was done using the formula (A0−At)/A) x 100%, where A0 represents the area of the wound at 0h and At represents the area of the wound at indicated time points as described (Holand et al., 2014). (B) Graph represents the summary of the average wound closure area + SD. Statistical analysis was performed using ANOVA, comparing the shEV empty vector control (CAL-EV), and cells overexpressing EP300 (CAL-EP300) and CDH1 overexpressing (CAL-CDH1), (P<0.05*, **P<0.01, ***P<0.001).

Figure 8.2a is a visual representation of one well analysed for this experiment in MDA-MB-231. The area highlighted in yellow, represents the wound. Each panel represents the respective conditions and the time point of 0 h at the start and 24 h at the end of the experiment. **Figure 8.2b** shows the compiled data for three replicates for MDA-MB-231 and demonstrates a decrease in wound closure when EP300 and CDH1 is reintroduced into the cell line. At 2 h the control sample is 14% wound closure, MDA-EP300 has 4% wound closure and MDA-CDH1 has 9%. EP300 overexpression decreases wound closure by 10% ($p<0.01$), while CDH1 overexpression decreases wound closure by 5% ($p<0.01$) compared to the control.

When comparing EP300 with CDH1, EP300 is 5% less than CDH1 ($p<0.01$). At 4 h the control sample is 28% wound closure, EP300 has 10% wound closure and CDH1 has 22%. EP300 is the only significant result at this timepoint, having decreased wound closure by 18% ($p<0.001$). At 6 h the control sample is 39% wound closure, EP300 has 14% wound closure and CDH1 has 32%. EP300 is the only significant result at this timepoint, having decreased wound closure by 25% ($p<0.001$). At 8 h the control sample is 54% wound closure, EP300 has 11% wound closure and CDH1 has 41%. EP300 is the only significant result at this timepoint, having decreased wound closure by 43% ($p<0.001$). At 10 h the control sample is 63% wound closure, EP300 has 18% wound closure and CDH1 has 56%. EP300 decreases wound closure by 45% ($p<0.001$), while CDH1 decreases it by 7% ($p<0.01$). When comparing both EP300 and CDH1, EP300 has less wound closure by 11% ($p<0.001$). At 12 h the control sample is 68% wound closure, EP300 has 19% wound closure and CDH1 has 55%. EP300 decreases wound closure by 49% ($p<0.001$), while CDH1 decreases it by 13% ($p<0.01$). When comparing both EP300 and CDH1, EP300 has less wound closure by 36% ($p<0.001$). At 14 h the control sample is 77% wound closure, EP300 has 25% wound closure and CDH1 has 62%. EP300 decreases wound closure by 52% ($p<0.001$), while CDH1 decreases it by 15% ($p<0.01$). When comparing both EP300 and CDH1, EP300 has less wound closure by 37% ($p<0.001$). At 16 h the control sample is 82% wound closure, EP300 has 32% wound closure and CDH1 has 69%. EP300 decreases wound closure by 50% ($p<0.001$), while CDH1 decreases it by 13% ($p<0.01$). When comparing both EP300 and CDH1, EP300 has less wound closure by 37% ($p<0.001$). At 18 h the control sample is 87% wound closure, EP300 has 35% wound closure and CDH1 has 74%. EP300 is the only significant result at this time point, having decreased wound closure by 52% ($p<0.001$). At 20 h the control sample is 90% wound closure, EP300 has 39% wound closure and CDH1 has 80%. EP300 is the only significant result at this time point, having decreased wound closure by 51% ($p<0.001$). At 22 h the control sample is 94% wound closure, EP300 has 43% wound closure and CDH1 has 85%. EP300 decreases wound closure by 51% ($p<0.001$),

while CDH1 decreases it by 9% ($p<0.05$). When comparing both EP300 and CDH1, EP300 has less wound closure by 42% ($p<0.001$). At 24 h the control sample is 98% wound closure, EP300 has 48% wound closure and CDH1 has 90%. EP300 decreases wound closure by 50% ($p<0.001$), while CDH1 decreases it by 8% ($p<0.01$). When comparing both EP300 and CDH1, EP300 has less wound closure by 42 % ($p<0.001$). Overall EP300 overexpression decreased wound healing more significantly than CDH1 overexpression in MDA-MB-231 cells.

To summarise, this section we can see that in both CAL51 and MDA-MB-231, the overexpression of EP300 and subsequent upregulation of CDH1, leads to the decreased directional migration.

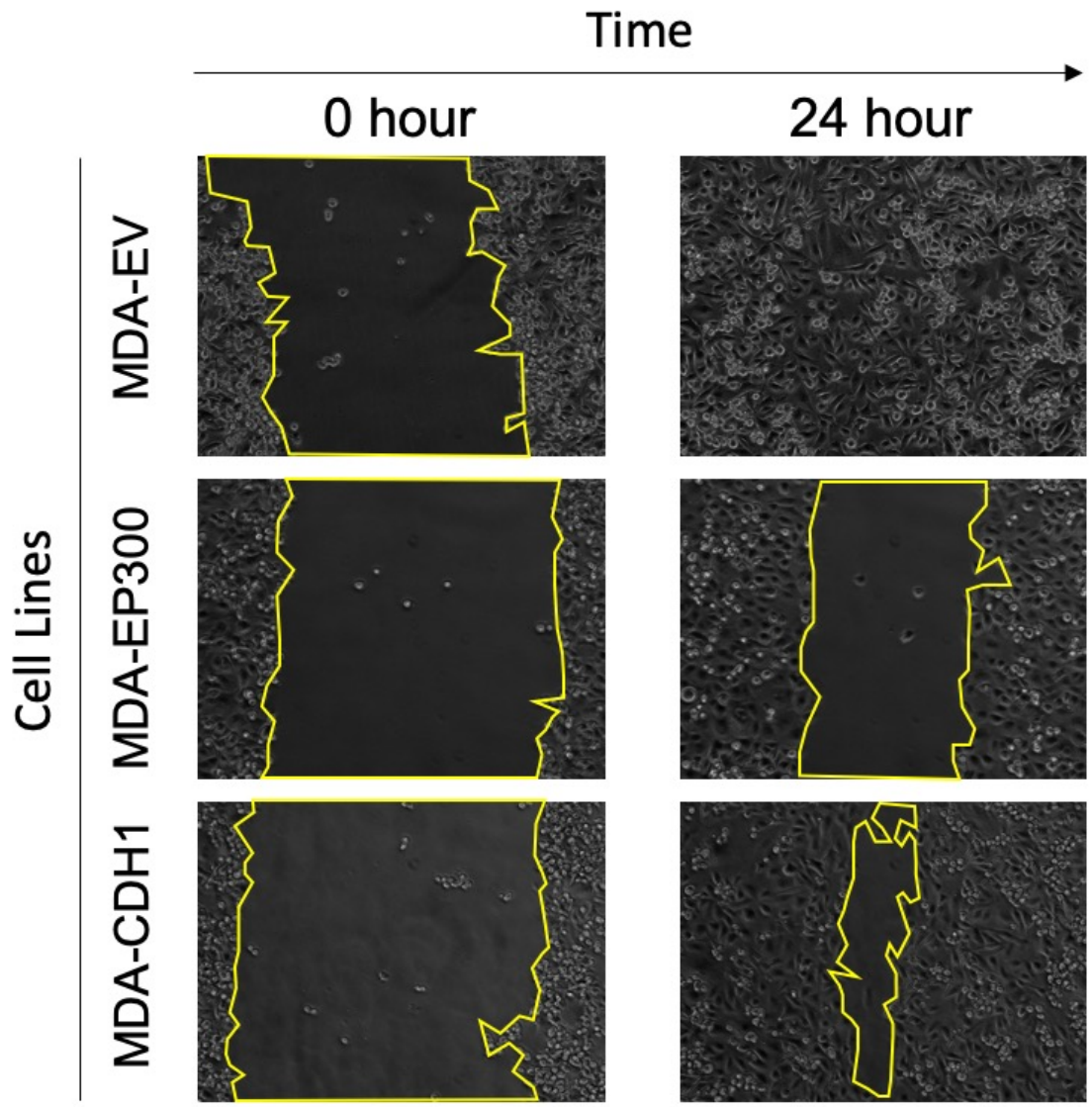

(a)

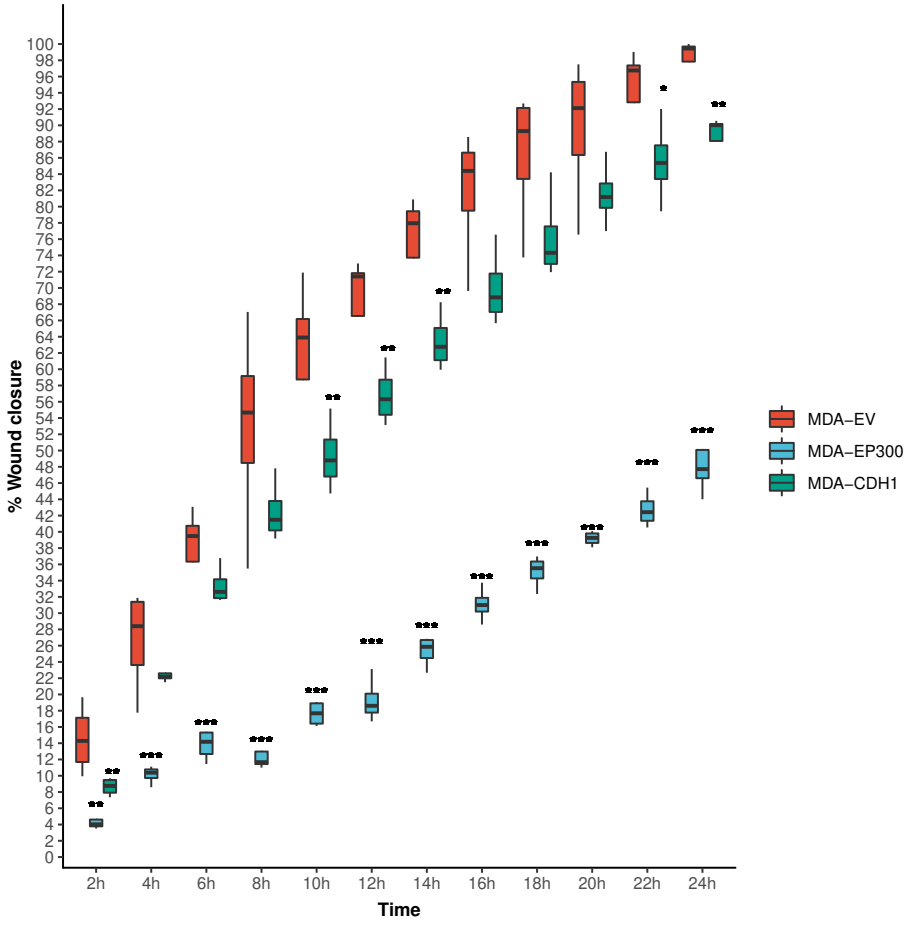

(b)

Fig. 8.2 Overexpression of EP300 decreases wound healing in MDA-MB-231 breast cancer cells. (A) Images show MDA-MB-231 cell lines transfected with empty vector control (MDA-EV), EP300 overexpressing (MDA-EP300), and CDH1 overexpressing (MDA-CDH1), plated onto 6 well plates and imaged over 24 h, over a 2-hour interval. Quantification of the wound closure was done using the formula (A0−At)/A) x 100%, where A0 represents the area of the wound at 0 h and At represents the area of the wound at indicated time points as described (Holand et al., 2014). (B) Graph represents the summary of the average wound closure area + SD. Statistical analysis was performed using ANOVA, comparing the shEV empty vector control (MDA-EV), and cells overexpressing EP300 (MDA-EP300) and E-cadherin (MDA-CDH1), (P<0.05*, **P<0.01, ***P<0.001).

Downregulation of EP300 leads to increased directional migration in epithelial breast cancer cell lines.

In order to study the effects of EP300 on wound closure, we used some of the cell lines we had used previously for our gene expression analysis in **Chapter 4**. The hypothesis was tested in a epithelial breast cancer cell line MCF7 and T47D in context of EP300 downregulation and compared to the basal expression in the same cell line with a control empty vector. In **Figure 8.3**, we observe the breast cancer cell line MCF7 in three conditions: a control sample with an empty vector (MCF7-EV), an EP300 knockdown (sh EP300 I) and a second EP300 knockdown with a different vector (sh EP300 II). **Figure 8.4** we observe the breast cancer cell line T47D in three conditions: a control sample with an empty vector (T47D-EV), an EP300 knockdown (sh EP300 I) and a second EP300 knockdown with a different vector (sh EP300 II). All three samples were seeded at a density of 100,000 cells per well into a 96 well plate, from which 5 positions were selected, and 1 image was taken for each well and respective position every 30 minutes for 24 hours. The images were then analysed, by monitoring the wound closure using the formula : $(A0-At)/ (A0 \times 100\%)$, where A0 represents the area of the scratch at 0 h, and At represents the area of the wound at indicated time point.

Figure 8.3a is a visual representation of one well analysed for this experiment in MCF7 cells. The area highlighted in yellow, represents the wound. Each panel represents the respective conditions and the time point of 0 h at the start and 24 h at the end of the experiment. **Figure 8.3b** shows the compiled data for three replicates for MCF7 and demonstrates an increase in wound closure when EP300 (sh EP300 I and sh EP300 II) is downregulated in the cell line. At 12 h the control sample is 6% wound closure, sh EP300 I has 13% wound closure and sh EP300 II has 12%. There is no significant difference between the control and the other conditions at this time point. At 48 h the control has 21% wound closure, sh EP300 I has 23%, while sh EP300 II has 26%. There is no significant difference between the control and the other conditions at this time point. However there seems to be a trend that overexpression results in more wound closure.

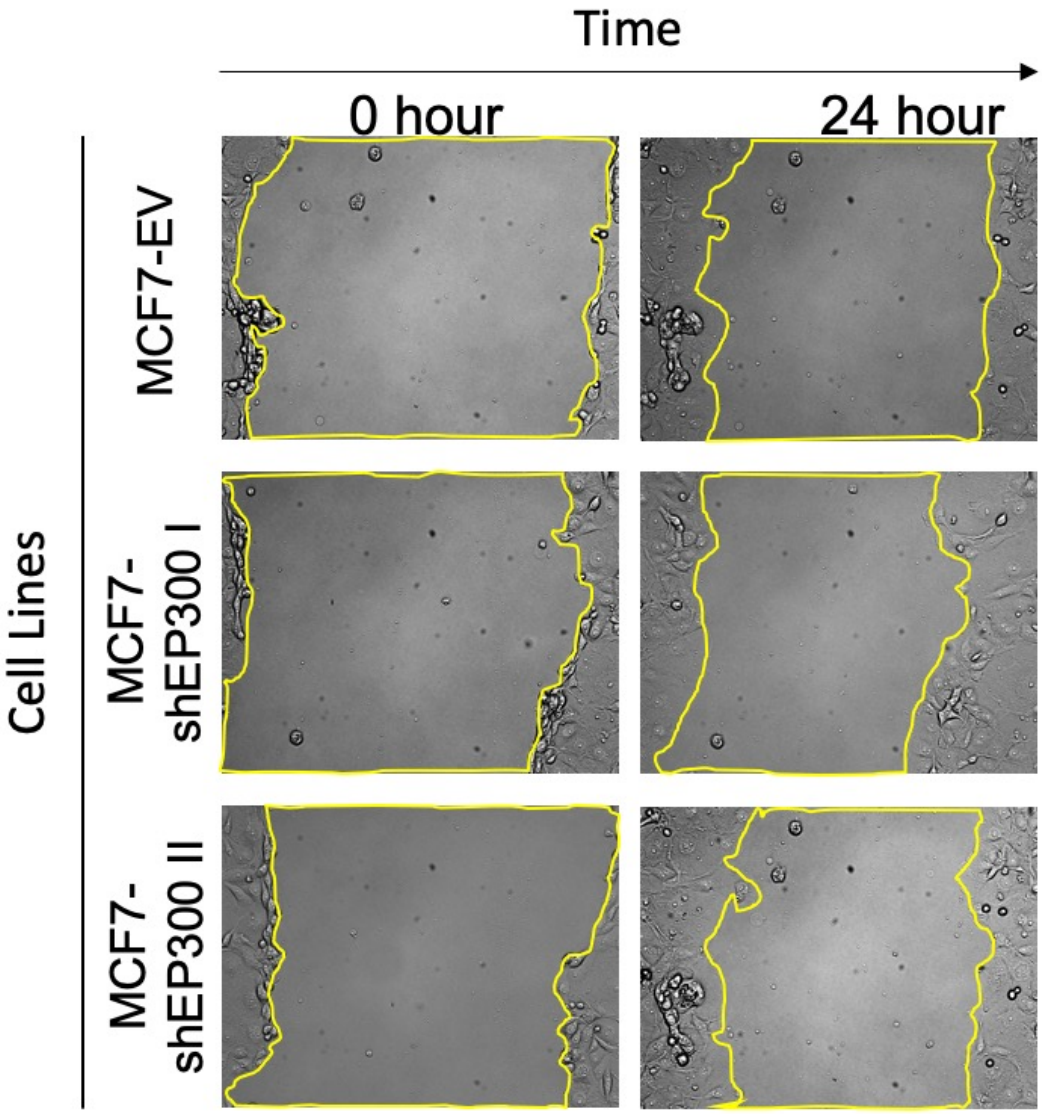
Time
0 hour
24 hour
Cell Lines
MCF7-EV
MCF7-shEP300 I
MCF7-shEP300 II

(a)

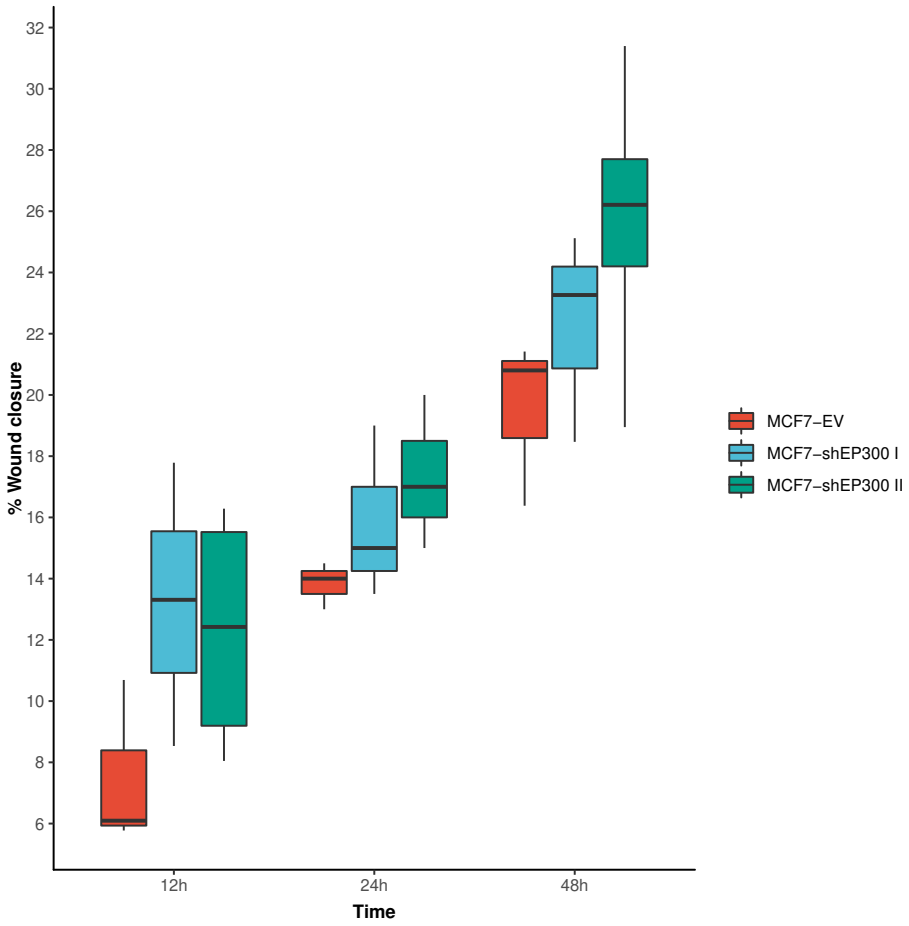

(b)

Fig. 8.3 Downregulation of EP300 increases wound healing in MCF7 breast cancer cells. (A) Images show MCF7 cell lines transfected with empty vector control (MCF7-EV), and two vectors for EP300 downregulation (MCF7-shEP300 I & MCF7-shEP300 II), plated onto 6 well plates and imaged over 24 h, over a 2-hour interval. Quantification of the wound closure was done using the formula (A0−t)/A) x 100%, where A0 represents the area of the wound at 0 h and At represents the area of the wound at indicated time points as described (Holand et al., 2014). (B) Graph represents the summary of the average wound closure area + SD. Statistical analysis was performed using ANOVA, comparing the shEV empty vector control (MCF7-EV), and cells with EP300 downregulation (MCF7-shEP300 I & MCF7-shEP300 II), (P<0.05*, **P<0.01, ***P<0.001).

Figure 8.4a is a visual representation of one well analysed for this experiment in T47D cells. The area highlighted in yellow, represents the wound. Each panel represents the respective conditions and the time point of 0 h at the start and 24 h at the end of the experiment. **Figure 8.4b** shows the compiled data for three replicates for T47D and demonstrates a decrease in wound closure when EP300 (sh EP300 I and sh EP300 II) is knocked down in the cell line. At 12 h the control sample is 16% wound closure, sh EP300 I has 8% wound closure and sh EP300 II has 9%. Wound closure is significantly decreased by 8% in sh EP300 I ($p<0.05$) and by 7% in sh EP300 II when compared to the control. However no significant difference is seen between sh EP300 I and sh EP300 II. At 4 8h the control has 23% wound closure, sh EP300 I has 18%, while sh EP300 II has 19%. There is no significant difference between the control and sh EP300 II or between sh EP300 I and sh EP300 II. While there is a significant difference between the control and sh EP300 I, which results in a 5% decrease ($p<0.01$). Overall there seems to be a trend for decreased wound closure with the knockdown of EP300 in T47D cells.

To summarise, it seems that the downregulation of EP300 promotes proinvasive/migratory traits in epithelial breast cancer cell lines T47D and MCF7. Which links our hypothesis of EP300 modulation of CDH1 and its effect on EMT traits.

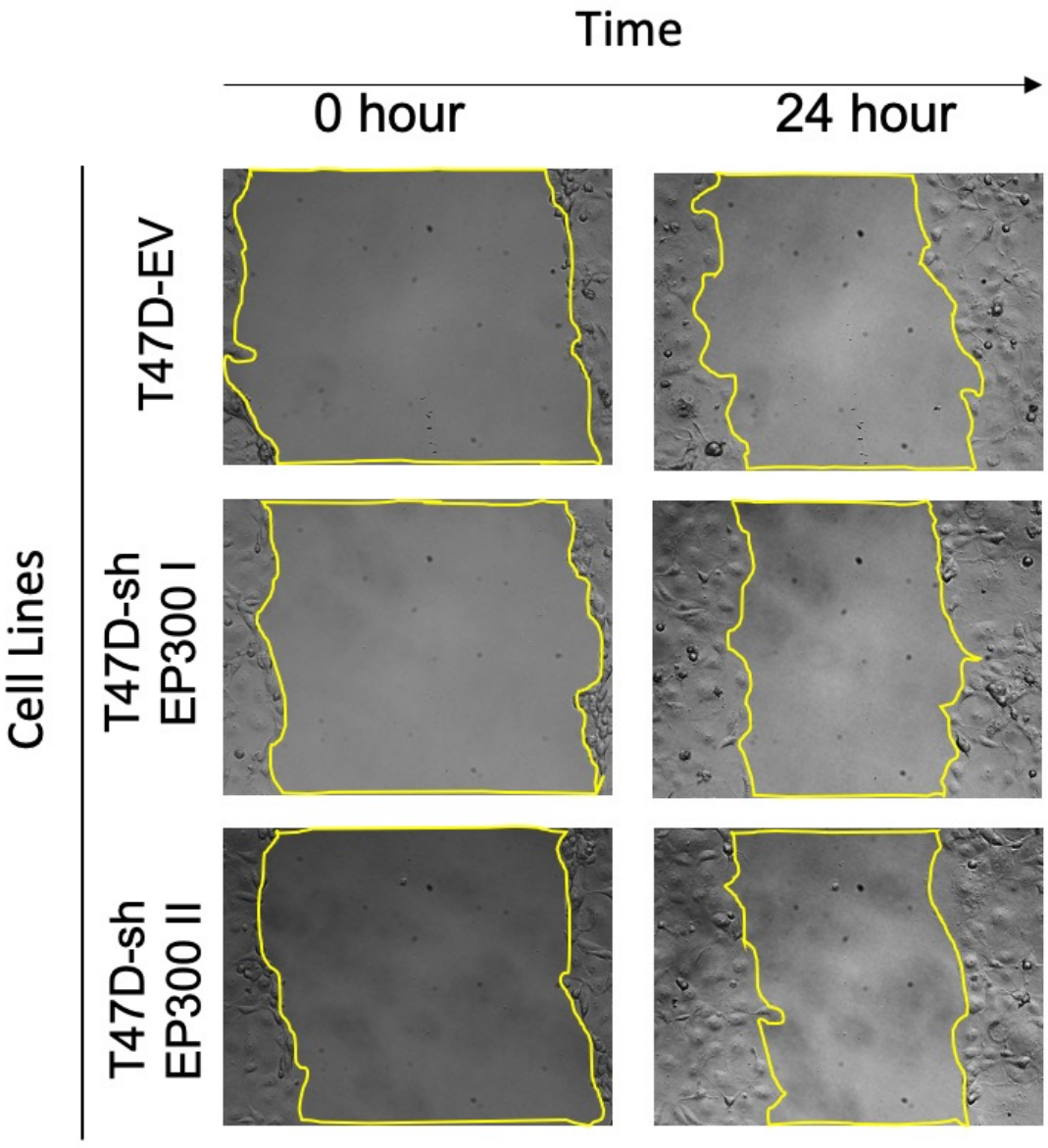
Time
0 hour
24 hour
Cell Lines
T47D-EV
T47D-sh EP300 I
T47D-sh EP300 II

(a)

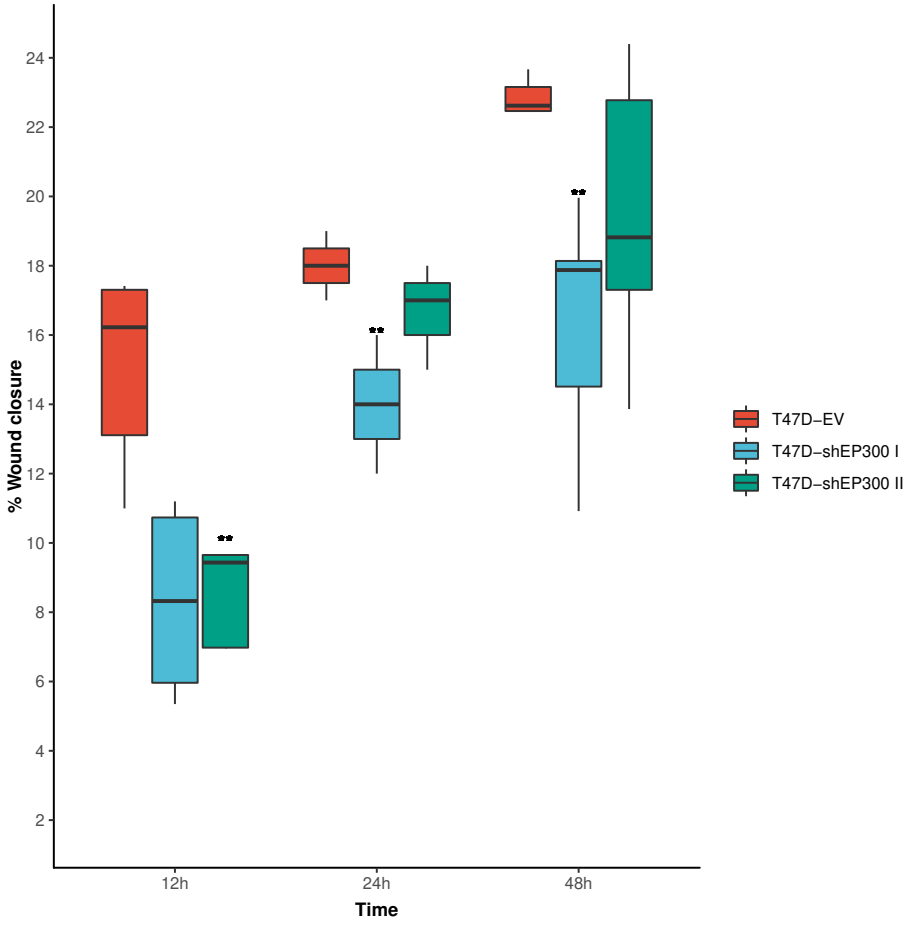

(b)

Fig. 8.4 Downregulation of EP300 increases wound healing in T47D breast cancer cells. (A) Images show T47D cell lines transfected with empty vector control (T47D-EV), and two vectors for EP300 downregulation (T47D-shEP300 I & T47D-shEP300 II), plated onto 6 well plates and imaged over 24 h, over a 2-hour interval. Quantification of the wound closure was done using the formula (A0−At)/A) x 100%, where A0 represents the area of the wound at 0 h and At represents the area of the wound at indicated time points as described (Holand et al., 2014). (B) Graph represents the summary of the average wound closure area + SD. Statistical analysis was performed using ANOVA, comparing the shEV empty vector control (T47D-EV), and cells with EP300 downregulation T47D-shEP300 I & T47D-shEP300 II (P<0.05*, **P<0.01, ***P<0.001).

Knockout of EP300 leads to decreased directional migration in colorectal cancer cell lines.

In order to study the effects of EP300 on wound closure, we used some of the cell lines we had used previously for our gene expression analysis in **Chapter 4**. The hypothesis was tested in a colorectal cancer cell line HCT116 in context of EP300 knockout and compared to the basal expression in the same cell line with a control empty vector.

Figure 8.5a is a visual representation of one well analysed for this experiment in HCT116. The area highlighted in yellow, represents the wound. Each panel represents the respective conditions and the time point of 0 h at the start and 24 h at the end of the experiment. **Figure 8.5b** shows the compiled data for three replicates for HCT116 and demonstrates a decrease in wound closure when EP300 (KO EP300) is knocked out in the cell line. At 12 h the control sample is 8% wound closure, KO EP300 has 26% wound closure. Wound closure is significantly increased by 18% in KO EP300 ($p<0.001$). At 24 h the control sample is 16% wound closure, KO EP300 has 45% wound closure. Wound closure is significantly increased by 29% in KO EP300 ($p<0.001$). At 48 h the control sample is 29% wound closure, KO EP300 has 75% wound closure. Wound closure is significantly increased by 46% in KO EP300 ($p<0.001$). Overall there seems to be a trend for an increase in wound closure after EP300 knockout in HCT116 colon carcinoma cells.

Therefore in colorectal cancer, EP300 functions as a promoter of directional migration as its knockdown abrogated this function in the HCT116 cell line.

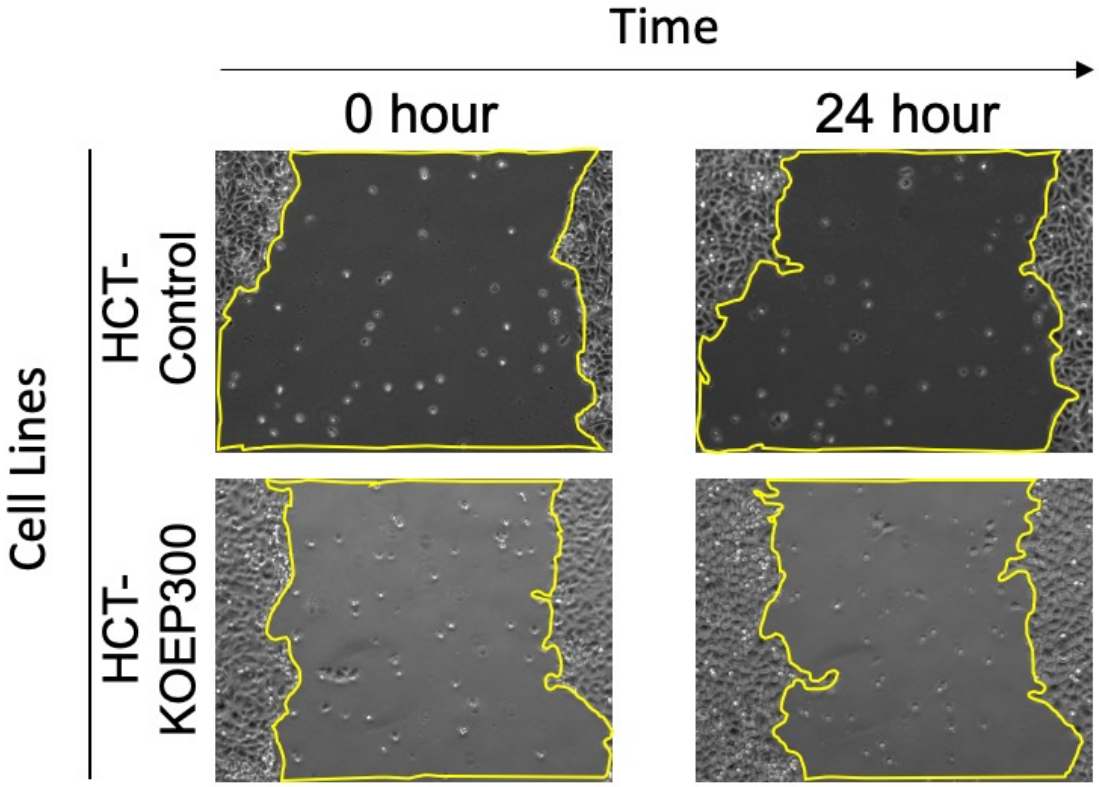

(a)

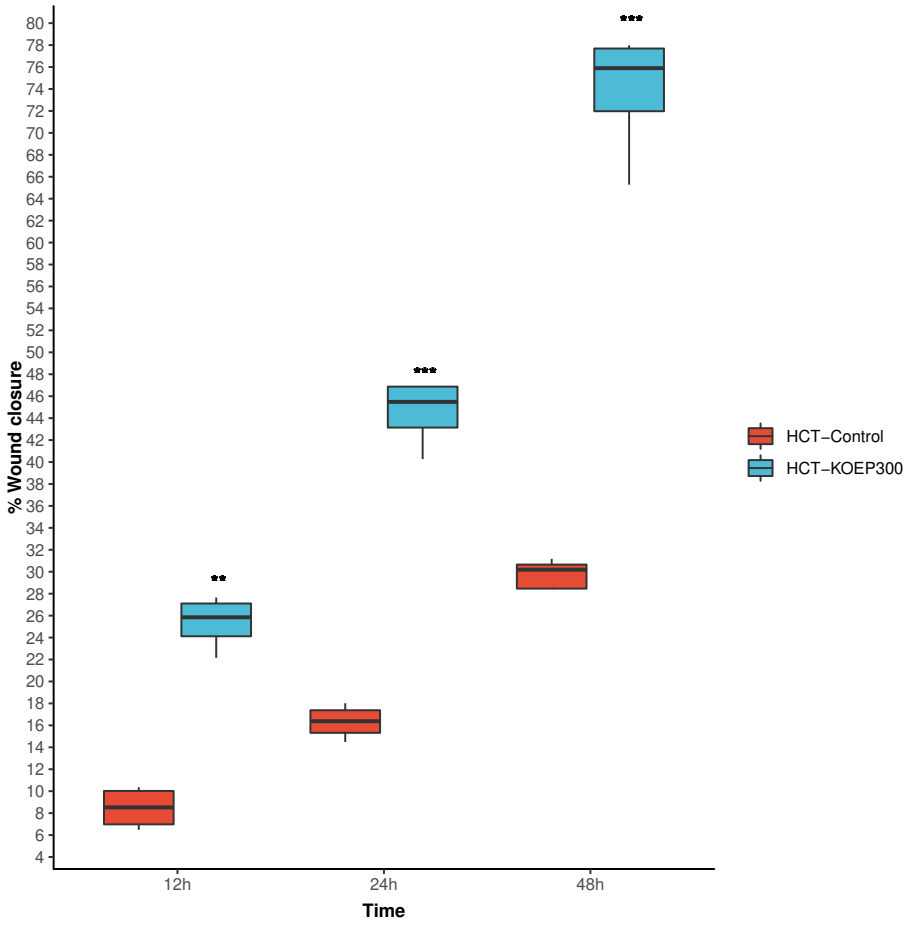

(b)

Fig. 8.5 Knockout of EP300 increases wound healing in HCT116 colorectal cancer cells. (A) Images show HCT116 cells (HCT-Control), and EP300 knockout (HCT-KOEP300), plated onto 6 well plates and imaged over 24 h, over a 2-hour interval. Quantification of the wound closure was done using the formula (A0−At)/A) x 100%, where A0 represents the area of the wound at 0 h and At represents the area of the wound at indicated time points as described (Holand et al., 2014). (B) Graph represents the summary of the average wound closure area + SD. Statistical analysis was performed using ANOVA, comparing the wild type HCT116 control (HCT-Control), and HCT116 cells with EP300 knockout (HCT-KOEP300) (P<0.05*, **P<0.01, ***P<0.001).

Overexpression of EP300 and CDH1 leads to decreased random migration in mesenchymal breast cancer cell lines.

Both random and directed migration are characterised by constant velocity or persistent direction (Gail et al., 1970), the fundamental difference between them seems to rest on the presence and activity of lamellipodia which act as a stabiliser (Andrew & Insall., 2007). These llamelipodia are regulated by multiple control mechanisms such as: external signaling, ECM matrix topography, cell polarity, cell adhesion receptors, which all act on the cells internal Rho GTPase signalling. The latter responsible for the cell cytoskeleton, lamellipodia formation, integrin cycling and focal adhesion kinase links with the ECM. For example, the presence of lateral lamellipodia can induce random migration, which also seems to persist more on 2D surfaces (Petrie et al., 2010). Furthermore a number of signaling mechanisms influence this, such as signalling by the partitioning defective complex, which conntexts to Rho GTPases and is responsible for cell polarity between the leading and trailing edge of the cell (Iden et al., 2008). Experimental models of wound healing in fibroblasts have also demonstrated a role for the WNT pathway in establishing cell polarisaiotn by exerting control over this partitioning defective complex, as well as CDC42, which is a recruiter for this complex (Nomachi et al., 2008)

In order to study the effects of EP300 and CDH1 on random migration, we used some of the cell lines we had used previously for our gene expression analysis in **Chapter 4**. The hypothesis was tested in mesenchymal breast cancer cell lines CAL51 and MDA-MB-231 in context of EP300 overexpression, CDH1 overexpression and compared to the basal expression in the same cell line with a control empty vector.

In **Figure 8.6**, we observe the breast cancer cell line CAL51 in three conditions: a control sample with an empty vector (CAL-EV), an EP300 overexpression (CAL-EP300) and a CDH1 overexpression (CAL-CDH1). While in **Figure 8.7** we observe the breast cancer cell line MDA-MB-231 in three conditions: a control sample with an empty vector (MDA-EV), an EP300 overexpression (MDA-EP300) and a CDH1 overexpression (MDA-CDH1).

The protocol was based on previously published research by (Pardo et al., 2016).All three samples were seeded at a density of 100,000 cells per well into a 96 well plate, from which 5 positions were selected, and 1 image was taken for each well and respective position every 10 minutes. These images were then analysed using a cell tracking package created by Dr. Olivier Pardo (Imperial College London) in which 8 cells were selected from each position and their movement monitored from the start (10 minute) to end position (18 hours). The raw data was converted into arbitrary units of movement (A.U) relative to the control. An example of this code can be seen in appendix 2.

Figure 8.6a is a visual tracking of one well analysed for this experiment in CAL51 cells. The graphical representation of random migration in A.U is shown for the control (**Figure 8.6b**), EP300 overexpression (**Figure 8.6c**) and CDH1 overexpression (**Figure 8.6d**). A bar chart was constructed from this data and shown in **Figure 8.6e**, data represents three biological replicates.

We can see that the movement of this cell line does have movement as demonstrated by several selected cells (**Figure 8.6a**), this movement seems to be restricted to a very small area, with little differences between conditions (**Figures 8.6b to 8.6d**). The graph representing these data (**8.6e**) shows that there is a small difference in random migration between the control and EP300 overexpression by 0.019 AU ($p<0.01$), and the control and CDH1 overexpression by 0.041 AU ($p<0.01$). And a small difference between EP300 overexpression and CDH1 overexpression by 0.021 AU ($p<0.01$). Overall, the overexpression of EP300 does not influence random migration more than CDH1 overexpression.

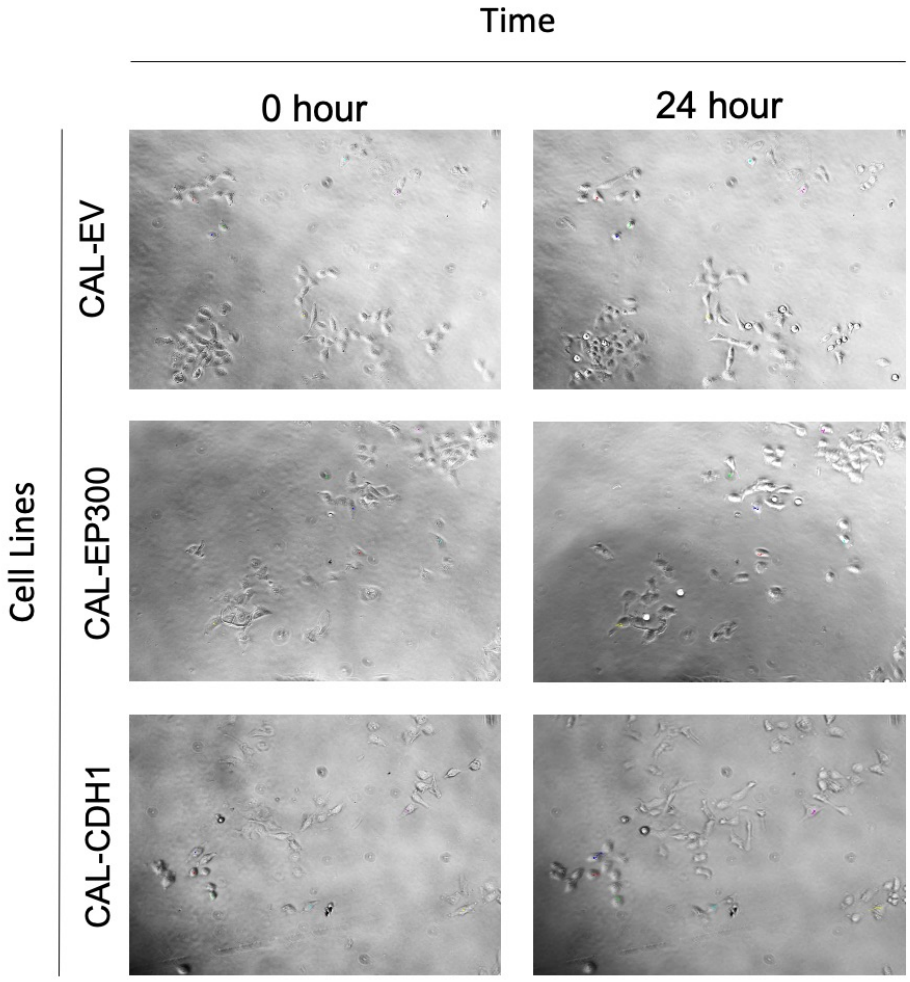

(a)

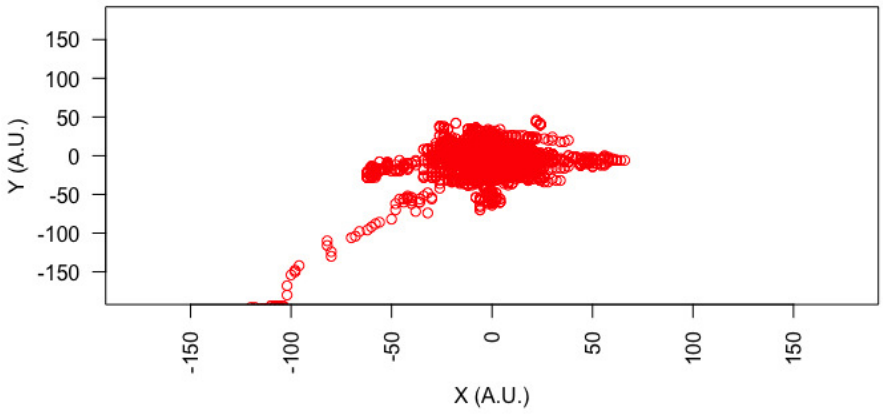

(b) CAL-EV

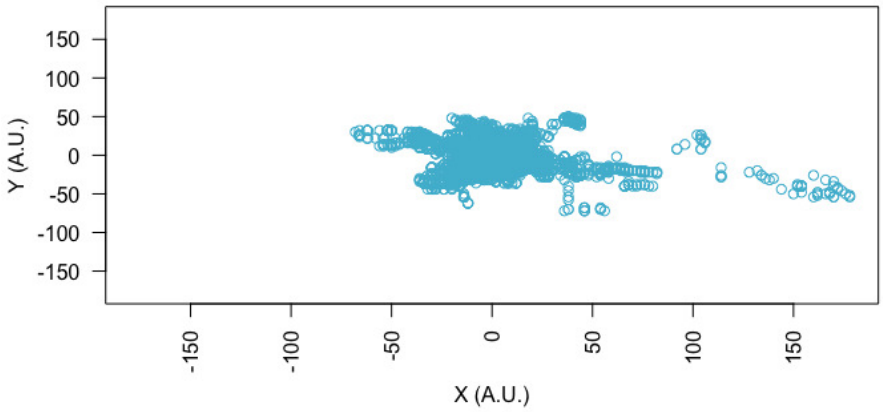

(c) CAL-EP300

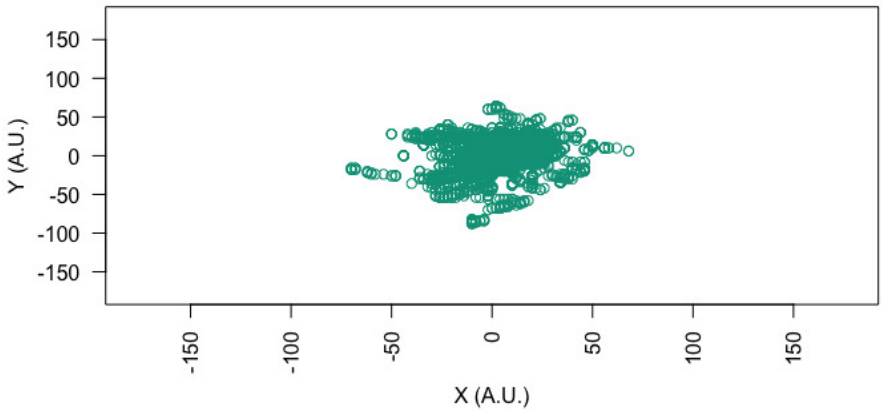

(d) CAL-CDH1

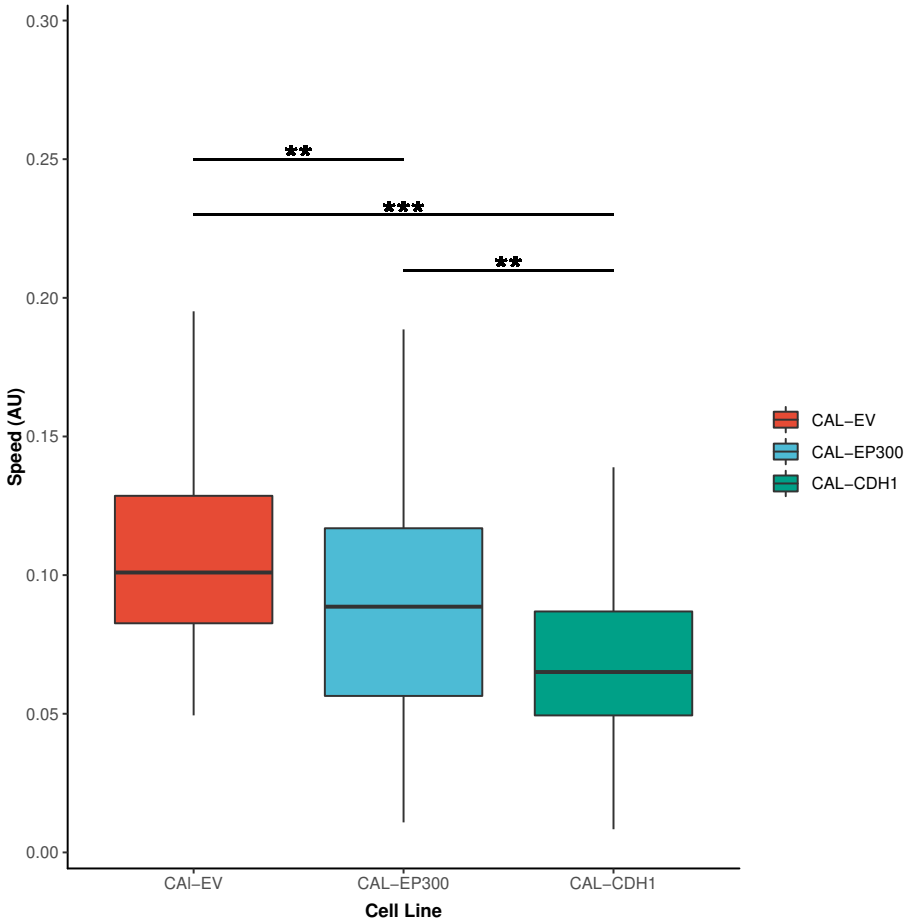

(e)

Fig. 8.6 Overexpression of EP300 decreases random migration in CAL51 breast cancer cells. CAL51 cell lines were transfected with empty vector control (CAL-EV), EP300 overexpressing (CAL-EP300) and CDH1 overexpressing (CAL-CDH1) and time lapse imaging was performed for 18 h. (A) Shows a representative cell population and their overlaid trajectories travelled. (C-D) Plots show overlays of representative trajectories travelled. The distance of migration was quantified and represented as the mean + SEM of values normalized to the respective control condition. (E) Shows a bar chart representing the mean + SD of the speed of cell migration in arbitrary units (AU). Statistical analysis was performed using one-way ANOVA, comparing CAL51 with shEV empty vector control (CAL-EV), to EP300 overexpressing (CAL-EP300) and CDH1 overexpressing (CAL-CDH1) transfected cells. (**P<0.01, ***P<0.001). Data represents 3 experimental replicates (n=3).

Figure 8.7a is a visual tracking of one well analysed for this experiment in MDA-MB-231 cells. The graphical representation of random migration in A.U is shown for the control (**Figure 8.7b**), EP300 overexpression (**Figure 8.7c**) and CDH1 overexpression (**Figure 8.7d**). A bar chart was constructed from this data and shown in **Figure 8.7e**, data represents three biological replicates.

We can see that the movement of this cell line does have movement as demonstrated by several selected cells (**Figure 8.7a**), this movement seems to be restricted to a very small area. The control (**Figure 8.7b**) is spread out around the center, and CDH1 overexpression matches this movement pattern (**Figure 8.7d**), while EP300 overexpression shows the movement restricted (**Figure 8.7c**). The graph representing these data (**Figure 8.7e**) indicates that there is decreased random migration between the control and EP300 overexpression by 0.142 AU ($p<0.05$), and the control and CDH1 overexpression by 0.057 AU ($p<0.05$). There is also a larger decrease in random migration with EP300 overexpression than CDh1 overexpression by 0.085 AU ($p<0.05$). Overall, the overexpression of EP300 impacts random migration more than CDH1 overexpression.

To summarise, the effects of EP300 on random migration, we can see that as these cells favour directional migration, the overexpression of EP300 decreases random migration, probably by exerting control ovr lamellipodia and cell polarity.

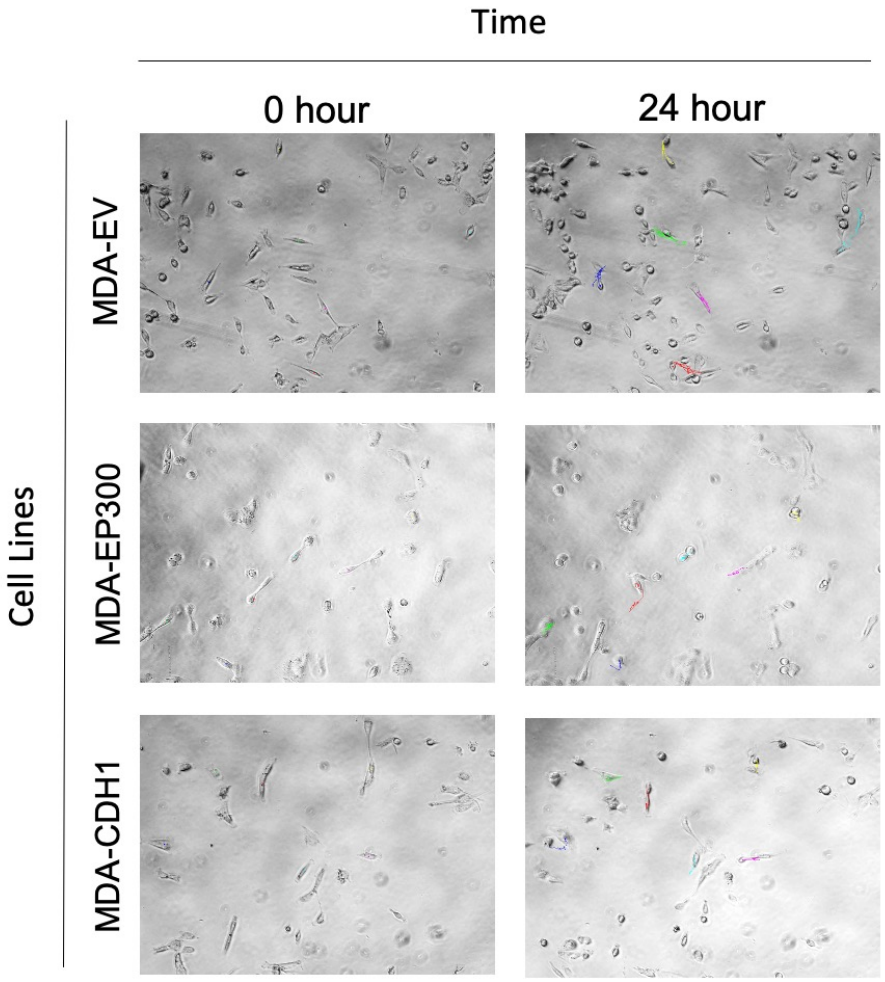

(a)

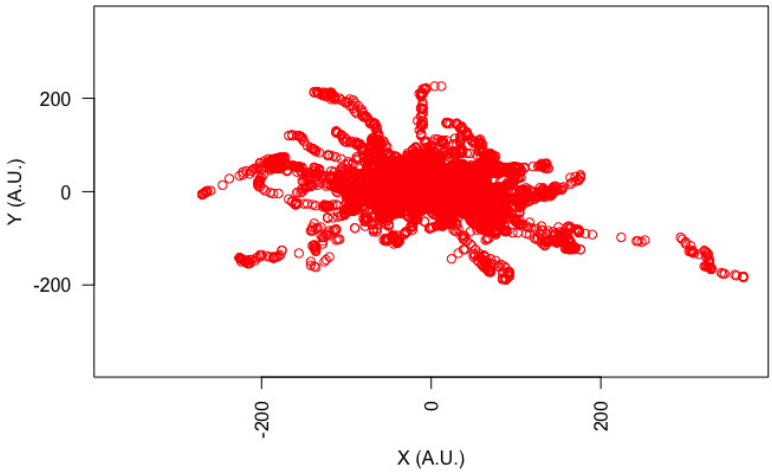

(b) MDA-EV

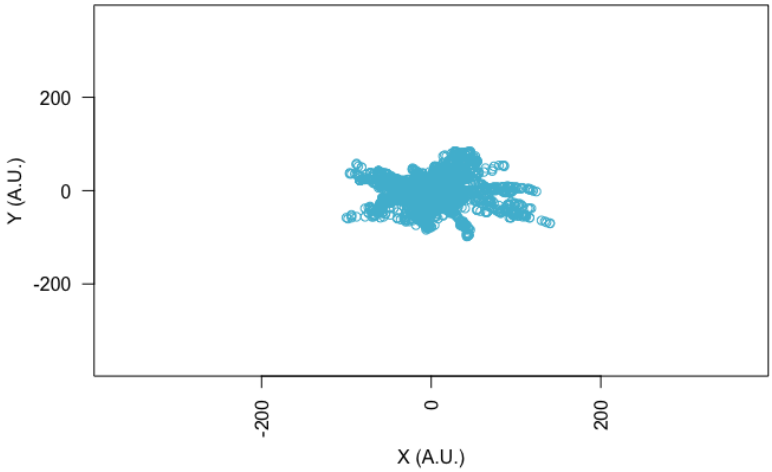

(c) MDA-EP300

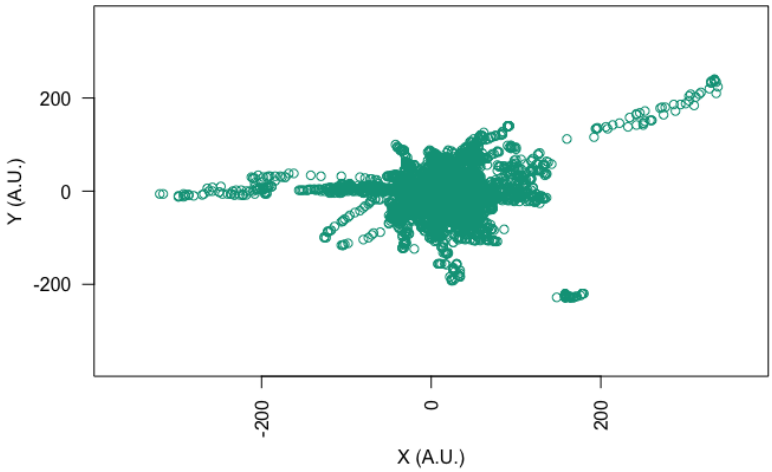

(d) MDA-CDH1

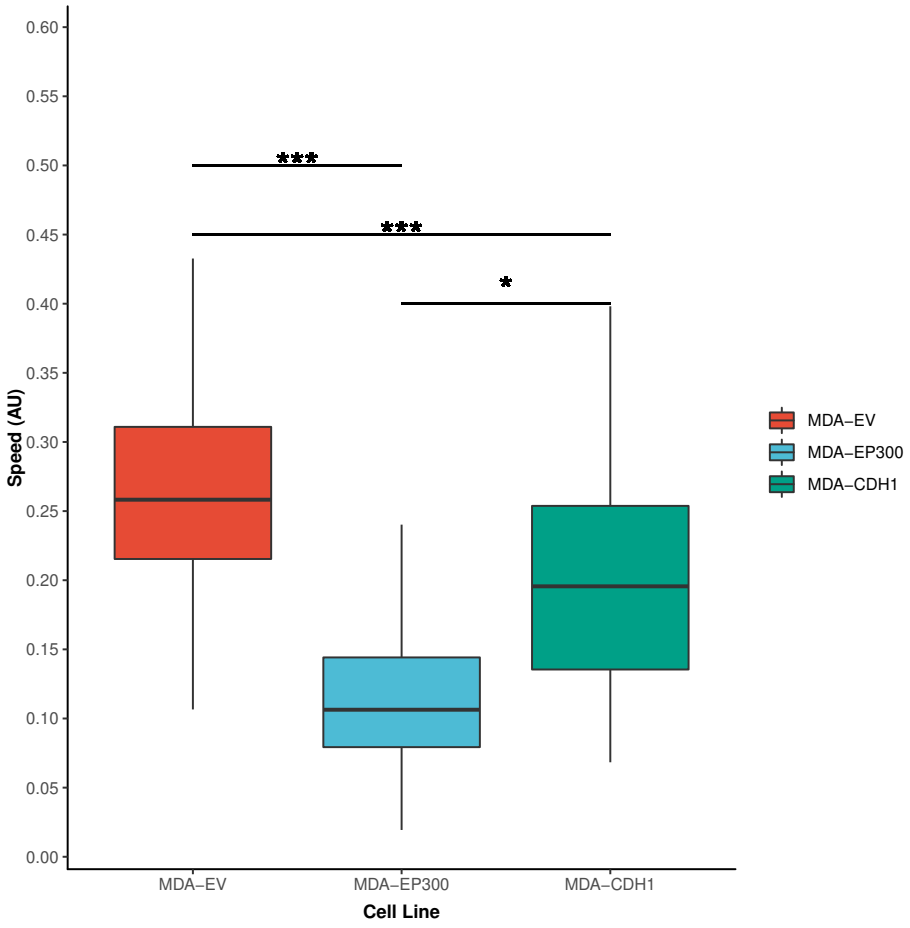

(e)

Fig. 8.7 Overexpression of EP300 decreases random migration in MDA-MB-231 breast cancer cells. MDA-MB-231 cell lines were transfected with empty vector control (MDA-EV),EP300 overexpressing (MDA-EP300) and CDH1 overexpressing (MDA-CDH1) and time lapse imaging was performed for 18 h. (A) Shows a representative cell population and their overlaid trajectories travelled. (C-D) Plots show overlays of representative trajectories travelled. The distance of migration was quantified and represented as the mean + SEM of values normalized to the respective control condition. (E) Shows a bar chart representing the mean + SD of the speed of cell migration in arbitrary units (AU). Statistical analysis was performed using one-way ANOVA, comparing MDA-MB-231 with shEV empty vector control (MDA-EV), to EP300 overexpressing (MDA-EP300) and CDH1 overexpressing (MDA-CDH1) transfected cells. (**P<0.01, ***P<0.001). Data represents 3 experimental replicates (n=3).

Knockout of EP300 leads to decreased random migration in colorectal cancer cell lines.

In order to study the effects of EP300 knockout on random migration, we used some of the cell lines we had used previously for our gene expression analysis in **Chapter 4**. The hypothesis was tested in colorectal cancer cell line HCT116 in context of EP300 knockout compared to the basal expression in the same cell line with a control empty vector. In Figure 8, we observe the colorectal cancer cell line HCT116 in two conditions: a control HCT116 naïve cells (Control), an EP300 knockout (KO EP300). All samples were seeded at a density of 100,000 cells per well into a 96 well plate, from which 5 positions were selected, and 1 image was taken for each well and respective position every 10 minutes. These images were then analysed using a cell tracking package created by Dr. Olivier Pardo (Imperial College London). In which 8 cells were selected from each position and their movement monitored from the start (10 minute) to end position (18 hours). The raw data was converted into arbitrary units of movement (A.U) relative to the control.

Figure 8.8a is a visual tracking of one well analysed for this experiment in HCT116 cells. The graphical representation of random migration in A.U is shown for the control (**Figure 8.8b**), EP300 knockout (**Figure 8.8c**). A bar chart was constructed from this data and shown in **Figure 8.8d**, data represents three biological replicates. We can see that the movement of this cell line does have movement as demonstrated by several selected cells (**Figure 8.8a**), this movement seems to be restricted to a very small area, with little differences between conditions shown in **Figures 8.8b** to **Figure 8.8c**. The graph representing these data (**Figure 8.8d**) shows that there is significant difference in random migration between the control and KOEP300 by 0.038 AU ($p<0.01$). Overall, the knockout of EP300 seems to reduce random migration, probably through the presence of less lateral lamellipodia or other signalling pathways which regulate Rho GTPase.

Thus to summarise there is a decrease in random migration in the HTC116 cell line associated with the knockout of EP300.

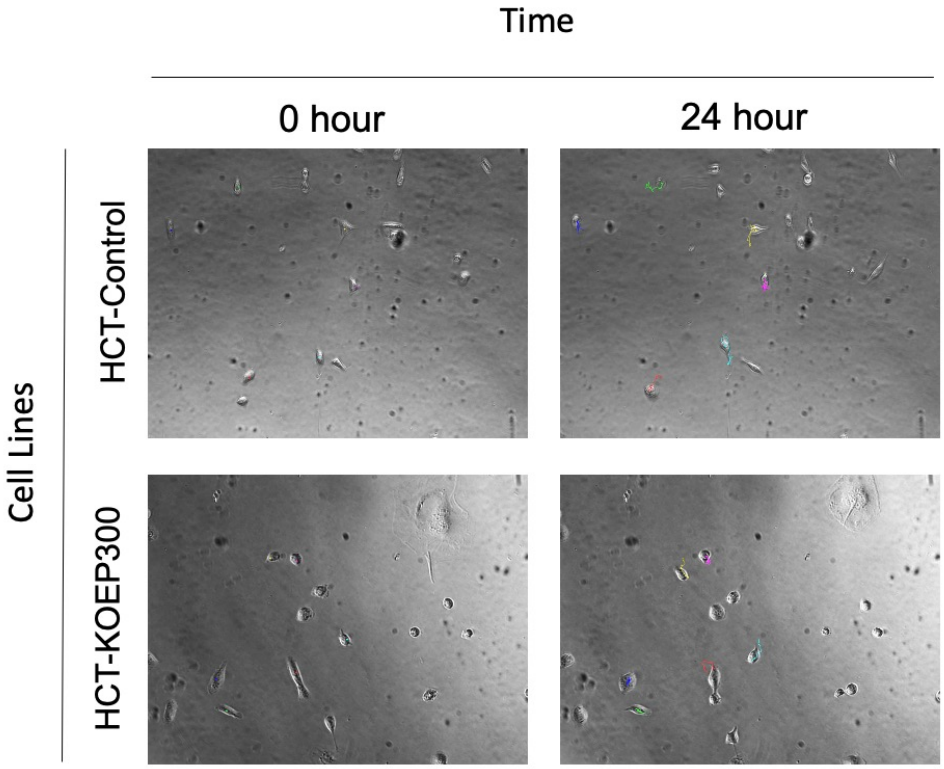

(a)

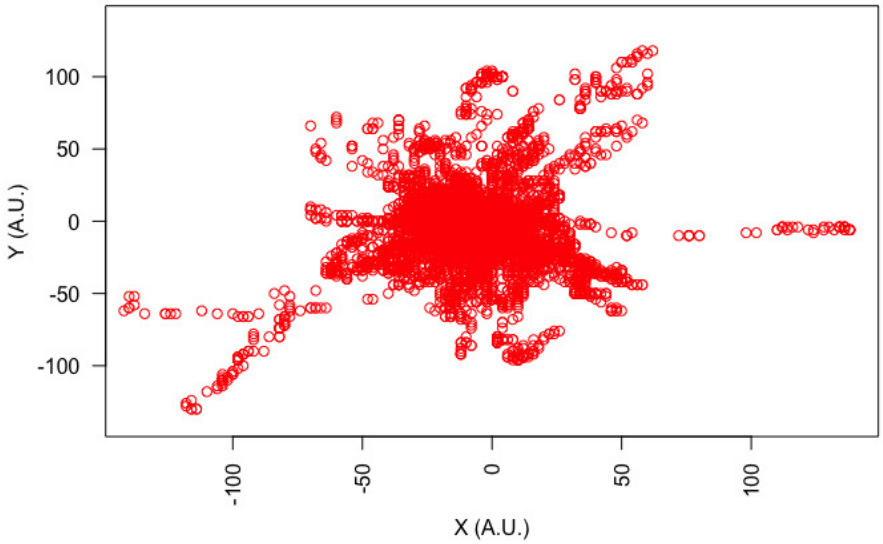

(b) HCT-EV

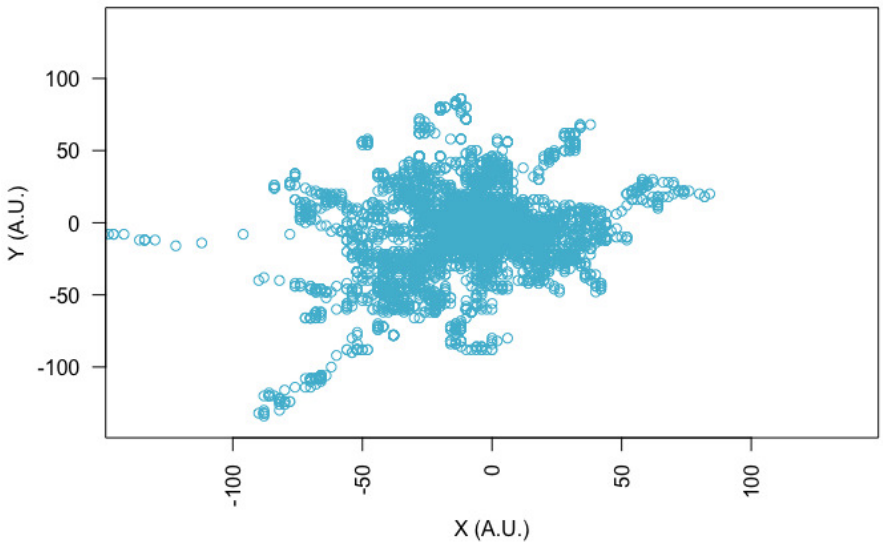

(c) HCT-KOEP300

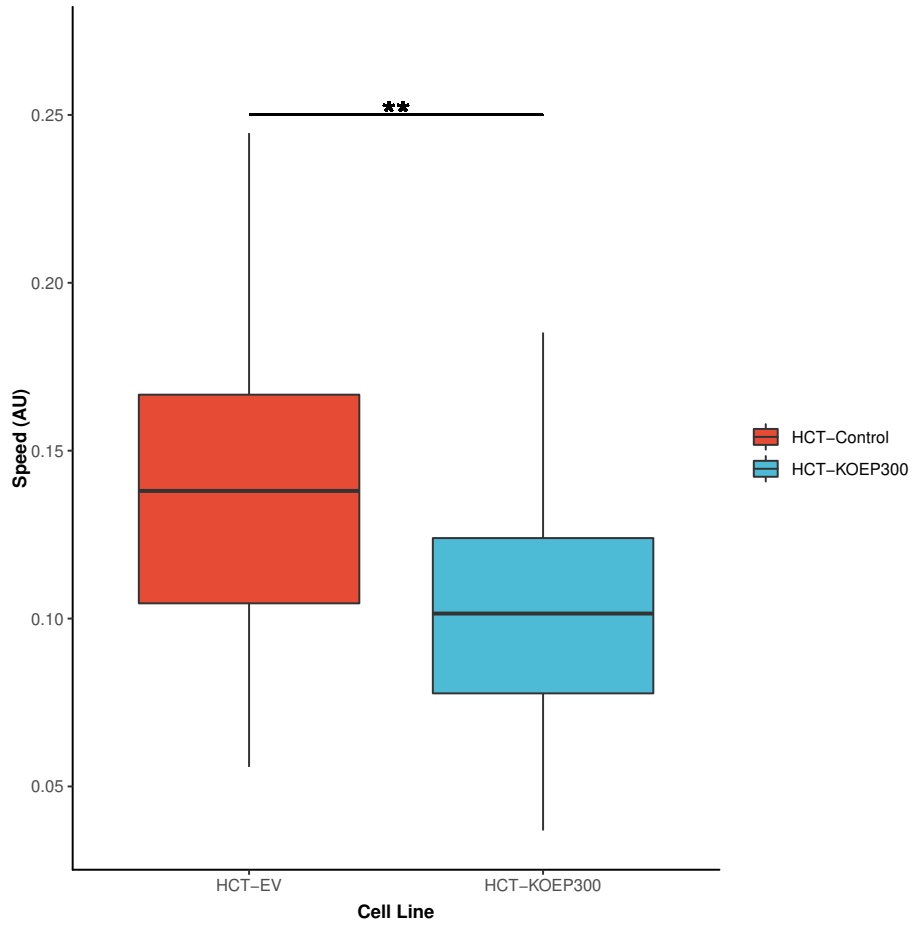

(d)

Fig. 8.8 Knockout of EP300 decreases random migration in HCT116 colorectal cancer cells. HCT116 cells (HCT-Control) and EP300 knockout (HCT-KOEP300) and time lapse imaging was performed for 18 h. (A) Shows a representative cell population and their overlaid trajectories travelled. (B-C) Plots show overlays of representative trajectories travelled. The distance of migration was quantified and represented as the mean + SEM of values normalized to the respective control condition. (D) Shows a bar chart representing the mean + SD of the speed of cell migration in arbitrary units (AU). Statistical analysis was performed using one-way ANOVA, comparing HCT116 wild type control (HCT-Control), to HCT116 with EP300 knockout (HCT-KOEP300). (**P<0.01, ***P<0.001). Data represents 3 experimental replicates (n=3).

Downregulation of EP300 leads to increased random migration in epithelial breast cancer cell lines.

In order to study the effects of EP300 on random migration, we used some of the cell lines we had used previously for our gene expression analysis in **Chapter 4**. The hypothesis was tested in mesenchymal breast cancer cell lines MCF7 and T47D in context of EP300 downregulation, and compared to the basal expression in the same cell line with a control empty vector. In **Figure 8.9**, we observe the breast cancer cell line MCF7 in three conditions: a control sample with an empty vector (MCF7-EV), an EP300 knockdown (sh EP300 I) and a second EP300 knockdown (sh EP300 II). While in **Figure 8.10** we observe the breast cancer cell line T47D in three conditions: a control sample with an empty vector (T47D-EV), an EP300 knockdown (sh EP300 I) and a EP300 knockdown with a second vector hairpin (sh EP300 II).

All three samples were seeded at a density of 100,000 cells per well into a 96 well plate, from which 5 positions were selected, and 1 image was taken for each well and respective position every 10 minutes. These images were then analysed using a cell tracking package created by Dr. Olivier Pardo (Imperial College London) in which 8 cells were selected from each position and their movement monitored from the start (10 minute) to end position (18 hours). The raw data was converted into arbitrary units of movement (A.U) relative to the control. **Figure 8.9a** is a visual tracking of one well analysed for this experiment in MCF7 cells. The graphical representation of random migration in A.U is shown for the control (**Figure 8.9b**), EP300 downregulation (**Figure 8.9c**) and the second EP300 downregulation (**Figure 8.9d**). A bar chart was constructed from this data and shown in **Figure 8.9e**, data represents three biological replicates.

We can see that the movement of this cell line does have movement as demonstrated by several selected cells (**Figure 8.9a**), this movement seems to be restricted to a very small area, with the downregulation of EP300 (**Figures 8.9b** to **8.9d**). The graph representing these data (**Figure 8.9e**) shows that there is significant decrease in random migration between the control and sh EP300 I by 0.092 AU ($p<0.001$), and sh EP300 II by 0.076 AU ($P<0.001$). There seems to be no difference between the two knockdowns of EP300. Overall, the downregulation of EP300 seems impact random migration by restricting the movement.

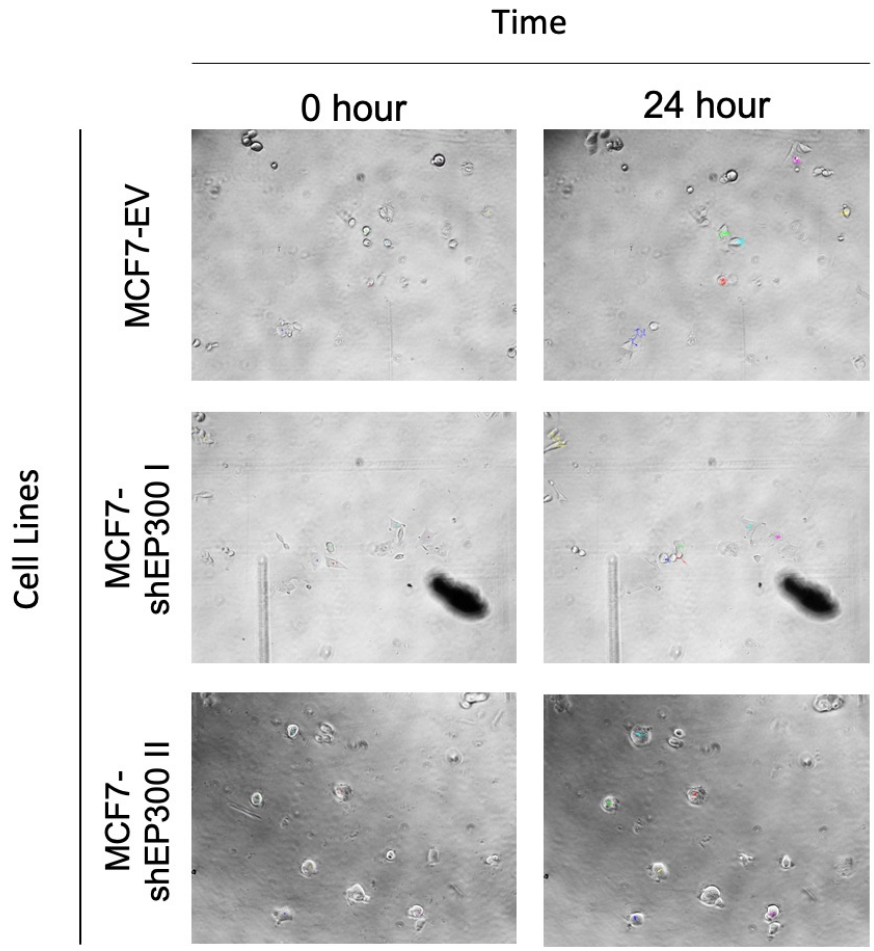
Time
0 hour
24 hour
Cell Lines
MCF7-EV
MCF7-shEP300 I
MCF7-shEP300 II

(a)

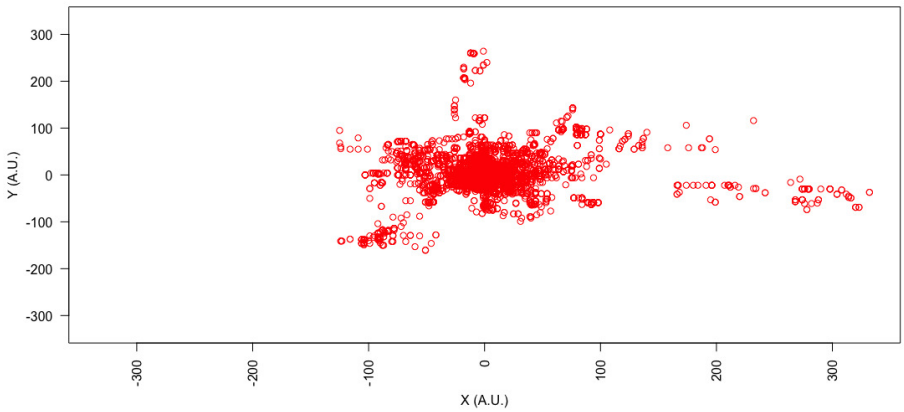

(b) MCF7-EV

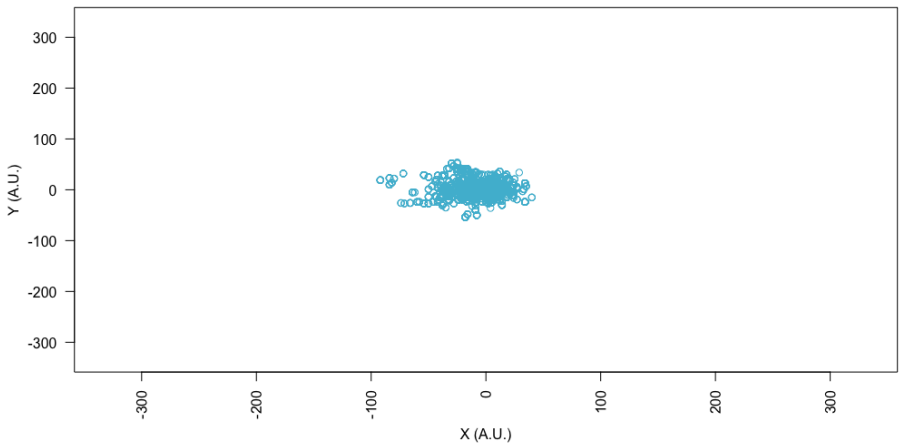

(c) MCF7-shEP300 I

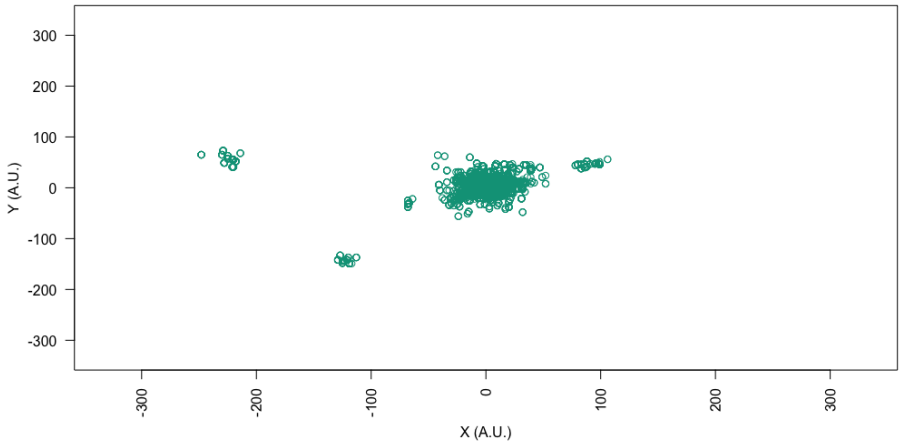

(d) MCF7-shEP300 II

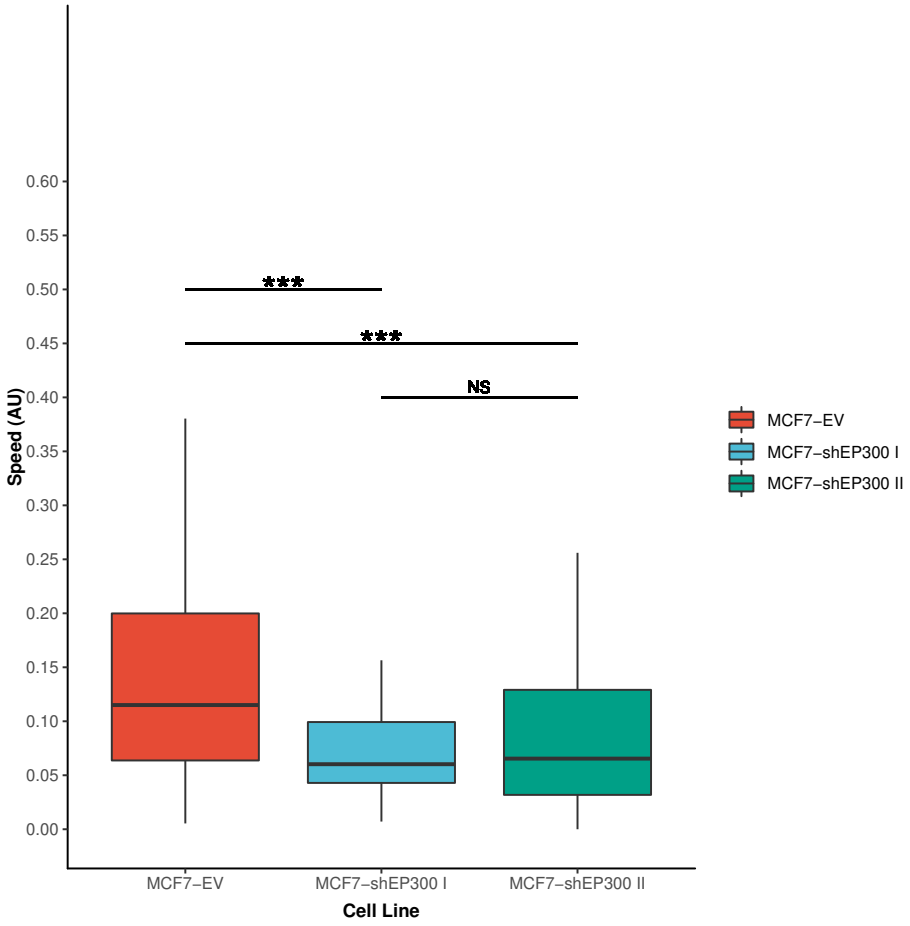

(e)

Fig. 8.9 Downregulation of EP300 decreases random migration in MCF7 breast cancer cells. MCF7 cell lines were transfected with empty vector control (MCF7-EV) and two vectors for EP300 downregulation (MCF7shP300 I & MCF7-shEP300 II) and time lapse imaging was performed for 18 h. (A) Shows a representative cell population and their overlaid trajectories travelled. (B-D) Plots show overlays of representative trajectories travelled. The distance of migration was quantified and represented as the mean + SEM of values normalized to the respective control condition. (E) Shows a bar chart representing the mean + SD of the speed of cell migration in arbitrary units (AU). Statistical analysis was performed using one-way ANOVA, comparing MCF7 with shEV empty vector control (MCF7-EV), to the two EP300 downregulations in MCF7 (MCF7shP300 I & MCF7-shEP300 II). (**P<0.01, ***P<0.001). Data represents 3 experimental replicates (n=3).

Figure 8.10a is a visual tracking of one well analysed for this experiment in T47D cells. The graphical representation of random migration in A.U is shown for the control (**Figure 8.10b**), EP300 downregulation (**Figure 8.10c**) and the second EP300 downregulation (**Figure 8.10d**). A bar chart was constructed from this data and shown in **Figure 8.10e**, data represents three biological replicates. We can see that the movement of this cell line does have movement as demonstrated by several selected cells (**Figure 8.10a**), this movement seems to be restricted to a very small area, with the knockdown of EP300 (**Figures 8.10b** to **8.10d**). The graph representing this data (**8.10e**) shows that there is significant decrease in random migration between the control and sh EP300 I by 0.052 AU ($p<0.01$), and no significant difference with sh EP300 II by 0.02 AU. There seems to be a small difference between the two knockdowns of EP300 by 0.032 AU ($p<0.01$). Overall, the downregulation of EP300 seems impact random migration by restricting the movement.

Thus to summarise, EP300 downregulation, promotes random migration in epithelial cell lines. Meaning that cells tend to lose directionality and perhaps have disrupted signalling with the Rho GTPase machinery.

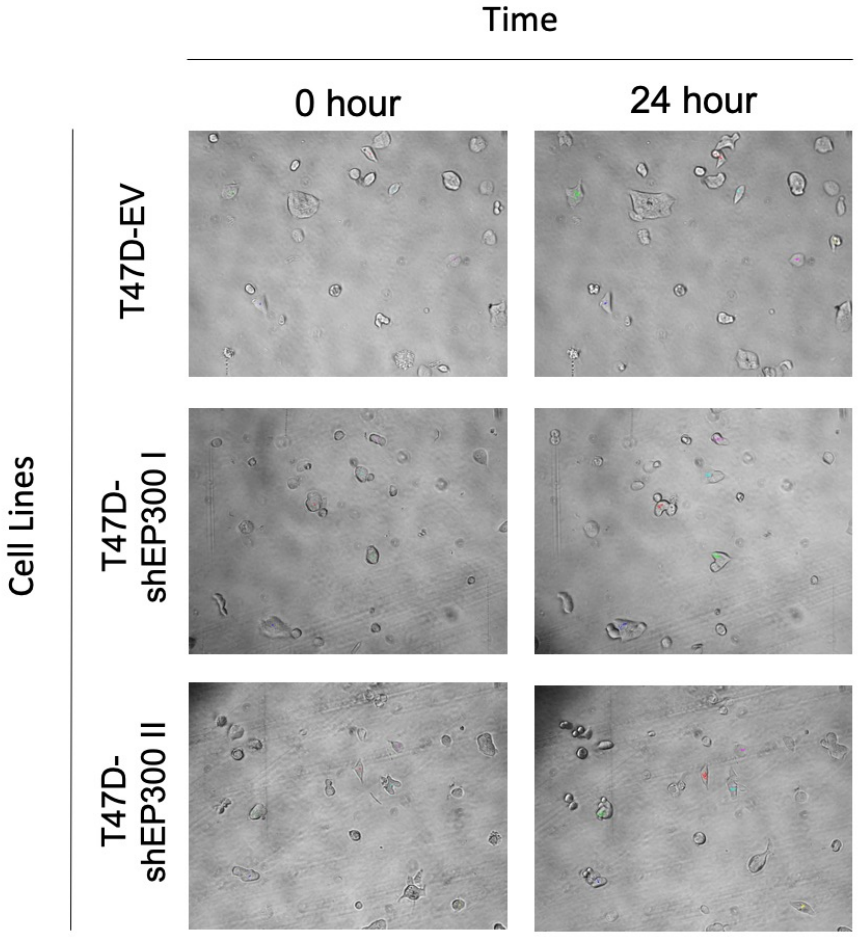
Time
0 hour
24 hour
Cell Lines
T47D-EV
T47D-shEP300 I
T47D-shEP300 II

(a)

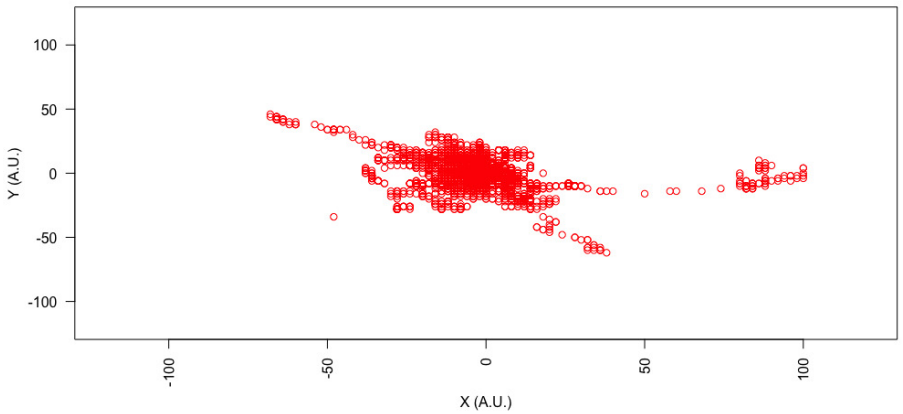

(b) T47D-EV

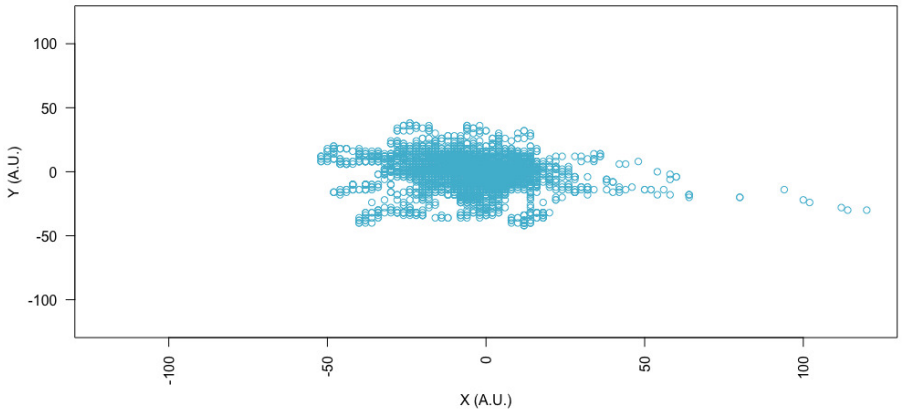

(c) T47D-shEP300 I

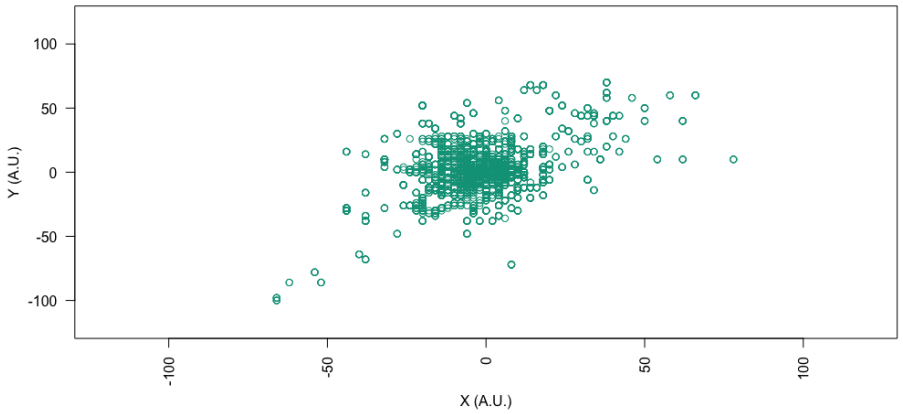

(d) T47D-shEP300 II

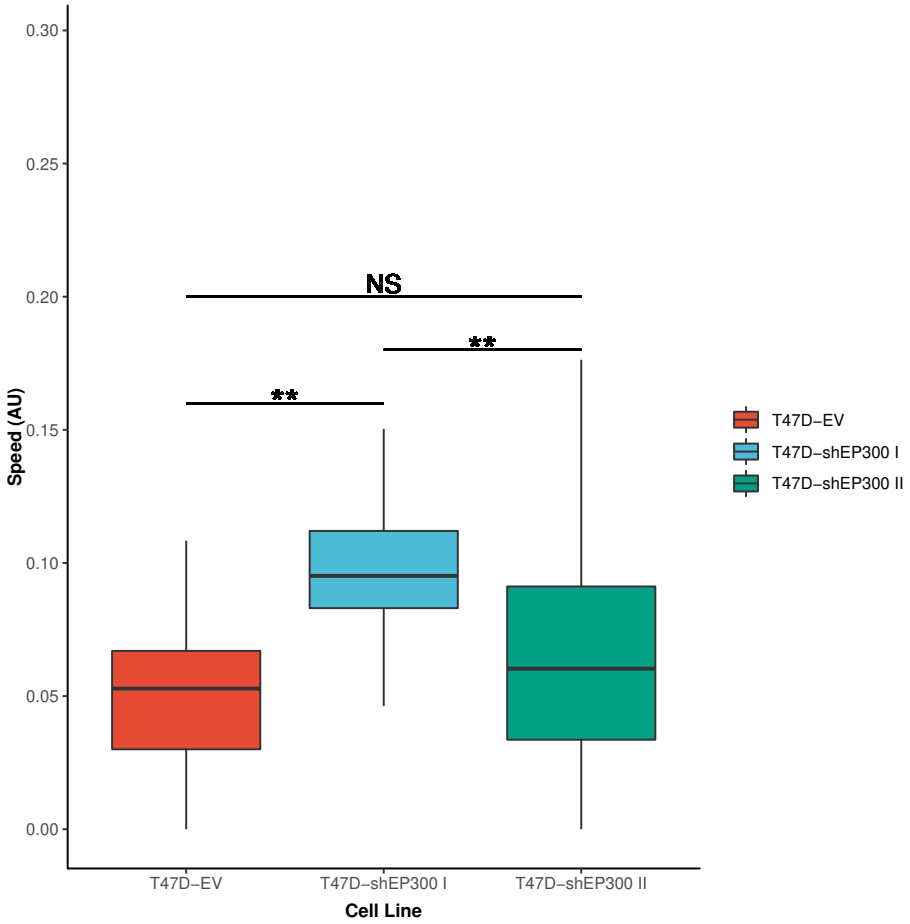

(e)

Fig. 8.10 Downregulation of EP300 decreases random migration in T47D breast cancer cells. T47D cell lines were transfected with control (T47D-EV empty vector) and two vectors for EP300 knockdown (T47D-shP300 I & T47D-shEP300 II) and time lapse imaging was performed for 18 h. (A) Shows a representative cell population and their overlaid trajectories travelled. (B-D) Plots show overlays of representative trajectories travelled. The distance of migration was quantified and represented as the mean + SEM of values normalized to the respective control condition. (E) Shows a bar chart representing the mean + SD of the speed of cell migration in arbitrary units (AU). Statistical analysis was performed using one-way ANOVA, comparing control (T47D-EV empty vector), to the two EP300 knockdowns (T47D-shEP300 I & T47D-shEP300 II). (**P<0.01, ***P<0.001). Data represents 3 experimental replicates (n=3).

Overexpression of EP300 and CDH1 leads to decreased invasion in mesenchymal breast cancer cell lines.

In order to study the effects of EP300 and CDH1 on directional migration, we used some of the cell lines we had used previously for our gene expression analysis in **Chapter 4**. The hypothesis was tested in a mesenchymal breast cancer cell line MDA-MB-231 in context of EP300 overexpression, CDH1 overexpression and compared to the basal expression in the same cell line with a control empty vector.

In **Figure 8.11**, we observe the breast cancer cell line MDA-MB-231 in three conditions: a control sample with an empty vector control (MDA-EV), an EP300 overexpression (MDA-EP300) and a CDH1 overexpression (MDA-CDH1). All three samples were seeded at a density of 10,000 cells per well into a black bottomed 96 well plate, which was then covered in type IV collagen with a chemoattractant (EGF) on top. Cells were allowed to migrate over 48 hours and then fixed using sytox green nuclear stain with paraformaldehyde. From these plates, 9 sites were selected per condition, and image stacks of 500 nm were taken in each condition. Images were then processed using deconvolution software and their 3D movement was analysed using Fiji Image J to generate distances from the surface of the Matrigel in μm.

Figure 8.11a is the side view of the representative 3D image stack for each condition for this experiment in MDA-MB-231 cells after 48 h of invasion through the collagen. **Figure 8.11b** shows a bar chart which was constructed from this data, the data represents three biological replicates. We can see based on the side profile, the cells all migrate towards the chemoattractant after a 48 h period (**Figure 8.11a**). There is also a decrease in invasion between the control and EP300 overexpression by a distance of 10% ($p<0.05$) and the control and CDH1 overexpression by ($p<0.01$). CDH1 expressing cells have the least invasive capability, and when comparing to EP300 it is less by 20% ($p<0.05$). When comparing EP300 to CDH1 overexpression we see a difference in 9% ($p<0.05$) as seen in **Figure 8.11b**.

Leading to conclude that EP300 overexpression is effective to decrease invasive capabilities in the MDA-MB-231 cell line. Potentially due to its higher adhesive properties and cell to cell contacts due to the higher expression of CDH1 which is promoted by EP300. Leading us to believe this cell line has undergone an EMT to MET shift.

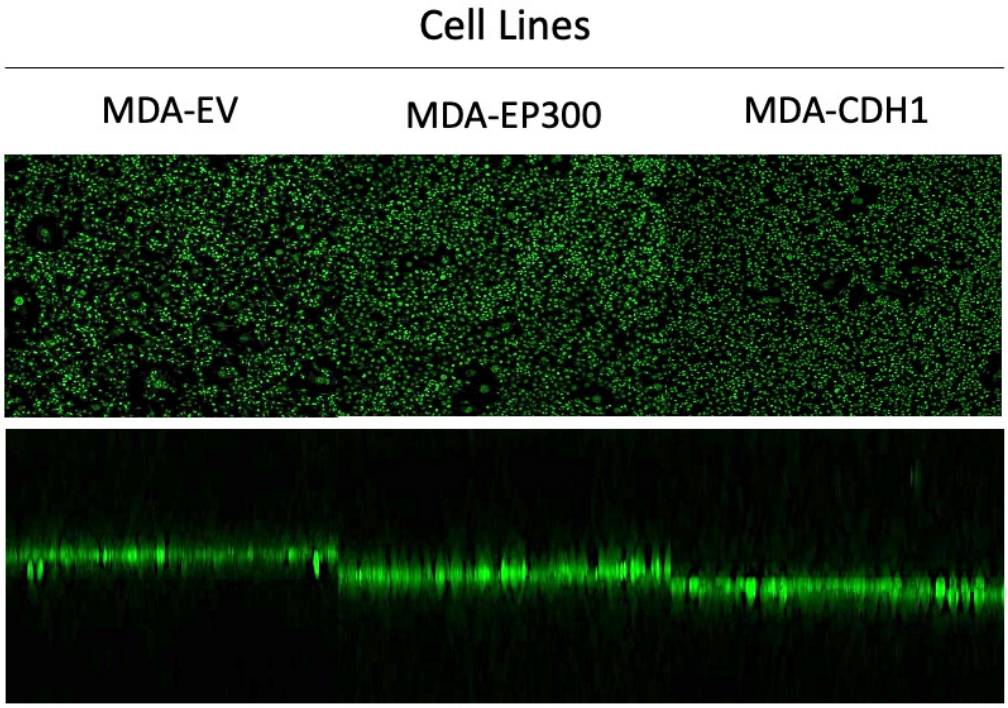

(a)

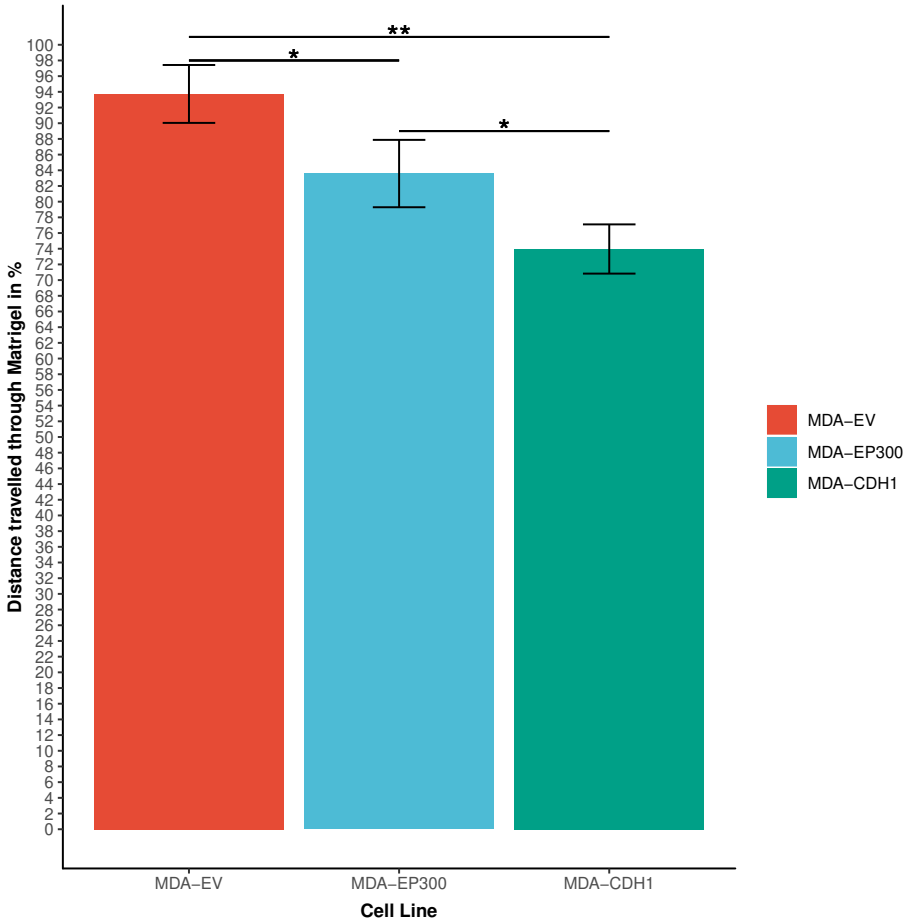

(b)

Fig. 8.11 Overexpression of EP300 decreases invasion in breast cancer cells. EP300 expression inhibits invasion in MDA-MB-231 cells. MDA-MB-231 cell lines were transfected with empty vector control (MDA-EV), EP300 overexpressing (MDA-EP300) and CDH1 overexpressing (MDA-CDH1) and seeded into a Matrigel and allowed to migrate for 48 hours. Cells were then fixed in 4% paraforlamdehyde supplemented with 1.25μM sytox green nuclear stain. (A) Shows 40x magnification of cells after 48 h of migration at 488 nm. (B) Data represent the summary of the average distance to the surface of the matrigel (μm) through collagen membrane + SD. Statistical analysis was performed using ANOVA, comparing MDA-MB-231 with shEV empty vector control (MDA-EV), and MDA-MB-231 cells overexpressing EP300 (MDA-EP300) and MDA-MB-231 cells overexpressing CDH1 (MDA-CDH1), (**P<0.01,***P<0.001).

Knockout of EP300 leads to increased invasion in a colorectal cancer cell line.

The hypothesis was tested in a colorectal cancer cell line HCT116 in context of EP300 knockout (HCT-KOEP300) and compared to the basal expression in the naive wild type cells (HCT116-Control). **Figure 8.12a** is the side view of the representative 3D image stack for each condition for this experiment in HCT116 cells after 48 h of invasion through the collagen. **Figure 8.12b** shows a bar chart which was constructed from this data, the data represents three biological replicates. We can see based on the side profile, the cells all migrate towards the chemoattractant after 48 h (**Figure 8.12a**). There is also an increase in invasion between the control and knocked out EP300 cells by 12% ($p<0.01$) as seen in **Figure 8.12b**.

This increased invasion as a response to EP300 knockout is an anomalous result when looking in context of directional and random migration, which was shown to be downregulated. Perhaps this difference is due to the differences between 2D and 3D models, which have shown to influence results (Petrie et al., 2010). Which somewhat complicates our conclusion in this cell line. Alternative models must be used to confirm these findings.

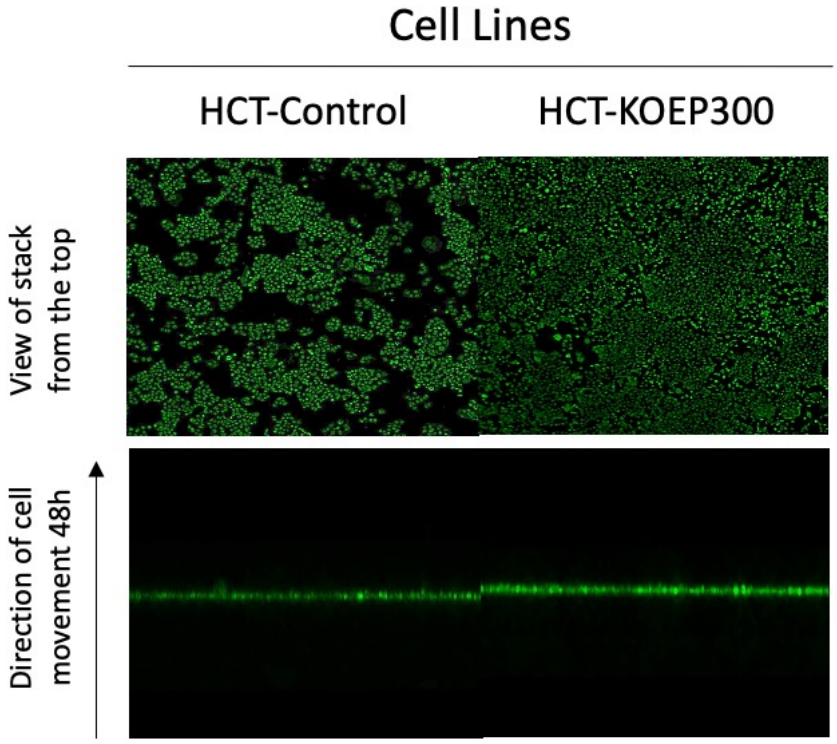
Cell Lines
HCT-Control
HCT-KOEP300
View of stack from the top
Direction of cell movement 48h

(a)

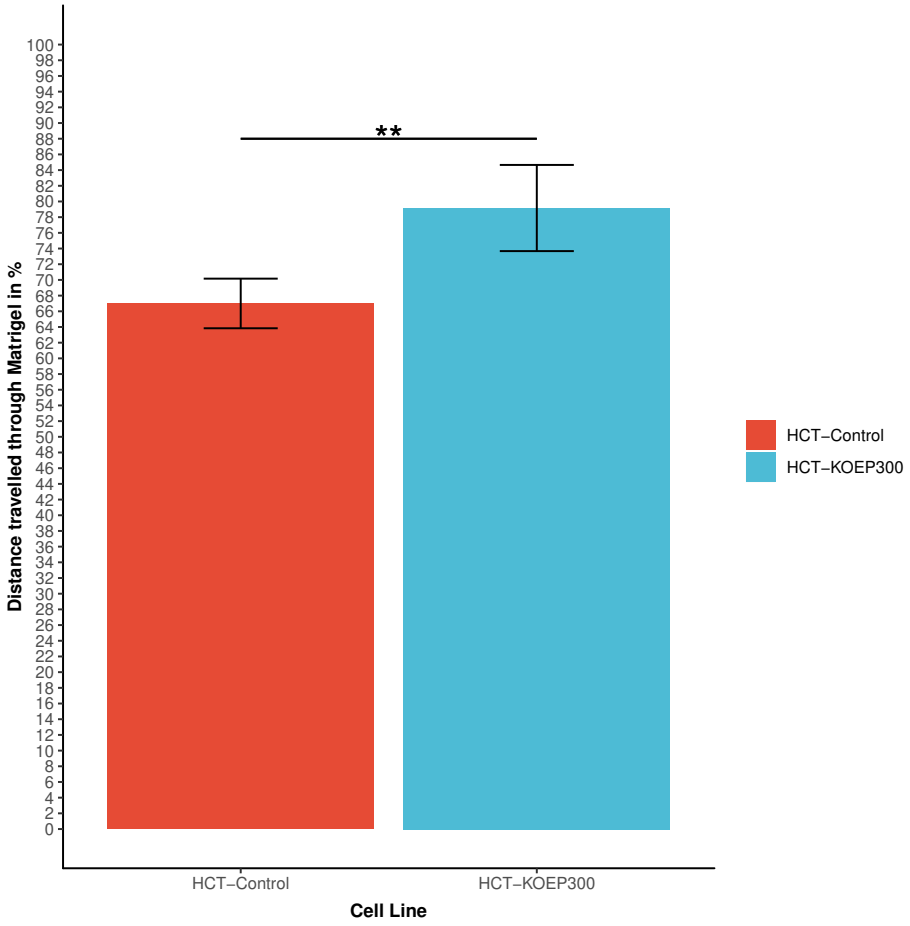

(b)

Fig. 8.12 EP300 knockout inhibits invasion in HCT116 cells. Wild type HCT116 cell lines (HCT-Control) and EP300 knockout (HCT-KOEP300) were seeded into a 400μm matrigel and allowed to migrate for 48 hours. Cells were then fixed in 4% paraforlamdehyde supplemented with 1.25μm sytox green nuclear stain. (A) Shows 40x magnification of cells after 48h of migration at 488 nm. (B) Data represents the summary of the average distance to the surface of the matrigel (μm) through collagen membrane + SD. Statistical analysis was performed using ANOVA, comparing the wild type HCT116 control (HCT-Control), and cells with EP300 knockout (HCT-KOEP300) and E-cadherin (CDH1)), (**P<0.01,***P<0.001).

8.2.4 Discussion

In this chapter, we aim to answer whether modulated expression of EP300 has any effect on the migration and invasion characteristics. As described earlier in this chapter, they are a hallmark of cancer and responsible for metastasis to other organs. It stands to reason that if cells are not able to migrate from their primary site, then there would be less tumour burden and less chemotherapy cycles for the patient, which will improve their quality of life and overall survival (Xu et al., 2018).

Mesenchymal breast cancer effects on migration.

We first set out by taking two mesenchymal breast cancer cell lines: CAL51 and MDA-MB-231 with EP300 overexpressed and tested their response to wound healing, a classical model routinely used to test migration in the laboratory. Once a wound or scratch is generated in the cell lawn, the cells at both edges would attempt to rejoin and form cell-cell contacts/ adherens junctions/ desmosomes etc. The more invasive or higher migratory potential cell lines are mesenchymal while epithelial cell lines are slower because they are maintaining more cell contacts through the expression of E-cadherin among others. While the EMT shift would upregulate invasive characteristics through the expression of SNAI1/ SNAI2/ TWIST, activation of Rac Family Small GTPase 1 (RAC)/Ras Homolog Family Member A (RHoA), combining an increase in focal adhesions and integrin cycling, give an increased cell movement.

The results show that with EP300 overexpression in CAL51, there is a decrease in the total wound healing area that the cells are able to cover versus the control. The same is seen in the MDA-MB-231 cell line, the overexpression of EP300 reduces the wound healing area covered by the cells. The rate of wound closure is much higher in MDA-MB-231, leading to the conclusion that this cell line has much higher migration capability. This has been demonstrated by another study where MDA-MB-231 had wound closure within 8 h (Kabala-Dzik et al., 2017; Pires et al., 2017; Cui et al., 2016), of which NF-κB was shown to be one of the primary drivers of this behaviour (Pires et al., 2017). Our previously published paper showed that the overexpression of EP300 in both of these cell lines resulted in decreased anchorage independence (Asaduzzaman et al., 2017). This would suggest that there would also be an impeded migration and invasion capability.

Interestingly, this EMT phenotype has been investigated and linked to HER2 (ERBB2) expression. Cell lines such as CAL51 and MDA-MB-231 lack expression of ERBB2 which was highly correlated with the mesenchymal phenotype (Nami et al., 2020). This phenotype and its effects on EMT could be explained by clear differences in the epigenetic landscape

through histone marker expression. Differences such as epithelial cell lines display higher 3D chromatin interaction with the ERBB2 promoter region and enrichment for mesenchymal transcription factors in its absence (Nami et al., 2020). The study also shows that epithelial cell lines with high HER2 are enriched for the ubiquitination of lysine 120 on histone H2 (H2BK120ub), methylation on lysine 39 on histone 3 (H3K39me5), and trimethylation at lysine 79 on histone 3 (H3K79me3), as well as higher open access chromatin enhancer marks at ERBB2 gene such as acetylation on lysine 9 on histone 3 (H3K9ac), H3K27ac and H4K8ac (Nami et al., 2020).

It is our hypothesis that EP300 might play a different role in context of these EMT traits between epithelial and mesenchymal cell lines. The same study showed that the EMT phenotype in the mesenchymal cells was not due to the presence of inactivator histone marks, but just the absence of H2BK120ub, H3K39me5, H3K79me3, H3K9ac, H3K27ac and H4K8ac (Nami et al., 2020). This would suggest that EP300 could either activate the acetylation histone marks in epithelial cells or act as a repressor of the EMT transcription factors. It's absence in mesenchymal cells could be what promotes transcription factors. Additionally, its reintroduction into the mesenchymal cells would not affect the histone marks but only affect the transcription factors influencing EMT, potentially also those influenced by HER2. The role of HER2 is more interesting due to studies showing that E-cadherin loss was not necessary for HER2 induced EMT and somewhat explains EMT in absence of EGFR signalling (Nilsson et al., 2014; Ingthorsson et al., 2016), and linking HER2 with a breast cancer stemness which enforces the EMT phenotype (Nami et al., 2017). The connection of EMT with stemness is something which we have hypothesised in this study. This would be another avenue worth exploring, in whether the active promoter region of ERRB2 is affected by EP300 presence.

As we assume that EP300 is one of the main effectors or regulators of E-cadherin through the CDH1 gene, we suppose that this migration characteristic could be also controlled through its expression. This is the logic behind the CDH1 overexpression in this cell line, as mesenchymal cells lack E-cadherin, its reintroduction should reverse the EMT migratory characteristics. With these two cell lines (CAL51 and MDA-MB-231), there are mixed findings: while both cell lines result in a decreased wound healing response with CDH1 overexpression, only CAL51s overexpression of CDH1 results in the lowest wound healing response, whereas MDA-MB-231 cells have the lowest wound healing response with EP300 overexpression. This likely reflects different activated pathways and perhaps EP300 is a more relevant target in this cell line. We also have still yet to confirm whether there is a direct or indirect relationship between the two in this case. We could attempt to inactivate

the bromodomain of EP300 and reintroduce CDH1 on its own and vice versa, to see whether this effect is mainly coming from CDH1 or not.

A study shows that in CAL-51 and MDA-MB-231 cell lines E-cadherin promoter is not deleted, hypermethylated or mutated. It was also found that in those cell lines with absence of CDH1, synthetic lethality could be achieved via inhibition of ROS1 (Bejrami et al., 2018). We should study whether our cell lines with reintroduced EP300 have any effect on ROS Proto-Oncogene 1, Receptor Tyrosine Kinase (ROS1). When it comes to CAL51, there is a specific link between cell migration dynamics and the expression of YAP (Nardone et al., 2017). This study shows that this expression of YAP influences focal adhesion interaction of the cells by directly influencing focal adhesion genes. Its nuclear localisation influences cell spreading area, and has transcriptional regulation of focal adhesions, as well as influencing the cytoskeleton dynamics and ECM adhesion (Nardone et al., 2017). This makes this protein very important for migration and invasion, and it could also potentially be influenced by EP300 and should be further looked into. The MDA-MB-231 and MCF7 models showed the implication of SAI1/2 and anillin which inhibits the cell migration in these cell lines (Wang et al., 2020; Yang et al., 2020). Furthermore, an attempt to reverse the EMT phenotype has also been shown with an HDAC inhibitor Panobinostat (LBH589), this reversal of invasive properties is mainly through the overexpression of CDH1 and downregulation of ZEB1 and ZEB2 (Rhodes et al., 2014).

Random migration and mesenchymal breast cancer cell lines.

While we weren't able to demonstrate our wound healing reversal solely with EP300 overexpression, we decided to apply a second model to show its relevance and importance in this characteristic. In this instance, we used the same mesenchymal breast cancer cell lines: CAL51 and MDA-MB-231 with the same conditions as with the wound healing assay. For the manual tracking of migration, we plated cells so they have as little or no cell-cell contact and recorded their movement by a camera. The images were then being analysed using a manual tracking software where a good portion of cells were selected and the average movement rate was determined. The CAL51 model did not display a lot of movement so it was difficult to estimate whether EP300 and CDH1 had an effect on these characteristics. However, EP300 overexpression does seem to decrease movement in this cell line, as does the overexpression of CDH1. Again, CDH1 overexpression seems to have more impact on the migration characteristics. The opposite is seen in the MDA-MB-231 cells. This cell line seems to be the better candidate for this assay because its overall movement was higher, as previously shown by our wound healing assay results. Our findings show that EP300 overexpression significantly reduces random migration in this cell line, and this effect is

larger than that with CDH1 overexpression. This could suggest that E-cadherin, while a pivotal EMT switch, might not be the only crucial component for this cell line, and might implicate EP300 as a more important target.

Cells behave in different ways and the presence or lack of ECM ligands might show a different response, as an empty flat plate surface might not accurately reflect in vivo models (Stuelten et al., 2018). Similarly, we mentioned previously that 2D/ 3D models show differences in mammosphere formations and stemness characteristics (Reynolds et al., 2017). As this was shown to affect invasive characteristics and filopodia formation (Yan et al., 2013), therefore, it stands to reason that using 3D models of migration and invasion would be a more accurate result.

Epithelial breast cancer and wound healing.

Using the same principle as before for the mesenchymal cell lines, we adopted this technique for epithelial cell lines. We downregulated EP300 aiming to induce EMT, which should stimulate higher migratory capability and wound healing. In our findings, it is demonstrated that as hypothesised, the epithelial cell lines overall show a very low capacity to migrate even with overexpression of EP300. The low migratory capacity of MCF7 and T47D cell lines has already been demonstrated by another study using the same methodology (Sun et al., 2016; Uchino et al., 2010). Potentially, we should increase the time necessary for this assay up to 72 hours to see a more pronounced effect with this assay. The migratory capacity of these cell lines seems largely due to the effects of estrogen (Lymperatou et al., 2013). There is also some evidence of androgens positively regulating migration characteristics of T47D cells through the expression of myosin cytoskeletal components (Montt-Guevara et al., 2016). Also, there is potential for the epithelial cell lines to have a different mechanism by which EMT can be activated reversed to induce migration, ROCK inhibition has been shown to induce migration independently of EMT (Yang et al., 2014).

Nonetheless, there is still a slightly higher wound closure with EP300 overexpression, when compared to the control. The findings are inconclusive when it comes to generalising this effect across epithelial cells. We used another epithelial cell line, T47D, which shares luminal A characteristics with MCF7 cells. In theory, we would have expected a similar response to EP300 overexpression. Our results show however, that there is an opposite response in T47D, in which both instances of EP300 overexpression result in a slightly decreased wound healing response. This might be due to the imprecision and manual nature of the technique. Some wounds can be larger than others, and therefore much smaller differences would be negated by this, while hypoxia seems to uniformly influence both mesenchymal and epithelial cells to induce higher migration (Barrak et al., 2020).

Random migration and epithelial breast cancer cell lines.

Similar with the mesenchymal cells, we tried to see whether our luminal A subtype cell lines had a different response in another migration assay. Same concept applies like before, where movement was tracked by using imaging techniques earlier described. In this case, we noticed EP300 downregulation in MCF7 cells results in a relatively similar or decreased migration, while T47D cells display an opposite response of increased migration with both instances of EP300 knockdown.

Colorectal cancer and wound healing.

To take this concept further, we recognise that all cancers behave differently across subtypes and even sit on primary tumours. We tested our concept of EMT reversal on a cell line that has a high expression of EP300. In this way, we see if our concept is applicable outside the domain of breast cancer. While we haven't managed to demonstrate a distinct role for EP300 between breast cancer subtypes, when looking at a different model of an invasive cancer such as colorectal cancer, we clearly see that, its knockdown results in an increased migration and wound healing response in the HCT116 cell line. This could suggest that EP300 is a repressor of sorts in this cell line, and its knockdown results in upregulation of pathways that were otherwise shut down. It should be noted that while its knockout results in an increase in wound healing, its regular expression does not fully repress these traits as this cell line still has migration, albeit at a very slow pace. The slow pace of migration has been previously demonstrated by other studies (Chung et al., 2018; Zhu et al., 2016). The activation of EMT traits is likely following a different model in this cell line compared to breast cancer, and the effects of EP300 are more likely to be through β-catenin. The induction of EMT with the loss of E-cadherin in this cell line has been shown to be through β-catenin, and is responsible for decreased cell-cell junctions (Kim et al., 2019).

Colorectal Cancer and Random Migration

Paradoxically, while we mentioned that our wound healing response is higher in HCT116 with EP300 knockout, we see the opposite effect on random migration, whereby its knockout reduces movement. It is hard to speculate the reason for this, it potentially responds better in this experiment, or simply the differences are too small to be significant and are just a statistical anomaly. We can see that the relative arbitrary units for speed are much lower for both conditions when comparing other cell lines we used, which reflects the relatively low speed of wound closure we saw in our previous model.

Invasion assay and mesenchymal breast cancer cell line.

As the hallmark of cancer is both invasion and migration, we could not demonstrate one without the other. Due to the nature of the assay, we opted for cells which would be easiest to estimate cell doubling time and with a higher rate of proliferation. Therefore, we chose MDA-MB-231 cells which have demonstrated a high rate of migration, and a demonstrable effect of EP300 and CDH1 overexpression on this characteristic. The second is a colorectal cancer model using HCT116 cells. We realised that at the outset, a better demonstration of our EP300 model would be within breast cancer and between cancer subtypes, but due to time constraints of this method, we opted for the faster cell lines to see whether this was a viable technique. The classical way of demonstrating invasion is by using transwell migration assays (Eccles et al., 2005), which while effective, are variable in quality and pore size between manufacturers. And due to different sizes of cell lines, can have a result that is more down to gravity than any genetic differences. There are also difficulties during the preparation of these assays as excessive trypsinization can lead to cell clumping during the single cell suspension step (Staton et al., 2009). There are also issues with automation of cell counting due to the way cell staining does not always provide clear cell boundaries if cells are too close together (Staton et al., 2009).

The method begins with plating cells in a 96 well plate, then coated with type IV rat tail collagen, which is allowed to solidify before the EGF is administered on top. The cells are then left to migrate towards the surface and fixed with PFA and a cell dye. This invasion/migration is captured by an imaging technique after, which records the image of the collagen gel in slices, or Z-stacks which are captured at multiple locations in the well. This step is crucial as it would normalise or accentuate any deformation in the gel, as the experiment requires a uniform gel height without any bubbles to accurately measure invasion.

This results in a 3D image of the cells, which requires an automated deconvolution step using Huygens deconvolution software, and significant computing power and time to process each image. This deconvolution step is necessary to improve contrast and decrease any autofluorescence so that we can accurately see cells. Due to the nature of some cells fluorescing more than others depending on what cell cycle they are in and whether they have more than one nucleus. After this step, a section is taken and converted to an 8-bit image, which we opted for using an automated procedure in Fiji for Image J. The final automated procedure in the same software uses an automated script by a threshold value differentiated cells from stroma and counts them on every level of the Z stack. We then used an averaged Z-score value to measure the amount of cells which invaded the surface. This method is similar in its approach to one used by a previous study (Benbow et al., 2000)

Our method relies on a migration against gravity on a chemotactic concentration gradient towards EGF. Similarly, we try to emulate the stromal environment by using a collagen type IV ligand structure, which results in a more porous, less straight environment where the cells would have to navigate. This is not without its drawbacks however, as the optimal thickness of collagen gel must be determined for each cell line, as well as optimal cell number and time point for stopping the experiment. Further complications arise in the analysis of the results as multiple steps require adoption of the protocol.

Our results show that the MDA-MB-231 cell line seems to invade more in the control and the overexpression of EP300 impedes its progress, more so than with the overexpression of CDH1. Together with their increased ability of migration demonstrated by the wound healing assay and cell tracking, this suggests that EP300 regulate these traits. It would be worth checking the cells for expression of MMPs during this invasion phase to see whether they express more and whether that helps them navigate. The opposite is seen in our HCT116 model showing that the knockout of EP300 in this cell line results in increased invasion. This likely reflects the differences between the activated pathways in these cancers.

8.2.5 Future Potential Work

One way in which the migration assays could be taken further is by taking a similar approach to (Wang et al., 2019), where the migration characteristics and leading edge will be monitored according to increasing concentrations of paclitaxel and doxorubicin used in **Chapter 7**.

While these methods are easy to handle, fast and reproducible, along with the utility of software, like Image J, allow for robust analysis to be done on a variety of cell properties. Some limitations, as mentioned earlier, include that the pipette tip could potentially not offer the most accurate wound that can be compared. A commercial kit: CellPlayer™ Migration Assay from Essen Bioscience exists to improve this accuracy and works by an automated wound marker tool (Hayes et al., 2010). However, this comes at a great cost due to a need for a specialised imaging tool. Otherwise, an alternative exists to combine the wound healing assay with an invasive component, by overlaying a matrigel on the wound healing area or by coating the plate surface with an ECM component to test both characteristics (Kam et al., 2008; Vogt et al., 2010). This might also improve cell motility on some of the slower moving cell lines in our study.

Another option is to test migration with the microfluidics chamber assay (Meyvantsson et al., 2008), in which cells are added and adhered onto the chamber, and a gradient is set up by which the cells migrate. This can be further improved upon by making a 3D ECM environment through which the cells must migrate through (Echeverria et al., 2010). The

advantage of this is low reagent costs but also due to the small size of the assay, constant monitoring and required hands-on approach, therefore adding a time cost to the assay.

A further potential assay is a cell exclusion zone assay which circumvents some limitations of the wound healing assay, such as the release of cell death cytokines during the wound scratch procedure from cell debris (Poujade et al., 2007). In this assay, cells are seeded around a stopper, and once the object is removed, the cells rejoin the area, which is then monitored. All of the assays above could also be improved upon by using MMP inhibitors and perhaps utilising high throughput screening which would be able to monitor the molecular changes that are happening during migration. Recent studies also used a combination of molecular profile of kinases involved in migration coupled with functional assays like micropatterning (Thakuri et al., 2020)

There is also potential to take this analysis further by first determining the leading edge healing speed and moving on to individual cell migration analysis (De Pascalis, Etienne-Manneville et al., 2017). As mentioned earlier, invasion assays such as transwell are problematic and require testing on each cell line if they do not penetrate the membrane horizontally (Trepat et al., 2012). Nevertheless, this assay could also be used. We could have also opted for using a fluorescent microscope to track the cell movement as some of our cells are GFP tagged, but also pose a challenge due to potential for photo-toxicity (Icha et al., 2017). Another limitation of these methods is due to the vast amount of images generated, we were forced to automate some steps using scripts written for Image J and Huygens. Some steps generalise the analysis and are less accurate than done by hand but are not feasible otherwise and in any case, they are accurate enough for the analysis we performed. For migration, it would be probably easier to use less manual methods, which would decrease human error but also allow for streamline procedure. Currently, there is IncuCyte ZOOM live cell analyzer (Essen Biomedics) that does automated image capture, along with data analysis (Martin et al., 2017)

The role of EP300 in migration and invasion is still yet to be demonstrated but some evidence already suggests that there is potential for this. A study has shown modulation of acetylation states by CBP, influences EMT by targeting promoters of known pro EMT genes like SNAI1 (Dai et al., 2020).CBP and EP300 both share their bromodomain structure (Ebrahimi et al., 2019). It is reasonable to assume that EP300 would have similar effects. The evidence of acetylation marks expression differences between epithelial and mesenchymal breast cancer cell lines, which makes it an interesting target (Nami et al., 2020). Apart from transcription factors involved in EMT, as migration is controlled by cytoskeletal interactions with the ECM and stroma, the acetylation of the cytoskeletal component is also vitally important. We have outlined a number of these among ezrin (Song et al., 2020), particularly

interactions with the microenvironment and acetylation of its influencers such as ArfGAP with coiled-coil, ankyrin repeat and PH domains 4 (ACAP4) (Song et al., 2018).

8.2.6 Overall Conclusion

In conclusion, the effect of EP300 is not clear on migration and invasion between subtypes of breast cancer, and seems to have a different impact between colorectal cancer and breast cancer. However, due to similar results in wound healing assay for mesenchymal cells CAL-51 and MDA-MB-231, it leads us to believe there is some potential for this as a therapeutic target. This needs to be validated with more robust reproducible models, perhaps using the aqueous two phase printing technique by (Thakuri et al., 2020).

Chapter 9

Concluding Remarks

Throughout this study, we have aimed to draw a conclusive role for EP300, a histone acetyltransferase as a master regulator of CDH1. We initially decided to approach this as a gain of function and loss of function experiment by looking at epithelial to mesenchymal transition. Most studies agree that the loss of CDH1 results in this EMT switch and has a cascade effect on many of the genes involved in metastasis, drug resistance and stemness. The experimental design involved categorising CAL-51 and MDA-MB-231 as mesenchymal subtypes, which would have EP300 overexpressed and T47D and MCF7 as epithelial subtypes with EP300 knocked down. This showed that in mesenchymal models, EP300 would be expected to have a repressive role on EMT and therefore its knockdown in an epithelial cell line should promote EMT. We also utilised an alternative model of colorectal cancer-HCT116, in which we knocked out EP300 and showed that EP300 is applicable to other cancers, as well as having alternative effects on epithelial cell lines of other cancers.

Throughout this thesis, we hypothesised that EP300 affects the expression of CDH1. We went through several investigations to show this effect. In **Chapter 3**, we looked at the effect of miRs, in particular miR-25 on promoting FOXO3a expression and positively regulating CDH1. In **Chapter 4**, we attempted to follow-up on our published work by taking a gene signature previously found in our MCF7 model of EP300 downregulation and seeing if there is any differential expression of these genes between molecular subtypes and modulated EP300 expression. In **Chapter 5**, we tackled the problem two-fold, we first looked into whether the expression of either CDH1 or EP300 has any positive effect on patient survival through Kaplan Meier analysis, investigating the same gene signature in the TCGA RNA-seq dataset to see whether breast cancer subtypes, express this signature differently. In **Chapter 6**, we began to look into some of the cancer survival traits such as drug resistance, and whether modulated expression of EP300 could prevent this resistance. In **Chapter 7**, we looked into the CSCs, a trait often linked to EMT, drug resistance, and whether modulating

EP300 in our cell line models, could affect the expression of ALDH+ and $CD44^{high}/CD24^{low}$ CSC populations. Finally, in **Chapter 8** we tackled invasion and migration, one of the hallmarks of cancer and traits which enable metastasis. In this chapter, we opted for wound healing and other microscopy techniques to manually track cell movement and invasion through Matrigel barriers to reflect their invasion in tissues in vivo in context of modulating EP300. The same cell lines also experienced a decrease in random migration. In this chapter, we found that in context of mesenchymal cells, EP300 acts as a repressor of directional migration while in epithelial cell lines it is a promoter. When investigating the same traits in a colorectal cancer model, we saw that EP300 knockdown decreases both directional and random migration. This suggested that there might be a dramatic effect on lamellipodia formation and potentially interruption in the Rho GTPase control on cell polarity. However, as demonstrated by our invasion model, this cell line experiences an increase in invasion as a response to EP300 knockdown.

The beginning of the study focused more on miRs 27a, 23a and 25 as potential upstream effectors that would target various genes such as, FOXA1, RUNX1 and GATA3 to affect the EP300 network. **Chapter 3** concluded with miR-25 being our most promising target. Despite a body of evidence showing all three miRs are involved in EMT, drug resistance and CSC traits, our RTqPCR results concluded with us dismissing miR-27a and miR-23a due to a potential transfection problem. MiR-25 demonstrated through RTqPCR that it regulates EP300, GATA3 and FOXO3a in our MTMEC model. All of these genes in some form regulate CDH1, e.g. FOXO3a is a pioneer transcription factor and repressor of its FOXM1 counterpart which mediates downregulation of CDH1. This is important for potential therapeutic purposes, as if our hypothesis with EP300 is proved to be incorrect, miRs could be used to circumvent signalling pathways and directly influence CDH1 levels.

This also prompted us to investigate the miR transcriptional landscape in context of drug resistance. Overall, the commonly used chemotherapeutic agents such as doxorubicin and paclitaxel, affect the expression of all 3 miRs. While we have dismissed the transfection results of miRs 27a and 23a, doxorubicin and paclitaxel both seem to downregulate miR-27a and upregulate miR-23a in our MTMEC wild type. The significance of which is yet to be determined but likely yields a different response to these therapies through the modulation of CDH1. We also tested a platinum-based inhibitor Lapatinib, which showed its own unique modulation of these aforementioned miRs. Both miR-27a and miR-23a were upregulated in its resistance, likely reflecting their close proximity to chromosome 19, as well as downregulation of miR-25. All this suggested that monitoring the effects of chemotherapy is complex but might be worthwhile to pursue investigation into their differential expression across molecular subtypes of breast cancer.

This led us to analysing basal expression levels of our miRs. Our results showed that epithelial cell lines such as T47D and MCF7 express all 3 miRs at low levels. However, there was no universal expression among the mesenchymal subtype as all MDA-MB-231, CAL-51 and Hs578T seem to have their own unique expression patterns, though all commonly overexpress miR-27a. The outcome of this portion was inconclusive and required more in depth study into protein levels and potential gain/loss of function experiments with miRs. This was out of the scope of the study and was left for follow-up at a later point in time.

As our investigation into miRs provided some interesting preliminary results into a connection with EP300 and CDH1 signalling network, in **chapter 4** we proceeded to use our cell lines with modulated EP300 and CDH1 levels through lentiviral overexpression and knockdown. All of our models showed that this transfection was successful and the overexpression of both EP300 and CDH1 in CAL-51 and MDA-MB-231 both affected the levels of CDH1. Going back to our hypothesis with CDH1 being the EMT switch, as levels of CDH1 were directly modulated by EP300, we assumed that there could be some knock-on effect on EMT. However, both cell lines resulted in different gene expression patterns, which likely reflected the heterogeneity of cancer even among molecular subtypes. Of which, the direct overexpression of CDH1 seemed to have a more dramatic effect than EP300 on its own. We also confirmed a successful downregulation of EP300 in our T47D model which echoed with previously published data on MCF7 (Asaduzzaman et al., 2017). This potentially could promote EMT in these cell lines. We could potentially investigate this through the effects on CDH1 and GATA3, which were the most prominently affected genes. The most puzzling was the different gene expression between two vectors which we used to target EP300 (shEP300 I and shEP300 II). We think that this could be attributed to different isolation time points and cell cycle states. Our attempt to look into a colorectal cancer cell line HCT116 showed that knockout of EP300 affected some pro invasive genes. Overall, the gene expression signature we focused on in this chapter did not yield any patterns between cancer subtypes or different cancers. This suggested that while these genes are significantly affected, no conclusive pattern can be drawn. Therefore, when taken into account with the results of chapter 5, we abandoned the idea of a novel gene signature to be of any prognostic significance. In this chapter, we also began to focus on the hallmarks of cancer. While the distinct gene signature of EP300 has not yet been revealed, we attempted to investigate its effects on these hallmark traits. The first of which, is uncontrolled cell proliferation. It seemed not to be controlled by EP300 as all of our cell lines showed no effect on proliferation.

Chapter 5 was our attempt to establish prognostic value of EP300 and CDH1 in patient datasets. By using the KM-plot analysis of Metabric and TCGA datasets, we found that high CDH1 expression had improved overall survival. This is likely due to its suppression

of pro invasive and drug resistance genes, whereas high expression of EP300 conferred higher relapse free survival in the triple negative, luminal A and luminal B subtypes; high CDH1 expression improved relapse free survival in the HER2 subtype. These findings confirmed that these two genes are worth looking into as they might have a therapeutic benefit. Together with observed results from chapter 4, we concluded with the investigation of our gene signature in a RNA-seq analysis of the publicly available TCGA dataset. The results of which conclusively proved the gene signature to have no value for any molecular subtype. It is likely that other expression patterns exist, and potentially other genes need to be investigated both in TCGA and by our RTqPCR analysis. We also suggested that as EP300 is an acetyltransferase, it might be worth looking into its effects on histone acetylation marks, promoter hypermethylation of CDH1, as well as other computational analysis.

Continuing with the theme of hallmarks of cancer, we investigated the drug resistance traits and whether modulation of EP300 has any effect on reversing this trait. **Chapter 6** concluded with MDA-MB-231 overexpressing EP300 and CDH1 seem to regain sensitivity at 10-16nM. While the same overexpression of EP300 shows improved sensitivity to doxorubicin between 313-405nM. We have also demonstrated that EP300 and CDH1 both affect drug resistance and therefore worthwhile therapeutic targets in context of drug resistance. We then looked into long term drug resistance to paclitaxel and found that drug resistant clones decreased with EP300 and CDH1 overexpression when treated at a concentration range of 8-10nM. While we have not determined the ideal concentration of paclitaxel or doxorubicin, we have arrived at a potentially ideal range where we can continue the investigation in the mesenchymal cell lines. Finally, the T47D knockdown of EP300 was inconclusive, while we see a decrease in cell survival, we are yet to determine the optimal concentration of paclitaxel. Therefore, further testing is necessary in this cell line to draw any conclusion to epithelial cell line drug resistance.

As drug resistance traits are linked with cancer stem cells, the origin of which is debated. Nevertheless, we opted for flow cytometry analysis of two classical markers of stemness ALDH+ and $CD44^{high}/CD24^{low}$ subpopulations in **Chapter 7**. We used the same cell lines for this experiment, EP300 overexpression in mesenchymal cell lines MDA-MB-231 and CAL51 to decrease the presence of ALDH+ subpopulations. However, when it comes to the $CD44^{high}/CD24^{low}$ subpopulation, EP300 overexpression increased the proportion of cells expressing this phenotype; whereas, CAL51 expressed a very small percentage of $CD44^{high}/CD24^{low}$, instead favoured $CD44^{low}/CD24^{low}$ phenotype with EP300 overexpression. Similarly in the MCF7 and T47D downregulation of EP300. In MCF7, there was no conclusive effect on ALDH+ cells as both shEp300 I and sh EP300 II have opposite effects. We also saw both cell lines did not express $CD44^{high}CD24^{low}$, instead favoured

the $CD44^{high}/CD24^{high}$ and $CD44^{low}/CD24^{high}$ phenotypes. The knockout of EP300 in the colorectal cancer cell line HCT116 increases the expression of ALDH+ subpopulations. However, the knockout did not have a big influence on the presence of $CD44^{high}/CD24^{low}$ subpopulations, as a large portion still remained despite having an effect. While we initially decided on these two markers, our conclusion is that we could not state whether EP300 had an effect on promoting CSCs in mesenchymal breast cancer cell lines. What we discovered is that it affected one of the markers, ALDH. Also, while there was no direct relationship with $CD44^{high}/CD24^{low}$, some studies showed that the various surface expression patterns of CD44 and CD24 correspond to higher and lower invasive capabilities and presence of filopodia (Yan et al., 2013). Furthermore, the mixture of CD44 and CD24 expression patterns is better explained in the context of 3D environment, where leading edge or necrotic core of 3D structures, had more of the $CD44^{high}/CD24^{low}$ phenotype (Reynolds et al., 2017). This could potentially connect EP300 and control invasion, another hallmark of cancer. We also tested the effects of long-term drug resistance on the expression of these markers, to see if there was a correlation. Both doxorubicin and paclitaxel influence the expression of ALDH in opposite effects, probably due to their mode of action. Paclitaxel has a positive influence on decreasing this subpopulation of cells. However, both drug treatments increased the proportion of $CD44^{high}/CD24^{low}$ cells, suggesting that chemotherapy can induce a drug resistant phenotype in epithelial breast cancers. Overall, while EP300 overexpression did not fully confirm the presence of CSCs, we can see that its expression can affect the presence of stem cell markers. To fully explore this effect, we should use mammosphere assays or explore other markers.

The final chapter (**Chapter 8**), it dealt with one other hallmark of cancer, invasion and migration. While breast cancer cell line subtype effects were cell line specific, we did see a trend towards decreasing random and directional migration in MDA-MB-231, and a decrease in invasion. CAL51, while decreasing directional migration, had a decrease in random migration. The reason why both have different responses is probably due to the mechanism which both utilised to form leading/trailing edge movement. This suggests CAL-51 favoured the random migration. The opposite effect was seen in MCF7 and T47D epithelial cell lines, which showed an increase in both directional and random migration. With our knockout model of EP300 in HCT116, we saw both an increase in invasion and directional migration, as well as a decrease in random migration. The discrepancy could be that overall, EP300 knockout increased invasion and migration, and it favoured a more directional migration pattern with more filopodia formation.

Therefore, to summarise all findings, it seemed that EP300 directly modulates the expression of CDH1, therefore influencing the status of EMT, drug resistance and stemness

characteristics. In particular, this is shown well with the mesenchymal cell lines MDA-MB-231 and CAL51, and our downregulation in T47D and MCF7 using the sh EP300 I and II vectors. This showed EP300 as a viable therapeutic model which should be investigated further through the use of mouse models and other sequencing technology, in order to show a full effect on the pathways and acetylation/ methylation states it influences through the action of enhancer regions and active promoters. The study of this protein is still incomplete and requires more in depth analysis to reveal its true impact on the drug resistance, EMT and CSC landscape.

Chapter 10

References

Abraham, B.K., Fritz, P., McClellan, M., Hauptvogel, P., Athelogou, M. and Brauch, H.,2005. Prevalence of CD44+/CD24−/low cells in breast cancer may not be associated with clinical outcome but may favor distant metastasis. Clinical cancer research, 11(3), pp.1154-1159.

Aigner, K., Dampier, B., Descovich, L., Mikula, M., Sultan, A., Schreiber, M., Mikulits, W., Brabletz, T., Strand, D., Obrist, P. and Sommergruber, W., 2007. The transcription factor ZEB1 (δ EF1) promotes tumour cell dedifferentiation by repressing master regulators of epithelial polarity. Oncogene, 26(49), pp.6979-6988.

Al Harras, M.F., Houssen, M.E., Shaker, M.E., Farag, K., Farouk, O., Monir, R., El Mahdy, R. and Abo Hashem, E.M., 2016. Polymorphisms of glutathione S-transferase π 1 and toll-like receptors 2 and 9: Association with breast cancer susceptibility. Oncology letters, 11(3), pp.2182-2188.

Alcázar-Román, A.R., Tran, E.J., Guo, S. and Wente, S.R., 2006. Inositol hexakisphosphate and Gle1 activate the DEAD-box protein Dbp5 for nuclear mRNA export. Nature cell biology, 8(7), pp.711-716.

Alotaibi, K.D., Schoenau, J.J., Kar, G., Peak, D. and Fonstad, T., 2018. Phosphorus speciation in a prairie soil amended with MBM and DDG ash: Sequential chemical extraction and synchrotron-based XANES spectroscopy investigations. Scientific reports, 8(1), pp.1-9.

An, J., Lv, J., Li, A., Qiao, J., Fang, L., Li, Z., Li, B., Zhao, W., Chen, H. and Wang, L., 2015. Constitutive expression of Bcl-2 induces epithelial-Mesenchymal transition in mammary epithelial cells. BMC cancer, 15(1), pp.1-8.

An, T., Qin, S., Xu, Y., Tang, Y., Huang, Y., Situ, B., Inal, J.M. and Zheng, L., 2015. Exosomes serve as tumour markers for personalized diagnostics owing to their important role in cancer metastasis. Journal of extracellular vesicles, 4(1), p.27522.

An, Y., Zhang, Z., Shang, Y., Jiang, X., Dong, J., Yu, P., Nie, Y. and Zhao, Q., 2015. miR-23b 3p regulates the chemoresistance of gastric cancer cells by targeting ATG12 and HMGB2. Cell death & disease, 6(5), pp.e1766-e1766.

Ananthakrishnan, P. and Lucas, A., 2008. Options and considerations in the timing of breast reconstruction after mastectomy. Cleveland Clinic journal of medicine, 75(1), p.S30.

Anders, C.K., Hsu, D.S., Broadwater, G., Acharya, C.R., Foekens, J.A., Zhang, Y., Wang, Y., Marcom, P.K., Marks, J.R., Febbo, P.G. and Nevins, J.R., 2008. Young age at diagnosis correlates with worse prognosis and defines a subset of breast cancers with shared patterns of gene expression. Journal of clinical oncology, 26(20), pp.3324-3330.

André, F., Bachelot, T., Campone, M., Dalenc, F., Perez-Garcia, J.M., Hurvitz, S.A., Turner, N., Rugo, H., Smith, J.W., Deudon, S. and Shi, M., 2013. Targeting FGFR with dovitinib (TKI258): preclinical and clinical data in breast cancer. Clinical cancer research, 19(13), pp.3693-3702.

Andre, F., Berrada, N. and Desmedt, C., 2010. Implication of tumor microenvironment in the resistance to chemotherapy in breast cancer patients. Current opinion in oncology, 22(6), pp.547-551.

Ansieau, S., Bastid, J., Doreau, A., Morel, A.P., Bouchet, B.P., Thomas, C., Fauvet, F., Puisieux, I., Doglioni, C., Piccinin, S. and Maestro, R., 2008. Induction of EMT by twist proteins as a collateral effect of tumor-promoting inactivation of premature senescence. Cancer cell, 14(1), pp.79-89.

Antón, I.M., Lu, W., Mayer, B.J., Ramesh, N. and Geha, R.S., 1998. The Wiskott-Aldrich syndrome protein-interacting protein (WIP) binds to the adaptor protein Nck. Journal of Biological Chemistry, 273(33), pp.20992-20995.

Anzai, E., Hirata, K., Shibazaki, M., Yamada, C., Morii, M., Honda, T., Yamaguchi, N. and Yamaguchi, N., 2017. FOXA1 induces E-cadherin expression at the protein level via suppression of slug in epithelial breast cancer cells. Biological and Pharmaceutical Bulletin, 40(9), pp.1483-1489.

Aomatsu, N., Yashiro, M., Kashiwagi, S., Takashima, T., Ishikawa, T., Ohsawa, M., Wakasa, K. and Hirakawa, K., 2012. CD133 is a useful surrogate marker for predicting chemosensitivity to neoadjuvant chemotherapy in breast cancer. PloS one, 7(9), p.e45865.

Arco, A., Favaloro, A., Gioffrè, M., Santoro, G., Speciale, F., Vermiglio, G. and Cutroneo, G., 2012. Sarcoglycans in the normal and pathological breast tissue of humans: an immunohistochemical and molecular study. Cells Tissues Organs, 195(6), pp.550-562.

Arfuso, F., Millward, M., Dharmarajan, A. and Warrier, S., 2015. Secreted frizzled-related protein 4 inhibits glioma stem-like cells by reversing epithelial to mesenchymal

transition, inducing apoptosis and decreasing cancer stem cell properties. PloS one, 10(6), p.e0127517.

Arienti, C., Tesei, A., Carloni, S., Ulivi, P., Romeo, A., Ghigi, G., Menghi, E., Sarnelli, A., Parisi, E., Silvestrini, R. and Zoli, W., 2013. SLUG silencing increases radiosensitivity of melanoma cells in vitro. Cellular Oncology, 36(2), pp.131-139.

Arjonen, A., Kaukonen, R., Mattila, E., Rouhi, P., Högnäs, G., Sihto, H., Miller, B.W., Morton, J.P., Bucher, E., Taimen, P. and Virtakoivu, R., 2014. Mutant p53–associated myosin-X upregulation promotes breast cancer invasion and metastasis. The Journal of clinical investigation, 124(3), pp.1069-1082.

Armesto-Jimenez, A.U., Arason, A.J., Stefasson, O.A., Gudmundsson, G., Gudjonsson, T. and Magnusson, M.K., 2019. A MUC5B polymorphism associated with Idiopathic Pulmonary Fibrosis mediates overexpression through decreased CpG methylation and C/EBPb transcriptional activation. bioRxiv.

Arnott, C.H., Scott, K.A., Moore, R.J., Robinson, S.C., Thompson, R.G. and Balkwill, F.R., 2004. Expression of both TNF-α receptor subtypes is essential for optimal skin tumour development. Oncogene, 23(10), pp.1902-1910.

Arpin, M., Friederich, E., Algrain, M., Vernel, F. and Louvard, D., 1994. Functional differences between L-and T-plastin isoforms. The Journal of cell biology, 127(6), pp.1995-2008.

Arthur, J.S.C. and Ley, S.C., 2013. Mitogen-activated protein kinases in innate immunity. Nature Reviews Immunology, 13(9), pp.679-692.

Arwert, E.N., Harney, A.S., Entenberg, D., Wang, Y., Sahai, E., Pollard, J.W. and Condeelis, J.S., 2018. A unidirectional transition from migratory to perivascular macrophage is required for tumor cell intravasation. Cell reports, 23(5), pp.1239-1248.

Atiyeh, B., Dibo, S., Zgheib, E. and Abbas, J., 2014. Skin sparing/skin reducing mastectomy (SSM/SRM) and the concept of oncoplastic breast surgery. International Journal of Surgery, 12(10), pp.1115-1122.

Attwood, K., Fleyshman, D., Prendergast, L., Paszkiewicz, G., Omilian, A.R., Bshara, W. and Gurova, K., 2017. Prognostic value of histone chaperone FACT subunits expression in breast cancer. Breast Cancer: Targets and Therapy, 9, p.301.

Augustine, C.K., Yoshimoto, Y., Gupta, M., Zipfel, P.A., Selim, M.A., Febbo, P., Pendergast, A.M., Peters, W.P. and Tyler, D.S., 2008. Targeting N-cadherin enhances antitumor activity of cytotoxic therapies in melanoma treatment. Cancer research, 68(10), pp.3777-3784.

Avruch, J., Hara, K., Lin, Y., Liu, M., Long, X., Ortiz-Vega, S. and Yonezawa, K., 2006. Insulin and amino-acid regulation of mTOR signaling and kinase activity through the Rheb GTPase. Oncogene, 25(48), pp.6361-6372.

Avvaru, S.P., Noolvi, M.N., Aminbhavi, T.M., Chkraborty, S., Dash, A. and Shukla, S.S., 2018. Aromatase inhibitors evolution as potential class of drugs in the treatment of postmenopausal breast cancer women. Mini Reviews in Medicinal Chemistry, 18(7), pp.609-621.

Awad, O., Yustein, J.T., Shah, P., Gul, N., Katuri, V., O'Neill, A., Kong, Y., Brown, M.L., Toretsky, J.A. and Loeb, D.M., 2010. High ALDH activity identifies chemotherapy-resistant Ewing's sarcoma stem cells that retain sensitivity to EWS-FLI1 inhibition. PloS one, 5(11), p.e13943.

Azim, H.A., Michiels, S., Bedard, P.L., Singhal, S.K., Criscitiello, C., Ignatiadis, M., Haibe Kains, B., Piccart, M.J., Sotiriou, C. and Loi, S., 2012. Elucidating prognosis and biology of breast cancer arising in young women using gene expression profiling. Clinical cancer research, 18(5), pp.1341-1351.

Baccelli, I., Schneeweiss, A., Riethdorf, S., Stenzinger, A., Schillert, A., Vogel, V., Klein, C., Saini, M., Bäuerle, T., Wallwiener, M. and Holland-Letz, T., 2013. Identification of a population of blood circulating tumor cells from breast cancer patients that initiates metastasis in a xenograft assay. Nature biotechnology, 31(6), pp.539-544.

Baccelli, I., Schneeweiss, A., Riethdorf, S., Stenzinger, A., Schillert, A., Vogel, V., Klein, C., Saini, M., Bäuerle, T., Wallwiener, M. and Holland-Letz, T., 2013. Identification of a population of blood circulating tumor cells from breast cancer patients that initiates metastasis in a xenograft assay. Nature biotechnology, 31(6), pp.539-544.

Bach, D.H., Kim, D., An, Y.J., Park, S., Park, H.J. and Lee, S.K., 2018. BMP4 upregulation is associated with acquired drug resistance and fatty acid metabolism in EGFR-mutant non-small-cell lung cancer cells. Molecular Therapy-Nucleic Acids, 12, pp.817-828.

Bachelder, R.E., Yoon, S.O., Franci, C., de Herreros, A.G. and Mercurio, A.M., 2005. Glycogen synthase kinase-3 is an endogenous inhibitor of Snail transcription: implications for the epithelial–mesenchymal transition. The Journal of cell biology, 168(1), pp.29-33.

Bader, A.G., Brown, D. and Winkler, M., 2010. The promise of microRNA replacement therapy. Cancer research, 70(18), pp.7027-7030. Bader, A.G., Kang, S., Zhao, L. and Vogt, P.K., 2005. Oncogenic PI3K deregulates transcription and translation. Nature Reviews Cancer, 5(12), pp.921-929.

Badouel, C. and McNeill, H., 2011. SnapShot: The hippo signaling pathway. Cell, 145(3), pp.484-484.

Badve, S., Turbin, D., Thorat, M.A., Morimiya, A., Nielsen, T.O., Perou, C.M., Dunn, S., Huntsman, D.G. and Nakshatri, H., 2007. FOXA1 expression in breast cancer—correlation with luminal subtype A and survival. Clinical cancer research, 13(15), pp.4415-4421.

Baeriswyl, V. and Christofori, G., 2009, October. The angiogenic switch in carcinogenesis. In Seminars in cancer biology (Vol. 19, No. 5, pp. 329-337). Academic Press.

Bai, J.W., Chen, M.N., Wei, X.L., Li, Y.C., Lin, H.Y., Chen, M., Li, J.W., Du, C.W., Man, K. and Zhang, G.J., 2017. The zinc-finger transcriptional factor Slug transcriptionally downregulates ERα by recruiting lysine-specific demethylase 1 in human breast cancer. Oncogenesis, 6(5), pp.e330-e330.

Bai, W.D., Ye, X.M., Zhang, M.Y., Zhu, H.Y., Xi, W.J., Huang, X., Zhao, J., Gu, B., Zheng, G.X., Yang, A.G. and Jia, L.T., 2014. MiR-200c suppresses TGF-β signaling and counteracts trastuzumab resistance and metastasis by targeting ZNF217 and ZEB1 in breast cancer. International journal of cancer, 135(6), pp.1356-1368.

Bajrami, I., Marlow, R., van de Ven, M., Brough, R., Pemberton, H.N., Frankum, J., Song, F., Rafiq, R., Konde, A., Krastev, D.B. and Menon, M., 2018. E-cadherin/ROS1 inhibitor synthetic lethality in breast cancer. Cancer discovery, 8(4), pp.498-515.

Bakin, A.V., Rinehart, C., Tomlinson, A.K. and Arteaga, C.L., 2002. p38 mitogen-activated protein kinase is required for TGFβ-mediated fibroblastic transdifferentiation and cell migration. Journal of cell science, 115(15), pp.3193-3206.

Bakiri, L., Macho-Maschler, S., Custic, I., Niemiec, J., Guio-Carrion, A., Hasenfuss, S.C., Eger, A., Müller, M., Beug, H. and Wagner, E.F., 2015. Fra-1/AP-1 induces EMT in mammary epithelial cells by modulating Zeb1/2 and TGF β expression. Cell Death & Differentiation, 22(2), pp.336-350.

Balaji, S.A., Udupa, N., Chamallamudi, M.R., Gupta, V. and Rangarajan, A., 2016. Role of the drug transporter ABCC3 in breast cancer chemoresistance. PloS one, 11(5), p.e0155013.

Balko, J.M., Schwarz, L.J., Bhola, N.E., Kurupi, R., Owens, P., Miller, T.W., Gómez, H., Cook, R.S. and Arteaga, C.L., 2013. Activation of MAPK pathways due to DUSP4 loss promotes cancer stem cell-like phenotypes in basal-like breast cancer. Cancer research, 73(20), pp.6346-6358.

Bao, Y., Chen, Z., Guo, Y., Feng, Y., Li, Z., Han, W., Wang, J., Zhao, W., Jiao, Y., Li, K. and Wang, Q., 2014. Tumor suppressor microRNA-27a in colorectal carcinogenesis and progression by targeting SGPP1 and Smad2. PloS one, 9(8), p.e105991.

Bao, Y., Chen, Z., Guo, Y., Feng, Y., Li, Z., Han, W., Wang, J., Zhao, W., Jiao, Y., Li, K. and Wang, Q., 2014. Tumor suppressor microRNA-27a in colorectal carcinogenesis and progression by targeting SGPP1 and Smad2. PloS one, 9(8), p.e105991.

Bao, Y., Chen, Z., Guo, Y., Feng, Y., Li, Z., Han, W., Wang, J., Zhao, W., Jiao, Y., Li, K. and Wang, Q., 2014. Tumor suppressor microRNA-27a in colorectal carcinogenesis and progression by targeting SGPP1 and Smad2. PloS one, 9(8), p.e105991.

Bargagna-Mohan, P., Hamza, A., Kim, Y.E., Ho, Y.K.A., Mor-Vaknin, N., Wendschlag, N., Liu, J., Evans, R.M., Markovitz, D.M., Zhan, C.G. and Kim, K.B., 2007. The tumor inhibitor and antiangiogenic agent withaferin A targets the intermediate filament protein vimentin. Chemistry & biology, 14(6), pp.623-634.

Bargou, R.C., Jürchott, K., Wagener, C., Bergmann, S., Metzner, S., Bommert, K., Mapara, M.Y., Winzer, K.J., Dietel, M., Dörken, B. and Royer, H.D., 1997. Nuclear localization and increased levels of transcription factor YB-1 in primary human breast cancers are associated with intrinsic MDR1 gene expression. Nature medicine, 3(4), pp.447-450.

Barkan, D., Kleinman, H., Simmons, J.L., Asmussen, H., Kamaraju, A.K., Hoenorhoff, M.J., Liu, Z.Y., Costes, S.V., Cho, E.H., Lockett, S. and Khanna, C., 2008. Inhibition of metastatic outgrowth from single dormant tumor cells by targeting the cytoskeleton. Cancer research, 68(15), pp.6241-6250.

Barkauskaite, E., Jankevicius, G. and Ahel, I., 2015. Structures and mechanisms of enzymes employed in the synthesis and degradation of PARP-dependent protein ADP-ribosylation. Molecular cell, 58(6), pp.935-946.

Barlow, J., Yandell, D., Weaver, D., Casey, T. and Plaut, K., 2003. Higher stromal expression of transforming growth factor-beta type II receptors is associated with poorer prognosis breast tumors. Breast cancer research and treatment, 79(2), pp.149-159.

Barrak, N.H., Khajah, M.A. and Luqmani, Y.A., 2020. Hypoxic environment may enhance migration/penetration of endocrine resistant MCF7-derived breast cancer cells through monolayers of other non-invasive cancer cells in vitro. Scientific reports, 10(1), pp.1-14.

Barrallo-Gimeno, A. and Nieto, M.A., 2005. The Snail genes as inducers of cell movement and survival: implications in development and cancer. Development, 132(14), pp.3151-3161.

Barrow-McGee, R., Kishi, N., Joffre, C., Ménard, L., Hervieu, A., Bakhouche, B.A., Noval, A.J., Mai, A., Guzmán, C., Robbez-Masson, L. and Iturrioz, X., 2016. Beta 1-integrin–c-Met cooperation reveals an inside-in survival signalling on autophagy-related endomembranes. Nature communications, 7, p.11942.

Bartel, D.P., 2004. MicroRNAs: genomics, biogenesis, mechanism, and function. cell, 116(2), pp.281-297.

Bartelink, H., Maingon, P., Poortmans, P., Weltens, C., Fourquet, A., Jager, J., Schinagl, D., Oei, B., Rodenhuis, C., Horiot, J.C. and Struikmans, H., 2015. Whole-breast irradiation

with or without a boost for patients treated with breast-conserving surgery for early breast cancer: 20-year follow-up of a randomised phase 3 trial. The lancet oncology, 16(1), pp.47-56.

Bassez, G., Camand, O.J., Cacheux, V., Kobetz, A., Dastot-Le Moal, F., Marchant, D., Catala, M., Abitbol, M. and Goossens, M., 2004. Pleiotropic and diverse expression of ZFHX1B gene transcripts during mouse and human development supports the various clinical manifestations of the "Mowat–Wilson" syndrome. Neurobiology of disease, 15(2), pp.240-250.

Bastien, R.R., Rodríguez-Lescure, Á., Ebbert, M.T., Prat, A., Munárriz, B., Rowe, L., Miller, P., Ruiz-Borrego, M., Anderson, D., Lyons, B. and Álvarez, I., 2012. PAM50 breast cancer subtyping by RT-qPCR and concordance with standard clinical molecular markers. BMC medical genomics, 5(1), p.44. Bates, D.L., Chen, Y., Kim, G., Guo, L. and Chen, L., 2008. Crystal structures of multiple GATA zinc fingers bound to DNA reveal new insights into DNA recognition and self-association by GATA. Journal of molecular biology, 381(5), pp.1292-1306.

Batlle, E., Sancho, E., Francí, C., Domínguez, D., Monfar, M., Baulida, J. and De Herreros, A.G., 2000. The transcription factor snail is a repressor of E-cadherin gene expression in epithelial tumour cells. Nature cell biology, 2(2), pp.84-89.

Baum, O., Hlushchuk, R., Forster, A., Greiner, R., Clézardin, P., Zhao, Y., Djonov, V. and Gruber, G., 2007. Increased invasive potential and up-regulation of MMP-2 in MDA-MB-231 breast cancer cells expressing the $\beta 3$ integrin subunit. International journal of oncology, 30(2), pp.325-332.

Baumann, P., Cremers, N., Kroese, F., Orend, G., Chiquet-Ehrismann, R., Uede, T., Yagita, H. and Sleeman, J.P., 2005. CD24 expression causes the acquisition of multiple cellular properties associated with tumor growth and metastasis. Cancer research, 65(23), pp.10783-10793.

Bayraktar, S., Royce, M., Stork-Sloots, L., de Snoo, F. and Glück, S., 2014. Molecular subtyping predicts pathologic tumor response in early-stage breast cancer treated with neoadjuvant docetaxel plus capecitabine with or without trastuzumab chemotherapy. Medical oncology, 31(10), p.163.

Beach, J.R., Hussey, G.S., Miller, T.E., Chaudhury, A., Patel, P., Monslow, J., Zheng, Q., Keri, R.A., Reizes, O., Bresnick, A.R. and Howe, P.H., 2011. Myosin II isoform switching mediates invasiveness after TGF-β–induced epithelial–mesenchymal transition. Proceedings of the National Academy of Sciences, 108(44), pp.17991-17996.

Beauchemin, N. and Arabzadeh, A., 2013. Carcinoembryonic antigen-related cell adhesion molecules (CEACAMs) in cancer progression and metastasis. Cancer and Metastasis Reviews, 32(3-4), pp.643-671.

Beck, S., Sommer, P., Silva, E.D.S., Blin, N. and Gott, P., 1999. Hepatocyte nuclear factor 3 (winged helix domain) activates trefoil factor gene TFF1 through a binding motif adjacent to the TATAA box. DNA and cell biology, 18(2), pp.157-164.

Bedford, D.C. and Brindle, P.K., 2012. Is histone acetylation the most important physiological function for CBP and p300?. Aging (Albany NY), 4(4), p.247.

Bellucci, L., Dalvai, M., Kocanova, S., Moutahir, F. and Bystricky, K., 2013. Activation of p21 by HDAC inhibitors requires acetylation of H2A. Z. PloS one, 8(1), p.e54102.

Ben-Porath, I., Thomson, M.W., Carey, V.J., Ge, R., Bell, G.W., Regev, A. and Weinberg, R.A., 2008. An embryonic stem cell–like gene expression signature in poorly differentiated aggressive human tumors. Nature genetics, 40(5), p.499.

Benbow, U., Orndorff, K.A., Brinckerhoff, C.E. and Givan, A.L., 2000. Confocal assay for invasion: use of propidium iodide fluorescence and laser reflectance to quantify the rate of migration of cells through a matrix. Cytometry: The Journal of the International Society for Analytical Cytology, 40(4), pp.253-259.

Benchimol, S., Fuks, A., Jothy, S., Beauchemin, N., Shirota, K. and Stanners, C.P., 1989. Carcinoembryonic antigen, a human tumor marker, functions as an intercellular adhesion molecule. Cell, 57(2), pp.327-334.

Beretta, G.L., Cassinelli, G., Pennati, M., Zuco, V. and Gatti, L., 2017. Overcoming ABC transporter-mediated multidrug resistance: the dual role of tyrosine kinase inhibitors as multitargeting agents. European journal of medicinal chemistry, 142, pp.271-289.

Bergert, M., Chandradoss, S.D., Desai, R.A. and Paluch, E., 2012. Cell mechanics control rapid transitions between blebs and lamellipodia during migration. Proceedings of the National Academy of Sciences, 109(36), pp.14434-14439.

Bernardo, G.M. and Keri, R.A., 2012. FOXA1: a transcription factor with parallel functions in development and cancer. Bioscience reports, 32(2), pp.113-130.

Bernardo, G.M., Lozada, K.L., Miedler, J.D., Harburg, G., Hewitt, S.C., Mosley, J.D., Godwin, A.K., Korach, K.S., Visvader, J.E., Kaestner, K.H. and Abdul-Karim, F.W., 2010. FOXA1 is an essential determinant of ERα expression and mammary ductal morphogenesis. Development, 137(12), pp.2045-2054.

Berois, N., Varangot, M., Sonora, C., Zarantonelli, L., Pressa, C., LAVIna, R., Rodríguez, J.L., Delgado, F., Porchet, N., Aubert, J.P. and Osinaga, E., 2003. Detection of bone marrow-disseminated breast cancer cells using an RT-PCR assay of MUC5B mRNA. International journal of cancer, 103(4), pp.550-555.

Berx, G. and Van Roy, F., 2009. Involvement of members of the cadherin superfamily in cancer. Cold Spring Harbor perspectives in biology, 1(6), p.a003129.

Bharadwaj, R. and Yu, H., 2004. The spindle checkpoint, aneuploidy, and cancer. Oncogene, 23(11), pp.2016-2027.

Bhat-Nakshatri, P., Appaiah, H., Ballas, C., Pick-Franke, P., Goulet, R., Badve, S., Srour, E.F. and Nakshatri, H., 2010. SLUG/SNAI2 and tumor necrosis factor generate breast cells with CD44+/CD24-phenotype. BMC cancer, 10(1), p.411. Bhowmick, N.A., Ghiassi, M., Bakin, A., Aakre, M., Lundquist, C.A., Engel, M.E., Arteaga, C.L. and Moses, H.L., 2001. Transforming growth factor-β1 mediates epithelial to mesenchymal transdifferentiation through a RhoA-dependent mechanism. Molecular biology of the cell, 12(1), pp.27-36.

Bhowmick, N.A., Zent, R., Ghiassi, M., McDonnell, M. and Moses, H.L., 2001. Integrin β1 signaling is necessary for transforming growth factor-β activation of p38MAPK and epithelial plasticity. Journal of Biological Chemistry, 276(50), pp.46707-46713.

Bi, Y., Kong, P., Zhang, L., Cui, H., Xu, X., Chang, F., Yan, T., Li, J., Cheng, C., Song, B. and Niu, X., 2019. EP300 as an oncogene correlates with poor prognosis in esophageal squamous carcinoma. Journal of Cancer, 10(22), p.5413.

Bibikova, M., Barnes, B., Tsan, C., Ho, V., Klotzle, B., Le, J.M., Delano, D., Zhang, L., Schroth, G.P., Gunderson, K.L. and Fan, J.B., 2011. High density DNA methylation array with single CpG site resolution. Genomics, 98(4), pp.288-295.

Bierie, B. and Moses, H.L. (2006). TGFβ: the molecular Jekyll and Hyde of cancer. Nature Reviews Cancer, 6(7), pp.506–520.

Bierie, B., Pierce, S.E., Kroeger, C., Stover, D.G., Pattabiraman, D.R., Thiru, P., Donaher, J.L., Reinhardt, F., Chaffer, C.L., Keckesova, Z. and Weinberg, R.A., 2017. Integrin-β4 identifies cancer stem cell-enriched populations of partially mesenchymal carcinoma cells. Proceedings of the National Academy of Sciences, 114(12), pp.E2337-E2346.

Bierie, B., Stover, D.G., Abel, T.W., Chytil, A., Gorska, A.E., Aakre, M., Forrester, E., Yang, L., Wagner, K.U. and Moses, H.L., 2008. Transforming growth factor–β regulates mammary carcinoma cell survival and interaction with the adjacent microenvironment. Cancer research, 68(6), pp.1809-1819.

Birchmeier, W. and Behrens, J., 1994. Cadherin expression in carcinomas: role in the formation of cell junctions and the prevention of invasiveness. Biochimica et Biophysica Acta (BBA)-Reviews on Cancer, 1198(1), pp.11-26.

Blumenthal, R.D., Leon, E., Hansen, H.J. and Goldenberg, D.M. (2007). Expression patterns of CEACAM5 and CEACAM6 in primary and metastatic cancers. BMC Cancer, 7(1).

Bogusławska, J., Rodzik, K., Popławski, P., Kędzierska, H., Rybicka, B., Sokół, E., Tański, Z. and Piekiełko-Witkowska, A., 2018. TGF-β1 targets a microRNA network that regulates cellular adhesion and migration in renal cancer. Cancer Letters, 412, pp.155–169.

Bonnans, C., Chou, J. and Werb, Z., 2014. Remodelling the extracellular matrix in development and disease. Nature reviews Molecular cell biology, 15(12), pp.786-801.

Borrie, S.C., Brems, H., Legius, E. and Bagni, C., 2017. Cognitive dysfunctions in intellectual disabilities: the contributions of the Ras-MAPK and PI3K-AKT-mTOR pathways. Annual review of genomics and human genetics, 18, pp.115-142.

Bretscher, A. and Weber, K., 1980. Fimbrin, a new microfilament-associated protein present in microvilli and other cell surface structures. The Journal of cell biology, 86(1), pp.335-340.

Bronsert, P., Enderle-Ammour, K., Bader, M., Timme, S., Kuehs, M., Csanadi, A., Kayser, G., Kohler, I., Bausch, D., Hoeppner, J. and Hopt, U.T., 2014. Cancer cell invasion and EMT marker expression: a three-dimensional study of the human cancer–host interface. The Journal of pathology, 234(3), pp.410-422.

Broughton, J.P., Lovci, M.T., Huang, J.L., Yeo, G.W. and Pasquinelli, A.E., 2016. Pairing beyond the seed supports microRNA targeting specificity. Molecular cell, 64(2), pp.320-333.

Bryan, E.J., Jokubaitis, V.J., Chamberlain, N.L., Baxter, S.W., Dawson, E., Choong, D.Y. and Campbell, I.G., 2002. Mutation analysis of EP300 in colon, breast and ovarian carcinomas. International journal of cancer, 102(2), pp.137-141.

Bryan, E.J., Jokubaitis, V.J., Chamberlain, N.L., Baxter, S.W., Dawson, E., Choong, D.Y. and Campbell, I.G., 2002. Mutation analysis of EP300 in colon, breast and ovarian carcinomas. International journal of cancer, 102(2), pp.137-141.

Bryant, D.M. and Stow, J.L., 2004. The ins and outs of E-cadherin trafficking. Trends in cell biology, 14(8), pp.427-434.

Bublil, E.M. and Yarden, Y., 2007. The EGF receptor family: spearheading a merger of signaling and therapeutics. Current opinion in cell biology, 19(2), pp.124-134.

Bueno, M.J., 2010. G mez de Cedr n ó ó M, Laresgoiti U, Fern ndez-Piqueras á J, Zubiaga AM, Malumbres M. Multiple E2F-induced microRNAs prevent replicative stress in response to mitogenic signaling. Mol Cell Biol, 30, pp.2983-2995.

Burch, M.L., Yang, S.N., Ballinger, M.L., Getachew, R., Osman, N. and Little, P.J., 2010. TGF-β stimulates biglycan synthesis via p38 and ERK phosphorylation of the linker region of Smad2. Cellular and Molecular Life Sciences, 67(12), pp.2077-2090.

Burgess, A.W., 2008. EGFR family: structure physiology signalling and therapeutic targets. Growth factors, 26(5), pp.263-274.

Burgess, R.J. and Zhang, Z., 2013. Histone chaperones in nucleosome assembly and human disease. Nature structural & molecular biology, 20(1), p.14.

Bürglin, T.R. and Affolter, M., 2016. Homeodomain proteins: an update. Chromosoma, 125(3), pp.497-521.

Burk, U., Schubert, J., Wellner, U., Schmalhofer, O., Vincan, E., Spaderna, S. and Brabletz, T., 2008. A reciprocal repression between ZEB1 and members of the miR-200 family promotes EMT and invasion in cancer cells. EMBO reports, 9(6), pp.582-589.

Burkhart, D.L. and Sage, J., 2008. Cellular mechanisms of tumour suppression by the retinoblastoma gene. Nature Reviews Cancer, 8(9), pp.671-682.

Butt, S., Harlid, S., Borgquist, S., Ivarsson, M., Landberg, G., Dillner, J., Carlson, J. and Manjer, J., 2012. Genetic predisposition, parity, age at first childbirth and risk for breast cancer. BMC research notes, 5(1), p.414.

Byron, S.A., Chen, H., Wortmann, A., Loch, D., Gartside, M.G., Dehkhoda, F., Blais, S.P., Neubert, T.A., Mohammadi, M. and Pollock, P.M., 2013. The N550K/H mutations in FGFR2 confer differential resistance to PD173074, dovitinib, and ponatinib ATP-competitive inhibitors. Neoplasia, 15(8), pp.975-IN30.

Cadoo, K.A., Gucalp, A. and Traina, T.A., 2014. Palbociclib: an evidence-based review of its potential in the treatment of breast cancer. Breast Cancer: Targets and Therapy, 6, p.123.

Cagnet, S., Faraldo, M.M., Kreft, M., Sonnenberg, A., Raymond, K. and Glukhova, M.A., 2014. Signaling events mediated by $\alpha 3\beta 1$ integrin are essential for mammary tumorigenesis. Oncogene, 33(34), pp.4286-4295.

Cai, S., Chen, R., Li, X., Cai, Y., Ye, Z., Li, S., Li, J., Huang, H., Peng, S., Wang, J. and Tao, Y., 2015. Downregulation of microRNA-23a suppresses prostate cancer metastasis by targeting the PAK6-LIMK1 signaling pathway. Oncotarget, 6(6), p.3904.

Calaf, G.M., Ponce-Cusi, R. and Carrión, F., 2018. Curcumin and paclitaxel induce cell death in breast cancer cell lines. Oncology reports, 40(4), pp.2381-2388.

Calin, G.A., Ferracin, M., Cimmino, A., Di Leva, G., Shimizu, M., Wojcik, S.E., Iorio, M.V., Visone, R., Sever, N.I., Fabbri, M. and Iuliano, R., 2005. A MicroRNA signature associated with prognosis and progression in chronic lymphocytic leukemia. New England Journal of Medicine, 353(17), pp.1793-1801.

Calin, G.A., Sevignani, C., Dumitru, C.D., Hyslop, T., Noch, E., Yendamuri, S., Shimizu, M., Rattan, S., Bullrich, F., Negrini, M. and Croce, C.M., 2004. Human microRNA genes are frequently located at fragile sites and genomic regions involved in cancers. Proceedings of the National Academy of Sciences, 101(9), pp.2999-3004.

Calle, Y., Anton, I.M., Thrasher, A.J. and Jones, G.E., 2008. WASP and WIP regulate podosomes in migrating leukocytes. Journal of microscopy, 231(3), pp.494-505.

Camaj, P., Seeliger, H., Ischenko, I., Krebs, S., Blum, H., De Toni, E.N., Faktorova, D., Jauch, K.W. and Bruns, C.J., 2009. EFEMP1 binds the EGF receptor and activates MAPK and Akt pathways in pancreatic carcinoma cells. Biological chemistry, 390(12), pp.1293-1302.

Campbell, K.M. and Lumb, K.J., 2002. Structurally distinct modes of recognition of the KIX domain of CBP by Jun and CREB. Biochemistry, 41(47), pp.13956-13964.

Campbell, K.P. and Kahl, S.D., 1989. Association of dystrophin and an integral membrane glycoprotein. Nature, 338(6212), pp.259-262.

Campbell, T.M., Castro, M.A., de Santiago, I., Fletcher, M.N., Halim, S., Prathalingam, R., Ponder, B.A. and Meyer, K.B., 2016. FGFR2 risk SNPs confer breast cancer risk by augmenting oestrogen responsiveness. Carcinogenesis, 37(8), pp.741-750.

Canagarajah, B., Leskow, F.C., Ho, J.Y.S., Mischak, H., Saidi, L.F., Kazanietz, M.G. and Hurley, J.H., 2004. Structural mechanism for lipid activation of the Rac-specific GAP, β2-chimaerin. Cell, 119(3), pp.407-418.

Cancello, G., Maisonneuve, P., Rotmensz, N., Viale, G., Mastropasqua, M.G., Pruneri, G., Montagna, E., Iorfida, M., Mazza, M., Balduzzi, A. and Veronesi, P., 2013. Progesterone receptor loss identifies Luminal B breast cancer subgroups at higher risk of relapse. Annals of oncology, 24(3), pp.661-668.

Cancer Genome Atlas Network, 2012. Comprehensive molecular portraits of human breast tumours. Nature, 490(7418), p.61. Cancer.org. 2014. [online] Available at: https://www.cancer.org/cancer/breastcancer/treatment/hormone-therapy-for-breast-cancer.html

Canel, M., Serrels, A., Miller, D., Timpson, P., Serrels, B., Frame, M.C. and Brunton, V.G., 2010. Quantitative in vivo imaging of the effects of inhibiting integrin signaling via Src and FAK on cancer cell movement: effects on E-cadherin dynamics. Cancer research, 70(22), pp.9413-9422.

Canettieri, G., Di Marcotullio, L., Greco, A., Coni, S., Antonucci, L., Infante, P., Pietrosanti, L., De Smaele, E., Ferretti, E., Miele, E. and Pelloni, M., 2010. Histone deacetylase and Cullin3–REN KCTD11 ubiquitin ligase interplay regulates Hedgehog signalling through Gli acetylation. Nature cell biology, 12(2), pp.132-142.

Cano, A., Pérez-Moreno, M.A., Rodrigo, I., Locascio, A., Blanco, M.J., del Barrio, M.G., Portillo, F. and Nieto, M.A., 2000. The transcription factor snail controls epithelial–mesenchymal transitions by repressing E-cadherin expression. Nature cell biology, 2(2), pp.76-83.

Cantley, L.C. and Neel, B.G., 1999. New insights into tumor suppression: PTEN suppresses tumor formation by restraining the phosphoinositide 3-kinase/AKT pathway. Proceedings of the National Academy of Sciences, 96(8), pp.4240-4245.

Cao, M., Li, Y., Lu, H., Meng, Q., Wang, L., Cai, L. and Dong, X., 2014. MiR-23a-mediated migration/invasion is rescued by its target, IRS-1, in non-small cell lung cancer cells. Journal of cancer research and clinical oncology, 140(10), pp.1661-1670

Cao, M., Seike, M., Soeno, C., Mizutani, H., Kitamura, K., Minegishi, Y., Noro, R., Yoshimura, A., Cai, L. and Gemma, A., 2012. MiR-23a regulates TGF-β-induced epithelial-mesenchymal transition by targeting E-cadherin in lung cancer cells. International journal of oncology, 41(3), pp.869-875.

Cao, X., Geradts, J., Dewhirst, M.W. and Lo, H.W., 2012. Upregulation of VEGF-A and CD24 gene expression by the tGLI1 transcription factor contributes to the aggressive behavior of breast cancer cells. Oncogene, 31(1), pp.104-115.

Cao, Y., Slaney, C.Y., Bidwell, B.N., Parker, B.S., Johnstone, C.N., Rautela, J., Eckhardt, B.L. and Anderson, R.L., 2014. BMP4 inhibits breast cancer metastasis by blocking myeloid-derived suppressor cell activity. Cancer research, 74(18), pp.5091-5102.

Capaccione, K.M. and Pine, S.R., 2013. The Notch signaling pathway as a mediator of tumor survival. Carcinogenesis, 34(7), pp.1420-1430.

Capell, A., Kaether, C., Edbauer, D., Shirotani, K., Merkl, S., Steiner, H. and Haass, C., 2003. Nicastrin interacts with γ-secretase complex components via the N-terminal part of its transmembrane domain. Journal of Biological Chemistry, 278(52), pp.52519-52523.

Capriotti, E., Vonderheid, E.C., Thoburn, C.J., Wasik, M.A., Bahler, D.W. and Hess, A.D., 2008. Expression of T-plastin, FoxP3 and other tumor-associated markers by leukemic T-cells of cutaneous T-cell lymphoma. Leukemia & lymphoma, 49(6), pp.1190-1201.

Cardone, R.A., Casavola, V. and Reshkin, S.J., 2005. The role of disturbed pH dynamics and the Na+/H+ exchanger in metastasis. Nature Reviews Cancer, 5(10), pp.786-795.

Carmona, F.J., Villanueva, A., Vidal, A., Muñoz, C., Puertas, S., Penin, R.M., Gomà, M., Lujambio, A., Piulats, J.M., Mesía, R. and Sánchez-Céspedes, M., 2012. Epigenetic disruption of cadherin-11 in human cancer metastasis. The Journal of pathology, 228(2), pp.230-240.

Carnero, A. and Paramio, J.M., 2014. The PTEN/PI3K/AKT pathway in vivo, cancer mouse models. Frontiers in oncology, 4, p.252.

Carrera, I. and Treisman, J.E., 2008. Message in a nucleus: signaling to the transcriptional machinery. Current opinion in genetics & development, 18(5), pp.397-403.

Carrington, J.C. and Ambros, V., 2003. Role of microRNAs in plant and animal development. Science, 301(5631), pp.336-338.

Carroll, J.S. and Brown, M., 2006. Estrogen receptor target gene: an evolving concept. Molecular Endocrinology, 20(8), pp.1707-1714.

Carstens, R.P., Eaton, J.V., Krigman, H.R., Walther, P.J. and Garcia-Blanco, M.A., 1997. Alternative splicing of fibroblast growth factor receptor 2 (FGF-R2) in human prostate cancer. Oncogene, 15(25), pp.3059-3065.

Casas, E., Kim, J., Bendesky, A., Ohno-Machado, L., Wolfe, C.J. and Yang, J., 2011. Snail2 is an essential mediator of Twist1-induced epithelial mesenchymal transition and metastasis. Cancer research, 71(1), pp.245-254.

Castillo-Lluva, S., Hontecillas-Prieto, L., Blanco-Gómez, A., del Mar Sáez-Freire, M., García-Cenador, B., García-Criado, J., Pérez-Andrés, M., Orfao, A., Cañamero, M., Mao, J.H. and Gridley, T., 2015. A new role of SNAI2 in postlactational involution of the mammary gland links it to luminal breast cancer development. Oncogene, 34(36), pp.4777-4790.

Cataldo, A., Cheung, D.G., Balsari, A., Tagliabue, E., Coppola, V., Iorio, M.V., Palmieri, D. and Croce, C.M., 2016. miR-302b enhances breast cancer cell sensitivity to cisplatin by regulating E2F1 and the cellular DNA damage response. Oncotarget, 7(1), p.786.

Cavallaro, U.G.O. and Christofori, G., 2004. Multitasking in tumor progression: signalling functions of cell adhesion molecules. Annals of the New York Academy of Sciences, 1014(1), pp.58-66.

Cavard, C., Audebourg, A., Letourneur, F., Audard, V., Beuvon, F., Cagnard, N., Radenen, B., Varlet, P., Vacher-Lavenu, M.C., Perret, C. and Terris, B., 2009. Gene expression profiling provides insights into the pathways involved in solid pseudopapillary neoplasm of the pancreas. The Journal of Pathology: A Journal of the Pathological Society of Great Britain and Ireland, 218(2), pp.201-209.

Cernilogar, F.M., Onorati, M.C., Kothe, G.O., Burroughs, A.M., Parsi, K.M. and Breiling, A., Lo Sardo F, Saxena A, Miyoshi K, Siomi H, et al. 2011. Chromatin-associated RNA interference components contribute to transcriptional regulation in Drosophila. Nature, 480, pp.391-395.

Chaffanet, M., Gressin, L., Preudhomme, C., Soenen-Cornu, V., Birnbaum, D. and Pébusque, M.J., 2000. MOZ is fused to p300 in an acute monocytic leukemia with t (8; 22). Genes, Chromosomes and Cancer, 28(2), pp.138-144.

Chaffer, C.L. and Weinberg, R.A., 2011. A perspective on cancer cell metastasis. Science, 331(6024), pp.1559-1564.

Chaffer, C.L., Brueckmann, I., Scheel, C., Kaestli, A.J., Wiggins, P.A., Rodrigues, L.O., Brooks, M., Reinhardt, F., Su, Y., Polyak, K. and Arendt, L.M., 2011. Normal and neoplastic nonstem cells can spontaneously convert to a stem-like state. Proceedings of the National Academy of Sciences, 108(19), pp.7950-7955.

Chaffer, C.L., Dopheide, B., Savagner, P., Thompson, E.W. and Williams, E.D., 2007. Aberrant fibroblast growth factor receptor signaling in bladder and other cancers. Differentiation, 75(9), pp.831-842.

Chaffer, C.L., Marjanovic, N.D., Lee, T., Bell, G., Kleer, C.G., Reinhardt, F., D'Alessio, A.C., Young, R.A. and Weinberg, R.A., 2013. Poised chromatin at the ZEB1 promoter enables breast cancer cell plasticity and enhances tumorigenicity. Cell, 154(1), pp.61-74.

Chakrabarti, R., Hwang, J., Blanco, M.A., Wei, Y., Lukačišin, M., Romano, R.A., Smalley, K., Liu, S., Yang, Q., Ibrahim, T. and Mercatali, L., 2012. Elf5 inhibits the epithelial–mesenchymal transition in mammary gland development and breast cancer metastasis by transcriptionally repressing Snail2. Nature cell biology, 14(11), pp.1212-1222.

Chakravarti, D., LaMorte, V.J., Nelson, M.C., Nakajima, T., Schulman, I.G., Juguilon, H., Montminy, M. and Evans, R.M., 1996. Role of CBP/P300 in nuclear receptor signalling. Nature, 383(6595), pp.99-103.

Chambard, J.C., Lefloch, R., Pouysségur, J. and Lenormand, P., 2007. ERK implication in cell cycle regulation. Biochimica et Biophysica Acta (BBA)-Molecular Cell Research, 1773(8), pp.1299-1310.

Chan, B.K., Wiseberg-Firtell, J.A., Jois, R.H., Jensen, K. and Audisio, R.A., 2015. Localization techniques for guided surgical excision of non-palpable breast lesions. Cochrane Database of Systematic Reviews, (12).

Chan, C.E. and Odde, D.J., 2008. Traction dynamics of filopodia on compliant substrates. Science, 322(5908), pp.1687-1691.

Chan, C.H., Lee, S.W., Li, C.F., Wang, J., Yang, W.L., Wu, C.Y., Wu, J., Nakayama, K.I., Kang, H.Y., Huang, H.Y. and Hung, M.C., 2010. Deciphering the transcriptional complex critical for RhoA gene expression and cancer metastasis. Nature cell biology, 12(5), pp.457-467.

Chan, H.M. and La Thangue, N.B., 2001. p300/CBP proteins: HATs for transcriptional bridges and scaffolds. Journal of cell science, 114(13), pp.2363-2373.

Chandramohan, V., Mineva, N.D., Burke, B., Jeay, S., Wu, M., Shen, J., Yang, W., Hann, S.R. and Sonenshein, G.E., 2008. c-Myc represses FOXO3a-mediated transcription of the gene encoding the p27Kip1 cyclin dependent kinase inhibitor. Journal of cellular biochemistry, 104(6), pp.2091-2106.

Chandran, P.A., Keller, A., Weinmann, L., Adel Seida, A., Braun, M., Andreev, K., Fischer, B., Horn, E., Schwinn, S., Junker, M. and Houben, R., 2014. The TGF-β-inducible miR-23a cluster attenuates IFN-γ levels and antigen-specific cytotoxicity in human CD8+ T cells. Journal of leukocyte biology, 96(4), pp.633-645.

Chang, E.C., Frasor, J., Komm, B. and Katzenellenbogen, B.S., 2006. Impact of Estrogen Receptor β on Gene Networks Regulated by Estrogen Receptor α in Breast Cancer Cells. Endocrinology, 147(10), pp.4831–4842.

Chang, H., Balenci, L., Okolowsky, N., Muller, W.J. and Hamel, P.A., 2012. Mammary epithelial-restricted expression of activated c-src rescues the block to mammary gland morphogenesis due to the deletion of the C-terminus of Patched-1. Developmental biology, 370(2), pp.187-197.

Chang, T.H., Tsai, M.F., Su, K.Y., Wu, S.G., Huang, C.P., Yu, S.L., Yu, Y.L., Lan, C.C., Yang, C.H., Lin, S.B. and Wu, C.P., 2011. Slug confers resistance to the epidermal growth factor receptor tyrosine kinase inhibitor. American journal of respiratory and critical care medicine, 183(8), pp.1071-1079.

Chang, Y.W., Hung, M.C. and Su, J.L., 2014. The anti-tumor activity of E1A and its implications in cancer therapy. Archivum immunologiae et therapiae experimentalis, 62(3), pp.195-204.

Chanmee, T., Ontong, P. and Itano, N., 2016. Hyaluronan: A modulator of the tumor microenvironment. Cancer letters, 375(1), pp.20-30.

Charafe-Jauffret, E., Ginestier, C., Iovino, F., Wicinski, J., Cervera, N., Finetti, P., Hur, M.H., Diebel, M.E., Monville, F., Dutcher, J. and Brown, M., 2009. Breast cancer cell lines contain functional cancer stem cells with metastatic capacity and a distinct molecular signature. Cancer research, 69(4), pp.1302-1313.

Chen, C, C., Chu, C, B., Liu, K, J., Huang, C, Y, F., Chang, J, Y., Pan, W, Y., et al. (2013). Gene expression profiling for analysis acquired oxaliplatin resistant factors in human gastric carcinoma TSGH-S3 cells: the role of IL-6 signaling and Nrf2/AKR1C axis identification, Biochem. Pharmacol. 86(7), 872–887.

Chen, H., Pan, H., Qian, Y., Zhou, W. and Liu, X., 2018. MiR-25-3p promotes the proliferation of triple negative breast cancer by targeting BTG2. Molecular cancer, 17(1), pp.1-11.

Chou, C.H., Chang, N.W., Shrestha, S., Hsu, S.D., Lin, Y.L., Lee, W.H., Yang, C.D., Hong, H.C., Wei, T.Y., Tu, S.J. and Tsai, T.R., 2016. miRTarBase 2016: updates to the experimentally validated miRNA-target interactions database. Nucleic acids research, 44(D1), pp.D239-D247.

Chu, P.Y., Hu, F.W., Yu, C.C., Tsai, L.L., Yu, C.H., Wu, B.C., Chen, Y.W., Huang, P.I. and Lo, W.L., 2013. Epithelial–mesenchymal transition transcription factor ZEB1/ZEB2 co-expression predicts poor prognosis and maintains tumor-initiating properties in head and neck cancer. Oral Oncology, 49(1), pp.34-41.

Chung, S., Jin, Y., Han, B., Qu, Y., Gao, B., Giuliano, A.E. and Cui, X., 2017. Identification of EGF-NF-κB-FOXC1 signaling axis in basal-like breast cancer. Cell Communication and Signaling, 15(1), p.22.

Comerford, K.M., Wallace, T.J., Karhausen, J., Louis, N.A., Montalto, M.C. and Colgan, S.P., 2002. Hypoxia-inducible factor-1-dependent regulation of the multidrug resistance (MDR1) gene. Cancer research, 62(12), pp.3387-3394.

Dai, M., Al-Odaini, A.A., Arakelian, A., Rabbani, S.A., Ali, S. and Lebrun, J.J., 2012. A novel function for p21Cip1 and acetyltransferase p/CAF as critical transcriptional regulators of TGFβ-mediated breast cancer cell migration and invasion. Breast Cancer Research, 14(5), pp.1-22. De Palma, M. and Lewis, C.E., 2011. Macrophages limit chemotherapy. Nature, 472(7343), pp.303-304.

De Zeng, Y.X., Zhu, J., Peng, C., Liang, W. and Lin, H., 2019. Knockdown of nucleophosmin 1 suppresses proliferation of triple-negative breast cancer cells through activating CDH1/Skp2/p27kip1 pathway. Cancer Management and Research, 11, p.143.

Deift, P., Kriecherbauer, T., McLaughlin, K.T.R., Venakides, S. and Zhou, X., 1999. Uniform asymptotics for polynomials orthogonal with respect to varying exponential weights and applications to universality questions in random matrix theory. Communications on Pure and Applied Mathematics: A Journal Issued by the Courant Institute of Mathematical Sciences, 52(11), pp.1335-1425.

Derynck, R. and Zhang, Y.E. (2003). Smad- dependent and Smad-independent pathways in TGF-β family signalling. Nature, 425(6958), pp.577–584

Descalzo, D.L.M., Satoorian, T.S., Walker, L.M., Sparks, N.R., Pulyanina, P.Y. and Zur Nieden, N.I., 2016. Glucose-induced oxidative stress reduces proliferation in embryonic stem cells via FOXO3A/β-catenin-dependent transcription of p21cip1. Stem Cell Reports, 7(1), pp.55-68.

Dong, Y., Tang, L., Letterio, J.J. and Benveniste, E.N., 2001. The Smad3 protein is involved in TGF-β inhibition of class II transactivator and class II MHC expression. The Journal of Immunology, 167(1), pp.311-319.

Dou, X.W., Liang, Y.K., Lin, H.Y., Wei, X.L., Zhang, Y.Q., Bai, J.W., Chen, C.F., Chen, M., Du, C.W., Li, Y.C. and Tian, J., 2017. Notch3 maintains luminal phenotype and suppresses tumorigenesis and metastasis of breast cancer via trans-activating estrogen receptor-α. Theranostics, 7(16), p.4041.

Droufakou, S., Deshmane, V., Roylance, R., Hanby, A., Tomlinson, I., Hart, I, R. (2001). Multiple ways of silencing E-cadherin gene expression in lobular carcinoma of the breast, Int. J. Cancer 92 (3), 404–408.

Dufraine, J., Funahashi, Y. and Kitajewski, J., 2008. Notch signaling regulates tumor angiogenesis by diverse mechanisms. Oncogene, 27(38), pp.5132-5137.

Eilken, H.M. and Adams, R.H., 2010. Dynamics of endothelial cell behavior in sprouting angiogenesis. Current opinion in cell biology, 22(5), pp.617-625.

El Kerch, F., Ratbi, I., Sbiti, A., Laarabi, F.Z., Barkat, A. and Sefiani, A., 2014. Carrier frequency of the c. 525delT mutation in the SGCG gene and estimated prevalence of limb girdle muscular dystrophy type 2C among the Moroccan population. Genetic testing and molecular biomarkers, 18(4), pp.253-256.

Emery, J.G., McDonnell, P., Burke, M.B., Deen, K.C., Lyn, S., Silverman, C., Dul, E., Appelbaum, E.R., Eichman, C., DiPrinzio, R., Dodds, R.A., James, I.E., Rosenberg, M., Lee, J.C. and Young, P.R. (1998). Osteoprotegerin Is a Receptor for the Cytotoxic Ligand TRAIL. Journal of Biological Chemistry, 273(23), pp.14363–14367.

European Pharmaceutical Review. (2010). Advances in two-dimensional cell migration assay technologies. [online] Available at: https://www.europeanpharmaceuticalreview.com /article/4346/advances-in-two-dimensional-cell-migration-assay-technologies/

Fang, X., Zheng, P., Tang, J. and Liu, Y., 2010. CD24: from A to Z. Cellular & molecular immunology, 7(2), pp.100-103.

Feeley, B.T., Gamradt, S.C., Hsu, W.K., Liu, N., Krenek, L., Robbins, P., Huard, J. and Lieberman, J.R., 2005. Influence of BMPs on the formation of osteoblastic lesions in metastatic prostate cancer. Journal of Bone and Mineral Research, 20(12), pp.2189-2199.

Feng, X., Jiang, J., Shi, S., Xie, H., Zhou, L. and Zheng, S., 2016. Knockdown of miR-25 increases the sensitivity of liver cancer stem cells to TRAIL-induced apoptosis via PTEN/PI3K/Akt/Bad signaling pathway. International journal of oncology, 49(6), pp.2600-2610.

Fernandez-Valdivia, R., Mukherjee, A., Ying, Y., Li, J., Paquet, M., DeMayo, F.J. and Lydon, J.P. (2009). The RANKL signaling axis is sufficient to elicit ductal side-branching and alveologenesis in the mammary gland of the virgin mouse. Developmental Biology, 328(1), pp.127–139.

FG, G., 1999. Ruoslahti E. Integrin signaling. Science, 285, pp.1028-1032.

Fuchs, H., Theuser, M., Wruck, W. and Adjaye, J., 2014. miR-27 negatively regulates pluripotency-associated genes in human embryonal carcinoma cells. PLoS One, 9(11), p.e111637.

Gao, L., Yang, Y., Song, S., Hong, H., Zhao, X. and Li, D., 2013. The association between genetic variant of MDR1 gene and breast cancer risk factors in Chinese women. International immunopharmacology, 17(1), pp.88-91.

Gayther, S.A., Batley, S.J., Linger, L., Bannister, A., Thorpe, K., Chin, S.F., Daigo, Y., Russell, P., Wilson, A., Sowter, H.M. and Delhanty, J.D., 2000. Mutations truncating the EP300 acetylase in human cancers. Nature genetics, 24(3), pp.300-303.

Ge, Y.F., Sun, J., Jin, C.J., Cao, B.Q., Jiang, Z.F. and Shao, J.F., 2013. AntagomiR-27a targets FOXO3a in glioblastoma and suppresses U87 cell growth in vitro and in vivo. Asian Pac J Cancer Prev, 14(2), pp.963-8.

Geng, J., Luo, H., Pu, Y., Zhou, Z., Wu, X., Xu, W. and Yang, Z., 2012. Methylation mediated silencing of miR-23b expression and its role in glioma stem cells. Neuroscience letters, 528(2), pp.185-189.

Gerhardt, H., Golding, M., Fruttiger, M., Ruhrberg, C., Lundkvist, A., Abramsson, A., Jeltsch, M., Mitchell, C., Alitalo, K., Shima, D. and Betsholtz, C., 2003. VEGF guides angiogenic sprouting utilizing endothelial tip cell filopodia. The Journal of cell biology, 161(6), pp.1163-1177.

Gertler, F. and Condeelis, J., 2011. Metastasis: tumor cells becoming MENAcing. Trends in cell biology, 21(2), pp.81-90.

Gévry, N., Chan, H.M., Laflamme, L., Livingston, D.M. and Gaudreau, L., 2007. p21 transcription is regulated by differential localization of histone H2A. Z. Genes & development, 21(15), pp.1869-1881.

Ghajar, C.M., Peinado, H., Mori, H., Matei, I.R., Evason, K.J., Brazier, H., Almeida, D., Koller, A., Hajjar, K.A., Stainier, D.Y. and Chen, E.I., 2013. The perivascular niche regulates breast tumour dormancy. Nature cell biology, 15(7), pp.807-817.

Ghebeh, H., Sleiman, G.M., Manogaran, P.S., Al-Mazrou, A., Barhoush, E., Al-Mohanna, F.H., Tulbah, A., Al-Faqeeh, K. and Adra, C.N., 2013. Profiling of normal and malignant breast tissue show CD44 high/CD24 low phenotype as a predominant stem/progenitor marker when used in combination with Ep-CAM/CD49f markers. BMC cancer, 13(1), pp.1-14.

Ghods, A., Ghaderi, A., Shariat, M., Talei, A.R. and Mehdipour, F., 2019. TNFR2 but not TNFR1 is the main TNFR expressed by B and T lymphocytes in breast cancer draining lymph nodes. Immunology letters, 209, pp.36-44.

Ghosh, S., Taylor, A., Chin, M., Huang, H.R., Conery, A.R., Mertz, J.A., Salmeron, A., Dakle, P.J., Mele, D., Cote, A. and Jayaram, H., 2016. Regulatory T cell modulation by CBP/EP300 bromodomain inhibition. Journal of Biological Chemistry, 291(25), pp.13014-13027.

Giampieri, S., Manning, C., Hooper, S., Jones, L., Hill, C.S. and Sahai, E., 2009. Localized and reversible TGFβ signalling switches breast cancer cells from cohesive to single cell motility. Nature cell biology, 11(11), pp.1287-1296. Giancotti, F.G., 2013. Mechanisms governing metastatic dormancy and reactivation. Cell, 155(4), pp.750-764.

Giannakou, M.E. and Partridge, L., 2004. The interaction between FOXO and SIRT1: tipping the balance towards survival. Trends in cell biology, 14(8), pp.408-412.

Giannopoulou, L., Kasimir-Bauer, S. and Lianidou, E.S., 2018. Liquid biopsy in ovarian cancer: recent advances on circulating tumor cells and circulating tumor DNA. Clinical Chemistry and Laboratory Medicine (CCLM), 56(2), pp.186-197.

Gibbons, D.L., Lin, W., Creighton, C.J., Rizvi, Z.H., Gregory, P.A., Goodall, G.J., Thilaganathan, N., Du, L., Zhang, Y., Pertsemlidis, A. and Kurie, J.M., 2009. Contextual extracellular cues promote tumor cell EMT and metastasis by regulating miR-200 family expression. Genes & development, 23(18), pp.2140-2151.

Gidlöf, O., Van Der Brug, M., Öhman, J., Gilje, P., Olde, B., Wahlestedt, C. and Erlinge, D., 2013. Platelets activated during myocardial infarction release functional miRNA, which can be taken up by endothelial cells and regulate ICAM1 expression. Blood, The Journal of the American Society of Hematology, 121(19), pp.3908-3917.

Giganti, A., Plastino, J., Janji, B., Van Troys, M., Lentz, D., Ampe, C., Sykes, C. and Friederich, E., 2005. Actin-filament cross-linking protein T-plastin increases Arp2/3-mediated actin-based movement. Journal of cell science, 118(6), pp.1255-1265.

Gilles, C., Polette, M., Mestdagt, M., Nawrocki-Raby, B., Ruggeri, P., Birembaut, P. and Foidart, J.M., 2003. Transactivation of vimentin by β-catenin in human breast cancer cells. Cancer research, 63(10), pp.2658-2664.

Gillet, J.P. and M Gottesman, M., 2011. Advances in the molecular detection of ABC transporters involved in multidrug resistance in cancer. Current pharmaceutical biotechnology, 12(4), pp.686-692.

Ginestier, C., Hur, M.H., Charafe-Jauffret, E., Monville, F., Dutcher, J., Brown, M., Jacquemier, J., Viens, P., Kleer, C.G., Liu, S. and Schott, A., 2007. ALDH1 is a marker of normal and malignant human mammary stem cells and a predictor of poor clinical outcome. Cell stem cell, 1(5), pp.555-567.

Girdwood, D., Bumpass, D., Vaughan, O.A., Thain, A., Anderson, L.A., Snowden, A.W., Garcia-Wilson, E., Perkins, N.D. and Hay, R.T., 2003. P300 transcriptional repression is mediated by SUMO modification. Molecular cell, 11(4), pp.1043-1054.

Gkountela, S., Castro-Giner, F., Szczerba, B.M., Vetter, M., Landin, J., Scherrer, R., Krol, I., Scheidmann, M.C., Beisel, C., Stirnimann, C.U. and Kurzeder, C., 2019. Circulating tumor cell clustering shapes DNA methylation to enable metastasis seeding. Cell, 176(1-2), pp.98-112.

Gligorijevic, B., Bergman, A. and Condeelis, J., 2014. Multiparametric classification links tumor microenvironments with tumor cell phenotype. PLoS Biol, 12(11), p.e1001995.

Gobbi, H., Arteaga, C.L., Jensen, R.A., Simpson, J.F., Dupont, W.D., Olson, S.J., Schuyler, P.A., Plummer Jr, W.D. and Page, D.L., 2000. Loss of expression of transforming growth factor beta type II receptor correlates with high tumour grade in human breast in-situ and invasive carcinomas. Histopathology, 36(2), pp.168-177.

Goel, H.L., Pursell, B., Chang, C., Shaw, L.M., Mao, J., Simin, K., Kumar, P., Kooi, C.W.V., Shultz, L.D., Greiner, D.L. and Norum, J.H., 2013. GLI1 regulates a novel neuropilin-2/$\alpha 6\beta 1$ integrin based autocrine pathway that contributes to breast cancer initiation. EMBO molecular medicine, 5(4), pp.488-508.

Gold, P., 1998. The carcinoembryonic antigen (CEA): past, present, and future. McGill J Med, 3, pp.46-66.

Goldie, K.N., Wedig, T., Mitra, A.K., Aebi, U., Herrmann, H. and Hoenger, A., 2007. Dissecting the 3-D structure of vimentin intermediate filaments by cryo-electron tomography. Journal of structural biology, 158(3), pp.378-385.

Goldstein, D., Djeu, J., Latter, G., Burbeck, S. and Leavitt, J., 1985. Abundant synthesis of the transformation-induced protein of neoplastic human fibroblasts, plastin, in normal lymphocytes. Cancer research, 45(11 Part 2), pp.5643-5647.

Goll, D.E., Thompson, V.F., Li, H., Wei, W.E.I. and Cong, J., 2003. The calpain system. Physiological reviews.

Gomis, R.R., Alarcón, C., Nadal, C., Van Poznak, C. and Massagué, J., 2006. C/EBPβ at the core of the TGFβ cytostatic response and its evasion in metastatic breast cancer cells. Cancer cell, 10(3), pp.203-214.

Gong, C., Yao, Y., Wang, Y., Liu, B., Wu, W., Chen, J., Su, F., Yao, H. and Song, E., 2011. Up-regulation of miR-21 mediates resistance to trastuzumab therapy for breast cancer. Journal of Biological Chemistry, 286(21), pp.19127-19137.

Gong, L., Cai, Y., Zhou, X. and Yang, H., 2012. Activated platelets interact with lung cancer cells through P-selectin glycoprotein ligand-1. Pathology & Oncology Research, 18(4), pp.989-996. Gonzalez-Angulo, A.M., Ferrer-Lozano, J., Stemke-Hale, K., Sahin, A., Liu, S., Barrera, J.A., Burgues, O., Lluch, A.M., Chen, H., Hortobagyi, G.N. and Mills, G.B., 2011. PI3K pathway mutations and PTEN levels in primary and metastatic breast cancer. Molecular cancer therapeutics, 10(6), pp.1093-1101.

Gonzalez-Angulo, A.M., Sneige, N., Buzdar, A.U., Valero, V., Kau, S.W., Broglio, K., Yamamura, Y., Hortobagyi, G.N. and Cristofanilli, M., 2004. p53 expression as a prognostic marker in inflammatory breast cancer. Clinical cancer research, 10(18), pp.6215-6221.

Goodman, R.H. and Smolik, S., 2000. CBP/p300 in cell growth, transformation, and development. Genes & development, 14(13), pp.1553-1577.

Goossens, S., Radaelli, E., Blanchet, O., Durinck, K., Van der Meulen, J., Peirs, S., Taghon, T., Tremblay, C.S., Costa, M., Ghahremani, M.F. and De Medts, J., 2015. ZEB2 drives immature T-cell lymphoblastic leukaemia development via enhanced tumour-initiating potential and IL-7 receptor signalling. Nature communications, 6(1), pp.1-12.

Gorden, B.H., Kim, J.H., Sarver, A.L., Frantz, A.M., Breen, M., Lindblad-Toh, K., O'Brien, T.D., Sharkey, L.C., Modiano, J.F. and Dickerson, E.B., 2014. Identification of three molecular and functional subtypes in canine hemangiosarcoma through gene expression profiling and progenitor cell characterization. The American journal of pathology, 184(4), pp.985-995.

Gorringe, K.L. and Fox, S.B., 2017. Ductal carcinoma in situ biology, biomarkers, and diagnosis. Frontiers in Oncology, 7, p.248. Gorsch, S.M., Memoli, V.A., Stukel, T.A., Gold, L.I. and Arrick, B.A., 1992. Immunohistochemical staining for transforming growth factor β1 associates with disease progression in human breast cancer. Cancer research, 52(24), pp.6949-6952.

Gottesman, M.M., Fojo, T. and Bates, S.E., 2002. Multidrug resistance in cancer: role of ATP–dependent transporters. Nature Reviews Cancer, 2(1), pp.48-58.

Gottfried, E., Kreutz, M. and Mackensen, A., 2008. Tumor-induced modulation of dendritic cell function. Cytokine & growth factor reviews, 19(1), pp.65-77.

Gradishar, W.J., Anderson, B.O., Balassanian, R., Blair, S.L., Burstein, H.J., Cyr, A., Elias, A.D., Farrar, W.B., Forero, A., Giordano, S.H. and Goetz, M., 2015. Breast cancer, version 1.2016. Journal of the National Comprehensive Cancer Network, 13(12), pp.1475-1485.

Gralow, J.R., Burstein, H.J., Wood, W., Hortobagyi, G.N., Gianni, L., Von Minckwitz, G., Buzdar, A.U., Smith, I.E., Symmans, W.F., Singh, B. and Winer, E.P., 2008. Preoperative therapy in invasive breast cancer: pathologic assessment and systemic therapy issues in operable disease. Journal of Clinical Oncology, 26(5), pp.814-819.

Grände, M., Franzen, Å., Karlsson, J.O., Ericson, L.E., Heldin, N.E. and Nilsson, M., 2002. Transforming growth factor-β and epidermal growth factor synergistically stimulate epithelial to mesenchymal transition (EMT) through a MEK-dependent mechanism in primary cultured pig thyrocytes. Journal of cell science, 115(22), pp.4227-4236.

Gray, A.M. and Mason, A.J., 1990. Requirement for activin A and transforming growth factor–beta 1 pro-regions in homodimer assembly. Science, 247(4948), pp.1328-1330.

Greaves, M. and Maley, C.C., 2012. Clonal evolution in cancer. Nature, 481(7381), pp.306-313.

Green, K.J., Böhringer, M., Gocken, T. and Jones, J.C., 2005. Intermediate filament associated proteins. In Advances in protein chemistry (Vol. 70, pp. 143-202). Academic Press.

Greenman, C., Stephens, P., Smith, R., Dalgliesh, G.L., Hunter, C., Bignell, G., Davies, H., Teague, J., Butler, A., Stevens, C. and Edkins, S., 2007. Patterns of somatic mutation in human cancer genomes. Nature, 446(7132), pp.153-158.

Greer, E.L. and Shi, Y., 2012. Histone methylation: a dynamic mark in health, disease and inheritance. Nature Reviews Genetics, 13(5), pp.343-357.

Grell, M., Becke, F.M., Wajant, H., Männel, D.N. and Scheurich, P., 1998. Tumor necrosis factor (TNF) receptor type 2 mediates thymocyte proliferation independently of TNF receptor type 1. European journal of immunology, 28(1), pp.257-263.

Grell, M., Wajant, H., Zimmermann, G. and Scheurich, P., 1998. The type 1 receptor (CD120a) is the high-affinity receptor for soluble tumor necrosis factor. Proceedings of the National Academy of Sciences, 95(2), pp.570-575.

Grimshaw, M.J., Cooper, L., Papazisis, K., Coleman, J.A., Bohnenkamp, H.R., Chiapero Stanke, L., Taylor-Papadimitriou, J. and Burchell, J.M., 2008. Mammosphere culture of metastatic breast cancer cells enriches for tumorigenic breast cancer cells. Breast Cancer Research, 10(3), p.R52.

Grönroos, E., Hellman, U., Heldin, C.H. and Ericsson, J., 2002. Control of Smad7 stability by competition between acetylation and ubiquitination. Molecular cell, 10(3), pp.483-493.

Gross, K.M., Zhou, W., Breindel, J.L., Ouyang, J., Jin, D.X., Sokol, E.S., Gupta, P.B., Huber, K., Zou, L. and Kuperwasser, C., 2019. Loss of slug compromises DNA damage repair and accelerates stem cell aging in mammary epithelium. Cell reports, 28(2), pp.394-407.

Grossman, S.R., Perez, M., Kung, A.L., Joseph, M., Mansur, C., Xiao, Z.X., Kumar, S., Howley, P.M. and Livingston, D.M., 1998. p300/MDM2 complexes participate in MDM2-mediated p53 degradation. Molecular cell, 2(4), pp.405-415.

Grotowski, M. and Wojtuń, S., 2003. CEA, CA-19-9 and IL-8, sTNFRII and sIL-2R in persons at high risk of colorectal cancer. Polski Merkuriusz Lekarski: Organ Polskiego Towarzystwa Lekarskiego, 14(82), pp.327-330.

Grunstein, M., 1997. Histone acetylation in chromatin structure and transcription. Nature, 389(6649), pp.349-352.

Gryaznova, T., Kropyvko, S., Burdyniuk, M., Gubar, O., Kryklyva, V., Tsyba, L. and Rynditch, A., 2015. Intersectin adaptor proteins are associated with actin-regulating protein WIP in invadopodia. Cellular Signalling, 27(7), pp.1499-1508.

Gu, J., Wang, Y., Wang, X., Zhou, D., Wang, X., Zhou, M. and He, Z., 2018. Effect of the LncRNA GAS5-MiR-23a-ATG3 axis in regulating autophagy in patients with breast cancer. Cellular Physiology and Biochemistry, 48(1), pp.194-207.

Gu, X., Niu, J., Dorahy, D.J., Scott, R. and Agrez, M.V., 2002. Integrin αvβ6-associated ERK2 mediates MMP-9 secretion in colon cancer cells. British journal of cancer, 87(3), pp.348-351.

Gu, Y., Forostyan, T., Sabbadini, R. and Rosenblatt, J., 2011. Epithelial cell extrusion requires the sphingosine-1-phosphate receptor 2 pathway. Journal of Cell Biology, 193(4), pp.667-676.

Guiu, S., Michiels, S., André, F., Cortes, J., Denkert, C., Di Leo, A., Hennessy, B.T., Sorlie, T., Sotiriou, C., Turner, N. and Van de Vijver, M., 2012. Molecular subclasses of breast cancer: how do we define them? The IMPAKT 2012 Working Group Statement. Annals of oncology, 23(12), pp.2997-3006.

Gulyaeva, L.F. and Kushlinskiy, N.E., 2016. Regulatory mechanisms of microRNA expression. Journal of translational medicine, 14(1), p.143.

Gumbiner, B.M. and Kim, N.G., 2014. The Hippo-YAP signaling pathway and contact inhibition of growth. Journal of cell science, 127(4), pp.709-717.

Günhan-Bilgen, I., Memis, A., Üstün, E.E., Zekioglu, O. and Özdemir, N., 2002.Metaplastic carcinoma of the breast: clinical, mammographic, and sonographic findings with histopathologic correlation. American Journal of Roentgenology, 178(6), pp.1421-1425.

Guo, D., Huang, J. and Gong, J., 2012. Bone morphogenetic protein 4 (BMP4) is required for migration and invasion of breast cancer. Molecular and cellular biochemistry, 363(1-2), pp.179-190.

Guo, J.P., Tian, W., Shu, S., Xin, Y., Shou, C. and Cheng, J.Q., 2013. IKBKE phosphorylation and inhibition of FOXO3a: a mechanism of IKBKE oncogenic function. PLoS One, 8(5), p.e63636.

Guo, P., Chen, W., Li, H., Li, M. and Li, L., 2018. The histone acetylation modifications of breast cancer and their therapeutic implications. Pathology & Oncology Research, 24(4), pp.807-813.

Guo, W., Keckesova, Z., Donaher, J.L., Shibue, T., Tischler, V., Reinhardt, F., Itzkovitz, S., Noske, A., Zürrer-Härdi, U., Bell, G. and Tam, W.L., 2012. Slug and Sox9 cooperatively determine the mammary stem cell state. Cell, 148(5), pp.1015-1028.

Guo, X. and Wang, X.F., 2009. Signaling cross-talk between TGF-β/BMP and other pathways. Cell research, 19(1), pp.71-88.

Gupta, P.B., Chaffer, C.L. and Weinberg, R.A., 2009. Cancer stem cells: mirage or reality?. Nature medicine, 15(9), pp.1010-1012.

Gupta, P.B., Onder, T.T., Jiang, G., Tao, K., Kuperwasser, C., Weinberg, R.A. and Lander, E.S., 2009. Identification of selective inhibitors of cancer stem cells by high-throughput screening. Cell, 138(4), pp.645-659.

Gurdon, J.B., 1960. The developmental capacity of nuclei taken from differentiating endoderm cells of Xenopus laevis. Development, 8(4), pp.505-526.

Guttilla, I.K. and White, B.A., 2009. Coordinate regulation of FOXO1 by miR-27a, miR-96, and miR-182 in breast cancer cells. Journal of Biological Chemistry, 284(35), pp.23204-23216. Ha, M., J., and V.,. N. Kim. 2014. Regulation of microRNA biogenesis. Nat. Rev. Mol. Cell Biol, 15, pp.509-24.

Habashy, H.O., Rakha, E.A., Aleskandarany, M., Ahmed, M.A., Green, A.R., Ellis, I.O. and Powe, D.G., 2011. FOXO3a nuclear localisation is associated with good prognosis in luminal-like breast cancer. Breast cancer research and treatment, 129(1), pp.11-21.

Hachim, I.Y., Villatoro, M., Canaff, L., Hachim, M.Y., Boudreault, J., Haiub, H., Ali, S. and Lebrun, J.J., 2017. Transforming growth factor-beta regulation of ephrin type-A receptor 4 signaling in breast cancer cellular migration. Scientific Reports, 7(1), pp.1-15.

Hachim, M.Y., Hachim, I.Y., Dai, M., Ali, S. and Lebrun, J.J., 2018. Differential expression of TGFβ isoforms in breast cancer highlights different roles during breast cancer progression. Tumor Biology, 40(1), p.1010428317748254.

Hafner, C., Schmitz, G., Meyer, S., Bataille, F., Hau, P., Langmann, T., Dietmaier, W., Landthaler, M. and Vogt, T., 2004. Differential gene expression of Eph receptors and ephrins in benign human tissues and cancers. Clinical chemistry, 50(3), pp.490-499.

Hah, N., Benner, C., Chong, L.W., Ruth, T.Y., Downes, M. and Evans, R.M., 2015. Inflammation-sensitive super enhancers form domains of coordinately regulated enhancer RNAs. Proceedings of the National Academy of Sciences, 112(3), pp.E297-E302.

Hajra, K.M., Chen, D.Y. and Fearon, E.R., 2002. The SLUG zinc-finger protein represses E cadherin in breast cancer. Cancer research, 62(6), pp.1613-1618.

Hałasa, M., Wawruszak, A., Przybyszewska, A., Jaruga, A., Guz, M., Kałafut, J., Stepulak, A. and Cybulski, M., 2019. H3K18Ac as a marker of cancer progression and potential target of anti-cancer therapy. Cells, 8(5), p.485.

Halder, S.K., Beauchamp, R.D. and Datta, P.K. (2005). Smad7 induces tumorigenicity by blocking TGF-β-induced growth inhibition and apoptosis. Experimental Cell Research, 307(1), pp.231–246.

Hamada, S., Satoh, K., Hirota, M., Kanno, A., Umino, J., Ito, H., Masamune, A., Kikuta, K., Kume, K. and Shimosegawa, T., 2012. The homeobox gene MSX2 determines chemosensitivity of pancreatic cancer cells via the regulation of transporter gene ABCG2. Journal of cellular physiology, 227(2), pp.729-738.

Hamamori, Y., Sartorelli, V., Ogryzko, V., Puri, P.L., Wu, H.Y., Wang, J.Y., Nakatani, Y. and Kedes, L., 1999. Regulation of histone acetyltransferases p300 and PCAF by the bHLH protein twist and adenoviral oncoprotein E1A. Cell, 96(3), pp.405-413.

Hamidi, A., Song, J., Thakur, N., Itoh, S., Marcusson, A., Bergh, A., Heldin, C.-H. and Landström, M. (2017). TGF-β promotes PI3K-AKT signaling and prostate cancer cell migration through the TRAF6-mediated ubiquitylation of p85α. Science Signaling, 10(486), p.eaal4186.

Hamidi, H. and Ivaska, J., 2018. Every step of the way: integrins in cancer progression and metastasis. Nature Reviews Drug Discovery, 17(3), pp.31-46.

Hammarström, S., 1999, April. The carcinoembryonic antigen (CEA) family: structures, suggested functions and expression in normal and malignant tissues. In Seminars in cancer biology(Vol. 9, No. 2, pp. 67-81). Academic Press.

Hammon, M., Dankerl, P., Janka, R., Wachter, D.L., Hartmann, A., Schulz-Wendtland, R., Uder, M. and Wenkel, E., 2015. Fine needle aspiration cytology of lymph nodes in breast cancer follow-up is a feasible alternative to watchful waiting and to histology. BMC Women's Health, 15(1), pp.1-8.

Han, B., Qu, Y., Jin, Y., Yu, Y., Deng, N., Wawrowsky, K., Zhang, X., Li, N., Bose, S., Wang, Q. and Sakkiah, S., 2015. FOXC1 activates smoothened-independent hedgehog signaling in basal-like breast cancer. Cell reports, 13(5), pp.1046-1058.

Han, G., Lu, S.L., Li, A.G., He, W., Corless, C.L., Kulesz-Martin, M. and Wang, X.J., 2005. Distinct mechanisms of TGF-β1–mediated epithelial-to-mesenchymal transition and metastasis during skin carcinogenesis. The Journal of clinical investigation, 115(7), pp.1714-1723.

Han, L., Diehl, A., Nguyen, N.K., Korangath, P., Teo, W., Cho, S., Kominsky, S., Huso, D.L., Feigenbaum, L., Rein, A. and Argani, P., 2014. The Notch pathway inhibits TGFβ signaling in breast cancer through HEYL-mediated crosstalk. Cancer research, 74(22), pp.6509-6518.

Han, Z., Zhou, X., Li, S., Qin, Y., Chen, Y. and Liu, H., 2017. Inhibition of miR-23a increases the sensitivity of lung cancer stem cells to erlotinib through PTEN/PI3K/Akt pathway. Oncology reports, 38(5), pp.3064-3070.

Hanahan, D. and Weinberg, R.A., 2000. The hallmarks of cancer. cell, 100(1), pp.57-70.

Hanahan, D. and Weinberg, R.A., 2011. Hallmarks of cancer: the next generation. cell, 144(5), pp.646-674.

Hancock, L.A., Hennessy, C.E., Solomon, G.M., Dobrinskikh, E., Estrella, A., Hara, N., Hill, D.B., Kissner, W.J., Markovetz, M.R., Villalon, D.E.G. and Voss, M.E., 2018. Muc5b

overexpression causes mucociliary dysfunction and enhances lung fibrosis in mice. Nature communications, 9(1), pp.1-10.

Hanein, D., Volkmann, N., Goldsmith, S., Michon, A.M., Lehman, W., Craig, R., DeRosier, D., Almo, S. and Matsudaira, P., 1998. An atomic model of fimbrin binding to F-actin and its implications for filament crosslinking and regulation. Nature structural biology, 5(9), pp.787-792.

Hanker, A.B., Estrada, M.V., Bianchini, G., Moore, P.D., Zhao, J., Cheng, F., Koch, J.P., Gianni, L., Tyson, D.R., Sánchez, V. and Rexer, B.N., 2017. Extracellular matrix/integrin signaling promotes resistance to combined inhibition of HER2 and PI3K in HER2+ breast cancer. Cancer research, 77(12), pp.3280-3292.

Hannafon, B.N., Cai, A., Calloway, C.L., Xu, Y.F., Zhang, R., Fung, K.M. and Ding, W.Q., 2019. miR-23b and miR-27b are oncogenic microRNAs in breast cancer: evidence from a CRISPR/Cas9 deletion study. BMC cancer, 19(1), p.642.

Hannon, G.J., 1994. Beach, 0. pb5INK4B is a potentialTGFp-induced cell cycle arrest. Nature (Lend.), 371, pp.257-261.

Hanrahan, E.O., Gonzalez-Angulo, A.M., Giordano, S.H., Rouzier, R., Broglio, K.R., Hortobagyi, G.N. and Valero, V., 2007. Overall survival and cause-specific mortality of patients with stage T1a, bN0M0 breast carcinoma. Journal of clinical oncology, 25(31), pp.4952-4960.

Hanrahan, K., O'Neill, A., Prencipe, M., Bugler, J., Murphy, L., Fabre, A., Puhr, M., Culig, Z., Murphy, K. and Watson, R.W., 2017. The role of epithelial–mesenchymal transition drivers ZEB1 and ZEB2 in mediating docetaxel-resistant prostate cancer. Molecular oncology, 11(3), pp.251-265.

Hanstein, B., Eckner, R., DiRenzo, J., Halachmi, S., Liu, H., Searcy, B., Kurokawa, R. and Brown, M., 1996. p300 is a component of an estrogen receptor coactivator complex. Proceedings of the National Academy of Sciences, 93(21), pp.11540-11545.

Hardwick, J.C., Kodach, L.L., Offerhaus, G.J. and Van Den Brink, G.R., 2008. Bone morphogenetic protein signalling in colorectal cancer. Nature Reviews Cancer, 8(10), pp.806-812.

Hardy, K.M., Booth, B.W., Hendrix, M.J., Salomon, D.S. and Strizzi, L., 2010. ErbB/EGF signaling and EMT in mammary development and breast cancer. Journal of mammary gland biology and neoplasia, 15(2), pp.191-199.

Harney, A.S., Arwert, E.N., Entenberg, D., Wang, Y., Guo, P., Qian, B.Z., Oktay, M.H., Pollard, J.W., Jones, J.G. and Condeelis, J.S., 2015. Real-time imaging reveals local, transient vascular permeability, and tumor cell intravasation stimulated by TIE2hi macrophage–derived VEGFA. Cancer discovery, 5(9), pp.932-943.

Harris, L., Fritsche, H., Mennel, R., Norton, L., Ravdin, P., Taube, S., Somerfield, M.R., Hayes, D.F. and Bast Jr, R.C., 2007. American Society of Clinical Oncology 2007 update of recommendations for the use of tumor markers in breast cancer. Journal of clinical oncology, 25(33), pp.5287-5312.

Harris, L.G., Pannell, L.K., Singh, S., Samant, R.S. and Shevde, L.A., 2012. Increased vascularity and spontaneous metastasis of breast cancer by hedgehog signaling mediated upregulation of cyr61. Oncogene, 31(28), pp.3370-3380.

Harrison, H., Simões, B.M., Rogerson, L., Howell, S.J., Landberg, G. and Clarke, R.B., 2013. Oestrogen increases the activity of oestrogen receptor negative breast cancer stem cells through paracrine EGFR and Notch signalling. Breast Cancer Research, 15(2), pp.1-12.

Harshman, S.W., Hoover, M.E., Huang, C., Branson, O.E., Chaney, S.B., Cheney, C.M., Rosol, T.J., Shapiro, C.L., Wysocki, V.H., Huebner, K. and Freitas, M.A., 2014. Histone H1 phosphorylation in breast cancer. Journal of proteome research, 13(5), pp.2453-2467.

Hartwell, K.A., Muir, B., Reinhardt, F., Carpenter, A.E., Sgroi, D.C. and Weinberg, R.A., 2006. The Spemann organizer gene, Goosecoid, promotes tumor metastasis. Proceedings of the National Academy of Sciences, 103(50), pp.18969-18974.

Haslehurst, A.M., Koti, M., Dharsee, M., Nuin, P., Evans, K., Geraci, J., Childs, T., Chen, J., Li, J., Weberpals, J. and Davey, S., 2012. EMT transcription factors snail and slug directly contribute to cisplatin resistance in ovarian cancer. BMC cancer, 12(1), p.91.

Hata, S., Abe, M., Suzuki, H., Kitamura, F., Toyama-Sorimachi, N., Abe, K., Sakimura, K. and Sorimachi, H., 2010. Calpain 8/nCL-2 and calpain 9/nCL-4 constitute an active protease complex, G-calpain, involved in gastric mucosal defense. PLoS Genet, 6(7), p.e1001040.

Hay, D.A., Fedorov, O., Martin, S., Singleton, D.C., Tallant, C., Wells, C., Picaud, S., Philpott, M., Monteiro, O.P., Rogers, C.M. and Conway, S.J., 2014. Discovery and optimization of small-molecule ligands for the CBP/p300 bromodomains. Journal of the American Chemical Society, 136(26), pp.9308-9319.

Hayashi, I., Takatori, S., Urano, Y., Miyake, Y., Takagi, J., Sakata-Yanagimoto, M., Iwanari, H., Osawa, S., Morohashi, Y., Li, T. and Wong, P.C., 2012. Neutralization of the γ-secretase activity by monoclonal antibody against extracellular domain of nicastrin. Oncogene, 31(6), pp.787-798.

Hayes, N.V., Blackburn, E., Boyle, M.M., Russell, G.A., Frost, T.M., Morgan, B.J. and Gullick, W.J., 2011. Expression of neuregulin 4 splice variants in normal human tissues and prostate cancer and their effects on cell motility. Endocrine-related cancer, 18(1), p.39.

Hazarika, M., Chuk, M.K., Theoret, M.R., Mushti, S., He, K., Weis, S.L., Putman, A.H., Helms, W.S., Cao, X., Li, H. and Zhao, H., 2017. US FDA approval summary: nivolumab

for treatment of unresectable or metastatic melanoma following progression on ipilimumab. Clinical Cancer Research, 23(14), pp.3484-3488.

He, H.C., Zhu, J.G., Chen, X.B., Chen, S.M., Han, Z.D., Dai, Q.S., Ling, X.H., Fu, X., Lin, Z.Y., Deng, Y.H. and Qin, G.Q., 2012. MicroRNA-23b downregulates peroxiredoxin III in human prostate cancer. Febs Letters, 586(16), pp.2451-2458.

He, J., Qi, H., Chen, F. and Cao, C., 2017. MicroRNA 25 contributes to cisplatin resistance in gastric cancer cells by inhibiting forkhead box O3a. Oncology Letters, 14(5), pp.6097-6102.

He, J., Ye, J., Cai, Y., Riquelme, C., Liu, J.O., Liu, X., Han, A. and Chen, L., 2011. Structure of p300 bound to MEF2 on DNA reveals a mechanism of enhanceosome assembly. Nucleic acids research, 39(10), pp.4464-4474.

He, X.X., Kuang, S.Z., Liao, J.Z., Xu, C.R., Chang, Y., Wu, Y.L., Gong, J., Tian, D.A., Guo, A.Y. and Lin, J.S., 2015. The regulation of microRNA expression by DNA methylation in hepatocellular carcinoma. Molecular bioSystems, 11(2), pp.532-539.

He, Y.J., Wu, J.Z., Ji, M.H., Ma, T., Qiao, E.Q., Ma, R. and Tang, J.H., 2013. miR 342 is associated with estrogen receptor α expression and response to tamoxifen in breast cancer. Experimental and therapeutic medicine, 5(3), pp.813-818.

Hecht, A. and Stemmler, M.P., 2003. Identification of a promoter-specific transcriptional activation domain at the C terminus of the Wnt effector protein T-cell factor 4. Journal of Biological Chemistry, 278(6), pp.3776-3785.

Hedges, J.C., Dechert, M.A., Yamboliev, I.A., Martin, J.L., Hickey, E., Weber, L.A. and Gerthoffer, W.T., 1999. A role for p38MAPK/HSP27 pathway in smooth muscle cell migration. Journal of Biological Chemistry, 274(34), pp.24211-24219.

Heemann, C., Kreuz, M., Stoller, I., Schoof, N., von Bonin, F., Ziepert, M., Löffler, M., Jung, W., Pfreundschuh, M., Trümper, L. and Kube, D., 2012. Circulating Levels of TNF Receptor II Are Prognostic for Patients with Peripheral T-cell Non–Hodgkin Lymphoma. Clinical Cancer Research, 18(13), pp.3637-3647.

Helleman, J., Jansen, M.P., Burger, C., van der Burg, M.E. and Berns, E.M., 2010. Integrated genomics of chemotherapy resistant ovarian cancer: a role for extracellular matrix, TGFbeta and regulating microRNAs. The international journal of biochemistry & cell biology, 42(1), pp.25-30.

Hellström M., Phng L. and Gerhardt H., 2014. VEGF and Notch Signalling. Cell Adhesion & Migration, 1(3), pp. 133–136. Helsten, T., Elkin, S., Arthur, E., Tomson, B.N., Carter, J. and Kurzrock, R., 2016. The FGFR landscape in cancer: analysis of 4,853 tumors by next-generation sequencing. Clinical cancer research, 22(1), pp.259-267.

Hennessy, B.T., Gonzalez-Angulo, A.M., Stemke-Hale, K., Gilcrease, M.Z., Krishnamurthy, S., Lee, J.S., Fridlyand, J., Sahin, A., Agarwal, R., Joy, C. and Liu, W., 2009. Characterization of a naturally occurring breast cancer subset enriched in epithelial-to-mesenchymal transition and stem cell characteristics. Cancer research, 69(10), pp.4116-4124.

Hennessy, B.T., Smith, D.L., Ram, P.T., Lu, Y. and Mills, G.B., 2005. Exploiting the PI3K/AKT pathway for cancer drug discovery. Nature reviews Drug discovery, 4(12), pp.988-1004.

Hernandez-Aya, L.F. and Gonzalez-Angulo, A.M., 2013. Adjuvant systemic therapies in breast cancer. Surgical Clinics, 93(2), pp.473-491.

Hesari, A., Azizian, M., Darabi, H., Nesaei, A., Hosseini, S.A., Salarinia, R., Motaghi, A.A. and Ghasemi, F., 2019. Expression of circulating miR-17, miR-25, and miR-133 in breast cancer patients. Journal of cellular biochemistry, 120(5), pp.7109-7114.

Hicks, D.G., Short, S.M., Prescott, N.L., Tarr, S.M., Coleman, K.A., Yoder, B.J., Crowe, J.P., Choueiri, T.K., Dawson, A.E., Budd, G.T. and Tubbs, R.R., 2006. Breast cancers with brain metastases are more likely to be estrogen receptor negative, express the basal cytokeratin CK5/6, and overexpress HER2 or EGFR. The American journal of surgical pathology, 30(9), pp.1097-1104.

Hicks, D.G., Short, S.M., Prescott, N.L., Tarr, S.M., Coleman, K.A., Yoder, B.J., Crowe, J.P., Choueiri, T.K., Dawson, A.E., Budd, G.T. and Tubbs, R.R., 2006. Breast cancers with brain metastases are more likely to be estrogen receptor negative, express the basal cytokeratin CK5/6, and overexpress HER2 or EGFR. The American journal of surgical pathology, 30(9), pp.1097-1104.

Hill, C.S., 2009. Nucleocytoplasmic shuttling of Smad proteins. Cell research, 19(1), pp.36-46.

Hill, L., Browne, G. and Tulchinsky, E., 2013. ZEB/miR-200 feedback loop: at the crossroads of signal transduction in cancer. International journal of cancer, 132(4), pp.745-754.

Hillgren, K.M., Keppler, D., Zur, A.A., Giacomini, K.M., Stieger, B., Cass, C.E., Zhang, L. and International Transporter Consortium, 2013. Emerging transporters of clinical importance: an update from the International Transporter Consortium. Clinical Pharmacology & Therapeutics, 94(1), pp.52-63.

Himanen, J.P., Chumley, M.J., Lackmann, M., Li, C., Barton, W.A., Jeffrey, P.D., Vearing, C., Geleick, D., Feldheim, D.A., Boyd, A.W. and Henkemeyer, M., 2004. Repelling class discrimination: ephrin-A5 binds to and activates EphB2 receptor signaling. Nature neuroscience, 7(5), pp.501-509.

Himanen, J.P., Chumley, M.J., Lackmann, M., Li, C., Barton, W.A., Jeffrey, P.D., Vearing, C., Geleick, D., Feldheim, D.A., Boyd, A.W. and Henkemeyer, M., 2004. Repelling class discrimination: ephrin-A5 binds to and activates EphB2 receptor signaling. Nature neuroscience, 7(5), pp.501-509.

Himanen, J.P., Saha, N. and Nikolov, D.B., 2007. Cell–cell signaling via Eph receptors and ephrins. Current opinion in cell biology, 19(5), pp.534-542.

Hinohara, K., Kobayashi, S., Kanauchi, H., Shimizu, S., Nishioka, K., Tsuji, E.I., Tada, K.I., Umezawa, K., Mori, M., Ogawa, T. and Inoue, J.I., 2012. ErbB receptor tyrosine kinase/NF-κB signaling controls mammosphere formation in human breast cancer. Proceedings of the National Academy of Sciences, 109(17), pp.6584-6589.

Hinshelwood, R.A., Huschtscha, L.I., Melki, J., Stirzaker, C., Abdipranoto, A., Vissel, B., Ravasi, T., Wells, C.A., Hume, D.A., Reddel, R.R. and Clark, S.J., 2007. Concordant epigenetic silencing of transforming growth factor-β signaling pathway genes occurs early in breast carcinogenesis. Cancer research, 67(24), pp.11517-11527.

Hirohashi, S., 1998. Inactivation of the E-cadherin-mediated cell adhesion system in human cancers. The American journal of pathology, 153(2), pp.333-339.

Hirschhaeuser, F., Menne, H., Dittfeld, C., West, J., Mueller-Klieser, W. and Kunz Schughart, L.A., 2010. Multicellular tumor spheroids: an underestimated tool is catching up again. Journal of biotechnology, 148(1), pp.3-15.

Hisamatsu, Y., Tokunaga, E., Yamashita, N., Akiyoshi, S., Okada, S., Nakashima, Y., Aishima, S., Morita, M., Kakeji, Y. and Maehara, Y., 2012. Impact of FOXA1 expression on the prognosis of patients with hormone receptor-positive breast cancer. Annals of surgical oncology, 19(4), pp.1145-1152.

Hisano, T., Ono, M., Nakayama, M., Naito, S., Kuwano, M. and Wada, M., 1996. Increased expression of T-plastin gene in cisplatin-resistant human cancer cells: identification by mRNA differential display. FEBS letters, 397(1), pp.101-107.

HL, B.B.M., 2006. Tumour microenvironment: TGFβ: the molecular Jekyll and Hyde of cancer. Nat Rev Cancer, 6(7), pp.506-20.

Hnisz, D., Abraham, B.J., Lee, T.I., Lau, A., Saint-André, V., Sigova, A.A., Hoke, H.A. and Young, R.A., 2013. Super-enhancers in the control of cell identity and disease. Cell, 155(4), pp.934-947.

Ho, K.K., McGuire, V.A., Koo, C.Y., Muir, K.W., de Olano, N., Maifoshie, E., Kelly, D.J., McGovern, U.B., Monteiro, L.J., Gomes, A.R. and Nebreda, A.R., 2012. Phosphorylation of FOXO3a on Ser-7 by p38 promotes its nuclear localization in response to doxorubicin. Journal of Biological Chemistry, 287(2), pp.1545-1555.

Hodgkinson, C.L., Morrow, C.J., Li, Y., Metcalf, R.L., Rothwell, D.G., Trapani, F., Polanski, R., Burt, D.J., Simpson, K.L., Morris, K. and Pepper, S.D., 2014. Tumorigenicity and genetic profiling of circulating tumor cells in small-cell lung cancer. Nature medicine, 20(8), pp.897-903.

Hoelper, D., Huang, H., Jain, A.Y., Patel, D.J. and Lewis, P.W., 2017. Structural and mechanistic insights into ATRX-dependent and-independent functions of the histone chaperone DAXX. Nature communications, 8(1), pp.1-13.

Hofman, J., Malcekova, B., Skarka, A., Novotna, E., Wsol, V. (2014). Anthracycline resistance mediated by reductive metabolism in cancer cells: the role of aldo-keto reductase 1C3, Toxicol. Appl. Pharmacol. 278(3), 238–248.

Hohenester, E. and Yurchenco, P.D., 2013. Laminins in basement membrane assembly. Cell adhesion & migration, 7(1), pp.56-63.

Hollenbach, A.D., McPherson, C.J., Mientjes, E.J., Iyengar, R. and Grosveld, G., 2002. Daxx and histone deacetylase II associate with chromatin through an interaction with core histones and the chromatin-associated protein Dek. Journal of cell science, 115(16), pp.3319-3330.

Hollestelle, A., Peeters, J.K., Smid, M., Timmermans, M., Verhoog, L.C., Westenend, P.J., Heine, A.A., Chan, A., Sieuwerts, A.M., Wiemer, E.A. and Klijn, J.G., 2013. Loss of E-cadherin is not a necessity for epithelial to mesenchymal transition in human breast cancer. Breast cancer research and treatment, 138(1), pp.47-57.

Holohan, C., Van Schaeybroeck, S., Longley, D.B. and Johnston, P.G., 2013. Cancer drug resistance: an evolving paradigm. Nature Reviews Cancer, 13(10), pp.714-726.

Holton, S.E., Bergamaschi, A., Katzenellenbogen, B.S. and Bhargava, R., 2014. Integration of molecular profiling and chemical imaging to elucidate fibroblast-microenvironment impact on cancer cell phenotype and endocrine resistance in breast cancer. PLoS One, 9(5), p.e96878.

Hong, S., Kim, C.Y., Lee, J.E. and Seong, G.J., 2009. Agmatine protects cultured retinal ganglion cells from tumor necrosis factor-alpha-induced apoptosis. Life sciences, 84(1-2), pp.28-32.

Hood, J.D. and Cheresh, D.A., 2002. Role of integrins in cell invasion and migration. Nature Reviews Cancer, 2(2), pp.91-100.

Horst, A.K., Ito, W.D., Dabelstein, J., Schumacher, U., Sander, H., Turbide, C., Brümmer, J., Meinertz, T., Beauchemin, N. and Wagener, C., 2006. Carcinoembryonic antigen–related cell adhesion molecule 1 modulates vascular remodeling in vitro and in vivo. The Journal of clinical investigation, 116(6), pp.1596-1605.

Hoshi, H., Sawada, T., Uchida, M., Saito, H., Iijima, H., Toda-Agetsuma, M., Wada, T., Yamazoe, S., Tanaka, H., Kimura, K. and Kakehashi, A., 2011. Tumor-associated MUC5AC stimulates in vivo tumorigenicity of human pancreatic cancer. International journal of oncology, 38(3), pp.619-627.

Hoshino, A., Costa-Silva, B., Shen, T.L., Rodrigues, G., Hashimoto, A., Mark, M.T., Molina, H., Kohsaka, S., Di Giannatale, A., Ceder, S. and Singh, S., 2015. Tumour exosome integrins determine organotropic metastasis. Nature, 527(7578), pp.329-335.

Hosoya-Ohmura, S., Lin, Y.H., Herrmann, M., Kuroha, T., Rao, A., Moriguchi, T., Lim, K.C., Hosoya, T. and Engel, J.D., 2011. An NK and T cell enhancer lies 280 kilobase pairs 3 to the gata3 structural gene. Molecular and cellular biology, 31(9), pp.1894-1904.

Hossain, M.M., Crish, J.F., Eckert, R.L., Lin, J.J.C. and Jin, J.P., 2005. h2-Calponin is regulated by mechanical tension and modifies the function of actin cytoskeleton. Journal of Biological Chemistry, 280(51), pp.42442-42453.

Hossain, M.M., Wang, X., Bergan, R.C. and Jin, J.P., 2014. Diminished expression of h2 calponin in prostate cancer cells promotes cell proliferation, migration and the dependence of cell adhesion on substrate stiffness. FEBS open bio, 4, pp.627-636.

Hossini, A.M., Quast, A.S., Plötz, M., Grauel, K., Exner, T., Küchler, J., Stachelscheid, H., Eberle, J., Rabien, A., Makrantonaki, E. and Zouboulis, C.C., 2016. PI3K/AKT signaling pathway is essential for survival of induced pluripotent stem cells. PloS one, 11(5), p.e0154770.

Hotary, K.B., Allen, E.D., Brooks, P.C., Datta, N.S., Long, M.W. and Weiss, S.J., 2003. Membrane type I matrix metalloproteinase usurps tumor growth control imposed by the three-dimensional extracellular matrix. Cell, 114(1), pp.33-45.

Hou, C., Kaspari, M., Vander Zanden, H.B. and Gillooly, J.F., 2010. Energetic basis of colonial living in social insects. Proceedings of the National Academy of Sciences, 107(8), pp.3634-3638.

Hou, J., Wang, X., Li, Y., Liu, X., Wang, Z., An, J., Yang, L. and He, Y., 2012. 17beta estradiol induces both up-regulation and processing of cyclin E in a calpain-dependent manner in MCF-7 breast cancer cells. FEBS letters, 586(6), pp.892-896.

Howard, E.W. and Yang, X., 2018. microRNA regulation in estrogen receptor-positive breast cancer and endocrine therapy. Biological procedures online, 20(1), pp.1-19.

Howe, L.R. and Brown, A.M., 2004. Wnt signaling and breast cancer. Cancer biology & therapy, 3(1), pp.36-41.

Hsu, Y.L., Hung, J.Y., Chang, W.A., Lin, Y.S., Pan, Y.C., Tsai, P.H., Wu, C.Y. and Kuo, P.L., 2017. Hypoxic lung cancer-secreted exosomal miR-23a increased angiogenesis

and vascular permeability by targeting prolyl hydroxylase and tight junction protein ZO-1. Oncogene, 36(34), pp.4929-4942.

Hu, B., Thirtamara-Rajamani, K.K., Sim, H. and Viapiano, M.S., 2009. Fibulin-3 is uniquely upregulated in malignant gliomas and promotes tumor cell motility and invasion. Molecular cancer research, 7(11), pp.1756-1770.

Hu, B.R., Liu, C.L. and Park, D.J., 2000. Alteration of MAP kinase pathways after transient forebrain ischemia. Journal of Cerebral Blood Flow & Metabolism, 20(7), pp.1089-1095.

Hu, F., Wang, C., Du, J., Sun, W., Yan, J., Mi, D., Zhang, J., Qiao, Y., Zhu, T. and Yang, S., 2010. δEF1 promotes breast cancer cell proliferation through down-regulating p21 expression. Biochimica et Biophysica Acta (BBA)-Molecular Basis of Disease, 1802(2), pp.301-312.

Hu, H., Li, S., Cui, X., Lv, X., Jiao, Y., Yu, F., Yao, H., Song, E., Chen, Y., Wang, M. and Lin, L., 2013. The overexpression of hypomethylated miR-663 induces chemotherapy resistance in human breast cancer cells by targeting heparin sulfate proteoglycan 2 (HSPG2). Journal of Biological Chemistry, 288(16), pp.10973-10985.

Hu, J., Guo, H., Li, H., Liu, Y., Liu, J., Chen, L., Zhang, J. and Zhang, N., 2012. MiR-145 regulates epithelial to mesenchymal transition of breast cancer cells by targeting Oct4. PloS one, 7(9), p.e45965.

Hu, J., Xie, W., Shang, L., Yang, X., Li, Q., Xu, M., Dou, J., Zhou, Y., Niu, W. and Wu, Y., 2017. Knockdown of calponin 2 suppressed cell growth in gastric cancer cells. Tumor Biology, 39(7), p.1010428317706455.

Hu, M., Xia, M., Chen, X., Lin, Z., Xu, Y., Ma, Y. and Su, L., 2010. MicroRNA-141 regulates Smad interacting protein 1 (SIP1) and inhibits migration and invasion of colorectal cancer cells. Digestive diseases and sciences, 55(8), pp.2365-2372.

Hu, M.C., Wasserman, D., Hartwig, S. and Rosenblum, N.D., 2004. p38MAPK acts in the BMP7-dependent stimulatory pathway during epithelial cell morphogenesis and is regulated by Smad1. Journal of Biological Chemistry, 279(13), pp.12051-12059

Hu, T., Zhou, R., Zhao, Y. and Wu, G., 2016. Integrin α6/Akt/Erk signaling is essential for human breast cancer resistance to radiotherapy. Scientific reports, 6, p.33376.

Hu, X., Wang, Y., Liang, H., Fan, Q., Zhu, R., Cui, J., Zhang, W., Zen, K., Zhang, C.Y., Hou, D. and Zhou, Z., 2017. miR-23a/b promote tumor growth and suppress apoptosis by targeting PDCD4 in gastric cancer. Cell death & disease, 8(10), pp.e3059-e3059. Hu, Y., Guo, R., Wei, J., Zhou, Y., Ji, W., Liu, J., Zhi, X. and Zhang, J., 2015. Effects of PI3K inhibitor NVP-BKM120 on overcoming drug resistance and eliminating cancer stem cells in human breast cancer cells. Cell death & disease, 6(12), pp.e2020-e2020.

Hu, Y., Li, K., Asaduzzaman, M., Cuella, R., Shi, H., Raguz, S., Coombes, R.C., Zhou, Y. and Yagüe, E., 2016. miR-106b 25 cluster regulates multidrug resistance in an ABC transporter-independent manner via downregulation of EP300. Oncology reports, 35(2), pp.1170-1178.

Hu, Y.Y., Zheng, M.H., Zhang, R., Liang, Y.M. and Han, H., 2012. Notch signaling pathway and cancer metastasis. In Notch Signaling in Embryology and Cancer (pp. 186-198). Springer, New York, NY. Hu, Z., Huang, G., Sadanandam, A., Gu, S., Lenburg, M.E., Pai, M., Bayani, N., Blakely, E.A., Gray, J.W. and Mao, J.H., 2010. The expression level of HJURP has an independent prognostic impact and predicts the sensitivity to radiotherapy in breast cancer. Breast cancer research, 12(2), p.R18.

Hua, S., Kallen, C.B., Dhar, R., Baquero, M.T., Mason, C.E., Russell, B.A., Shah, P.K., Liu, J., Khramtsov, A., Tretiakova, M.S. and Krausz, T.N., 2008. Genomic analysis of estrogen cascade reveals histone variant H2A. Z associated with breast cancer progression. Molecular systems biology, 4(1), p.188.

Huang, D., Duan, H., Huang, H., Tong, X., Han, Y., Ru, G., Qu, L., Shou, C. and Zhao, Z., 2016. Cisplatin resistance in gastric cancer cells is associated with HER2 upregulation-induced epithelial-mesenchymal transition. Scientific reports, 6, p.20502.

Huang, E.H., Hynes, M.J., Zhang, T., Ginestier, C., Dontu, G., Appelman, H., Fields, J.Z., Wicha, M.S. and Boman, B.M., 2009. Aldehyde dehydrogenase 1 is a marker for normal and malignant human colonic stem cells (SC) and tracks SC overpopulation during colon tumorigenesis. Cancer research, 69(8), pp.3382-3389.

Huang, F.Y., Wong, D.K.H., Seto, W.K., Lai, C.L. and Yuen, M.F., 2015. Estradiol induces apoptosis via activation of miRNA-23a and p53: implication for gender difference in liver cancer development. Oncotarget, 6(33), p.34941.

Huang, Q.Q., Hossain, M.M., Wu, K., Parai, K., Pope, R.M. and Jin, J.P., 2008. Role of H2 calponin in regulating macrophage motility and phagocytosis. Journal of Biological Chemistry, 283(38), pp.25887-25899.

Huang, T.T., Ping, Y.H., Wang, A.M., Ke, C.C., Fang, W.L., Huang, K.H., Lee, H.C., Chi, C.W. and Yeh, T.S., 2015. The reciprocal regulation loop of Notch2 pathway and miR-23b in controlling gastric carcinogenesis. Oncotarget, 6(20), p.18012.

Huang, Y.T., Lan, Q., Lorusso, G., Duffey, N. and Rüegg, C., 2017. The matricellular protein CYR61 promotes breast cancer lung metastasis by facilitating tumor cell extravasation and suppressing anoikis. Oncotarget, 8(6), p.9200.

Huber, M.A., Kraut, N. and Beug, H., 2005. Molecular requirements for epithelial mesenchymal transition during tumor progression. Current opinion in cell biology, 17(5), pp.548-558.

Huck, L., Pontier, S.M., Zuo, D.M. and Muller, W.J., 2010. β1-integrin is dispensable for the induction of ErbB2 mammary tumors but plays a critical role in the metastatic phase of tumor progression. Proceedings of the National Academy of Sciences, 107(35), pp.15559-15564.

Hui, A.B., Shi, W., Boutros, P.C., Miller, N., Pintilie, M., Fyles, T., McCready, D., Wong, D., Gerster, K., Jurisica, I. and Penn, L.Z., 2009. Robust global micro-RNA profiling with formalin-fixed paraffin-embedded breast cancer tissues. Laboratory investigation, 89(5), pp.597-606.

Hulpiau, P. and Van Roy, F., 2009. Molecular evolution of the cadherin superfamily. The international journal of biochemistry & cell biology, 41(2), pp.349-369.

Humphries, J.D., Byron, A. and Humphries, M.J., 2006. Integrin ligands at a glance. Journal of cell science, 119(19), pp.3901-3903.

Hunter, D.J., Kraft, P., Jacobs, K.B., Cox, D.G., Yeager, M., Hankinson, S.E., Wacholder, S., Wang, Z., Welch, R., Hutchinson, A. and Wang, J., 2007. A genome-wide association study identifies alleles in FGFR2 associated with risk of sporadic postmenopausal breast cancer. Nature genetics, 39(7), pp.870-874.

Hurtado, A., Holmes, K.A., Ross-Innes, C.S., Schmidt, D. and Carroll, J.S., 2011. FOXA1 is a key determinant of estrogen receptor function and endocrine response. Nature genetics, 43(1), pp.27-33.

Hussein, H.A., Walker, L.R., Abdel-Raouf, U.M., Desouky, S.A., Montasser, A.K.M. and Akula, S.M., 2015. Beyond RGD: virus interactions with integrins. Archives of virology, 160(11), pp.2669-2681.

Hwang, W.L., Jiang, J.K., Yang, S.H., Huang, T.S., Lan, H.Y., Teng, H.W., Yang, C.Y., Tsai, Y.P., Lin, C.H., Wang, H.W. and Yang, M.H., 2014. MicroRNA-146a directs the symmetric division of Snail-dominant colorectal cancer stem cells. Nature cell biology, 16(3), pp.268-280.

Hyndman, B.D., Thompson, P., Bayly, R., Côté, G.P. and LeBrun, D.P., 2012. E2A proteins enhance the histone acetyltransferase activity of the transcriptional co-activators CBP and p300. Biochimica et Biophysica Acta (BBA)-Gene Regulatory Mechanisms, 1819(5), pp.446-453.

Hynes, R.O., 2002. Integrins: bidirectional, allosteric signaling machines. cell, 110(6), pp.673-687.

Icha, J., Weber, M., Waters, J.C. and Norden, C., 2017. Phototoxicity in live fluorescence microscopy, and how to avoid it. Bioessays, 39(8), p.1700003.

Iden, S., Rehder, D., August, B., Suzuki, A., Wolburg-Buchholz, K., Wolburg, H., Ohno, S., Behrens, J., Vestweber, D. and Ebnet, K., 2006. A distinct PAR complex associates

physically with VE-cadherin in vertebrate endothelial cells. EMBO reports, 7(12), pp.1239-1246.

Iftikhar, H. and Carney, G.E., 2016. Evidence and potential in vivo functions for biofluid miRNAs: From expression profiling to functional testing: Potential roles of extracellular miRNAs as indicators of physiological change and as agents of intercellular information exchange. Bioessays, 38(4), pp.367-378.

Ikeda, J.I., Tian, T., Wang, Y., Hori, Y., Honma, K., Wada, N. and Morii, E., 2013. Expression of FoxO3a in clinical cases of malignant lymphoma. Pathology-Research and Practice, 209(11), pp.716-720.

Ikeda, K., Horie-Inoue, K., Ueno, T., Suzuki, T., Sato, W., Shigekawa, T., Osaki, A., Saeki, T., Berezikov, E., Mano, H. and Inoue, S., 2015. miR-378a-3p modulates tamoxifen sensitivity in breast cancer MCF-7 cells through targeting GOLT1A. Scientific reports, 5, p.13170.

Ilina, O., Bakker, G.J., Vasaturo, A., Hoffman, R.M. and Friedl, P., 2011. Two-photon laser-generated microtracks in 3D collagen lattices: principles of MMP-dependent and-independent collective cancer cell invasion. Physical biology, 8(1), p.015010.

Imai, T., Hieshima, K., Haskell, C., Baba, M., Nagira, M., Nishimura, M., Kakizaki, M., Takagi, S., Nomiyama, H., Schall, T.J. and Yoshie, O., 1997. Identification and molecular characterization of fractalkine receptor CX3CR1, which mediates both leukocyte migration and adhesion. Cell, 91(4), pp.521-530.

Imai, T., Horiuchi, A., Wang, C., Oka, K., Ohira, S., Nikaido, T. and Konishi, I., 2003. Hypoxia attenuates the expression of E-cadherin via up-regulation of SNAIL in ovarian carcinoma cells. The American journal of pathology, 163(4), pp.1437-1447.

Imamichi, Y., König, A., Gress, T. and Menke, A., 2006. Collagen type I-induced Smad interacting protein 1 expression downregulates E-cadherin in pancreatic cancer. Oncogene, 26(16), pp.2381–2385.

Ingham, P.W., 2001. Hedgehog signaling in animal development: paradigms and principles. Genes & Development, [online] 15(23), pp.3059–3087. Available at: http://genesdev.cshlp.org/content/1

Ingthorsson, S., Andersen, K., Hilmarsdottir, B., Maelandsmo, G.M., Magnusson, M.K. and Gudjonsson, T., 2015. HER2 induced EMT and tumorigenicity in breast epithelial progenitor cells is inhibited by coexpression of EGFR. Oncogene, 35(32), pp.4244–4255.

International Agency for Research on Cancer, 2012. Cervical cancer estimated incidence, mortality and prevalence worldwide in 2012. World Health Organization. International Agency for Research on Cancer, 2012. GLOBOCAN 2012: estimated cancer incidence, mortality and prevalence worldwide in 2012. Iorio, M.V., Ferracin, M., Liu, C.-G., Veronese, A., Spizzo, R., Sabbioni, S., Magri, E., Pedriali, M., Fabbri, M., Campiglio, M., Ménard, S.,

Palazzo, J.P., Rosenberg, A., Musiani, P., Volinia, S., Nenci, I., Calin, G.A., Querzoli, P., Negrini, M. and Croce, C.M., 2005. MicroRNA Gene Expression Deregulation in Human Breast Cancer. Cancer Research, 65(16), pp.7065–7070

Ipsaro, J.J. and Joshua-Tor, L., 2015. From guide to target: molecular insights into eukaryotic RNA-interference machinery. Nature Structural & Molecular Biology, 22(1), pp.20–28

Iso, T., Sartorelli, V., Poizat, C., Iezzi, S., Wu, H.-Y., Chung, G., Kedes, L. and Hamamori, Y., 2001. HERP, a Novel Heterodimer Partner of HES/E(spl) in Notch Signaling. Molecular and Cellular Biology, 21(17), pp.6080–6089.

Ito, T., Ikehara, T., Nakagawa, T., Kraus, W. L., & Muramatsu, M., 2000. p300-mediated acetylation facilitates the transfer of histone H2A-H2B dimers from nucleosomes to a histone chaperone. Genes & development, 14(15), 1899–1907.

Ivaska, J., Pallari, H.-M., Nevo, J. and Eriksson, J.E., 2007. Novel functions of vimentin in cell adhesion, migration, and signaling. Experimental Cell Research, 313(10), pp.2050–2062.

Jack, X.Y., Sieuwerts, A.M., Zhang, Y., Martens, J.W., Smid, M., Klijn, J.G., Wang, Y. and Foekens, J.A., 2007. Pathway analysis of gene signatures predicting metastasis of node-negative primary breast cancer. BMC cancer, 7(1), p.182.

Jackson, A.M., Mulcahy, L.A., Porte, J., Franks, H.A., El Refaee, M., Wang, Q., Shah, S., Zhu, X. and Patel, P.M., 2010. Role of mitogen-activated protein kinase and PI3K pathways in the regulation of IL-12-family cytokines in dendritic cells and the generation of T H-responses. European cytokine network, 21(4), pp.319-328.

Jaggupilli, A. and Elkord, E., 2012. Significance of CD44 and CD24 as cancer stem cell markers: an enduring ambiguity. Clinical and Developmental Immunology, 2012.

Jahangiri, A., Nguyen, A., Chandra, A., Sidorov, M.K., Yagnik, G., Rick, J., Han, S.W., Chen, W., Flanigan, P.M., Schneidman-Duhovny, D. and Mascharak, S., 2017. Cross-activating c-Met/β1 integrin complex drives metastasis and invasive resistance in cancer. Proceedings of the National Academy of Sciences, 114(41), pp.E8685-E8694.

Jamaladdin, S., Kelly, R.D., O'Regan, L., Dovey, O.M., Hodson, G.E., Millard, C.J., Portolano, N., Fry, A.M., Schwabe, J.W. and Cowley, S.M., 2014. Histone deacetylase (HDAC) 1 and 2 are essential for accurate cell division and the pluripotency of embryonic stem cells. Proceedings of the National Academy of Sciences, 111(27), pp.9840-9845.

Jamaleddine, M., Harris, M.S., Liyanage, L. and Cook, G.A., 2020. Expression, purification, and structural analysis of the full-length human integral membrane protein γ-sarcoglycan. Protein Expression and Purification, 167, p.105525.

Janni, W., Rack, B., Schindlbeck, C., Strobl, B., Rjosk, D., Braun, S., Sommer, H., Pantel, K., Gerber, B. and Friese, K., 2005. The persistence of isolated tumor cells in bone

marrow from patients with breast carcinoma predicts an increased risk for recurrence. Cancer: Interdisciplinary International Journal of the American Cancer Society, 103(5), pp.884-891.

Jechlinger, M., Sommer, A., Moriggl, R., Seither, P., Kraut, N., Capodiecci, P., Donovan, M., Cordon-Cardo, C., Beug, H. and Grünert, S., 2006. Autocrine PDGFR signaling promotes mammary cancer metastasis. The Journal of clinical investigation, 116(6), pp.1561-1570.

Jeng, K.S., Sheen, I.S., Jeng, W.J., Yu, M.C., Hsiau, H.I. and Chang, F.Y., 2014. High expression of Sonic Hedgehog signaling pathway genes indicates a risk of recurrence of breast carcinoma. OncoTargets and therapy, 7, p.79.

Jeong, Y.J., Kang, J.S., Lee, S.I., So, D.M., Yun, J., Baek, J.Y., Kim, S.K., Lee, K. and Park, S.K., 2016. Breast cancer cells evade paclitaxel-induced cell death by developing resistance to dasatinib. Oncology letters, 12(3), pp.2153-2158. Jeter, C.R., Liu, B., Liu, X., Chen, X., Liu, C., Calhoun-Davis, T., Repass, J., Zaehres, H., Shen, J.J. and Tang, D.G., 2011. NANOG promotes cancer stem cell characteristics and prostate cancer resistance to androgen deprivation. Oncogene, 30(36), pp.3833-3845.

Ji, T., Ma, F., Huo, L., Guo, X., Chen, B. and Zhou, Q., 2015. Calponin h2 is upregulated in the tissues and plasma of patients with breast cancer. Molecular Medicine Reports, 12(2), pp.2886-2892. Ji, Z., Mei, F.C., Xie, J. and Cheng, X., 2007. Oncogenic KRAS activates hedgehog signalling pathway in pancreatic cancer cells. Journal of Biological Chemistry, 282(19), pp.14048-14055.

Jia, Y., Yun, C.H., Park, E., Ercan, D., Manuia, M., Juarez, J., Xu, C., Rhee, K., Chen, T., Zhang, H. and Palakurthi, S., 2016. Overcoming EGFR (T790M) and EGFR (C797S) resistance with mutant-selective allosteric inhibitors. Nature, 534(7605), pp.129-132.

Jiang, B.H. and Liu, L.Z., 2009. PI3K/PTEN signaling in angiogenesis and tumorigenesis. Advances in cancer research, 102, pp.19-65. Jiang, G., Shi, W., Fang, H. and Zhang, X., 2018. miR 27a promotes human breast cancer cell migration by inducing EMT in a FBXW7 dependent manner. Molecular Medicine Reports, 18(6), pp.5417-5426.

Jiang, J., Gusev, Y., Aderca, I., Mettler, T.A., Nagorney, D.M., Brackett, D.J., Roberts, L.R. and Schmittgen, T.D., 2008. Association of MicroRNA expression in hepatocellular carcinomas with hepatitis infection, cirrhosis, and patient survival. Clinical cancer research, 14(2), pp.419-427.

Jiang, T., Dong, P., Li, L., Ma, X., Xu, P., Zhu, H., Wang, Y., Yang, B., Liu, K., Liu, J. and Xue, J., 2017. MicroRNA-200c regulates cisplatin resistance by targeting ZEB2 in human gastric cancer cells. Oncology reports, 38(1), pp.151-158.

Jiang, W.R., Cady, G., Hossain, M.M., Huang, Q.Q., Wang, X. and Jin, J.P., 2014. Mechanoregulation of h2-calponin gene expression and the role of Notch signaling. Journal of Biological Chemistry, 289(3), pp.1617-1628.

Jiang, Y., Duan, Y. and Zhou, H., 2015. MicroRNA 27a directly targets KRAS to inhibit cell proliferation in esophageal squamous cell carcinoma. Oncology letters, 9(1), pp.471-477.

Jiang, Y., Zou, L., Lu, W.Q., Zhang, Y. and Shen, A.G., 2013. Foxo3a expression is a prognostic marker in breast cancer. PloS one, 8(8), p.e70746.

Jin, A.H. and Wei, Z.L., 2015. Molecular mechanism of increased sensitivity of cisplatin to ovarian cancer by inhibition of microRNA-23a expression. International journal of clinical and experimental medicine, 8(8), p.13329.

Jin, A.H., Zhou, X.P. and Zhou, F.Z., 2015. Inhibition of microRNA-23a increases cisplatin sensitivity of ovarian cancer cells: The possible molecular mechanisms. Nan fang yi ke da xue xue bao= Journal of Southern Medical University, 35(1), pp.125-128.

Jin, L., Garcia, J., Chan, E., de la Cruz, C., Segal, E., Merchant, M., Kharbanda, S., Raisner, R., Haverty, P.M., Modrusan, Z. and Ly, J., 2017. Therapeutic targeting of the CBP/p300 bromodomain blocks the growth of castration-resistant prostate cancer. Cancer research, 77(20), pp.5564-5575.

Jin, L., Wessely, O., Marcusson, E.G., Ivan, C., Calin, G.A. and Alahari, S.K., 2013. Prooncogenic factors miR-23b and miR-27b are regulated by Her2/Neu, EGF, and TNF-α in breast cancer. Cancer research, 73(9), pp.2884-2896.

Jing, X., Liang, H., Hao, C., Yang, X. and Cui, X., 2019. Overexpression of MUC1 predicts poor prognosis in patients with breast cancer. Oncology reports, 41(2), pp.801-810.

Jo, M.H., Shin, S., Jung, S.R., Kim, E., Song, J.J. and Hohng, S., 2015. Human Argonaute 2 has diverse reaction pathways on target RNAs. Molecular cell, 59(1), pp.117-124.

Johnston, S.J. and Carroll, J.S., 2015. Transcription factors and chromatin proteins as therapeutic targets in cancer. Biochimica et Biophysica Acta (BBA)-Reviews on Cancer, 1855(2), pp.183-192.

Jöhrer, K., Janke, K., Krugmann, J., Fiegl, M. and Greil, R., 2004. Transendothelial migration of myeloma cells is increased by tumor necrosis factor (TNF)-α via TNF receptor 2 and autocrine up-regulation of MCP-1. Clinical cancer research, 10(6), pp.1901-1910.

Joly, E. and Hudrisier, D., 2003. What is trogocytosis and what is its purpose?. Nature immunology, 4(9), pp.815-815.

Jonckheere, N., Skrypek, N. and Van Seuningen, I., 2014. Mucins and tumor resistance to chemotherapeutic drugs. Biochimica et Biophysica Acta (BBA)-Reviews on Cancer, 1846(1), pp.142-151.

Jonker, J.W., Smit, J.W., Brinkhuis, R.F., Maliepaard, M., Beijnen, J.H., Schellens, J.H. and Schinkel, A.H., 2000. Role of breast cancer resistance protein in the bioavailability and fetal penetration of topotecan. Journal of the National Cancer Institute, 92(20), pp.1651-1656.

Jung, S.Y., Jeong, J., Shin, S.H., Kwon, Y., Kim, E.A., Ko, K.L., Shin, K.H., Ro, J., Lee, K.S., Park, I.H. and Lee, S., 2011. Accumulation of p53 determined by immunohistochemistry as a prognostic marker in node negative breast cancer; analysis according to St Gallen consensus and intrinsic subtypes. Journal of surgical oncology, 103(3), pp.207-211.

Junttila, M.R. and de Sauvage, F.J., 2013. Influence of tumour micro-environment heterogeneity on therapeutic response. Nature, 501(7467), pp.346-354.

Jurkovicova, D., Smolkova, B., Magyerkova, M., Sestakova, Z., Kajabova, V.H., Kulcsar, L., Zmetakova, I., Kalinkova, L., Krivulcik, T., Karaba, M. and Benca, J., 2017. Down-regulation of traditional oncomiRs in plasma of breast cancer patients. Oncotarget, 8(44), p.77369.

Kabała-Dzik, A., Rzepecka-Stojko, A., Kubina, R., Jastrzębska-Stojko, Ż., Stojko, R., Wojtyczka, R.D. and Stojko, J., 2017. Migration rate inhibition of breast cancer cells treated by caffeic acid and caffeic acid phenethyl ester: An in vitro comparison study. Nutrients, 9(10), p.1144.

Kabashima-Niibe, A., Higuchi, H., Takaishi, H., Masugi, Y., Matsuzaki, Y., Mabuchi, Y., Funakoshi, S., Adachi, M., Hamamoto, Y., Kawachi, S. and Aiura, K., 2013. Mesenchymal stem cells regulate epithelial–mesenchymal transition and tumor progression of pancreatic cancer cells. Cancer science, 104(2), pp.157-164.

Kageyama, R., Ishibashi, M., Takebayashi, K. and Tomita, K., 1997. bHLH transcription factors and mammalian neuronal differentiation. The international journal of biochemistry & cell biology, 29(12), pp.1389-1399.

Kakarala, M. and Wicha, M.S., 2008. Implications of the cancer stem-cell hypothesis for breast cancer prevention and therapy. Journal of clinical oncology: official journal of the American Society of Clinical Oncology, 26(17), p.2813.

Kalkhoven, E., 2004. CBP and p300: HATs for different occasions. Biochemical pharmacology, 68(6), pp.1145-1155.

Kalkhoven, E., Roelen, B.A., De Winter, J.P., Mummery, C.L., Van den Eijnden-Van Raaij, A.J., Van der Saag, P.T. and Van der Burg, B., 1995. Resistance to Transforming Growth Factor and Activin Due to Reduced Receptor Expression in Human Breast Tumor Cell Lines. Cell Growth and Differentiation-Publication American Association for Cancer Research, 6(9), pp.1151-1162.

Kallergi, G., Papadaki, M.A., Politaki, E., Mavroudis, D., Georgoulias, V. and Agelaki, S., 2011. Epithelial to mesenchymal transition markers expressed in circulating tumour cells of early and metastatic breast cancer patients. Breast Cancer Research, 13(3), p.R59.

Kalluri, R. and Weinberg, R.A., 2009. The basics of epithelial-mesenchymal transition. The Journal of clinical investigation, 119(6), pp.1420-1428.

Kam, Y., Guess, C., Estrada, L., Weidow, B. and Quaranta, V., 2008. A novel circular invasion assay mimics in vivo invasive behavior of cancer cell lines and distinguishes single-cell motility in vitro. BMC cancer, 8(1), pp.1-12.

Kampan, N.C., Madondo, M.T., McNally, O.M., Quinn, M. and Plebanski, M., 2015. Paclitaxel and its evolving role in the management of ovarian cancer. BioMed research international, 2015.

Kan, T., Sato, F., Ito, T., Matsumura, N., David, S., Cheng, Y., Agarwal, R., Paun, B.C., Jin, Z., Olaru, A.V. and Selaru, F.M., 2009. The miR-106b-25 polycistron, activated by genomic amplification, functions as an oncogene by suppressing p21 and Bim. Gastroenterology, 136(5), pp.1689-1700.

Kan, T., Sato, F., Ito, T., Matsumura, N., David, S., Cheng, Y., Agarwal, R., Paun, B.C., Jin, Z., Olaru, A.V., Selaru, F.M., Hamilton, J.P., Yang, J., Abraham, J.M., Mori, Y. and Meltzer, S.J. (2009). The miR-106b-25 Polycistron, Activated by Genomic Amplification, Functions as an Oncogene by Suppressing p21 and Bim. Gastroenterology, 136(5), pp.1689–1700.

Kanda, R., Kawahara, A., Watari, K., Murakami, Y., Sonoda, K., Maeda, M., Fujita, H., Kage, M., Uramoto, H., Costa, C. and Kuwano, M., 2013. Erlotinib resistance in lung cancer cells mediated by integrin β1/Src/Akt-driven bypass signaling. Cancer research, 73(20), pp.6243-6253.

Kang, M.-I., Kim, H.-S., Jung, Y.-C., Kim, Y.-H., Hong, S.-J., Kim, M.-K., Baek, K.-H., Kim, C. and Rhyu, M.-G. (2007). Transitional CpG methylation between promoters and retroelements of tissue-specific genes during human mesenchymal cell differentiation. Journal of Cellular Biochemistry, 102(1), pp.224–239.

Kang, S.H., Bang, Y.J., Im, Y.H., Yang, H.K., Lee, D.A., Lee, H.Y., Lee, H.S., Kim, N.K. and Kim, S.J., 1999. Transcriptional repression of the transforming growth factor-β type I receptor gene by DNA methylation results in the development of TGF-β resistance in human gastric cancer. Oncogene, 18(51), pp.7280-7286.

Kang, S.Y., Halvorsen, O.J., Gravdal, K., Bhattacharya, N., Lee, J.M., Liu, N.W., Johnston, B.T., Johnston, A.B., Haukaas, S.A., Aamodt, K. and Yoo, S., 2009. Prosaposin inhibits tumor metastasis via paracrine and endocrine stimulation of stromal p53 and Tsp-1. Proceedings of the National Academy of Sciences, 106(29), pp.12115-12120.

Kang, Y., He, W., Tulley, S., Gupta, G.P., Serganova, I., Chen, C.R., Manova-Todorova, K., Blasberg, R., Gerald, W.L. and Massagué, J., 2005. Breast cancer bone metastasis mediated by the Smad tumor suppressor pathway. Proceedings of the National Academy of Sciences, 102(39), pp.13909-13914.

Kang, Y.K., Guermah, M., Yuan, C.X. and Roeder, R.G., 2002. The TRAP/Mediator coactivator complex interacts directly with estrogen receptors α and β through the TRAP220 subunit and directly enhances estrogen receptor function in vitro. Proceedings of the National Academy of Sciences, 99(5), pp.2642-2647.

Kanwar, S.S., Yu, Y., Nautiyal, J., Patel, B.B. and Majumdar, A.P., 2010. The Wnt/β catenin pathway regulates growth and maintenance of colonospheres. Molecular cancer, 9(1), pp.1-13.

Kao, J., Salari, K., Bocanegra, M., Choi, Y.L., Girard, L., Gandhi, J., Kwei, K.A., Hernandez Boussard, T., Wang, P., Gazdar, A.F. and Minna, J.D., 2009. Molecular profiling of breast cancer cell lines defines relevant tumor models and provides a resource for cancer gene discovery. PloS one, 4(7), p.e6146.

Kaplan, R.N., Riba, R.D., Zacharoulis, S., Bramley, A.H., Vincent, L., Costa, C., MacDonald, D.D., Jin, D.K., Shido, K., Kerns, S.A. and Zhu, Z., 2005. VEGFR1-positive haematopoietic bone marrow progenitors initiate the pre-metastatic niche. Nature, 438(7069), pp.820-827.

Kappes, F., Waldmann, T., Mathew, V., Yu, J., Zhang, L., Khodadoust, M.S., Chinnaiyan, A.M., Luger, K., Erhardt, S., Schneider, R. and Markovitz, D.M., 2011. The DEK oncoprotein is a Su (var) that is essential to heterochromatin integrity. Genes & development, 25(7), pp.673-678.

Karadedou, C.T., Gomes, A.R., Chen, J., Petkovic, M., Ho, K.K., Zwolinska, A.K., Feltes, A., Wong, S.Y., Chan, K.Y., Cheung, Y.N. and Tsang, J.W., 2012. FOXO3a represses VEGF expression through FOXM1-dependent and-independent mechanisms in breast cancer. Oncogene, 31(14), pp.1845-1858.

Karagiannis, G.S., Pastoriza, J.M., Wang, Y., Harney, A.S., Entenberg, D., Pignatelli, J., Sharma, V.P., Xue, E.A., Cheng, E., D'Alfonso, T.M. and Jones, J.G., 2017. Neoadjuvant chemotherapy induces breast cancer metastasis through a TMEM-mediated mechanism. Science translational medicine, 9(397).

Karamanou, K., Franchi, M., Piperigkou, Z., Perreau, C., Maquart, F.X., Vynios, D.H. and Brézillon, S., 2017. Lumican effectively regulates the estrogen receptors-associated functional properties of breast cancer cells, expression of matrix effectors and epithelial-to-mesenchymal transition. Scientific reports, 7, p.45138.

Karamboulas, C. and Ailles, L., 2013. Developmental signaling pathways in cancer stem cells of solid tumors. Biochimica et Biophysica Acta (BBA)-General Subjects, 1830(2), pp.2481-2495.

Karihtala, P., Auvinen, P., Kauppila, S., Haapasaari, K.M., Jukkola-Vuorinen, A. and Soini, Y., 2013. Vimentin, zeb1 and Sip1 are up-regulated in triple-negative and basal-like

breast cancers: association with an aggressive tumour phenotype. Breast cancer research and treatment, 138(1), pp.81-90.

Karnoub, A.E., Dash, A.B., Vo, A.P., Sullivan, A., Brooks, M.W., Bell, G.W., Richardson, A.L., Polyak, K., Tubo, R. and Weinberg, R.A., 2007. Mesenchymal stem cells within tumour stroma promote breast cancer metastasis. Nature, 449(7162), pp.557-563.

Kashima, T., Nakamura, K., Kawaguchi, J., Takanashi, M., Ishida, T., Aburatani, H., Kudo, A., Fukayama, M. and Grigoriadis, A.E., 2003. Overexpression of cadherins suppresses pulmonary metastasis of osteosarcoma in vivo. International journal of cancer, 104(2), pp.147-154.

Kato, T., Sato, N., Hayama, S., Yamabuki, T., Ito, T., Miyamoto, M., Kondo, S., Nakamura, Y. and Daigo, Y., 2007. Activation of Holliday Junction–Recognizing Protein involved in the chromosomal stability and immortality of cancer cells. Cancer research, 67(18), pp.8544-8553.

Kato, Y., Lambert, C.A., Colige, A.C., Mineur, P., Noël, A., Frankenne, F., Foidart, J.M., Baba, M., Hata, R.I., Miyazaki, K. and Tsukuda, M., 2005. Acidic extracellular pH induces matrix metalloproteinase-9 expression in mouse metastatic melanoma cells through the phospholipase D-mitogen-activated protein kinase signaling. Journal of Biological Chemistry, 280(12), pp.10938-10944.

Katoh, M. and Katoh, M., 2006. Cross-talk of WNT and FGF signaling pathways at GSK3ß to regulate ß-catenin and SNAIL signaling cascades. Cancer biology & therapy, 5(9), pp.1059-1064.

Katoh, M. and Katoh, M., 2006. FGF signaling network in the gastrointestinal tract. International journal of oncology, 29(1), pp.163-168.

Katoh, M. and Nakagama, H., 2014. FGF receptors: cancer biology and therapeutics. Medicinal research reviews, 34(2), pp.280-300.

Katoh, M. and Terada, M., 1993. Oncogenes and tumor suppressor genes. In Gastric cancer (pp. 196-208). Springer, Tokyo.

Katoh, M., 2007. Dysregulation of stem cell signaling network due to germline mutation, SNP, Helicobacter pylori infection, epigenetic change, and genetic alteration in gastric cancer. Cancer biology & therapy, 6(6), pp.832-839.

Katsumura, K.R., Bresnick, E.H. and GATA Factor Mechanisms Group, 2017. The GATA factor revolution in hematology. Blood, The Journal of the American Society of Hematology, 129(15), pp.2092-2102.

Katsuno, Y., Meyer, D.S., Zhang, Z., Shokat, K.M., Akhurst, R.J., Miyazono, K. and Derynck, R., 2019. Chronic TGF-β exposure drives stabilized EMT, tumor stemness, and

cancer drug resistance with vulnerability to bitopic mTOR inhibition. Science signaling, 12(570), p.eaau8544.

Kaur, A., Ecker, B.L., Douglass, S.M., Kugel, C.H., Webster, M.R., Almeida, F.V., Somasundaram, R., Hayden, J., Ban, E., Ahmadzadeh, H. and Franco-Barraza, J., 2019. Remodeling of the collagen matrix in aging skin promotes melanoma metastasis and affects immune cell motility. Cancer discovery, 9(1), pp.64-81.

Kaur, H., Phillips-Mason, P.J., Burden-Gulley, S.M., Kerstetter-Fogle, A.E., Basilion, J.P., Sloan, A.E. and Brady-Kalnay, S.M., 2012. Cadherin-11, a marker of the mesenchymal phenotype, regulates glioblastoma cell migration and survival in vivo. Molecular Cancer Research, 10(3), pp.293-304.

Kawase, M., Toyama, T., Takahashi, S., Sato, S., Yoshimoto, N., Endo, Y., Asano, T., Kobayashi, S., Fujii, Y. and Yamashita, H., 2015. FOXA1 expression after neoadjuvant chemotherapy is a prognostic marker in estrogen receptor-positive breast cancer. Breast cancer, 22(3), pp.308-316.

Keeley, D.P. and Sherwood, D.R., 2019. Tissue linkage through adjoining basement membranes: the long and the short term of it. Matrix Biology, 75, pp.58-71.

Kehrl, J.H., Wakefield, L.M., Roberts, A.B., Jakowlew, S., Alvarez-Mon, M., Derynck, R.B.S.M., Sporn, M.B. and Fauci, A.S., 1986. Production of transforming growth factor beta by human T lymphocytes and its potential role in the regulation of T cell growth. The Journal of experimental medicine, 163(5), pp.1037-1050.

Kele Arruda Macedo, J., W Fox, J. and de Souza Castro, M., 2015. Disintegrins from snake venoms and their applications in cancer research and therapy. Current protein and peptide science, 16(6), pp.532-548.

Keller, P.J., Arendt, L.M., Skibinski, A., Logvinenko, T., Klebba, I., Dong, S., Smith, A.E., Prat, A., Perou, C.M., Gilmore, H. and Schnitt, S., 2012. Defining the cellular precursors to human breast cancer. Proceedings of the National Academy of Sciences, 109(8), pp.2772-2777.

Kenny, P.A., Lee, G.Y., Myers, C.A., Neve, R.M., Semeiks, J.R., Spellman, P.T., Lorenz, K., Lee, E.H., Barcellos-Hoff, M.H., Petersen, O.W. and Gray, J.W., 2007. The morphologies of breast cancer cell lines in three-dimensional assays correlate with their profiles of gene expression. Molecular oncology, 1(1), pp.84-96.

Kesanakurti, D., Chetty, C., Dinh, D.H., Gujrati, M. and Rao, J.S., 2013. Role of MMP-2 in the regulation of IL-6/Stat3 survival signaling via interaction with $\alpha 5\beta 1$ integrin in glioma. Oncogene, 32(3), pp.327-340.

Ketolainen, J.M., Alarmo, E.L., Tuominen, V.J. and Kallioniemi, A., 2010. Parallel inhibition of cell growth and induction of cell migration and invasion in breast cancer cells by bone morphogenetic protein 4. Breast cancer research and treatment, 124(2), pp.377-386.

Khalil, A.A. and Friedl, P., 2010. Determinants of leader cells in collective cell migration. Integrative biology, 2(11-12), pp.568-574.

Khongkow, M., Olmos, Y., Gong, C., Gomes, A.R., Monteiro, L.J., Yagüe, E., Cavaco, T.B., Khongkow, P., Man, E.P., Laohasinnarong, S. and Koo, C.Y., 2013. SIRT6 modulates paclitaxel and epirubicin resistance and survival in breast cancer. Carcinogenesis, 34(7), pp.1476-1486.

Kikutake, C., Yoshihara, M., Sato, T., Saito, D. and Suyama, M., 2018. Intratumor heterogeneity of HMCN1 mutant alleles associated with poor prognosis in patients with breast cancer. Oncotarget, 9(70), p.33337.

Kim, E.J., Lee, S.Y., Woo, M.K., Choi, S.I., Kim, T.R., Kim, M.J., Kim, K.C., Cho, E.W. and Kim, I.G., 2012. Fibulin-3 promoter methylation alters the invasive behavior of non-small cell lung cancer cell lines via MMP-7 and MMP-2 regulation. International journal of oncology, 40(2), pp.402-408.

Kim, E.K., Kim, H.A., Koh, J.S., Kim, M.S., Kim, K.I., Lee, J.I., Moon, N.M., Ko, E. and Noh, W.C., 2011. Phosphorylated S6K1 is a possible marker for endocrine therapy resistance in hormone receptor-positive breast cancer. Breast cancer research and treatment, 126(1), pp.93-99.

Kim, E.Y., Priatel, J.J., Teh, S.J. and Teh, H.S., 2006. TNF receptor type 2 (p75) functions as a costimulator for antigen-driven T cell responses in vivo. The Journal of Immunology, 176(2), pp.1026-1035.

Kim, H.J., Yoon, S.L., Young, C.K., Hwan, Y.K., Ju, W. and Cheol, S.K., 2017. Subcellular localization of FOXO3a as a potential biomarker of response to combined treatment with inhibitors of PI3K and autophagy in PIK3CA-mutant cancer cells. Oncotarget, 8(4), p.6608.

Kim, J., Shin, Y., Lee, S., Kim, M., Punj, V., Lu, J.F., Shin, H., Kim, K., Ulmer, T.S., Koh, J. and Jeong, D., 2018. Regulation of breast cancer-induced osteoclastogenesis by MacroH2A1. 2 involving EZH2-mediated H3K27me3. Cell reports, 24(1), pp.224-237.

Kim, K., Lu, Z. and Hay, E.D., 2002. Direct evidence for a role of β-catenin/LEF-1 signaling pathway in induction of EMT. Cell biology international, 26(5), pp.463-476.

Kim, M.Y., Oskarsson, T., Acharyya, S., Nguyen, D.X., Zhang, X.H.F., Norton, L. and Massagué, J., 2009. Tumor self-seeding by circulating cancer cells. Cell, 139(7), pp.1315-1326.

Kim, S., Lee, J., Jeon, M., Nam, S.J. and Lee, J.E., 2015. Elevated TGF-β1 and-β2 expression accelerates the epithelial to mesenchymal transition in triple-negative breast cancer cells. Cytokine, 75(1), pp.151-158.

Kim, S.J., Im, Y.H., Markowitz, S.D. and Bang, Y.J., 2000. Molecular mechanisms of inactivation of TGF-β receptors during carcinogenesis. Cytokine & growth factor reviews, 11(1-2), pp.159-168.

Kim, W.K., Kwon, Y., Jang, M., Park, M., Kim, J., Cho, S., Jang, D.G., Lee, W.B., Jung, S.H., Choi, H.J. and Min, B.S., 2019. β-catenin activation down-regulates cell-cell junction-related genes and induces epithelial-to-mesenchymal transition in colorectal cancers. Scientific reports, 9(1), pp.1-15.

Kim, Y.K., Kim, N.H., Hwang, J.W., Song, Y.J., Park, Y.S., Seo, D.W., Lee, H.Y., Choi, W.S., Han, J.W. and Kim, S.N., 2008. Histone deacetylase inhibitor apicidin-mediated drug resistance: involvement of P-glycoprotein. Biochemical and biophysical research communications, 368(4), pp.959-964.

Kim, Y.R., Yoo, J.K., Jeong, C.W. and Choi, J.W., 2018. Selective killing of circulating tumor cells prevents metastasis and extends survival. Journal of hematology & oncology, 11(1), pp.1-4.

Klarmann, G.J., Decker, A. and Farrar, W.L., 2008. Epigenetic gene silencing in the Wnt pathway in breast cancer. Epigenetics, 3(2), pp.59-63.

Klein, M.G., Shi, W., Ramagopal, U., Tseng, Y., Wirtz, D., Kovar, D.R., Staiger, C.J. and Almo, S.C., 2004. Structure of the actin crosslinking core of fimbrin. Structure, 12(6), pp.999-1013.

Klein, R., 2001. Excitatory Eph receptors and adhesive ephrin ligands. Current opinion in cell biology, 13(2), pp.196-203.

Klopp, A.H., Spaeth, E.L., Dembinski, J.L., Woodward, W.A., Munshi, A., Meyn, R.E., Cox, J.D., Andreeff, M. and Marini, F.C., 2007. Tumor irradiation increases the recruitment of circulating mesenchymal stem cells into the tumor microenvironment. Cancer research, 67(24), pp.11687-11695.

Knott, S.R., Wagenblast, E., Khan, S., Kim, S.Y., Soto, M., Wagner, M., Turgeon, M.O., Fish, L., Erard, N., Gable, A.L. and Maceli, A.R., 2018. Asparagine bioavailability governs metastasis in a model of breast cancer. Nature, 554(7692), pp.378-381.

Kobayashi, A., Okuda, H., Xing, F., Pandey, P.R., Watabe, M., Hirota, S., Pai, S.K., Liu, W., Fukuda, K., Chambers, C. and Wilber, A., 2011. Bone morphogenetic protein 7 in dormancy and metastasis of prostate cancer stem-like cells in bone. Journal of Experimental Medicine, 208(13), pp.2641-2655.

Kobayashi, N., Kostka, G., Garbe, J.H., Keene, D.R., Bächinger, H.P., Hanisch, F.G., Markova, D., Tsuda, T., Timpl, R., Chu, M.L. and Sasaki, T., 2007. A comparative analysis of the fibulin protein family biochemical characterization, binding interactions, and tissue localization. Journal of Biological Chemistry, 282(16), pp.11805-11816.

Koboldt, D.C., Fulton, R.S., McLellan, M.D., Schmidt, H., Kalicki-Veizer, J., McMichael, J.F., Fulton, L.L., Dooling, D.J., Ding, L., Mardis, E.R., Wilson, R.K., Ally, A., Balasundaram, M., Butterfield, Y.S.N., Carlsen, R., Carter, C., Chu, A., Chuah, E., Chun, H.-J.E., Coope, R.J.N., Dhalla, N., Guin, R., Hirst, C., Hirst, M., Holt, R.A., Lee, D., Li, H.I., Mayo, M., Moore, R.A., Mungall, A.J., Pleasance, E., Gordon Robertson, A., Schein, J.E., Shafiei, A., Sipahimalani, P., Slobodan, J.R., Stoll, D., Tam, A., Thiessen, N., Varhol, R.J., Wye, N., Zeng, T., Zhao, Y., Birol, I., Jones, S.J.M., Marra, M.A., Cherniack, A.D., Saksena, G., Onofrio, R.C., Pho, N.H., Carter, S.L., Schumacher, S.E., Tabak, B., Hernandez, B., Gentry, J., Nguyen, H., Crenshaw, A., Ardlie, K., Beroukhim, R., Winckler, W., Getz, G., Gabriel, S.B., Meyerson, M., Chin, L., Park, P.J., Kucherlapati, R., Hoadley, K.A., Todd Auman, J., Fan, C., Turman, Y.J., Shi, Y., Li, L., Topal, M.D., He, X., Chao, H.-H., Prat, A., Silva, G.O., Iglesia, M.D., Zhao, W., Usary, J., Berg, J.S., Adams, M., Booker, J., Wu, J., Gulabani, A., Bodenheimer, T., Hoyle, A.P., Simons, J.V., Soloway, M.G., Mose, L.E., Jefferys, S.R., Balu, S., Parker, J.S., Neil Hayes, D., Perou, C.M., Malik, S., Mahurkar, S., Shen, H., Weisenberger, D.J., Triche Jr, T., Lai, P.H., Bootwalla, M.S., Maglinte, D.T., Berman, B.P., Van Den Berg, D.J., Baylin, S.B., Laird, P.W., Creighton, C.J., Donehower, L.A., Getz, G., Noble, M., Voet, D., Saksena, G., Gehlenborg, N., DiCara, D., Zhang, J., Zhang, H., Wu, C.-J., Yingchun Liu, S., Lawrence, M.S., Zou, L., Sivachenko, A., Lin, P., Stojanov, P., Jing, R., Cho, J., Sinha, R., Park, R.W., Nazaire, M.-D., Robinson, J., Thorvaldsdottir, H., Mesirov, J., Park, P.J., Chin, L., Reynolds, S., Kreisberg, R.B., Bernard, B., Bressler, R., Erkkila, T., Lin, J., Thorsson, V., Zhang, W., Shmulevich, I., Ciriello, G., Weinhold, N., Schultz, N., Gao, J., Cerami, E., Gross, B., Jacobsen, A., Sinha, R., Arman Aksoy, B., Antipin, Y., Reva, B., Shen, R., Taylor, B.S., Ladanyi, M., Sander, C., Anur, P., Spellman, P.T., Lu, Y., Liu, W., Verhaak, R.R.G., Mills, G.B., Akbani, R., Zhang, N., Broom, B.M., Casasent, T.D., Wakefield, C., Unruh, A.K., Baggerly, K., Coombes, K., Weinstein, J.N., Haussler, D., Benz, C.C., Stuart, J.M., Benz, S.C., Zhu, J., Szeto, C.C., Scott, G.K., Yau, C., Paull, E.O., Carlin, D., Wong, C., Sokolov, A., Thusberg, J., Mooney, S., Ng, S., Goldstein, T.C., Ellrott, K., Grifford, M., Wilks, C., Ma, S., Craft, B., Yan, C., Hu, Y., Meerzaman, D., Gastier-Foster, J.M., Bowen, J., Ramirez, N.C., Black, A.D., XPATH ERROR: unknown variable “tname”., R.E., White, P., Zmuda, E.J., Frick, J., Lichtenberg, T.M., Brookens, R., George, M.M., Gerken, M.A., Harper, H.A., Leraas, K.M., Wise, L.J., Tabler, T.R., McAllister, C., Barr, T., Hart-Kothari, M., Tarvin, K., Saller, C., Sandusky, G., Mitchell, C., Iacocca, M.V., Brown, J., Rabeno,

B., Czerwinski, C., Petrelli, N., Dolzhansky, O., Abramov, M., Voronina, O., Potapova, O., Marks, J.R., Suchorska, W.M., Murawa, D., Kycler, W., Ibbs, M., Korski, K., Spychała, A., Murawa, P., Brzeziński, J.J., Perz, H., Łaźniak, R., Teresiak, M., Tatka, H., Leporowska, E., Bogusz-Czerniewicz, M., Malicki, J., Mackiewicz, A., Wiznerowicz, M., Van Le, X., Kohl, B., Viet Tien, N., Thorp, R., Van Bang, N., Sussman, H., Duc Phu, B., Hajek, R., Phi Hung, N., Viet The Phuong, T., Quyet Thang, H., Zaki Khan, K., Penny, R., Mallery, D., Curley, E., Shelton, C., Yena, P., Ingle, J.N., Couch, F.J., Lingle, W.L., King, T.A., Maria Gonzalez-Angulo, A., Mills, G.B., Dyer, M.D., Liu, S., Meng, X., Patangan, M., Waldman, F., Stöppler, H., Kimryn Rathmell, W., Thorne, L., Huang, M., Boice, L., Hill, A., Morrison, C., Gaudioso, C., Bshara, W., Daily, K., Egea, S.C., Pegram, M.D., Gomez-Fernandez, C., Dhir, R., Bhargava, R., Brufsky, A., Shriver, C.D., Hooke, J.A., Leigh Campbell, J., Mural, R.J., Hu, H., Somiari, S., Larson, C., Deyarmin, B., Kvecher, L., Kovatich, A.J., Ellis, M.J., King, T.A., Hu, H., Couch, F.J., Mural, R.J., Stricker, T., White, K., Olopade, O., Ingle, J.N., Luo, C., Chen, Y., Marks, J.R., Waldman, F., Wiznerowicz, M., Bose, R., Chang, L.-W., Beck, A.H., Maria Gonzalez-Angulo, A., Pihl, T., Jensen, M., Sfeir, R., Kahn, A., Chu, A., Kothiyal, P., Wang, Z., Snyder, E., Pontius, J., Ayala, B., Backus, M., Walton, J., Baboud, J., Berton, D., Nicholls, M., Srinivasan, D., Raman, R., Girshik, S., Kigonya, P., Alonso, S., Sanbhadti, R., Barletta, S., Pot, D., Sheth, M., Demchok, J.A., Mills Shaw, K.R., Yang, L., Eley, G., Ferguson, M.L., Tarnuzzer, R.W., Zhang, J., Dillon, L.A.L., Buetow, K., Fielding, P., Ozenberger, B.A., Guyer, M.S., Sofia, H.J. and Palchik, J.D. (2012). Comprehensive molecular portraits of human breast tumours. Nature, 490(7418), pp.61–70.

Kochneva, G.V., Babkina, I.N., Lupan, T.A., Grazhdantseva, A.A., Iudin, P.V., Sivolobova, G.F., Shvalov, A.N., Popov, E.G., Babkin, I.V., Netesov, S.V. and Chumakov, P.M., 2013. Apoptin enhances the oncolytic activity of vaccinia virus. Molekuliarnaia biologiia, 47(5), pp.842-852.

Kodera, Y., Takeyama, K.I., Murayama, A., Suzawa, M., Masuhiro, Y. and Kato, S., 2000. Ligand type-specific interactions of peroxisome proliferator-activated receptor γ with transcriptional coactivators. Journal of Biological Chemistry, 275(43), pp.33201-33204.

Koedoot, E., Fokkelman, M., Rogkoti, V.M., Smid, M., van de Sandt, I., de Bont, H., Pont, C., Klip, J.E., Wink, S., Timmermans, M.A. and Wiemer, E.A., 2019. Uncovering the signaling landscape controlling breast cancer cell migration identifies novel metastasis driver genes. Nature communications, 10(1), pp.1-16.

Köhler, S., Ullrich, S., Richter, U. and Schumacher, U., 2010. E-/P-selectins and colon carcinoma metastasis: first in vivo evidence for their crucial role in a clinically relevant model of spontaneous metastasis formation in the lung. British journal of cancer, 102(3), pp.602-609.

Koike, Y., Ohta, Y., Saitoh, W., Yamashita, T., Kanomata, N., Moriya, T. and Kurebayashi, J., 2017. Anti-cell growth and anti-cancer stem cell activities of the non-canonical hedgehog inhibitor GANT61 in triple-negative breast cancer cells. Breast Cancer, 24(5), pp.683-693.

Kokkinos, M.I., Wafai, R., Wong, M.K., Newgreen, D.F., Thompson, E.W. and Waltham, M., 2007. Vimentin and epithelial-mesenchymal transition in human breast cancer–observations in vitro and in vivo. Cells Tissues Organs, 185(1-3), pp.191-203.

Kondo, K. and Kaelin Jr, W.G., 2001. The von Hippel–Lindau tumor suppressor gene. Experimental cell research, 264(1), pp.117-125.

Kong, D., Li, Y., Wang, Z. and Sarkar, F.H., 2011. Cancer stem cells and epithelial-to mesenchymal transition (EMT)-phenotypic cells: are they cousins or twins?. Cancers, 3(1), pp.716-729.

Kong, K.Y., Owens, K.S., Rogers, J.H., Mullenix, J., Velu, C.S., Grimes, H.L. and Dahl, R., 2010. MIR-23A microRNA cluster inhibits B-cell development. Experimental hematology, 38(8), pp.629-640.

Kong, W., He, L., Coppola, M., Guo, J., Esposito, N.N., Coppola, D. and Cheng, J.Q., 2010. MicroRNA-155 regulates cell survival, growth, and chemosensitivity by targeting FOXO3a in breast cancer. Journal of Biological Chemistry, 285(23), pp.17869-17879.

Kong, W., Yang, H., He, L., Zhao, J.J., Coppola, D., Dalton, W.S. and Cheng, J.Q., 2008. MicroRNA-155 is regulated by the transforming growth factor β/Smad pathway and contributes to epithelial cell plasticity by targeting RhoA. Molecular and cellular biology, 28(22), pp.6773-6784.

Koo, E.H. and Kopan, R., 2004. Potential role of presenilin-regulated signaling pathways in sporadic neurodegeneration. Nature medicine, 10(7), pp.S26-S33.

Koo, P, K., Ploenzke, M. (2020). Deep learning for inferring transcription factor binding sites. Current Opinion in Systems Biology. 19. 10.1016/j.coisb.2020.04.001.

Kopp, H.G., Placke, T. and Salih, H.R., 2009. Platelet-derived transforming growth factor β down-regulates NKG2D thereby inhibiting natural killer cell antitumor reactivity. Cancer research, 69(19), pp.7775-7783.

Koren, S., Reavie, L., Couto, J.P., De Silva, D., Stadler, M.B., Roloff, T., Britschgi, A., Eichlisberger, T., Kohler, H., Aina, O. and Cardiff, R.D., 2015. PIK3CA H1047R induces multipotency and multi-lineage mammary tumours. Nature, 525(7567), pp.114-118.

Korenbaum, E. and Rivero, F., 2002. Calponin homology domains at a glance. Journal of Cell Science, 115(18), pp.3543-3545.

Korkaya, H., Paulson, A., Iovino, F. and Wicha, M.S., 2008. HER2 regulates the mammary stem/progenitor cell population driving tumorigenesis and invasion. Oncogene, 27(47), pp.6120-6130.

Korpal, M., Lee, E.S., Hu, G. and Kang, Y., 2008. The miR-200 family inhibits epithelial mesenchymal transition and cancer cell migration by direct targeting of E-cadherin transcriptional repressors ZEB1 and ZEB2. Journal of Biological Chemistry, 283(22), pp.14910-14914.

Korsching, E., Packeisen, J., Liedtke, C., Hungermann, D., Wülfing, P., van Diest, P.J., Brandt, B., Boecker, W. and Buerger, H., 2005. The origin of vimentin expression in invasive breast cancer: epithelial–mesenchymal transition, myoepithelial histogenesis or histogenesis from progenitor cells with bilinear differentiation potential?. The Journal of Pathology: A Journal of the Pathological Society of Great Britain and Ireland, 206(4), pp.451-457.

Kort, A., Durmus, S., Sparidans, R.W., Wagenaar, E., Beijnen, J.H. and Schinkel, A.H., 2015. Brain and testis accumulation of regorafenib is restricted by breast cancer resistance protein (BCRP/ABCG2) and P-glycoprotein (P-GP/ABCB1). Pharmaceutical research, 32(7), pp.2205-2216.

Kotiyal, S. and Bhattacharya, S. (2014). Breast cancer stem cells, EMT and therapeutic targets. Biochemical and Biophysical Research Communications, 453(1), pp.112–116.

Kouros-Mehr, H., Bechis, S.K., Slorach, E.M., Littlepage, L.E., Egeblad, M., Ewald, A.J., Pai, S.Y., Ho, I.C. and Werb, Z., 2008. GATA-3 links tumor differentiation and dissemination in a luminal breast cancer model. Cancer cell, 13(2), pp.141-152.

Kouros-Mehr, H., Slorach, E.M., Sternlicht, M.D. and Werb, Z., 2006. GATA-3 maintains the differentiation of the luminal cell fate in the mammary gland. Cell, 127(5), pp.1041-1055.

Kouros-Mehr, H. and Werb, Z., 2006. Candidate regulators of mammary branching morphogenesis identified by genome-wide transcript analysis. Developmental dynamics: an official publication of the American Association of Anatomists, 235(12), pp.3404-3412.

Koussounadis, A., Langdon, S.P., Um, I.H., Harrison, D.J. and Smith, V.A., 2015. Relationship between differentially expressed mRNA and mRNA-protein correlations in a xenograft model system. Scientific reports, 5, p.10775.

Kouzarides, T., 2007. Chromatin modifications and their function. Cell, 128(4), pp.693-705.

Kovalchuk, O., Filkowski, J., Meservy, J., Ilnytskyy, Y., Tryndyak, V.P., Vasyl'F, C. and Pogribny, I.P., 2008. Involvement of microRNA-451 in resistance of the MCF-7 breast cancer cells to chemotherapeutic drug doxorubicin. Molecular cancer therapeutics, 7(7), pp.2152-2159.

Krampera, M., Franchini, M., Pizzolo, G. and Aprili, G., 2007. Mesenchymal stem cells: from biology to clinical use. Blood Transfusion, 5(3), p.120.

Kristiansen, G., Winzer, K.J., Mayordomo, E., Bellach, J., Schlüns, K., Denkert, C., Dahl, E., Pilarsky, C., Altevogt, P., Guski, H. and Dietel, M., 2003. CD24 expression is a new prognostic marker in breast cancer. Clinical cancer research, 9(13), pp.4906-4913.

Krokan, H.E. and Bjørås, M., 2013. Base excision repair. Cold Spring Harbor perspectives in biology, 5(4), p.a012583.

Krubasik, D., Iyer, N.G., English, W.R., Ahmed, A.A., Vias, M., Roskelley, C., Brenton, J.D., Caldas, C. and Murphy, G., 2006. Absence of p300 induces cellular phenotypic changes characteristic of epithelial to mesenchyme transition. British journal of cancer, 94(9), pp.1326-1332.

Kruijtzer, C.M.F., Beijnen, J.H., Rosing, H., ten Bokkel Huinink, W.W., Schot, M., Jewell, R.C., Paul, E.M. and Schellens, J.H.M., 2002. Increased oral bioavailability of topotecan in combination with the breast cancer resistance protein and P-glycoprotein inhibitor GF120918. Journal of Clinical Oncology, 20(13), pp.2943-2950.

Krutzfeldt, J., 2005. Rajewsky N, Braich R, Rajeev KG, Tuschl T, Manoharan M, Stoffel M. Silencing of microRNAs in vivo with 'antagomirs'. Nature, 438, pp.685-689.

Kryczek, I., Liu, S., Roh, M., Vatan, L., Szeliga, W., Wei, S., Banerjee, M., Mao, Y., Kotarski, J., Wicha, M.S. and Liu, R., 2012. Expression of aldehyde dehydrogenase and CD133 defines ovarian cancer stem cells. International journal of cancer, 130(1), pp.29-39.

Kuehbacher, A., Urbich, C., Zeiher, A.M. and Dimmeler, S., 2007. Role of Dicer and Drosha for endothelial microRNA expression and angiogenesis. Circulation research, 101(1), pp.59-68. Kuespert, K., Pils, S. and Hauck, C.R., 2006. CEACAMs: their role in physiology and pathophysiology. Current opinion in cell biology, 18(5), pp.565-571.

Kumar, M., Lu, Z., Takwi, A.A.L., Chen, W., Callander, N.S., Ramos, K.S., Young, K.H. and Li, Y., 2011. Negative regulation of the tumor suppressor p53 gene by microRNAs. Oncogene, 30(7), pp.843-853.

Kunii, K., Davis, L., Gorenstein, J., Hatch, H., Yashiro, M., Di Bacco, A., Elbi, C. and Lutterbach, B., 2008. FGFR2-amplified gastric cancer cell lines require FGFR2 and Erbb3 signaling for growth and survival. Cancer research, 68(7), pp.2340-2348.

Kuo, K.K., Jian, S.F., Li, Y.J., Wan, S.W., Weng, C.C., Fang, K., Wu, D.C. and Cheng, K.H., 2015. Epigenetic inactivation of transforming growth factor-β1 target gene HEYL, a novel tumor suppressor, is involved in the P53-induced apoptotic pathway in hepatocellular carcinoma. Hepatology Research, 45(7), pp.782-793.

Kwak, J.H., Lee, N.H., Lee, H.Y., Hong, I.S. and Nam, J.S., 2016. HIF2α/EFEMP1 cascade mediates hypoxic effects on breast cancer stem cell hierarchy. Oncotarget, 7(28), p.43518.

Kwon, Y.J., Hurst, D.R., Steg, A.D., Yuan, K., Vaidya, K.S., Welch, D.R. and Frost, A.R., 2011. Gli1 enhances migration and invasion via up-regulation of MMP-11 and promotes metastasis in ERα negative breast cancer cell lines. Clinical & experimental metastasis, 28(5), p.437.

Labelle, M. and Hynes, R.O., 2012. The initial hours of metastasis: the importance of cooperative host–tumor cell interactions during hematogenous dissemination. Cancer discovery, 2(12), pp.1091-1099.

Lacroix, M., 2006. Significance, detection and markers of disseminated breast cancer cells. Endocrine-related cancer, 13(4), pp.1033-1067.

Laffin, B., Wellberg, E., Kwak, H.I., Burghardt, R.C., Metz, R.P., Gustafson, T., Schedin, P. and Porter, W.W., 2008. Loss of singleminded-2s in the mouse mammary gland induces an epithelial-mesenchymal transition associated with up-regulation of slug and matrix metalloprotease 2. Molecular and cellular biology, 28(6), pp.1936-1946.

Lagas, J.S., Fan, L., Wagenaar, E., Vlaming, M.L., van Tellingen, O., Beijnen, J.H. and Schinkel, A.H., 2010. P-glycoprotein (P-gp/Abcb1), Abcc2, and Abcc3 determine the pharmacokinetics of etoposide. Clinical Cancer Research, 16(1), pp.130-140.

Lahdaoui, F., Messager, M., Vincent, A., Hec, F., Gandon, A., Warlaumont, M., Renaud, F., Leteurtre, E., Piessen, G., Jonckheere, N. and Mariette, C., 2017. Depletion of MUC5B mucin in gastrointestinal cancer cells alters their tumorigenic properties: implication of the Wnt/β-catenin pathway. Biochemical Journal, 474(22), pp.3733-3746.

Lai, Y., Zhang, X., Zhang, Z., Shu, Y., Luo, X., Yang, Y., Wang, X., Yang, G., Li, L. and Feng, Y., 2013. The microRNA-27a: ZBTB10-specificity protein pathway is involved in follicle stimulating hormone-induced VEGF, Cox2 and survivin expression in ovarian epithelial cancer cells. International journal of oncology, 42(2), pp.776-784.

Lakshmanan, G., Lieuw, K.H., Lim, K.C., Gu, Y., Grosveld, F., Engel, J.D. and Karis, A., 1999. Localization of distant urogenital system-, central nervous system-, and endocardium-specific transcriptional regulatory elements in the GATA-3 locus. Molecular and Cellular Biology, 19(2), pp.1558-1568.

Lal, S., Wong, Z.W., Sandanaraj, E., Xiang, X., Ang, P.C.S., Lee, E.J. and Chowbay, B., 2008. Influence of ABCB1 and ABCG2 polymorphisms on doxorubicin disposition in Asian breast cancer patients. Cancer science, 99(4), pp.816-823.

Lala, P.K. and Orucevic, A., 1998. Role of nitric oxide in tumor progression: lessons from experimental tumors. Cancer and Metastasis Reviews, 17(1), pp.91-106.

Lam, E.W.F., Brosens, J.J., Gomes, A.R. and Koo, C.Y., 2013. Forkhead box proteins: tuning forks for transcriptional harmony. Nature reviews Cancer, 13(7), pp.482-495.

Lammens, T., Swerts, K., Derycke, L., De Craemer, A., De Brouwer, S., De Preter, K., Van Roy, N., Vandesompele, J., Speleman, F., Philippe, J. and Benoit, Y., 2012. N-cadherin in neuroblastoma disease: expression and clinical significance. PLoS One, 7(2), p.e31206.

Lamouille, S. and Derynck, R. (2007). Cell size and invasion in TGF-β–induced epithelial to mesenchymal transition is regulated by activation of the mTOR pathway. The Journal of Cell Biology, 178(3), pp.437–451.

Lamouille, S., Connolly, E., Smyth, J.W., Akhurst, R.J. and Derynck, R., 2012. TGF-β induced activation of mTOR complex 2 drives epithelial–mesenchymal transition and cell invasion. Journal of cell science, 125(5), pp.1259-1273.

Laprise, P., Viel, A. and Rivard, N., 2004. Human homolog of disc-large is required for adherens junction assembly and differentiation of human intestinal epithelial cells. Journal of Biological Chemistry, 279(11), pp.10157-10166.

Larrivée, B., Prahst, C., Gordon, E., del Toro, R., Mathivet, T., Duarte, A., Simons, M. and Eichmann, A., 2012. ALK1 signaling inhibits angiogenesis by cooperating with the Notch pathway. Developmental cell, 22(3), pp.489-500.

Larue, L. and Bellacosa, A., 2005. Epithelial–mesenchymal transition in development and cancer: role of phosphatidylinositol 3' kinase/AKT pathways. Oncogene, 24(50), pp.7443-7454.

Latres, E., Chiaur, D.S. and Pagano, M., 1999. The human F box protein β-Trcp associates with the Cul1/Skp1 complex and regulates the stability of β-catenin. Oncogene, 18(4), pp.849-854.

Lau, L.F., 2016. Cell surface receptors for CCN proteins. Journal of cell communication and signaling, 10(2), pp.121-127.

Lavigne, A.C., Castells, M., Mermet, J., Kocanova, S., Dalvai, M. and Bystricky, K., 2014. Increased macroH2A1. 1 expression correlates with poor survival of triple-negative breast cancer patients. PloS one, 9(6), p.e98930.

Lazarova, D. and Bordonaro, M., 2017. ZEB1 mediates drug resistance and EMT in p300 deficient CRC. Journal of Cancer, 8(8), p.1453.

Leavitt, J., 1994. Discovery and characterization of two novel human cancer-related proteins using two-dimensional gel electrophoresis. Electrophoresis, 15(1), pp.345-357.

Leavitt, J., Goldman, D., Merril, C. and Kakunaga, T., 1982. Changes in gene expression accompanying chemically-induced malignant transformation of human fibroblasts. Carcinogenesis, 3(1), pp.61-70.

Lecka-Czernik, B., Lumpkin, C.K. and Goldstein, S., 1995. An overexpressed gene transcript in senescent and quiescent human fibroblasts encoding a novel protein in the

epidermal growth factor-like repeat family stimulates DNA synthesis. Molecular and cellular biology, 15(1), pp.120-128.

Lee, E., Wang, J., Yumoto, K., Jung, Y., Cackowski, F.C., Decker, A.M., Li, Y., Franceschi, R.T., Pienta, K.J. and Taichman, R.S., 2016. DNMT1 regulates epithelial-mesenchymal transition and cancer stem cells, which promotes prostate cancer metastasis. Neoplasia, 18(9), pp.553-566.

Lee, E.J., Gusev, Y., Jiang, J., Nuovo, G.J., Lerner, M.R., Frankel, W.L., Morgan, D.L., Postier, R.G., Brackett, D.J. and Schmittgen, T.D., 2007. Expression profiling identifies microRNA signature in pancreatic cancer. International journal of cancer, 120(5), pp.1046-1054.

Lee, G.R., Fields, P.E. and Flavell, R.A., 2001. Regulation of IL-4 gene expression by distal regulatory elements and GATA-3 at the chromatin level. Immunity, 14(4), pp.447-459.

Lee, H.J., Seo, A.N., Park, S.Y., Kim, J.Y., Park, J.Y., Yu, J.H., Ahn, J.H. and Gong, G., 2014. Low prognostic implication of fibroblast growth factor family activation in triple-negative breast cancer subsets. Annals of surgical oncology, 21(5), pp.1561-1568.

Lee, H.J., Tomioka, S., Kinbara, K., Masumoto, H., Jeong, S.Y., Sorimachi, H., Ishiura, S. and Suzuki, K., 1999. Characterization of a human digestive tract-specific calpain, nCL-4, expressed in the baculovirus system. Archives of biochemistry and biophysics, 362(1), pp.22-31.

Lee, J.M., Dedhar, S., Kalluri, R. and Thompson, E.W., 2006. The epithelial–mesenchymal transition: new insights in signaling, development, and disease. Journal of Cell Biology, 172(7), pp.973-981.

Lee, J.Y., Kinch, L.N., Borek, D.M., Wang, J., Wang, J., Urbatsch, I.L., Xie, X.S., Grishin, N.V., Cohen, J.C., Otwinowski, Z. and Hobbs, H.H., 2016. Crystal structure of the human sterol transporter ABCG5/ABCG8. Nature, 533(7604), pp.561-564.

Lee, K.K. and Workman, J.L., 2007. Histone acetyltransferase complexes: one size doesn't fit all. Nature reviews Molecular cell biology, 8(4), pp.284-295.

Lee, R.C., Feinbaum, R.L. and Ambros, V., 1993. The C. elegans heterochronic gene lin-4 encodes small RNAs with antisense complementarity to lin-14. cell, 75(5), pp.843-854.

Lee, S.H., Oh, S.Y., Do, S.I., Lee, H.J., Kang, H.J., Rho, Y.S., Bae, W.J. and Lim, Y.C., 2014. SOX2 regulates self-renewal and tumorigenicity of stem-like cells of head and neck squamous cell carcinoma. British journal of cancer, 111(11), pp.2122-2130.

Lee, Y.H., Bedford, M.T. and Stallcup, M.R., 2011. Regulated recruitment of tumor suppressor BRCA1 to the p21 gene by coactivator methylation. Genes & development, 25(2), pp.176-188.

Lee, Y.H., Coonrod, S.A., Kraus, W.L., Jelinek, M.A. and Stallcup, M.R., 2005. Regulation of coactivator complex assembly and function by protein arginine methylation and demethylimination. Proceedings of the National Academy of Sciences, 102(10), pp.3611-3616.

Lehmann, B.D., Bauer, J.A., Chen, X., Sanders, M.E., Chakravarthy, A.B., Shyr, Y. and Pietenpol, J.A., 2011. Identification of human triple-negative breast cancer subtypes and preclinical models for selection of targeted therapies. The Journal of clinical investigation, 121(7), pp.2750-2767.

Lehtinen, M.K., Yuan, Z., Boag, P.R., Yang, Y., Villén, J., Becker, E.B., DiBacco, S., de la Iglesia, N., Gygi, S., Blackwell, T.K. and Bonni, A., 2006. A conserved MST-FOXO signaling pathway mediates oxidative-stress responses and extends life span. Cell, 125(5), pp.987-1001.

Lei, J., Fan, L., Wei, G., Chen, X., Duan, W., Xu, Q., Sheng, W., Wang, K. and Li, X., 2015. Gli-1 is crucial for hypoxia-induced epithelial-mesenchymal transition and invasion of breast cancer. Tumor Biology, 36(4), pp.3119-3126.

Leimeister, C., Externbrink, A., Klamt, B. and Gessler, M., 1999. Hey genes: a novel subfamily of hairy-and Enhancer of split related genes specifically expressed during mouse embryogenesis. Mechanisms of development, 85(1-2), pp.173-177.

Leong, K.G., Niessen, K., Kulic, I., Raouf, A., Eaves, C., Pollet, I. and Karsan, A., 2007. Jagged1-mediated Notch activation induces epithelial-to-mesenchymal transition through Slug-induced repression of E-cadherin. The Journal of experimental medicine, 204(12), pp.2935-2948.

Lester, R.D., Jo, M., Montel, V., Takimoto, S. and Gonias, S.L., 2007. uPAR induces epithelial–mesenchymal transition in hypoxic breast cancer cells. Journal of Cell Biology, 178(3), pp.425-436.

Letterio, J.J. and Roberts, A.B., 1998. Regulation of immune responses by TGF-β. Annual review of immunology, 16(1), pp.137-161.

Levaggi, A., Poggio, F. and Lambertini, M., 2014. The burden of breast cancer from China to Italy. Journal of thoracic disease, 6(6), p.591.

Levine, B. and Kroemer, G., 2008. Autophagy in the pathogenesis of disease. Cell, 132(1), pp.27-42.

Lewis, M., Tartaglia, L.A., Lee, A., Bennett, G.L., Rice, G.C., Wong, G.H., Chen, E.Y. and Goeddel, D.V., 1991. Cloning and expression of cDNAs for two distinct murine tumor necrosis factor receptors demonstrate one receptor is species specific. Proceedings of the National Academy of Sciences, 88(7), pp.2830-2834.

Li, B., Zheng, Y.W., Sano, Y. and Taniguchi, H., 2011. Evidence for mesenchymal−epithelial transition associated with mouse hepatic stem cell differentiation. PloS one, 6(2), p.e17092.

Li, C., Heidt, D.G., Dalerba, P., Burant, C.F., Zhang, L., Adsay, V., Wicha, M., Clarke, M.F. and Simeone, D.M., 2007. Identification of pancreatic cancer stem cells. Cancer research, 67(3), pp.1030-1037.

Li, C.I., Uribe, D.J. and Daling, J.R., 2005. Clinical characteristics of different histologic types of breast cancer. British journal of cancer, 93(9), pp.1046-1052.

Li, H., Chen, Y., Zhou, B., Peng, Y., Bai, W. and Rao, L., 2012. RNT4 3'-UTR insertion/deletion polymorphisms are not associated with atrial septal defect in Chinese Han population: a brief communication. DNA and cell biology, 31(6), pp.1121-1124.

Li, H.J., Reinhardt, F., Herschman, H.R. and Weinberg, R.A., 2012. Cancer-stimulated mesenchymal stem cells create a carcinoma stem cell niche via prostaglandin E2 signaling. Cancer discovery, 2(9), pp.840-855.

Li, J., Sutter, C., Parker, D.S., Blauwkamp, T., Fang, M. and Cadigan, K.M., 2007. CBP/p300 are bimodal regulators of Wnt signaling. The EMBO journal, 26(9), pp.2284-2294.

Li, L., Fang, R., Liu, B., Shi, H., Wang, Y., Zhang, W., Zhang, X. and Ye, L., 2016. Deacetylation of tumor-suppressor MST1 in Hippo pathway induces its degradation through HBXIP-elevated HDAC6 in promotion of breast cancer growth. Oncogene, 35(31), pp.4048-4057.

Li, L., Liu, Y., Guo, Y., Liu, B., Zhao, Y., Li, P., Song, F., Zheng, H., Yu, J., Song, T. and Niu, R., 2015. Regulatory MiR-148a-ACVR1/BMP circuit defines a cancer stem cell-like aggressive subtype of hepatocellular carcinoma. Hepatology, 61(2), pp.574-584.

Li, L., Ying, J., Li, H., Zhang, Y., Shu, X., Fan, Y., Tan, J., Cao, Y., Tsao, S.W., Srivastava, G. and Chan, A.T.C., 2012. The human cadherin 11 is a pro-apoptotic tumor suppressor modulating cell stemness through Wnt/β-catenin signaling and silenced in common carcinomas. Oncogene, 31(34), pp.3901-3912.

Li, L.T., Jiang, G., Chen, Q. and Zheng, J.N., 2015. Ki67 is a promising molecular target in the diagnosis of cancer. Molecular medicine reports, 11(3), pp.1566-1572.

Li, M., Han, Y., Zhou, H., Li, X., Lin, C., Zhang, E., Chi, X., Hu, J. and Xu, H., 2018. Transmembrane protein 170B is a novel breast tumorigenesis suppressor gene that inhibits the Wnt/β-catenin pathway. Cell death & disease, 9(2), pp.1-15.

Li, M.Z., Wang, J.J., Yang, S.B., Li, W.F., Xiao, L.B., He, Y.L. and Song, X.M., 2017. ZEB2 promotes tumor metastasis and correlates with poor prognosis of human colorectal cancer. American journal of translational research, 9(6), p.2838.

Li, P., Nijhawan, D., Budihardjo, I., Srinivasula, S.M., Ahmad, M., Alnemri, E.S. and Wang, X., 1997. Cytochrome c and dATP-dependent formation of Apaf-1/caspase-9 complex initiates an apoptotic protease cascade. Cell, 91(4), pp.479-489.

Li, Q., Zou, C., Zou, C., Han, Z., Xiao, H., Wei, H., Wang, W., Zhang, L., Zhang, X., Tang, Q. and Zhang, C., 2013. MicroRNA-25 functions as a potential tumor suppressor in colon cancer by targeting Smad7. Cancer letters, 335(1), pp.168-174.

Li, S., Li, S., Sun, Y. and Li, L., 2014. The expression of β-catenin in different subtypes of breast cancer and its clinical significance. Tumor Biology, 35(8), pp.7693-7698.

Li, W., Liu, C., Tang, Y., Li, H., Zhou, F. and Lv, S., 2011. Overexpression of Snail accelerates adriamycin induction of multidrug resistance in breast cancer cells. Asian Pac J Cancer Prev, 12(10), pp.2575-2580.

Li, W., Liu, Z., Zhao, C. and Zhai, L., 2015. Binding of MMP-9-degraded fibronectin to β6 integrin promotes invasion via the FAK-Src-related Erk1/2 and PI3K/Akt/Smad-1/5/8 pathways in breast cancer. Oncology reports, 34(3), pp.1345-1352.

Li, W., Ma, H., Zhang, J., Zhu, L., Wang, C. and Yang, Y., 2017. Unraveling the roles of CD44/CD24 and ALDH1 as cancer stem cell markers in tumorigenesis and metastasis. Scientific reports, 7(1), pp.1-15.

Li, X., Li, X., Liao, D., Wang, X., Wu, Z., Nie, J., Bai, M., Fu, X., Mei, Q. and Han, W., 2015. Elevated microRNA-23a expression enhances the chemoresistance of colorectal cancer cells with microsatellite instability to 5-fluorouracil by directly targeting ABCF1. Current Protein and Peptide Science, 16(4), pp.301-309.

Li, X., Liu, X., Xu, W., Zhou, P., Gao, P., Jiang, S., Lobie, P.E. and Zhu, T., 2013. c-MYC regulated miR-23a/24-2/27a cluster promotes mammary carcinoma cell invasion and hepatic metastasis by targeting Sprouty2. Journal of Biological Chemistry, 288(25), pp.18121-18133.

Li, X., Mertens-Talcott, S.U., Zhang, S., Kim, K., Ball, J. and Safe, S., 2010. MicroRNA-27a indirectly regulates estrogen receptor α expression and hormone responsiveness in MCF-7 breast cancer cells. Endocrinology, 151(6), pp.2462-2473.

Li, X., Wang, Z., Ma, Q., Xu, Q., Liu, H., Duan, W., Lei, J., Ma, J., Wang, X., Lv, S. and Han, L., 2014. Sonic hedgehog paracrine signaling activates stromal cells to promote perineural invasion in pancreatic cancer. Clinical Cancer Research, 20(16), pp.4326-4338.

Li, X., Xu, M., Ding, L. and Tang, J., 2019. MiR-27a: a novel biomarker and potential therapeutic target in tumors. Journal of Cancer, 10(12), p.2836.

Li, Y., Li, J., Sun, X., Chen, J., Sun, X., Zheng, J. and Chen, R., 2016. MicroRNA 27a functions as a tumor suppressor in renal cell carcinoma by targeting epidermal growth factor receptor. Oncology letters, 11(6), pp.4217-4223.

Li, Y., Tan, W., Neo, T.W., Aung, M.O., Wasser, S., Lim, S.G. and Tan, T.M., 2009. Role of the miR-106b-25 microRNA cluster in hepatocellular carcinoma. Cancer science, 100(7), pp.1234-1242.

Li, Y., Wang, X., Ao, M., Gabrielson, E., Askin, F., Zhang, H. and Li, Q.K., 2013. Aberrant Mucin5B expression in lung adenocarcinomas detected by iTRAQ labeling quantitative proteomics and immunohistochemistry. Clinical proteomics, 10(1), p.15.

Li, Z., Hu, S., Wang, J., Cai, J., Xiao, L., Yu, L. and Wang, Z., 2010. MiR-27a modulates MDR1/P-glycoprotein expression by targeting HIPK2 in human ovarian cancer cells. Gynecologic oncology, 119(1), pp.125-130.

Li, Z.W. and Dalton, W.S., 2006. Tumor microenvironment and drug resistance in hematologic malignancies. Blood reviews, 20(6), pp.333-342.

Liang, T., Yu, J., Liu, C. and Guo, L. (2014). An Exploration of Evolution, Maturation, Expression and Function Relationships in Mir-23∼27∼24 Cluster. PLoS ONE, 9(8), p.e106223.

Liang, Z., Wu, H., Xia, J., Li, Y., Zhang, Y., Huang, K., Wagar, N., Yoon, Y., Cho, H.T., Scala, S. and Shim, H., 2010. Involvement of miR-326 in chemotherapy resistance of breast cancer through modulating expression of multidrug resistance-associated protein 1. Biochemical pharmacology, 79(6), pp.817-824.

Liao, M.J., Zhang, C.C., Zhou, B., Zimonjic, D.B., Mani, S.A., Kaba, M., Gifford, A., Reinhardt, F., Popescu, N.C., Guo, W. and Eaton, E.N., 2007. Enrichment of a population of mammary gland cells that form mammospheres and have in vivo repopulating activity. Cancer research, 67(17), pp.8131-8138.

Libusova, L., Stemmler, M.P., Hierholzer, A., Schwarz, H. and Kemler, R., 2010. N cadherin can structurally substitute for E-cadherin during intestinal development but leads to polyp formation. Development, 137(14), pp.2297-2305.

Lien, W.H. and Fuchs, E., 2014. Wnt some lose some: transcriptional governance of stem cells by Wnt/β-catenin signaling. Genes & development, 28(14), pp.1517-1532.

Likhite, V.S., Stossi, F., Kim, K., Katzenellenbogen, B.S. and Katzenellenbogen, J.A., 2006. Kinase-specific phosphorylation of the estrogen receptor changes receptor interactions with ligand, deoxyribonucleic acid, and coregulators associated with alterations in estrogen and tamoxifen activity. Molecular endocrinology, 20(12), pp.3120-3132.

Lim, J.C., Kania, K.D., Wijesuriya, H., Chawla, S., Sethi, J.K., Pulaski, L., Romero, I.A., Couraud, P.O., Weksler, B.B., Hladky, S.B. and Barrand, M.A., 2008. Activation of β-catenin signalling by GSK-3 inhibition increases p-glycoprotein expression in brain endothelial cells. Journal of neurochemistry, 106(4), pp.1855-1865.

Lim, S., Becker, A., Zimmer, A., Lu, J., Buettner, R. and Kirfel, J., 2013. SNAI1-mediated epithelial-mesenchymal transition confers chemoresistance and cellular plasticity by regulating genes involved in cell death and stem cell maintenance. PloS one, 8(6), p.e66558.

Lim, S., Janzer, A., Becker, A., Zimmer, A., Schüle, R., Buettner, R. and Kirfel, J., 2010. Lysine-specific demethylase 1 (LSD1) is highly expressed in ER-negative breast cancers and a biomarker predicting aggressive biology. Carcinogenesis, 31(3), pp.512-520.

Lin, C.S., Aebersold, R.H., Kent, S.B., Varma, M.A.D.H.U. and Leavitt, J., 1988. Molecular cloning and characterization of plastin, a human leukocyte protein expressed in transformed human fibroblasts. Molecular and cellular biology, 8(11), pp.4659-4668.

Lin, C.S., Lau, A., Huynh, T. and Lue, T.F., 1999. Differential regulation of human T-plastin gene in leukocytes and non-leukocytes: identification of the promoter, enhancer, and CpG island. DNA and cell biology, 18(1), pp.27-37.

Lin, C.S., Park, T., Chen, Z.P. and Leavitt, J., 1993. Human plastin genes. Comparative gene structure, chromosome location, and differential expression in normal and neoplastic cells. Journal of Biological Chemistry, 268(4), pp.2781-2792.

Lin, C.S., Shen, W., Chen, Z.P., Tu, Y.H. and Matsudaira, P., 1994. Identification of I plastin, a human fimbrin isoform expressed in intestine and kidney. Molecular and Cellular Biology, 14(4), pp.2457-2467.

Lin, C.Y., Lee, Y.E., Tian, Y.F., Sun, D.P., Sheu, M.J., Lin, C.Y., Li, C.F., Lee, S.W., Lin, L.C., Chang, I.W. and Wang, C.T., 2017. High expression of EphA4 predicted lesser degree of tumor regression after neoadjuvant chemoradiotherapy in rectal cancer. Journal of Cancer, 8(6), p.1089.

Lin, E.Y., 2002. Gouon-Evans G, Nguyen AV, and Pollard JW. The macrophage growth factor CSF-1 in mammary gland development and tumor progression. J Mammary Gland Biol Neoplasia, 7, pp.147-162.

Lin, H., Dai, T., Xiong, H., Zhao, X., Chen, X., Yu, C., Li, J., Wang, X. and Song, L., 2010. Unregulated miR-96 induces cell proliferation in human breast cancer by downregulating transcriptional factor FOXO3a. PloS one, 5(12), p.e15797.

Lin, M., Pan, J., Chen, Q., Xu, Z., Lin, X. and Shi, C., 2018. Overexpression of FOXA1 inhibits cell proliferation and EMT of human gastric cancer AGS cells. Gene, 642, pp.145-151.

Lin, M.H., Pope III, B.D., Sasaki, T., Keeley, D.P., Sherwood, D.R. and Miner, J.H., 2020. Mammalian hemicentin 1 is assembled into tracks in the extracellular matrix of multiple tissues. Developmental Dynamics.

Lin, Q., Gao, Z., Alarcon, R.M., Ye, J. and Yun, Z., 2009. A role of miR-27 in the regulation of adipogenesis. The FEBS journal, 276(8), pp.2348-2358.

Lin, R., Chen, L., Chen, G., Hu, C., Jiang, S., Sevilla, J., Wan, Y., Sampson, J.H., Zhu, B. and Li, Q.J., 2014. Targeting miR-23a in CD8+ cytotoxic T lymphocytes prevents tumor dependent immunosuppression. The Journal of clinical investigation, 124(12), pp.5352-5367.

Lin, S.C., Kao, C.Y., Lee, H.J., Creighton, C.J., Ittmann, M.M., Tsai, S.J., Tsai, S.Y. and Tsai, M.J., 2016. Dysregulation of miRNAs-COUP-TFII-FOXM1-CENPF axis contributes to the metastasis of prostate cancer. Nature communications, 7(1), pp.1-14.

Lin, S.Y. and Elledge, S.J., 2003. Multiple tumor suppressor pathways negatively regulate telomerase. Cell, 113(7), pp.881-889.

Lin, S.Y., Xia, W., Wang, J.C., Kwong, K.Y., Spohn, B., Wen, Y., Pestell, R.G. and Hung, M.C., 2000. β-catenin, a novel prognostic marker for breast cancer: its roles in cyclin D1 expression and cancer progression. Proceedings of the National Academy of Sciences, 97(8), pp.4262-4266.

Lin, T., Ponn, A., Hu, X., Law, B.K. and Lu, J., 2010. Requirement of the histone demethylase LSD1 in Snai1-mediated transcriptional repression during epithelial-mesenchymal transition. Oncogene, 29(35), pp.4896-4904.

Liu, C.C., Prior, J., Piwnica-Worms, D. and Bu, G., 2010. LRP6 overexpression defines a class of breast cancer subtype and is a target for therapy. Proceedings of the National Academy of Sciences, 107(11), pp.5136-5141.

Liu, C.L., Pan, H.W., Torng, P.L., Fan, M.H. and Mao, T.L., 2019. SRPX and HMCN1 regulate cancer associated fibroblasts to promote the invasiveness of ovarian carcinoma. Oncology Reports, 42(6), pp.2706-2715.

Liu, H.B., Gao, X.X., Zhang, Q., Liu, J., Cui, Y., Zhu, Y. and Liu, Y.F., 2015. Expression and prognostic implications of FOXO3a and Ki67 in lung adenocarcinomas. Asian Pac J Cancer Prev, 16(4), pp.1443-8.

Liu, J., Lichtenberg, T., Hoadley, K.A., Poisson, L.M., Lazar, A.J., Cherniack, A.D., Kovatich, A.J., Benz, C.C., Levine, D.A., Lee, A.V. and Omberg, L., 2018. An integrated TCGA pan-cancer clinical data resource to drive high-quality survival outcome analytics. Cell, 173(2), pp.400-416.

Liu, J., Taylor, D.W. and Taylor, K.A., 2004. A 3-D reconstruction of smooth muscle α actinin by CryoEm reveals two different conformations at the actin-binding region. Journal of molecular biology, 338(1), pp.115-125.

Liu, L., Xu, Q., Cheng, L., Ma, C., Xiao, L., Xu, D., Gao, Y., Wang, J. and Song, H., 2015. NPY1R is a novel peripheral blood marker predictive of metastasis and prognosis in breast cancer patients. Oncology letters, 9(2), pp.891-896.

Liu, L.K., Jiang, X.Y., Zhou, X.X., Wang, D.M., Song, X.L. and Jiang, H.B., 2010. Upregulation of vimentin and aberrant expression of E-cadherin/β-catenin complex in oral squamous cell carcinomas: correlation with the clinicopathological features and patient outcome. Modern Pathology, 23(2), pp.213-224.

Liu, N., Li, S., Wu, N. and Cho, K.S., 2017. Acetylation and deacetylation in cancer stem like cells. Oncotarget, 8(51), p.89315.

Liu, P., Wang, C., Ma, C., Wu, Q., Zhang, W. and Lao, G., 2016. MicroRNA-23a regulates epithelial-to-mesenchymal transition in endometrial endometrioid adenocarcinoma by targeting SMAD3. Cancer cell international, 16(1), p.67.

Liu, R. and Jin, J.P., 2015. Calponin: A mechanical tension-modulated regulator of cytoskeleton and cell motility. Current Topics in Biochemical Research, 16, pp.1-15.

Liu, S., Clouthier, S.G. and Wicha, M.S., 2012. Role of microRNAs in the regulation of breast cancer stem cells. Journal of mammary gland biology and neoplasia, 17(1), pp.15-21.

Liu, S., Cong, Y., Wang, D., Sun, Y., Deng, L., Liu, Y., Martin-Trevino, R., Shang, L., McDermott, S.P., Landis, M.D. and Hong, S., 2014. és mtsai. Breast cancer stem cells transition between epithelial and mesenchymal states reflective of their normal counterparts. Stem cell reports. Elsevier, 2, pp.78-91.

Liu, S., Dontu, G. and Wicha, M.S., 2005. Mammary stem cells, self-renewal pathways, and carcinogenesis. Breast cancer research, 7(3), p.86.

Liu, S., Dontu, G., Mantle, I.D., Patel, S., Ahn, N.S., Jackson, K.W., Suri, P. and Wicha, M.S., 2006. Hedgehog signaling and Bmi-1 regulate self-renewal of normal and malignant human mammary stem cells. Cancer research, 66(12), pp.6063-6071.

Liu, S., Ginestier, C., Charafe-Jauffret, E., Foco, H., Kleer, C.G., Merajver, S.D., Dontu, G. and Wicha, M.S., 2008. BRCA1 regulates human mammary stem/progenitor cell fate. Proceedings of the National Academy of Sciences, 105(5), pp.1680-1685.

Liu, S., Ginestier, C., Ou, S.J., Clouthier, S.G., Patel, S.H., Monville, F., Korkaya, H., Heath, A., Dutcher, J., Kleer, C.G. and Jung, Y., 2011. Breast cancer stem cells are regulated by mesenchymal stem cells through cytokine networks. Cancer research, 71(2), pp.614-624.

Liu, S., Patel, S.H., Ginestier, C., Ibarra, I., Martin-Trevino, R., Bai, S., McDermott, S.P., Shang, L., Ke, J., Ou, S.J. and Heath, A., 2012. MicroRNA93 regulates proliferation and differentiation of normal and malignant breast stem cells. PLoS Genet, 8(6), p.e1002751.

Liu, W., Huang, Y.J., Liu, C., Yang, Y.Y., Liu, H., Cui, J.G., Cheng, Y., Gao, F., Cai, J.M. and Li, B.L., 2014. Inhibition of TBK1 attenuates radiation-induced epithelial–mesenchymal transition of A549 human lung cancer cells via activation of GSK-3 β and repression of ZEB1. Laboratory Investigation, 94(4), pp.362-370.

Liu, W., Qian, K., Wei, X., Deng, H., Zhao, B., Chen, Q., Zhang, J. and Liu, H., 2017. miR 27a promotes proliferation, migration, and invasion of colorectal cancer by targeting FAM172A and acts as a diagnostic and prognostic biomarker. Oncology reports, 37(6), pp.3554-3564.

Liu, X., Jiao, T., Wang, Y., Su, W., Tang, Z. and Han, C., 2016. Long non-coding RNA GAS5 acts as a molecular sponge to regulate miR-23a in gastric cancer. Int J Exp Pathol, 9, pp.11412-11419.

Liu, X., Jutooru, I., Lei, P., Kim, K., Lee, S.O., Brents, L.K., Prather, P.L. and Safe, S., 2012. Betulinic acid targets YY1 and ErbB2 through cannabinoid receptor-dependent disruption of microRNA-27a: ZBTB10 in breast cancer. Molecular cancer therapeutics, 11(7), pp.1421-1431.

Liu, X., Liu, Q., Fan, Y., Wang, S., Liu, X., Zhu, L., Liu, M. and Tang, H., 2014. Downregulation of PPP2R5E expression by miR-23a suppresses apoptosis to facilitate the growth of gastric cancer cells. FEBS letters, 588(17), pp.3160-3169.

Liu, X., Wang, L., Zhao, K., Thompson, P.R., Hwang, Y., Marmorstein, R. and Cole, P.A., 2008. The structural basis of protein acetylation by the p300/CBP transcriptional coactivator. Nature, 451(7180), pp.846-850.

Liu, Y., El-Naggar, S., Darling, D.S., Higashi, Y. and Dean, D.C., 2008. Zeb1 links epithelial mesenchymal transition and cellular senescence. Development, 135(3), pp.579-588.

Liu, Y., Gu, Y., Han, Y., Zhang, Q., Jiang, Z., Zhang, X., Huang, B., Xu, X., Zheng, J. and Cao, X., 2016. Tumor exosomal RNAs promote lung pre-metastatic niche formation by activating alveolar epithelial TLR3 to recruit neutrophils. Cancer cell, 30(2), pp.243-256.

Liu, Y., Nenutil, R., Appleyard, M.V., Murray, K., Boylan, M., Thompson, A.M. and Coates, P.J., 2014. Lack of correlation of stem cell markers in breast cancer stem cells. British journal of cancer, 110(8), pp.2063-2071.

Liu, Y., Zeng, X., He, Z. and Zou, Q., 2016. Inferring microRNA-disease associations by random walk on a heterogeneous network with multiple data sources. IEEE/ACM transactions on computational biology and bioinformatics, 14(4), pp.905-915.

Liu, Y.N., Lee, W.W., Wang, C.Y., Chao, T.H., Chen, Y. and Chen, J.H., 2005. Regulatory mechanisms controlling human E-cadherin gene expression. Oncogene, 24(56), pp.8277-8290.

Liu, Z., Xu, J., He, J., Zheng, Y., Li, H., Lu, Y., Qian, J., Lin, P., Weber, D.M., Yang, J. and Yi, Q., 2014. A critical role of autocrine sonic hedgehog signaling in human CD138+ myeloma cell survival and drug resistance. Blood, The Journal of the American Society of Hematology, 124(13), pp.2061-2071.

Lo, H.W., Hsu, S.C., Xia, W., Cao, X., Shih, J.Y., Wei, Y., Abbruzzese, J.L., Hortobagyi, G.N. and Hung, M.C., 2007. Epidermal growth factor receptor cooperates with signal transducer and activator of transcription 3 to induce epithelial-mesenchymal transition in cancer cells via up-regulation of TWIST gene expression. Cancer research, 67(19), pp.9066-9076.

Lobo, N.A., Shimono, Y., Qian, D. and Clarke, M.F., 2007. The biology of cancer stem cells. Annu. Rev. Cell Dev. Biol., 23, pp.675-699.

Locksley, R.M., Killeen, N. and Lenardo, M.J., 2001. The TNF and TNF receptor superfamilies: integrating mammalian biology. Cell, 104(4), pp.487-501.

Lohrisch, C., Paltiel, C., Gelmon, K., Speers, C., Taylor, S., Barnett, J. and Olivotto, I.A., 2006. Impact on survival of time from definitive surgery to initiation of adjuvant chemotherapy for early-stage breast cancer. Journal of clinical oncology, 24(30), pp.4888-4894.

Lombaerts, M., Van Wezel, T., Philippo, K., Dierssen, J.W.F., Zimmerman, R.M.E., Oosting, J., Van Eijk, R., Eilers, P.H., van De Water, B., Cornelisse, C.J. and Cleton-Jansen, A.M., 2006. E-cadherin transcriptional downregulation by promoter methylation but not mutation is related to epithelial-to-mesenchymal transition in breast cancer cell lines. British journal of cancer, 94(5), pp.661-671.

Lombardo, Y., Filipović, A., Molyneux, G., Periyasamy, M., Giamas, G., Hu, Y., Trivedi, P.S., Wang, J., Yagüe, E., Michel, L. and Coombes, R.C., 2012. Nicastrin regulates breast cancer stem cell properties and tumor growth in vitro and in vivo. Proceedings of the National Academy of Sciences, 109(41), pp.16558-16563.

López-Mateo, I., Arruabarrena-Aristorena, A., Artaza-Irigaray, C., López, J.A., Calvo, E. and Belandia, B., 2016. HEY1 functions are regulated by its phosphorylation at Ser-68. Bioscience Reports, 36(3).

Lovén, J., Hoke, H.A., Lin, C.Y., Lau, A., Orlando, D.A., Vakoc, C.R., Bradner, J.E., Lee, T.I. and Young, R.A., 2013. Selective inhibition of tumor oncogenes by disruption of super-enhancers. Cell, 153(2), pp.320-334.

Lü, M., K. Ding, G. Zhang, M. Yin, G. Yao, and H. Tian. "MicroRNA-320a sensitizes tamoxifen-resistant breast cancer cells to tamoxifen by targeting ARPP-19 and ERRγ. Sci Rep 2015; 5: 8735." GSEA enrichment plots for “ESTROGEN_RESPONSE_EARLY”(upper panel) and “ESTROGEN_RESPONSE_LATE”(lower panel) pathways associated with PSF expression in E2-treated group. E and F, Effect of PSF knockdown on GREB1 induction by E2 treatment (10 nmol/L) in MCF-7.

Lu, M., Zhao, Y., Xu, F., Wang, Y., Xiang, J. and Chen, D., 2012. The expression and prognosis of FOXO3a and Skp2 in human ovarian cancer. Medical Oncology, 29(5), pp.3409-3415.

Lu, T., Burdelya, L.G., Swiatkowski, S.M., Boiko, A.D., Howe, P.H., Stark, G.R. and Gudkov, A.V., 2004. Secreted transforming growth factor β2 activates NFκB, blocks apoptosis, and is essential for the survival of some tumor cells. Proceedings of the National Academy of Sciences, 101(18), pp.7112-7117.

Lunning, M.A. and Green, M.R., 2015. Mutation of chromatin modifiers; an emerging hallmark of germinal center B-cell lymphomas. Blood cancer journal, 5(10), pp.e361-e361.

Luo, J., Liang, A., Liang, M., Xia, R., Rizvi, Y., Wang, Y. and Cheng, J., 2016. Serum Glucocorticoid–Regulated Kinase 1 Blocks CKD–Induced Muscle Wasting Via Inactivation of FoxO3a and Smad2/3. Journal of the American Society of Nephrology, 27(9), pp.2797-2808.

Luo, W., Zhang, D., Ma, S., Wang, C., Zhang, Q., Wang, H., He, K. and Liu, Z., 2018. miR 27a is highly expressed in H1650 cancer stem cells and regulates proliferation, migration, and invasion. Journal of Cancer Research and Therapeutics, 14(12), p.1004.

Lv, Z.M., Wang, Q., Wan, Q., Lin, J.G., Hu, M.S., Liu, Y.X. and Wang, R., 2011. The role of the p38 MAPK signaling pathway in high glucose-induced epithelial-mesenchymal transition of cultured human renal tubular epithelial cells. PloS one, 6(7), p.e22806.

Lyman, G.H., Temin, S., Edge, S.B., Newman, L.A., Turner, R.R., Weaver, D.L., Benson, A.3., Bosserman, L.D., Burstein, H.J., Cody, H. and Hayman, J., 2014. Sentinel lymph node biopsy for patients with early-stage breast cancer: American Society of Clinical Oncology clinical practice guideline update. J Clin Oncol, 32(13), pp.1365-1383.

Lymperatou, D., Giannopoulou, E., Koutras, A.K. and Kalofonos, H.P., 2013. The exposure of breast cancer cells to fulvestrant and tamoxifen modulates cell migration differently. BioMed research international, 2013.

Lyons, J.G., Lobo, E., Martorana, A.M. and Myerscough, M.R., 2008. Clonal diversity in carcinomas: its implications for tumour progression and the contribution made to it by epithelial-mesenchymal transitions. Clinical & experimental metastasis, 25(6), pp.665-677.

Ma, F., Li, W., Liu, C., Li, W., Yu, H., Lei, B., Ren, Y., Li, Z., Pang, D. and Qian, C., 2017. MiR-23a promotes TGF-β1-induced EMT and tumor metastasis in breast cancer cells by directly targeting CDH1 and activating Wnt/β-catenin signaling. Oncotarget, 8(41), p.69538.

Ma, L., Young, J., Prabhala, H., Pan, E., Mestdagh, P., Muth, D., Teruya-Feldstein, J., Reinhardt, F., Onder, T.T., Valastyan, S. and Westermann, F., 2010. miR-9, a MYC/MYCN-

activated microRNA, regulates E-cadherin and cancer metastasis. Nature cell biology, 12(3), pp.247-256.

Ma, M., Yin, Z., Zhong, H., Liang, T. and Guo, L., 2019. Analysis of the expression, function, and evolution of miR-27 isoforms and their responses in metabolic processes. Genomics, 111(6), pp.1249-1257.

Ma, S., Liu, M., Xu, Z., Li, Y., Guo, H., Ge, Y., Liu, Y., Zheng, D. and Shi, J., 2016. A double feedback loop mediated by microRNA-23a/27a/24-2 regulates M1 versus M2 macrophage polarization and thus regulates cancer progression. Oncotarget, 7(12), p.13502.

Ma, S., Liu, M., Xu, Z., Li, Y., Guo, H., Ge, Y., Liu, Y., Zheng, D. and Shi, J., 2016. A double feedback loop mediated by microRNA-23a/27a/24-2 regulates M1 versus M2 macrophage polarization and thus regulates cancer progression. Oncotarget, 7(12), p.13502.

Ma, Y., Lai, W., Zhao, M., Yue, C., Shi, F., Li, R. and Hu, Z., 2019. Plastin 3 down regulation augments the sensitivity of MDA-MB-231 cells to paclitaxel via the p38 MAPK signalling pathway. Artificial Cells, Nanomedicine, and Biotechnology, 47(1), pp.684-694.

Mabuchi, K., Li, B., Ip, W. and Tao, T., 1997. Association of calponin with desmin intermediate filaments. Journal of Biological Chemistry, 272(36), pp.22662-22666.

Macaluso, M., Cinti, C., Russo, G., Russo, A. and Giordano, A., 2003. pRb2/p130-E2F4/5 HDAC1-SUV39H1-p300 and pRb2/p130-E2F4/5-HDAC1-SUV39H1-DNMT1 multimolecular complexes mediate the transcription of estrogen receptor-α in breast cancer. Oncogene, 22(23), pp.3511-3517.

Madureira, P.A., Varshochi, R., Constantinidou, D., Francis, R.E., Coombes, R.C., Yao, K.M. and Lam, E.W.F., 2006. The Forkhead box M1 protein regulates the transcription of the estrogen receptor α in breast cancer cells. Journal of Biological Chemistry, 281(35), pp.25167-25176.

Maeda, G., Chiba, T., Okazaki, M., Satoh, T., Taya, Y., Aoba, T., Kato, K., Kawashiri, S. and Imai, K., 2005. Expression of SIP1 in oral squamous cell carcinomas: implications for E-cadherin expression and tumor progression. International journal of oncology, 27(6), pp.1535-1541.

Maetzel, D., Denzel, S., Mack, B., Canis, M., Went, P., Benk, M., Kieu, C., Papior, P., Baeuerle, P.A., Munz, M. and Gires, O., 2009. Nuclear signalling by tumour-associated antigen EpCAM. Nature cell biology, 11(2), pp.162-171.

Majid, S. and Dahiya, R., 2014. MicroRNA based therapeutic strategies for cancer: Emphasis on advances in renal cell carcinoma. In MicroRNA Targeted Cancer Therapy (pp. 175-188). Springer, Cham.

Majumder, A., Syed, K.M., Mukherjee, A., Lankadasari, M.B., Azeez, J.M., Sreeja, S., Harikumar, K.B., Pillai, M.R. and Dutta, D., 2018. Enhanced expression of histone chaperone APLF associate with breast cancer. Molecular cancer, 17(1), pp.1-9.

Malanchi, I., Santamaria-Martínez, A., Susanto, E., Peng, H., Lehr, H.A., Delaloye, J.F. and Huelsken, J., 2012. Interactions between cancer stem cells and their niche govern metastatic colonization. Nature, 481(7379), pp.85-89.

Manandhar, S., Kim, C.G., Lee, S.H., Kang, S.H., Basnet, N. and Lee, Y.M., 2017. Exostosin 1 regulates cancer cell stemness in doxorubicin-resistant breast cancer cells. Oncotarget, 8(41), p.70521.

Mani, S.A., Guo, W., Liao, M.J., Eaton, E.N., Ayyanan, A., Zhou, A.Y., Brooks, M., Reinhard, F., Zhang, C.C., Shipitsin, M. and Campbell, L.L., 2008. The epithelial-mesenchymal transition generates cells with properties of stem cells. Cell, 133(4), pp.704-715.

Mani, S.A., Guo, W., Liao, M.J., Eaton, E.N., Ayyanan, A., Zhou, A.Y., Brooks, M., Reinhard, F., Zhang, C.C., Shipitsin, M. and Campbell, L.L., 2008. The epithelial-mesenchymal transition generates cells with properties of stem cells. Cell, 133(4), pp.704-715.

Mani, S.A., Yang, J., Brooks, M., Schwaninger, G., Zhou, A., Miura, N., Kutok, J.L., Hartwell, K., Richardson, A.L. and Weinberg, R.A., 2007. Mesenchyme Forkhead 1 (FOXC2) plays a key role in metastasis and is associated with aggressive basal-like breast cancers. Proceedings of the National Academy of Sciences, 104(24), pp.10069-10074.

Manning, B.D. and Cantley, L.C., 2007. AKT/PKB signaling: navigating downstream. Cell, 129(7), pp.1261-1274.

Mansour, S.F. and Atwa, M.M., 2015. Clinicopathological significance of CD133 and ALDH1 cancer stem cell marker expression in invasive ductal breast carcinoma. Asian Pac J Cancer Prev, 16(17), pp.7491-7496.

Mao, Q. and Unadkat, J.D., 2015. Role of the breast cancer resistance protein (BCRP/ABCG2) in drug transport—an update. The AAPS journal, 17(1), pp.65-82.

Mao, Q., Zhang, Y., Fu, X., Xue, J., Guo, W., Meng, M., Zhou, Z., Mo, X. and Lu, Y., 2013. A tumor hypoxic niche protects human colon cancer stem cells from chemotherapy. Journal of cancer research and clinical oncology, 139(2), pp.211-222.

Mao, R., Fan, Y., Mou, Y., Zhang, H., Fu, S. and Yang, J., 2011. TAK1 lysine 158 is required for TGF-β-induced TRAF6-mediated Smad-independent IKK/NF-κB and JNK/AP-1 activation. Cellular signalling, 23(1), pp.222-227.

Maquart, F.X., Pasco, S., Ramont, L., Hornebeck, W. and Monboisse, J.C., 2004. An introduction to matrikines: extracellular matrix-derived peptides which regulate cell activity: implication in tumor invasion. Critical reviews in oncology/hematology, 49(3), pp.199-202.

Maragoudakis, M.E., Kraniti, N., Giannopoulou, E., Alexopoulos, K. and Matsoukas, J., 2001. Modulation of angiogenesis and progelatinase a by thrombin receptor mimetics and antagonists. Endothelium, 8(3), pp.195-206.

Marcath, L.A., Kidwell, K.M., Vangipuram, K., Gersch, C.L., Rae, J.M., Burness, M.L., Griggs, J.J., Van Poznak, C., Hayes, D.F., Smith, E.M.L. and Henry, N.L., 2020. Genetic variation in EPHA contributes to sensitivity to paclitaxel-induced peripheral neuropathy. British Journal of Clinical Pharmacology, 86(5), pp.880-890.

Marcato, P., Dean, C.A., Pan, D., Araslanova, R., Gillis, M., Joshi, M., Helyer, L., Pan, L., Leidal, A., Gujar, S. and Giacomantonio, C.A., 2011. Aldehyde dehydrogenase activity of breast cancer stem cells is primarily due to isoform ALDH1A3 and its expression is predictive of metastasis. Stem cells, 29(1), pp.32-45.

Mareel, M. and Leroy, A., 2003. Clinical, cellular, and molecular aspects of cancer invasion. Physiological reviews, 83(2), pp.337-376.

Marin, F., Luquet, G., Marie, B. and Medakovic, D., 2007. Molluscan shell proteins: primary structure, origin, and evolution. Current topics in developmental biology, 80, pp.209-276.

Marrazzo, E., Frusone, F., Milana, F., Sagona, A., Gatzemeier, W., Barbieri, E., Bottini, A., Canavese, G., Rubino, A.O., Eboli, M.G. and Rossetti, C.M., 2020. Mucinous breast cancer: A narrative review of the literature and a retrospective tertiary single-centre analysis. The Breast, 49, pp.87-92.

Marteijn, J.A., Lans, H., Vermeulen, W. and Hoeijmakers, J.H., 2014. Understanding nucleotide excision repair and its roles in cancer and ageing. Nature reviews Molecular cell biology, 15(7), pp.465-481.

Martin, C.M., Ferdous, A., Gallardo, T., Humphries, C., Sadek, H., Caprioli, A., Garcia, J.A., Szweda, L.I., Garry, M.G. and Garry, D.J., 2008. Hypoxia-inducible factor-2α transactivates Abcg2 and promotes cytoprotection in cardiac side population cells. Circulation research, 102(9), pp.1075-1081.

Martin, L.A., Ribas, R., Simigdala, N., Schuster, E., Pancholi, S., Tenev, T., Gellert, P., Buluwela, L., Harrod, A., Thornhill, A. and Nikitorowicz-Buniak, J., 2017. Discovery of naturally occurring ESR1 mutations in breast cancer cell lines modelling endocrine resistance. Nature communications, 8(1), pp.1-15.

Martinez-Outschoorn, U.E., Goldberg, A.F., Lin, Z., Ko, Y.H., Flomenberg, N., Wang, C., Pavlides, S., Pestell, R.G., Howell, A., Sotgia, F. and Lisanti, M.P., 2011. Anti-estrogen resistance in breast cancer is induced by the tumor microenvironment and can be overcome by inhibiting mitochondrial function in epithelial cancer cells. Cancer biology & therapy, 12(10), pp.924-938.

Martinez-Perez, C., Turnbull, A.K. and Dixon, J.M., 2019. The evolving role of receptors as predictive biomarkers for metastatic breast cancer. Expert review of anticancer therapy, 19(2), pp.121-138.

Martinez-Rico, C., Pincet, F., Thiery, J.P. and Dufour, S., 2010. Integrins stimulate E cadherin-mediated intercellular adhesion by regulating Src-kinase activation and actomyosin contractility. Journal of cell science, 123(5), pp.712-722.

Maruyama, R., Choudhury, S., Kowalczyk, A., Bessarabova, M., Beresford-Smith, B., Conway, T., Kaspi, A., Wu, Z., Nikolskaya, T., Merino, V.F. and Lo, P.K., 2011. Epigenetic regulation of cell type–specific expression patterns in the human mammary epithelium. PLoS Genet, 7(4), p.e1001369.

Mason, W.P., 2015. End of the road: confounding results of the CORE trial terminate the arduous journey of cilengitide for glioblastoma. Masumi, A. and Ozato, K., 2001. Coactivator p300 acetylates the interferon regulatory factor-2 in U937 cells following phorbol ester treatment. Journal of Biological Chemistry, 276(24), pp.20973-20980.

Matloubian, M., Lo, C.G., Cinamon, G., Lesneski, M.J., Xu, Y., Brinkmann, V., Allende, M.L., Proia, R.L. and Cyster, J.G., 2004. Lymphocyte egress from thymus and peripheral lymphoid organs is dependent on S1P receptor 1. Nature, 427(6972), pp.355-360.

Mato, E., Gonzalez, C., Moral, A., Perez, J.I., Bell, O., Lerma, E. and de Leiva, A., 2014. ABCG2/BCRP gene expression is related to epithelial-mesenchymal transition inducer genes in a papillary thyroid carcinoma cell line (TPC-1). J Mol Endocrinol, 52(3), pp.289-300.

Matsudaira, P.T. and Burgess, D.R., 1979. Identification and organization of the components in the isolated microvillus cytoskeleton. The Journal of cell biology, 83(3), pp.667-673.

Maturi, V., Enroth, S., Heldin, C.-H. and Moustakas, A. (2018). Genome-wide binding of transcription factor ZEB1 in triple-negative breast cancer cells. Journal of Cellular Physiology, 233(10), pp.7113–7127.

Maxwell, P.J., Neisen, J., Messenger, J. and Waugh, D.J., 2014. Tumor-derived CXCL8 signaling augments stroma-derived CCL2-promoted proliferation and CXCL12-mediated invasion of PTEN-deficient prostate cancer cells. Oncotarget, 5(13), p.4895.

Mayer, I.A. and Arteaga, C.L., 2016. The PI3K/AKT pathway as a target for cancer treatment. Annual review of medicine, 67, pp.11-28.

McAllister, S.S., Gifford, A.M., Greiner, A.L., Kelleher, S.P., Saelzler, M.P., Ince, T.A., Reinhardt, F., Harris, L.N., Hylander, B.L., Repasky, E.A. and Weinberg, R.A., 2008. Systemic endocrine instigation of indolent tumor growth requires osteopontin. Cell, 133(6), pp.994-1005.

McAndrews, K.M., McGrail, D.J., Ravikumar, N. and Dawson, M.R., 2015. Mesenchymal stem cells induce directional migration of invasive breast cancer cells through TGF-β. Scientific reports, 5, p.16941.

McDonald, O.G., Wu, H., Timp, W., Doi, A. and Feinberg, A.P., 2011. Genome-scale epigenetic reprogramming during epithelial-to-mesenchymal transition. Nature structural & molecular biology, 18(8), p.867.

McGovern, S.L., Qi, Y., Pusztai, L., Symmans, W.F. and Buchholz, T.A., 2012. Centromere protein-A, an essential centromere protein, is a prognostic marker for relapse in estrogen receptor-positive breast cancer. Breast Cancer Research, 14(3), p.R72.

McGovern, S.L., Qi, Y., Pusztai, L., Symmans, W.F. and Buchholz, T.A., 2012. Centromere protein-A, an essential centromere protein, is a prognostic marker for relapse in estrogen receptor-positive breast cancer. Breast Cancer Research, 14(3), p.R72.

McGowan, S.E. and McCoy, D.M., 2013. Platelet-derived growth factor-A regulates lung fibroblast S-phase entry through p27 kip1 and FoxO3a. Respiratory research, 14(1), p.68.

McGrogan, B.T., Gilmartin, B., Carney, D.N. and McCann, A. (2008). Taxanes, microtubules and chemoresistant breast cancer. Biochimica et Biophysica Acta (BBA) - Reviews on Cancer, 1785(2), pp.96–132.

McLachlan, R.W., 2007. Not so simple: the complexity of phosphotyrosine signaling at cadherin adhesive contacts. Journal of Molecular Medicine, 85(6), pp.545-554.

McLean, K., Gong, Y., Choi, Y., Deng, N., Yang, K., Bai, S., Cabrera, L., Keller, E., McCauley, L., Cho, K.R. and Buckanovich, R.J., 2011. Human ovarian carcinoma–associated mesenchymal stem cells regulate cancer stem cells and tumorigenesis via altered BMP production. The Journal of clinical investigation, 121(8), pp.3206-3219.

Mege, R.M., Gavard, J. and Lambert, M., 2006. Regulation of cell–cell junctions by the cytoskeleton. Current opinion in cell biology, 18(5), pp.541-548.

Meidhof, S., Brabletz, S., Lehmann, W., Preca, B., Mock, K., Ruh, M., Schüler, J., Berthold, M., Weber, A., Burk, U., Lübbert, M., Puhr, M., Culig, Z., Wellner, U., Keck, T., Bronsert, P., Küsters, S., Hopt, U.T., Stemmler, M.P. and Brabletz, T. (2015). ZEB 1-associated drug resistance in cancer cells is reversed by the class I HDAC inhibitor mocetinostat. EMBO Molecular Medicine, 7(6), pp.831–847.

Meijnen, P., Oldenburg, H.S., Peterse, J.L., Bartelink, H. and Emiel, J.T., 2008. Clinical outcome after selective treatment of patients diagnosed with ductal carcinoma in situ of the breast. Annals of Surgical Oncology, 15(1), pp.235-243.

Memmi, E.M., Sanarico, A.G., Giacobbe, A., Peschiaroli, A., Frezza, V., Cicalese, A., Pisati, F., Tosoni, D., Zhou, H., Tonon, G. and Antonov, A., 2015. p63 Sustains self-renewal

of mammary cancer stem cells through regulation of Sonic Hedgehog signaling. Proceedings of the National Academy of Sciences, 112(11), pp.3499-3504.

Mertens-Talcott, S.U., Chintharlapalli, S., Li, X. and Safe, S., 2007. The oncogenic microRNA-27a targets genes that regulate specificity protein transcription factors and the G2-M checkpoint in MDA-MB-231 breast cancer cells. Cancer research, 67(22), pp.11001-11011.

Mertz, J.A., Conery, A.R., Bryant, B.M., Sandy, P., Balasubramanian, S., Mele, D.A., Bergeron, L. and Sims, R.J., 2011. Targeting MYC dependence in cancer by inhibiting BET bromodomains. Proceedings of the National Academy of Sciences, 108(40), pp.16669-16674.

Messica, Y., Laser-Azogui, A., Volberg, T., Elisha, Y., Lysakovskaia, K., Eils, R., Gladilin, E., Geiger, B. and Beck, R., 2017. The role of vimentin in regulating cell invasive migration in dense cultures of breast carcinoma cells. Nano letters, 17(11), pp.6941-6948.

Messier, T.L., Gordon, J.A., Boyd, J.R., Tye, C.E., Browne, G., Stein, J.L., Lian, J.B. and Stein, G.S., 2016. Histone H3 lysine 4 acetylation and methylation dynamics define breast cancer subtypes. Oncotarget, 7(5), p.5094.

Metzger, E., Wissmann, M., Yin, N., Müller, J.M., Schneider, R., Peters, A.H., Günther, T., Buettner, R. and Schüle, R., 2005. LSD1 demethylates repressive histone marks to promote androgen-receptor-dependent transcription. Nature, 437(7057), pp.436-439.

Meyer, M.J., Fleming, J.M., Ali, M.A., Pesesky, M.W., Ginsburg, E. and Vonderhaar, B.K., 2009. Dynamic regulation of CD24 and the invasive, CD44 pos CD24 neg phenotype in breast cancer cell lines. Breast Cancer Research, 11(6), p.R82.

Meyvantsson, I. and Beebe, D.J., 2008. Cell culture models in microfluidic systems. Annu. Rev. Anal. Chem., 1, pp.423-449.

Mi, Y.J., Liang, Y.J., Huang, H.B., Zhao, H.Y., Wu, C.P., Wang, F., Tao, L.Y., Zhang, C.Z., Dai, C.L., Tiwari, A.K. and Ma, X.X., 2010. Apatinib (YN968D1) reverses multidrug resistance by inhibiting the efflux function of multiple ATP-binding cassette transporters. Cancer research, 70(20), pp.7981-7991.

Michalak, E.M. and Visvader, J.E., 2016. Dysregulation of histone methyltransferases in breast cancer–Opportunities for new targeted therapies?. Molecular oncology, 10(10), pp.1497-1515.

Miettinen, P.J., Ebner, R., Lopez, A.R. and Derynck, R., 1994. TGF-beta induced transdifferentiation of mammary epithelial cells to mesenchymal cells: involvement of type I receptors. The Journal of cell biology, 127(6), pp.2021-2036.

Min, S., Li, L., Zhang, M., Zhang, Y., Liang, X., Xie, Y., He, Q., Li, Y., Sun, J., Liu, Q. and Jiang, X., 2012. TGF-β-associated miR-27a inhibits dendritic cell-mediated

differentiation of Th1 and Th17 cells by TAB3, p38 MAPK, MAP2K4 and MAP2K7. Genes and immunity, 13(8), pp.621-631.

Minciacchi, V.R., Freeman, M.R. and Di Vizio, D., 2015, April. Extracellular vesicles in cancer: exosomes, microvesicles and the emerging role of large oncosomes. In Seminars in cell & developmental biology (Vol. 40, pp. 41-51). Academic Press.

Minderman, H., O'Loughlin, K.L., Pendyala, L. and Baer, M.R., 2004. VX-710 (biricodar) increases drug retention and enhances chemosensitivity in resistant cells overexpressing P-glycoprotein, multidrug resistance protein, and breast cancer resistance protein. Clinical Cancer Research, 10(5), pp.1826-1834.

Mironchik, Y., Winnard Jr, P.T., Vesuna, F., Kato, Y., Wildes, F., Pathak, A.P., Kominsky, S., Artemov, D., Bhujwalla, Z., Van Diest, P. and Burger, H., 2005. Twist Overexpression Induces. Mistry, D.S., Chen, Y., Wang, Y., Zhang, K. and Sen, G.L., 2014. SNAI2 controls the undifferentiated state of human epidermal progenitor cells. Stem Cells, 32(12), pp.3209-3218.

Mitra, A.K., Sawada, K., Tiwari, P., Mui, K., Gwin, K. and Lengyel, E., 2011. Ligand independent activation of c-Met by fibronectin and α 5 β 1-integrin regulates ovarian cancer invasion and metastasis. Oncogene, 30(13), pp.1566-1576

Miyazono, K., Hellman, U., Wernstedt, C. and Heldin, C.H., 1988. Latent high molecular weight complex of transforming growth factor beta 1. Purification from human platelets and structural characterization. Journal of Biological Chemistry, 263(13), pp.6407-6415.

Moarii, M., Boeva, V., Vert, J.P. and Reyal, F., 2015. Changes in correlation between promoter methylation and gene expression in cancer. BMC genomics, 16(1), pp.1-14.

Moitra, K. and Dean, M., 2011. Evolution of ABC transporters by gene duplication and their role in human disease. Biological chemistry, 392(1-2), pp.29-37.

Moldoveanu, T., Campbell, R.L., Cuerrier, D. and Davies, P.L. (2004). Crystal Structures of Calpain–E64 and –Leupeptin Inhibitor Complexes Reveal Mobile Loops Gating the Active Site. Journal of Molecular Biology, 343(5), pp.1313–1326.

Moldoveanu, T., Grace, C.R., Llambi, F., Nourse, A., Fitzgerald, P., Gehring, K., Kriwacki, R.W. and Green, D.R., 2013. BID-induced structural changes in BAK promote apoptosis. Nature structural & molecular biology, 20(5), p.589.

Molyneux, G., Geyer, F.C., Magnay, F.A., McCarthy, A., Kendrick, H., Natrajan, R., MacKay, A., Grigoriadis, A., Tutt, A., Ashworth, A. and Reis-Filho, J.S., 2010. BRCA1 basal-like breast cancers originate from luminal epithelial progenitors and not from basal stem cells. Cell stem cell, 7(3), pp.403-417.

Montero, A.J., Escobar, M., Lopes, G., Glück, S. and Vogel, C., 2012. Bevacizumab in the treatment of metastatic breast cancer: friend or foe?. Current oncology reports, 14(1), pp.1-11.

Montt-Guevara, M.M., Shortrede, J.E., Giretti, M.S., Giannini, A., Mannella, P., Russo, E., Genazzani, A.D. and Simoncini, T., 2016. Androgens regulate T47D cells motility and invasion through actin cytoskeleton remodeling. Frontiers in endocrinology, 7, p.136.

Moore, K.M., Thomas, G.J., Duffy, S.W., Warwick, J., Gabe, R., Chou, P., Ellis, I.O., Green, A.R., Haider, S., Brouilette, K. and Saha, A., 2014. Therapeutic targeting of integrin αvβ6 in breast cancer. JNCI: Journal of the National Cancer Institute, 106(8).

Morales, S., Monzo, M. and Navarro, A., 2017. Epigenetic regulation mechanisms of microRNA expression. Biomolecular concepts, 8(5-6), pp.203-212.

Moran, T., Gat, Y. and Fass, D., 2015. Laminin L4 domain structure resembles adhesion modules in ephrin receptor and other transmembrane glycoproteins. The FEBS journal, 282(14), pp.2746-2757.

Moreau, V., Frischknecht, F., Reckmann, I., Vincentelli, R., Rabut, G., Stewart, D. and Way, M., 2000. A complex of N-WASP and WIP integrates signalling cascades that lead to actin polymerization. Nature cell biology, 2(7), pp.441-448.

Morel, A.P., Ginestier, C., Pommier, R.M., Cabaud, O., Ruiz, E., Wicinski, J., Devouassoux Shisheboran, M., Combaret, V., Finetti, P., Chassot, C. and Pinatel, C., 2017. A stemness-related ZEB1–MSRB3 axis governs cellular pliancy and breast cancer genome stability. Nature medicine, 23(5), p.568.

Morel, A.P., Lièvre, M., Thomas, C., Hinkal, G., Ansieau, S. and Puisieux, A., 2008. Generation of breast cancer stem cells through epithelial-mesenchymal transition. PloS one, 3(8), p.e2888.

Morel, A.P., Lièvre, M., Thomas, C., Hinkal, G., Ansieau, S. and Puisieux, A., 2008. Generation of breast cancer stem cells through epithelial-mesenchymal transition. PloS one, 3(8), p.e2888.

Morley, S.C., 2012. The actin-bundling protein L-plastin: a critical regulator of immune cell function. International journal of cell biology, 2012.

Morley, S.C., 2013. The actin-bundling protein L-plastin supports T-cell motility and activation. Immunological reviews, 256(1), pp.48-62.

Morozov, V.M., Massoll, N.A., Vladimirova, O.V., Maul, G.G. and Ishov, A.M., 2008. Regulation of c-met expression by transcription repressor Daxx. Oncogene, 27(15), pp.2177-2186.

Morrissey, M.A., Keeley, D.P., Hagedorn, E.J., McClatchey, S.T., Chi, Q., Hall, D.H. and Sherwood, D.R., 2014. B-LINK: a hemicentin, plakin, and integrin-dependent adhesion

system that links tissues by connecting adjacent basement membranes. Developmental cell, 31(3), pp.319-331.

Morrow, D., Sweeney, C., Birney, Y.A., Cummins, P.M., Walls, D., Redmond, E.M. and Cahill, P.A., 2005. Cyclic strain inhibits Notch receptor signaling in vascular smooth muscle cells in vitro. Circulation research, 96(5), pp.567-575.

Moses, H.L., Yang, E.Y. and Pietenpol, J.A., 1990. TGF-β stimulation and inhibition of cell proliferation: new mechanistic insights. Cell, 63(2), pp.245-247.

Moss, L.A.S., Jensen-Taubman, S. and Stetler-Stevenson, W.G., 2012. Matrix metalloproteinases: changing roles in tumor progression and metastasis. The American journal of pathology, 181(6), pp.1895-1899.

Moulder, S.L., Symmans, W.F., Booser, D.J., Madden, T.L., Lipsanen, C., Yuan, L., Brewster, A.M., Cristofanilli, M., Hunt, K.K., Buchholz, T.A. and Zwiebel, J., 2008. Phase I/II study of G3139 (Bcl-2 antisense oligonucleotide) in combination with doxorubicin and docetaxel in breast cancer. Clinical Cancer Research, 14(23), pp.7909-7916. Moustakas, A. and Heldin, C.-H. (2009). The regulation of TGF signal transduction. Development, 136(22), pp.3699–3714.

Moustakas, A., 2005. Heldin CH. Non-Smad TGF-beta signals. J Cell Sci, 118, pp.3573 3584.

Muhammad, N., Bhattacharya, S., Steele, R., Phillips, N. and Ray, R.B., 2017. Involvement of c-Fos in the promotion of cancer stem-like cell properties in head and neck squamous cell carcinoma. Clinical Cancer Research, 23(12), pp.3120-3128.

Mukai, Y., Nakamura, T., Yoshikawa, M., Yoshioka, Y., Tsunoda, S.I., Nakagawa, S., Yamagata, Y. and Tsutsumi, Y., 2010. Solution of the structure of the TNF-TNFR2 complex. Science signaling, 3(148), pp.ra83-ra83.

Müller, A., Homey, B., Soto, H., Ge, N., Catron, D., Buchanan, M.E., McClanahan, T., Murphy, E., Yuan, W., Wagner, S.N. and Barrera, J.L., 2001. Involvement of chemokine receptors in breast cancer metastasis. nature, 410(6824), pp.50-56.

Müller, M., Meijer, C.J.L.M., Zaman, G.J., Borst, P., Scheper, R.J., Mulder, N.H., De Vries, E.G. and Jansen, P.L., 1994. Overexpression of the gene encoding the multidrug resistance-associated protein results in increased ATP-dependent glutathione S-conjugate transport. Proceedings of the National Academy of Sciences, 91(26), pp.13033-13037.

Muluhngwi, P. and Klinge, C.M., 2015. Roles for miRNAs in endocrine resistance in breast cancer. Endocrine-related cancer, 22(5), p.R279.

Munagala, R., Aqil, F. and Gupta, R.C., 2011. Promising molecular targeted therapies in breast cancer. Indian journal of pharmacology, 43(3), p.236.

Munshi, H.G. and Stack, M.S., 2006. Reciprocal interactions between adhesion receptor signaling and MMP regulation. Cancer and Metastasis Reviews, 25(1), pp.45-56.

Murakami, M., Takahashi, K. and Yamanaka, S. (2005). Role of the phosphoinositide 3-kinase pathway in mouse embryonic stem (ES) cells. Biochemical Society Transactions, 33(6), p.1522.

Muraoka, M., Konishi, M., Kikuchi−Yanoshita, R., Tanaka, K., Shitara, N., Chong, J.M., Iwama, T. and Miyaki, M., 1996. p300 gene alterations in colorectal and gastric carcinomas. oncogene, 12(7), p.1565.

Murray, C.J. and Lopez, A.D., 1997. Mortality by cause for eight regions of the world: Global Burden of Disease Study. The lancet, 349(9061), pp.1269-1276.

Mylona, E., Giannopoulou, I., Fasomytakis, E., Nomikos, A., Magkou, C., Bakarakos, P. and Nakopoulou, L., 2008. The clinicopathologic and prognostic significance of CD44+/CD24−/low and CD44−/CD24+ tumor cells in invasive breast carcinomas. Human pathology, 39(7), pp.1096-1102.

Nadler, Y., Camp, R.L., Giltnane, J.M., Moeder, C., Rimm, D.L., Kluger, H.M. and Kluger, Y., 2008. Expression patterns and prognostic value of Bag-1 and Bcl-2 in breast cancer. Breast Cancer Research, 10(2), p.R35.

Nagano, M., Hoshino, D., Koshikawa, N., Akizawa, T. and Seiki, M., 2012. Turnover of focal adhesions and cancer cell migration. International journal of cell biology, 2012.

Nair, N.U., Das, A., Rogkoti, V.M., Fokkelman, M., Marcotte, R., de Jong, C.G., Koedoot, E., Lee, J.S., Meilijson, I., Hannenhalli, S. and Neel, B.G., 2019. Migration rather than proliferation transcriptomic signatures are strongly associated with breast cancer patient survival. Scientific reports, 9(1), pp.1-12.

Nair, V.A., Al-khayyal, N.A., Sivaperumal, S. and Abdel-Rahman, W.M., 2019. Calponin 3 promotes invasion and drug resistance of colon cancer cells. World Journal of Gastrointestinal Oncology, 11(11), p.971.

Naito, S. (2011). p300 mediates cellular resistance to doxorubicin in bladder cancer. Molecular Medicine Reports. Nakajima, G., Patiño-Garcia, A., Bruheim, S., Xi, Y., San Julian, M., Lecanda, F., Sierrasesumaga, L., Müller, C., Fodstad, O. and Ju, J., 2008. CDH11 expression is associated with survival in patients with osteosarcoma. Cancer Genomics-Proteomics, 5(1), pp.37-42.

Nakanishi, T. and Ross, D.D., 2012. Breast cancer resistance protein (BCRP/ABCG2): its role in multidrug resistance and regulation of its gene expression. Chinese journal of cancer, 31(2), p.73.

Nakayama, S., Torikoshi, Y., Takahashi, T., Yoshida, T., Sudo, T., Matsushima, T., Kawasaki, Y., Katayama, A., Gohda, K., Hortobagyi, G.N. and Noguchi, S., 2009. Prediction

of paclitaxel sensitivity by CDK1 and CDK2 activity in human breast cancer cells. Breast Cancer Research, 11(1), p.R12.

Nami, B. and Wang, Z., 2017. HER2 in breast cancer stemness: A negative feedback loop towards trastuzumab resistance. Cancers, 9(5), p.40.

Nami, B., Ghanaeian, A. and Wang, Z., 2020. Epigenetic downregulation of HER2 during EMT leads to tumor resistance to HER2-targeted therapies in breast cancer. bioRxiv. Naor, D., Wallach-Dayan, S.B., Zahalka, M.A. and Sionov, R.V., 2009. Involvement of CD44, a molecule with a thousand faces, in cancer dissemination. In Hyaluronan in Cancer Biology (pp. 127-146). Academic Press.

Nardone, G., Oliver-De La Cruz, J., Vrbsky, J., Martini, C., Pribyl, J., Skládal, P., Pešl, M., Caluori, G., Pagliari, S., Martino, F. and Maceckova, Z., 2017. YAP regulates cell mechanics by controlling focal adhesion assembly. Nature communications, 8(1), pp.1-13.

Naudé, P.J., den Boer, J.A., Luiten, P.G. and Eisel, U.L., 2011. Tumor necrosis factor receptor cross-talk. The FEBS journal, 278(6), pp.888-898.

Nawijn, M.C., Ferreira, R., Dingjan, G.M., Kahre, O., Drabek, D., Karis, A., Grosveld, F. and Hendriks, R.W., 2001. Enforced expression of GATA-3 during T cell development inhibits maturation of CD8 single-positive cells and induces thymic lymphoma in transgenic mice. The Journal of Immunology, 167(2), pp.715-723.

Nawrocki-Raby, B., Gilles, C., Polette, M., Bruyneel, E., Laronze, J.Y., Bonnet, N., Foidart, J.M., Mareel, M. and Birembaut, P., 2003. Upregulation of MMPs by soluble E-cadherin in human lung tumor cells. International journal of cancer, 105(6), pp.790-795.

Nayak, S.R., Harrington, E., Boone, D., Hartmaier, R., Chen, J., Pathiraja, T.N., Cooper, K.L., Fine, J.L., Sanfilippo, J., Davidson, N.E. and Lee, A.V., 2015. A role for histone H2B variants in endocrine-resistant breast cancer. Hormones and Cancer, 6(5-6), pp.214-224.

NCCN. 2014. NCCN Guidelines for Patients. Stage 0 Breast Cancer. Fort Washington, PA, National Comprehensive Cancer Network (NCCN) Foundation. Neelakantan, D., Drasin, D.J. and Ford, H.L., 2015. Intratumoral heterogeneity: clonal cooperation in epithelial-to-mesenchymal transition and metastasis. Cell adhesion & migration, 9(4), pp.265-276.

Neilsen, C.T., Goodall, G.J. and Bracken, C.P., 2012. IsomiRs–the overlooked repertoire in the dynamic microRNAome. Trends in genetics, 28(11), pp.544-549.

Neve, R.M., Chin, K., Fridlyand, J., Yeh, J., Baehner, F.L., Fevr, T., Clark, L., Bayani, N., Coppe, J.P., Tong, F. and Speed, T., 2006. A collection of breast cancer cell lines for the study of functionally distinct cancer subtypes. Cancer cell, 10(6), pp.515-527.

Nho, R.S., Im, J., Ho, Y.Y. and Hergert, P., 2014. MicroRNA-96 inhibits FoxO3a function in IPF fibroblasts on type I collagen matrix. American Journal of Physiology-Lung Cellular and Molecular Physiology, 307(8), pp.L632-L642.

Nicholson, S., Wright, C., Sainsbury, J.R.C., Halcrow, P., Kelly, P., Angus, B., FarnVon, J.R. and Harris, A.L., 1990. Epidermal growth factor receptor (EGFr) as a marker for poor prognosis in node-negative breast cancer patients: neu and tamoxifen failure. The Journal of Steroid Biochemistry and Molecular Biology, 37(6), pp.811-814.

Nieminen, M., Henttinen, T., Merinen, M., Marttila–Ichihara, F., Eriksson, J.E. and Jalkanen, S., 2006. Vimentin function in lymphocyte adhesion and transcellular migration. Nature cell biology, 8(2), pp.156-162.

Nieto, M.A., 2009. Epithelial-Mesenchymal Transitions in development and disease: old views and new perspectives. International Journal of Developmental Biology, 53(8-9-10), pp.1541-1547.

Niimura, M., Isoo, N., Takasugi, N., Tsuruoka, M., Ui-Tei, K., Saigo, K., Morohashi, Y., Tomita, T. and Iwatsubo, T., 2005. Aph-1 contributes to the stabilization and trafficking of the γ-secretase complex through mechanisms involving intermolecular and intramolecular interactions. Journal of Biological Chemistry, 280(13), pp.12967-12975.

Nikitaki, Z., Michalopoulos, I. and Georgakilas, A.G., 2015. Molecular inhibitors of DNA repair: searching for the ultimate tumor killing weapon. Future medicinal chemistry, 7(12), pp.1543-1558.

Nilsson, G., Akhtar, N., Kannius-Janson, M. and Baeckström, D., 2014. Loss of E-cadherin expression is not a prerequisite for c-erbB2-induced epithelial-mesenchymal transition. International journal of oncology, 45(1), pp.82-94.

Niv, Y., 2008. MUC1 and colorectal cancer pathophysiology considerations. World Journal of Gastroenterology: WJG, 14(14), p.2139.

Noble, M.E., Endicott, J.A. and Johnson, L.N., 2004. Protein kinase inhibitors: insights into drug design from structure. Science, 303(5665), pp.1800-1805.

Noblitt, L.W., Bangari, D.S., Shukla, S., Mohammed, S. and Mittal, S.K., 2005. Immunocompetent mouse model of breast cancer for preclinical testing of EphA2-targeted therapy. Cancer gene therapy, 12(1), pp.46-53.

Nomoto, S., Kanda, M., Okamura, Y., Nishikawa, Y., Qiyong, L., Fujii, T., Sugimoto, H., Takeda, S. and Nakao, A., 2010. Epidermal growth factor-containing fibulin-like extracellular matrix protein 1, EFEMP1, a novel tumor-suppressor gene detected in hepatocellular carcinoma using double combination array analysis. Annals of surgical oncology, 17(3), pp.923-932.

Norman, P.J., Norberg, S.J., Guethlein, L.A., Nemat-Gorgani, N., Royce, T., Wroblewski, E.E., Dunn, T., Mann, T., Alicata, C., Hollenbach, J.A. and Chang, W., 2017. Sequences of 95 human MHC haplotypes reveal extreme coding variation in genes other than highly polymorphic HLA class I and II. Genome research, 27(5), pp.813-823.

O'Brien, S.K., Chen, L., Zhong, W., Armellino, D., Yu, J., Loreth, C., Follettie, M. and Damelin, M., 2015. Breast cancer cells respond differentially to modulation of TGFβ2 signaling after exposure to chemotherapy or hypoxia. Cancer research, 75(21), pp.4605-4616.

Ocaña, O.H., Córcoles, R., Fabra, Á., Moreno-Bueno, G., Acloque, H., Vega, S., Barrallo Gimeno, A., Cano, A. and Nieto, M.A., 2012. Metastatic colonization requires the repression of the epithelial-mesenchymal transition inducer Prrx1. Cancer cell, 22(6), pp.709-724.

Oda, H. and Takeichi, M., 2011. Structural and functional diversity of cadherin at the adherens junction. Journal of Cell Biology, 193(7), pp.1137-1146.

Ogryzko, V.V., Schiltz, R.L., Russanova, V., Howard, B.H. and Nakatani, Y., 1996. The transcriptional coactivators p300 and CBP are histone acetyltransferases. Cell, 87(5), pp.953-959.

Oh, D.S., Troester, M.A., Usary, J., Hu, Z., He, X., Fan, C., Wu, J., Carey, L.A. and Perou, C.M., 2006. Estrogen-regulated genes predict survival in hormone receptor-positive breast cancers. J Clin Oncol, 24(11), pp.1656-1664.

Ohashi, S., Natsuizaka, M., Wong, G.S., Michaylira, C.Z., Grugan, K.D., Stairs, D.B., Kalabis, J., Vega, M.E., Kalman, R.A., Nakagawa, M. and Klein-Szanto, A.J., 2010. Epidermal growth factor receptor and mutant p53 expand an esophageal cellular subpopulation capable of epithelial-to-mesenchymal transition through ZEB transcription factors. Cancer research, 70(10), pp.4174-4184.

Ohata, Y., Shimada, S., Akiyama, Y., Mogushi, K., Nakao, K., Matsumura, S., Aihara, A., Mitsunori, Y., Ban, D., Ochiai, T. and Kudo, A., 2017. Acquired resistance with epigenetic alterations under long-term antiangiogenic therapy for hepatocellular carcinoma. Molecular cancer therapeutics, 16(6), pp.1155-1165.

Ohnishi, H., Taki, T., Yoshino, H., Takita, J., Ida, K., Ishii, M., Nishida, K., Hayashi, Y., Taniwaki, M., Bessho, F. and Watanabe, T., 2008. A complex t (1; 22; 11)(q44; q13; q23) translocation causing MLL-p300 fusion gene in therapy-related acute myeloid leukemia. European journal of haematology, 81(6), pp.475-480.

Ohta, M., Massague, J., Anklesaria, P., FitzGerald, T.J. and Greenberger, J.S., 1987. Type β transforming growth factor (TGF-β) regulates differentiation and proliferation of multipotential hematopoietic progenitor cells. Nature, 329, pp.539-541.

Oida, K., Matsuda, A., Jung, K., Xia, Y., Jang, H., Amagai, Y., Ahn, G., Nishikawa, S., Ishizaka, S., Jensen-Jarolim, E. and Matsuda, H., 2014. Nuclear factor-κB plays a critical role in both intrinsic and acquired resistance against endocrine therapy in human breast cancer cells. Scientific reports, 4(1), pp.1-8.

Oikawa, S., Inuzuka, C., Kuroki, M., Matsuoka, Y., Kosaki, G. and Nakazato, H., 1989. Cell adhesion activity of non-specific cross-reacting antigen (NCA) and carcinoembryonic

antigen (CEA) expressed on CHO cell surface: homophilic and heterophilic adhesion. Biochemical and biophysical research communications, 164(1), pp.39-45.

Okuda, H., Kobayashi, A., Xia, B., Watabe, M., Pai, S.K., Hirota, S., Xing, F., Liu, W., Pandey, P.R., Fukuda, K. and Modur, V., 2012. Hyaluronan synthase HAS2 promotes tumor progression in bone by stimulating the interaction of breast cancer stem–like cells with macrophages and stromal cells. Cancer research, 72(2), pp.537-547.

Okugawa, Y., Toiyama, Y., Tanaka, K., Matsusita, K., Fujikawa, H., Saigusa, S., Ohi, M., Inoue, Y., Mohri, Y., Uchida, K. and Kusunoki, M., 2012. Clinical significance of zinc finger E-box binding homeobox 1 (ZEB1) in human gastric cancer. Journal of surgical oncology, 106(3), pp.280-285.

Onder, T.T., Gupta, P.B., Mani, S.A., Yang, J., Lander, E.S. and Weinberg, R.A., 2008. Loss of E-cadherin promotes metastasis via multiple downstream transcriptional pathways. Cancer research, 68(10), pp.3645-3654.

Ono, M., Kosaka, N., Tominaga, N., Yoshioka, Y., Takeshita, F., Takahashi, R.U., Yoshida, M., Tsuda, H., Tamura, K. and Ochiya, T., 2014. Exosomes from bone marrow mesenchymal stem cells contain a microRNA that promotes dormancy in metastatic breast cancer cells. Science signaling, 7(332), pp.ra63-ra63.

Ono, Y. and Sorimachi, H., 2012. Calpains—An elaborate proteolytic system. Biochimica et Biophysica Acta (BBA)-Proteins and Proteomics, 1824(1), pp.224-236.

Oppong, B.A. and King, T.A., 2011. Recommendations for women with lobular carcinoma in situ (LCIS). Oncology, 25(11).

Ordoñez, C., Screaton, R.A., Ilantzis, C. and Stanners, C.P., 2000. Human carcinoembryonic antigen functions as a general inhibitor of anoikis. Cancer research, 60(13), pp.3419-3424.

Orecchioni, S., Gregato, G., Martin-Padura, I., Reggiani, F., Braidotti, P., Mancuso, P., Calleri, A., Quarna, J., Marighetti, P., Aldeni, C. and Pruneri, G., 2013. Complementary populations of human adipose CD34+ progenitor cells promote growth, angiogenesis, and metastasis of breast cancer. Cancer research, 73(19), pp.5880-5891.

Ørom, U.A., Nielsen, F.C. and Lund, A.H., 2008. MicroRNA-10a binds the 5' UTR of ribosomal protein mRNAs and enhances their translation. Molecular cell, 30(4), pp.460-471.

Ortega, S., Ittmann, M., Tsang, S.H., Ehrlich, M. and Basilico, C., 1998. Neuronal defects and delayed wound healing in mice lacking fibroblast growth factor 2. Proceedings of the National Academy of Sciences, 95(10), pp.5672-5677.

Ota, T., Fujii, M., Sugizaki, T., Ishii, M., Miyazawa, K., Aburatani, H. and Miyazono, K. (2002). Targets of transcriptional regulation by two distinct type I receptors for transforming

growth factor-? in human umbilical vein endothelial cells. Journal of Cellular Physiology, 193(3), pp.299–318.

Otani, H., Otsuka, F., Inagaki, K., Takeda, M., Miyoshi, T., Suzuki, J., Mukai, T., Ogura, T. and Makino, H., 2007. Antagonistic effects of bone morphogenetic protein-4 and-7 on renal mesangial cell proliferation induced by aldosterone through MAPK activation. American Journal of Physiology-Renal Physiology, 292(5), pp.F1513-F1525.

Oudin, M.J., Barbier, L., Schäfer, C., Kosciuk, T., Miller, M.A., Han, S., Jonas, O., Lauffenburger, D.A. and Gertler, F.B., 2017. MENA confers resistance to paclitaxel in triple-negative breast cancer. Molecular cancer therapeutics, 16(1), pp.143-155.

Ozdamar, B., Bose, R., Barrios-Rodiles, M., Wang, H.R., Zhang, Y. and Wrana, J.L., 2005. Regulation of the polarity protein Par6 by TGFß receptors controls epithelial cell plasticity. Science, 307(5715), pp.1603-1609.

Padmanaban, V., Krol, I., Suhail, Y., Szczerba, B.M., Aceto, N., Bader, J.S. and Ewald, A.J., 2019. E-cadherin is required for metastasis in multiple models of breast cancer. Nature, 573(7774), pp.439-444.

Padua, D., Zhang, X.H.F., Wang, Q., Nadal, C., Gerald, W.L., Gomis, R.R. and Massagué, J., 2008. TGFβ primes breast tumors for lung metastasis seeding through angiopoietin-like 4. Cell, 133(1), pp.66-77.

Palasuberniam, P., Yang, X., Kraus, D., Jones, P., Myers, K.A. and Chen, B., 2015. ABCG2 transporter inhibitor restores the sensitivity of triple negative breast cancer cells to aminolevulinic acid-mediated photodynamic therapy. Scientific reports, 5(1), pp.1-12.

Palumbo, J.S., Talmage, K.E., Massari, J.V., La Jeunesse, C.M., Flick, M.J., Kombrinck, K.W., Jirousková, M. and Degen, J.L., 2005. Platelets and fibrin (ogen) increase metastatic potential by impeding natural killer cell–mediated elimination of tumor cells. Blood, 105(1), pp.178-185.

Pan, S.T., Li, Z.L., He, Z.X., Qiu, J.X. and Zhou, S.F., 2016. Molecular mechanisms for tumour resistance to chemotherapy. Clinical and Experimental Pharmacology and Physiology, 43(8), pp.723-737.

Pan, Y., Lu, F., Xiong, P., Pan, M., Zhang, Z., Lin, X., Pan, M. and Huang, H., 2018. WIPF1 antagonizes the tumor suppressive effect of miR-141/200c and is associated with poor survival in patients with PDAC. Journal of Experimental & Clinical Cancer Research, 37(1), p.167.

Pantel, K., Alix-Panabières, C. and Riethdorf, S., 2009. Cancer micrometastases. Nature reviews Clinical oncology, 6(6), pp.339-351.

Pardossi-Piquard, R., Dunys, J., Giaime, E., Guillot-Sestier, M.V., St. George-Hyslop, P., Checler, F. and Alves da Costa, C., 2009. p53-Dependent control of cell death by nicastrin:

lack of requirement for presenilin-dependent γ-secretase complex. Journal of neurochemistry, 109(1), pp.225-237.

Park, C.C., Mitsumori, M., Nixon, A., Recht, A., Connolly, J., Gelman, R., Silver, B., Hetelekidis, S., Abner, A., Harris, J.R. and Schnitt, S.J., 2000. Outcome at 8 years after breast-conserving surgery and radiation therapy for invasive breast cancer: influence of margin status and systemic therapy on local recurrence. Journal of Clinical Oncology, 18(8), pp.1668-1675.

Park, C.C., Zhang, H.J., Yao, E.S., Park, C.J. and Bissell, M.J., 2008. β1 integrin inhibition dramatically enhances radiotherapy efficacy in human breast cancer xenografts. Cancer research, 68(11), pp.4398-4405.

Park, I.K., Morrison, S.J. and Clarke, M.F., 2004. Bmi1, stem cells, and senescence regulation. The Journal of clinical investigation, 113(2), pp.175-179.

Park, J.I., Venteicher, A.S., Hong, J.Y., Choi, J., Jun, S., Shkreli, M., Chang, W., Meng, Z., Cheung, P., Ji, H. and McLaughlin, M., 2009. Telomerase modulates Wnt signalling by association with target gene chromatin. Nature, 460(7251), pp.66-72.

Park, S.J., Wu, C.H., Gordon, J.D., Zhong, X., Emami, A. and Safa, A.R., 2004. Taxo induces caspase-10-dependent apoptosis. Journal of Biological Chemistry, 279(49), pp.51057-51067.

Park, S.M., Gaur, A.B., Lengyel, E. and Peter, M.E., 2008. The miR-200 family determines the epithelial phenotype of cancer cells by targeting the E-cadherin repressors ZEB1 and ZEB2. Genes & development, 22(7), pp.894-907.

Park, S.Y., Kim, H.M. and Koo, J.S., 2015. Differential expression of cancer-associated fibroblast-related proteins according to molecular subtype and stromal histology in breast cancer. Breast cancer research and treatment, 149(3), pp.727-741.

Park, S.Y., Lee, H.E., Li, H., Shipitsin, M., Gelman, R. and Polyak, K., 2010. Heterogeneity for stem cell–related markers according to tumor subtype and histologic stage in breast cancer. Clinical Cancer Research, 16(3), pp.876-887.

Parvani, J.G., Galliher-Beckley, A.J., Schiemann, B.J. and Schiemann, W.P., 2013. Targeted inactivation of β1 integrin induces β3 integrin switching, which drives breast cancer metastasis by TGF-β. Molecular biology of the cell, 24(21), pp.3449-3459.

Pasquale, E.B., 2008. Eph-ephrin bidirectional signaling in physiology and disease. Cell, 133(1), pp.38-52.

Pasqualucci, L., Dominguez-Sola, D., Chiarenza, A., Fabbri, G., Grunn, A., Trifonov, V., Kasper, L.H., Lerach, S., Tang, H., Ma, J. and Rossi, D., 2011. Inactivating mutations of acetyltransferase genes in B-cell lymphoma. Nature, 471(7337), pp.189-195.

Passi, A., Vigetti, D., Buraschi, S. and Iozzo, R.V., 2019. Dissecting the role of hyaluronan synthases in the tumor microenvironment. The FEBS journal, 286(15), pp.2937-2949.

Paszek, M.J., Zahir, N., Johnson, K.R., Lakins, J.N., Rozenberg, G.I., Gefen, A., Reinhart King, C.A., Margulies, S.S., Dembo, M., Boettiger, D. and Hammer, D.A., 2005. Tensional homeostasis and the malignant phenotype. Cancer cell, 8(3), pp.241-254.

Patel, A.G. and Kaufmann, S.H., 2012. Cancer: How does doxorubicin work?. Elife, 1, p.e00387.

Pearson, K.L., Hunter, T. and Janknecht, R., 1999. Activation of Smad1-mediated transcription by p300/CBP. Biochimica et Biophysica Acta (BBA)-Gene Structure and Expression, 1489(2-3), pp.354-364.

Pece, S., Serresi, M., Santolini, E., Capra, M., Hulleman, E., Galimberti, V., Zurrida, S., Maisonneuve, P., Viale, G. and Di Fiore, P.P. (2004). Loss of negative regulation by Numb over Notch is relevant to human breast carcinogenesis. Journal of Cell Biology, 167(2), pp.215–221.

Peinado, H., Olmeda, D. and Cano, A., 2007. Snail, Zeb and bHLH factors in tumour progression: an alliance against the epithelial phenotype?. Nature reviews cancer, 7(6), pp.415-428.

Peinado, H., Quintanilla, M. and Cano, A., 2003. Transforming growth factor β-1 induces Snail transcription factor in epithelial cell lines mechanisms for epithelial mesenchymal transitions. Journal of Biological Chemistry, 278(23), pp.21113-21123.

Pellegrino, L., Stebbing, J., Braga, V.M., Frampton, A.E., Jacob, J., Buluwela, L., Jiao, L.R., Periyasamy, M., Madsen, C.D., Caley, M.P. and Ottaviani, S., 2013. miR-23b regulates cytoskeletal remodeling, motility and metastasis by directly targeting multiple transcripts. Nucleic acids research, 41(10), pp.5400-5412.

Pérez-Losada, J., Sánchez-Martın, M., Rodrıguez-Garcıa, A., Sánchez, M.L., Orfao, A., Flores, T. and Sánchez-Garcıa, I., 2002. Zinc-finger transcription factor Slug contributes to the function of the stem cell factor c-kit signaling pathway. Blood, The Journal of the American Society of Hematology, 100(4), pp.1274-1286.

Perez-Moreno, M., Jamora, C. and Fuchs, E., 2003. Sticky business: orchestrating cellular signals at adherens junctions. Cell, 112(4), pp.535-548.

Pérez-Moreno, M.A., Locascio, A., Rodrigo, I., Dhondt, G., Portillo, F., Nieto, M.A. and Cano, A., 2001. A new role for E12/E47 in the repression ofe-cadherin expression and epithelial-mesenchymal transitions. Journal of Biological Chemistry, 276(29), pp.27424-27431.

Perez-Vilar J, Hill RL (2004). "Mucin Family of Glycoproteins". Encyclopedia of Biological Chemistry (Lennarz & Lane, EDs.). Oxford: Academic Press/Elsevier. 2: 758–764

Perlson, E., Michaelevski, I., Kowalsman, N., Ben-Yaakov, K., Shaked, M., Seger, R., Eisenstein, M. and Fainzilber, M., 2006. Vimentin binding to phosphorylated Erk sterically hinders enzymatic dephosphorylation of the kinase. Journal of molecular biology, 364(5), pp.938-944.

Perrais, M., Chen, X., Perez-Moreno, M. and Gumbiner, B.M., 2007. E-cadherin homophilic ligation inhibits cell growth and epidermal growth factor receptor signaling independently of other cell interactions. Molecular biology of the cell, 18(6), pp.2013-2025.

Perrin, B.J., 2002. Huttenlocher A. Calpain. Int J Biochem Cell Biol, 34, pp.722-725.

Pessah, M., Prunier, C., Marais, J., Ferrand, N., Mazars, A., Lallemand, F., Gauthier, J.M. and Atfi, A., 2001. c-Jun interacts with the corepressor TG-interacting factor (TGIF) to suppress Smad2 transcriptional activity. Proceedings of the National Academy of Sciences, 98(11), pp.6198-6203.

Petrocca, F., Visone, R., Onelli, M.R., Shah, M.H., Nicoloso, M.S., de Martino, I., Iliopoulos, D., Pilozzi, E., Liu, C.G., Negrini, M. and Cavazzini, L., 2008. E2F1-regulated microRNAs impair TGFβ-dependent cell-cycle arrest and apoptosis in gastric cancer. Cancer cell, 13(3), pp.272-286.

Petros, A.M., Nettesheim, D.G., Wang, Y., Olejniczak, E.T., Meadows, R.P., Mack, J., Swift, K., Matayoshi, E.D., Zhang, H., Fesik, S.W. and Thompson, C.B., 2000. Rationale for Bcl-xL/Bad peptide complex formation from structure, mutagenesis, and biophysical studies. Protein Science, 9(12), pp.2528-2534.

Peuhu, E., Virtakoivu, R., Mai, A., Wärri, A. and Ivaska, J., 2017. Epithelial vimentin plays a functional role in mammary gland development. Development, 144(22), pp.4103-4113.

Pham, C.G., Bubici, C., Zazzeroni, F., Knabb, J.R., Papa, S., Kuntzen, C. and Franzoso, G., 2007. Upregulation of Twist-1 by NF-κB blocks cytotoxicity induced by chemotherapeutic drugs. Molecular and cellular biology, 27(11), pp.3920-3935.

Pham, P.V., Phan, N.L., Nguyen, N.T., Truong, N.H., Duong, T.T., Le, D.V., Truong, K.D. and Phan, N.K., 2011. Differentiation of breast cancer stem cells by knockdown of CD44: promising differentiation therapy. Journal of translational medicine, 9(1), p.209.

Phua, D.C., Humbert, P.O. and Hunziker, W., 2009. Vimentin regulates scribble activity by protecting it from proteasomal degradation. Molecular biology of the cell, 20(12), pp.2841-2855.

Piasecka, D., Kitowska, K., Czaplinska, D., Mieczkowski, K., Mieszkowska, M., Turczyk, L., Skladanowski, A.C., Zaczek, A.J., Biernat, W., Kordek, R. and Romanska, H.M., 2016. Fibroblast growth factor signalling induces loss of progesterone receptor in breast cancer cells. Oncotarget, 7(52), p.86011.

Pichiorri, F., Suh, S.S., Ladetto, M., Kuehl, M., Palumbo, T., Drandi, D., Taccioli, C., Zanesi, N., Alder, H., Hagan, J.P. and Munker, R., 2008. MicroRNAs regulate critical genes associated with multiple myeloma pathogenesis. Proceedings of the National Academy of Sciences, 105(35), pp.12885-12890.

Pickup, M.W., Hover, L.D., Guo, Y., Gorska, A.E., Chytil, A., Novitskiy, S.V., Moses, H.L. and Owens, P., 2015. Deletion of the BMP receptor BMPR1a impairs mammary tumor formation and metastasis. Oncotarget, 6(26), p.22890.

Pietraszek, K., Chatron-Colliet, A., Brézillon, S., Perreau, C., Jakubiak-Augustyn, A., Krotkiewski, H., Maquart, F.X. and Wegrowski, Y., 2014. Lumican: a new inhibitor of matrix metalloproteinase-14 activity. FEBS letters, 588(23), pp.4319-4324.

Pignatelli, J., Tumbarello, D.A., Schmidt, R.P. and Turner, C.E., 2012. Hic-5 promotes invadopodia formation and invasion during TGF-β–induced epithelial–mesenchymal transition. Journal of Cell Biology, 197(3), pp.421-437.

Pires, B.R., Mencalha, A.L., Ferreira, G.M., de Souza, W.F., Morgado-Díaz, J.A., Maia, A.M., Corrêa, S. and Abdelhay, E.S., 2017. NF-kappaB is involved in the regulation of EMT genes in breast cancer cells. PloS one, 12(1), p.e0169622.

Plas, D.R. and Thompson, C.B., 2003. Akt activation promotes degradation of tuberin and FOXO3a via the proteasome. Journal of Biological Chemistry, 278(14), pp.12361-12366.

Pogribny, I.P., Filkowski, J.N., Tryndyak, V.P., Golubov, A., Shpyleva, S.I. and Kovalchuk, O., 2010. Alterations of microRNAs and their targets are associated with acquired resistance of MCF-7 breast cancer cells to cisplatin. International journal of cancer, 127(8), pp.1785-1794.

Poliseno, L., Salmena, L., Riccardi, L., Fornari, A., Song, M.S., Hobbs, R.M., Sportoletti, P., Varmeh, S., Egia, A., Fedele, G. and Rameh, L., 2010. Identification of the miR-106b 25 microRNA cluster as a proto-oncogenic PTEN-targeting intron that cooperates with its host gene MCM7 in transformation. Science signaling, 3(117), pp.ra29-ra29.

Polizio, A.H., Chinchilla, P., Chen, X., Kim, S., Manning, D.R. and Riobo, N.A., 2011. Heterotrimeric Gi proteins link Hedgehog signaling to activation of Rho small GTPases to promote fibroblast migration. Journal of Biological Chemistry, 286(22), pp.19589-19596.

Pollard, J.W., 2008. Macrophages define the invasive microenvironment in breast cancer. Journal of leukocyte biology, 84(3), pp.623-630.

Polyak, K. and Weinberg, R.A., 2009. Transitions between epithelial and mesenchymal states: acquisition of malignant and stem cell traits. Nature Reviews Cancer, 9(4), pp.265-273.

Polyak, K., Kato, J.Y., Solomon, M.J., Sherr, C.J., Massague, J., Roberts, J.M. and Koff, A., 1994. p27Kip1, a cyclin-Cdk inhibitor, links transforming growth factor-beta and contact inhibition to cell cycle arrest. Genes & development, 8(1), pp.9-22.

Pommier, Y., Leo, E., Zhang, H. and Marchand, C., 2010. DNA topoisomerases and their poisoning by anticancer and antibacterial drugs. Chemistry & biology, 17(5), pp.421-433.

Ponta, H., Sherman, L. and Herrlich, P.A., 2003. CD44: from adhesion molecules to signalling regulators. Nature reviews Molecular cell biology, 4(1), pp.33-45.

Pontiggia, O., Sampayo, R., Raffo, D., Motter, A., Xu, R., Bissell, M.J., de Kier Joffé, E.B. and Simian, M., 2012. The tumor microenvironment modulates tamoxifen resistance in breast cancer: a role for soluble stromal factors and fibronectin through β1 integrin. Breast cancer research and treatment, 133(2), pp.459-471.

Porsch, H., Bernert, B., Mehić, M., Theocharis, A.D., Heldin, C.H. and Heldin, P., 2013. Efficient TGFβ-induced epithelial–mesenchymal transition depends on hyaluronan synthase HAS2. Oncogene, 32(37), pp.4355-4365.

Postigo, A.A., 2003. Opposing functions of ZEB proteins in the regulation of the TGFβ/BMP signaling pathway. The EMBO journal, 22(10), pp.2443-2452.

Poudineh, M., Sargent, E.H., Pantel, K. and Kelley, S.O., 2018. Profiling circulating tumour cells and other biomarkers of invasive cancers. Nature Biomedical Engineering, 2(2), pp.72-84.

Poujade, M., Grasland-Mongrain, E., Hertzog, A., Jouanneau, J., Chavrier, P., Ladoux, B., Buguin, A. and Silberzan, P., 2007. Collective migration of an epithelial monolayer in response to a model wound. Proceedings of the National Academy of Sciences, 104(41), pp.15988-15993.

Pouponnot, C., Jayaraman, L. and Massagué, J., 1998. Physical and functional interaction of SMADs and p300/CBP. Journal of Biological Chemistry, 273(36), pp.22865-22868.

Powell, E., Shao, J., Picon, H.M., Bristow, C., Ge, Z., Peoples, M., Robinson, F., Jeter Jones, S.L., Schlosberg, C., Grzeskowiak, C.L. and Yang, F., 2018. A functional genomic screen in vivo identifies CEACAM5 as a clinically relevant driver of breast cancer metastasis. NPJ breast cancer, 4(1), pp.1-12.

Poyyakkara, A., Raji, G.R., Kunhiraman, H., Edatt, L. and Kumar, S.V., 2018. ER stress mediated regulation of miR23a confer Hela cells better adaptability to utilize glycolytic pathway. Journal of cellular biochemistry, 119(6), pp.4907-4917.

Prakash, R., Zhang, Y., Feng, W. and Jasin, M., 2015. Homologous recombination and human health: the roles of BRCA1, BRCA2, and associated proteins. Cold Spring Harbor perspectives in biology, 7(4), p.a016600.

Prenzel, T., Begus-Nahrmann, Y., Kramer, F., Hennion, M., Hsu, C., Gorsler, T., Hintermair, C., Eick, D., Kremmer, E., Simons, M. and Beissbarth, T., 2011. Estrogen-dependent gene transcription in human breast cancer cells relies upon proteasome-dependent monoubiquitination of histone H2B. Cancer research, 71(17), pp.5739-5753.

Prince, M.E., Sivanandan, R., Kaczorowski, A., Wolf, G.T., Kaplan, M.J., Dalerba, P., Weissman, I.L., Clarke, M.F. and Ailles, L.E., 2007. Identification of a subpopulation of cells with cancer stem cell properties in head and neck squamous cell carcinoma. Proceedings of the National Academy of Sciences, 104(3), pp.973-978.

Proia, T.A., Keller, P.J., Gupta, P.B., Klebba, I., Jones, A.D., Sedic, M., Gilmore, H., Tung, N., Naber, S.P., Schnitt, S. and Lander, E.S., 2011. Genetic predisposition directs breast cancer phenotype by dictating progenitor cell fate. Cell stem cell, 8(2), pp.149-163.

Provenzano, P.P., Eliceiri, K.W., Campbell, J.M., Inman, D.R., White, J.G. and Keely, P.J., 2006. Collagen reorganization at the tumor-stromal interface facilitates local invasion. BMC medicine, 4(1), pp.1-15.

Puisieux, A., Brabletz, T. and Caramel, J., 2014. Oncogenic roles of EMT-inducing transcription factors. Nature cell biology, 16(6), pp.488-494.

Qadir, F., Aziz, M.A., Sari, C.P., Ma, H., Dai, H., Wang, X., Raithatha, D., Da Silva, L.G.L., Hussain, M., Poorkasreiy, S.P. and Hutchison, I.L., 2018. Transcriptome reprogramming by cancer exosomes: identification of novel molecular targets in matrix and immune modulation. Molecular cancer, 17(1), p.97.

Qadir, M., O'Loughlin, K.L., Fricke, S.M., Williamson, N.A., Greco, W.R., Minderman, H. and Baer, M.R., 2005. Cyclosporin A is a broad-spectrum multidrug resistance modulator. Clinical Cancer Research, 11(6), pp.2320-2326.

Qi, P., Xu, M.D., Shen, X.H., Ni, S.J., Huang, D., Tan, C., Weng, W.W., Sheng, W.Q., Zhou, X.Y. and Du, X., 2015. Reciprocal repression between TUSC 7 and mi R-23b in gastric cancer. International journal of cancer, 137(6), pp.1269-1278.

Qian, X., Anzovino, A., Kim, S., Suyama, K., Yao, J., Hulit, J., Agiostratidou, G., Chandiramani, N., McDaid, H.M., Nagi, C. and Cohen, H.W., 2014. N-cadherin/FGFR promotes metastasis through epithelial-to-mesenchymal transition and stem/progenitor cell-like properties. Oncogene, 33(26), pp.3411-3421.

Qian, Z., Ren, L., Wu, D., Yang, X., Zhou, Z., Nie, Q., Jiang, G., Xue, S., Weng, W., Qiu, Y. and Lin, Y., 2017. Overexpression of FoxO3a is associated with glioblastoma progression and predicts poor patient prognosis. International journal of cancer, 140(12), pp.2792-2804.

Qin, B.Y., Liu, C., Srinath, H., Lam, S.S., Correia, J.J., Derynck, R. and Lin, K., 2005. Crystal structure of IRF-3 in complex with CBP. Structure, 13(9), pp.1269-1277.

Qiu, Z., Chu, Y., Xu, B., Wang, Q., Jiang, M., Li, X., Wang, G., Yu, P., Liu, G., Wang, H. and Kang, H., 2017. Increased expression of calponin 2 is a positive prognostic factor in pancreatic ductal adenocarcinoma. Oncotarget, 8(34), p.56428.

Qu, W.Q., Liu, L. and Yu, Z., 2015. Clinical value of microRNA-23a upregulation in non small cell lung cancer. International journal of clinical and experimental medicine, 8(8), p.13598.

Quayle, L.A., Ottewell, P.D. and Holen, I., 2018. Chemotherapy resistance and stemness in mitotically quiescent human breast cancer cells identified by fluorescent dye retention. Clinical & experimental metastasis, 35(8), pp.831-846.

Quenet, D., 2018. Histone variants and disease. In International Review of Cell and Molecular Biology (Vol. 335, pp. 1-39). Academic Press. Quinlan, A.R., Boland, M.J., Leibowitz, M.L., Shumilina, S., Pehrson, S.M., Baldwin, K.K. and Hall, I.M., 2011. Genome sequencing of mouse induced pluripotent stem cells reveals retroelement stability and infrequent DNA rearrangement during reprogramming. Cell stem cell, 9(4), pp.366-373.

Quintás-Cardama, A., Kantarjian, H.M. and Cortes, J.E., 2009. Mechanisms of primary and secondary resistance to imatinib in chronic myeloid leukemia. Cancer control, 16(2), pp.122-131.

R Prosperi, J. and H Goss, K., 2010. A Wnt-ow of opportunity: targeting the Wnt/β catenin pathway in breast cancer. Current drug targets, 11(9), pp.1074-1088.

Raab-Westphal, S., Marshall, J.F. and Goodman, S.L., 2017. Integrins as therapeutic targets: successes and cancers. Cancers, 9(9), p.110.

Rack, J.G., Lutter, T., Bjerga, G.E.K., Guder, C., Ehrhardt, C., Värv, S., Ziegler, M. and Aasland, R., 2014. The PHD finger of p300 influences its ability to acetylate histone and non-histone targets. Journal of molecular biology, 426(24), pp.3960-3972.

Radisky, D.C., Levy, D.D., Littlepage, L.E., Liu, H., Nelson, C.M., Fata, J.E., Leake, D., Godden, E.L., Albertson, D.G., Nieto, M.A. and Werb, Z., 2005. Rac1b and reactive oxygen species mediate MMP-3-induced EMT and genomic instability. Nature, 436(7047), pp.123-127.

Raffel, C., Jenkins, R.B., Frederick, L., Hebrink, D., Alderete, B., Fults, D.W. and James, C.D., 1997. Sporadic medulloblastomas contain PTCH mutations. Cancer research, 57(5), pp.842-845.

Raguz, S. and Yagüe, E., 2008. Resistance to chemotherapy: new treatments and novel insights into an old problem. British journal of cancer, 99(3), pp.387-391.

Raguz, S., Adams, C., Masrour, N., Rasul, S., Papoutsoglou, P., Hu, Y., Cazzanelli, G., Zhou, Y., Patel, N., Coombes, C. and Yagüe, E., 2013. Loss of O6-methylguanine-DNA methyltransferase confers collateral sensitivity to carmustine in topoisomerase II-mediated

doxorubicin resistant triple negative breast cancer cells. Biochemical pharmacology, 85(2), pp.186-196.

Ramaswamy, B., Lu, Y., Teng, K.Y., Nuovo, G., Li, X., Shapiro, C.L. and Majumder, S., 2012. Hedgehog signaling is a novel therapeutic target in tamoxifen-resistant breast cancer aberrantly activated by PI3K/AKT pathway. Cancer research, 72(19), pp.5048-5059.

Ramesh, N., Antón, I.M., Hartwig, J.H. and Geha, R.S., 1997. WIP, a protein associated with Wiskott–Aldrich syndrome protein, induces actin polymerization and redistribution in lymphoid cells. Proceedings of the National Academy of Sciences, 94(26), pp.14671-14676.

Ramirez, N.E. and Zutter, M.M., The alpha2beta1 integrin is a metastasis suppressor in mouse models and human cancer (J Clin Invest, 2011, 121: 226-237).

Ramovs, V., te Molder, L. and Sonnenberg, A., 2017. The opposing roles of laminin binding integrins in cancer. Matrix Biology, 57, pp.213-243.

Ramsundar, B., Eastman, P., Walters, P., Pande, V. (2019). Deep Learning for the Life Sciences. United States of America. O'Reilly Media, Inc.

Ranganath, S. and Murphy, K.M., 2001. Structure and specificity of GATA proteins in Th2 development. Molecular and cellular biology, 21(8), pp.2716-2725.

Rangasamy, D., 2010. Histone variant H2A. Z can serve as a new target for breast cancer therapy. Current medicinal chemistry, 17(28), pp.3155-3161.

Rangaswami, H., Bulbule, A. and Kundu, G.C., 2006. Osteopontin: role in cell signalling and cancer progression. Trends in cell biology, 16(2), pp.79-87.

Rangel, N., Fortunati, N., Osella-Abate, S., Annaratone, L., Isella, C., Catalano, M.G., Rinella, L., Metovic, J., Boldorini, R., Balmativola, D. and Ferrando, P., 2018. FOXA1 and AR in invasive breast cancer: new findings on their co-expression and impact on prognosis in ER-positive patients. BMC cancer, 18(1), p.703.

Rankin, E.B. and Giaccia, A.J., 2016. Hypoxic control of metastasis. Science, 352(6282), pp.175-180.

RAO, P., HSU, K.C. and CHAO, M.V., 1995. Upregulation of NF-κB-dependent gene expression mediated by the p75 tumor necrosis factor receptor. Journal of interferon & cytokine research, 15(2), pp.171-177.

Rao, T.P. and Kühl, M., 2010. An updated overview on Wnt signaling pathways: a prelude for more. Circulation research, 106(12), pp.1798-1806. Raphael, J., Desautels, D., Pritchard, K.I., Petkova, E. and Shah, P.S., 2018. Phosphoinositide 3-kinase inhibitors in advanced breast cancer: A systematic review and meta-analysis. European Journal of Cancer, 91, pp.38-46.

Rasul, S., Balasubramanian, R., Filipović, A., Slade, M.J., Yagüe, E. and Coombes, R.C., 2009. Inhibition of γ-secretase induces G2/M arrest and triggers apoptosis in breast cancer cells. British journal of cancer, 100(12), pp.1879-1888.

Rathore, M.G., Saumet, A., Rossi, J.F., De Bettignies, C., Tempé, D., Lecellier, C.H. and Villalba, M., 2012. The NF-κB member p65 controls glutamine metabolism through miR-23a. The international journal of biochemistry & cell biology, 44(9), pp.1448-1456.

Ray, P.S., Wang, J., Qu, Y., Sim, M.S., Shamonki, J., Bagaria, S.P., Ye, X., Liu, B., Elashoff, D., Hoon, D.S. and Walter, M.A., 2010. FOXC1 is a potential prognostic biomarker with functional significance in basal-like breast cancer. Cancer research, 70(10), pp.3870-3876.

Razumilava, N., Bronk, S.F., Smoot, R.L., Fingas, C.D., Werneburg, N.W., Roberts, L.R. and Mott, J.L., 2012. miR-25 targets TNF-related apoptosis inducing ligand (TRAIL) death receptor-4 and promotes apoptosis resistance in cholangiocarcinoma. Hepatology, 55(2), pp.465-475.

Razumilava, N., Gradilone, S.A., Smoot, R.L., Mertens, J.C., Bronk, S.F., Sirica, A.E. and Gores, G.J., 2014. Non-canonical Hedgehog signaling contributes to chemotaxis in cholangiocarcinoma. Journal of hepatology, 60(3), pp.599-605.

Reddy, K.B., 2011. Triple-negative breast cancers: an updated review on treatment options. Current oncology, 18(4), p.e173.

Reed, A.E.M., Kutasovic, J.R., Lakhani, S.R. and Simpson, P.T., 2015. Invasive lobular carcinoma of the breast: morphology, biomarkers and'omics. Breast cancer research, 17(1), p.12. Regenbrecht, C.R., Lehrach, H. and Adjaye, J., 2008. Stemming cancer: functional genomics of cancer stem cells in solid tumors. Stem cell reviews, 4(4), pp.319-328.

Rehman, A., Kim, Y., Kim, H., Sim, J., Ahn, H., Chung, M.S., Shin, S.J. and Jang, K., 2018. FOXO3a expression is associated with lymph node metastasis and poor disease-free survival in triple-negative breast cancer. Journal of clinical pathology, 71(9), pp.806-813.

Reid, G., Kao, S.C., Pavlakis, N., Brahmbhatt, H., MacDiarmid, J., Clarke, S., Boyer, M. and van Zandwijk, N., 2016. Clinical development of TargomiRs, a miRNA mimic-based treatment for patients with recurrent thoracic cancer. Epigenomics, 8(8), pp.1079-1085.

Reinhold, W, C., Reimers, M, A., Maunakea, A, K. Kim, S., Lababidi, S., Scherf, U., et al. (2007) .Detailed DNA methylation profiles of the E-cadherin promoter in the NCI-60 cancer cells, Mol. Cancer Ther. 6 (2),391–403.

Reis-Filho, J.S., Simpson, P.T., Turner, N.C., Lambros, M.B., Jones, C., Mackay, A., Grigoriadis, A., Sarrio, D., Savage, K., Dexter, T. and Iravani, M., 2006. FGFR1 emerges as a potential therapeutic target for lobular breast carcinomas. Clinical Cancer Research, 12(22), pp.6652-6662.

Remacle, J.E., Kraft, H., Lerchner, W., Wuytens, G., Collart, C., Verschueren, K., Smith, J.C. and Huylebroeck, D., 1999. New mode of DNA binding of multi-zinc finger transcription factors: δEF1 family members bind with two hands to two target sites. The EMBO journal, 18(18), pp.5073-5084.

Renoir, J.M., Marsaud, V. and Lazennec, G., 2013. Estrogen receptor signaling as a target for novel breast cancer therapeutics. Biochemical pharmacology, 85(4), pp.449-465.

Resop, R.S., Douaisi, M., Craft, J., Jachimowski, L.C., Blom, B. and Uittenbogaart, C.H., 2016. Sphingosine-1-phosphate/sphingosine-1-phosphate receptor 1 signaling is required for migration of naive human T cells from the thymus to the periphery. Journal of Allergy and Clinical Immunology, 138(2), pp.551-557.

Rexer, B.N. and Arteaga, C.L., 2012. Intrinsic and acquired resistance to HER2-targeted therapies in HER2 gene-amplified breast cancer: mechanisms and clinical implications. Critical Reviews™ in Oncogenesis, 17(1).

Reya, T., Morrison, S.J., Clarke, M.F. and Weissman, I.L., 2001. Stem cells, cancer, and cancer stem cells. nature, 414(6859), pp.105-111.

Reynolds, D.S., Tevis, K.M., Blessing, W.A., Colson, Y.L., Zaman, M.H. and Grinstaff, M.W., 2017. Breast cancer spheroids reveal a differential cancer stem cell response to chemotherapeutic treatment. Scientific reports, 7(1), pp.1-12.

Reynolds, D.S., Tevis, K.M., Blessing, W.A., Colson, Y.L., Zaman, M.H. and Grinstaff, M.W. (2017). Breast Cancer Spheroids Reveal a Differential Cancer Stem Cell Response to Chemotherapeutic Treatment. Scientific Reports, 7(1).

Rezaeian, A.H., Li, C.F., Wu, C.Y., Zhang, X., Delacerda, J., You, M.J., Han, F., Cai, Z., Jeong, Y.S., Jin, G. and Phan, L., 2017. A hypoxia-responsive TRAF6–ATM–H2AX signalling axis promotes HIF1α activation, tumorigenesis and metastasis. Nature cell biology, 19(1), pp.38-51.

Rhee, S. and Grinnell, F., 2007. Fibroblast mechanics in 3D collagen matrices. Advanced drug delivery reviews, 59(13), pp.1299-1305.

Rhodes, L.V., Tate, C.R., Segar, H.C., Burks, H.E., Phamduy, T.B., Hoang, V., Elliott, S., Gilliam, D., Pounder, F.N., Anbalagan, M. and Chrisey, D.B., 2014. Suppression of triple-negative breast cancer metastasis by pan-DAC inhibitor panobinostat via inhibition of ZEB family of EMT master regulators. Breast cancer research and treatment, 145(3), pp.593-604.

Riaz, S.K., Ke, Y., Wang, F., Kayani, M.A. and Malik, M.F.A., 2019. Influence of SHH/GLI1 axis on EMT mediated migration and invasion of breast cancer cells. Scientific reports, 9(1), pp.1-13.

Ribatti, D., 2009. Endogenous inhibitors of angiogenesis: a historical review. Leukemia research, 33(5), pp.638-644.

Ricard, N., Ciais, D., Levet, S., Subileau, M., Mallet, C., Zimmers, T.A., Lee, S.J., Bidart, M., Feige, J.J. and Bailly, S., 2012. BMP9 and BMP10 are critical for postnatal retinal vascular remodeling. Blood, The Journal of the American Society of Hematology, 119(25), pp.6162-6171.

Ricardo, S., Vieira, A.F., Gerhard, R., Leitao, D., Pinto, R., Cameselle-Teijeiro, J.F., Milanezi, F., Schmitt, F. and Paredes, J. (2011). Breast cancer stem cell markers CD44, CD24 and ALDH1: expression distribution within intrinsic molecular subtype. Journal of Clinical Pathology, 64(11), pp.937–946.

Ricardo, S., Vieira, A.F., Gerhard, R., Leitão, D., Pinto, R., Cameselle-Teijeiro, J.F., Milanezi, F., Schmitt, F. and Paredes, J., 2011. Breast cancer stem cell markers CD44, CD24 and ALDH1: expression distribution within intrinsic molecular subtype. Journal of clinical pathology, 64(11), pp.937-946.

Richardson, A.M., Havel, L.S., Koyen, A.E., Konen, J.M., Shupe, J., Wiles, W.4., Martin, W.D., Grossniklaus, H.E., Sica, G., Gilbert-Ross, M. and Marcus, A.I., 2018. Vimentin is required for lung adenocarcinoma metastasis via heterotypic tumor cell–cancer-associated fibroblast interactions during collective invasion. Clinical Cancer Research, 24(2), pp.420-432.

Rivas, M.A., Carnevale, R.P., Proietti, C.J., Rosemblit, C., Beguelin, W., Salatino, M., Charreau, E.H., Frahm, I., Sapia, S., Brouckaert, P. and Elizalde, P.V., 2008. TNFα acting on TNFR1 promotes breast cancer growth via p42/P44 MAPK, JNK, Akt and NF-κB-dependent pathways. Experimental cell research, 314(3), pp.509-529.

Rizzo, S., Cangemi, A., Galvano, A., Fanale, D., Buscemi, S., Ciaccio, M., Russo, A., Castorina, S. and Bazan, V., 2017. Analysis of miRNA expression profile induced by short term starvation in breast cancer cells treated with doxorubicin. Oncotarget, 8(42), p.71924.

Roberts, A.B., Sporn, M.B., Assoian, R.K., Smith, J.M., Roche, N.S., Wakefield, L.M., Heine, U.I., Liotta, L.A., Falanga, V. and Kehrl, J.H., 1986. Transforming growth factor type beta: rapid induction of fibrosis and angiogenesis in vivo and stimulation of collagen formation in vitro. Proceedings of the National Academy of Sciences, 83(12), pp.4167-4171.

Robey, R.W., Steadman, K., Polgar, O., Morisaki, K., Blayney, M., Mistry, P. and Bates, S.E., 2004. Pheophorbide a is a specific probe for ABCG2 function and inhibition. Cancer research, 64(4), pp.1242-1246.

Robinson, B.D., Sica, G.L., Liu, Y.F., Rohan, T.E., Gertler, F.B., Condeelis, J.S. and Jones, J.G., 2009. Tumor microenvironment of metastasis in human breast carcinoma: a

potential prognostic marker linked to hematogenous dissemination. Clinical cancer research, 15(7), pp.2433-2441.

Robinson, D.R., Kalyana-Sundaram, S., Wu, Y.M., Shankar, S., Cao, X., Ateeq, B., Asangani, I.A., Iyer, M., Maher, C.A., Grasso, C.S. and Lonigro, R.J., 2011. Functionally recurrent rearrangements of the MAST kinase and Notch gene families in breast cancer. Nature medicine, 17(12), pp.1646-1651.

Robinson, D.R., Wu, Y.M., Lonigro, R.J., Vats, P., Cobain, E., Everett, J., Cao, X., Rabban, E., Kumar-Sinha, C., Raymond, V. and Schuetze, S., 2017. Integrative clinical genomics of metastatic cancer. Nature, 548(7667), pp.297-303.

Rodriguez-Aguayo, C., del C Monroig, P., Redis, R.S., Bayraktar, E., Almeida, M.I., Ivan, C., Fuentes-Mattei, E., Rashed, M.H., Chavez-Reyes, A., Ozpolat, B. and Mitra, R., 2017. Regulation of hnRNPA1 by microRNAs controls the miR-18a–K-RAS axis in chemotherapy-resistant ovarian cancer. Cell discovery, 3(1), pp.1-14.

Roh-Johnson, M., Bravo-Cordero, J.J., Patsialou, A., Sharma, V.P., Guo, P., Liu, H., Hodgson, L. and Condeelis, J., 2014. Macrophage contact induces RhoA GTPase signaling to trigger tumor cell intravasation. Oncogene, 33(33), pp.4203-4212.

Rohan, T.E., Xue, X., Lin, H.M., D'Alfonso, T.M., Ginter, P.S., Oktay, M.H., Robinson, B.D., Ginsberg, M., Gertler, F.B., Glass, A.G. and Sparano, J.A., 2014. Tumor microenvironment of metastasis and risk of distant metastasis of breast cancer. Journal of the National Cancer Institute, 106(8), p.dju136.

Romagnani, S. (2006). Regulation of the T cell response. Clinical & Experimental Allergy, 36(11), pp.1357–1366.

Romano, L.A. and Runyan, R.B. (2000). Slug is an Essential Target of TGFβ2 Signaling in the Developing Chicken Heart. Developmental Biology, 223(1), pp.91–102.

ROSEN, V. (2006). BMP and BMP Inhibitors in Bone. Annals of the New York Academy of Sciences, 1068(1), pp.19–25

Rosivatz, E., Becker, I., Specht, K., Fricke, E., Luber, B., Busch, R., Höfler, H. and Becker, K.-F. (2002). Differential Expression of the Epithelial-Mesenchymal Transition Regulators Snail, SIP1, and Twist in Gastric Cancer. The American Journal of Pathology, 161(5), pp.1881–1891.

Rossetto, D., Avvakumov, N. and Côté, J. (2012). Histone phosphorylation. Epigenetics, [online] 7(10), pp.1098–1108. Available at: https://www.ncbi.nlm.nih.gov/pmc/articles/PMC3469451/

Rossow, K.L. and Janknecht, R. (2003). Synergism between p68 RNA helicase and the transcriptional coactivators CBP and p300. Oncogene, 22(1), pp.151–156.

Rothe, M., Pan, M.-G., Henzel, W.J., Ayres, T.M. and V. Goeddel, D. (1995). The TNFR2 TRAF signaling complex contains two novel proteins related to baculoviral inhibitor of apoptosis proteins. Cell, 83(7), pp.1243–1252.

Rubashkin, M.G., Cassereau, L., Bainer, R., DuFort, C.C., Yui, Y., Ou, G., Paszek, M.J., Davidson, M.W., Chen, Y.-Y. and Weaver, V.M. (2014). Force Engages Vinculin and Promotes Tumor Progression by Enhancing PI3K Activation of Phosphatidylinositol (3,4,5)-Triphosphate. Cancer Research, 74(17), pp.4597–4611.

Ruby, J.G., Jan, C.H. and Bartel, D.P. (2007). Intronic microRNA precursors that bypass Drosha processing. Nature, 448(7149), pp.83–86.

Rybakovsky, E., Valenzano, M.C., DiGuilio, K.M., Buleza, N.B., Moskalenko, D.V., Harty, R.N. and Mullin, J.M. (2019). Improving Transient Transfection Efficiency in a Differentiated, Polar Epithelial Cell Layer. Journal of Biomolecular Techniques: JBT, 30(2), pp.19–24.

Ryder, C., McColl, K., Zhong, F. and Distelhorst, C.W. (2012). Acidosis Promotes Bcl-2 Family-mediated Evasion of Apoptosis. Journal of Biological Chemistry, 287(33), pp.27863–27875.

Saadatmand, S., De Kruijf, E.M., Sajet, A., Dekker-Ensink, N.G., Van Nes, J.G., Putter, H., Smit, V.T., Van De Velde, C.J., Liefers, G.J. and Kuppen, P.J., 2013. Expression of cell adhesion molecules and prognosis in breast cancer. Br J Surg, 100(2), pp.252-260.

Sachdeva, M., Wu, H., Ru, P., Hwang, L., Trieu, V. and Mo, Y.Y., 2011. MicroRNA-101 mediated Akt activation and estrogen-independent growth. Oncogene, 30(7), pp.822-831.

Sadr-Nabavi, A., Ramser, J., Volkmann, J., Naehrig, J., Wiesmann, F., Betz, B., Hellebrand, H., Engert, S., Seitz, S., Kreutzfeld, R. and Sasaki, T., 2009. Decreased expression of angiogenesis antagonist EFEMP1 in sporadic breast cancer is caused by aberrant promoter methylation and points to an impact of EFEMP1 as molecular biomarker. International journal of cancer, 124(7), pp.1727-1735.

Saez, M.E., Ramirez-Lorca, R., Moron, F.J. and Ruiz, A., 2006. The therapeutic potential of the calpain family: new aspects. Drug discovery today, 11(19-20), pp.917-923.

Sahlgren, C., Gustafsson, M.V., Jin, S., Poellinger, L. and Lendahl, U., 2008. Notch signaling mediates hypoxia-induced tumor cell migration and invasion. Proceedings of the National Academy of Sciences, 105(17), pp.6392-6397.

Sakamoto, M., Hirata, H., Ohtsuka, T., Bessho, Y. and Kageyama, R., 2003. The basic helix-loop-helix genes Hesr1/Hey1 and Hesr2/Hey2 regulate maintenance of neural precursor cells in the brain. Journal of Biological Chemistry, 278(45), pp.44808-44815.

Salah, Z., Arafeh, R., Maximov, V., Galasso, M., Khawaled, S., Abou-Sharieha, S., Volinia, S., Jones, K.B., Croce, C.M. and Aqeilan, R.I., 2015. miR-27a and miR-27a* contribute to metastatic properties of osteosarcoma cells. Oncotarget, 6(7), p.4920.

Salas, N.R., González, E.G. and Amat, C.G., 2010. Breast cancer stem cell hypothesis: clinical relevance (answering breast cancer clinical features). Clinical and Translational Oncology, 12(6), pp.395-400.

Salhia, B., Kiefer, J., Ross, J.T., Metapally, R., Martinez, R.A., Johnson, K.N., DiPerna, D.M., Paquette, K.M., Jung, S., Nasser, S. and Wallstrom, G., 2014. Integrated genomic and epigenomic analysis of breast cancer brain metastasis. PloS one, 9(1), p.e85448.

Salinas Vera, Y.M., Marchat, L.A., Gallardo Rincón, D., Ruiz García, E., Echavarría Zepeda, R. and López Camarillo, C., 2019. AngiomiRs: MicroRNAs driving angiogenesis in cancer. International journal of molecular medicine, 43(2), pp.657-670.

Salvador, M.A., Wicinski, J., Cabaud, O., Toiron, Y., Finetti, P., Josselin, E., Lelièvre, H., Kraus-Berthier, L., Depil, S., Bertucci, F. and Collette, Y., 2013. The histone deacetylase inhibitor abexinostat induces cancer stem cells differentiation in breast cancer with low Xist expression. Clinical cancer research, 19(23), pp.6520-6531.

Samanta, D., Gilkes, D.M., Chaturvedi, P., Xiang, L. and Semenza, G.L., 2014. Hypoxia inducible factors are required for chemotherapy resistance of breast cancer stem cells. Proceedings of the National Academy of Sciences, 111(50), pp.E5429-E5438.

Sanchez-Tillo, E., Lazaro, A., Torrent, R., Cuatrecasas, M., Vaquero, E.C., Castells, A., Engel, P. and Postigo, A., 2010. ZEB1 represses E-cadherin and induces an EMT by recruiting the SWI/SNF chromatin-remodeling protein BRG1. Oncogene, 29(24), pp.3490-3500.

Sanchez, A.M., Csibi, A., Raibon, A., Cornille, K., Gay, S., Bernardi, H. and Candau, R., 2012. AMPK promotes skeletal muscle autophagy through activation of forkhead FoxO3a and interaction with Ulk1. Journal of cellular biochemistry, 113(2), pp.695-710.

Sander, J.D. and Joung, J.K. (2014). CRISPR-Cas systems for editing, regulating and targeting genomes. Nature Biotechnology, 32(4), pp.347–355.

Sanphui, P. and Biswas, S.C., 2013. FoxO3a is activated and executes neuron death via Bim in response to βamyloid. Cell death & disease, 4(5), pp.e625-e625.

Santamaria, P.G. and Nebreda, A.R., 2010. Deconstructing ERK signaling in tumorigenesis. Molecular cell, 38(1), pp.3-5.

Santer, F.R., Höschele, P.P., Oh, S.J., Erb, H.H., Bouchal, J., Cavarretta, I.T., Parson, W., Meyers, D.J., Cole, P.A. and Culig, Z., 2011. Inhibition of the acetyltransferases p300 and CBP reveals a targetable function for p300 in the survival and invasion pathways of prostate cancer cell lines. Molecular cancer therapeutics, 10(9), pp.1644-1655.

Sanz-Moreno, V., Gadea, G., Ahn, J., Paterson, H., Marra, P., Pinner, S., Sahai, E. and Marshall, C.J., 2008. Rac activation and inactivation control plasticity of tumor cell movement. Cell, 135(3), pp.510-523.

Saravia, C.H., Flores, C., Schwarz, L.J., Bravo, L., Zavaleta, J., Araujo, J., Neciosup, S. and Pinto, J.A., 2019. Patterns of mutation enrichment in metastatic triple-negative breast cancer. Clinical Medicine Insights: Oncology, 13, p.1179554919868482.

Sarkadi, B., Homolya, L., Szakács, G. and Váradi, A., 2006. Human multidrug resistance ABCB and ABCG transporters: participation in a chemoimmunity defense system. Physiological reviews, 86(4), pp.1179-1236.

Sarrio, D., Moreno-Bueno, G., Hardisson, D., Sanchez-Estevez, C., Guo, M, Z., Herman, J, G., et al. (2003). Epigenetic and genetic alterations of APC and CDH1 genes in lobular breast cancer: relationships with abnormal E-cadherin and catenin expres- sion and microsatellite instability, Int. J. Cancer 106(2), 208–215.

Sarver, A.L., French, A.J., Borralho, P.M., Thayanithy, V., Oberg, A.L., Silverstein, K.A., Morlan, B.W., Riska, S.M., Boardman, L.A., Cunningham, J.M. and Subramanian, S., 2009. Human colon cancer profiles show differential microRNA expression depending on mismatch repair status and are characteristic of undifferentiated proliferative states. BMC cancer, 9(1), pp.1-15.

Satapathy, S., Kumar, C. and Singh, R.K., 2019. MicroRNAs as Key Regulators of Ovarian Cancers. Cell Medicine, 11, p.2155179019873849.

Satherley, L.K., Sun, P.H., Ji, K.E., Mason, M., Hargest, R., Jiang, W.G. and Ye, L., 2016. Prostate Apoptosis Response-4 (PAR4) Suppresses Growth and Invasion of Breast Cancer Cells and Is Positively Associated with Patient Survival. Anticancer Research, 36(3), pp.1227-1235.

Sathyanarayanan, A., Chandrasekaran, K.S. and Karunagaran, D., 2017. microRNA-145 modulates epithelial-mesenchymal transition and suppresses proliferation, migration and invasion by targeting SIP1 in human cervical cancer cells. Cellular Oncology, 40(2), pp.119-131.

Sato, Y. and Rifkin, D.B., 1988. Autocrine activities of basic fibroblast growth factor: regulation of endothelial cell movement, plasminogen activator synthesis, and DNA synthesis. The Journal of Cell Biology, 107(3), pp.1199-1205.

Savita, U. and Karunagaran, D. (2013). MicroRNA-106b-25 cluster targets β-TRCP2, increases the expression of Snail and enhances cell migration and invasion in H1299 (non small cell lung cancer) cells. Biochemical and Biophysical Research Communications, 434(4), pp.841–847.

Sawaki, M., Shien, T. and Iwata, H., 2019. TNM classification of malignant tumors (Breast Cancer Study Group). Japanese journal of clinical oncology, 49(3), pp.228-231.

SC Wilson, M., J Brosens, J., DC Schwenen, H. and W-F Lam, E., 2011. FOXO and FOXM1 in cancer: the FOXO-FOXM1 axis shapes the outcome of cancer chemotherapy. Current drug targets, 12(9), pp.1256-1266.

Scaltriti, M., Eichhorn, P.J., Cortés, J., Prudkin, L., Aura, C., Jiménez, J., Chandarlapaty, S., Serra, V., Prat, A., Ibrahim, Y.H. and Guzmán, M., 2011. Cyclin E amplification/overexpression is a mechanism of trastuzumab resistance in HER2+ breast cancer patients. Proceedings of the National Academy of Sciences, 108(9), pp.3761-3766.

Schabath, H., Runz, S., Joumaa, S. and Altevogt, P., 2006. CD24 affects CXCR4 function in pre-B lymphocytes and breast carcinoma cells. Journal of cell science, 119(2), pp.314-325.

Schaefer, A., Jung, M., Mollenkopf, H.J., Wagner, I., Stephan, C., Jentzmik, F., Miller, K., Lein, M., Kristiansen, G. and Jung, K., 2010. Diagnostic and prognostic implications of microRNA profiling in prostate carcinoma. International journal of cancer, 126(5), pp.1166-1176.

Schafer, J.M., Liu, H., Bentrem, D.J., Zapf, J.W. and Jordan, V.C., 2000. Allosteric silencing of activating function 1 in the 4-hydroxytamoxifen estrogen receptor complex is induced by substituting glycine for aspartate at amino acid 351. Cancer Research, 60(18), pp.5097-5105.

Schäfer, M.K. and Altevogt, P., 2010. L1CAM malfunction in the nervous system and human carcinomas. Cellular and molecular life sciences, 67(14), pp.2425-2437.

Scheel, C. and Weinberg, R.A., 2012, October. Cancer stem cells and epithelial mesenchymal transition: concepts and molecular links. In Seminars in cancer biology (Vol. 22, No. 5-6, pp. 396-403). Academic Press.

Scheel, C., Eaton, E.N., Li, S.H.J., Chaffer, C.L., Reinhardt, F., Kah, K.J., Bell, G., Guo, W., Rubin, J., Richardson, A.L. and Weinberg, R.A., 2011. Paracrine and autocrine signals induce and maintain mesenchymal and stem cell states in the breast. Cell, 145(6), pp.926-940.

Scheffzek, K., Ahmadian, M.R. and Wittinghofer, A., 1998. GTPase-activating proteins: helping hands to complement an active site. Trends in biochemical sciences, 23(7), pp.257-262.

Scherbakov, A.M., Andreeva, O.E., Shatskaya, V.A. and Krasil'nikov, M.A. (2012). The relationships between snail1 and estrogen receptor signaling in breast cancer cells. Journal of Cellular Biochemistry, 113(6), pp.2147–2155.

Scherz-Shouval, R., Santagata, S., Mendillo, M.L., Sholl, L.M., Ben-Aharon, I., Beck, A.H., Dias-Santagata, D., Koeva, M., Stemmer, S.M., Whitesell, L. and Lindquist, S., 2014.

The reprogramming of tumor stroma by HSF1 is a potent enabler of malignancy. Cell, 158(3), pp.564-578.

Schiffers, P.M.H., Henrion, D., Boulanger, C.M., Colucci-Guyon, E., Langa-Vuves, F., Van Essen, H., Fazzi, G.E., Levy, B.I. and De Mey, J.G.R., 2000. Altered flow–induced arterial remodeling in vimentin-deficient mice. Arteriosclerosis, thrombosis, and vascular biology, 20(3), pp.611-616.

Schiller, H.B. and Fässler, R., 2013. Mechanosensitivity and compositional dynamics of cell–matrix adhesions. EMBO reports, 14(6), pp.509-519.

Schmierer, B. and Hill, C.S., 2007. TGFβ–SMAD signal transduction: molecular specificity and functional flexibility. Nature reviews Molecular cell biology, 8(12), pp.970-982.

Schwitalla, S., Fingerle, A.A., Cammareri, P., Nebelsiek, T., Göktuna, S.I., Ziegler, P.K., Canli, O., Heijmans, J., Huels, D.J., Moreaux, G. and Rupec, R.A., 2013. Intestinal tumorigenesis initiated by dedifferentiation and acquisition of stem-cell-like properties. Cell, 152(1-2), pp.25-38.

Scott, G.K., Mattie, M.D., Berger, C.E., Benz, S.C. and Benz, C.C., 2006. Rapid alteration of microRNA levels by histone deacetylase inhibition. Cancer research, 66(3), pp.1277-1281.

Sefrioui, D., Blanchard, F., Toure, E., Basile, P., Beaussire, L., Dolfus, C., Perdrix, A., Paresy, M., Antonietti, M., Iwanicki-Caron, I. and Alhameedi, R., 2017. Diagnostic value of CA19. 9, circulating tumour DNA and circulating tumour cells in patients with solid pancreatic tumours. British journal of cancer, 117(7), pp.1017-1025.

Segovia-Mendoza, M., González-González, M.E., Barrera, D., Díaz, L. and García-Becerra, R., 2015. Efficacy and mechanism of action of the tyrosine kinase inhibitors gefitinib, lapatinib and neratinib in the treatment of HER2-positive breast cancer: preclinical and clinical evidence. American journal of cancer research, 5(9), p.2531.

Seguin, L., Desgrosellier, J.S., Weis, S.M. and Cheresh, D.A., 2015. Integrins and cancer: regulators of cancer stemness, metastasis, and drug resistance. Trends in cell biology, 25(4), pp.234-240.

Senfter, D., Holzner, S., Kalipciyan, M., Staribacher, A., Walzl, A., Huttary, N., Krieger, S., Brenner, S., Jäger, W., Krupitza, G. and Dolznig, H., 2015. Loss of miR-200 family in 5-fluorouracil resistant colon cancer drives lymphendothelial invasiveness in vitro. Human molecular genetics, 24(13), pp.3689-3698.

Senkus, E., Kyriakides, S., Ohno, S., Penault-Llorca, F., Poortmans, P., Rutgers, E., Zackrisson, S. and Cardoso, F., 2015. Primary breast cancer: ESMO Clinical Practice

Guidelines for diagnosis, treatment and follow-up. Annals of oncology, 26(suppl_5), pp.v8-v30.

Seoane, J., Le, H.V., Shen, L., Anderson, S.A. and Massagué, J., 2004. Integration of Smad and forkhead pathways in the control of neuroepithelial and glioblastoma cell proliferation. Cell, 117(2), pp.211-223.

Sethi, N., Dai, X., Winter, C.G. and Kang, Y., 2011. Tumor-derived JAGGED1 promotes osteolytic bone metastasis of breast cancer by engaging notch signaling in bone cells. Cancer cell, 19(2), pp.192-205.

Seto, M., Ohta, M., Asaoka, Y., Ikenoue, T., Tada, M., Miyabayashi, K., Mohri, D., Tanaka, Y., Ijichi, H., Tateishi, K. and Kanai, F., 2009. Regulation of the hedgehog signaling by the mitogen-activated protein kinase cascade in gastric cancer. Molecular Carcinogenesis: Published in cooperation with the University of Texas MD Anderson Cancer Center, 48(8), pp.703-712.

Seymour, T., Twigger, A.J. and Kakulas, F., 2015. Pluripotency genes and their functions in the normal and aberrant breast and brain. International journal of molecular sciences, 16(11), pp.27288-27301.

Shaikh, F., He, J., Bhadra, P., Chen, X. and Siu, S.W., 2018. TNF receptor type II as an emerging drug target for the treatment of cancer, autoimmune diseases, and graft-versus-host disease: current perspectives and in silico search for small molecule binders. Frontiers in immunology, 9, p.1382.

Shamas-Din, A., Brahmbhatt, H., Leber, B. and Andrews, D.W., 2011. BH3-only proteins: Orchestrators of apoptosis. Biochimica et Biophysica Acta (BBA)-Molecular Cell Research, 1813(4), pp.508-520.

Shames, D.S., Girard, L., Gao, B., Sato, M., Lewis, C.M., Shivapurkar, N., Jiang, A., Perou, C.M., Kim, Y.H., Pollack, J.R. and Fong, K.M., 2006. A genome-wide screen for promoter methylation in lung cancer identifies novel methylation markers for multiple malignancies. PLoS Med, 3(12), p.e486.

Shang, J., Yang, F., Wang, Y., Wang, Y., Xue, G., Mei, Q., Wang, F. and Sun, S., 2014. MicroRNA-23a antisense enhances 5-fluorouracil chemosensitivity through APAF-1/caspase-9 apoptotic pathway in colorectal cancer cells. Journal of cellular biochemistry, 115(4), pp.772-784.

Sharff, K.A., Song, W.X., Luo, X., Tang, N., Luo, J., Chen, J., Bi, Y., He, B.C., Huang, J., Li, X. and Jiang, W., 2009. Hey1 basic helix-loop-helix protein plays an important role in mediating BMP9-induced osteogenic differentiation of mesenchymal progenitor cells. Journal of Biological Chemistry, 284(1), pp.649-659.

Sharma, P., Hu-Lieskovan, S., Wargo, J.A. and Ribas, A., 2017. Primary, adaptive, and acquired resistance to cancer immunotherapy. Cell, 168(4), pp.707-723.

Sharma, S.V., Lee, D.Y., Li, B., Quinlan, M.P., Takahashi, F., Maheswaran, S., McDermott, U., Azizian, N., Zou, L., Fischbach, M.A. and Wong, K.K., 2010. A chromatin-mediated reversible drug-tolerant state in cancer cell subpopulations. Cell, 141(1), pp.69-80.

Sharom, F.J., 2008. ABC multidrug transporters: structure, function and role in chemoresistance. Sharom, F.J., 2011. The P-glycoprotein multidrug transporter. Essays in biochemistry, 50, pp.161-178.

Sharov, A.A., Mardaryev, A.N., Sharova, T.Y., Grachtchouk, M., Atoyan, R., Byers, H.R., Seykora, J.T., Overbeek, P., Dlugosz, A. and Botchkarev, V.A., 2009. Bone morphogenetic protein antagonist noggin promotes skin tumorigenesis via stimulation of the Wnt and Shh signaling pathways. The American journal of pathology, 175(3), pp.1303-1314.

Shaw, R.J., 2009. Tumor suppression by LKB1: SIK-ness prevents metastasis. Science signaling, 2(86), pp.pe55-pe55.

Shen, H., Zhang, L., Zhou, J., Chen, Z., Yang, G., Liao, Y. and Zhu, M., 2017. Epidermal growth factor-containing fibulin-like extracellular matrix protein 1 (EFEMP1) acts as a potential diagnostic biomarker for prostate cancer. Medical science monitor: international medical journal of experimental and clinical research, 23, p.216.

Shen, Y., Quan, J., Wang, M., Li, S., Yang, J., Lv, M., Chen, Z., Zhang, L., Zhao, X. and Yang, J., 2017. Tumor vasculogenic mimicry formation as an unfavorable prognostic indicator in patients with breast cancer. Oncotarget, 8(34), p.56408.

Sheridan, C., Kishimoto, H., Fuchs, R.K. and Mehrotra, S., 2006. Turner CH, Goulet R, Badve S and Nakshatri H CD44+/CD24-breast cancer cells exhibit enhanced invasive properties: an early step necessary for metastasis. Breast Cancer Res, 8, p.R59.

Sheridan, C., Kishimoto, H., Fuchs, R.K., Mehrotra, S., Bhat-Nakshatri, P., Turner, C.H., Goulet, R., Badve, S. and Nakshatri, H., 2006. CD44+/CD24-breast cancer cells exhibit enhanced invasive properties: an early step necessary for metastasis. Breast Cancer Research, 8(5), pp.1-13.

Sheridan, C., Kishimoto, H., Fuchs, R.K., Mehrotra, S., Bhat-Nakshatri, P., Turner, C.H., Goulet, R., Badve, S. and Nakshatri, H., 2006. CD44+/CD24-breast cancer cells exhibit enhanced invasive properties: an early step necessary for metastasis. Breast Cancer Research, 8(5), pp.1-13.

Sherman, B.T. and Lempicki, R.A., 2009. Systematic and integrative analysis of large gene lists using DAVID bioinformatics resources. Nature protocols, 4(1), p.44.

Sherr, C.J. and McCormick, F., 2002. The RB and p53 pathways in cancer. Cancer cell, 2(2), pp.103-112.

Sherwood, D.R. and Plastino, J., 2018. Invading, leading and navigating cells in caenorhabditis elegans: Insights into cell movement in vivo. Genetics, 208(1), pp.53-78.

Shi, F., Ma, Y., Qian, Y., Wang, Y., Wang, Z., Zhao, M. and Hu, Z., 2019. A Novel Peptide Probe for Identification of PLS3-Expressed Cancer Cells. Analytical chemistry, 91(15), pp.9640-9647.

Shi, J., Zhang, L., Shen, A., Zhang, J., Wang, Y., Zhao, Y., Zou, L., Ke, Q., He, F., Wang, P. and Cheng, C., 2010. Clinical and biological significance of forkhead class box O 3a expression in glioma: mediation of glioma malignancy by transcriptional regulation of p27 kip1. Journal of neuro-oncology, 98(1), pp.57-69.

Shi, W., Gerster, K., Alajez, N.M., Tsang, J., Waldron, L., Pintilie, M., Hui, A.B., Sykes, J., P'ng, C., Miller, N. and McCready, D., 2011. MicroRNA-301 mediates proliferation and invasion in human breast cancer. Cancer research, 71(8), pp.2926-2937.

Shi, Y., 2003. Massague J. Mechanisms of TGF-beta signaling from cell membrane to the nucleus. Cell, 113, pp.685-700.

Shi, Y., Du, L., Lin, L. and Wang, Y., 2017. Tumour-associated mesenchymal stem/stromal cells: emerging therapeutic targets. Nature reviews Drug discovery, 16(1), pp.35-52.

Shi, Y., Sawada, J.I., Sui, G., Affar, E.B., Whetstine, J.R., Lan, F., Ogawa, H., Luke, M.P.S., Nakatani, Y. and Shi, Y., 2003. Coordinated histone modifications mediated by a CtBP co-repressor complex. Nature, 422(6933), pp.735-738.

Shibue, T. and Weinberg, R.A., 2017. EMT, CSCs, and drug resistance: the mechanistic link and clinical implications. Nature reviews Clinical oncology, 14(10), p.611.

Shigeno, K., Yoshida, H., Pan, L., Luo, J.M., Fujisawa, S., Naito, K., Nakamura, S., Shinjo, K., Takeshita, A., Ohno, R. and Ohnishi, K., 2004. Disease-related potential of mutations in transcriptional cofactors CREB-binding protein and p300 in leukemias. Cancer letters, 213(1), pp.11-20.

Shih, W. and Yamada, S., 2012. N-cadherin-mediated cell–cell adhesion promotes cell migration in a three-dimensional matrix. Journal of cell science, 125(15), pp.3661-3670.

Shima, Y., Shima, T., Chiba, T., Irimura, T., Pandolfi, P.P. and Kitabayashi, I., 2008. PML activates transcription by protecting HIPK2 and p300 from SCFFbx3-mediated degradation. Molecular and cellular biology, 28(23), pp.7126-7138.

Shimo, T., Nakanishi, T., Nishida, T., Asano, M., Sasaki, A., Kanyama, M., Kuboki, T., Matsumura, T. and Takigawa, M. (2001). Involvement of CTGF, a Hypertrophic Chondrocyte-Specific Gene Product, in Tumor Angiogenesis. Oncology, 61(4), pp.315–322.

Shinnakasu, R., Yamashita, M., Shinoda, K., Endo, Y., Hosokawa, H., Hasegawa, A., Ikemizu, S. and Nakayama, T., 2006. Critical YxKxHxxxRP motif in the C-terminal region

of GATA3 for its DNA binding and function. The Journal of Immunology, 177(9), pp.5801-5810.

Shinomiya, H., Hagi, A., Fukuzumi, M., Mizobuchi, M., Hirata, H. and Utsumi, S., 1995. Complete primary structure and phosphorylation site of the 65-kDa macrophage protein phosphorylated by stimulation with bacterial lipopolysaccharide. The Journal of Immunology, 154(7), pp.3471-3478.

Shintani, Y., Fukumoto, Y., Chaika, N., Grandgenett, P.M., Hollingsworth, M.A., Wheelock, M.J. and Johnson, K.R., 2008. ADH-1 suppresses N-cadherin-dependent pancreatic cancer progression. International journal of cancer, 122(1), pp.71-77.

Shintani, Y., Fukumoto, Y., Chaika, N., Svoboda, R., Wheelock, M.J. and Johnson, K.R., 2008. Collagen I–mediated up-regulation of N-cadherin requires cooperative signals from integrins and discoidin domain receptor 1. The Journal of cell biology, 180(6), pp.1277-1289.

Shintani, Y., Hollingsworth, M.A., Wheelock, M.J. and Johnson, K.R., 2006. Collagen I promotes metastasis in pancreatic cancer by activating c-Jun NH2-terminal kinase 1 and up-regulating N-cadherin expression. Cancer research, 66(24), pp.11745-11753.

Shiota, M., Yokomizo, A., Kashiwagi, E., Tada, Y., Inokuchi, J., Tatsugami, K., Kuroiwa, K., Uchiumi, T., Seki, N. and Naito, S., 2010. Foxo3a expression and acetylation regulate cancer cell growth and sensitivity to cisplatin. Cancer science, 101(5), pp.1177-1185.

Shipitsin, M., Campbell, L.L., Argani, P., Weremowicz, S., Bloushtain-Qimron, N., Yao, J., Nikolskaya, T., Serebryiskaya, T., Beroukhim, R., Hu, M. and Halushka, M.K., 2007. Molecular definition of breast tumor heterogeneity. Cancer cell, 11(3), pp.259-273.

Shirakihara, T., Horiguchi, K., Miyazawa, K., Ehata, S., Shibata, T., Morita, I., Miyazono, K. and Saitoh, M., 2011. TGFβ regulates isoform switching of FGF receptors and epithelial–mesenchymal transition. The EMBO journal, 30(4), pp.783-795.

Shively, J.E. and Beatty, J.D., 1985. CEA-related antigens: molecular biology and clinical significance. Critical reviews in oncology/hematology, 2(4), pp.355-399.

Shon, S.K., Kim, A., Kim, J.Y., Kim, K.I., Yang, Y. and Lim, J.S., 2009. Bone morphogenetic protein-4 induced by NDRG2 expression inhibits MMP-9 activity in breast cancer cells. Biochemical and biophysical research communications, 385(2), pp.198-203.

Shou, J., Massarweh, S., Osborne, C.K., Wakeling, A.E., Ali, S., Weiss, H. and Schiff, R., 2004. Mechanisms of tamoxifen resistance: increased estrogen receptor-HER2/neu cross-talk in ER/HER2–positive breast cancer. Journal of the National Cancer Institute, 96(12), pp.926-935.

Shou, Z., Lin, L., Liang, J., Li, J.L. and Chen, H.Y., 2012. Expression and prognosis of FOXO3a and HIF-1α in nasopharyngeal carcinoma. Journal of cancer research and clinical oncology, 138(4), pp.585-593.

Simpson, E.R. (2003). Sources of estrogen and their importance. The Journal of Steroid Biochemistry and Molecular Biology, [online] 86(3–5), pp.225–230. Available at: https://www.ncbi.nlm.nih.gov/pubmed/14623515/

Sin, W.C. and Lim, C.L. (2017). Breast cancer stem cells—from origins to targeted therapy. Stem Cell Investigation, 4(12), pp.96–96.

Singh, A. and Settleman, J. (2010). EMT, cancer stem cells and drug resistance: an emerging axis of evil in the war on cancer. Oncogene, 29(34), pp.4741–4751.

Singh, R., Bassett, E., Chakravarti, A. and Parthun, M.R. (2018). Replication-dependent histone isoforms: a new source of complexity in chromatin structure and function. Nucleic Acids Research, 46(17), pp.8665–8678.

Singh, T. R., Shankar, S., Chen, X., Asim, M., & Srivastava, R. K. (2003). Synergistic interactions of chemotherapeutic drugs and tumor necrosis factor-related apoptosis-inducing ligand/Apo-2 ligand on apoptosis and on regression of breast carcinoma in vivo. Cancer research, 63(17), pp. 5390–5400.

Singla, N., Goldgur, Y., Xu, K., Paavilainen, S., Nikolov, D.B. and Himanen, J.P. (2010). Crystal structure of the ligand-binding domain of the promiscuous EphA4 receptor reveals two distinct conformations. Biochemical and Biophysical Research Communications, 399(4), pp.555–559.

Sippl, C., Zeilbeck, L.F., Fuchshofer, R. and Tamm, E.R. (2014). Optineurin associates with the podocyte Golgi complex to maintain its structure. Cell and Tissue Research, 358(2), pp.567–583.

Sjöblom, T., Jones, S., Wood, L.D., Parsons, D.W., Lin, J., Barber, T.D., Mandelker, D., Leary, R.J., Ptak, J., Silliman, N., Szabo, S., Buckhaults, P., Farrell, C., Meeh, P., Markowitz, S.D., Willis, J., Dawson, D., Willson, J.K.V., Gazdar, A.F., Hartigan, J., Wu, L., Liu, C., Parmigiani, G., Park, B.H., Bachman, K.E., Papadopoulos, N., Vogelstein, B., Kinzler, K.W. and Velculescu, V.E. (2006). The consensus coding sequences of human breast and colorectal cancers. Science (New York, N.Y.), 314(5797), pp.268–74. Available at: https://www.ncbi.nlm.nih.gov/pubmed/16959974

Skurk, C., Izumiya, Y., Maatz, H., Razeghi, P., Shiojima, I., Sandri, M., Sato, K., Zeng, L., Schiekofer, S., Pimentel, D., Lecker, S., Taegtmeyer, H., Goldberg, A.L. and Walsh, K. (2005). The FOXO3a Transcription Factor Regulates Cardiac Myocyte Size Downstream of AKT Signaling. Journal of Biological Chemistry, 280(21), pp.20814–20823.

Smith, A., Robinson, V., Patel, K. and Wilkinson, D.G. (1997). The EphA4 and EphB1 receptor tyrosine kinases and ephrin-B2 ligand regulate targeted migration of branchial neural crest cells. Current Biology, 7(8), pp.561–570.

Smith, I.E. and Dowsett, M. (2003). Aromatase Inhibitors in Breast Cancer. New England Journal of Medicine, 348(24), pp.2431–2442.

So, J.Y., Lee, H.J., Smolarek, A.K., Paul, S., Wang, C.-X., Maehr, H., Uskokovic, M., Zheng, X., Conney, A.H., Cai, L., Liu, F. and Suh, N. (2010). A Novel Gemini Vitamin D Analog Represses the Expression of a Stem Cell Marker CD44 in Breast Cancer. Molecular Pharmacology, 79(3), pp.360–367.

Soares, R., Balogh, G., Guo, S., Gartner, F., Russo, J. and Schmitt, F., 2004. Evidence for the notch signaling pathway on the role of estrogen in angiogenesis. Molecular endocrinology, 18(9), pp.2333-2343.

Sodani, K., Patel, A., Kathawala, R.J. and Chen, Z.S., 2012. Multidrug resistance associated proteins in multidrug resistance. Chinese journal of cancer, 31(2), p.58.

Soeth, E., Wirth, T., List, H. J., Kumbhani, S., Petersen, A., Neumaier, M., Czubayko, F., & Juhl, H. (2001). Controlled ribozyme targeting demonstrates an antiapoptotic effect of carcinoembryonic antigen in HT29 colon cancer cells. Clinical cancer research : an official journal of the American Association for Cancer Research, 7(7), pp. 2022–2030.

Soler, A., Cayrefourcq, L., Mazard, T., Babayan, A., Lamy, P.-J., Assou, S., Assenat, E., Pantel, K. and Alix-Panabières, C. (2018). Autologous cell lines from circulating colon cancer cells captured from sequential liquid biopsies as model to study therapy-driven tumor changes. Scientific Reports, 8(1).

Sommer, A., Kopitz, C., Schatz, C.A., Nising, C.F., Mahlert, C., Lerchen, H.-G., Stelte Ludwig, B., Hammer, S., Greven, S., Schuhmacher, J., Braun, M., Zierz, R., Wittemer-Rump, S., Harrenga, A., Dittmer, F., Reetz, F., Apeler, H., Jautelat, R., Huynh, H., Ziegelbauer, K. and Kreft, B. (2016). Preclinical Efficacy of the Auristatin-Based Antibody–Drug Conjugate BAY 1187982 for the Treatment of FGFR2-Positive Solid Tumors. Cancer Research, 76(21), pp.6331–6339.

Song, B., Park, S.-H., Zhao, J.C., Fong, K., Li, S., Lee, Y., Yang, Y.A., Sridhar, S., Lu, X., Abdulkadir, S.A., Vessella, R.L., Morrissey, C., Kuzel, T.M., Catalona, W., Yang, X. and Yu, J. (2018). Targeting FOXA1-mediated repression of TGF-β signaling suppresses castration-resistant prostate cancer progression. Journal of Clinical Investigation, 129(2), pp.569–582.

Song, L.-B., Li, J., Liao, W.-T., Feng, Y., Yu, C.-P., Hu, L.-J., Kong, Q.-L., Xu, L.-H., Zhang, X., Liu, W.-L., Li, M.-Z., Zhang, L., Kang, T.-B., Fu, L.-W., Huang, W.-L., Xia, Y.-F., Tsao, S.W., Li, M., Band, V., Band, H., Shi, Q.-H., Zeng, Y.-X. and Zeng, M.-S. (2009). The polycomb group protein Bmi-1 represses the tumor suppressor PTEN and induces epithelial-mesenchymal transition in human nasopharyngeal epithelial cells. Journal of Clinical Investigation, 119(12), pp.3626–3636.

Song, X., Liu, W., Yuan, X., Jiang, J., Wang, W., Mullen, M., Zhao, X., Zhang, Y., Liu, F., Du, S. and Rehman, A., 2018. Acetylation of ACAP4 regulates CCL18-elicited breast cancer cell migration and invasion. Journal of molecular cell biology, 10(6), pp.559-572.

Song, X., Wang, W., Wang, H., Yuan, X., Yang, F., Zhao, L., Mullen, M., Du, S., Zohbi, N., Muthusamy, S. and Cao, Y., 2020. Acetylation of ezrin regulates membrane–cytoskeleton interaction underlying CCL18-elicited cell migration. Journal of molecular cell biology, 12(6), pp.424-437.

Song, Y., Washington, M.K. and Crawford, H.C. (2010). Loss of FOXA1/2 Is Essential for the Epithelial-to-Mesenchymal Transition in Pancreatic Cancer. Cancer Research, 70(5), pp.2115–2125.

Soria, J.-C., DeBraud, F., Bahleda, R., Adamo, B., Andre, F., Dientsmann, R., Delmonte, A., Cereda, R., Isaacson, J., Litten, J., Allen, A., Dubois, F., Saba, C., Robert, R., D'Incalci, M., Zucchetti, M., Camboni, M.G. and Tabernero, J. (2014). Phase I/IIa study evaluating the safety, efficacy, pharmacokinetics, and pharmacodynamics of lucitanib in advanced solid tumors. Annals of Oncology, 25(11), pp.2244–2251.

Sorlie, T., Perou, C.M., Tibshirani, R., Aas, T., Geisler, S., Johnsen, H., Hastie, T., Eisen, M.B., van de Rijn, M., Jeffrey, S.S., Thorsen, T., Quist, H., Matese, J.C., Brown, P.O., Botstein, D., Lonning, P.E. and Borresen-Dale, A.-L. (2001). Gene expression patterns of breast carcinomas distinguish tumor subclasses with clinical implications. Proceedings of the National Academy of Sciences, 98(19), pp.10869–10874.

Sorrentino, A., Thakur, N., Grimsby, S., Marcusson, A., von Bulow, V., Schuster, N., Zhang, S., Heldin, C.-H. and Landström, M. (2008). The type I TGF-β receptor engages TRAF6 to activate TAK1 in a receptor kinase-independent manner. Nature Cell Biology, 10(10), pp.1199–1207.

Sparano, J., O'Neill, A., Alpaugh, K., Wolff, A.C., Northfelt, D.W., Dang, C.T., Sledge, G.W. and Miller, K.D. (2018). Association of Circulating Tumor Cells With Late Recurrence of Estrogen Receptor–Positive Breast Cancer. JAMA Oncology, 4(12), p.1700.

Sparmann, A. and van Lohuizen, M. (2006). Polycomb silencers control cell fate, development and cancer. Nature Reviews Cancer, 6(11), pp.846–856.

Spivak-Kroizman, T.R., Hostetter, G., Posner, R., Aziz, M., Hu, C., Demeure, M.J., Von Hoff, D., Hingorani, S.R., Palculict, T.B., Izzo, J., Kiriakova, G.M., Abdelmelek, M., Bartholomeusz, G., James, B.P. and Powis, G. (2013). Hypoxia Triggers Hedgehog-Mediated Tumor-Stromal Interactions in Pancreatic Cancer. Cancer Research, 73(11), pp.3235–3247.

Sprowl, J.A., Reed, K., Armstrong, S.R., Lanner, C., Guo, B., Kalatskaya, I., Stein, L., Hembruff, S.L., Tam, A. and Parissenti, A.M. (2012). Alterations in tumor necrosis factor

signaling pathways are associated with cytotoxicity and resistance to taxanes: a study in isogenic resistant tumor cells. Breast Cancer Research, 14(1).

Stacy, A.E., Jansson, P.J. and Richardson, D.R. (2013). Molecular Pharmacology of ABCG2 and Its Role in Chemoresistance. Molecular Pharmacology, 84(5), pp.655–669.

Stankiewicz, T.R., Gray, J.J., Winter, A.N. and Linseman, D.A. (2014). C-terminal binding proteins: central players in development and disease. Biomolecular Concepts, 5(6), pp.489–511.

Stanners, C. (2007). Recent Advances in Tumor Biology of the GPI-Anchored Carcinoembryonic Antigen Family Members CEACAM5 and CEACAM6. Current Oncology, 14(2), pp.70–73.

Staton, C.A., Reed, M.W.R. and Brown, N.J. (2009). A critical analysis of current in vitro and in vivo angiogenesis assays. International Journal of Experimental Pathology, 90(3), pp.195–221.

Staub, E., Groene, J., Heinze, M., Mennerich, D., Roepcke, S., Klaman, I., Hinzmann, B., Castanos-Velez, E., Pilarsky, C., Mann, B., Brümmendorf, T., Weber, B., Buhr, H.-J. and Rosenthal, A. (2009). An expression module of WIPF1-coexpressed genes identifies patients with favorable prognosis in three tumor types. Journal of Molecular Medicine, 87(6), pp.633–644.

Stecca, B., Mas, C., Clement, V., Zbinden, M., Correa, R., Piguet, V., Beermann, F. and Ruiz i Altaba, A. (2007). Melanomas require HEDGEHOG-GLI signaling regulated by interactions between GLI1 and the RAS-MEK/AKT pathways. Proceedings of the National Academy of Sciences, 104(14), pp.5895–5900.

Steeg, P.S. (2016). Targeting metastasis. Nature Reviews Cancer, 16(4), pp.201–218.

Stehbens, S.J., Ju, R.J., Adams, M.N., Perry, S.R., Haass, N.K., Bryant, D.M. and Pollock, P.M. (2018). FGFR2-activating mutations disrupt cell polarity to potentiate migration and invasion in endometrial cancer cell models. Journal of Cell Science, 131(15), p.jcs213678.

Stemke-Hale, K., Gonzalez-Angulo, A.M., Lluch, A., Neve, R.M., Kuo, W.-L., Davies, M., Carey, M., Hu, Z., Guan, Y., Sahin, A., Symmans, W.F., Pusztai, L., Nolden, L.K., Horlings, H., Berns, K., Hung, M.-C., van de Vijver, M.J., Valero, V., Gray, J.W., Bernards, R., Mills, G.B. and Hennessy, B.T. (2008). An integrative genomic and proteomic analysis of PIK3CA, PTEN, and AKT mutations in breast cancer. Cancer research, 68(15), pp.6084–91.

Stoletov, K., Kato, H., Zardouzian, E., Kelber, J., Yang, J., Shattil, S. and Klemke, R. (2010). Visualizing extravasation dynamics of metastatic tumor cells. Journal of Cell Science, 123(13), pp.2332–2341.

Storci, G., Sansone, P., Mari, S., D'Uva, G., Tavolari, S., Guarnieri, T., Taffurelli, M., Ceccarelli, C., Santini, D., Chieco, P., Marcu, K.B. and Bonafè, M. (2010). TNFalpha

up-regulates SLUG via the NF-kappaB/HIF1alpha axis, which imparts breast cancer cells with a stem cell-like phenotype. Journal of Cellular Physiology, 225(3), pp.682–691.

Storr, S.J., Lee, K.W., Woolston, C.M., Safuan, S., Green, A.R., Macmillan, R.D., Benhasouna, A., Parr, T., Ellis, I.O. and Martin, S.G. (2012). Calpain system protein expression in basal-like and triple-negative invasive breast cancer. Annals of Oncology, 23(9), pp.2289–2296.

Strasser, A., Harris, A.W., Bath, M.L. and Cory, S. (1990). Novel primitive lymphoid tumours induced in transgenic mice by cooperation between myc and bcl-2. Nature, 348(6299), pp.331–333.

Strathdee, G. (2002). Epigenetic versus genetic alterations in the inactivation of E cadherin. Seminars in Cancer Biology, 12(5), pp.373–379.

Strilic, B. and Offermanns, S. (2017). Intravascular Survival and Extravasation of Tumor Cells. Cancer Cell, 32(3), pp.282–293.

Strippoli, R., Benedicto, I., Foronda, M., Perez-Lozano, M.L., Sanchez-Perales, S., Lopez Cabrera, M. and del Pozo, M.A. (2010). p38 maintains E-cadherin expression by modulating TAK1-NF- B during epithelial-to-mesenchymal transition. Journal of Cell Science, 123(24), pp.4321–4331.

Stuelten, C.H., Mertins, S.D., Busch, J.I., Gowens, M., Scudiero, D.A., Burkett, M.W., Hite, K.M., Alley, M., Hollingshead, M., Shoemaker, R.H. and Niederhuber, J.E., 2010. Complex display of putative tumor stem cell markers in the NCI60 tumor cell line panel. Stem cells, 28(4), pp.649-660.

Stuelten, C.H., Parent, C.A. and Montell, D.J. (2018). Cell motility in cancer invasion and metastasis: insights from simple model organisms. Nature Reviews Cancer, 18(5), pp.296–312.

Stumm, S., Meyer, A., Lindner, M., Bastert, G., Wallwiener, D. and Gückel, B. (2004). Paclitaxel Treatment of Breast Cancer Cell Lines Modulates Fas/Fas Ligand Expression and Induces Apoptosis Which Can Be Inhibited through the CD40 Receptor. Oncology, 66(2), pp.101–111.

Su, B., Liu, H., Wang, X., Chen, S.G., Siedlak, S.L., Kondo, E., Choi, R., Takeda, A., Castellani, R.J., Perry, G., Smith, M.A., Zhu, X. and Lee, H. (2009). Ectopic localization of FOXO3a protein in Lewy bodies in Lewy body dementia and Parkinson's disease. Molecular Neurodegeneration, 4(1), p.32.

Su, C., Huang, D., Liu, J., Liu, W. and Cao, Y. (2019). miR-27a-3p regulates proliferation and apoptosis of colon cancer cells by potentially targeting BTG1. Oncology Letters.

Su, L. and Liu, M. (2018). Correlation analysis on the expression levels of microRNA-23a and microRNA-23b and the incidence and prognosis of ovarian cancer. Oncology Letters.

Su, R., Dong, L., Zou, D., Zhao, H., Ren, Y., Li, F., Yi, P., Li, L., Zhu, Y., Ma, Y., Wang, J., Wang, F. and Yu, J. (2016). microRNA-23a, -27a and -24 synergistically regulate JAK1/Stat3 cascade and serve as novel therapeutic targets in human acute erythroid leukemia. Oncogene, 35(46), pp.6001–6014.

Su, T., Dan, S. and Wang, Y. (2014). Akt–Oct4 regulatory circuit in pluripotent stem cells. Chinese Science Bulletin, 59(10), pp.936–943.

Su, Y., Hopfinger, N.R., Nguyen, T.D., Pogash, T.J., Santucci-Pereira, J. and Russo, J. (2018). Epigenetic reprogramming of epithelial mesenchymal transition in triple negative breast cancer cells with DNA methyltransferase and histone deacetylase inhibitors. Journal of Experimental & Clinical Cancer Research, 37(1).

Su, Y., Li, J., Witkiewicz, A.K., Brennan, D., Neill, T., Talarico, J. and Radice, G.L. (2011). N cadherin haploinsufficiency increases survival in a mouse model of pancreatic cancer. Oncogene, 31(41), pp.4484–4489.

Sudarsanam, S., & Johnson, D. E. (2010). Functional consequences of mTOR inhibition. Current opinion in drug discovery & development, 13(1), pp. 31–40.

Sugase, K., Dyson, H.J. and Wright, P.E. (2007). Mechanism of coupled folding and binding of an intrinsically disordered protein. Nature, 447(7147), pp.1021–1025.

Suh, S.S., Yoo, J.Y., Nuovo, G.J., Jeon, Y.J., Kim, S., Lee, T.J., Kim, T., Bakàcs, A., Alder, H., Kaur, B. and Aqeilan, R.I., 2012. MicroRNAs/TP53 feedback circuitry in glioblastoma multiforme. Proceedings of the National Academy of Sciences, 109(14), pp.5316-5321.

Sui, M., Huang, Y., Park, B.H., Davidson, N.E. and Fan, W. (2007). Estrogen Receptor α Mediates Breast Cancer Cell Resistance to Paclitaxel through Inhibition of Apoptotic Cell Death. Cancer Research, 67(11), pp.5337–5344.

Sulaiman, A., Sulaiman, B., Khouri, L., McGarry, S., Nessim, C., Arnaout, A., Li, X., Addison, C., Dimitroulakos, J. and Wang, L. (2016). Both bulk and cancer stem cell subpopulations in triple-negative breast cancer are susceptible to Wnt, HDAC, and ERα coinhibition. FEBS Letters, 590(24), pp.4606–4616.

Sun, C., Olopade, O.I. and Di Rienzo, A. (2010). rs2981582 is associated with FGFR2 expression in normal breast. Cancer Genetics and Cytogenetics, 197(2), pp.193–194.

Sun, J., Fu, X., Wang, Y., Liu, Y., Zhang, Y., Hao, T., & Hu, X. (2016). Erianin inhibits the proliferation of T47D cells by inhibiting cell cycles, inducing apoptosis and suppressing migration. American journal of translational research, 8(7), pp. 3077–3086.

Sun, L., Ke, J., He, Z., Chen, Z., Huang, Q., Ai, W., Wang, G., Wei, Y., Zou, X., Zhang, S., Lan, P. and Hong, C. (2017). HES1 Promotes Colorectal Cancer Cell Resistance To 5-Fu by Inducing Of EMT and ABC Transporter Proteins. Journal of Cancer, 8(14), pp.2802–2808.

Sun, S., Jiang, Y., Zhang, G., Song, H., Zhang, X., Zhang, Y., Liang, X., Sun, Q. and Pang, D. (2011). Increased expression of fibroblastic growth factor receptor 2 is correlated with poor prognosis in patients with breast cancer. Journal of Surgical Oncology, 105(8), pp.773–779.

Sun, Y., Qian, J., Lu, M. and Xu, H. (2016). Lower and reduced expression of EphA4 is associated with advanced TNM stage, lymph node metastasis, and poor survival in breast carcinoma. Pathology International, 66(9), pp.506–510.

Sunderkötter, C., Goebeler, M., Schulze-Osthoff, K., Bhardwaj, R. and Sorg, C., 1991. Macrophage-derived angiogenesis factors. Pharmacology & therapeutics, 51(2), pp.195-216.

Suyama, K., Shapiro, I., Guttman, M. and Hazan, R.B. (2002). A signaling pathway leading to metastasis is controlled by N-cadherin and the FGF receptor. Cancer Cell, 2(4), pp.301–314.

Suzuki, H.I., Katsura, A., Matsuyama, H. and Miyazono, K. (2014). MicroRNA regulons in tumor microenvironment. Oncogene, 34(24), pp.3085–3094.

Swaminathan, V., Kishore, A.H., Febitha, K.K. and Kundu, T.K. (2005). Human Histone Chaperone Nucleophosmin Enhances Acetylation-Dependent Chromatin Transcription. Molecular and Cellular Biology, 25(17), pp.7534–7545.

Switzer, C.H., Cheng, R.Y.S., Vitek, T.M., Christensen, D.J., Wink, D.A. and Vitek, M.P. (2011). Targeting SET/I2PP2A oncoprotein functions as a multi-pathway strategy for cancer therapy. Oncogene, 30(22), pp.2504–2513.

Swope, D.L., Mueller, C.L. and Chrivia, J.C. (1996). CREB-binding Protein Activates Transcription through Multiple Domains. Journal of Biological Chemistry, 271(45), pp.28138–28145.

Symonds, H., Krall, L., Remington, L., Saenz-Robles, M., Lowe, S., Jacks, T. and Van Dyke, T. (1994). p53-Dependent apoptosis suppresses tumor growth and progression in vivo. Cell, 78(4), pp.703–711.

Szerlong, H.J. and Hansen, J.C. (2011). Nucleosome distribution and linker DNA: connecting nuclear function to dynamic chromatin structure This paper is one of a selection of papers published in a Special Issue entitled 31st Annual International Asilomar Chromatin and Chromosomes Conference, and has undergone the Journal's usual peer review process. Biochemistry and Cell Biology, 89(1), pp.24–34.

Szymanski, P.T. and Tao, T. (1997). Localization of Protein Regions Involved in the Interaction between Calponin and Myosin. Journal of Biological Chemistry, 272(17), pp.11142–11146.

Tacar, O., Sriamornsak, P. and Dass, C.R. (2012). Doxorubicin: an update on anticancer molecular action, toxicity and novel drug delivery systems. Journal of Pharmacy and Pharmacology, 65(2), pp.157–170.

Taherian-Fard, A., Srihari, S. and Ragan, M.A., 2015. Breast cancer classification: linking molecular mechanisms to disease prognosis. Briefings in BIOINFORMATICS, 16(3), pp.461-474.

Tahiri, A., Leivonen, S.-K., Lüders, T., Steinfeld, I., Ragle Aure, M., Geisler, J., Mäkelä, R., Nord, S., Riis, M.L.H., Yakhini, Z., Kleivi Sahlberg, K., Børresen-Dale, A.-L., Perälä, M., Bukholm, I.R.K. and Kristensen, V.N. (2013). Deregulation of cancer-related miRNAs is a common event in both benign and malignant human breast tumors. Carcinogenesis, 35(1), pp.76–85.

Taipale, J., Miyazono, K., Heldin, C.H. and Keski-Oja, J. (1994). Latent transforming growth factor-beta 1 associates to fibroblast extracellular matrix via latent TGF-beta binding protein. The Journal of cell biology, 124(1–2), pp.171–81.

Tajadura-Ortega, V., Gambardella, G., Skinner, A., Halim, A., Van Coillie, J., Schjoldager, K.T.-B.G., Beatson, R., Graham, R., Achkova, D., Taylor-Papadimitriou, J., Ciccarelli, F.D. and Burchell, J.M. (2020). O-linked mucin-type glycosylation regulates the transcriptional programme downstream of EGFR. Glycobiology. Takahashi, K., Hiwada, K. and Kokubu, T. (1986). Isolation and characterization of a 34000-dalton calmodulin- and F-actin-binding protein from chicken gizzard smooth muscle. Biochemical and Biophysical Research Communications, 141(1), pp.20–26.

Takeichi, M. (1990). Cadherins: A Molecular Family Important in Selective Cell-Cell Adhesion. Annual Review of Biochemistry, 59(1), pp.237–252.

Talmadge, J.E. and Fidler, I.J. (2010). AACR Centennial Series: The Biology of Cancer Metastasis: Historical Perspective. Cancer Research, 70(14), pp.5649–5669.

Tamaki, A., Ierano, C., Szakacs, G., Robey, R.W. and Bates, S.E. (2011). The controversial role of ABC transporters in clinical oncology. Essays in Biochemistry, 50, pp.209–232.

Tamilzhalagan, S., Rathinam, D. and Ganesan, K., 2017. Amplified 7q21-22 gene MCM7 and its intronic miR-25 suppress COL1A2 associated genes to sustain intestinal gastric cancer features. Molecular carcinogenesis, 56(6), pp.1590-1602.

Tamoxifen After Adjuvant Chemotherapy for Premenopausal Women With Lymph Node Positive Breast Cancer: International Breast Cancer Study Group Trial 13-93., 2006. J ournal of Clinical Oncology, 24(9), pp.1332–1341.

Tanaka, H., Kono, E., Tran, C.P., Miyazaki, H., Yamashiro, J., Shimomura, T., Fazli, L., Wada, R., Huang, J., Vessella, R.L., An, J., Horvath, S., Gleave, M., Rettig, M.B., Wainberg,

Z.A. and Reiter, R.E. (2010). Monoclonal antibody targeting of N-cadherin inhibits prostate cancer growth, metastasis and castration resistance. Nature Medicine, 16(12), pp.1414–1420.

Tanaka, K., Miyata, H., Sugimura, K., Fukuda, S., Kanemura, T., Yamashita, K., Miyazaki, Y., Takahashi, T., Kurokawa, Y., Yamasaki, M. and Wada, H., 2015. miR-27 is associated with chemoresistance in esophageal cancer through transformation of normal fibroblasts to cancer-associated fibroblasts. Carcinogenesis, 36(8), pp.894-903.

Tanei, T., Morimoto, K., Shimazu, K., Kim, S.J., Tanji, Y., Taguchi, T., Tamaki, Y. and Noguchi, S. (2009). Association of Breast Cancer Stem Cells Identified by Aldehyde Dehydrogenase 1 Expression with Resistance to Sequential Paclitaxel and Epirubicin-Based Chemotherapy for Breast Cancers. Clinical Cancer Research, 15(12), pp.4234–4241.

Tang, Hai-lin & Deng, Min & Liao, Qian-jin & Zeng, xi & Zhou, Xiu-tian & Su, Qi. (2012). Expression and clinical significance of miR-23a and metastasis suppressor 1 in colon carcinoma. Zhonghua bing li xue za zhi Chinese journal of pathology. 41. Pp. 28-32.

Tang, J., Hu, G., Hanai, J., Yadlapalli, G., Lin, Y., Zhang, B., Galloway, J., Bahary, N., Sinha, S., Thisse, B., Thisse, C., Jin, J.-P., Zon, L.I. and Sukhatme, V.P. (2005). A Critical Role for Calponin 2 in Vascular Development. Journal of Biological Chemistry, 281(10), pp.6664–6672.

Tang, W., Yu, F., Yao, H., Cui, X., Jiao, Y., Lin, L., Chen, J., Yin, D., Song, E. and Liu, Q. (2013). miR-27a regulates endothelial differentiation of breast cancer stem like cells. Oncogene, 33(20), pp.2629–2638.

Tang, W., Zhu, J., Su, S., Wu, W., Liu, Q., Su, F. and Yu, F. (2012). MiR-27 as a Prognostic Marker for Breast Cancer Progression and Patient Survival. PLoS ONE, 7(12), p.e51702.

Tang, X., Zhang, H., Long, Y., Hua, H., Jiang, Y. and Jing, J. (2018). PARP9 is overexpressed in human breast cancer and promotes cancer cell migration. Oncology Letters.

Tanimura, Y., Kokuryo, T., Tsunoda, N., Yamazaki, Y., Oda, K., Nimura, Y., Naing Mon, N., Huang, P., Nakanuma, Y., Chen, M.-F., Jan, Y.-Y., Yeh, T.-S., Chiu, C.-T., Hsieh, L.-L. and Hamaguchi, M. (2005). Tumor necrosis factor α promotes invasiveness of cholangiocarcinoma cells via its receptor, TNFR2. Cancer Letters, 219(2), pp.205–213.

Tarragona, M., Pavlovic, M., Arnal-Estapé, A., Urosevic, J., Morales, M., Guiu, M., Planet, E., González-Suárez, E. and Gomis, R.R. (2012). Identification ofNOGas a Specific Breast Cancer Bone Metastasis-supporting Gene. Journal of Biological Chemistry, 287(25), pp.21346–21355.

Tasdogan, A., Faubert, B., Ramesh, V., Ubellacker, J.M., Shen, B., Solmonson, A., Murphy, M.M., Gu, Z., Gu, W., Martin, M., Kasitinon, S.Y., Vandergriff, T., Mathews, T.P., Zhao, Z., Schadendorf, D., DeBerardinis, R.J. and Morrison, S.J. (2019). Metabolic

heterogeneity confers differences in melanoma metastatic potential. Nature, 577(7788), pp.115–120.

Tate, C.M., Pallini, R., Ricci-Vitiani, L., Dowless, M., Shiyanova, T., D'Alessandris, G.Q., Morgante, L., Giannetti, S., Larocca, L.M., di Martino, S., Rowlinson, S.W., De Maria, R. and Stancato, L. (2012). A BMP7 variant inhibits the tumorigenic potential of glioblastoma stem-like cells. Cell Death & Differentiation, 19(10), pp.1644–1654.

Taylor, K.L., Henderson, A.M. and Hughes, C.C.W. (2002). Notch Activation during Endothelial Cell Network Formation in Vitro Targets the Basic HLH Transcription Factor HESR-1 and Downregulates VEGFR-2/KDR Expression. Microvascular Research, 64(3), pp.372–383.

Taylor, N.M.I., Manolaridis, I., Jackson, S.M., Kowal, J., Stahlberg, H. and Locher, K.P. (2017). Structure of the human multidrug transporter ABCG2. Nature, 546(7659), pp.504–509.

Taymaz-Nikerel, H., Karabekmez, M.E., Eraslan, S. and Kırdar, B. (2018). Doxorubicin induces an extensive transcriptional and metabolic rewiring in yeast cells. Scientific Reports, 8(1). Teicher, B.A. (2001). Cancer and Metastasis Reviews, 20(1/2), pp.133–143.

Tekel, S.J. and Haynes, K.A. (2017). Molecular structures guide the engineering of chromatin. Nucleic Acids Research, 45(13), pp.7555–7570.

Tempé, D., Casas, M., Karaz, S., Blanchet-Tournier, M.-F. and Concordet, J.-P. (2006). Multisite Protein Kinase A and Glycogen Synthase Kinase 3β Phosphorylation Leads to Gli3 Ubiquitination by SCFβTrCP. Molecular and Cellular Biology, 26(11), pp.4316–4326.

ten Dijke, P., Hansen, P., Iwata, K.K., Pieler, C. and Foulkes, J.G. (1988). Identification of another member of the transforming growth factor type beta gene family. Proceedings of the National Academy of Sciences, 85(13), pp.4715–4719.

Tenbaum, S.P., Ordóñez-Morán, P., Puig, I., Chicote, I., Arqués, O., Landolfi, S., Fernández, Y., Herance, J.R., Gispert, J.D., Mendizabal, L., Aguilar, S., Cajal, S.R. y, Schwartz, S., Vivancos, A., Espín, E., Rojas, S., Baselga, J., Tabernero, J., Muñoz, A. and Palmer, H.G. (2012). β-catenin confers resistance to PI3K and AKT inhibitors and subverts FOXO3a to promote metastasis in colon cancer. Nature Medicine, 18(6), pp.892–901.

Terzi, F., Henrion, D., Colucci-Guyon, E., Federici, P., Babinet, C., Levy, B.I., Briand, P. and Friedlander, G. (1997). Reduction of renal mass is lethal in mice lacking vimentin. Role of endothelin-nitric oxide imbalance. Journal of Clinical Investigation, 100(6), pp.1520–1528.

Thakuri, P.S., Gupta, M., Singh, S., Joshi, R., Glasgow, E., Lekan, A., Agarwal, S., Luker, G.D. and Tavana, H., 2020. Phytochemicals inhibit migration of triple negative breast cancer cells by targeting kinase signaling. BMC cancer, 20(1), pp.1-14. Thiery, J.P. (2002).

Epithelial–mesenchymal transitions in tumour progression. Nature Reviews Cancer, 2(6), pp.442–454.

Thiery, J.P., Acloque, H., Huang, R.Y.J. and Nieto, M.A. (2009). Epithelial-Mesenchymal Transitions in Development and Disease. Cell, 139(5), pp.871–890.

Thomas, P., Gangopadhyay, A., Steele, G., Andrews, C., Nakazato, H., Oikawa, S. and Jessup, J.M. (1995). The effect of transfection of the CEA gene on the metastatic behavior of the human colorectal cancer cell line MIP-101. Cancer Letters, 92(1), pp.59–66.

Thompson, J.A., Grunert, F. and Zimmermann, W. (1991). Carcinoembryonic antigen gene family: Molecular biology and clinical perspectives. Journal of Clinical Laboratory Analysis, 5(5), pp.344–366.

Thorn, C.F., Oshiro, C., Marsh, S., Hernandez-Boussard, T., McLeod, H., Klein, T.E. and Altman, R.B. (2011). Doxorubicin pathways. Pharmacogenetics and Genomics, 21(7), pp.440–446.

Thuault, S., Tan, E.-J., Peinado, H., Cano, A., Heldin, C.-H. and Moustakas, A. (2008). HMGA2 and Smads Co-regulate SNAIL1 Expression during Induction of Epithelial-to-Mesenchymal Transition. Journal of Biological Chemistry, 283(48), pp.33437–33446.

Thuault, S., Valcourt, U., Petersen, M., Manfioletti, G., Heldin, C.H. and Moustakas, A., 2006. Transforming growth factor-β employs HMGA2 to elicit epithelial–mesenchymal transition. The Journal of cell biology, 174(2), pp.175-183.

Thul, P.J., Åkesson, L., Wiking, M., Mahdessian, D., Geladaki, A., Ait Blal, H., Alm, T., Asplund, A., Björk, L., Breckels, L.M., Bäckström, A., Danielsson, F., Fagerberg, L., Fall, J., Gatto, L., Gnann, C., Hober, S., Hjelmare, M., Johansson, F., Lee, S., Lindskog, C., Mulder, J., Mulvey, C.M., Nilsson, P., Oksvold, P., Rockberg, J., Schutten, R., Schwenk, J.M., Sivertsson, Å., Sjöstedt, E., Skogs, M., Stadler, C., Sullivan, D.P., Tegel, H., Winsnes, C., Zhang, C., Zwahlen, M., Mardinoglu, A., Pontén, F., von Feilitzen, K., Lilley, K.S., Uhlén, M. and Lundberg, E. (2017). A subcellular map of the human proteome. Science, 356(6340), p.eaal3321.

Tian, H., Liu, J., Chen, J., Gatza, M.L. and Blobe, G.C. (2015). Fibulin-3 is a novel TGF-β pathway inhibitor in the breast cancer microenvironment. Oncogene, 34(45), pp.5635–5647.

Tian, K., Di, R. and Wang, L. (2015). MicroRNA-23a enhances migration and invasion through PTEN in osteosarcoma. Cancer Gene Therapy, 22(7), pp.351–359.

Tian, L., Fang, Y., Xue, J. and Chen, J. (2013). Four MicroRNAs Promote Prostate Cell Proliferation with Regulation of PTEN and Its Downstream Signals In Vitro. PLoS ONE, 8(9), p.e75885. Tie, Y., Liu, B., Fu, H. and Zheng, X. (2009). Circulating miRNA and cancer diagnosis. Science in China Series C: Life Sciences, 52(12), pp.1117–1122.

Tikhanovich, I., Cox, J. and Weinman, S.A. (2013). Forkhead box class O transcription factors in liver function and disease. Journal of Gastroenterology and Hepatology, 28, pp.125–131.

Timmerman, L.A. (2004). Notch promotes epithelial-mesenchymal transition during cardiac development and oncogenic transformation. Genes & Development, 18(1), pp.99–115.

Timpl, R., Sasaki, T., Kostka, G. and Chu, M.-L. (2003). Fibulins: a versatile family of extracellular matrix proteins. Nature Reviews Molecular Cell Biology, 4(6), pp.479–489.

Tindemans, I., Serafini, N., Di Santo, J.P. and Hendriks, R.W. (2014). GATA-3 Function in Innate and Adaptive Immunity. Immunity, 41(2), pp.191–206.

Tirino, V., Desiderio, V., Paino, F., De Rosa, A., Papaccio, F., La Noce, M., Laino, L., De Francesco, F. and Papaccio, G. (2012). Cancer stem cells in solid tumors: an overview and new approaches for their isolation and characterization. The FASEB Journal, 27(1), pp.13–24.

Tiwari, A.K., Sodani, K., Wang, S.-R., Kuang, Y.-H., Ashby, C.R., Chen, X. and Chen, Z.-S. (2009). Nilotinib (AMN107, Tasigna®) reverses multidrug resistance by inhibiting the activity of the ABCB1/Pgp and ABCG2/BCRP/MXR transporters. Biochemical Pharmacology, 78(2), pp.153–161.

To, K.K.W., Polgar, O., Huff, L.M., Morisaki, K. and Bates, S.E. (2008). Histone Modifications at the ABCG2 Promoter following Treatment with Histone Deacetylase Inhibitor Mirror Those in Multidrug-Resistant Cells. Molecular Cancer Research, 6(1), pp.151–164.

Toffoli, B., Zennaro, C., Winkler, C., Giordano Attianese, G.M.P., Bernardi, S., Carraro, M., Gilardi, F. and Desvergne, B. (2018). Hemicentin 1 influences podocyte dynamic changes in glomerular diseases. American Journal of Physiology-Renal Physiology, 314(6), pp.F1154–F1165.

Tomczak, K., Czerwińska, P. and Wiznerowicz, M. (2015). Review The Cancer Genome Atlas (TCGA): an immeasurable source of knowledge. Współczesna Onkologia, 1A, pp.68–77.

Tomita, K., van Bokhoven, A., van Leenders, G. J., Ruijter, E. T., Jansen, C. F., Bussemakers, M. J., & Schalken, J. A. (2000). Cadherin switching in human prostate cancer progression. Cancer research, 60(13), pp. 3650–3654.

Tong, J., Jiao, N., Wang, Y., Zhang, Y. And Han, F. (2011). Downregulation of fibulin-3 gene by promoter methylation in colorectal cancer predicts adverse prognosis. Neoplasma, 58(5), pp.441–448.

Topper, J.N., DiChiara, M.R., Brown, J.D., Williams, A.J., Falb, D., Collins, T. and Gimbrone, M.A. (1998). CREB binding protein is a required coactivator for Smad-dependent,

transforming growth factor β transcriptional responses in endothelial cells. Proceedings of the National Academy of Sciences, 95(16), pp.9506–9511.

Toss, A. and Cristofanilli, M. (2015). Molecular characterization and targeted therapeutic approaches in breast cancer. Breast Cancer Research, 17(1).

Touat, M., Ileana, E., Postel-Vinay, S., André, F. and Soria, J.-C. (2015). Targeting FGFR Signaling in Cancer. Clinical Cancer Research, 21(12), pp.2684–2694.

Tradonsky, A., Rubin, T., Beck, R., Ring, B., Seitz, R. and Mair, S. (2012). A Search for Reliable Molecular Markers of Prognosis in Prostate Cancer. American Journal of Clinical Pathology, 137(6), pp.918–930.

Truesdell, S.S., Mortensen, R.D., Seo, M., Schroeder, J.C., Lee, J.H., LeTonqueze, O. and Vasudevan, S. (2012). MicroRNA-mediated mRNA Translation Activation in Quiescent Cells and Oocytes Involves Recruitment of a Nuclear microRNP. Scientific Reports, 2(1).

Truong, H.H., Xiong, J., Ghotra, V.P.S., Nirmala, E., Haazen, L., Le Devedec, S.E., Balcio lu, H.E., He, S., Snaar-Jagalska, B.E., Vreugdenhil, E., Meerman, J.H.N., van de Water, B. and Danen, E.H.J. (2014). 1 Integrin Inhibition Elicits a Prometastatic Switch Through the TGF -miR-200-ZEB Network in E-Cadherin-Positive Triple-Negative Breast Cancer. Science Signaling, 7(312), pp.ra15–ra15.

Trusolino, L., Bertotti, A. and Comoglio, P.M. (2001). A Signaling Adapter Function for $\alpha 6\beta 4$ Integrin in the Control of HGF-Dependent Invasive Growth. Cell, 107(5), pp.643–654.

Tsai, K., Yang, S., Lei, Y., Tsai, C., Chen, H., Hsu, C., Chen, L., Wang, H., Miller, S.A., Chiou, S., Hung, M. and Hung, S. (2011). Mesenchymal Stem Cells Promote Formation of Colorectal Tumors in Mice. Gastroenterology, 141(3), pp.1046–1056.

Tsang, J., Zhu, J. and van Oudenaarden, A. (2007). MicroRNA-Mediated Feedback and Feedforward Loops Are Recurrent Network Motifs in Mammals. Molecular Cell, 26(5), pp.753–767.

Tse, J.M., Cheng, G., Tyrrell, J.A., Wilcox-Adelman, S.A., Boucher, Y., Jain, R.K. and Munn, L.L. (2012). Mechanical compression drives cancer cells toward invasive phenotype. Proceedings of the National Academy of Sciences, 109(3), pp.911–916.

Tsopanoglou, N.E. and Maragoudakis, M.E. (1999). On the Mechanism of Thrombin induced Angiogenesis. Journal of Biological Chemistry, 274(34), pp.23969–23976.

Tsou, S.-H., Chen, T.-M., Hsiao, H.-T. and Chen, Y.-H. (2015). A Critical Dose of Doxorubicin Is Required to Alter the Gene Expression Profiles in MCF-7 Cells Acquiring Multidrug Resistance. PLOS ONE, 10(1), p.e0116747.

Tucker, R., Shipley, G., Moses, H. and Holley, R. (1984). Growth inhibitor from BSC-1 cells closely related to platelet type beta transforming growth factor. Science, 226(4675), pp.705–707.

Turner, N. and Grose, R. (2010). Fibroblast growth factor signalling: from development to cancer. Nature Reviews Cancer, 10(2), pp.116–129.

Turner, N., Lambros, M.B., Horlings, H.M., Pearson, A., Sharpe, R., Natrajan, R., Geyer, F.C., van Kouwenhove, M., Kreike, B., Mackay, A., Ashworth, A., van de Vijver, M.J. and Reis-Filho, J.S. (2010). Integrative molecular profiling of triple negative breast cancers identifies amplicon drivers and potential therapeutic targets. Oncogene, 29(14), pp.2013–2023.

Uchibori, K., Kasamatsu, A., Sunaga, M., Yokota, S., Sakurada, T., Kobayashi, E., Yoshikawa, M., Uzawa, K., Ueda, S., Tanzawa, H. And Sato, N. (2011). Establishment and characterization of two 5-fluorouracil-resistant hepatocellular carcinoma cell lines. International Journal of Oncology, 40(4), pp.1005–1010.

Uchino, M., Kojima, H., Wada, K., Imada, M., Onoda, F., Satofuka, H., Utsugi, T. and Murakami, Y. (2010). Nuclear β-catenin and CD44 upregulation characterize invasive cell populations in non-aggressive MCF-7 breast cancer cells. BMC Cancer, 10(1).

Ueda, S., Takanashi, M., Sudo, K., Kanekura, K. and Kuroda, M. (2020). miR-27a ameliorates chemoresistance of breast cancer cells by disruption of reactive oxygen species homeostasis and impairment of autophagy. Laboratory Investigation, 100(6), pp.863–873.

Ueo, H., Sugimachi, K., Gorges, T.M., Bartkowiak, K., Yokobori, T., Müller, V., Shinden, Y., Ueda, M., Ueo, H., Mori, M., Kuwano, H., Maehara, Y., Ohno, S., Pantel, K. and Mimori, K. (2015). Circulating tumour cell-derived plastin3 is a novel marker for predicting long-term prognosis in patients with breast cancer. British Journal of Cancer, 112(9), pp.1519–1526.

Uhlen, M., Zhang, C., Lee, S., Sjöstedt, E., Fagerberg, L., Bidkhori, G., Benfeitas, R., Arif, M., Liu, Z., Edfors, F., Sanli, K., von Feilitzen, K., Oksvold, P., Lundberg, E., Hober, S., Nilsson, P., Mattsson, J., Schwenk, J.M., Brunnström, H., Glimelius, B., Sjöblom, T., Edqvist, P.-H., Djureinovic, D., Micke, P., Lindskog, C., Mardinoglu, A. and Ponten, F. (2017). A pathology atlas of the human cancer transcriptome. Science, 357(6352), p.eaan2507.

Ujihira, T., Ikeda, K., Suzuki, T., Yamaga, R., Sato, W., Horie-Inoue, K., Shigekawa, T., Osaki, A., Saeki, T., Okamoto, K., Takeda, S. and Inoue, S. (2015). MicroRNA-574-3p, identified by microRNA library-based functional screening, modulates tamoxifen response in breast cancer. Scientific Reports, 5(1).

Urbich, C., Kaluza, D., Frömel, T., Knau, A., Bennewitz, K., Boon, R.A., Bonauer, A., Doebele, C., Boeckel, J.-N., Hergenreider, E., Zeiher, A.M., Kroll, J., Fleming, I. and Dimmeler, S. (2012). MicroRNA-27a/b controls endothelial cell repulsion and angiogenesis by targeting semaphorin 6A. Blood, 119(6), pp.1607–1616.

Ursin, G., Hovanessian-Larsen, L., Parisky, Y.R., Pike, M.C. and Wu, A.H. (2005). Greatly increased occurrence of breast cancers in areas of mammographically dense tissue. Breast Cancer Research, 7(5).

Vaidyanathan, A., Sawers, L., Gannon, A.-L., Chakravarty, P., Scott, A.L., Bray, S.E., Ferguson, M.J. and Smith, G. (2016). ABCB1 (MDR1) induction defines a common resistance mechanism in paclitaxel- and olaparib-resistant ovarian cancer cells. British Journal of Cancer, 115(4), pp.431–441.

Vainzof, M. (1996). The sarcoglycan complex in the six autosomal recessive limb-girdle muscular dystrophies. Human Molecular Genetics, 5(12), pp.1963–1969.

Vaksman, O., Tropé, C., Davidson, B. and Reich, R. (2014). Exosome-derived miRNAs and ovarian carcinoma progression. Carcinogenesis, 35(9), pp.2113–2120.

Valastyan, S. and Weinberg, R.A. (2011). Tumor Metastasis: Molecular Insights and Evolving Paradigms. Cell, 147(2), pp.275–292.

Valderrama-Carvajal, H., Cocolakis, E., Lacerte, A., Lee, E.H., Krystal, G., Ali, S. and Lebrun, J.J., 2002. Activin/TGF-β induce apoptosis through Smad-dependent expression of the lipid phosphatase SHIP. Nature cell biology, 4(12), pp.963-969.

Valieva, M.E., Feofanov, A.V. and Studitsky, V.M. (2016). Histone chaperones: Variety and functions. Moscow University Biological Sciences Bulletin, 71(3), pp.165–169.

Valor, L., Viosca, J., Lopez-Atalaya, J. and Barco, A. (2013). Lysine Acetyltransferases CBP and p300 as Therapeutic Targets in Cognitive and Neurodegenerative Disorders. Current Pharmaceutical Design, 19(28), pp.5051–5064.

Valque, H., Gouyer, V., Gottrand, F. and Desseyn, J.-L. (2012). MUC5B Leads to Aggressive Behavior of Breast Cancer MCF7 Cells. PLoS ONE, 7(10), p.e46699.

van 't Veer, L.J., Dai, H., van de Vijver, M.J., He, Y.D., Hart, A.A.M., Mao, M., Peterse, H.L., van der Kooy, K., Marton, M.J., Witteveen, A.T., Schreiber, G.J., Kerkhoven, R.M., Roberts, C., Linsley, P.S., Bernards, R. and Friend, S.H. (2002). Gene expression profiling predicts clinical outcome of breast cancer. Nature, 415(6871), pp.530–536.

Van Dyck, F., Declercq, J., Braem, C. and Van de Ven, W. (2007). PLAG1, the prototype of the PLAG gene family: Versatility in tumour development (Review). International Journal of Oncology. Van Keymeulen, A., Rocha, A.S., Ousset, M., Beck, B., Bouvencourt, G., Rock, J., Sharma, N., Dekoninck, S. and Blanpain, C. (2011). Distinct stem cells contribute to mammary gland development and maintenance. Nature, 479(7372), pp.189–193.

Van Nguyen, A. and Pollard, J.W. (2002). Colony Stimulating Factor-1 Is Required to Recruit Macrophages into the Mammary Gland to Facilitate Mammary Ductal Outgrowth. Developmental Biology, 247(1), pp.11–25.

van Roy, F. and Berx, G. (2008). The cell-cell adhesion molecule E-cadherin. Cellular and molecular life sciences: CMLS, 65(23), pp.3756–3788.

van Schooneveld, E., Wildiers, H., Vergote, I., Vermeulen, P.B., Dirix, L.Y. and Van Laere, S.J. (2015). Dysregulation of microRNAs in breast cancer and their potential role as prognostic and predictive biomarkers in patient management. Breast Cancer Research, 17(1).

Vande Pol, S.B. and Klingelhutz, A.J. (2013). Papillomavirus E6 oncoproteins. Virology, 445(1–2), pp.115–137.

Vandewalle, C. (2005). SIP1/ZEB2 induces EMT by repressing genes of different epithelial cell-cell junctions. Nucleic Acids Research, 33(20), pp.6566–6578.

Vandewalle, C., Van Roy, F. and Berx, G. (2008). The role of the ZEB family of transcription factors in development and disease. Cellular and Molecular Life Sciences, 66(5), pp.773–787.

Varambally, S., Cao, Q., Mani, R.-S., Shankar, S., Wang, X., Ateeq, B., Laxman, B., Cao, X., Jing, X., Ramnarayanan, K., Brenner, J.C., Yu, J., Kim, J.H., Han, B., Tan, P., Kumar-Sinha, C., Lonigro, R.J., Palanisamy, N., Maher, C.A. and Chinnaiyan, A.M. (2008). Genomic Loss of microRNA-101 Leads to Overexpression of Histone Methyltransferase EZH2 in Cancer. Science, 322(5908), pp.1695–1699.

Varjosalo, M., Björklund, M., Cheng, F., Syvänen, H., Kivioja, T., Kilpinen, S., Sun, Z., Kallioniemi, O., Stunnenberg, H.G., He, W.-W., Ojala, P. and Taipale, J. (2008). Application of Active and Kinase-Deficient Kinome Collection for Identification of Kinases Regulating Hedgehog Signaling. Cell, 133(3), pp.537–548.

Varner, J.A. and Cheresh, D.A. (1996). Integrins and cancer. Current Opinion in Cell Biology, 8(5), pp.724–730.

Varshavsky, A., Kessler, O., Abramovitch, S., Kigel, B., Zaffryar, S., Akiri, G. and Neufeld, G. (2008). Semaphorin-3B Is an Angiogenesis Inhibitor That Is Inactivated by Furin-Like Pro-Protein Convertases. Cancer Research, 68(17), pp.6922–6931. Vassalli, G. (2019). Aldehyde Dehydrogenases: Not Just Markers, but Functional Regulators of Stem Cells. Stem Cells International, 2019, pp.1–15.

Vaught, D., Brantley-Sieders, D.M. and Chen, J. (2008). Eph receptors in breast cancer: roles in tumor promotion and tumor suppression. Breast Cancer Research, 10(6).

Vaux, D.L., Cory, S. and Adams, J.M. (1988). Bcl-2 gene promotes haemopoietic cell survival and cooperates with c-myc to immortalize pre-B cells. Nature, 335(6189), pp.440–442.

Veliceasa, D., Biyashev, D., Qin, G., Misener, S., Mackie, A.R., Kishore, R. and Volpert, O.V. (2015). Therapeutic manipulation of angiogenesis with miR-27b. Vascular Cell, 7(1).

Venkatesh, S. and Workman, J.L. (2015). Histone exchange, chromatin structure and the regulation of transcription. Nature Reviews Molecular Cell Biology, 16(3), pp.178–189.

Ventura, A., Young, A.G., Winslow, M.M., Lintault, L., Meissner, A., Erkeland, S.J., Newman, J., Bronson, R.T., Crowley, D., Stone, J.R., Jaenisch, R., Sharp, P.A. and Jacks, T. (2008). Targeted Deletion Reveals Essential and Overlapping Functions of the miR-17∼92 Family of miRNA Clusters. Cell, 132(5), pp.875–886.

Verde, P., Casalino, L., Talotta, F., Yaniv, M. and Weitzman, J.B. (2007). Deciphering AP-1 Function in Tumorigenesis: Fra-ternizing on Target Promoters. Cell Cycle, 6(21), pp.2633–2639.

Verdone, L., Agricola, E., Caserta, M. and Di Mauro, E. (2006). Histone acetylation in gene regulation. Briefings in Functional Genomics, 5(3), pp.209–221.

Vermeulen, L., De Sousa E Melo, F., van der Heijden, M., Cameron, K., de Jong, J.H., Borovski, T., Tuynman, J.B., Todaro, M., Merz, C., Rodermond, H., Sprick, M.R., Kemper, K., Richel, D.J., Stassi, G. and Medema, J.P. (2010). Wnt activity defines colon cancer stem cells and is regulated by the microenvironment. Nature Cell Biology, 12(5), pp.468–476.

Vesuna, F., van Diest, P., Chen, J.H. and Raman, V. (2008). Twist is a transcriptional repressor of E-cadherin gene expression in breast cancer. Biochemical and Biophysical Research Communications, 367(2), pp.235–241.

Villunger, A. (2003). p53- and Drug-Induced Apoptotic Responses Mediated by BH3-Only Proteins Puma and Noxa. Science, 302(5647), pp.1036–1038.

Vinogradov, S. and Wei, X. (2012). Cancer stem cells and drug resistance: the potential of nanomedicine. Nanomedicine (London, England), 7(4), pp.597–615.

Virrey, J.J., Guan, S., Li, W., Schönthal, A.H., Chen, T.C. and Hofman, F.M., 2008. Increased survivin expression confers chemoresistance to tumor-associated endothelial cells. The American journal of pathology, 173(2), pp.575-585.

Vishnoi, M., Peddibhotla, S., Yin, W., T. Scamardo, A., George, G.C., Hong, D.S. and Marchetti, D. (2015). The isolation and characterization of CTC subsets related to breast cancer dormancy. Scientific Reports, 5(1). Visvader, J.E. and Lindeman, G.J., 2008. Cancer stem cells in solid tumours: accumulating evidence and unresolved questions. Nature reviews cancer, 8(10), pp.755-768.

Vleugel, M.M., Greijer, A.E., Bos, R., van der Wall, E. and van Diest, P.J. (2006). c-Jun activation is associated with proliferation and angiogenesis in invasive breast cancer. Human Pathology, 37(6), pp.668–674.

Voduc, K.D., Cheang, M.C.U., Tyldesley, S., Gelmon, K., Nielsen, T.O. and Kennecke, H. (2010). Breast Cancer Subtypes and the Risk of Local and Regional Relapse. Journal of Clinical Oncology, 28(10), pp.1684–1691.

Vogel, B.E., Muriel, J.M., Dong, C. and Xu, X. (2006). Hemicentins: What have we learned from worms? Cell Research, 16(11), pp.872–878.

Volkman, B.F., Prehoda, K.E., Scott, J.A., Peterson, F.C. and Lim, W.A. (2002). Structure of the N-WASP EVH1 Domain-WIP Complex. Cell, 111(4), pp.565–576.

von Burstin, J., Eser, S., Paul, M.C., Seidler, B., Brandl, M., Messer, M., von Werder, A., Schmidt, A., Mages, J., Pagel, P., Schnieke, A., Schmid, R.M., Schneider, G. and Saur, D. (2009). E-Cadherin Regulates Metastasis of Pancreatic Cancer In Vivo and Is Suppressed by a SNAIL/HDAC1/HDAC2 Repressor Complex. Gastroenterology, 137(1), pp.361-371.e5.

Voorneveld, P.W., Kodach, L.L., Jacobs, R.J., van Noesel, C.J.M., Peppelenbosch, M.P., Korkmaz, K.S., Molendijk, I., Dekker, E., Morreau, H., van Pelt, G.W., Tollenaar, R.A.E.M., Mesker, W., Hawinkels, L.J.A.C., Paauwe, M., Verspaget, H.W., Geraets, D.T., Hommes, D.W., Offerhaus, G.J.A., van den Brink, G.R., ten Dijke, P. and Hardwick, J.C.H. (2014). The BMP pathway either enhances or inhibits the Wnt pathway depending on the SMAD4 and p53 status in CRC. British Journal of Cancer, 112(1), pp.122–130.

Vora, H.H., Patel, N.A., Rajvik, K.N., Mehta, S.V., Brahmbhatt, B.V., Shah, M.J., Shukla, S.N. and Shah, P.M. (2009). Cytokeratin and Vimentin Expression in Breast Cancer. The International Journal of Biological Markers, 24(1), pp.38–46.

Voulgari, A. and Pintzas, A. (2009). Epithelial–mesenchymal transition in cancer metastasis: Mechanisms, markers and strategies to overcome drug resistance in the clinic. Biochimica et Biophysica Acta (BBA) - Reviews on Cancer, 1796(2), pp.75–90.

Vtorushin, S.V., Khristenko, K.Y., Zavyalova, M.V., Perelmuter, V.M., Litviakov, N.V., Denisov, E.V., Dulesova, A.Y. and Cherdyntseva, N.V., 2014. The phenomenon of multi-drug resistance in the treatment of malignant tumors. Experimental oncology. Vuoriluoto, K., Haugen, H., Kiviluoto, S., Mpindi, J.-P., Nevo, J., Gjerdrum, C., Tiron, C., Lorens, J.B. and Ivaska, J. (2010). Vimentin regulates EMT induction by Slug and oncogenic H-Ras and migration by governing Axl expression in breast cancer. Oncogene, 30(12), pp.1436–1448.

W Robey, R., Ierano, C., Zhan, Z. and E Bates, S., 2011. The challenge of exploiting ABCG2 in the clinic. Current pharmaceutical biotechnology, 12(4), pp.595-608.

Wainwright, E.N. and Scaffidi, P., 2017. Epigenetics and cancer stem cells: unleashing, hijacking, and restricting cellular plasticity. Trends in cancer, 3(5), pp.372-386.

Wajant, H., Pfizenmaier, K. and Scheurich, P., 2003. Tumor necrosis factor signaling. Cell Death & Differentiation, 10(1), pp.45-65.

Wakabayashi, Y., Mao, J.H., Brown, K., Girardi, M. and Balmain, A., 2007. Promotion of Hras-induced squamous carcinomas by a polymorphic variant of the Patched gene in FVB mice. Nature, 445(7129), pp.761-765.

Wang, B., Hsu, S.H., Frankel, W., Ghoshal, K. and Jacob, S.T., 2012. Stat3-mediated activation of microRNA-23a suppresses gluconeogenesis in hepatocellular carcinoma by down-regulating Glucose-6-phosphatase and peroxisome proliferator-activated receptor gamma, coactivator 1 alpha. Hepatology, 56(1), pp.186-197.

Wang, B., Zhang, Z., Xia, S.A., Jiang, M. and Wang, Y., 2019. Expression of γ-H2AX and patient prognosis in breast cancer cohort. Journal of Cellular Biochemistry, 120(8), pp.12958-12965.

Wang, C., Wang, X., Su, Z., Fei, H., Liu, X. and Pan, Q., 2015. MiR-25 promotes hepatocellular carcinoma cell growth, migration and invasion by inhibiting RhoGDI1. Oncotarget, 6(34), p.36231.

Wang, D., Naydenov, N.G., Dozmorov, M.G., Koblinski, J.E. and Ivanov, A.I., 2020. Anillin regulates breast cancer cell migration, growth, and metastasis by non-canonical mechanisms involving control of cell stemness and differentiation. Breast Cancer Research, 22(1), pp.1-19.

Wang, F., Marshall, C.B. and Ikura, M., 2013. Transcriptional/epigenetic regulator CBP/p300 in tumorigenesis: structural and functional versatility in target recognition. Cellular and Molecular Life Sciences, 70(21), pp.3989-4008.

Wang, F., Marshall, C.B., Yamamoto, K., Li, G.Y., Gasmi-Seabrook, G.M., Okada, H., Mak, T.W. and Ikura, M., 2012. Structures of KIX domain of CBP in complex with two FOXO3a transactivation domains reveal promiscuity and plasticity in coactivator recruitment. Proceedings of the National Academy of Sciences, 109(16), pp.6078-6083.

Wang, F., Marshall, C.B., Yamamoto, K., Li, G.Y., Plevin, M.J., You, H., Mak, T.W. and Ikura, M., 2008. Biochemical and structural characterization of an intramolecular interaction in FOXO3a and its binding with p53. Journal of molecular biology, 384(3), pp.590-603.

Wang, J., Guan, X., Zhang, Y., Ge, S., Zhang, L., Li, H., Wang, X., Liu, R., Ning, T., Deng, T. and Zhang, H., 2018. Exosomal miR-27a derived from gastric cancer cells regulates the transformation of fibroblasts into cancer-associated fibroblasts. Cellular Physiology and Biochemistry, 49(3), pp.869-883.

Wang, J., Ray, P.S., Sim, M.S., Zhou, X.Z., Lu, K.P., Lee, A.V., Lin, X., Bagaria, S.P., Giuliano, A.E. and Cui, X., 2012. FOXC1 regulates the functions of human basal-like breast cancer cells by activating NF-κB signaling. Oncogene, 31(45), pp.4798-4802.

Wang, J., Zhu, B., Zhang, Y., Saiyin, H., Wumaier, R., Yu, L., Sun, L. and Xiao, Q., 2019. HEY2 acting as a co-repressor with smad3 and smad4 interferes with the response of TGF-beta in hepatocellular carcinoma. American journal of translational research, 11(7), p.4367.

Wang, K. and Li, P.F., 2010. Foxo3a regulates apoptosis by negatively targeting miR-21. Journal of Biological Chemistry, 285(22), pp.16958-16966.

Wang, K., Zhang, Q., Li, D., Ching, K., Zhang, C., Zheng, X., Ozeck, M., Shi, S., Li, X., Wang, H. and Rejto, P., 2015. PEST domain mutations in Notch receptors comprise an oncogenic driver segment in triple-negative breast cancer sensitive to a γ-secretase inhibitor. Clinical cancer research, 21(6), pp.1487-1496.

Wang, N., Zhu, M., Tsao, S.W., Man, K., Zhang, Z. and Feng, Y., 2013. MiR-23a-mediated inhibition of topoisomerase 1 expression potentiates cell response to etoposide in human hepatocellular carcinoma. Molecular Cancer, 12(1), pp.1-10.

Wang, R.A., Li, Z.S., Zhang, H.Z., Zheng, P.J., Li, Q.L., Shi, J.G., Yan, Q.G., Ye, J., Wang, J.B., Guo, Y. and Huang, X.F., 2013. Invasive cancers are not necessarily from preformed in situ tumours—an alternative way of carcinogenesis from misplaced stem cells. Journal of Cellular and Molecular Medicine, 17(7), pp.921-926.

Wang, S., Tsui, S.T., Liu, C., Song, Y. and Liu, D., 2016. EGFR C797S mutation mediates resistance to third-generation inhibitors in T790M-positive non-small cell lung cancer. Journal of hematology & oncology, 9(1), pp.1-5.

Wang, S.X., Elder, P.K., Zheng, Y., Strauch, A.R. and Kelm, R.J., 2005. Cell cycle-mediated regulation of smooth muscle α-actin gene transcription in fibroblasts and vascular smooth muscle cells involves multiple adenovirus E1A-interacting cofactors. Journal of Biological Chemistry, 280(7), pp.6204-6214.

Wang, W., Cheng, B., Miao, L., Mei, Y. and Wu, M., 2013. Mutant p53-R273H gains new function in sustained activation of EGFR signaling via suppressing miR-27a expression. Cell death & disease, 4(4), pp.e574-e574.

Wang, X., Belguise, K., Kersual, N., Kirsch, K.H., Mineva, N.D., Galtier, F., Chalbos, D. and Sonenshein, G.E., 2007. Oestrogen signalling inhibits invasive phenotype by repressing RelB and its target BCL2. Nature cell biology, 9(4), pp.470-478.

Wang, X., Bo, J., Bridges, T., Dugan, K.D., Pan, T.C., Chodosh, L.A. and Montell, D.J., 2006. Analysis of cell migration using whole-genome expression profiling of migratory cells in the Drosophila ovary. Developmental cell, 10(4), pp.483-495.

Wang, X., Decker, C.C., Zechner, L., Krstin, S. and Wink, M., 2019. In vitro wound healing of tumor cells: inhibition of cell migration by selected cytotoxic alkaloids. BMC Pharmacology and Toxicology, 20(1), pp.1-12.

Wang, X., Hu, S. and Liu, L., 2017. Phosphorylation and acetylation modifications of FOXO3a: Independently or synergistically?. Oncology letters, 13(5), pp.2867-2872.

Wang, X., Zheng, M., Liu, G., Xia, W., McKeown-Longo, P.J., Hung, M.C. and Zhao, J., 2007. Krüppel-like factor 8 induces epithelial to mesenchymal transition and epithelial cell invasion. Cancer research, 67(15), pp.7184-7193.

Wang, Y. and Zhou, B.P., 2011. Epithelial-mesenchymal transition in breast cancer progression and metastasis. Chinese journal of cancer, 30(9), p.603.

Wang, Y., Bu, F., Royer, C., Serres, S., Larkin, J.R., Soto, M.S., Sibson, N.R., Salter, V., Fritzsche, F., Turnquist, C. and Koch, S., 2014. ASPP2 controls epithelial plasticity and inhibits metastasis through β-catenin-dependent regulation of ZEB1. Nature cell biology, 16(11), pp.1092-1104.

Wang, Y., Klijn, J.G., Zhang, Y., Sieuwerts, A.M., Look, M.P., Yang, F., Talantov, D., Timmermans, M., Meijer-van Gelder, M.E., Yu, J. and Jatkoe, T., 2005. Gene-expression profiles to predict distant metastasis of lymph-node-negative primary breast cancer. The Lancet, 365(9460), pp.671-679.

Wang, Y., Lee, A.T., Ma, J.Z., Wang, J., Ren, J., Yang, Y., Tantoso, E., Li, K.B., Ooi, L.L.J., Tan, P. and Lee, C.G., 2008. Profiling microRNA expression in hepatocellular carcinoma reveals microRNA-224 up-regulation and apoptosis inhibitor-5 as a microRNA-224-specific target. Journal of Biological Chemistry, 283(19), pp.13205-13215.

Wang, Z., Chen, Y., Lin, Y., Wang, X., Cui, X., Zhang, Z., Xian, G. and Qin, C., 2017. Novel crosstalk between KLF4 and ZEB1 regulates gemcitabine resistance in pancreatic ductal adenocarcinoma. International Journal of Oncology, 51(4), pp.1239-1248.

Wang, Z., Li, T.E., Chen, M., Pan, J.J. and Shen, K.W., 2020. miR-106b-5p contributes to the lung metastasis of breast cancer via targeting CNN1 and regulating Rho/ROCK1 pathway. Aging (Albany NY), 12(2), p.1867.

Wang, Z., Shen, Z., Li, Z., Duan, J., Fu, S., Liu, Z., Bai, H., Zhang, Z., Zhao, J., Wang, X. and Wang, J., 2015. Activation of the BMP-BMPR pathway conferred resistance to EGFR-TKIs in lung squamous cell carcinoma patients with EGFR mutations. Proceedings of the National Academy of Sciences, 112(32), pp.9990-9995.

Wang, Z., Wang, N., Liu, P., Chen, Q., Situ, H., Xie, T., Zhang, J., Peng, C., Lin, Y. and Chen, J., 2014. MicroRNA-25 regulates chemoresistance-associated autophagy in breast cancer cells, a process modulated by the natural autophagy inducer isoliquiritigenin. Oncotarget, 5(16), p.7013.

Ward, A., Balwierz, A., Zhang, J.D., Küblbeck, M., Pawitan, Y., Hielscher, T., Wiemann, S. and Sahin, Ö., 2013. Re-expression of microRNA-375 reverses both tamoxifen resistance and accompanying EMT-like properties in breast cancer. Oncogene, 32(9), pp.1173-1182.

Wasif, N., Maggard, M.A., Ko, C.Y. and Giuliano, A.E., 2010. Invasive lobular vs. ductal breast cancer: a stage-matched comparison of outcomes. Annals of surgical oncology, 17(7), pp.1862-1869.

Watanabe, A., Yasuhira, S., Inoue, T., Kasai, S., Shibazaki, M., Takahashi, K., Akasaka, T., Masuda, T. and Maesawa, C., 2013. BCL 2 and BCL xL are key determinants of resistance to antitubulin chemotherapeutics in melanoma cells. Experimental dermatology, 22(8), pp.518-523.

Watanabe, N., Tomita, T., Sato, C., Kitamura, T., Morohashi, Y. and Iwatsubo, T., 2005. Pen-2 is incorporated into the γ-secretase complex through binding to transmembrane domain 4 of presenilin 1. Journal of Biological Chemistry, 280(51), pp.41967-41975.

Weaver, B.A., 2014. How Taxol/paclitaxel kills cancer cells. Molecular biology of the cell, 25(18), pp.2677-2681. Weedon, M.N., Lango, H., Lindgren, C.M., Wallace, C., Evans, D.M., Mangino, M., Freathy, R.M., Perry, J.R., Stevens, S., Hall, A.S. and Samani, N.J., 2008. Genome-wide association analysis identifies 20 loci that influence adult height. Nature genetics, 40(5), p.575.

Ween, M.P., Armstrong, M.A., Oehler, M.K. and Ricciardelli, C., 2015. The role of ABC transporters in ovarian cancer progression and chemoresistance. Critical reviews in oncology/hematology, 96(2), pp.220-256.

Wei-Wei, S.H.I., Yong, L.I., Zhen, W.A.N.G., Rong-Guang, S.H.A.O., Dian-Dong, L.I. and Qi Yang, H.E., 2009. Role of prosurvival molecules in the action of lidamycin toward human tumor cells. Biomedical and Environmental Sciences, 22(3), pp.244-252.

Wei, J., Yang, Y., Lu, M., Lei, Y., Xu, L., Jiang, Z., Xu, X., Guo, X., Zhang, X., Sun, H. and You, Q., 2018. Recent Advances in the Discovery of HIF-1α-p300/CBP Inhibitors as Anti-Cancer Agents. Mini reviews in medicinal chemistry, 18(4), pp.296-309.

Wei, W., Liu, W., Serra, S., Asa, S.L. and Ezzat, S., 2015. The breast cancer susceptibility FGFR2 provides an alternate mode of HER2 activation. Oncogene, pp.1-9.

Weidle, U.H., Dickopf, S., Hintermair, C., Kollmorgen, G., Birzele, F. and Brinkmann, U., 2018. The role of micro RNAs in breast cancer metastasis: preclinical validation and potential therapeutic targets. Cancer Genomics-Proteomics, 15(1), pp.17-39.

Weigelt, B., Peterse, J.L. and Van't Veer, L.J., 2005. Breast cancer metastasis: markers and models. Nature reviews cancer, 5(8), pp.591-602. Weinberg, O.K., Marquez-Garban, D.C. and Pietras, R.J., 2005. New approaches to reverse resistance to hormonal therapy in human breast cancer. Drug resistance updates, 8(4), pp.219-233.

Weinberg, R.A., 2014. Coming full circle—from endless complexity to simplicity and back again. Cell, 157(1), pp.267-271.

Welch-Reardon, K.M., Ehsan, S.M., Wang, K., Wu, N., Newman, A.C., Romero-Lopez, M., Fong, A.H., George, S.C., Edwards, R.A. and Hughes, C.C., 2014. Angiogenic sprouting is regulated by endothelial cell expression of Slug. Journal of cell science, 127(9), pp.2017-2028.

Wellner, U., Brabletz, T. and Keck, T., 2010. ZEB1 in pancreatic cancer. Cancers, 2(3), pp.1617-1628.

Wellner, U., Schubert, J., Burk, U.C., Schmalhofer, O., Zhu, F., Sonntag, A., Waldvogel, B., Vannier, C., Darling, D., Zur Hausen, A. and Brunton, V.G., 2009. The EMT-activator ZEB1 promotes tumorigenicity by repressing stemness-inhibiting microRNAs. Nature cell biology, 11(12), pp.1487-1495.

Wesche, J., Haglund, K. and Haugsten, E.M., 2011. Fibroblast growth factors and their receptors in cancer. Biochemical Journal, 437(2), pp.199-213.

Wheler, J.J., Janku, F., Naing, A., Li, Y., Stephen, B., Zinner, R., Subbiah, V., Fu, S., Karp, D., Falchook, G.S. and Tsimberidou, A.M., 2016. Cancer therapy directed by comprehensive genomic profiling: a single center study. Cancer research, 76(13), pp.3690-3701.

White, D.E., Kurpios, N.A., Zuo, D., Hassell, J.A., Blaess, S., Mueller, U. and Muller, W.J., 2004. Targeted disruption of β1-integrin in a transgenic mouse model of human breast cancer reveals an essential role in mammary tumor induction. Cancer cell, 6(2), pp.159-170.

Whittaker, C.A. and Hynes, R.O., 2002. Distribution and evolution of von Willebrand/integrin A domains: widely dispersed domains with roles in cell adhesion and elsewhere. Molecular biology of the cell, 13(10), pp.3369-3387.

Whyte, P., Williamson, N.M. and Harlow, E.D., 1989. Cellular targets for transformation by the adenovirus E1A proteins. cell, 56(1), pp.67-75.

Whyte, W.A., Orlando, D.A., Hnisz, D., Abraham, B.J., Lin, C.Y., Kagey, M.H., Rahl, P.B., Lee, T.I. and Young, R.A., 2013. Master transcription factors and mediator establish super-enhancers at key cell identity genes. Cell, 153(2), pp.307-319.

Wilbur, M.A., Shih, I.M., Segars, J.H. and Fader, A.N., 2017, January. Cancer implications for patients with endometriosis. In Seminars in reproductive medicine (Vol. 35, No. 01, pp. 110-116). Thieme Medical Publishers.

Wilhelm, B., Meinhardt, A. and Seitz, J., 1996. Transglutaminases: purification and activity assays. Journal of Chromatography B: Biomedical Sciences and Applications, 684(1-2), pp.163-177.

Wilk, G. and Braun, R., 2018. regQTLs: Single nucleotide polymorphisms that modulate microRNA regulation of gene expression in tumors. PLoS genetics, 14(12), p.e1007837.

Williams, T.M., Moolten, D., Burlein, J., Romano, J., Bhaerman, R., Godillot, A., Mellon, M., Rauscher, F.D. and Kant, J.A., 1991. Identification of a zinc finger protein that inhibits IL-2 gene expression. Science, 254(5039), pp.1791-1794.

Wilson, A.R.M., Marotti, L., Bianchi, S., Biganzoli, L., Claassen, S., Decker, T., Frigerio, A., Goldhirsch, A., Gustafsson, E.G., Mansel, R.E. and Orecchia, R., 2013. The requirements of a specialist Breast Centre. European journal of cancer, 49(17), pp.3579-3587.

Winograd-Katz, S.E., Fässler, R., Geiger, B. and Legate, K.R., 2014. The integrin adhesome: from genes and proteins to human disease. Nature reviews Molecular cell biology, 15(4), pp.273-288.

Winter, J., Jung, S., Keller, S., Gregory, R.I. and Diederichs, S., 2009. Many roads to maturity: microRNA biogenesis pathways and their regulation. Nature cell biology, 11(3), pp.228-234.

Wipff, P.J. and Hinz, B., 2008. Integrins and the activation of latent transforming growth factor β1–an intimate relationship. European journal of cell biology, 87(8-9), pp.601-615.

Witt, A.E., Lee, C.W., Lee, T.I., Azzam, D.J., Wang, B., Caslini, C., Petrocca, F., Grosso, J., Jones, M., Cohick, E.B. and Gropper, A.B., 2017. Identification of a cancer stem cell-specific function for the histone deacetylases, HDAC1 and HDAC7, in breast and ovarian cancer. Oncogene, 36(12), pp.1707-1720.

Wojciak, J.M., Martinez-Yamout, M.A., Dyson, H.J. and Wright, P.E., 2009. Structural basis for recruitment of CBP/p300 coactivators by STAT1 and STAT2 transactivation domains. The EMBO journal, 28(7), pp.948-958.

Wolf, I., Bose, S., Williamson, E.A., Miller, C.W., Karlan, B.Y. and Koeffler, H.P., 2007. FOXA1: Growth inhibitor and a favorable prognostic factor in human breast cancer. International journal of cancer, 120(5), pp.1013-1022.

Wolfe, M.S., Xia, W., Ostaszewski, B.L., Diehl, T.S., Kimberly, W.T. and Selkoe, D.J., 1999. Two transmembrane aspartates in presenilin-1 required for presenilin endoproteolysis and γ-secretase activity. Nature, 398(6727), pp.513-517.

Wong, H.K.A., Veremeyko, T., Patel, N., Lemere, C.A., Walsh, D.M., Esau, C., Vanderburg, C. and Krichevsky, A.M., 2013. De-repression of FOXO3a death axis by microRNA-132 and-212 causes neuronal apoptosis in Alzheimer's disease. Human molecular genetics, 22(15), pp.3077-3092.

Wright, M.H., Calcagno, A.M., Salcido, C.D., Carlson, M.D., Ambudkar, S.V. and Varticovski, L., 2008. Brca1 breast tumors contain distinct CD44+/CD24-and CD133+ cells with cancer stem cell characteristics. Breast Cancer Research, 10(1), p.R10.

Wu, D.C., Zhang, M.F., Su, S.G., Fang, H.Y., Wang, X.H., He, D., Xie, Y.Y. and Liu, X.H., 2016. HEY2, a target of miR-137, indicates poor outcomes and promotes cell proliferation and migration in hepatocellular carcinoma. Oncotarget, 7(25), p.38052.

Wu, F., Li, J., Guo, N., Wang, X.H. and Liao, Y.Q., 2017. MiRNA-27a promotes the proliferation and invasion of human gastric cancer MGC803 cells by targeting SFRP1 via Wnt/β-catenin signaling pathway. American journal of cancer research, 7(3), p.405.

Wu, G., Li, Z., Jiang, P., Zhang, X., Xu, Y., Chen, K. and Li, X., 2017. MicroRNA-23a promotes pancreatic cancer metastasis by targeting epithelial splicing regulator protein 1. Oncotarget, 8(47), p.82854.

Wu, J., Sun, Z., Sun, H. and Li, Y., 2018. MicroRNA 27a promotes tumorigenesis via targeting AKT in triple negative breast cancer. Molecular medicine reports, 17(1), pp.562-570.

Wu, M., Cao, M., He, Y., Liu, Y., Yang, C., Du, Y., Wang, W. and Gao, F., 2015. A novel role of low molecular weight hyaluronan in breast cancer metastasis. The FASEB Journal, 29(4), pp.1290-1298.

Wu, M.Y., Fu, J., Xiao, X., Wu, J. and Wu, R.C., 2014. MiR-34a regulates therapy resistance by targeting HDAC1 and HDAC7 in breast cancer. Cancer letters, 354(2), pp.311-319.

Wu, M.Z., Cheng, W.C., Chen, S.F., Nieh, S., O'Connor, C., Liu, C.L., Tsai, W.W., Wu, C.J., Martin, L., Lin, Y.S. and Wu, K.J., 2017. miR-25/93 mediates hypoxia-induced immunosuppression by repressing cGAS. Nature cell biology, 19(10), pp.1286-1296.

Wu, Q., Wang, C., Lu, Z., Guo, L. and Ge, Q., 2012. Analysis of serum genome-wide microRNAs for breast cancer detection. Clinica chimica acta, 413(13-14), pp.1058-1065.

Wu, Q., Yang, Z., Nie, Y., Shi, Y. and Fan, D., 2014. Multi-drug resistance in cancer chemotherapeutics: mechanisms and lab approaches. Cancer letters, 347(2), pp.159-166.

Wu, T., Chen, W., Kong, D., Li, X., Lu, H., Liu, S., Wang, J., Du, L., Kong, Q., Huang, X. and Lu, Z. (2015). miR-25 targets the modulator of apoptosis 1 gene in lung cancer. Carcinogenesis, 36(8), pp.925–935.

Wu, W.S., Heinrichs, S., Xu, D., Garrison, S.P., Zambetti, G.P., Adams, J.M. and Look, A.T., 2005. Slug antagonizes p53-mediated apoptosis of hematopoietic progenitors by repressing puma. Cell, 123(4), pp.641-653.

Wu, Y.M., Su, F., Kalyana-Sundaram, S., Khazanov, N., Ateeq, B., Cao, X., Lonigro, R.J., Vats, P., Wang, R., Lin, S.F. and Cheng, A.J., 2013. Identification of targetable FGFR gene fusions in diverse cancers. Cancer discovery, 3(6), pp.636-647.

Wu, Z.Q., Li, X.Y., Hu, C.Y., Ford, M., Kleer, C.G. and Weiss, S.J., 2012. Canonical Wnt signaling regulates Slug activity and links epithelial–mesenchymal transition with epigenetic

Breast Cancer 1, Early Onset (BRCA1) repression. Proceedings of the National Academy of Sciences, 109(41), pp.16654-16659.

Wyllie, A.H., Kerr, J.R. and Currie, A.R., 1980. Cell death: the significance of apoptosis. In International review of cytology (Vol. 68, pp. 251-306). Academic Press.

Xi, Q., Wang, Z., Zaromytidou, A.I., Zhang, X.H.F., Chow-Tsang, L.F., Liu, J.X., Kim, H., Barlas, A., Manova-Todorova, K., Kaartinen, V. and Studer, L., 2011. A poised chromatin platform for TGF-β access to master regulators. Cell, 147(7), pp.1511-1524.

Xian, S., Jilu, L., Zhennan, T., Yang, Z., Yang, H., Jingshu, G. and Songbin, F., 2014. BMP-4 genetic variants and protein expression are associated with platinum-based chemotherapy response and prognosis in NSCLC. BioMed research international, 2014. Xie, D., Nakachi, K., Wang, H., Elashoff, R. and Koeffler, H.P., 2001. Elevated levels of connective tissue growth factor, WISP-1, and CYR61 in primary breast cancers associated with more advanced features. Cancer research, 61(24), pp.8917-8923.

Xie, G.X. and Palmer, P.P., 2007. How regulators of G protein signaling achieve selective regulation. Journal of molecular biology, 366(2), pp.349-365.

Xie, L., Law, B.K., Chytil, A.M., Brown, K.A., Aakre, M.E. and Moses, H.L., 2004. Activation of the Erk pathway is required for TGF-β1-induced EMT in vitro. Neoplasia, 6(5), pp.603-610.

Xie, M., Li, M., Vilborg, A., Lee, N., Shu, M.D., Yartseva, V., Šestan, N. and Steitz, J.A., 2013. Mammalian 5-capped microRNA precursors that generate a single microRNA. Cell, 155(7), pp.1568-1580.

Xie, Y., Wolff, D.W., Wei, T., Wang, B., Deng, C., Kirui, J.K., Jiang, H., Qin, J., Abel, P.W. and Tu, Y., 2009. Breast cancer migration and invasion depend on proteasome degradation of regulator of G-protein signaling 4. Cancer research, 69(14), pp.5743-5751.

Xie, Z.Y., Lv, K., Xiong, Y. and Guo, W.H., 2014. ABCG2-meditated multidrug resistance and tumor-initiating capacity of side population cells from colon cancer. Oncology research and treatment, 37(11), pp.666-672.

Xiong, Z., Ye, L., Zhenyu, H., Li, F., Xiong, Y., Lin, C., Wu, X., Deng, G., Shi, W., Song, L. and Yuan, Z., 2018. ANP 32E induces tumorigenesis of triple-negative breast cancer cells by upregulating E2F1. Molecular oncology, 12(6), pp.896-912.

Xishan, Z., Xianjun, L., Ziying, L., Guangxin, C. and Gang, L., 2014. The malignancy suppression role of miR-23a by targeting the BCR/ABL oncogene in chromic myeloid leukemia. Cancer gene therapy, 21(9), pp.397-404.

Xu, J., Prosperi, J.R., Choudhury, N., Olopade, O.I. and Goss, K.H., 2015. β-Catenin is required for the tumorigenic behavior of triple-negative breast cancer cells. PloS one, 10(2), p.e0117097.

Xu, K., Tzvetkova-Robev, D., Xu, Y., Goldgur, Y., Chan, Y.P., Himanen, J.P. and Nikolov, D.B., 2013. Insights into Eph receptor tyrosine kinase activation from crystal structures of the EphA4 ectodomain and its complex with ephrin-A5. Proceedings of the National Academy of Sciences, 110(36), pp.14634-14639.

Xu, L., Fukumura, D. and Jain, R.K., 2002. Acidic extracellular pH induces vascular endothelial growth factor (VEGF) in human glioblastoma cells via ERK1/2 MAPK signaling pathway Mechanism of low pH-induced VEGF. Journal of Biological Chemistry, 277(13), pp.11368-11374.

Xu, L., Gordon, R., Farmer, R., Pattanayak, A., Binkowski, A., Huang, X., Avram, M., Krishna, S., Voll, E., Pavese, J. and Chavez, J., 2018. Precision therapeutic targeting of human cancer cell motility. Nature communications, 9(1), pp.1-14.

Xu, M., Zhu, C., Zhao, X., Chen, C., Zhang, H., Yuan, H., Deng, R., Dou, J., Wang, Y., Huang, J. and Chen, Q., 2015. Atypical ubiquitin E3 ligase complex Skp1-Pam-Fbxo45 controls the core epithelial-to-mesenchymal transition-inducing transcription factors. Oncotarget, 6(2), p.979.

Xu, R.H., Pelicano, H., Zhou, Y., Carew, J.S., Feng, L., Bhalla, K.N., Keating, M.J. and Huang, P., 2005. Inhibition of glycolysis in cancer cells: a novel strategy to overcome drug resistance associated with mitochondrial respiratory defect and hypoxia. Cancer research, 65(2), pp.613-621.

Xu, Y. and Yu, Q., 2003. E-cadherin negatively regulates CD44-hyaluronan interaction and CD44-mediated tumor invasion and branching morphogenesis. Journal of Biological Chemistry, 278(10), pp.8661-8668.

Yagi, T. and Takeichi, M., 2000. Cadherin superfamily genes: functions, genomic organization, and neurologic diversity. Genes & development, 14(10), pp.1169-1180.

Yagüe, E. and Raguz, S., 2010. Multidrug Resistance. In Methods of Cancer Diagnosis, Therapy, and Prognosis (pp. 121-133). Springer, Dordrecht.

Yagüe, E., Arance, A., Kubitza, L., O'Hare, M., Jat, P., Ogilvie, C.M., Hart, I.R., Higgins, C.F. and Raguz, S., 2007. Ability to acquire drug resistance arises early during the tumorigenesis process. Cancer research, 67(3), pp.1130-1137.

Yagüe, E., Arance, A., Kubitza, L., O'Hare, M., Jat, P., Ogilvie, C.M., Hart, I.R., Higgins, C.F. and Raguz, S., 2007. Ability to acquire drug resistance arises early during the tumorigenesis process. Cancer research, 67(3), pp.1130-1137.

Yahata, T., de Caestecker, M.P., Lechleider, R.J., Andriole, S., Roberts, A.B., Isselbacher, K.J. and Shioda, T., 2000. The MSG1 non-DNA-binding transactivator binds to the p300/CBP coactivators, enhancing their functional link to the Smad transcription factors. Journal of Biological Chemistry, 275(12), pp.8825-8834.

Yamada, T., Sakisaka, T., Hisata, S., Baba, T. and Takai, Y., 2005. RA-RhoGAP, Rap activated Rho GTPase-activating protein implicated in neurite outgrowth through Rho. Journal of Biological Chemistry, 280(38), pp.33026-33034.

Yamaguchi, H. and Condeelis, J., 2007. Regulation of the actin cytoskeleton in cancer cell migration and invasion. Biochimica et Biophysica Acta (BBA)-Molecular Cell Research, 1773(5), pp.642-652.

Yamaguchi, H., Lorenz, M., Kempiak, S., Sarmiento, C., Coniglio, S., Symons, M., Segall, J., Eddy, R., Miki, H., Takenawa, T. and Condeelis, J., 2005. Molecular mechanisms of invadopodium formationAbbreviations used in this paper: CBD, cortactin-binding domain; FN, fibronectin; N-WASP, neural WASP; RNAi, RNA interference; siRNA, small interference RNA; WBD, N-WASP binding domain. the role of the N-WASP–Arp2/3 complex pathway and cofilin. The Journal of Cell Biology, 168(3), pp.441-452.

Yamaguchi, K., Shirakabe, K., Shibuya, H., Irie, K., Oishi, I., Ueno, N., Taniguchi, T., Nishida, E. and Matsumoto, K., 1995. Identification of a member of the MAPKKK family as a potential mediator of TGF-β signal transduction. Science, 270(5244), pp.2008-2011.

Yamaguchi, N., Nakayama, Y. and Yamaguchi, N., 2017. Down-regulation of Forkhead box protein A1 (FOXA1) leads to cancer stem cell-like properties in tamoxifen-resistant breast cancer cells through induction of interleukin-6. Journal of Biological Chemistry, 292(20), pp.8136-8148.

Yamamoto, M., Taguchi, Y., Ito-Kureha, T., Semba, K., Yamaguchi, N. and Inoue, J.I., 2013. NF-κB non-cell-autonomously regulates cancer stem cell populations in the basal-like breast cancer subtype. Nature communications, 4(1), pp.1-13.

Yamamoto, N., Kinoshita, T., Nohata, N., Itesako, T., Yoshino, H., Enokida, H., Nakagawa, M., Shozu, M. and Seki, N., 2013. Tumor suppressive microRNA-218 inhibits cancer cell migration and invasion by targeting focal adhesion pathways in cervical squamous cell carcinoma. International journal of oncology, 42(5), pp.1523-1532.

Yamamoto, Y., Yoshioka, Y., Minoura, K., Takahashi, R.U., Takeshita, F., Taya, T., Horii, R., Fukuoka, Y., Kato, T., Kosaka, N. and Ochiya, T., 2011. An integrative genomic analysis revealed the relevance of microRNA and gene expression for drug-resistance in human breast cancer cells. Molecular cancer, 10(1), pp.1-16.

Yamamura, Y., Lee, W.L., Inoue, K.I., Ida, H. and Ito, Y., 2006. RUNX3 cooperates with FoxO3a to induce apoptosis in gastric cancer cells. Journal of Biological Chemistry, 281(8), pp.5267-5276.

Yamashita, H., Nishio, M., Toyama, T., Sugiura, H., Zhang, Z., Kobayashi, S. and Iwase, H., 2003. Coexistence of HER2 over-expression and p53 protein accumulation is a strong prognostic molecular marker in breast cancer. Breast Cancer Research, 6(1), p.R24.

Yamashita, M., Fatyol, K., Jin, C., Wang, X., Liu, Z. and Zhang, Y.E., 2008. TRAF6 mediates Smad-independent activation of JNK and p38 by TGF-β. Molecular cell, 31(6), pp.918-924.

Yamashita, M., Ogawa, T., Zhang, X., Hanamura, N., Kashikura, Y., Takamura, M., Yoneda, M. and Shiraishi, T., 2012. Role of stromal myofibroblasts in invasive breast cancer: stromal expression of alpha-smooth muscle actin correlates with worse clinical outcome. Breast cancer, 19(2), pp.170-176.

Yamashita, N., Tokunaga, E., Kitao, H., Tanaka, K., Taketani, K., Saeki, H., Aishima, S., Oki, E., Morita, M. and Maehara, Y., 2013. Significance of the vimentin expression in triple-negative breast cancer.

Yamazoe, S., Tanaka, H., Sawada, T., Amano, R., Yamada, N., Ohira, M. and Hirakawa, K., 2010. RNA interference suppression of mucin 5AC (MUC5AC) reduces the adhesive and invasive capacity of human pancreatic cancer cells. Journal of Experimental & Clinical Cancer Research, 29(1), p.53.

Yan, K., Wu, Q., Yan, D.H., Lee, C.H., Rahim, N., Tritschler, I., DeVecchio, J., Kalady, M.F., Hjelmeland, A.B. and Rich, J.N., 2014. Glioma cancer stem cells secrete Gremlin1 to promote their maintenance within the tumor hierarchy. Genes & development, 28(10), pp.1085-1100.

Yan, W., Cao, Q.J., Arenas, R.B., Bentley, B. and Shao, R., 2010. GATA3 inhibits breast cancer metastasis through the reversal of epithelial-mesenchymal transition. Journal of Biological Chemistry, 285(18), pp.14042-14051.

Yan, W., Chen, Y., Yao, Y., Zhang, H. and Wang, T., 2013. Increased invasion and tumorigenicity capacity of CD44+/CD24-breast cancer MCF7 cells in vitro and in nude mice. Cancer cell international, 13(1), pp.1-7.

Yanaihara, N., Caplen, N., Bowman, E., Seike, M., Kumamoto, K., Yi, M., Stephens, R.M., Okamoto, A., Yokota, J., Tanaka, T. and Calin, G.A., 2006. Unique microRNA molecular profiles in lung cancer diagnosis and prognosis. Cancer cell, 9(3), pp.189-198.

Yang, C., He, P., Liu, Y., He, Y., Yang, C., Du, Y., Zhou, M., Wang, W., Zhang, G., Wu, M. and Gao, F. (2015). Down-regulation of CEACAM1 in breast cancer. Acta Biochimica et Biophysica Sinica, 47(10), pp.788–794.

Yang, C., Zhao, X., Cui, N. and Liang, Y., 2017. Cadherins associate with distinct stem cell related transcription factors to coordinate the maintenance of stemness in triple-negative breast cancer. Stem cells international, 2017.

Yang, D.S., Tandon, A., Chen, F., Yu, G., Yu, H., Arawaka, S., Hasegawa, H., Duthie, M., Schmidt, S.D., Ramabhadran, T.V. and Nixon, R.A., 2002. Mature glycosylation and

trafficking of nicastrin modulate its binding to presenilins. Journal of Biological Chemistry, 277(31), pp.28135-28142.

Yang, F., Zhao, N. and Wu, N., 2017. TNFR2 promotes Adriamycin resistance in breast cancer cells by repairing DNA damage. Molecular medicine reports, 16(3), pp.2962-2968.

Yang, F., Zhao, Z. and Zhao, N., 2017. Clinical implications of tumor necrosis factor receptor 2 in breast cancer. Oncology Letters, 14(2), pp.2393-2398.

Yang, H., Pinello, C.E., Luo, J., Li, D., Wang, Y., Zhao, L.Y., Jahn, S.C., Saldanha, S.A.,Planck, J., Geary, K.R. and Ma, H., 2013. Small-molecule inhibitors of acetyltransferase p300 identified by high-throughput screening are potent anticancer agents. Molecular cancer therapeutics, 12(5), pp.610-620.

Yang, H.L., Thiyagarajan, V., Shen, P.C., Mathew, D.C., Lin, K.Y., Liao, J.W. and Hseu, Y.C., 2019. Anti-EMT properties of CoQ0 attributed to PI3K/AKT/NFKB/MMP-9 signaling pathway through ROS-mediated apoptosis. Journal of Experimental & Clinical Cancer Research, 38(1), pp.1-21.

Yang, J., Mani, S.A., Donaher, J.L., Ramaswamy, S., Itzykson, R.A., Come, C., Savagner, P., Gitelman, I., Richardson, A. and Weinberg, R.A., 2004. Twist, a master regulator of morphogenesis, plays an essential role in tumor metastasis. cell, 117(7), pp.927-939.

Yang, J.M., Vassil, A.D. and Hait, W.N., 2001. Activation of phospholipase C induces the expression of the multidrug resistance (MDR1) gene through the Raf-MAPK pathway. Molecular pharmacology, 60(4), pp.674-680.

Yang, J.S., Maurin, T., Robine, N., Rasmussen, K.D., Jeffrey, K.L., Chandwani, R., Papapetrou, E.P., Sadelain, M., O'Carroll, D. and Lai, E.C., 2010. Conserved vertebrate mir-451 provides a platform for Dicer-independent, Ago2-mediated microRNA biogenesis. Proceedings of the National Academy of Sciences, 107(34), pp.15163-15168.

Yang, J.Y. and Hung, M.C., 2009. A new fork for clinical application: targeting forkhead transcription factors in cancer. Clinical cancer research, 15(3), pp.752-757.

Yang, J.Y., Zong, C.S., Xia, W., Yamaguchi, H., Ding, Q., Xie, X., Lang, J.Y., Lai, C.C., Chang, C.J., Huang, W.C. and Huang, H., 2008. ERK promotes tumorigenesis by inhibiting FOXO3a via MDM2-mediated degradation. Nature cell biology, 10(2), pp.138-148.

Yang, L., Lin, F., Gao, Z., Chen, X., Zhang, H. and Dong, K., 2020. Anti-tumor peptide SA12 inhibits metastasis of MDA-MB-231 and MCF-7 breast cancer cells via increasing expression of the tumor metastasis suppressor genes, CDH1, nm23-H1 and BRMS1. Experimental and Therapeutic Medicine, 20(2), pp.1758-1763.

Yang, L., Qiu, J., Xiao, Y., Hu, X., Liu, Q., Chen, L., Huang, W., Li, X., Li, L., Zhang, J. and Ding, X., 2018. AP-2β inhibits hepatocellular carcinoma invasion and metastasis

through Slug and Snail to suppress epithelial-mesenchymal transition. Theranostics, 8(13), p.3707.

Yang, M.H., Hsu, D.S.S., Wang, H.W., Wang, H.J., Lan, H.Y., Yang, W.H., Huang, C.H., Kao, S.Y., Tzeng, C.H., Tai, S.K. and Chang, S.Y., 2010. Bmi1 is essential in Twist1-induced epithelial–mesenchymal transition. Nature cell biology, 12(10), pp.982-992.

Yang, M.H., Wu, M.Z., Chiou, S.H., Chen, P.M., Chang, S.Y., Liu, C.J., Teng, S.C. and Wu, K.J., 2008. Direct regulation of TWIST by HIF-1α promotes metastasis. Nature cell biology, 10(3), pp.295-305.

Yang, Q., Wang, Y., Lu, X., Zhao, Z., Zhu, L., Chen, S., Wu, Q., Chen, C. and Wang, Z., 2015. MiR-125b regulates epithelial-mesenchymal transition via targeting Sema4C in paclitaxel-resistant breast cancer cells. Oncotarget, 6(5), p.3268.

Yang, S., Lim, M., Pham, L.K., Kendall, S.E., Reddi, A.H., Altieri, D.C. and Roy-Burman, P., 2006. Bone morphogenetic protein 7 protects prostate cancer cells from stress-induced apoptosis via both Smad and c-Jun NH2-terminal kinase pathways. Cancer Research, 66(8), pp.4285-4290.

Yang, S., Murphy, R.L., Morishige, D.T., Klein, P.E., Rooney, W.L. and Mullet, J.E., 2014. Sorghum phytochrome B inhibits flowering in long days by activating expression of SbPRR37 and SbGHD7, repressors of SbEHD1, SbCN8 and SbCN12. PloS one, 9(8), p.e105352.

Yang, S.X., Polley, E.C. and Nguyen, D., 2017. Association of γH2AX at diagnosis with chemotherapy outcome in patients with breast cancer. Theranostics, 7(4), p.945.

Yang, Wenbo, Yu Holly Hong, Xi-Qiang Shen, Christy Frankowski, Heidi S. Camp, and Todd Leff. "Regulation of Transcription by AMP-activated Protein Kinase Phosphorylation Of p300 Blocks Its Interaction With Nuclear Receptors." Journal of Biological Chemistry 276, no. 42 (2001): 38341-38344.

Yang, X., Wang, D., Dong, W., Song, Z. and Dou, K., 2010. Inhibition of Na+/H+ exchanger 1 by 5-(N-ethyl-N-isopropyl) amiloride reduces hypoxia-induced hepatocellular carcinoma invasion and motility. Cancer letters, 295(2), pp.198-204.

Yang, X.J., Ogryzko, V.V., Nishikawa, J.I., Howard, B.H. and Nakatani, Y., 1996. A p300/CBP-associated factor that competes with the adenoviral oncoprotein E1A. Nature, 382(6589), pp.319-324.

Yang, Y., Li, D.P., Shen, N.A., Yu, X.C., Li, J.B., Song, Q.I. and Zhang, J.H., 2015. TPX2 promotes migration and invasion of human breast cancer cells. Asian Pacific journal of tropical medicine, 8(12), pp.1064-1070.

Yao, R., Jiang, H., Ma, Y., Wang, L., Wang, L., Du, J., Hou, P., Gao, Y., Zhao, L., Wang, G. and Zhang, Y., 2014. PRMT7 induces epithelial-to-mesenchymal transition and promotes metastasis in breast cancer. Cancer research, 74(19), pp.5656-5667.

Yao, T.P., Oh, S.P., Fuchs, M., Zhou, N.D., Ch'ng, L.E., Newsome, D., Bronson, R.T., Li, E., Livingston, D.M. and Eckner, R., 1998. Gene dosage–dependent embryonic development and proliferation defects in mice lacking the transcriptional integrator p300. Cell, 93(3), pp.361-372.

Yao, Y., Suo, A.L., Li, Z.F., Liu, L.Y., Tian, T., Ni, L., Zhang, W.G., Nan, K.J., Song, T.S. and Huang, C., 2009. MicroRNA profiling of human gastric cancer. Molecular medicine reports, 2(6), pp.963-970.

Yap, A.S. and Kovacs, E.M., 2003. Direct cadherin-activated cell signaling: a view from the plasma membrane. The Journal of cell biology, 160(1), p.11.

Ye, J., Wu, D., Shen, J., Wu, P., Ni, C., Chen, J., Zhao, J., Zhang, T., Wang, X. and Huang, J., 2012. Enrichment of colorectal cancer stem cells through epithelial-mesenchymal transition via CDH1 knockdown. Molecular medicine reports, 6(3), pp.507-512.

Ye, L., Lewis-Russell, J.M., Kynaston, H. and Jiang, W.G., 2007. Endogenous bone morphogenetic protein-7 controls the motility of prostate cancer cells through regulation of bone morphogenetic protein antagonists. The Journal of urology, 178(3), pp.1086-1091.

Ye, X.M., Zhu, H.Y., Bai, W.D., Wang, T., Wang, L., Chen, Y., Yang, A.G. and Jia, L.T., 2014. Epigenetic silencing of miR-375 induces trastuzumab resistance in HER2-positive breast cancer by targeting IGF1R. BMC cancer, 14(1), pp.1-12.

Yeh, H.W., Lee, S.S., Chang, C.Y., Lang, Y.D. and Jou, Y.S., 2019. A new switch for TGFβ in cancer. Cancer research, 79(15), pp.3797-3805.

Yen, M.F., Tabar, L., Vitak, B., Smith, R.A., Chen, H.H. and Duffy, S.W., 2003. Quantifying the potential problem of overdiagnosis of ductal carcinoma in situ in breast cancer screening. European journal of cancer, 39(12), pp.1746-1754.

Yin, Z., Haynie, J., Yang, X., Han, B., Kiatchoosakun, S., Restivo, J., Yuan, S., Prabhakar, N.R., Herrup, K., Conlon, R.A. and Hoit, B.D., 2002. The essential role of Cited2, a negative regulator for HIF-1α, in heart development and neurulation. Proceedings of the National Academy of Sciences, 99(16), pp.10488-10493.

Ying, X., Sun, Y. and He, P., 2015. Bone morphogenetic protein-7 inhibits EMT-associated genes in breast cancer. Cellular Physiology and Biochemistry, 37(4), pp.1271-1278.

Yokobori, T., Iinuma, H., Shimamura, T., Imoto, S., Sugimachi, K., Ishii, H., Iwatsuki, M., Ota, D., Ohkuma, M., Iwaya, T. and Nishida, N., 2013. Plastin3 is a novel marker for

circulating tumor cells undergoing the epithelial–mesenchymal transition and is associated with colorectal cancer prognosis. Cancer research, 73(7), pp.2059-2069.

Yokobori, T., Iinuma, H., Shimamura, T., Imoto, S., Sugimachi, K., Ishii, H., Iwatsuki, M., Ota, D., Ohkuma, M., Iwaya, T. and Nishida, N., 2013. Plastin3 is a novel marker for circulating tumor cells undergoing the epithelial–mesenchymal transition and is associated with colorectal cancer prognosis. Cancer research, 73(7), pp.2059-2069.

Yong, F.L., Wang, C.W., Roslani, A.C. and Law, C.W., 2014. The involvement of miR 23a/APAF1 regulation axis in colorectal cancer. International journal of molecular sciences, 15(7), pp.11713-11729.

Yoo, K.H. and Hennighausen, L., 2012. EZH2 methyltransferase and H3K27 methylation in breast cancer. International journal of biological sciences, 8(1), p.59.

Yoshida, R., Kimura, N., Harada, Y. and Ohuchi, N., 2001. The loss of E-cadherin, α-and β catenin expression is associated with metastasis and poor prognosis in invasive breast cancer. International journal of oncology, 18(3), pp.513-520.

Yoshioka, T., Masuko, T., Kotanagi, H., Aizawa, O., Saito, Y., Nakazato, H., Koyama, K. and Hashimoto, Y., 1998. Homotypic adhesion through carcinoembryonic antigen plays a role in hepatic metastasis development. Japanese journal of cancer research, 89(2), pp.177-185.

Yoshioka, T., Otero, J., Chen, Y., Kim, Y.M., Koutcher, J.A., Satagopan, J., Reuter, V., Carver, B., De Stanchina, E., Enomoto, K. and Greenberg, N.M., 2013. β4 Integrin signaling induces expansion of prostate tumor progenitors. The Journal of clinical investigation, 123(2), pp.682-699.

Yu, F., Yao, H., Zhu, P., Zhang, X., Pan, Q., Gong, C., Huang, Y., Hu, X., Su, F., Lieberman, J. and Song, E., 2007. let-7 regulates self renewal and tumorigenicity of breast cancer cells. Cell, 131(6), pp.1109-1123.

Yu, F.X. and Guan, K.L., 2013. The Hippo pathway: regulators and regulations. Genes & development, 27(4), pp.355-371.

Yu, G., Nishimura, M., Arawaka, S., Levitan, D., Zhang, L., Tandon, A., Song, Y.Q., Rogaeva, E., Chen, F., Kawarai, T. and Supala, A., 2000. Nicastrin modulates presenilin-mediated notch/glp-1 signal transduction and βAPP processing. Nature, 407(6800), pp.48-54.

Yu, M., Bardia, A., Aceto, N., Bersani, F., Madden, M.W., Donaldson, M.C., Desai, R., Zhu, H., Comaills, V., Zheng, Z. and Wittner, B.S., 2014. Ex vivo culture of circulating breast tumor cells for individualized testing of drug susceptibility. science, 345(6193), pp.216-220.

Yu, M., Bardia, A., Wittner, B.S., Stott, S.L., Smas, M.E., Ting, D.T., Isakoff, S.J., Ciciliano, J.C., Wells, M.N., Shah, A.M. and Concannon, K.F., 2013. Circulating breast tumor cells exhibit dynamic changes in epithelial and mesenchymal composition. science, 339(6119), pp.580-584.

Yu, Q. and Stamenkovic, I., 2000. Cell surface-localized matrix metalloproteinase-9 proteolytically activates TGF-β and promotes tumor invasion and angiogenesis. Genes & development, 14(2), pp.163-176.

Yu, S., Yu, Y., Sun, Y., Wang, X., Luo, R., Zhao, N., Zhang, W., Li, Q., Cui, Y., Wang, Y. and Li, W., 2015. Activation of FOXO3a suggests good prognosis of patients with radically resected gastric cancer. International journal of clinical and experimental pathology, 8(3), p.2963.

Yu, S.L., Chen, H.Y., Chang, G.C., Chen, C.Y., Chen, H.W., Singh, S., Cheng, C.L., Yu, C.J., Lee, Y.C., Chen, H.S. and Su, T.J., 2008. MicroRNA signature predicts survival and relapse in lung cancer. Cancer cell, 13(1), pp.48-57.

Yu, X., Luo, A., Liu, Y., Wang, S., Li, Y., Shi, W., Liu, Z. and Qu, X., 2015. MiR-214 increases the sensitivity of breast cancer cells to tamoxifen and fulvestrant through inhibition of autophagy. Molecular cancer, 14(1), pp.1-16.

Yuan, S., Liu, Q., Hu, Z., Zhou, Z., Wang, G., Li, C., Xie, W., Meng, G., Xiang, Y., Wu, N. and Wu, L., 2018. Long non-coding RNA MUC5B-AS1 promotes metastasis through mutually regulating MUC5B expression in lung adenocarcinoma. Cell death & disease, 9(5), pp.1-12.

Yuan, S., Liu, Q., Hu, Z., Zhou, Z., Wang, G., Li, C., Xie, W., Meng, G., Xiang, Y., Wu, N. and Wu, L., 2018. Long non-coding RNA MUC5B-AS1 promotes metastasis through mutually regulating MUC5B expression in lung adenocarcinoma. Cell death & disease, 9(5), pp.1-12.

Yue, J. and Mulder, K.M., 2000. Requirement of Ras/MAPK Pathway Activation by Transforming Growth Factor β for Transforming Growth Factor β1 Production in a Smad-dependent Pathway. Journal of Biological Chemistry, 275(40), pp.30765-30773.

Zaheed, O., Samson, J. and Dean, K., 2020. A bioinformatics approach to identify novel long, non-coding RNAs in breast cancer cell lines from an existing RNA-sequencing dataset. Non-coding RNA Research.

Zanotto-Filho, A., Braganhol, E., Schröder, R., de Souza, L.H.T., Dalmolin, R.J., Pasquali, M.A.B., Gelain, D.P., Battastini, A.M.O. and Moreira, J.C.F., 2011. NFκB inhibitors induce cell death in glioblastomas. Biochemical pharmacology, 81(3), pp.412-424.

Zaret, K.S. and Carroll, J.S., 2011. Pioneer transcription factors: establishing competence for gene expression. Genes & development, 25(21), pp.2227-2241.

Zasadil, L.M., Andersen, K.A., Yeum, D., Rocque, G.B., Wilke, L.G., Tevaarwerk, A.J., Raines, R.T., Burkard, M.E. and Weaver, B.A., 2014. Cytotoxicity of paclitaxel in breast cancer is due to chromosome missegregation on multipolar spindles. Science translational medicine, 6(229), pp.229ra43-229ra43.

Zavadil, J., Bitzer, M., Liang, D., Yang, Y.C., Massimi, A., Kneitz, S., Piek, E. and Böttinger, E.P., 2001. Genetic programs of epithelial cell plasticity directed by transforming growth factor-β. Proceedings of the National Academy of Sciences, 98(12), pp.6686-6691.

Zavadil, J., Cermak, L., Soto-Nieves, N. and Böttinger, E.P. (2004). Integration of TGF β/Smad and Jagged1/Notch signalling in epithelial-to-mesenchymal transition. The EMBO Journal, 23(5), pp.1155–1165.

Zeng, C, M., Chang, L, L., Ying, M, D., Cao, J., He, Q, J., Zhu, H., et al. (2017).Aldo-keto re-ductase AKR1C1-AKR1C4: functions, regulation, and intervention for anti-cancer therapy, Front. Pharmacol. 8 119.

Zeng, G., Xun, W., Wei, K., Yang, Y. and Shen, H., 2016. MicroRNA-27a-3p regulates epithelial to mesenchymal transition via targeting YAP1 in oral squamous cell carcinoma cells. Oncology reports, 36(3), pp.1475-1482.

Zeng, Z., Li, Y., Pan, Y., Lan, X., Song, F., Sun, J., Zhou, K., Liu, X., Ren, X., Wang, F. and Hu, J., 2018. Cancer-derived exosomal miR-25-3p promotes pre-metastatic niche formation by inducing vascular permeability and angiogenesis. Nature communications, 9(1), pp.1-14.

Zhan, T., Rindtorff, N. and Boutros, M., 2017. Wnt signaling in cancer. Oncogene, 36(11), pp.1461-1473.

Zhang, B., Zhao, R., He, Y., Fu, X., Fu, L., Zhu, Z., Fu, L. and Dong, J.T., 2016. Micro RNA 100 sensitizes luminal A breast cancer cells to paclitaxel treatment in part by targeting mTOR. Oncotarget, 7(5), p.5702.

Zhang, C.C., Pavlicek, A., Zhang, Q., Lira, M.E., Painter, C.L., Yan, Z., Zheng, X., Lee, N.V., Ozeck, M., Qiu, M. and Zong, Q., 2012. Biomarker and pharmacologic evaluation of the γ-secretase inhibitor PF-03084014 in breast cancer models. Clinical Cancer Research, 18(18), pp.5008-5019.

Zhang, G.J., Zhou, T., Tian, H.P., Liu, Z.L. and Xia, S.S., 2013. High expression of ZEB1 correlates with liver metastasis and poor prognosis in colorectal cancer. Oncology letters, 5(2), pp.564-568.

Zhang, H., Hao, Y., Yang, J., Zhou, Y., Li, J., Yin, S., Sun, C., Ma, M., Huang, Y. and Xi, J.J., 2011. Genome-wide functional screening of miR-23b as a pleiotropic modulator suppressing cancer metastasis. Nature communications, 2(1), pp.1-11.

Zhang, H., Li, M., Han, Y., Hong, L., Gong, T., Sun, L. and Zheng, X., 2010. Down regulation of miR-27a might reverse multidrug resistance of esophageal squamous cell carcinoma. Digestive diseases and sciences, 55(9), pp.2545-2551.

Zhang, H., Meng, F., Liu, G., Zhang, B., Zhu, J., Wu, F., Ethier, S.P., Miller, F. and Wu, G., 2011. Forkhead transcription factor foxq1 promotes epithelial–mesenchymal transition and breast cancer metastasis. Cancer research, 71(4), pp.1292-1301.

Zhang, H., Zuo, Z., Lu, X., Wang, L., Wang, H. and Zhu, Z., 2012. MiR-25 regulates apoptosis by targeting Bim in human ovarian cancer. Oncology reports, 27(2), pp.594-598.

Zhang, J., Cao, Z., Yang, G., You, L., Zhang, T. and Zhao, Y., 2019. MicroRNA-27a (miR 27a) in solid tumors: a review based on mechanisms and clinical observations. Frontiers in Oncology, 9, p.893.

Zhang, J., Chen, D., Liang, S., Wang, J., Liu, C., Nie, C., Shan, Z., Wang, L., Fan, Q. and Wang, F., 2018. miR-106b promotes cell invasion and metastasis via PTEN mediated EMT in ESCC. Oncology letters, 15(4), pp.4619-4626.

Zhang, J., Gong, X., Tian, K., Chen, D., Sun, J., Wang, G. and Guo, M., 2015. miR-25 promotes glioma cell proliferation by targeting CDKN1C. Biomedicine & Pharmacotherapy, 71, pp.7-14.

Zhang, J., Gong, X., Tian, K., Chen, D., Sun, J., Wang, G. and Guo, M., 2015. miR-25 promotes glioma cell proliferation by targeting CDKN1C. Biomedicine & Pharmacotherapy, 71, pp.7-14.

Zhang, J., Lu, C., Zhang, J., Kang, J., Cao, C. and Li, M., 2013. Involvement of ZEB1 and E cadherin in the invasion of lung squamous cell carcinoma. Molecular biology reports, 40(2), pp.949-956.

Zhang, J., Zhou, W., Liu, Y., Liu, T., Li, C. and Wang, L., 2018. Oncogenic role of microRNA 532 5p in human colorectal cancer via targeting of the 5'UTR of RUNX3. Oncology letters, 15(5), pp.7215-7220.

Zhang, L., Deng, L., Chen, F., Yao, Y., Wu, B., Wei, L., Mo, Q. and Song, Y., 2014. Inhibition of histone H3K79 methylation selectively inhibits proliferation, self-renewal and metastatic potential of breast cancer. Oncotarget, 5(21), pp.10665–10677.

Zhang, L., Guo, X., Zhang, L., Yang, F., Qin, L., Zhang, D. and Qin, Y., 2018. SLC34A2 regulates miR-25-Gsk3β signaling pathway to affect tumor progression in gastric cancer stem cell-like cells. Molecular carcinogenesis, 57(3), pp.440-450.

Zhang, L., Huang, J., Yang, N., Greshock, J., Megraw, M.S., Giannakakis, A., Liang, S., Naylor, T.L., Barchetti, A., Ward, M.R. and Yao, G., 2006. microRNAs exhibit high frequency genomic alterations in human cancer. Proceedings of the National Academy of Sciences, 103(24), pp.9136-9141.

Zhang, L., Ridgway, L.D., Wetzel, M.D., Ngo, J., Yin, W., Kumar, D., Goodman, J.C., Groves, M.D. and Marchetti, D., 2013. The identification and characterization of

breast cancer CTCs competent for brain metastasis. Science translational medicine, 5(180), pp.180ra48-180ra48.

Zhang, L., Tong, X., Li, J., Huang, Y., Hu, X., Chen, Y., Huang, J., Wang, J. and Liu, B., 2015. Apoptotic and autophagic pathways with relevant small-molecule compounds, in cancer stem cells. Cell proliferation, 48(4), pp.385-397.

Zhang, L.Y., Chen, Y., Jia, J., Zhu, X., He, Y. and Wu, L.M., 2019. MiR-27a promotes EMT in ovarian cancer through active Wnt/β-catenin signalling by targeting FOXO1. Cancer Biomarkers, 24(1), pp.31-42.

Zhang, P., Sun, Y. and Ma, L., 2015. ZEB1: at the crossroads of epithelial-mesenchymal transition, metastasis and therapy resistance. Cell cycle, 14(4), pp.481-487.

Zhang, P., Wang, L., Rodriguez-Aguayo, C., Yuan, Y., Debeb, B.G., Chen, D., Sun, Y., You, M.J., Liu, Y., Dean, D.C. and Woodward, W.A., 2014. miR-205 acts as a tumour radiosensitizer by targeting ZEB1 and Ubc13. Nature communications, 5(1), pp.1-10.

Zhang, P., Wei, Y., Wang, L., Debeb, B.G., Yuan, Y., Zhang, J., Yuan, J., Wang, M., Chen, D., Sun, Y. and Woodward, W.A., 2014. ATM-mediated stabilization of ZEB1 promotes DNA damage response and radioresistance through CHK1. Nature cell biology, 16(9), pp.864-875.

Zhang, T., Shen, X., Liu, R., Zhu, G., Bishop, J. and Xing, M., 2017. Epigenetically upregulated WIPF1 plays a major role in BRAF V600E-promoted papillary thyroid cancer aggressiveness. Oncotarget, 8(1), p.900.

Zhang, W., Cai, J., Chen, S., Zheng, X., Hu, S., Dong, W., Lu, J., Xing, J. and Dong, Y., 2015. Paclitaxel resistance in MCF-7/PTX cells is reversed by paeonol through suppression of the SET/phosphatidylinositol 3-kinase/Akt pathway. Molecular medicine reports, 12(1), pp.1506-1514.

Zhang, W., Li, C., Baguley, B.C., Zhou, F., Zhou, W., Shaw, J.P., Wang, Z., Wu, Z. and Liu, J., 2016. Optimization of the formation of embedded multicellular spheroids of MCF-7 cells: How to reliably produce a biomimetic 3D model. Analytical biochemistry, 515, pp.47-54.

Zhang, Y., Xu, L., Li, A. and Han, X., 2019. The roles of ZEB1 in tumorigenic progression and epigenetic modifications. Biomedicine & Pharmacotherapy, 110, pp.400-408.

Zhang, Z., Shiratsuchi, H., Palanisamy, N., Nagrath, S. and Ramnath, N., 2017. Expanded circulating tumor cells from a patient with ALK-positive lung cancer present with EML4-ALK rearrangement along with resistance mutation and enable drug sensitivity testing: a case study. Journal of Thoracic Oncology, 12(2), pp.397-402.

Zhang, Z., Tao, D., Zhang, P., Liu, X., Zhang, Y., Cheng, J., Yuan, H., Liu, L. and Jiang, H., 2016. Hyaluronan synthase 2 expressed by cancer-associated fibroblasts promotes oral cancer invasion. Journal of Experimental & Clinical Cancer Research, 35(1), pp.1-12.

Zhao, B., Li, L., Lei, Q. and Guan, K.L., 2010. The Hippo–YAP pathway in organ size control and tumorigenesis: an updated version. Genes & development, 24(9), pp.862-874.

Zhao, N., Sun, B.C., Zhao, X.L., Wang, Y., Sun, H.Z., Dong, X.Y., Meng, J. and Gu, Q., 2015. Changes in microRNAs associated with Twist-1 and Bcl-2 overexpression identify signaling pathways. Experimental and molecular pathology, 99(3), pp.524-532.

Zhao, N., Sun, H., Sun, B., Zhu, D., Zhao, X., Wang, Y., Gu, Q., Dong, X., Liu, F., Zhang, Y. and Li, X., 2016. miR-27a-3p suppresses tumor metastasis and VM by down-regulating VE-cadherin expression and inhibiting EMT: an essential role for Twist-1 in HCC. Scientific reports, 6(1), pp.1-16.

Zhao, S., Yang, H., Zhang, M., Zhang, D., Liu, Y., Liu, Y., Song, Y., Zhang, X., Li, H., Ma, W. and Zhang, Q., 2013. Circulating tumor cells (CTCs) detected by triple-marker EpCAM, CK19, and hMAM RT-PCR and their relation to clinical outcome in metastatic breast cancer patients. Cell biochemistry and biophysics, 65(2), pp.263-273.

Zhao, W., Luo, Y., Li, B. and Zhang, T., 2016. Tumorigenic lung tumorospheres exhibit stem-like features with significantly increased expression of CD133 and ABCG2. Molecular medicine reports, 14(3), pp.2598-2606.

Zhao, W., Zhao, J.J., Zhang, L., Xu, Q.F., Zhao, Y.M., Shi, X.Y. and Xu, A.G., 2015. Serum miR-21 level: a potential diagnostic and prognostic biomarker for non-small cell lung cancer. International journal of clinical and experimental medicine, 8(9), p.14759.

Zhao, X., Yang, L. and Hu, J., 2011. Down-regulation of miR-27a might inhibit proliferation and drug resistance of gastric cancer cells. Journal of experimental & clinical cancer research, 30(1), p.55.

Zhao, Y. and Adjei, A.A., 2015. Targeting angiogenesis in cancer therapy: moving beyond vascular endothelial growth factor. The oncologist, 20(6), p.660.

Zhao, Y., Lu, H., Yan, A., Yang, Y., Meng, Q., Sun, L., Pang, H., Li, C., Dong, X. and Cai, L., 2013. ABCC3 as a marker for multidrug resistance in non-small cell lung cancer. Scientific reports, 3, p.3120.

Zhao, Y.X., Sun, Y.Y., Huang, A.L., Li, X.F., Huang, C., Ma, T.T. and Li, J., 2018. MicroRNA 200a induces apoptosis by targeting ZEB2 in alcoholic liver disease. Cell Cycle, 17(2), pp.250-262.

Zhao, Z.N., Bai, J.X., Zhou, Q., Yan, B., Qin, W.W., Jia, L.T., Meng, Y.L., Jin, B.Q., Yao, L.B., Wang, T. and Yang, A.G., 2012. TSA suppresses miR-106b-93-25 cluster expression through downregulation of MYC and inhibits proliferation and induces apoptosis in human EMC. PLoS One, 7(9), p.e45133.

Zheng, A., Lamkin, M., Wu, C., Su, H., Gymrek, M. (2020).“Deep neural networks identify context-specific determinants of transcription factor binding affinity”. bioRxiv 2020.02.26.965343; doi: https://doi.org/10.1101/2020.02.26.965343

Zheng, H., Li, W., Wang, Y., Xie, T., Cai, Y., Wang, Z. and Jiang, B., 2014. miR-23a inhibits E-cadherin expression and is regulated by AP-1 and NFAT4 complex during Fas-induced EMT in gastrointestinal cancer. Carcinogenesis, 35(1), pp.173-183.

Zheng, H., Liu, J.Y., Song, F.J. and Chen, K.X., 2013. Advances in circulating microRNAs as diagnostic and prognostic markers for ovarian cancer. Cancer biology & medicine, 10(3), p.123.

Zheng, X., Carstens, J.L., Kim, J., Scheible, M., Kaye, J., Sugimoto, H., Wu, C.C., LeBleu, V.S. and Kalluri, R., 2015. Epithelial-to-mesenchymal transition is dispensable for metastasis but induces chemoresistance in pancreatic cancer. Nature, 527(7579), pp.525-530.

Zhou, B.B.S., Zhang, H., Damelin, M., Geles, K.G., Grindley, J.C. and Dirks, P.B., 2009. Tumour-initiating cells: challenges and opportunities for anticancer drug discovery. Nature reviews Drug discovery, 8(10), pp.806-823.

Zhou, B.P. and Hung, M.C., 2005. Wnt, hedgehog, and snail: sister pathways that control by GSK-3beta and beta-Trcp in the regulation of metastasis. Cell Cycle, 4(6), pp.772-776.

Zhou, B.P., Deng, J., Xia, W., Xu, J., Li, Y.M., Gunduz, M. and Hung, M.C., 2004. Dual regulation of Snail by GSK-3β-mediated phosphorylation in control of epithelial–mesenchymal transition. Nature cell biology, 6(10), pp.931-940.

Zhou, B.P., Hu, M.C.T., Miller, S.A., Yu, Z., Xia, W., Lin, S.Y. and Hung, M.C., 2000. HER 2/neu blocks tumor necrosis factor-induced apoptosis via the Akt/NF-κB pathway. Journal of Biological Chemistry, 275(11), pp.8027-8031.

Zhou, G. and Kuo, M.T., 1997. NF-κB-mediated induction of mdr1b expression by insulin in rat hepatoma cells. Journal of Biological Chemistry, 272(24), pp.15174-15183.

Zhou, L., Jiang, Y., Yan, T., Di, G., Shen, Z., Shao, Z. and Lu, J. (2010). The prognostic role of cancer stem cells in breast cancer: a meta-analysis of published literatures. Breast Cancer Research and Treatment, 122(3), pp.795–801.

Zhou, M., Liu, Z., Zhao, Y., Ding, Y., Liu, H., Xi, Y., Xiong, W., Li, G., Lu, J., Fodstad, O. and Riker, A.I., 2010. MicroRNA-125b confers the resistance of breast cancer cells to paclitaxel through suppression of pro-apoptotic Bcl-2 antagonist killer 1 (Bak1) expression. Journal of Biological Chemistry, 285(28), pp.21496-21507.

Zhou, Q., Gallagher, R., Ufret-Vincenty, R., Li, X., Olson, E.N. and Wang, S., 2011. Regulation of angiogenesis and choroidal neovascularization by members of microRNA-23$\sim$ 27$\sim$ 24 clusters. Proceedings of the national academy of sciences, 108(20), pp.8287-8292.

Zhou, S., Huang, Q., Zheng, S., Lin, K., You, J. and Zhang, X., 2016. miR-27a regulates the sensitivity of breast cancer cells to cisplatin treatment via BAK-SMAC/DIABLO-XIAP axis. Tumor Biology, 37(5), pp.6837-6845.

Zhou, S., Schuetz, J.D., Bunting, K.D., Colapietro, A.M., Sampath, J., Morris, J.J., Lagutina, I., Grosveld, G.C., Osawa, M., Nakauchi, H. and Sorrentino, B.P., 2001. The ABC transporter Bcrp1/ABCG2 is expressed in a wide variety of stem cells and is a molecular determinant of the side-population phenotype. Nature medicine, 7(9), pp.1028-1034.

Zhou, W., Ni, T.K., Wronski, A., Glass, B., Skibinski, A., Beck, A. and Kuperwasser, C., 2016. The SIRT2 deacetylase stabilizes slug to control malignancy of basal-like breast cancer. Cell reports, 17(5), pp.1302-1317.

Zhou, Y., Hu, Y., Yang, M., Jat, P., Li, K., Lombardo, Y., Xiong, D., Coombes, R.C., Raguz, S. and Yagüe, E., 2014. The miR-106b$\sim$ 25 cluster promotes bypass of doxorubicin-induced senescence and increase in motility and invasion by targeting the E-cadherin transcriptional activator EP300. Cell Death & Differentiation, 21(3), pp.462-474.

Zhou, Y.M., Cao, L., Li, B., Zhang, R.X., Sui, C.J., Yin, Z.F. and Yang, J.M., 2012. Clinicopathological significance of ZEB1 protein in patients with hepatocellular carcinoma. Annals of surgical oncology, 19(5), pp.1700-1706.

Zhou, Z., Zhang, L.U., Xie, B., Wang, X., Yang, X., Ding, N., Zhang, J., Liu, Q., Tan, G., Feng, D. and Sun, L.Q., 2015. FOXC2 promotes chemoresistance in nasopharyngeal carcinomas via induction of epithelial mesenchymal transition. Cancer Letters, 363(2), pp.137-145.

Zhu, G., Pei, L., Li, Y. and Gou, X., 2020. EP300 mutation is associated with tumor mutation burden and promotes antitumor immunity in bladder cancer patients. Aging (Albany NY), 12(3), p.2132.

Zhu, K., Chen, L., Han, X., Wang, J. and Wang, J., 2012. Short hairpin RNA targeting Twist1 suppresses cell proliferation and improves chemosensitivity to cisplatin in HeLa human cervical cancer cells. Oncology reports, 27(4), pp.1027-1034.

Zhu, L.H., Liu, T., Tang, H., Tian, R.Q., Su, C., Liu, M. and Li, X., 2010. MicroRNA-23a promotes the growth of gastric adenocarcinoma cell line MGC803 and downregulates interleukin-6 receptor. The FEBS journal, 277(18), pp.3726-3734.

Zhu, P., Zhao, N., Sheng, D., Hou, J., Hao, C., Yang, X., Zhu, B., Zhang, S., Han, Z., Wei, L. and Zhang, L., 2016. Inhibition of growth and metastasis of colon cancer by delivering 5-fluorouracil-loaded pluronic P85 copolymer micelles. Scientific reports, 6(1), pp.1-11.

Zhu, X.J., Liu, J., Xu, X.Y., Zhang, C.D. and Dai, D.Q., 2014. Novel tumor-suppressor gene epidermal growth factor containing fibulin like extracellular matrix protein 1 is epi-

genetically silenced and associated with invasion and metastasis in human gastric cancer. Molecular medicine reports, 9(6), pp.2283-2292.

Zhu, Y., Wu, J., Li, S., Ma, R., Cao, H., Ji, M., Jing, C. and Tang, J., 2013. The function role of miR-181a in chemosensitivity to adriamycin by targeting Bcl-2 in low-invasive breast cancer cells. Cellular physiology and biochemistry, 32(5), pp.1225-1237.

Ziauddin, M.F., Hua, D. and Tang, S.C., 2014. Erratum: Emerging strategies to overcome resistance to endocrine therapy for breast cancer [Cancer Metastasis Rev, 33,(2–3),(2014), 791–807. Cancer and Metastasis Reviews, 33(4).

Zielske, S.P., Spalding, A.C., Wicha, M.S. and Lawrence, T.S., 2011. Ablation of breast cancer stem cells with radiation. Translational oncology, 4(4), pp.227-233.

Zimmerlin, L., Donnenberg, A.D., Rubin, J.P., Basse, P., Landreneau, R.J. and Donnenberg, V.S., 2011. Regenerative therapy and cancer: in vitro and in vivo studies of the interaction between adipose-derived stem cells and breast cancer cells from clinical isolates. Tissue Engineering Part A, 17(1-2), pp.93-106.

Zoni, E., van der Pluijm, G., Gray, P.C. and Kruithof-de Julio, M., 2015. Epithelial plasticity in cancer: Unmasking a MicroRNA network for TGF-β-, Notch-, and Wnt-Mediated EMT. Journal of oncology, 2015.

Zoon, C.K., Starker, E.Q., Wilson, A.M., Emmert-Buck, M.R., Libutti, S.K. and Tangrea, M.A., 2009. Current molecular diagnostics of breast cancer and the potential incorporation of microRNA. Expert review of molecular diagnostics, 9(5), pp.455-466.

Zor, T., De Guzman, R.N., Dyson, H.J. and Wright, P.E., 2004. Solution structure of the KIX domain of CBP bound to the transactivation domain of c-Myb. Journal of molecular biology, 337(3), pp.521-534.

Zou, Q., Li, J., Hong, Q., Lin, Z., Wu, Y., Shi, H. and Ju, Y., 2015. Prediction of microRNA disease associations based on social network analysis methods. BioMed research international, 2015.

Zou, Y., Tsai, W.B., Cheng, C.J., Hsu, C., Chung, Y.M., Li, P.C., Lin, S.H. and Hu, M.C., 2008. Forkhead box transcription factor FOXO3a suppresses estrogen-dependent breast cancer cell proliferation and tumorigenesis. Breast Cancer Research, 10(1), p.R21.

Zujewski, J.A., 2016. Changing Paradigms in Breast Cancer Therapeutics. Medical Principles and Practice, 25(Suppl 2), p.73.

Zuo, J.H., Zhu, W., Li, M.Y., Li, X.H., Yi, H., Zeng, G.Q., Wan, X.X., He, Q.Y., Li, J.H., Qu, J.Q. and Chen, Y., 2011. Activation of EGFR promotes squamous carcinoma SCC10A cell migration and invasion via inducing EMT-like phenotype change and MMP-9-mediated degradation of E-cadherin. Journal of cellular biochemistry, 112(9), pp.2508-2517.

Zuo, J.H., Zhu, W., Li, M.Y., Li, X.H., Yi, H., Zeng, G.Q., Wan, X.X., He, Q.Y., Li, J.H., Qu, J.Q. and Chen, Y., 2011. Activation of EGFR promotes squamous carcinoma SCC10A cell migration and invasion via inducing EMT-like phenotype change and MMP-9-mediated degradation of E-cadherin. Journal of cellular biochemistry, 112(9), pp.2508-2517.

Chang, S., Yim, S., Park, H., 2019. The cancer driver genes IDH1/2, JARID1C/KDM5C, and UTX/KDM6A: crosstalk between histone demethylation and hypoxic reprogramming in cancer metabolism. Experimental and Molecular Medicine, 51, pp.1-17.

Appendix A

Conferences and Publications

A.1 Breast Cancer Now Conference 2016

Modulation of EP300 alters paclitaxel resistance and is accompanied by regulation of cancer stem cell markers in breast cancer

Roman Jugov, Muhammad Asaduzzaman, Stephanie Constantinou, Haoxiang Min, John Gallon, Meng-Lay, Charles Coombes, Eric Lam and Ernesto Yagüe

Division of Cancer, Faculty of Medicine, Imperial College London, Hammersmith Hospital Campus, London, UK

Abstract

There is an urgent need to understand how cancer cells spread and to identify markers of diagnostic and prognostic significance that can help in the development of novel therapeutics. We have recently described a novel pathway regulating drug resistance in breast cancer. The three miRs in the miR-106b 25 cluster (miR-106b, miR-93 and miR-25) target the 3'-UTR of EP300, a transcriptional activator of E-cadherin, down-regulating its expression and thus activating an EMT programme accompanied by acquisition of cancer stem cell (CSC) properties and drug resistance. Here, we have used a variety of breast cancer cell lines in which EP300 expression has been stably modulated (either down-regulated or over-expressed), as well as paclitaxel resistant derivatives. We find that absence of EP300 is directly linked to paclitaxel resistance and this is accompanied by an enrichment in breast cancer stem cell markers (i.e. enrichment of $CD44^{high}/CD24^{low}$ sub-population and ABCG2). Importantly, cells in which EP300 has been either down-regulated or knocked-out show an up-regulation of antiapoptotic BCL2. Interestingly, ectopic expression of EP300 in breast cancer cell lines with mesenchymal characteristics (MDA-MB-231, CAL51) rescues the phenotype, with depletion of the $CD44^{high}/CD24^{low}$ sub- population and resensitization to paclitaxel. Transcriptome profiling of MCF-7 cells with EP300 down-regulated confirms that

EP300 has an important role regulating a plethora of molecules involved in drug resistance, motility, invasion and differentiation.

Metaplastic breast carcinomas constitute a distinct aggressive form of invasive breast cancer characterized by lack of E-cadherin expression and elongated, "fibroblast-like" cells. It is not a common type of breast cancer, but is highly aggressive and has a poor clinical outcome. We have analyzed by immunohistochemistry a small sample of metaplastic breast cancers and found EP300 highly down-regulated, indicating that EP300 may play a role in the regulation of aggressive characteristics of this form of breast cancer.

A.2 Oncogenic EP300 can be targetted with inhibitors of aldo-keto reductases

Biochemical Pharmacology 163 (2019) 391–403

Contents lists available at ScienceDirect

Biochemical Pharmacology

journal homepage: www.elsevier.com/locate/biochempharm

Oncogenic EP300 can be targeted with inhibitors of aldo-keto reductases

Zimam Mahmud[a], Muhammad Asaduzzaman[a,1], Uttom Kumar[a], Nahal Masrour[a], Roman Jugov[a], R. Charles Coombes[a], Sami Shousha[b], Yunhui Hu[c], Eric W.-F. Lam[a], Ernesto Yagüe[a,*]

[a] Division of Cancer, Imperial College Faculty of Medicine, Hammersmith Hospital Campus, Du Cane Road, London W12 0NN, United Kingdom
[b] Centre for Pathology, Department of Medicine, Imperial College Faculty of Medicine, Charing Cross Hospital, Fulham Palace Rd, London W6 8RF, United Kingdom
[c] Department of Breast Cancer, China Tianjin Breast Cancer Prevention, Treatment and Research Center, Tianjin Medical University Cancer Institute and Hospital, National Clinical Research Center of Cancer, Huan Hu Xi Road, Ti Yuan Bei, He xi District, Tianjin 300060, PR China

ARTICLE INFO

Keywords:
Aldo-keto reductase
Breast cancer
E-cadherin
EP300
Epidermal-to-mesenchymal transition
Lymph node metastasis

ABSTRACT

E-cadherin transcriptional activator EP300 is down-regulated in metaplastic breast carcinoma, a rare form of triple negative and E-cadherin-negative aggressive breast cancer with a poor clinical outcome. In order to shed light on the regulation of E-cadherin by EP300 in breast cancer we analyzed by immunohistochemistry 41 cases of invasive breast cancer with both E-cadherin^{high} and E-cadherin^{low} expression levels, together with 20 non-malignant breast tissues. EP300 and E-cadherin showed a positive correlation in both non-malignant and cancer cases and both markers together were better predictors of lymph node metastasis than E-cadherin alone. These data support a metastasis suppressor role for EP300 in breast cancer. However, some reports suggest an oncogenic role for EP300. We generated a breast cancer cell model to study E-cadherin-independent effects of EP300 by over-expression of EP300 in HS578T cells which have E-cadherin promoter hypermethylated. In this cell system, EP300 led to up-regulation of mesenchymal (vimentin, Snail, Slug, Zeb1) and stemness (ALDH$^+$ and CD44^{high}/CD24^{low}) markers, increases in migration, invasion, anchorage-independent growth and drug resistance. Genome-wide expression profiling identified aldo-keto reductases AKR1C1-3 as effectors of stemness and drug resistance, since their pharmacological inhibition with flufenamic acid restored both doxorubicin and paclitaxel sensitivity and diminished mammosphere formation. Thus, in cells with a permissive E-cadherin promoter, EP300 acts as a tumour/metastasis supressor by up-regulating E-cadherin expression, maintenance of the epithelial phenotype and avoidance of an epithelial-to-mesenchymal transition. In cells in which the E-cadherin promoter is hypermethylated, EP300 functions as an oncogene via up-regulation of aldo-keto reductases. This offers the rationale of using current aldo-keto reductase inhibitors in breast cancer treatment.

1. Introduction

E-cadherin is an important transmembrane glycoprotein mediating epithelial cell–cell adhesion [1]. E-cadherin expression, which can be used as a biomarker for breast cancer diagnosis [2], becomes low or absent in some types of breast cancer such as metaplastic breast carcinoma, especially in the spindle subtype which shows characteristics of epithelial-to-mesenchymal transition (EMT) [3,4]. Unlike invasive lobular carcinoma (ILC), primary invasive, or infiltrating, ductal carcinoma (IDC) shows good immunoreactivity for E-cadherin if lymph nodes have not been invaded, but the staining is very weak when metastases have occurred [5]. In addition, E-cadherin has a metastasis suppressor role as its depletion triggers EMT, acquisition of stem cell-like properties and drug resistance [6,7].

Regulation of E-cadherin gene (*CDH1*) expression occurs at many levels and the mechanisms leading to its repression are well studied. Promoter hypermethylation as well as inactivating mutations spreading along the extracellular domain have all been reported in different cancers [8,9]. Negative regulation by transcription factors such as Snail, Slug, Twist and ZEB1/2, resulting in EMT is also well understood [10]. However, the role of activators of E-cadherin expression (such as FOXA1, RUNX1 and EP300 [11,12]) during EMT is less understood.

We have recently described a novel E-cadherin regulatory axis controlled by the miR-106b ~ 25 cluster which down-regulates the E-cadherin transcriptional activator EP300 [13,14]. Experimental depletion of EP300 in breast epithelial cancer cells down-regulates E-

* Corresponding author at: Division of Cancer, Imperial College Faculty of Medicine, Hammersmith Hospital Campus, Du Cane Road, London W12 0NN, United Kingdom.
E-mail address: ernesto.yague@imperial.ac.uk (E. Yagüe).
[1] Present address: Department of Clinical Pharmacy and Pharmacology, University of Dhaka, Dhaka 1000, Bangladesh.

https://doi.org/10.1016/j.bcp.2019.03.009
Received 15 January 2019; Accepted 7 March 2019
Available online 09 March 2019
0006-2952/

cadherin, triggers an EMT as well as an increase in cancer stem cell-like cells (CSCs) and drug resistance. Conversely, ectopic expression of EP300 in basal-like triple negative breast cancer cells rescues the mesenchymal-like phenotype, coupled with an increase in epithelial-like properties [15]. Similar results have also been reported in pancreatic [16] and colorectal cancer [17], and Kaplan-Meier plots using a large cohort (> 4000) of breast cancer patients, suggest that both EP300 and E-cadherin are good prognostic indicators [18]. However, other reports support an oncogenic role for EP300 in prostate [19], hepatocellular [20] or nasopharyngeal cancer [21].

Recently, we have demonstrated a strong down-regulation of both EP300 and E-cadherin in metaplastic breast carcinoma, a rare, but aggressive form of invasive breast cancer which has a poor clinical outcome [15]. Here we show a strong positive correlation between EP300 and E-cadherin expression by immunohistochemistry (IHC) in IDC and ILC, although some clinical samples were EP300^{high}/E-cadherin^{low}, and find that both markers taken together were better predictors of lymph node metastasis than E-cadherin alone. However, EP300 can act as an oncogene in a cell model with hypermethylation of the *CDH1* promoter, leading to an increase in EMT and CSC markers, migration, invasion, anchorage independence and drug resistance.

2. Material and methods

2.1. Clinical samples

A total of 61 archival formalin fixed paraffin embedded breast tissues were collected from Imperial College Healthcare Tissue Bank (R14086 and R17041) and Breast Cancer Now Tissue Bank (BCNTB-TR000054) after ethics approval by both institutions and complying with the 1964 Helsinki declaration and its later amendments or comparable ethical standards. For this type of study formal consent is not required. This study analyzed 20 non-malignant (14 cosmetic reduction mammoplasties, 3 fibroadenomas, 2 intra-ductal papillomas and 1 tubular adenoma) and 41 breast cancer cases (20 IDC and 21 ILC) selected after an initial screening for E-cadherin, so that both E-cadherin^{high} and E-cadherin^{low} samples would be included.

2.2. IHC

Immunohistochemical staining was performed using antibodies against EP300 (HPA003128, Sigma-Aldrich, St. Louis, MO, USA, dilution 1:200) and E-cadherin (Clone 36, #610181, BD Biosciences, San Jose, CA, USA, dilution 1:200). We have previously validated EP300 antibody specificity using a synthetic peptide, as well as described the standard operating procedure for immunohistochemical staining [15]. All sections were visualized with diaminobenzidine and counterstained with hematoxylin.

2.3. Scoring

EP300 and E-cadherin immunoreactivity was scored based on staining intensity ranging from 0 to +3: 0 = null, +1 = low, +2 = intermediate and +3 = high, as described [15]. More than six representative fields of each slide were analyzed for determining EP300 and E-cadherin expression levels. The percentage of EP300- or E-cadherin-positive tumour cells scored as high (+2 or +3 in at least 66% of cells) or low/none, was calculated for each slide by two investigators (MA and EY) and validated by a pathologist (SS) and clinical oncologist (RCC).

2.4. Cells

European Cell Culture Collection cell lines MCF-7 and HS578T cells were obtained from Sigma-Aldrich (St. Louis, MO, USA). All cells were maintained in Dulbecco's Modified Eagle Medium (DMEM) supplemented with 1 g/L glucose, 10% foetal calf serum and 4 mM L-glutamine (Thermo Fisher Scientific, Waltham, MA, USA). Medium for HS578T cells contained, in addition, 10 μg/ml recombinant human insulin (Sigma Aldrich, St. Louis, MO, USA). Over-expression of *EP300* was obtained by stable expression of a pcDNA3.1-derived construct carrying the full-length *EP300* cDNA (#23252, Addgene, Watertown, MA, USA) [22]. Plasmid DNA was linearized by *Pvu*I and transfected into HS578T cells using GenJet (SignaGen Laboratories, Rockville, MD, USA) following manufacturer's instructions and selected and maintained with 1 mg/mL G418 (Sigma-Aldrich, St. Louis, MO, USA). Pools of at least 200 G418-resistant clones were used in all cases. Where indicated, cells were treated with 5-Aza-2′-deoxycytidine (AzaC; Sigma Aldrich, St. Louis, MO, USA) daily in fresh medium for up to four days or with flufenamic acid (N-(α,α,α-Trifluoro-*m*-tolyl)-anthranilic acid; 2-[[3-(trifluoro-methyl) phenyl] amino]-Benzoic acid, FFA; Sigma Aldrich, St. Louis, MO, USA) as indicated. Drug resistant derivatives from HS-578 T cells were generated using drug pulses in an escalating manner essentially as described [13] until cells were able to proliferate after 3-day toxic pulses of paclitaxel (HS-TX cells) and doxorubicin (HS-DOX cells). Drug resistant cells were routinely grown drug free with drug treatments (25 nM paclitaxel or 100 nM doxorubicin) every 5 passages to maintain the resistant phenotype. A sulphorhodamine B (Sigma Aldrich, St. Louis, MO, USA) assay was used to screen for drug cytotoxicity as described [13].

2.5. Gene expression analysis

Total RNA, isolated using a RNeasy Mini kit (Qiagen, Paisley, UK) was reverse transcribed with Superscript III reverse transcriptase (Thermo Fisher Scientific, Whaltham, MA, USA) and real-time quantitative PCR was performed using SYBR-Green (Thermo Fisher Scientific, Whaltham, MA, USA) on a ABI PRISM 7900 HT Fast Real-time PCR System (Thermo Fisher Scientific, Whaltham, MA, USA). The cycling program included a 90 °C for 10 min initial step for enzyme activation followed by 40 cycles of denaturation and primer annealing/extension consisting of 95 °C for 3 s and 60 °C for 30 s, respectively. The ribosomal *RPL19* gene was used as a normalizer. A comparative threshold cycle was used to determine relative gene expression with standard curves for each gene as previously described [13]. Primers used for RT-qPCR were RPL19 forward: 5′-GCGGAAGGGTACAGCCAAT, reverse: 5′-GCAGCCG GCGCAAA; EP300 forward: 5′-AAAAATAAGAGCAGCCTGAG, reverse: 5′-AGACCTCTTTATGCTTCTTCC; CDH1 forward: 5′-GATTCTGCTGCTC TTGCT, reverse: 5′-GATTCTGCTGCTCTTGCT; Vimentin forward: 5′-AGTCCACTGAGTACCGGAGAC, reverse: 5′-CATTTCACGCATCTGGC CGTTC; N-cadherin forward: 5′-GCGTCTGTAGAGGCTTCTGG, reverse: 5′-AAATCTGCAGGCTCACTGCT; ZEB1 forward: 5′-TTACACCTTTGCAT ACAGAACCC, reverse: 5′-TTTACGATTACACCCAGACTGC; SNAI1 forward: 5′-AGGCCATGTCCGGACCCACA, reverse: 5′-GTGGAGCAGGGAC ATTCGGGA; SNAI2 forward: 5′-CAGTGATTATTTCCCCGTATC, reverse: 5′-CCCCAAAGATGAGGAGTATC; AKR1C1 forward: 5′-AGGTGGAATGT CATCCTTAC, reverse: 5′-CTATAGGCAACCAGAACAATG; AKR1C2 forward: 5′-CTCATGAGATCTGGTTGTTTG, reverse: 5′-GTAACATCATGAA GGAAGGTG; AKR1C3 forward: 5′-AAAGCTTTGGTCCACTTTTC, reverse: 5′-AAGATAGAGGTCAACATAGTCC.

2.6. Immunoblotting

Antibodies for immunodetection following standard immunoblotting procedures were 24E10 for E-cadherin, #4061 for N-cadherin, D21H3 for Vimentin, C15D3 for Snail, C19G7 for Slug (Cell Signaling Technology, Danvers, MA, USA); ab10485 for EP300 (Abcam, Cambridge, UK) and H-235 for β-tubulin (Santa Cruz Biotechnology, Dallas, TX, USA). Primary antibodies were detected using horseradish peroxidase linked anti-mouse, anti-goat or anti-rabbit secondary antibodies as appropriate (DAKO, Ely, UK), and visualized using the ECL detection system (Amersham Biosciences, Amersham, UK).

2.7. Drug resistance clonogenic assay

Cells (2–5 × 10^3) were seeded into 6-well plates, at least in duplicate, and, after 24 h, treated with paclitaxel or doxorubicin (Tocris Bioscience, Bristol, UK) for 3 days and 2 days, respectively. Cells were kept in culture for 28 days with drug-free medium changing every three days. At the end of this period, drug resistant clones were fixed with 1% formaldehyde in PBS, washed 3 times with PBS and stained with 0.5% (w/v) crystal violet. Pictures were taken and the stain was solubilised with 33% acetic acid and OD_{592} nm measured.

2.8. Anchorage independent growth assay

For soft agar assays, 5 × 10^4 cells were mixed with DMEM containing 0.3% agar noble (Difco Laboratories, Detroit, MI, USA) on 6 well plates with a bottom layer of solidified 0.6% agar noble in the same medium. Triplicate cultures for each cell type were maintained for 8 weeks at 37 °C in an atmosphere of 5% CO_2 and 95% air, with 300 µl fresh medium added twice a week. After 8 weeks, colonies larger than 20 µm in diameter were counted. For mammosphere formation assays, 3 × 10^3 cells / well were seeded, at least in duplicate, in ultra-low attachment 6-well plates (Corning, NY, USA) in DMEM/F12 medium supplemented with 20 ng/ml epidermal growth factor (EGF, Sino Biologicals, Wayne, PA, USA), 20 ng/ml basic fibroblast growth factor (bFGF, Thermo Fisher Scientific, Whaltham, MA, USA) and B27 (Thermo Fisher Scientific, Whaltham, MA, USA). Fresh medium (500 µl) was added every 3–5 days for two weeks after which the spherical clusters of cells were counted. Clone or sphere forming efficiency was calculated relative to the total number of plated cells x100. Mammosphere volume was calculated according to the formula volume = 0.5 × $width^2$ × length. Images were captured using an EVOS FL Cell Imaging System® (Thermo Fisher Scientific, Whaltham, MA, USA).

2.9. Flow cytometry

For stem cell markers, anti-CD44 (APC) and anti-CD24 (PE), both from BD Biosciences (San Jose, CA, USA), were used essentially as described [23]. Briefly, 1 × 10^6 cells were resuspended in 100 µl FACS buffer and anti-CD44 or anti-CD24 antibodies added and incubated for 30 min at 4 °C. Isotype APC or PE-labelled antibodies (BD Biosciences, San Jose, CA, USA) were used as control. An Aldefluor assay kit (StemCell Technologies, Vancouver, Canada) was used for the determination of aldehyde dehydrogenase (ALDH) activity by flow cytometry essentially as described [23]. Briefly, cells were resuspended in assay buffer (10^6 cells/ml). Activated Aldefluor substrate (5 µl) was added to samples and incubated at 37 °C for 45 min to allow substrate conversion. As a negative control for all experiments, an aliquot of Aldefluor-stained cells was immediately quenched with 1.5-mM diethylaminobenzaldehyde (DEAB), a specific ALDH inhibitor.

2.10. Transwell cell migration and invasion assay

Migration and invasion assays were performed essentially as described [24] using Corning Boyden chambers (24-well insert, 8 µm, Corning, NY, USA). Cells (2x10^4) were seeded on 24-well transwell plates containing DMEM media with 10% FBS in the lower chamber as the chemoattractant. After 24 h of seeding, cells migrated though the pores to the bottom surface of the transwell were fixed with 4% *para*-formaldehyde, washed with PBS and stained with 0.5% crystal violet and counted. Six random microscopic fields were counted for each group. Cell invasion was assayed in transwell coated with Matrigel (BD Biosciences, San Jose, CA, USA). Cells crossed the Matrigel-coated filter were fixed as above, stained with DAPI (4′,6-diamidino-2-phenylindole, Sigma-Aldrich, St. Louis, MO, USA) and counted. The stained cell images were captured by microscope (EVOS, Thermo Fisher Scientific, Whaltham, MA, USA), and five random fields at × 10 magnification were counted.

2.11. Microarray hybridization, processing and data analysis

Total RNA was prepared from three independent biological replicates of each cell line using a RNeasy Kit (Qiagen, Crawley, UK). RNA integrity was evaluated using an Agilent 2100 Bioanalyzer (Agilent Technologies, Santa Clara, CA, USA). cDNA synthesis and further processing was performed using GeneChip WT PLUS Reagent kit (Thermo Fisher Scientific, Whaltham, MA, USA). Hybridization to Clariom S arrays (Thermo Fisher Scientific, Whaltham, MA, USA) followed manufacturer's protocol. Data were analysed with Robust Multichip Analysis (RMA) algorithm using default analysis settings and global scaling as a normalisation method. Values presented are log2 RMA signal intensity. Microarray data were deposited at the NCBI Gene Expression Omnibus (http://ncbi.nlm.nih.gov/geo/) under accession number **GSE116370**.

2.12. Pyrosequencing

The methylation status of well-characterized 21 cytosine residues in the *CDH1* gene promoter [9] was determined following bisulphite modification of DNA essentially as described [25]. Briefly, genomic DNA was extracted from FFPE cancer samples using a QIAamp DNA FFPE Tissue Kit (Qiagen, Crawley, UK). Genomic DNA was bisulphite treated using EZ DNA Methylation kit (Zymo Research, Irvine, CA, USA) and PCR amplified with FastStart Taq DNA Polymerase (Roche, Basel, Switzerland) using annealing temperature of 58 °C for *CDH1* and 53 °C for *LINE1* for 45 cycles. Primers were designed using PyroMark Assay Design 2.0 (Qiagen) to amplify 4 regions in the proximal *CDH1* promoter. Primers were: Region 1 (Forward 5′-Biotin- TTTAGTAATTTTAGGTTAGAGGGTTA, Reverse 5′- TCACCTACCCACCACAACCAATCAACAA, Sequencing 5′- CAACAACCCCCAACCCCTCCCCA), Region 2 (Forward 5′- ATTGGTTGTGGTAGGTAGGTGAATT, Reverse 5′-Biotin- AACTTCCCCAAACTCACAAATACTTTAC, Sequencing 5′- GTAGGTGAATTTTTAGTTAA), Region 3 (Forward 5′- GGAATTGTAAAGTATTTGTGAGTTTG, Reverse 5′-Biotin- AAAAACTACCACTCCAAAAACCCATA, Sequencing 5′- GTTTGAGGAAGTTAGTTTAGATTTT), Region 4 (Forward 5′- Biotin- TGTGAGTTTGAGGAAGTTAGTTTAGAT, Reverse 5′- AAAAACTACCACTCCAAAAACCCATAAC, Sequencing 5′- CAAAAACCCATAACTAACC). *LINE* primers have been described [25]. The biotinylated strands of the amplicons were purified with streptavidin-coated Sepharose beads (GE Healthcare, Chalfont St Giles, UK) and Vacuum Prep Tool (Qiagen, Crawley, UK) and subsequently annealed to the sequencing primer. Pyrosequencing was performed using PyroGold Reagent kit (Qiagen, Crawley, UK) with Pyromark Q96 MD instrument. The percentage methylation at individual CG sites was analysed using Pyro Q-CpG software (Qiagen, Crawley, UK). All runs contained an unmethylated DNA standard curve prepared with normal human female DNA (Promega, Madison, Wisconsin, USA) that was whole-genome amplified (GE Healthcare Life Sciences, Little Chalfornt, UK). The methylated standard curve was prepared by diluting hypermethylated DNA (CpGenome Universal Methylated DNA, Millipore, Whatford, UK) in the whole genome amplified DNA. Untreated normal female DNA was used as a control.

2.13. Statistical analyses

The 2 × 2 contingency table of variables was examined by Chi-square test using the Analyse-it add-in (Analyse-it Software, Ltd., Leeds, UK) for Microsoft Excel. Other statistical evaluations were performed by Student's *t*-test for paired data. Best-fit curves were obtained using Graphpad Prism 6 (Graphpad Software, San Diego, CA, USA). Mammosphere volume and CpG methylation data were analyzed using the Mann-Whitney test. Statistical significance was considered when $P \leq 0.05$.

3. Results

3.1. Correlation of EP300 and E-cadherin in breast tissue

In non-malignant breast tissues, both EP300 and E-cadherin staining showed, as expected, intense signals. E-cadherin consistently showed membrane staining scoring 3 and EP300 showed a strong/intermediate nuclear signal in 18 out of 20 samples. The remaining two samples showed scores of 0 and 1 in the nucleus, but with intermediate staining (score 2) in the cytoplasm, and thus all cases were considered EP300^{high}/E-cadherin^{high}. When IDC cases were analysed, their IHC score varied from 1 to 3, indicating low to high expression for both EP300 and E-cadherin. Most cases were either EP300^{high}/E-cadherin^{high} or EP300^{low}/E-cadherin^{low}, 10 and 6, respectively, out of 20 (Fig. 1). Of the 21 ILCs, 6 cases were EP300^{high}/E-cadherin^{high}, 7 EP300^{low}/E-cadherin^{low} and, more importantly, 7 EP300^{high}/E-cadherin^{low}. Only 2 cases scored 3 for both E-cadherin and EP300, the remaining of the high cases with intermediate levels of expression (score 2) for both proteins (Fig. 1 and Table 1).

As EP300 is a transcriptional activator of E-cadherin expression, we hypothesized that IHC signals of both proteins would vary in parallel. Normal and non-malignant breast tissues showed, as expected, a consistent strong expression for both EP300 and E-cadherin. Importantly, we found a positive correlation in 80% (49 out of 61) of all samples analyzed with strongly significant concordance between EP300 and E-cadherin ($P < 0.0001$, Chi-square test; Table 1). When only cancer samples were considered, the concordance between EP300 and E-cadherin was maintained ($P = 0.0046$, Chi-square test; Table 1). These data with a relatively small cohort are strongly supported by the previous literature [11] and our laboratory studies demonstrating a positive E-cadherin control by EP300 [13,14,15]. However, we also found some cancer cases with a negative correlation, either EP300^{high}/E-cadherin^{low} (9 out of 41, 22%) or EP300^{low}/E-cadherin^{high} (3 out of 41, 7.3%; Table 1), indicating that in malignant tissues other factors may play a role in E-cadherin expression.

3.2. Loss of EP300 and E-cadherin expression correlates with metastatic lymph node invasion in breast cancer

As EP300 transcriptionally activates E-cadherin expression and E-cadherin is a key molecule in metastatic reprogramming [26], we analyzed the expression of these two markers in relation to the invasion of lymph nodes in breast cancer patients. In both IDC and ILC, we found, reassuringly, that, in the group with a positive correlation between both markers, lymph node metastasis was less frequent (3 versus 13, 18.7%) in the EP300^{high}/E-cadherin^{high} patients. Conversely, a EP300^{low}/E-cadherin^{low} phenotype led to a high frequency of lymph node metastasis (10 versus 3, 76.9%; $P = 0.006$, Chi-square test; Table 2). Importantly, both markers when applied together were better predictors of lymph node metastasis than E-cadherin alone ($P = 0.006$ vs. $P = 0.025$, respectively).

Overall, these data support an anti-metastatic role for EP300 *via* its activation of the tumour suppressor E-cadherin.

3.3. Generation of a cell model to study EP300 function independently of E-cadherin

In order to gain an insight into the potential dual role of EP300 as oncogene or tumour suppressor, we reasoned it would be necessary to differentiate it from its role in activating E-cadherin expression. Histone

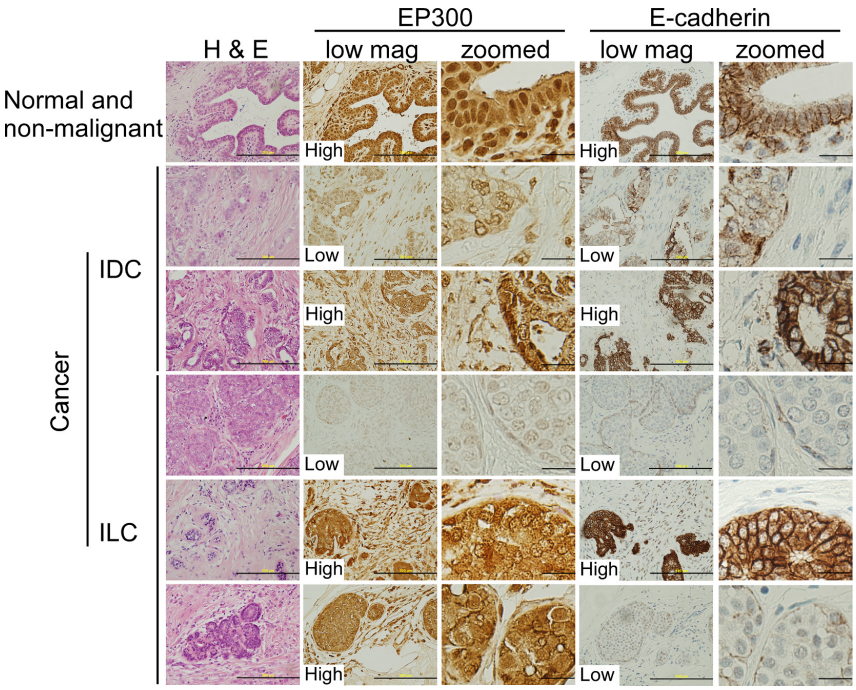

Fig. 1. EP300 and E-cadherin expression in breast tissue. Representative immunohistochemical images after staining for EP300 and E-cadherin. *IDC,* invasive ductal carcinoma; *ILC,* invasive lobular carcinoma. Scores have been included in the low magnification pictures. Most of the IDC cases were either EP300^{low}/E-cadherin^{low} or EP300^{high}/E-cadherin^{high} whereas in ILC the distribution of cases between EP300^{low}/E-cadherin^{low} , EP300^{high}/E-cadherin^{high} and EP300^{high}/E-cadherin^{low} was similar (Table 1). *H&E,* haematoxylin and eosin staining. Scale bar represents 200 μm in the low magnification pictures and 20 μm in the zoomed images.

Table 1
Expression of E-cadherin correlates with that of its transcriptional activator EP300 in both non-malignant and breast cancer.

	EP300 and E-cadherin expression				
	Positive correlation		Negative correlation		
Tissue	EP300^{high}/E-cadherin^{high}	EP300^{low}/E-cadherin^{low}	EP300^{high}/E-cadherin^{low}	EP300^{low}/E-cadherin^{high}	
Non-malignant	20	0	0	0	$n = 20$
IDC[a]	10	6	2	2	$n = 20$
ILC[b]	6	7	7	1	$n = 21$
Total	36	13	9	3	$P < 0.0001$[c]
Cancer total	16	13	9	3	$P = 0.0046$[c]

[a] invasive ductal breast carcinoma.
[b] invasive lobular breast carcinoma.
[c] Chi-square test.

Table 2
Correlation between EP300 and E-cadherin expression is a good predictor of lymph node metastasis.

	EP300 and E-cadherin markers				Single E-cadherin marker		
	Positive correlation		Negative correlation				
Lymph node metastasis	EP300^{high}/E-cadherin^{high}	EP300^{low}/E-cadherin^{low}	EP300^{high}/E-cadherin^{low}	EP300^{low}/E-cadherin^{high}	E-cadherin^{high}	E-cadherin^{low}	
Y[a]	**3**	**10**	**5**	**1**	**4**	**15**	$n = 19$
N	**13**	**3**	**4**	**2**	**15**	**7**	$n = 22$
	$P = 0.006$[b]		$P = 0.505$[b]		$P = 0.025$[b]		

[a] at least one lymph node invaded with cancer cells.
[b] Chi-square test of above 2x2 table highlighted in bold.

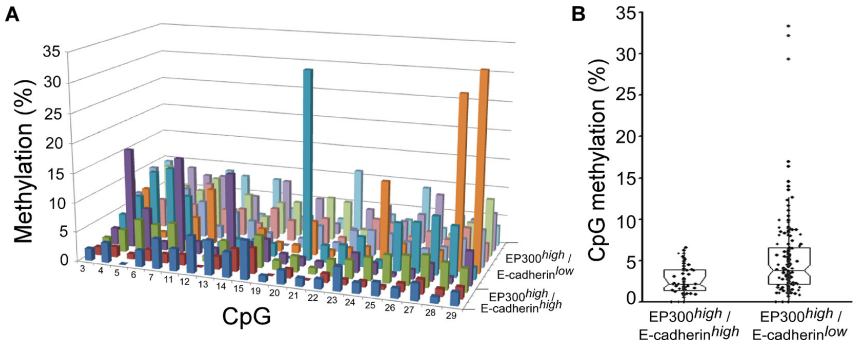

Fig. 2. E-cadherin promoter is methylated in EP300^{high}/E-cadherin^{low} tumours. Methylation at 21 CpGs in the proximal *CDH1* (E-cadherin) promoter was determined after bisulphite conversion and pyrosequencing in DNA isolated from EP300^{high}/E-cadherin^{high} ($n = 3$) and EP300^{high}/E-cadherin^{low} ($n = 8$) FFPE tissue samples. A) Individual methylation values in 21 CpGs. CpG numbering corresponds to that previously described [9]. B) Box plot representation of the methylation percentage in 21 CpGs in all patients analyzed. Box plot indicates the mean within the box at 95% confidence interval. Data were analyzed using the Mann-Whitney test ($p < 0.0001$).

acetyl transferases help to relax chromatin thus enabling gene expression, although this only occurs in not highly methylated loci [27]. *CDH1* (encoding E-cadherin) promoter has been found to be methylated in a proportion of breast cancer patients, where it may contribute to the repression of the locus [28]. We asked whether EP300^{high}/E-cadherin^{low} and EP300^{high}/E-cadherin^{high} patients tumours had a different methylation profile at the *CDH1* proximal promoter. For this we analyzed the methylation status of 21 CpGs by bisulphite conversion and pyrosequencing. As expected, methylation in EP300^{high}/E-cadherin^{high} samples was low and no CpG showed values above 6%. Conversely, EP300^{high}/E-cadherin^{low} samples showed a greater variation in the methylation percentage, with some CpGs as high as 33% (Fig. 2A). Taking all the CpGs analyzed, the overall percentage of methylation at the *CDH1* locus in EP300^{high}/E-cadherin^{low} was twice that found in EP300^{high}/E-cadherin^{high} samples (Fig. 2B). Thus, methylation of the E-cadherin promoter may explain, at least in part, the lack of E-cadherin expression in EP300^{high}/E-cadherin^{low} tumours.

E-cadherin promoter methylation is well characterized in some breast cancer cell lines and, in particular, HS578T cells which show an average of 47% methylation across 29 CpG sites with no, or minimal, E-cadherin expression [9]. Thus, we decided to use this cell line to overexpress EP300 and generate a cell model for EP300^{high}/E-cadherin^{low} breast cancer to test the role of EP300 in an E-cadherin-null background. Stably transfected HS578T cells overexpressing EP300 (HS-EP300) confirmed lack of E-cadherin activation (Fig. 3A and B). As expected, use of a demethylating agent (Aza-C) triggered E-cadherin expression in both control (HS-ev; carrying only empty vector) and HS-EP300 cells. Importantly, E-cadherin expression was higher in HS-EP300 than in control cells (Fig. 3C and D), indicating that EP300 is functional and could transcriptionally activate the demethylated *CDH1* locus. Thus, we have generated a cell model in which EP300 is over-expressed and functionally active but does not activate expression from

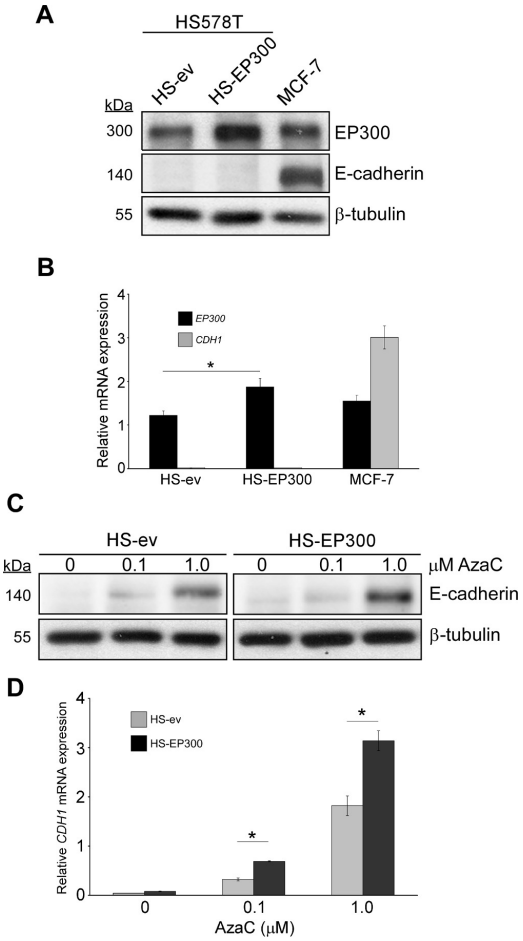

Fig. 3. Experimental overexpression of EP300 in E-cadherin-null HS578T cells. HS578T cells were stably transfected with an EP300 expression cassette cloned into pcDNA3.1 (HS-EP300). Transfected cells with the empty vector (HS-ev) served as control. Western blot analysis (*A*) and mRNA expression analysis by real-time PCR normalized to the expression of *RPL19* mRNA (*B*). MCF-7 cells serve as a positive control for E-cadherin expression. Cells were treated daily with the demethylating agent AzaC for 4 days and E-cadherin expression was determined by western blot (C) and real-time PCR (D). Numerical data represent the average ± SD of three different experiments ($^{*}P < 0.05$). Pictorial data shows a representative of three independent experiments.

the *CDH1* locus.

3.4. Epithelial-to-mesenchymal transition and cancer stem cell markers in EP300 overexpressing cells

EMT is the first step in the metastatic cascade and cells undergoing EMT present a set of characteristic markers accompanying the acquisition of mesenchymal-like phenotype [29]. HS-EP300 cells showed increased expression levels of N-cadherin (an adhesion molecule expressed in mesenchymal cells and neural tissues), vimentin (a mesenchymal intermediate filament), as well as the E-cadherin transcriptional repressors Snail, Slug and Zeb1 (Fig. 4A). Although control HS-ev cells expressed these molecules due to the triple-negative, basal-like, nature of HS578T cells, EP300 overexpression increased further both their RNA and protein levels.

As EMT generates cells with properties of stem cells [6], we also asked whether HS-EP300 cells would show an increase in two characteristic CSC markers, aldehyde dehydrogenase (ALDH) and CD44/CD24. Approximately 8% of HS-ev control cells were $ALDH^{+}$, which increased to approximately 16% in HS-EP300 cells (Fig. 4B). Breast CSCs are typically represented by a $CD44^{high}/CD24^{low}$ subpopulation that increased from 45% in HS-ev cells to 60% in HS-EP300 cells (Fig. 4C).

These results indicate that overexpression of EP300 in the E-cadherin-null background of HS578T cells increases EMT and CSC markers.

3.5. EP300 overexpressing cells gain motility, invasion, anchorage independence growth and become drug resistant

In order to assess the functional significance of the increase in EMT markers, we used *trans*-wells to determine the capacity of cells to migrate through in the presence or absence of Matrigel. Indeed, the motility of HS-EP300 cells increased approximately 6-fold with respect to control cells, whereas the capacity to invade through Matrigel increased approximately 3-fold (Fig. 5A and B).

CSCs are considered the tumour initiating sub-population [6] and thus its increase would lead to a higher number of tumours. In order to functionally test this, we used two methods to assess anchorage independence. Growth in soft agar showed that overexpression of EP300 led to an increase of approximately 1.5-fold in the number of clones (Fig. 5C). Equally, growth in low-attachment plates indicated an increase in the number of mammospheres (~2.2-fold) as well as their volume (~3.5-fold) in HS-EP300 cells (Fig. 5D).

EMT and CSCs are two phenomena tightly interlinked with drug resistance [30]. We then asked whether the increase in EMT and CSC characteristics gained by HS-EP300 cells was also accompanied by an increase in drug resistance. To test this, we treated both HS-ev and HS-EP300 cells with paclitaxel or doxorubicin and monitored the generation of surviving drug resistant clones. Indeed, 28 days after drug treatment HS-EP300 cells produced approximately four times more doxorubicin- and five times more paclitaxel-resistant clones than control HS-ev cells (Fig. 6).

Thus, EP300 activates an EMT programme characterized by acquisition of CSC properties and drug resistance in an E-cadherin non-permissive background.

3.6. Molecular signature of oncogenic EP300 indicates a major role of aldo–keto reductases

In order to gain insights into the molecular mechanisms underlying EP300 oncogenic function, we performed genome-wide transcriptome analysis of HS-EP300 cells. A total of 950 transcripts were differentially regulated between HS-EP300 and HS-ev control cells (GEO accession number **GSE116370**; a list of the most differentially regulated genes is shown in Table 3). *AKR1C1* (encoding Aldo-keto Reductase Family 1, Member C1) was the most up-regulated gene (5.5-fold), although members C2 and C3 (*AKR1C2* and *AKR1C3*) were also up-regulated by 3.5- and 3.0-fold, respectively. Aldo-keto reductases are a major superfamily of NAD(P)H-dependent oxidoreductases and family C members AKR1C1–AKR1C4, sharing a high percentage of amino-acid sequence identity (from 84 to 98%), are involved in progesterone, testosterone, prostaglandin, and xenobiotic ketones metabolism [31,32]. In addition, AKR1C members have been found to be up-regulated in many cancers [33] and be associated with therapy response [34].

RT-QPCR data indicated that *AKR1C1, AKR1C2* and *AKR1C3* were up-regulated by approximately 2.5-, 3.5- and 2-fold, respectively, upon EP300 overexpression in HS578T cells (Fig. 7A). Although quantitatively different to the fold values obtained with microarrays, as these

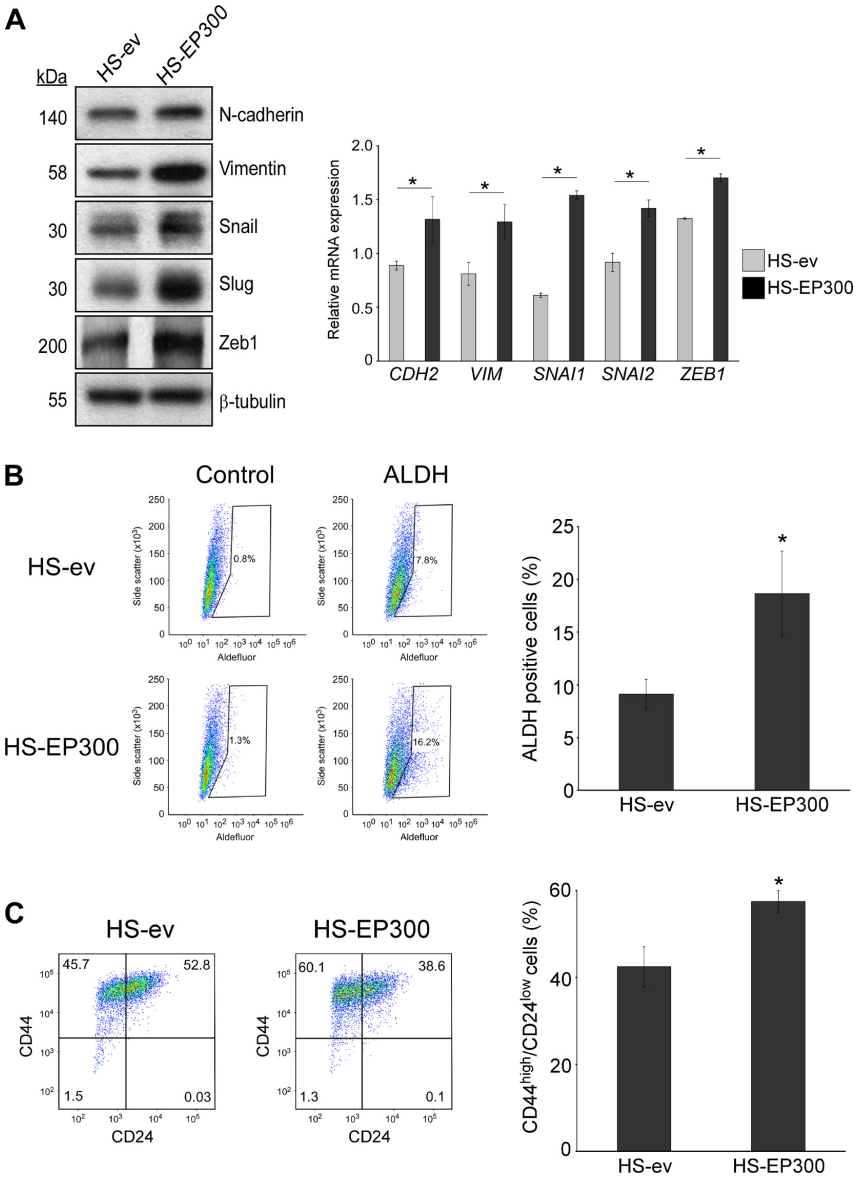

Fig. 4. Up-regulation of EMT and CSC markers in HS-EP300 cells. A) Expression of EMT markers by western blots (*left panel*) and real-time PCR normalized to the expression of *RPL19* mRNA (*right panel*). CSCs were determined by the presence of ALDH and $CD44^{high}/CD24^{low}$ markers. B) ALDH activity. Cells were treated with Aldefluor alone (*ALDH*) or in the presence of the ALDH inhibitor diethylaminobenzaldehyde (*Control*) and then analyzed by flow cytometry (*plots*). The gate was set up with the control cells to include approximately 1% of the population and was used to determine the percentage of ALDH-positive cells in the absence of the inhibitor (*histogram*). C) Flow cytometry analysis of CD24 and CD44 using phycoerythrin-conjugated anti CD24 IgG and APC-conjugated anti CD44 IgG. Quadrants were defined after plotting unstained cells and stained with isotype controls. The percentage of the population with a CSC-like phenotype ($CD44^{high}/CD24^{low}$) is indicated in the histogram. Pictorial data show representatives of at least three independent experiments. Numerical data represent the average ± SD of three different experiments ($^{*}P < 0.05$).

methods use completely different technologies, these data validate the up-regulation of *AKR1C1, AKR1C2* and *AKR1C3* in HS-EP300 cells. In addition, we have generated doxorubicin (HS-DOX, 5-fold resistance) and paclitaxel (HS-TX, 7.5-fold resistance) resistant cells from HS578T (Fig. 7B) and western blot analysis indicated that EP300 was up-regulated in both resistant cells (Fig. 7C). Reassuringly, aldo-keto reductases expression was also up-regulated in both resistant cells, although *AKR1C2* and *AKR1C3* were the most up-regulated (between 4- and 10-

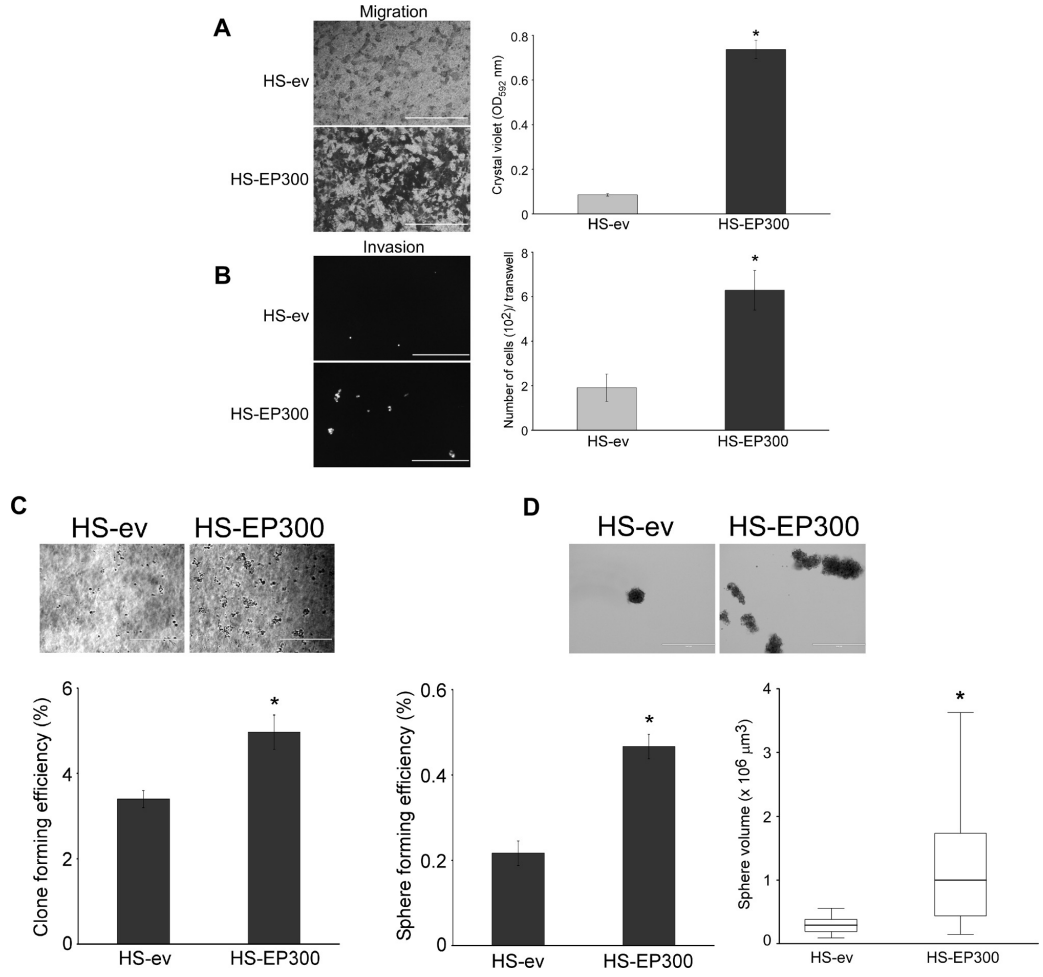

Fig. 5. HS-EP300 cells have increased migration, invasion and tumour formation capabilities. Up-regulation of EP300 increases the migration (A) and invasion (B) of HS578T cells. For the migration assays through transwells, cells were stained with crystal violet and for the invasion assays through transwells with Matrigel, cells were stained with DAPI. To obtain numerical data (*right panels*) crystal violet was solubilized and OD_{592} nm measured and DAPI-stained cells counted. Anchorage independence growth assays included mammospheres formation in low-attachment plates as well as colony formation in soft agar. C) Soft agar assay. Cells ($5x10^4$ / well) were seeded in 6-well dishes with medium containing soft agar and the formation of colonies determined after 8 weeks of culture. D) Mammosphere assay. Cells ($4x10^3$ / well) were grown in 6-well low attachment plates for two weeks and the number of spheres counted (*middle histogram*) and their volume calculated (*right box plot*). Clone or sphere forming efficiency calculated relative to the total number of plated cells x100. Pictorial data show representatives of at least three independent experiments. Numerical data represent the average ± SD of three different experiments (* $P < 0.05$). Bar represents 400 µm. Box plot indicates the median within the box at 95% confidence interval.

fold, respectively; Fig. 7D). Bioinformatic analyses of chromatin immunoprecipitation-sequencing data from The Encyclopedia of DNA Elements (ENCODE) [35] indicated that EP300 binds to *AKR1C1, AKR1C2* and *AKR1C3* promoters in A549, HeLa-S3, HepG2, MCF-7 and T47-D cells (data not shown). Thus, it is likely that during the generation of drug resistance, EP300 expression is activated, leading to up-regulation of *AKR1C1, AKR1C2* and *AKR1C3*.

3.7. Oncogenic EP300 can be targeted with FFA

In order to assess the role of *AKR1C1, AKR1C2* and *AKR1C3* in drug resistance we used a pharmacological approach. FFA is a non-steroid anti-inflammatory pan-AKR1C1-4 inhibitor [31] clinically used for a variety of rheumatic disorders [36]. For this we first performed drug sensitivity assays and determined that FFA concentrations up to 50 µM were not highly toxic for HS578T cells and drug resistant derivatives (Fig. 8A). Then, we asked whether FFA could resensitize drug resistant HS578T cells. For this we performed long-term clonogenic assays to identify cells that survive and proliferate after doxorubicin/paclitaxel treatment. Reassuringly, FFA did not produce any significant effect in the generation of clones from resistant cells in the absence of doxorubicin or paclitaxel. However, when drug resistant cells were treated with both FFA and chemotherapeutic drug (either doxorubicin or paclitaxel) the generation of resistant clones diminished dramatically

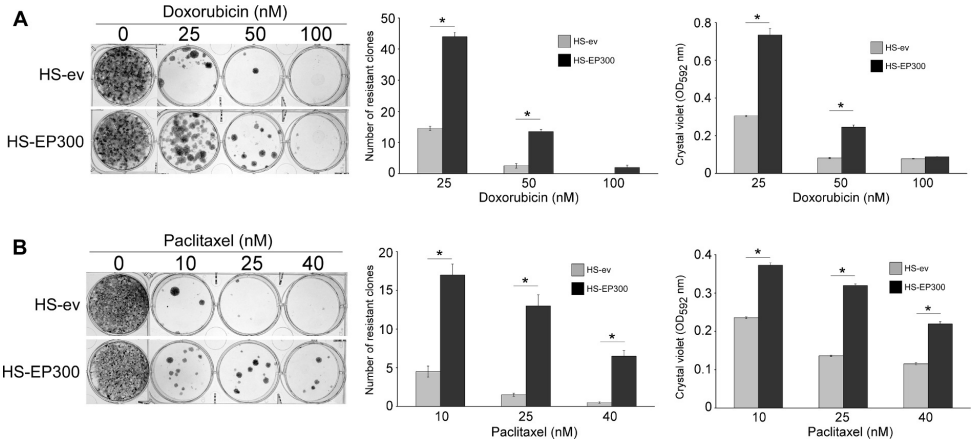

Fig. 6. Up-regulation of EP300 in an E-cadherin null background leads to drug resistance. Cells (3×10^3/well) were treated with doxorubicin for 2 days (A) or paclitaxel for 3 days (B) in 6-well dishes and drug-resistant, proliferating clones were stained with crystal violet after 4 weeks (1 week for the control), photographed (*left panels*), counted (*middle panels*) and crystal violet solubilized (*right panels*). Pictorial data show representatives of at least three independent experiments. Numerical data represent the average ± SD of three different experiments (*$P < 0.05$).

Table 3
Selection of most up-and down-regulated genes in HS-EP300 cells.

Gene	Description	Fold change[a]	*P*
AKR1C1	Aldo-keto reductase family 1, member C1	5.53	0.00002
ELF1	E74 Like ETS (E26 transformation-specific related) Transcription Factor	5.03	0.00450
MEF2C	Myocyte enhancer factor 2C	3.68	0.00020
UGT1	UDP glucuronosyltransferase 1 family, polypeptides A1, A6, A4, A10, A8, A7, A5, A3, A9	3.61	0.00002
KRT81	Keratin 81	3.61	0.00003
AKR1C2	Aldo-keto reductase family 1, member C2	3.50	0.00030
ALDH1A1	Aldehyde dehydrogenase 1 family, member A1	3.39	0.00360
AKR1C3	Aldo-keto reductase family 1, member C3	2.99	0.00010
CDH6	Cadherin 6	2.94	0.00010
NUDT6	Nudix hydrolase 6	2.85	0.01770
GORAB	Golgin, RAB6-interacting	2.69	0.04680
ARL4A	ADP-ribosylation factor like GTPase 4A	2.66	0.00350
ATP6V1C1	ATPase, H + transporting, lysosomal 42 kDa, V1 subunit C1	2.60	0.00110
AVEN	Apoptosis and caspase activation inhibitor	2.41	0.00080
ALDH1A2	Aldehyde dehydrogenase 1 family, member A2	2.27	0.00240
TP53INP1	Tumor protein p53 inducible nuclear protein 1	−2.26	0.00210
BIN3	Bridging integrator 3	−2.48	0.02100
IGFBP3	Insulin like growth factor binding protein 3	−2.54	0.00020
MXI1	MAX interactor 1, dimerization protein	−2.59	0.00020
BGN	Biglycan	−2.62	0.00030
TAGLN	Transgelin	−2.65	0.00040
KCTD11	Potassium channel tetramerization domain containing 11	−2.67	0.00010
POTEM; POTEG	POTE ankyrin domain family, members M and G	−2.72	0.00460
TUFT1	Tuftelin 1	−3.57	0.00100

[a] Positive expression values denote up-regulation and negative expression values denote down-regulation respect to HS-ev control cells.

(from ~45% in HS-DOX cells treated with 50 nM doxorubicin to ~10% when treated with 50 nM doxorubicin and 50 μM FFA; and from ~ 70% in HS-TX cells treated with 20 nM paclitaxel to ~30% when treated with 20 nM paclitaxel and 40 μM FFA; Fig. 8B and C). Thus, pharmacological inhibition of aldo–keto reductases resensitizes HS578T drug resistant cells.

As aldo–keto reductases, and particularly AKR1C3, reduce prostaglandins generating proliferating signals that may lead to breast cancer development [37], we asked whether their pharmacological inhibition with FFA might affect *in vitro* tumour initiation properties. Indeed, when HS-EP300 cells, which overexpress AKR1C1, AKR1C2 and AKR1C3, were treated with 50 μM FFA for 12 days, their mammosphere formation was reduced by 60%, whereas the reduction in control HS-ev cells was just 45%. Equally, there was a reduction in mammosphere volume upon FFA treatment of ~25% in HS-ev control cells that increased to ~70% in HS-EP300 cells (Fig. 8D).

Thus, the oncogenic, metastatic and drug resistance capacity of EP300 in a non-permissive E-cadherin background are due, at least in part, to the activation of aldo-keto reductases.

4. Discussion

Regulation of E-cadherin expression by transcriptional repressors, such as those belonging to the Snail family (Snail, Slug), the two-handed zinc factors ZEB1 and ZEB2, as well as the bHLH factors Twist and E47, is well understood. However, studies of E-cadherin transcriptional activators, such as EP300, are limited and in some cases with conflicting results [16,21]. We have recently demonstrated that both

EP300 and E-cadherin are down-regulated in metaplastic breast carcinoma [15], as would be expected for a positive regulator of E-cadherin. Here we demonstrate that, using two types of breast cancer, preselected

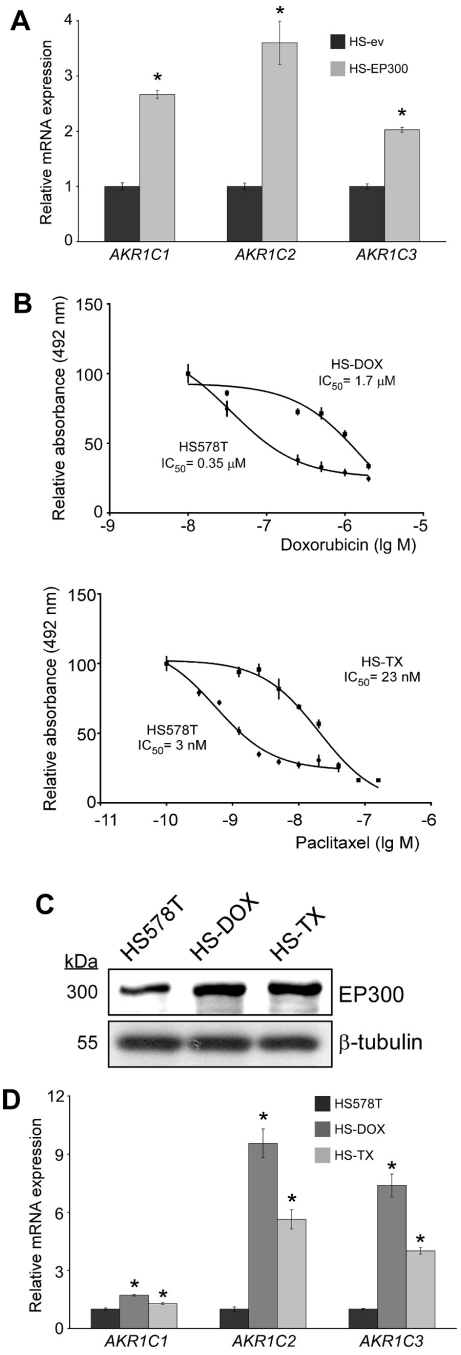

Fig. 7. Up-regulation of aldo-keto reductases. A) Determination of aldo–keto reductases mRNA levels in HS-EP300 and control HS-ev cells by real-time PCR normalized to the expression of *RPL19* mRNA. B) HS578T cells were used to generate doxorubicin (HS-DOX) and paclitaxel (HS-TX) resistant derivatives. Drug sensitivity best-fit curves determined by sulphorhodamine B assays. C) EP300 expression determined by western blot analysis in drug naive and resistant cells. D) Determination of aldo-keto reductases mRNA levels in drug naive and resistant cells HS578T cells by real-time PCR normalized to the expression of *RPL19* mRNA. Numerical data represent the average ± SD of three different experiments ($^{*}P < 0.05$). A representative immunoblot of three independent experiments is shown.

to comprise both E-cadherin^{low} and E-cadherin^{high} cases, the expression of these two markers correlates, reinforcing an EP300 positive regulatory role on E-cadherin expression. Importantly, using both markers together might be better at predicting lymph node metastasis than E-cadherin alone. These data agree with the well-established metastasis / tumour suppressor role of EP300 in a variety of cancers, including breast cancer reported by us [15] and others [16–18].

Interestingly, out of the 41 breast cancer cases analyzed, 9 showed E-cadherin low or null expression despite showing EP300 positivity. This reflects a complex scenario in the regulation of E-cadherin expression. In addition to the aforementioned transcriptional repressors, that may counteract EP300 activity, truncating mutations at the *CDH1* locus have been described in a few ILC cases [38,39], although mutation accounts for only a minority of cases of E-cadherin dysfunction in cancer [40]. E-cadherin absence can also be due to promoter hypermethylation, which has been demonstrated in ILC [41], acting as a dominant phenotype, as well as loss of heterozygosity, also high in ILC [42]. Reassuringly, E-cadherin proximal promoter shows a higher percentage of methylation in EP300^{high}/E-cadherin^{low} than in EP300^{high}/E-cadherin^{high} samples. However, this does not rule out a role of transcriptional repressors, potential *CDH1* mutations or loss of heterozygosity that might contribute to repression of E-cadherin expression. Nonetheless, this prompted us to ask whether EP300 might have a cancer role, independent of its activity on *CDH1* that could shed light on EP300 function to reconcile conflicting published reports. To tackle this, we decided to experimentally over-express EP300 in HS578T cells, a breast cancer cell line with hypermethylation of the *CDH1* locus, as EP300 is unable to transcriptionally activate its promoter. We have also previously over-expressed EP300 in E-cadherin-null MDA-MB-231 cells with a clear up-regulation of E-cadherin expression [15]. However, the average percentage of methylation in 29 CpG sites at the proximal *CDH1* promoter in MDA-MB-231 cells is just 13%, less than the 21% found in epithelial-like, E-cadherin expressing MCF-7 cells. In contrast, the *CDH1* promoter in HS578T cells is methylated by 47% [9]. This clearly explains the differential ability of EP300 activating the *CDH1* promoter in both cell lines and, confirms the suitability of this cell model to study EP300 oncogenic effects in an E-cadherin-independent manner.

Overexpression of EP300 in HS578T cells leads to a more aggressive phenotype, characterized by increases in the expression of mesenchymal markers (N-cadherin, vimentin) and repressors of E-cadherin expression (Snail, Slag, Zeb1), as well as an increase in the proportion of cells expressing stem cell-like markers (ALDH and CD44^{high}/CD24^{low}). This is accompanied by increases in motility, invasion and anchorage independence. Thus, in this breast cancer cell line, EP300 has a traditional oncogenic, metastasis promoting role. In PC3 prostate cancer cells, which have high levels of N-cadherin and low/null levels of E-cadherin [43], with only 15% methylation of *CDH1* promoter [9], experimental down-regulation of EP300 leads to apoptosis and reduction in motility and invasion [44]. Thus, oncogenic EP300 in PC3 cells may reflect more its inability to activate *CDH1* transcription and outcompete transcriptional repressors rather than the methylation status of *CDH1* promoter. In hepatocellular and nasopharyngeal carcinoma, EP300 acts as an oncogene, as high levels correlate with aggressive features and

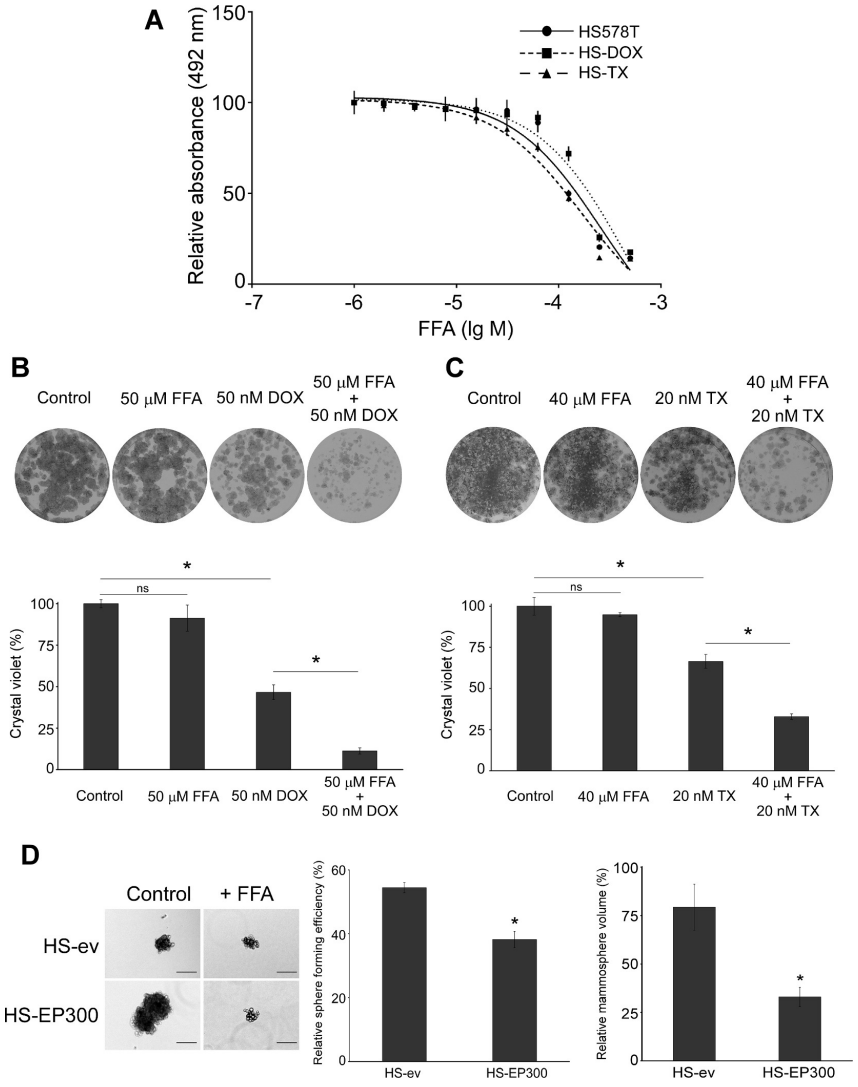

Fig. 8. Pharmacological inhibition of aldo–keto reductases reverts drug resistance and reduces anchorage independent growth. A) FFA toxicity best-fit curves in drug naive HS578T and doxorubicin (HS-DOX) and paclitaxel (HS-TX) resistant cells determined by sulforhodamine B staining. Cells ($3x10^3$ / well) were seeded in 96-well dishes and treated with increasing concentrations of FFA for 3 days before staining and measurement of optical density at 492 nm. Doxorubicin resistant HS-DOX cells (B) or placlitaxel resistant HS-TX cells (C) were seeded into 6-well plates ($1x10^3$ cells / well) and treated with FFA, doxorubicin (*DOX*) or placlitaxel (*TX*), or a combination of both drugs for 3 days. Clone growth was monitored after 15 days, stained with crystal violet (representative pictures on top) and absorbance at 592 nm determined (*bottom histograms*). D) Anchorage independence was monitored in HS-EP300 and control HS-ev cells by sphere formation in liquid medium using low attachment plates. Cells were seeded in 6 well plates ($4x10^3$ cells / well) and treated either with 50 μM FFA or vehicle control. Mammospheres were counted after 12 days (*middle histogram*) and their volume calculated (*right histogram* indicates relative volume of each cell line to the corresponding vehicle control). Bar represents 100 μm. Pictorial data show representatives of at least three independent experiments. Numerical data represent the average ± SD of three different experiments (* $P < 0.05$).

patient poor prognosis [45,46]. In some hepatocellular and nasopharyngeal carcinoma cell lines, experimental down-regulation of EP300 paradoxically leads to up-regulation of E-cadherin and down-regulation of EMT [20,21]. Whether this is a direct repression of the *CDH1* locus by EP300 [47], or an indirect effect, remains to be established. Thus, EP300 function as oncogene or tumour suppressor is clearly cancer/context dependent and can have both activation and repression roles on E-cadherin expression, controlling EMT and metastasis positively or negatively.

The EP300 oncogenic signature in HS-578T cells indicates its regulation of AKR1C1, AKR1C2 and AKR1C3, probably by direct transcriptional activation. AKR1C members have been found to be up-

regulated in many cancers, although in breast cancer this seems to be limited to AKR1C3 [33]. Aldo-keto reductases can detoxify anthracyclines, and AKR1C3 reduces doxorubicin to the corresponding C13 alcohol metabolite, doxorubicinol, which has less toxicity and DNA binding capacity [33,48]. This explains the doxorubicin resistant phenotype upon EP300 up-regulation in HS578T cells. It is uncertain whether paclitaxel is a substrate for aldo-keto reductases, although AKR1C1 confers resistance to a non-substrate, such as cisplatin, in gastric carcinoma cells, probably via indirect mechanisms [49]. Importantly, tumour initiation capacity is also dependent on aldo-keto reductase activity, as it decreases upon treatment with FFA. AKR1C3 is up-regulated in invasive ductal breast carcinoma and correlates with a worst prognosis [50]. AKR1C3 is involved in several metabolic reactions that may lead to the development of breast cancer by increasing estrogenic signals. However, in triple negative breast cancer, the reduction of prostaglandins has a more important role as it generates hormone-independent proliferative signals by increase in MAPK signaling, NFkB activity and decrease of PPARγ activity [37]. Although the development of novel aldo-keto reductase inhibitors specific for each isoform [33] would be a strategy to consider in cancer therapy, some caution must be exerted as aldo-keto reductases help relieve cardiac toxic effects of anthracyclins [51] and inhibitors might increase chemotherapy side effects. Whether aldo-keto reductases contribute also to the oncogenic effects of EP300 in different cancers and cell models, remains to be established.

In summary, EP300 acts as a tumour suppressor when able to activate E-cadherin expression. However, if E-cadherin expression is blocked, EP300 acts as an oncogene via up-regulation of aldo-keto reductases.

Conflict of interests

The authors declare no conflict of interest.

Acknowledgements

This study was partially funded by Breast Cancer Now (2014NovPhD326 to EY, EWFL and SS), Cancer Research UK (C37/A12011 to RCC, EWFL) and The Tianjin Natural Sciences Foundation (17JCQNJC09900 to YH). EWFL's work was also supported by The Medical Research Council (MR/N012097/1) and Breast Cancer Now (2012MayPR070 and 2012NovPhD016). The National Institute for Health Research Imperial Biomedical Research Centre, the Imperial Experimental Cancer Medicine Centre and the Cancer Research UK Imperial Centre at Imperial College London provided infrastructure support. Some tissue samples were provided by the Imperial College Healthcare NHS Trust Tissue Bank, which is funded by the National Institute for Health Research (NIHR) Biomedical Research Centre based at Imperial College Healthcare NHS Trust and Imperial College London. The views expressed are those of the authors and not necessarily those of the NHS, the NIHR or the Department of Health. ZM, MA and UK were supported by fellowships from the Commonwealth Scholarship Commission. RJ was supported by a fellowship from Breast Cancer Now.

References

[1] D. Hanahan, R.A. Weinberg, Hallmarks of cancer: the next generation, Cell 144 (5) (2011) 646–674.
[2] R. Singhai, V.W. Patil, S.R. Jaiswal, S.D. Patil, M.B. Tayade, A.V. Patil, E-Cadherin as a diagnostic biomarker in breast cancer, North Am. J. Med. Sci. 3 (5) (2011) 227–233, https://doi.org/10.4297/najms.2011.3227.
[3] Y. Zhang, K.A. Toy, C.G. Kleer, Metaplastic breast carcinomas are enriched in markers of tumor-initiating cells and epithelial to mesenchymal transition, Mod. Pathol. 25 (2) (2012) 178–184, https://doi.org/10.1038/modpathol.2011.167.
[4] B. Weigelt, C. Eberle, C.F. Cowell, C.K. Ng, J.S. Reis-Filho, Metaplastic breast carcinoma: more than a special type, Nat. Rev. Cancer 14 (3) (2014) 147–148.
[5] U. Jeschke, I. Mylonas, C. Kuhn, N. Shabani, C. Kunert-Keil, C. Schindlbeck, et al., Expression of E-cadherin in human ductal breast cancer carcinoma in situ, invasive carcinomas, their lymph node metastases, their distant metastases, carcinomas with recurrence and in recurrence, Anticancer Res. 27 (4A) (2007) 1969–1974.
[6] S.A. Mani, W. Guo, M.J. Liao, E.N. Eaton, A. Ayyanan, A.Y. Zhou, et al., The epithelial-mesenchymal transition generates cells with properties of stem cells, Cell 133 (4) (2008) 704–715, https://doi.org/10.1016/j.cell.2008.03.027.
[7] T.T. Onder, P.B. Gupta, S.A. Mani, J. Yang, E.S. Lander, R.A. Weinberg, Loss of E-Cadherin promotes metastasis via multiple downstream transcriptional pathways, Cancer Res. 68 (10) (2008) 3645–3654, https://doi.org/10.1158/0008-5472.can-07-2938.
[8] G. Berx, K.F. Becker, H. Hofler, F. van Roy, Mutations of the human E-cadherin (CDH1) gene, Hum. Mutat. 12 (4) (1998) 226–237.
[9] W.C. Reinhold, M.A. Reimers, A.K. Maunakea, S. Kim, S. Lababidi, U. Scherf, et al., Detailed DNA methylation profiles of the E-cadherin promoter in the NCI-60 cancer cells, Mol. Cancer Ther. 6 (2) (2007) 391–403.
[10] J. Yang, S.A. Mani, J.L. Donaher, S. Ramaswamy, R.A. Itzykson, C. Come, et al., Twist, a master regulator of morphogenesis, plays an essential role in tumor metastasis, Cell 117 (7) (2004) 927–939, https://doi.org/10.1016/j.cell.2004.06.006.
[11] Y.N. Liu, W.W. Lee, C.Y. Wang, T.H. Chao, Y. Chen, J.H. Chen, Regulatory mechanisms controlling human E-cadherin gene expression, Oncogene 24 (56) (2005) 8277–8290.
[12] F. van Roy, G. Berx, The cell-cell adhesion molecule E-cadherin, Cell. Mol. Life Sci.: CMLS 65 (23) (2008) 3756–3788, https://doi.org/10.1007/s00018-008-8281-1.
[13] Y. Zhou, Y. Hu, M. Yang, P. Jat, K. Li, Y. Lombardo, et al., The miR-106b~25 cluster promotes bypass of doxorubicin-induced senescence and increase in motility and invasion by targeting the E-cadherin transcriptional activator EP300, Cell Death Differ. 21 (3) (2014) 462–474, https://doi.org/10.1038/cdd.2013.167.
[14] Y. Hu, K. Li, M. Asaduzzaman, R. Cuella, H. Shi, S. Raguz, et al., miR-106b~25 cluster regulates multidrug resistance in an ABC transporter-independent manner via downregulation of EP300, Oncol. Rep. 35 (2016) 1170–1178, https://doi.org/10.3892/or.2015.4412.
[15] M. Asaduzzaman, S. Constantinou, H.X. Min, J. Gallon, M.L. Lin, P. Singh, et al., Tumour suppressor EP300, a modulator of paclitaxel resistance and stemness, is downregulated in metaplastic breast cancer, Breast Cancer Res. Treat. 163 (3) (2017) 461–474.
[16] S.T. Mees, W.A. Mardin, C. Wendel, N. Baeumer, E. Willscher, N. Senninger, et al., EP300–a miRNA-regulated metastasis suppressor gene in ductal adenocarcinomas of the pancreas, Int. J. Cancer 126 (1) (2010) 114–124.
[17] D. Krubasik, N.G. Iyer, W.R. English, A.A. Ahmed, M. Vias, C. Roskelley, et al., Absence of p300 induces cellular phenotypic changes characteristic of epithelial to mesenchyme transition, Br. J. Cancer 94 (9) (2006) 1326–1332, https://doi.org/10.1038/sj.bjc.6603101.
[18] B. Gyorffy, A. Lanczky, A.C. Eklund, C. Denkert, J. Budczies, Q.Y. Li, et al., An online survival analysis tool to rapidly assess the effect of 22,277 genes on breast cancer prognosis using microarray data of 1,809 patients, Breast Cancer Res. Treat. 123 (3) (2010) 725–731.
[19] F.R. Santer, P.P.S. Hoschele, S.J. Oh, H. Erb, J. Bouchal, I.T. Cavarretta, et al., Inhibition of the acetyltransferase p300 as a novel pro-apoptotic and anti-invasion approach for treatment of prostate cancer, Cancer Res. 71 (2011) 1622.
[20] C. Yokomizo, K. Yamaguchi, Y. Itoh, T. Nishimura, A. Umemura, M. Minami, et al., High expression of p300 in HCC predicts shortened overall survival in association with enhanced epithelial mesenchymal transition of HCC cells, Cancer Lett. 310 (2) (2011) 140–147.
[21] Z.W. Liao, L. Zhao, M.Y. Cai, M. Xi, L.R. He, F. Yu, et al., P300 promotes migration, invasion and epithelial-mesenchymal transition in a nasopharyngeal carcinoma cell line, Oncol. Lett. 13 (2) (2017) 763–769.
[22] L.F. Chen, Y. Mu, W.C. Greene, Acetylation of RelA at discrete sites regulates distinct nuclear functions of NF-kappaB, Embo J. 21 (23) (2002) 6539–6548.
[23] Y. Lombardo, A. Filipovic, G. Molyneux, M. Periyasamy, G. Giamas, Y. Hu, et al., Nicastrin regulates breast cancer stem cell properties and tumor growth in vitro and in vivo, Proc. Natl. Acad. Sci. U.S.A. 109 (41) (2012) 16558–16563, https://doi.org/10.1073/pnas.1206268109.
[24] Y.H. Hu, S.J. Li, M. Yang, C.H. Yan, D.M. Fan, Y. Zhou, et al., Sorcin silencing inhibits epithelial-to-mesenchymal transition and suppresses breast cancer metastasis in vivo, Breast Cancer Res. Treat. 143 (2) (2014) 287–299.
[25] S. Raguz, C. Adams, N. Masrour, S. Rasul, P. Papoutsoglou, Y. Hu, et al., Loss of O (6)-methylguanine-DNA methyltransferase confers collateral sensitivity to carmustine in topoisomerase II-mediated doxorubicin resistant triple negative breast cancer cells, Biochem. Pharmacol. 85 (2) (2013) 186–196, https://doi.org/10.1016/j.bcp.2012.10.020.
[26] N. Pecina-Slaus, Tumor suppressor gene E-cadherin and its role in normal and malignant cells, Cancer Cell. Int. 3 (1) (2003) 17, https://doi.org/10.1186/1475-2867-3-17.
[27] C.D. Allis, T. Jenuwein, The molecular hallmarks of epigenetic control, Nat. Rev. Genet. 17 (8) (2016) 487–500.
[28] M. Esteller, P.G. Corn, S.B. Baylin, J.G. Herman, A gene hypermethylation profile of human cancer, Cancer Res. 61 (8) (2001) 3225–3229.
[29] A.W. Lambert, D.R. Pattabiraman, R.A. Weinberg, Emerging biological principles of metastasis, Cell 168 (4) (2017) 670–691.
[30] Z. Wang, Y. Li, A. Ahmad, A.S. Azmi, D. Kong, S. Banerjee, et al., Targeting miRNAs involved in cancer stem cell and EMT regulation: An emerging concept in overcoming drug resistance, Drug Resist. Updat. 13 (4–5) (2010) 109–118.
[31] C.Z. Li, B. Lu, R.M. Garbaccio, E.S. Tasber, M.E. Fraley, G.D. Hartman, et al., Stereospecific reduction of a potent kinesin spindle protein (KSP) inhibitor in human tissues, Biochem. Pharmacol. 79 (10) (2010) 1526–1533.
[32] T.M. Penning, The aldo-keto reductases (AKRs): overview, Chem-Biol. Interact. 234

(2015) 236–246.
[33] C.M. Zeng, L.L. Chang, M.D. Ying, J. Cao, Q.J. He, H. Zhu, et al., Aldo-keto reductase AKR1C1-AKR1C4: functions, regulation, and intervention for anti-cancer therapy, Front. Pharmacol. 8 (2017) 119.
[34] R. Bortolozzi, S. Bresolin, E. Rampazzo, M. Paganin, F. Maule, E. Mariotto, et al., AKR1C enzymes sustain therapy resistance in paediatric T-ALL, Brit. J. Cancer 118 (7) (2018) 985–994.
[35] I. Dunham, A. Kundaje, S.F. Aldred, P.J. Collins, C.A. Davis, F. Doyle, et al., An integrated encyclopedia of DNA elements in the human genome, *Nature* (Article) 489 (2012) 57, https://doi.org/10.1038/nature11247.
[36] M. Asif, Study of anthranylic acid derivatives: mefenamic acid and its various analogues, Am. J. Med. Stud. 2 (1) (2014) 24–30.
[37] M.C. Byrns, T.M. Penning, Type 5 17 beta-hydroxysteroid dehydrogenase/prostaglandin F synthase (AKR1C3): Role in breast cancer and inhibition by non-steroidal anti-inflammatory drug analogs, Chem-Biol. Interact. 178 (1–3) (2009) 221–227.
[38] G. Berx, A.M. CletonJansen, F. Nollet, W.J.F. deLeeuw, M.J. vandeVijver, C. Cornelisse, et al., E-cadherin is a tumour invasion suppressor gene mutated in human lobular breast cancers, EMBO J. 14 (24) (1995) 6107–6115.
[39] S. Droufakou, V. Deshmane, R. Roylance, A. Hanby, I. Tomlinson, I.R. Hart, Multiple ways of silencing E-cadherin gene expression in lobular carcinoma of the breast, Int. J. Cancer 92 (3) (2001) 404–408.
[40] S.H.M. Wong, C.M. Fang, L.H. Chuah, C.O. Leong, S.C. Ngai, E-cadherin: its dysregulation in carcinogenesis and clinical implications, Crit. Rev. Oncol. Hemat. 121 (2018) 11–22.
[41] D. Sarrio, G. Moreno-Bueno, D. Hardisson, C. Sanchez-Estevez, M.Z. Guo, J.G. Herman, et al., Epigenetic and genetic alterations of APC and CDH1 genes in lobular breast cancer: relationships with abnormal E-cadherin and catenin expression and microsatellite instability, Int. J. Cancer 106 (2) (2003) 208–215.
[42] A.M. Cleton-Jansen, E-cadherin and loss of heterozygosity at chromosome 16 in breast carcinogenesis: different genetic pathways in ductal and lobular breast cancer? Breast Cancer Res. 4 (1) (2002) 5–8.
[43] A. Mishra, J.C. Wang, Y. Shiozawa, S. McGee, J. Kim, Y.H. Jung, et al., Hypoxia stabilizes GAS6/Axl signaling in metastatic prostate cancer, Mol. Cancer Res. 10 (6) (2012) 703–712.
[44] F.R. Santer, P.P.S. Hoschele, S.J. Oh, H.H.H. Erb, J. Bouchal, I.T. Cavarretta, et al., Inhibition of the acetyltransferases p300 and CBP reveals a targetable function for p300 in the survival and invasion pathways of prostate cancer cell lines, Mol. Cancer Ther. 10 (9) (2011) 1644–1655.
[45] M. Li, R.Z. Luo, J.W. Chen, Y. Cao, J.B. Lu, J.H. He, et al., High expression of transcriptional coactivator p300 correlates with aggressive features and poor prognosis of hepatocellular carcinoma, J. Transl. Med. 9 (2011) 5.
[46] Z.W. Liao, T.C. Zhou, X.J. Tan, X.L. Song, Y. Liu, X.Y. Shi, et al., High expression of p300 is linked to aggressive features and poor prognosis of Nasopharyngeal Carcinoma, J. Transl. Med. 10 (2012) 110.
[47] D. Girdwood, D. Bumpass, O.A. Vaughan, A. Thain, L.A. Anderson, A.W. Snowden, et al., P300 transcriptional repression is mediated by SUMO modification, Mol. Cell 11 (4) (2003) 1043–1054.
[48] J. Hofman, B. Malcekova, A. Skarka, E. Novotna, V. Wsol, Anthracycline resistance mediated by reductive metabolism in cancer cells: the role of aldo-keto reductase 1C3, Toxicol. Appl. Pharmacol. 278 (3) (2014) 238–248.
[49] C.C. Chen, C.B. Chu, K.J. Liu, C.Y.F. Huang, J.Y. Chang, W.Y. Pan, et al., Gene expression profiling for analysis acquired oxaliplatin resistant factors in human gastric carcinoma TSGH-S3 cells: the role of IL-6 signaling and Nrf2/AKR1C axis identification, Biochem. Pharmacol. 86 (7) (2013) 872–887.
[50] O.O. Oduwole, Y. Li, V.V. Isomaa, A. Mantyniemi, A.E. Pulkka, Y. Soini, et al., 17 beta-hydroxysteroid dehydrogenase type 1 is an independent prognostic marker in breast cancer, Cancer Res. 64 (20) (2004) 7604–7609.
[51] G. Minotti, P. Menna, E. Salvatorelli, G. Cairo, L. Gianni, Anthracyclines: molecular advances and pharmacologic developments in antitumor activity and cardiotoxicity, Pharmacol. Rev. 56 (2) (2004) 185–229.

Appendix B

Scripts

B.1 Migration Cell Tracking R Script

The R script was written by Dr Olivier Pardo, adapted and commented by me for the migration experiments used in this study.

```
#Set working directory to desired location e.g.
setwd("/Users/Documents/Migration_data/")
getwd()

#Enter the number treatment or conditions, add as required
Treatments<-c("Control","Treatment1","Treatment2")

#Count number of files in the working directory
list<-list.files()
nfiles<- as.numeric(length(list))

#Load libraries required for the code to run
library(xlsx)
library(data.table)
library(dplyr)
library(gplots)
library(tidyr)
library(reshape2)
library(plyr)
```

```
library(tidyverse)
library(ggsci)
library(ggpubr)
library(grid)
library(gridExtra)
library(ggsignif)

# CELL SPEED ANALYSIS #


#Create an empty dataframe
df<-data.table()

#Iterates through chosen directory and populates datafame
   with file contents
for(i in 1:nfiles){
    df_i<- read.table(list[i], sep="\t", header=TRUE)
    df_i$iTrack<-as.character(list[i])
    df<-rbind(df,df_i)
}

#Cleans dataframe by separating the "condition" name from "
   field number" and taking out the first negative speed
   measurement
df<-separate(data = df, col = iTrack, into = c("condition",
   "field"), sep = "\\_")
dfv<-df[df$Velocity!=-1,]

#Groups data by condition/track/field and creates a
   dataframe for "meanspeed" containing average speed for
   each field
by <- group_by(dfv, condition, Track.n., field)
meanspeed <- ddply(by, c("condition","field","Track.n.."),
   summarise, mean = mean(Velocity))
```

```
#Clean up the meanspeed dataframe by placing it into a
   temporary variable and assigning column names
tmp<-separate(data = meanspeed, col = field, into = c("field
   ", "xls"), sep = "\\.")
meanspeed$field<-tmp$field
colnames(meanspeed)=c("Condition", "Track", "Field", "Speed"
   )
meanspeed$Condition = factor(meanspeed$Condition,Treatments)

#Plot mean speed per condition as a boxplot
#Start PNG device and specify file name, image size and
   resolution
png("Figure_1_Migration_Speed_CAL.png", width=3000, height
   =3000, res=400)
#start ggplot package and group data by condition, and
   assign X and Y
p <- ggplot(meanspeed, aes(fill = Condition, y=Speed, x=
   Condition))
#Create boxplot
p <- p + geom_boxplot()
#Assign X and Y axis labels
p <- p + labs(x="Cell␣Line", y="Speed␣(AU)")+
#Make legend with blank background
p <- p + theme(legend.key = element_blank())
#Assign colour theme from chosen journal, choose from ggsci
   package based on preference
p <- p + scale_fill_npg()
#Make graph neater by having blank background and only
   outline of box
p <- p + theme(panel.grid.major = element_blank(), panel.
   grid.minor = element_blank(),
                  panel.background = element_blank()) +
#Adjust text size/font/colour on graph
  theme(plot.title=element_text(hjust = .5,vjust=2)) +
  theme(plot.title=element_text(size= 10,lineheight=.9, face
     ="bold", colour="black"))
```

```
p <- p + theme(axis.title.x = element_text(size=10,
   lineheight=.9,face="bold",color="black",vjust=-0.35),
                axis.title.y = element_text(size=10,
                   lineheight=.9,face="bold",color="black",
                   hjust=0.5,vjust=-0))
p <- p + theme(strip.text.x = element_text(size = 12),
                strip.text.y = element_text(size = 12))
p <- p + theme(axis.line.x = element_line(color="black",
   size = 0.5),
                axis.line.y = element_line(color="black",
                   size = 0.5))
#Adjust tick length
p <- p + theme(axis.ticks.length = unit(.5,))
#Adjust y scale
p <- p + scale_y_continuous(breaks=seq(0,0.6,0.05))
#Adjustments to labels on x axis can be done if needed
p <- p + scale_x_discrete(labels= c("CAL-EV", "CAL-EP300", "
   CAL-CDH1"))
#end  PNG device
dev.off()

#Associated statistics
aov.out = aov(Speed ~ Condition, data=meanspeed)
stats<-TukeyHSD(aov.out)

#Create a separate dataframe containing the summarised speed

meltmeanspeed<-melt(meanspeed,id=c("Condition"), measure.
   vars = "Speed")
summaryspeed<-dcast(meltmeanspeed, Condition ~variable, mean
   )


View(meanspeed)
View(stats[[1]])
View(summaryspeed)
```

```
# CELL TRACKS #


#Create a new dataframe copy of df
df1<-df

#Clean up df1 by creating the ID variable (containing
   Condition/field/track number) and deleting unused columns
df1<-separate(data = df1, col = field, into = c("field", "
   crap"), sep = "\\.")
df1[,crap:=NULL]
df1$ID<-paste(df1$condition,df1$field,df1$Track.n.)
df1[,Velocity:=NULL]
df1[,Pixel.Value:=NULL]
df1[,field:=NULL]
df1[,Track.n.:=NULL]
df1[,Distance:=NULL]

#Create a dataframe for the X positions
splx=split(df1$X,df1$ID)
splx1st<-lapply(splx, '[[', 1)
normsplx=mapply('-',splx, splx1st)
wrong_files=normsplx[lapply(normsplx, length) < 109]
wrong_files
xdf<-data.frame(normsplx)


#Create a dataframe for the Y positions
sply=split(df1$Y,df1$ID)
sply1st<-lapply(sply, '[[', 1)
normsply=mapply('-',sply, sply1st)
ydf<-data.frame(normsply)

#Rename the column names of the X and Y dataframes to only
   keep condition names
```

```
xnames<-colnames(xdf)
xtmp<-strsplit(xnames,"\\.")
xtmp1 = lapply(xtmp, function(l) l[[1]])
colnames(xdf)<-xtmp1

ynames<-colnames(ydf)
ytmp<-strsplit(ynames,"\\.")
ytmp1 = lapply(ytmp, function(l) l[[1]])
colnames(ydf)<-ytmp1

#Determine first and end column for each condition to plot
e<-c()
end<-c(0)
dforder<-unique(colnames(xdf))
lg<-length(dforder)
for(i in 1:lg){
  e[i]<-ncol(xdf[,colnames(xdf)==dforder[i]])
  end[i+1]=e[i]+end[i]
}

first<-c(1)
for(i in 1:lg){

  first<-c(first, e[i]+first[i])
}

#Plot the tracks
axismax<-max(max(xdf), max(ydf))

for(i in 1:lg){
  plot(normsplx[,first[i]:end[i+1]],normsply[,first[i]:end[i
      +1]], type = "p", main=dforder[i], xlab="X (A.U.)",
      ylab="Y (A.U.)", las=2, xlim = c(-axismax,axismax),
      ylim = c(-axismax,axismax))
}
```

B.2 Invasion Assay Image post processing on Fiji Macro Script

The Script was written by Steve Rothery, adapted and commented by me for the invasion experiments used in this study to reset the min max and convert the image files to 8-bit format.

```
#Finds the dimensions for each image
Stack.getDimensions(width, height, channels, slices, frames);
#Finds the middle z-slice
n=slices/2;
Stack.setSlice(n)
#Reset min and max signal threshold value
resetMinAndMax();
#Converts image to 8-bit
run("8-bit");
```

B.3 Invasion Assay Image Analysis Object Counter Fiji Macro Script

The Script was written by Steve Rothery, adapted and commented by me for the invasion experiments used in this study to count the numbers in the matrigel.

```
#Set the input and output file locations
//input = "H:\\macro\\";
//output = "H:\\macrores\\";

#Create function which will loop through the list
function action(input, output, list)
{
        stat = "Statistics for ";
        full = input + list[i];
        out = output + list[i] + ".csv";
        print(f);
        print (o);
        #Run Bioformats importer to automate process of
           image import
        run("Bio-Formats Importer", "open=full autoscale
           color_mode= Default view=Hyperstack stack_order=
           XYCZT");
        #Finds median stack
        run("Median...", "radius=3 stack");
        #Count number of cells using 3D object counter
        run("3D Objects Counter", thresh);
        run("3D Objects Counter", "threshold=250 slice=25
           min.=25 max.= 8000 exclude_objects_on_edges
           statistics");
        res = stat + list[i];
        print (w);
        selectWindow (res);
        #Saves count results to .csv
        saveAs("Results", out);
        run("Close");
```

```
        close();
}

#Enter file directory and get files for function
        input = getDirectory("Location␣of␣images")
        output = getDirectory("Location␣for␣results")
        list = getFileList(input);

#Main command to use input threshold and count cells
        x = getNumber("input␣threshold", 240)
        thresh = "threshold=" + x + "␣slice=25␣min.=25␣max
           .=8000␣exclude_objects_on_edges␣statistics␣
           summary"

        print(x);
        print(thresh);

#Creates loop to itereate through files
for (i = 0; i < list.length; i++)
    action(input, output, list);
```

B.4 TCGA Data Analysis R Script

The Script was adapted from scripts written by Dr Alex di Giorgio and Dr Jonathan Krell, adapted and commented by me for the analysis of mRNA in the TCGA dataset.

```
#Get the FASTQ file e.g.
wget https://portal.gdc.cancer.gov/

#Test the quality of the FASTQ files using fastqc package
Perl fastqc--format fastq R1.fastq R2.fastq

#Align data to hg19 human genome build
Tophat --transcriptome-index refFlat_hg19 --no-mixed
--p 4 hg19 R1.fastq R2.fastq

#Using cufflinks, assemble individual transcripts from mapped reads
cufflinks-- p 4-o cufflinks__output accepted_hits.bam

#Merge all assembled individual transcripts into one .txt file
Cuffmerge --g refFlat.gtf -- s hg19.fa --p 4 assemblies.txt
```